QUANTIFICATION OF ICHNOLOGICAL, PALEOECOLOGICAL, PALEOHYDROLOGICAL, AND PALEOCLIMATOLOGICAL INFORMATION FROM THE UPPER JURASSIC MORRISON FORMATION

BY

Brian Frederic Platt

Submitted to the graduate degree program in Geology and the
Graduate Faculty of the University of Kansas
in partial fulfillment of the requirements for the degree of
Doctor of Philosophy.

_____
Stephen T. Hasiotis, Chair

_____
Luis A. González

_____
Robert H. Goldstein

_____
Daniel R. Hirmas

_____
Larry D. Martin

Date Defended: April 13, 2012

The Dissertation Committee for Brian F. Platt certifies
that this is the approved version of the following dissertation:

QUANTIFICATION OF ICHNOLOGICAL, PALEOECOLOGICAL, PALEOHYDROLOGICAL, AND PALEOCLIMATOLOGICAL INFORMATION FROM THE UPPER JURASSIC MORRISON FORMATION

Committee:

_____
Stephen T. Hasiotis, Chair

_____
Luis A. González

_____
Robert H. Goldstein

_____
Daniel R. Hirmas

_____
Larry D. Martin

Date approved: April 13, 2012

ABSTRACT

This dissertation takes a multifaceted approach to interpreting paleoenvironments and paleoclimate represented by the strata of the Morrison Formation (MF). The MF has been the subject of geological and paleontological investigations for well over a century, but a number of confounding factors have limited interpretations. One problem with interpreting MF ichnology is uncertainty about the sedimentary conditions under which deep dinosaur tracks were made. To solve this problem, I developed new methods to measure trace fossils, including footprints. I used multistripe laser triangulation scanning to create three-dimensional digital models of traces, from which I improved precision of traditional ichnological techniques. I also performed neoichnological experiments with elephants to collect empirical trackmaking data, to which I applied multiple regression to derive a quantitative relationship between physical trackmaking variables. Results showed that many deep sauropod tracks were created in near saturated conditions.

Megafaunal track preservation was one factor taken into consideration when interpreting paleohydrology from moisture regimes represented by trace-fossil assemblages. I demonstrated the usefulness of ichnological moisture regimes by interpreting ichnocoenoses in MF avulsion deposits in the Bighorn Basin. I found a regular pattern of moisture profiles associated with crevassing that can be used to identify avulsion deposits in future ichnological studies.

Ichnological moisture regimes were incorporated with other pedogenic features to develop a soil moisture index that was combined with measures of carbonate content, carbonate mineralogy, total organic carbon, and stable isotopes of carbonates and organic carbon to construct a detailed vertical profile through the MF in the Henry Mountains, Utah. This profile is useful for paleoclimatic and paleoenvironmental interpretations as well as for correlation to

marine isotope records. I compared the vertical profile to paleoecological patterns determined from food-web network analyses and found a possible correlation between a global shift in organic carbon isotopes and an episode of biotic turnover. I also found that MF food webs were extremely stable, a factor that may have contributed to the success of dinosaur-dominated ecosystems during the Mesozoic.

ACKNOWLEDGMENTS

This dissertation represents the culmination of many years of research, which would not have been possible without the support of numerous mentors, colleagues, sponsors, friends, and family members. First and foremost, I thank my advisor, Steve Hasiotis, for his years of guidance and mentorship. I owe the development of my research, teaching, and writing skills to Steve's keen eye in the field, his thorough instruction in the classroom, and his careful editing in the office. I am grateful for everything Steve has done for me and appreciate his unfailing support during my graduate career.

I thank my committee members, Bob Goldstein, Luis González, Dan Hirmas, and Larry Martin, for their years of assistance, helpful advice, and editorial comments. I am grateful for the opportunities I've had to draw upon their expertise and I feel that my work has been greatly improved by their contributions. I also thank Bill Johnson, Bruce Lieberman, and Curt Sorenson, who were on previous iterations of my committee.

I thank the University of Kansas (KU) Geology Department for providing me with a graduate teaching assistantship during my first year of PhD research. I am deeply indebted to Madison and Lila Self for endowing the Self Graduate Fellowship (SGF), and to Cathy Dwigans, Sharon Graham, Jim Morrison, Howard Mossberg, and Patty Dannenberg, and the Self Fellows with whom I overlapped for providing me with many memorable experiences during my time in the SGF. I also thank Rick Devlin and Steve Hasiotis for their assistance with preparing my application for the SGF. I thank the KU Environmental Studies Program for providing me with a graduate teaching assistantship, during which I learned a great deal from my teaching mentors, Bob Hagen, Kelly Kindscher, and Phil Englehart. I am grateful to Greg Ludvigson for providing

me with a graduate research assistantship at the Kansas Geological Survey to help me through the final lap of my PhD journey. Lastly, I thank Luis González for appointing me instructor of the Geology Department's online historical geology, which provided me with valuable teaching experience in a medium that is becoming increasingly more prevalent in the realm of education.

Financial support for my research was provided internally by the KU Geology Department, a KU Natural History Museum and Biodiversity Research Center Panorama Society Small Grant Award, and a Leaman Harris Scholarship from the KU Biodiversity Institute. External support for my research was provided by the American Association of Petroleum Geologists, the Geological Society of America, the Jurassic Foundation, Paleontological Society Stephen J. Gould Grants, and Sigma Xi.

I am grateful to the staff of the Topeka Zoo and the Topeka Engineering Division for their cooperation, generosity, and patience during my elephant neoichnology research; this research would not have been possible without the efforts of Dawn Olson, Mike Coker, Fawn Moser, Daniel and Mindy Shute, Shawn Bruns, James Lopez, and Mike Briggs. I also thank Mark Bowen, Bill Johnson, John Kelly, Sara Platt, Julie Retrum, Ian Rowell, Jon Smith, Celina Suarez, Marina Suarez, Emily Tremain, and Terri Woodburn for their assistance with this project. My Morrison Formation research has been supported logistically through generous assistance in the field by a number of individuals, including Mary Kraus, Erik Kvale, Jim Farlow, Adam Huttenlocker, Cliff and Row Manuel, Chad Motter, Melissa Smeins, and Josh Schmerge. This fieldwork also would not have been possible without Brent Breithaupt and Dale Hanson of the Bureau of Land Management. I thank Greg Cane, Alvin Bonilla, Erin Dempsey, Greg Ludvigson, Laura Murphy, Celina Suarez, and Marina Suarez for their time spent on my laboratory training and help with sample analyses. My food-web research is the result of

generous assistance from Jennifer Dunne and Rich Williams. Finally, I thank Liana Silva at the KU Writing Center and my graduate student writing group for keeping me motivated while writing my dissertation.

I have been fortunate enough to share my PhD experiences with many graduate students, whose camaraderie I greatly value. These former and present students include Aisha Al-Suwaidi, Kenny Bader, Alvin Bonilla, Curtis Congreve, John Counts, Amanda Falk, Wes Gapp, Alan Halfen, Adam Jackson, Debra Jennings, Matt Jones, Wade Jones, Tony Layzell, Dave LoBue, Kim Metevier, Robin Moore, Cori Myers, Derek Raisanen, David Riese, Alicia Rosales, Erin Saupe-Finley, Pete Schillig, Josh and Maggie Schmerge, Alycia Stigall, Celina Suarez, Marina Suarez, Emily Tremain, and Sarah Wildermuth. I am especially grateful for the friendship of Jon Smith, Julie Retrum, and Dan Hembree, with whom I shared much of my time and many of my experiences in graduate school.

I would like to say a special thank you to the Smith family and the Cane family, who, like my wife, my son, and I, live very far from their immediate families and have become our surrogate families in Kansas.

I thank my parents, Fred and Joanne, for their love and support and for always encouraging me to follow my dreams. I also thank my brother, Adam, the rest of my family, and my friends in New Jersey and Pennsylvania for their support from afar and for their hospitality during those rare occasions when I was able to visit in person.

I owe so much to my wife, Sara, for her love, patience, and understanding. All of my accomplishments would not have been possible without her support and sacrifices over the years. I am truly appreciative of everything Sara has done for our family, especially as it has grown

with the birth of our son, Henry. Henry's natural curiosity is a constant reminder of why I became involved in science, and I thank him for helping me keep everything in perspective.

TABLE OF CONTENTS

CHAPTER 1: INTRODUCTION

The purpose of this dissertation is to interpret and reconstruct paleoenvironments, paleoecology, and paleoclimate recorded by deposits of the Upper Jurassic Morrison Formation (MF). My approach focuses on data collection and interpretation at several observational scales in order to build a more comprehensive picture from which to draw conclusions. The main body of the dissertation comprises five chapters written as individual papers intended for submission to peer-reviewed journals for publication. The chapters are arranged in approximate order of increasing scale, i.e., beginning with analyses of individual trace fossils and ending with a perspective on paleoenvironments, paleoclimate, and paleoecological progression throughout deposition of the entire formation. Following chapters two–six is a conclusion chapter that summarizes and synthesizes the results of the preceding chapters.

The MF is a laterally extensive unit found in the western interior of North America that is composed of a mosaic of largely continental facies. The MF is Late Jurassic in age, ranging from possibly the latest Oxfordian through the Tithonian (Kowallis et al., 1998). The MF has been the target of paleontological investigations since the late 1800s and is perhaps most famous for the abundant and diverse dinosaur fossils it contains (e.g., Foster, 2007). In addition to dinosaurs, a range of floral and faunal body and trace fossils have been recovered from the MF, which makes it an ideal unit to test for paleoecological responses to such external forcing factors as paleoclimate change and paleoenvironmental perturbations.

This dissertation begins with a laboratory-focused project meant to supplement the field-based MF projects in later chapters. Chapter two (Platt et al., 2010) presents new methods for quantifying multiple aspects of fossil and modern traces using multistripe laser triangulation

(MLT) technology. I test the capabilities of the NextEngine MLT scanner and outline potential applications to ichnology through multiple examples. The main contribution of the MLT scanning experiences to the goals of this dissertation is quantification of volumes of modern and fossil footprints, including dinosaur tracks in the MF. Track-measurement methods also complement methods used in chapter three to measure the volumes of elephant tracks.

The purpose of chapter three is to use empirical data from neoichnological experiments with elephants to develop an equation that quantifies the relationship between multiple track-making variables. My goal is to better understand the relative contributions of original physical properties to dimensions of megafaunal footprints created in various sediment types. Such an understanding will greatly aid interpretations of fossil megafaunal tracks, including those of sauropod dinosaurs. This chapter builds upon observations of deep sauropod dinosaur tracks in the MF and qualitative interpretations of original media consistency based on track preservation (Jennings et al., 2006; Platt and Hasiotis, 2006). Consideration of paleohydrological implications of sauropod tracks will enhance interpretations of tracks preserved in the field areas investigated in chapters four and five.

Chapter four tests the utility of ichnological moisture regimes (Hasiotis, 2004, 2008) for interpreting lateral variations in paleohydrology in sheet-sandstone bodies in the MF in the Bighorn Basin, Wyoming. I use GPS and GIS to quantitatively test ichnofossil assemblages observed in the field. Recurring assemblages, based on nearest neighbor analysis, justify definition of ichnocoenoses. Consistent moisture regimes represented by ichnocoenoses suggest bioturbation under specific paleohydraulic conditions. Patterns of ichnocoenoses within a single sheet sandstone indicate sediment-moisture conditions that persisted after deposition.

Chapter five builds upon the paleohydrological interpretations of trace fossils in chapter four and incorporates ichnology with paleopedology to reconstruct a semiquantitative soil drainage curve for a section through the MF in Garfield County, Utah. In addition, the vertical profile includes carbonate content, carbonate mineralogy, total organic carbon, and $\delta^{13}C_{org}$, $\delta^{18}O$, and $\delta^{13}C_{carb}$ data. The purpose of the chapter is to integrate all datasets to interpret paleoenvironment and paleoclimate through deposition of the MF. The significance of this chapter is that it provides quantitative evidence for environmental and climatic changes through time, which would have impacted local ecology. Broader applications of the data presented in this chapter are potential correlations between various localities in the MF and between the MF and the marine isotope record; such correlations are useful for constraints on timing of MF deposition.

Chapter six uses quantitative network analysis software to analyze properties of reconstructed MF food webs in multiple biostratigraphic zones to look for changes in paleoecology through time. Existing MF biostratigraphies suggest multiple biotic turnover events during MF deposition, which have been hypothesized to be the result of paleoenvironmental and/or paleoclimate change perturbations (e.g., Turner and Peterson, 1999). My goal is to compare food-web analysis results to paleoenvironmental and paleoclimatic interpretations from chapters four and five to look for possible driving factors behind paleoecological changes. Findings may be informative for predicting long-term ecological effects of present-day anthropogenic climate change and environmental degradation.

Chapter seven contains summaries of the findings of chapters two through six and draws larger conclusions, integrating information from the entire dissertation. The chapter also provides broader implications of my results and suggestions for future research directions.

Despite the long history of research in the MF, there are still many unanswered questions regarding its deposition and biota. My hope is to contribute solutions to some of those questions, provide impetus for further study and discussion, and raise additional questions that will sustain related scholarly endeavors well into the future.

REFERENCES

Foster, J.R., 2007, Jurassic West: Indiana University Press, Bloomington, Indiana, 389 p.

Hasiotis, S.T., 2004, Reconnaissance of Upper Jurassic Morrison Formation ichnofossils, Rocky Mountain region, USA: paleoenvironmental, stratigraphic, and paleoclimatic significance of terrestrial and freshwater ichnocoenoses: Sedimentary Geology, v. 167, p. 177–268.

Hasiotis, S.T., 2008, Reply to the comments by Bromley et al. of the paper "Reconnaissance of the Upper Jurassic Morrison Formation ichnofossils, Rocky Mountain Region, USA: Paleoenvironmental, stratigraphic, and paleoclimatic significance of terrestrial and freshwater ichnocoenoses" by Stephen T. Hasiotis: Sedimentary Geology, v. 208, p. 61–68.

Jennings, D.S., Platt, B.F., and Hasiotis, S.T., 2006, Distribution of vertebrate trace fossils, Upper Jurassic Morrison Formation, Wyoming, USA: implications for differentiating paleoecological and preservational bias: New Mexico Museum of Natural History and Science Bulletin, v. 36, p. 183–192.

Kowallis, B.J., Christiansen, E.H., Deino, A.L., Turner, C.E., Kunk, M.J., and Obradovich, J.D., 1998, The age of the Morrison Formation: Modern Geology, v. 22, p. 235–260.

Platt, B.F., and Hasiotis, S.T., 2006, Newly discovered sauropod dinosaur tracks with skin and foot-pad impressions from the Upper Jurassic Morrison Formation, Bighorn Basin, Wyoming, USA: PALAIOS, v. 21, p. 249–261.

Platt, B. F., Hasiotis, S.T., and Hirmas, D.R., 2010, Use of low-cost multistripe laser triangulation (MLT) scanning technology for three-dimensional, quantitative paleoichnological and neoichnological studies: Journal of Sedimentary Research, v. 80, p. 590–610.

Turner, C.E., and Peterson, F., 1999, Biostratigraphy of dinosaurs in the Upper Jurassic Morrison Formation of the western interior, U.S.A., *in* Gillette, D.D., ed., Vertebrate Paleontology in Utah: Utah Geological Survey Miscellaneous Publication 99-1, p. 77–114.

CHAPTER 2: USE OF LOW-COST MULTISTRIPE LASER TRIANGULATION (MLT) SCANNING TECHNOLOGY FOR THREE-DIMENSIONAL, QUANTITATIVE PALEOICHNOLOGICAL AND NEOICHNOLOGICAL STUDIES

Published as:

PLATT, B. F., HASIOTIS, S.T., AND HIRMAS, D.R., 2010, Use of low-cost multistripe laser triangulation (MLT) scanning technology for three-dimensional, quantitative paleoichnological and neoichnological studies: Journal of Sedimentary Research, v. 80, p. 590–610.

ABSTRACT

The purpose of this paper is to test the application of a new, low-cost ($2995.00 US), multistripe laser triangulation (MLT) scanner and three-dimensional (3D) software for semiquantitative and quantitative analyses of ichnofossils and modern traces. The goal of this research is to improve on existing analytical techniques and apply new methods to 3D digital models of ichnofossils and modern traces. Objectives are to (1) provide researchers with new ways to develop and test hypotheses quantitatively in the fields of paleoichnology, neoichnology, sedimentology, and soil science, and (2) discuss uses, advantages, and limitations of MLT technology related to ichnology. We scanned and created digital models of a variety of mostly continental ichnofossils and modern terrestrial traces produced by invertebrates and vertebrates. Visual methods applied include making uniformly colored specimen surfaces, stereo pairs, anaglyph stereo images, animations, and cross sections. Quantitative methods applied include measuring distances, tortuosity indices, and angles, and producing contour maps of tracks. Two

of the most useful properties measurable from digital models are surface area (SA) and volume (V); these are used rarely in ichnology because they are difficult to measure with traditional methods. We use SA to calculate area exploited and introduce a method of quantifying surface roughness adapted from research on soil surfaces. We measure V of burrows, tracks, and coprolites, as well as introduce a new measure termed volume exploited. We hypothesize that different tracemakers make burrows with characteristic V to SA ratios; this is partially supported by statistical tests of previously published data. We also use V to SA ratios to determine relative compactness—a metric adapted from building physics. Digital models ensure perpetuity of specimens because they preserve 3D data that can be used to make physical copies, placed in museums, and disseminated easily to researchers and educational institutions of all levels. Data from digital models can be used to interpret ichnocoenoses, bioturbation rates, and pedogenic properties and processes in soils and paleosols. Note that MLT scanning digitizes only surfaces of objects, so it is best suited for exogenic traces and casts of endogenic traces.

INTRODUCTION

The purpose of this paper is to explore the range of applications of a new multistripe laser triangulation (MLT) scanner, its proprietary software, and widely available third-party software to invertebrate and vertebrate paleoichnology and neoichnology. The MLT scanner is a relatively inexpensive ($2995.00 US), noncontact laser scanner that, along with associated three-dimensional (3D) software, makes the capture and manipulation of 3D data relatively easy. The scanner is fairly new to the market and is already being integrated into various scientific research programs (e.g., Strait et al. 2007; Rossi et al. 2008; Hirmas et al. 2009; DeSilva 2010). An instrument capable of recording and visually displaying 3D data is well suited for studies of 3D

trace fossils, especially burrows, cocoons, nests, and vertebrate tracks. Techniques aimed at preserving and expressing traces in 3D have been applied previously, but many of these are expensive, time intensive, and not regularly used by ichnologists. The portability and relatively low cost of the MLT scanner and ease of use of its software package promises to provide a reliable method for 3D ichnological studies into the future.

We recognize three categories of ichnological applications for MLT technology: visualization, quantification, and perpetuation of specimens. All three uses are important, but we concentrate mainly on quantitative applications because MLT technology holds the most potential in quantitative ichnology. New methods of data acquisition will enhance morphological and statistical analyses of trace fossils for ichnotaxonomic, paleopedological, paleobiological, paleoenvironmental, and paleohydrological interpretations.

BACKGROUND

Three-Dimensional Imaging in Ichnology

Many endogenic—originating within a medium (= substrate)—trace fossils (*sensu* Häntzschel 1980) are complex, 3D shapes that cannot be viewed completely in a single plane of exposure. Three-dimensional views of endogenic trace fossils, including burrows, nests, and subsurface features of vertebrate tracks, have been obtained from serial sectioning and polishing (e.g., Uchman 1995; Gatesy et al. 1999; Wetzel and Uchman 2001; Hasiotis 2002, 2004; Milàn et al. 2004), computer tomography (CT; Fu et al. 1994; Perez et al. 1999; Ekdale et al. 2006), and magnetic resonance imaging (MRI; Gingras et al. 2002). Naruse and Nifuku (2008) combined serial polishing and computer graphics to obtain 3D images of *Phycosiphon incertum*. All of these examples, however, involve imaging biogenic structures inside a rock sample; these types

of reconstructions are impossible using the methods described here and are beyond the scope of this paper. The only endogenic traces that can be scanned are natural or artificial casts, traces weathered in full relief, or outcrop exposures and bedding-plane surfaces with traces because MLT scanners can only scan surfaces of objects.

Endogenic trace fossils exposed in outcrop are often displayed in 3D with stereo pairs (e.g., Bown 1982; Bown and Kraus 1983; Bown et al. 1997; Groenewald et al. 2001). Stereo pairs typically are created from two photographs of an object taken from slightly different angles. Photographs are placed side by side and give the illusion of three-dimensionality when viewed through a stereoscope (Evitt 1949). The angle of rotation of the object between images determines the amount of vertical exaggeration when the image is viewed in 3D. The most realistic 3D views are created with an angle between 8° and 10° (Evitt 1949; Purnell 2003).

Exogenic—traces made on the surface of a medium—trace fossils (*sensu* Häntzschel 1980), for example, trackways and footprints, are well suited for analysis with MLT scanners. In previous studies, several 3D methods have been performed on tetrapod tracks to convey information not easily interpreted from monoscopic photographs or drawings. Cross sections of tracks have been generated with laser scanning and light detection and ranging (LiDAR) (Bates et al. 2008a; Falkingham et al. 2009). Two-dimensional images that portray the three-dimensionality of vertebrate tracks include stereo pairs (e.g., Sarjeant and Thulborn 1986; Gatesy 2003; Harris and Lacovara 2004; Fiorillo et al. 2009) and anaglyph stereo imaging (Gatesy et al. 2005). Anaglyph stereo images are created by colorizing and superimposing the left and right images of a stereo pair; the left image is typically colored red and the right is colored blue, green, or cyan so the illusion of three dimensionality is given when viewed through 3D glasses with one red lens and one blue, green, or cyan lens (Purnell 2003; Gatesy et al. 2005).

Quantitative Ichnological Methods

Distances and Angles.—Quantitative methods that can be performed or improved with MLT technology include such basic measurements as distances and angles in tracks, trackways, and burrows. Standard distance-measurement methods for tracks and trackways are described by Trewin (1994) for limbed invertebrates and by Leonardi (1987) for tetrapods. Typical distance measures for burrows and burrow segments include length, depth, and diameter. Maximum burrow depth is the distance between the burrow opening at the surface and the lowermost termination of the burrow, measured perpendicular to the original ground surface (Hembree and Hasiotis 2006). Measured distances are also used with burrows and burrow segments to compute tortuosity index, which is the average of the tortuosity of all burrow segments (Meadows 1991; Hembree and Hasiotis 2006). Tortuosity index (T) is calculated from the following equation:

$$T = (\sum_{i=0}^{s} u_i / v_i) / s \qquad (1)$$

where s = number of burrow segments, u = total length of a segment, and v = length of a straight line between the endpoints of a segment (Meadows 1991; Hembree and Hasiotis 2006).

Angles are used typically to measure invertebrate trails (e.g., Trewin 1994), divarication of digits in footprints (e.g., Sarjeant 1975; Leonardi 1987; Hasiotis et al. 2007), pace angles in tetrapod trackways (Leonardi 1987), ramps of helical burrows (Smith 1987), and branching tunnels and shafts in burrow systems (Ekdale et al. 1984).

Contour Maps.—Contour maps are used commonly to visually and quantitatively display relief of tetrapod tracks. They aid in such interpretations as trackmaker identification (e.g., Farlow and Lockley 1993; Fiorillo et al. 2009) and quantification of sediment deformation

(e.g., Bates et al. 2008a). Contour maps can be generated multiple ways, including moiré topography (Ishigaki and Fujisaki 1989), progressive immersion in water (Lim et al. 1989), and with computer software using 3D data collected from contact digitizers (Farlow 1993; Farlow and Lockley 1993; Graham et al. 1996), photogrammetry (Breithaupt and Matthews 2001; Matthews and Breithaupt 2001; Bates et al. 2008b), noncontact laser scanners (Breithaupt and Matthews 2001; Arakawa et al. 2002; Breithaupt et al. 2004), and LiDAR (Bates et al. 2008a; Bates et al. 2008b). The 3D data captured from digitizers, photogrammetry, laser scanners, and LiDAR have the added benefit that they can be manipulated in 3D space with software, providing a variety of views with the potential to quantify a variety of aspects of scanned traces.

Area Exploited.—Efficiency of a surface-mining organism is measured by calculating area exploited of a surface-grazing trail. Area exploited (AE) is expressed as a percent and compares the area utilized (AU)—the area between the origin, termination, and lateral margins of a trace—to the area available (AA)—the area of the polygon enclosed by lines connecting the margins of the AU (Orr 1999). Area exploited is calculated from the following equation:

$$AE = AU / AA * 100 \qquad (2)$$

Area exploited is rarely used in ichnology because its calculation involves comparing the surface areas of irregular shapes, which are difficult to measure directly.

Burrow Surface Area.—Surface area (SA) has been used to evaluate redox potential and microbial biomass on walls of subaqueous burrows (Dworschak 2001), area of water-sediment interface (e.g., Griffis and Suchanek 1991; Kinoshita 2002), phytoplankton removal

(Griffen et al. 2004), and O_2 consumption (Koike and Mukai 1983). Surface area is important in subaerial burrows for thermoregulation (Groenewald et al. 2001; Hasiotis et al. 2004).

Previous neoichnological studies have measured burrow SA by wrapping casts with a single layer of foil of known weight per unit area and weighing the foil (e.g., Atkinson and Chapman 1984; James et al. 1990; Dworschak 2001). Burrow SA has also been estimated by treating burrows as cylinders and using burrow lengths and diameters to calculate SA (e.g., Gerino and Stora 1991; Kinoshita 2002; Griffen et al. 2004).

Surficial Morphology.—Surficial morphology (i.e., bioglyph or fingerprint; Ekdale et al. 1984) of a trace fossil is a useful ichnotaxobase, at least for distinguishing ichnospecies (Bertling 2007), whereas others use it to define ichnogenera (e.g., Bown and Kraus 1983; Hasiotis and Mitchell 1993; Hasiotis et al. 1993a). In general, surface morphology is described qualitatively. Quantification of surface morphology typically involves measurements of such surficial features as pellet size (e.g., Frey et al. 1978; Bown and Kraus 1983) and scratch marks on burrow walls (e.g., Groenewald et al. 2001; Gobetz 2005). A possible standard way to quantify surficial features is to measure surface roughness; no method exists currently to do so.

Burrow Volume.—Studies of modern burrows in subaqueous sediments have used volume (V) to estimate sediment reworking (e.g., Lim 2006), bank stability of lakes and rivers (e.g., Rudnick et al. 2005), and sediment irrigation and flushing of salts around roots (Stieglitz et al. 2000). Burrow V in the continental realm is useful for estimating sediment turnover and mixing rates, which affect soil texture, structure, fertility, infiltration, aeration, runoff, maturity, and vegetative cover (Butler 1995, references therein; Langmaack et al. 1999). Volumes of modern burrows have been calculated by geometric estimates (e.g., Butler 1995; Bancroft et al. 2004) and estimated from casts by water displacement (e.g., Gerino and Stora 1991; Lim 2006),

cast weight, and density of the casting medium (e.g., Atkinson et al. 1987; James et al. 1990), and measuring V of casting medium required to fill a burrow (e.g., Stieglitz et al. 2000).

Tetrapod Footprint Volume.—Tetrapod tracks, especially deep ones, are properly viewed as 3D features (Allen 1989, 1997; Gatesy 2003; Manning 2004; Margetts et al. 2006) so volumes of true tracks may be more informative than depth, which can vary within an individual track. Track V can also be used to estimate sediment disturbance rates in a trampled area (e.g., Cohen et al. 1991) and interpret tracemaker acceleration and media consistency (e.g., Mossman et al. 2003; Platt and Hasiotis 2008). Track V can be estimated geometrically or measured from plaster casts. Mossman et al. (2003) measured track V by filling tracks with small pellets, which were then poured into a graduated cylinder. We attempted to measure by water displacement the V of dental-plaster casts of elephant tracks and found that V was underestimated because the plaster absorbed some of the water (Platt and Hasiotis, unpublished data).

Coprolite Volume.—Thulborn (1991) suggested using V as a standard measure of coprolites because the diversity of irregular shapes from fecal extrusion and deformation makes linear dimensions difficult to compare statistically. Northwood (2005) measured maximum length and V of multiple morphotypes of coprolites from two localities in the Early Triassic Arcadia Formation of Queensland, Australia. Most results of statistical analyses of coprolite data were nonsignificant; but, analysis of variance indicated a significant difference in V between two morphotypes of a given length at one locality (Northwood 2005). This evidence suggests that coprolite V can be a useful measure for future statistical analyses.

Coprolite and fecal V are measured typically by water displacement (Welch 1982; Northwood 2005). This introduces measurement errors with desiccated feces, however, because dry dung (Welch 1982) and poorly cemented coprolites absorb water. Errors can also be caused

by fecal masses that will not submerge completely and water-sensitive samples that disaggregate, resulting in destruction of samples.

MATERIALS AND METHODS

MLT Scanner and 3D Software

The MLT scanner we used is the NextEngine™ model 2020i desktop scanner housed in the University of Kansas Pedology Laboratory. Scanner hardware consists of twin arrays of four Class 1M, 10 mW solid-state lasers with a wavelength of 650 nm and twin 3.0 megapixel complementary metal-oxide-semiconductor (CMOS) image sensors (NextEngine, Inc. 2009). During operation, the scanner first captures a digital photograph of the object to be scanned. Then multiple, projected, vertical light stripes sweep across the object and are deformed by the object's surface. Distances from the scanner are calculated from detected differences in intensity of the light stripes (Knighton et al. 2005). The MLT technology of the NextEngine™ scanner has comparable scanning accuracy and precision when compared to more expensive, high-performance laser scanners (Guidi et al. 2007).

The laser scanner (Fig. 1A, B) is designed to be placed on a desktop and scan objects in front of it, but it can be placed on a tripod and pointed in any direction. The scanner can be connected to the AutoPositioner™, a base that automatically rotates an object to obtain a 360º scan. The PartGripper™ is a vertical rod with adjustable clamps that can be added to the AutoPositioner™ to hold objects for scanning (Fig. 1B). The standard ScanStudio™ software package allows scanning in two modes: macro and wide. Macro mode has a field of view of ~ 13 cm by 9.6 cm and an ideal focal distance of ~ 16.5 cm. Wide mode has a field of view of

about 34.2 cm by 25.6 cm and an ideal focal distance of 43 cm. Objects larger than this can be scanned in multiple parts and their digital representations assembled within the software.

The scanner is relatively portable, so it can be taken in the field and used with a laptop computer and generator. We used a custom four-legged table to scan footprints in the field (Fig. 1C–E). The table is made from ~ 1.3 cm (0.5 inch) thick PVC sheets. The scanner faces downward through a hole large enough so that the camera, lasers, and lights are not obscured. Four walls keep the scanner centered over the hole and prevent it from sliding off the table. The table has four legs made from PVC pipes angled away from the center so that they are not visible when scanning the ground surface. The legs have adjustable heights, so the table can be placed at different distances from and angles to the ground surface. The legs are removable for transport.

Data can be captured by the scanner at three speed settings, which limit the maximum resolution; the highest resolution possible is 400 DPI in macro mode and 150 DPI in wide mode (NextEngine, Inc. 2009). Our digital models averaged 213 DPI in macro mode and 88 DPI in wide mode. There are three possible scan types: single, bracket, and 360°; bracket and 360° scans require the AutoPositioner™. A single scan digitizes one view of an object. A bracket scan scans three views of an object, rotating it between each scan; this is best for scanning a surface with a lot of relief. A 360° scan takes multiple scans during the complete rotation of an object; the number of scans is adjustable. Multiple scans are aligned in virtual space using 3D software.

Each scan generates a series of 3D data that can be displayed as a point cloud, a wire mesh, a solid model with a rendered surface, or a solid model with photographs overlaying the points. Once the object is scanned, the scanner's software can be used to trim, align, and fuse

scans into a single mesh. Additional operations can be performed with expanded proprietary software packages and third-party 3D software.

Specimens and Digital Models

A variety of invertebrate and vertebrate trace fossils and modern traces were selected from the IchnoBioGeoScience (IBGS) research collections at the University of Kansas for laser scanning. The trace fossils are mostly from continental settings because of the nature of the collections. Modern traces include examples artificially cast in natural settings and during laboratory experiments. Some traces were selected specifically for a particular analysis, whereas other traces were chosen so that a variety of different techniques could be applied to a variety of trace morphologies. Many of the artificial casts of modern traces were already mounted on bases (Fig 1B), making them relatively easy to scan by rotating them 360º.

Traces were scanned with the laser scanner using the highest possible resolution setting. Bedding surfaces were bracket scanned, and 3D specimens were scanned using the 360º scan setting and the AutoPositioner™ and PartGripper™ when necessary. Additional views were added as needed with single or bracket scans. We scanned modern tracks in the field with the custom-made base (Fig. 1C), connected to a laptop computer, powered by a portable generator.

Individual scans of a given specimen were trimmed, aligned, and fused into digital models with the scanner's proprietary software. Photographic information was removed from the models to enhance visibility of surficial morphology; all figures show models displayed with solid rendered surfaces unless otherwise noted. Measurements were taken and operations were performed with a combination of the features available in ScanStudio HD™, ScanStudio CAD Tools™, and Adobe® 3D Reviewer (Table 1). Note that many of these operations can also be

performed with such free 3D software as Deep View (Right Hemisphere 2009) and Blender (Stichting Blender Foundation 2008). Adobe® 3D Reviewer was used because of its capabilities, simple user interface, and compatibility with Adobe® Reader®. We used R (R Development Core Team 2008) for all statistics on 3D data measured from digital models.

New Quantitative Ichnological Methods

Surface-Area Index.—If a regular surficial pattern is present that disrupts an otherwise smooth burrow wall, calculation of a surface roughness metric may be useful for ichnotaxonomic purposes. Surface-area index is used to quantify the roughness of soil surfaces (Jester and Klik 2005), and we adapted it for application to ichnology. Surface-area index (SAI) is calculated as

$$\text{SAI} = \text{total surface area} / \text{projected plot area} \qquad (3)$$

In soil applications, the projected plot area is calculated as a plane based on linear dimensions of the plot selected. The same principle can be applied to trace fossils, but instead of projected plot area, total surface area of a trace is compared to the surface area of the averaged or smoothed surface of the trace, i.e., after lowering of topographic highs and raising of lows. The scanner's proprietary software contains multiple smoothing functions that can be used to average the surface of a scanned object. The best way to smooth an object is to use the surface tool, which wraps a point cloud with a mesh composed of a specified number of polygons. Surfaces of objects become smoother as the number of polygons decreases.

Volume Exploited.—The principle behind AE can be extended to the third dimension, using V to calculate a metric we term volume exploited (VE). Volume exploited treats the

volume of the trace as the volume utilized (VU) and the volume of a prism enclosing the trace as the volume available (VA). We used a software-generated bounding box as VA; the bounding box is a rectangular prism. The equation for VE is

$$VE = VU / VA * 100 \qquad (4)$$

The bounding box for any one object, however, differs depending on the orientation of the coordinate system of the object. To calculate VE a standard reference system is needed for creating a bounding box. We defined the coordinate systems of each digital model so each vertical axis corresponded to the original vertical axis of the trace. We then rotated the model about the vertical axis, adjusting the horizontal dimensions of the bounding box until we reached the most compact prism possible. The only exceptions to this were traces created in aquaria; in those cases, we matched bounding-box orientation to the original orientation of the aquarium. The assumption that VA is a rectangular prism is not usually valid, but by measuring the minimum prism that encloses a trace, space usage between the extreme boundaries of the trace can be quantified. Patterns of space usage may be characteristic of certain tracemakers or behaviors; thus, VE may be useful for ichnotaxonomy. Volume exploited is most informative for burrows and burrow networks, where it essentially measures efficiency of space usage and burrow density. Note that a bounding box can also be created for field-cast burrows to find the ideal aquarium size for tracemakers for neoichnological experiments in the laboratory.

Relative Compactness.—Another quantitative measure we adapted for characterizing a burrow or burrow network is the concept of relative compactness (RC), introduced by Mahdavi and Gurtekin (2001) for building physics. Relative compactness compares the ratio of volume to

surface area (V:SA) of an object to V:SA of the most compact geometric shape—a sphere—with the same volume as the object (Appendix A). By comparing the ratio to a standard, problems of scale inherent in a single V:SA are eliminated. The equation to calculate RC is

$$RC \approx V^{2/3} * 4.84 / SA \qquad (5)$$

For example, three spheres with radii of 1 cm, 2 cm, and 3 cm have V:SA values of 0.333, 0.667, and 1, respectively. All three of these spheres have RC values of 1. Note that RC is essentially a measure of sphericity of an object. Relative compactness is not informative about such features as relationships between segments of burrow networks or tightness of coiling of spiral burrows, which are better described by VE.

RESULTS

Visualization

Uniform Surface Images.—Photography of fossil specimens is improved by coating specimen surfaces with powder or ink to obscure any color variation on the surface, clarifying surface morphology (e.g., Kier et al. 1965). Trace fossils may contain surficial discolorations (e.g., Kuban 1989), especially those preserved in paleosols with mottled, redoximorphic color variations that tend to obscure details of surficial morphology (e.g., Bown and Kraus 1983; Hasiotis et al. 1993b; Hasiotis 2002; Smith et al. 2008). By scanning such fossils to produce solidly rendered models, the fossil surface can be viewed as a uniform color. Visualization is also enhanced by the ability to adjust the position of the virtual light source in a 3D environment. For example, the latex mold of a tridactyl dinosaur track in convex hyporelief on the base of a

sheet sandstone from the Upper Jurassic Morrison Formation, Bighorn Basin, USA (Platt and Hasiotis 2006), was scanned (Fig. 2). The slab in which the track was preserved was too large to collect and too poorly lit for clear field photographs. Our latex mold of this track (Fig. 2A) is discolored from differences in thickness of the latex and adherence of debris from the original track surface. A bracket scan of the latex mold greatly enhances the clarity of the track (Fig. 2B), and lighting can be adjusted to achieve the best possible image.

Stereo Images and Movies.—The benefit of using digital models to create stereo pairs and stereo anaglyph images is the ideal angle of rotation between images can be achieved precisely. We created a stereo anaglyph image from the digital model of the latex mold of a tridactyl track in Figure 2A (Fig. 2C). We rotated the digital model exactly 8° between image captures and colorized and superimposed the images following Purnell (2003).

Animations enhance publications and presentations inasmuch as they convey more information than still photos or stereo pairs, and the window for a movie can occupy the two-dimensional (2D) space of a single photograph. We created movies of burrow casts of a tiger beetle larva (*Cicindela* sp.), marsh crab (*Sesarma* sp.), ghost crab (*Ocypode quadrata*), sand boa (*Eryx colubrinus*), brown scorpion (*Urodacus* sp.), desert skink (*Egernia inornata*), and latex mold of a tridactyl track in Fig. 2A. Movies are simple 360º rotations about a vertical axis through the center of each specimen. We created one movie with rotations about multiple axes through a natural sandstone cast of a tetradactyl dinosaur track from the Upper Jurassic Morrison Formation, Bighorn Basin, Wyoming, USA. The complete animation shows such features as striations, the impression of digit I, the horizontal and vertical curvature of the digits as they moved through the sediment, and a possible exit furrow (*sensu* Gatesy et al. 1999).

Cross-Sectional Shape.—Cross-sectional shape can be informative for ichnotaxonomy and for identifying potential tracemakers by comparison with modern organisms. Cross sections of scanned traces can be viewed easily along any plane through the rendered digital model. For example, a fossil burrow cast segment from the Lower Triassic Fremouw Formation, Kitching Ridge, Queen Maud Mountains, Antarctica (Miller et al. 2001; Hasiotis et al. 2004) (Fig. 3A), has a central groove and lateral ridges on an exposed end; these features are similar to those described from sectioned fossil *Trirachodon* burrows by Groenewald et al. (2001). To verify that the observed features persist throughout the entire length of the burrow we scanned the burrow cast (Fig. 3B) and sectioned it perpendicular to its long axis (Fig. 3C, D). The section shows that the groove and ridges are present throughout the entire length of the burrow cast.

We also compared the cross section of the Triassic trace fossil to a cross section of a cast of an *E. inornata* burrow from vegetated dune fields south of Alice Springs, Northern Territory, Australia (Fig. 3E–G). Both the modern and the Triassic burrows have a central ridge and lateral grooves that are characteristic of tetrapod burrows; however, there are distinct differences between the two. The *E. inornata* burrow cross section is shorter and wider than the fossil tetrapod burrow. The *E. inornata* burrow also has lateral wing-like extensions on the burrow walls (Fig. 3G, H) that are absent in the fossil burrow.

Quantification

Measuring Distances.—Routine measurements of linear distances are easy to take with calipers or a ruler, but there are many opportunities for measurement error when working with physical specimens. Surface relief can make it difficult to lay a ruler flat and can cause a tape measure to bend and twist. When measuring a cylindrical burrow cast, for example, burrow

length varies depending on the positions of the endpoints chosen (Fig. 4A). One standard way to measure length of a cylindrical object is along its long axis (Fig. 4B) at the intersection of two planes bisecting the cylinder. The long axis of an irregularly shaped object can be approximated from a scanned model by creating a series of planes perpendicular to the long axis, finding the approximate central point of each circular cross section, and linking those points (e.g., Fig. 4C). We used this technique to measure burrow length of the main shaft of an *O. quadrata* burrow cast (Fig. 4D, E; Table 2); the sum of segments u_1 and u_3 (Fig. 4E; Table 2) is 37.4 cm.

We also calculated T for the *O. quadrata* burrow using the same distance measurement technique. In this case, the burrow consists of three segments (i = 3; Fig. 4D). Using the total lengths of each segment (Fig. 4E; Table 2) and straight-line lengths of each segment (Fig. 4F; Table 2), we calculate T as (14.6 cm / 14.4 cm + 8.1 cm / 7.7 cm + 22.8 cm / 22.6 cm)/3 = 1.02. Taking measurements with 3D software allows restriction of measurements to a single plane. This is useful, for example, for measuring maximum burrow depth along a vertical axis or footprint length along a horizontal axis; this requires the coordinate system—x, y, and z axes—of the digital model to correspond to the original orientation of the trace. The default coordinate system of a digital model is determined by the orientation of the object during scanning, but the coordinate system can be redefined with 3D software. We checked the coordinate systems of all digital models and redefined them to original orientations where necessary. We measured maximum burrow depth for several burrow casts by restricting top-to-bottom measurement to the vertical axis of each (Fig. 4G–J). We also measured the diameters of three burrow openings by restricting measurement to the horizontal plane (Fig. 4G–I).

Measuring Angles.—As with distance measures, restricting measurement of angles to a single cross-sectional plane can increase precision. This is a tedious operation compared to the

other quantitative methods described here, but it is an improvement over holding a protractor up to a specimen to measure angles. As examples, we measured a ramp angle in a *Urodacus* sp. burrow (Fig. 4J) and the angles of divarication between the digits of a tetradactyl dinosaur track cast from the Upper Jurassic Morrison Formation, Bighorn Basin, Wyoming, USA (Fig. 4K).

Track Topography.—A contour map can be created from a digital model by making a series of parallel planar sections at regular intervals and then viewing the results from directly overhead. The thickness of intervals between sections controls the contour interval. As an example, we created a contour map of a tridactyl dinosaur track from the Upper Jurassic Morrison Formation, Bighorn Basin, Wyoming, USA (see Fig. 2C).

Area Exploited.—MLT scanning provides a more precise method of measuring surface areas than previously used methods. As an example, we bracket scanned the *Nerities*-bearing surface of a rock specimen from the Promina Beds, Benkovac, Croatia (Fig. 5A). The rock sample contains traces on multiple bedding surfaces. We trimmed the scan to isolate a single exposed surface to the boundaries of the trace fossil; this is AA (Fig. 5B), and 3D software measured its surface area as 32.54 cm^2. We then trimmed the AA down to the boundaries of the traces (Fig. 5C) to obtain a value for AU of 20.52 cm^2. We calculate AE as 20.52 cm^2 / 32.54 cm^2 * 100 = 63.1. This number represents the tracemaking organism's efficiency; i.e., the tracemaker was ~ 63% efficient in the area it exploited.

Burrow Surface Area.—Laser scanning and 3D software calculates the surface area of a burrow cast with much more accuracy and precision than other methods. When calculating SA, fusing the digital model into a single mesh is important or else the program will calculate and add the surface areas of each individual mesh, including overlap. Note that this requires a

surface to be rendered over any opening in the trace, for example, a burrow entrance. We calculated SA values for a variety of scanned trace fossils and modern traces (Tables 3, 4).

Surface-Area Index.—We performed several smoothing trials with different traces because the original size of the trace changes the appropriate number of polygons needed to smooth the surface. We selected six traces that represent a spectrum of different size, architecture, and surface roughness: (1) one small and one large specimen of *Edaphichnium lumbricatum* (Fig. 6A–E), a pelleted burrow fill from the Eocene Willwood Formation, Bighorn Basin, Wyoming, attributed to earthworms (Bown and Kraus 1983), (2) one small and one large specimen of *Eatonichnus claronensis* (Fig. 6F, G), interpreted as dung-beetle traces, from the Eocene Claron Formation, southwestern Utah (Bown et al. 1997), (3) one plaster cast of a partial burrow network (Fig. 6H) made in clay-rich soil in an aquarium by the limbless lizard *Amphisbaena camurea* (Hembree and Hasiotis 2006), and (4) one plaster cast of a burrow (Fig. 6I) made in coconut fiber and fine- to medium-grained sand in an aquarium by *E. colubrinus*.

Each scanned trace was fitted with different numbers of polygons ranging from a software-imposed maximum of 5,000 to a minimum of 25 or until the trace architecture became distorted due to too few surfaces to maintain the original shape. We plotted SAI against mesh resolution (Fig 6J). Mesh resolution equals original SA divided by the number of polygons in the smoothed mesh. We fit third-order polynomials to the data and calculated each inflection point. The inflection point represents the coarsest mesh resolution that maintains the integrity of the trace shape. Coarser mesh resolutions result in an overall size reduction of the model. This provides a standard and repeatable method for the determination of SAI for all traces. In this method, each trace needs to be treated separately because all of them respond differently during smoothing, i.e., have different original SA and inflection points when smoothed. Comparison of

the mesh with 5,000 surfaces and the smoothed mesh shows that the smoothing method achieved the desired results: the topographic highs were lowered and the lows were raised (Fig. 6D).

Results for SAI were 1.14 for the small *Edaphichnium*, 1.11 for the large *Edaphichnium*, 1.05 for the *E. colubrinus* burrow, 1.03 for the small *Eatonichnus*, 1.03 for the large *Eatonichnus*, and 1.03 for the *A. camurea* burrow. Results agree with qualitative observations that *Edaphichnium* has rougher surfaces. The range of SAI values is small, but we argue that these numbers are reliable because of the high precision of the laser scanned data (Fig. 6J).

Burrow Volume.—The V of digital models of fossil and burrow casts can be calculated with 3D software. To accurately measure V, however, all individual scans of a model must be fused into a single mesh devoid of holes. We calculated V for all scanned burrows (Tables 3, 4). We also used V to estimate the number of pellets in a pellet-filled burrow. We selected a specimen of *Edaphichnium* (Fig. 6A) with approximately uniform pellet size and made a 1:1 scale replica of a single pellet with clay. We scanned the pellet and measured its V as 0.13 cm^3. Dividing the specimen V of 51.8 cm^3 by the pellet V yields an estimate of ~ 398 pellets in the specimen. We take this as a maximum estimate because it does not account for pellet packing.

Tetrapod Footprint Volume.—Measuring V of a digital model of a track requires the model to be an enclosed shape; this is easier for a cast than for a footprint mold or an actual footprint, which require extra modifications before a measurement can be taken. As an example, we scanned the footprint of an African elephant (*Loxodonta africana*) at the Topeka Zoo, Topeka, Kansas, USA (Fig. 7A). We are interested in track V measured up to the original ground surface, so we used 3D software to isolate the track and trim away any features above the ground surface, i.e., marginal ridges (Fig. 7B, C). We then sealed the shaft (*sensu* Allen 1997;

Hasiotis et al. 2007) using the remesh tool in the scanner's proprietary software, essentially creating a virtual cast of the footprint (Fig. 7D). Volume was measured at this point (Table 4).

Coprolite Volume.—We scanned coprolites from the Eocene Willwood Formation, Wyoming, USA (Fig. 8A), Miocene of Washington, USA (Fig. 8B), and modern, desiccated fecal masses from an Asian elephant (*Elephas maximus*) (Fig. 8C) and a horse (*Equus ferus caballus*) (Fig. 8D). Volumes were 19.16 cm^3, 38.12 cm^3, 1682.46 cm^3, and 44.54 cm^3, respectively.

Volume Exploited.—We calculated VE for all scanned traces (Tables 3, 4). We used trace V as VU and bounding-box V as VA. Figure 9 shows bounding boxes used to measure VA for three traces. Particularly low VE values are 1.16 for the *Cicindela* sp. larva burrow cast (Fig. 4G), 1.93 for the *E. inornata* burrow cast (Fig. 9E, F), 2.38 for the *Urodacus* sp. burrow cast (Fig. 4J), 2.74 for the *O. quadrata* burrow cast (Fig. 4D), 2.80 for the *E. colubrinus* burrow cast (Fig. 9A, B), 3.82 for the *A. camurea* burrow cast (Fig. 6H), and 5.39 for the *Sesarma* sp. burrow cast (Fig. 9C, D). The highest VE values are 50.71 for the *E. maximus* dung (Fig. 8C), 52.89 for the fossil bee cell (Fig. 10A–D), and 54.39 for the fossil wasp cocoon (Fig. 10E, F).

The lowest VE values correspond to bounding boxes with the most unoccupied space; these resulted from burrow networks, burrows with high complexity, and cylindrical burrows with curves or projections that expanded their bounding boxes. The highest VE values resulted from the spherical elephant-dung bolus and ovoid bee cell and wasp cocoon, which conform well to the borders of their bounding boxes. Volume exploited may not seem useful for describing coprolites because they are not excavated features, but we nevertheless calculated VE for every specimen because it is easy to calculate and may prove to be informative for future studies.

Relative Compactness.—We calculated RC for all traces scanned (Tables 3, 4). The lowest RC values are 0.30 for the latex mold of a tridactyl dinosaur track (Fig. 2), 0.31 for the *Urodacus* sp. burrow cast (Fig. 4J), 0.31 for the *E. inornata* burrow cast (Fig. 9E, F), 0.34 for the *A. camurea* burrow cast (Fig. 6H), 0.34 for the *E. colubrinus* burrow cast (Fig. 9A, B), and 0.37 for the *Cicindela* sp. burrow cast (Fig. 4G). The highest RC values are 0.90 for the small specimen of *Eatonichnus*, 0.90 for the fossil bee cell (Fig. 10A–D), and 0.90 for the fossil wasp cocoon (Fig. 10E, F). As expected, the most spherical traces have the highest RC values and irregularly shaped traces have lower RC values.

DISCUSSION

Perpetuity of Specimens

Digital Specimens.—Digital 3D imagery and data allow specimen preservation, conservation, and dissemination at all educational levels. Specimens collected from the field or produced in the laboratory can be scanned so digital copies will exist in case original specimens are lost, damaged, destroyed, or stolen. Specimen molds and casts made from degradable media that could decompose through time or be altered due to aging can be preserved digitally. Traces impossible to collect from the field can be scanned in place with the laser scanner because it is relatively portable. Scans of specimens in public places or other areas in danger of damage by weathering or vandalism can also be preserved digitally (e.g., Bates et al. 2008b). Virtual specimens can be placed in a digital repository for preservation and easy access by other researchers (e.g., Smith and Strait 2008). Scanned data can be made available online or stored on CD or DVD, making dissemination to other researchers easy. This application also allows

multiple researchers to study the same specimens or data set at the same time from different locations, facilitating collaboration among widely dispersed colleagues.

Movies and images generated from 3D data can be used in classrooms and websites for scientific and educational purposes at all academic levels. Two main purposes for using these media are to illustrate (1) three-dimensionality of the architectural and surficial morphologies of a variety of modern and ancient traces, and (2) how organism behavior is manifest and visualized in 3D without any obstruction from the medium. This type of application is especially useful to teach others how to interpret the construction, form, and function of modern and ancient traces.

Model Production.—Another use of laser scanned traces is for the fabrication of physical 3D models from a digital model. This can be accomplished by exporting scanned files to a 3D printer (e.g., D'Urso et al. 2000) to produce replicas of traces that can be used for museum exhibits and teaching. A fabricated 3D model can also be placed in museum collections (e.g., Lak et al. 2008). The benefit of using this method is that it does not involve making a mold of a specimen, which requires putting molding medium in direct contact with the specimen.

Issues and Limitations

Specimen Size and Intricacy.—Larger scanned objects have larger file sizes and numbers of points that can slow operations, depending on the analyzing computer's capabilities. Handling such large files may require reduction of points in the mesh, which can decrease model detail. An object too large for a 360° scan can be easiest to handle as a series of single scans, but it can take many single scans to obtain enough views to create a full 3D model. If you have a large object that can be broken into pieces, e.g., a cast of a burrow network, you cannot easily scan the pieces and assemble them with the software because there will not be enough overlap of

parts to allow the software to combine the scans. Burrow networks and other large specimens should be fully assembled before scanning, though positioning such an object so that it can be scanned from every angle can be challenging and increases chances of damaging the specimen.

The smallest trace fossils scanned are a wasp cocoon from the Paleocene-Eocene Claron Formation in southwestern Utah, USA (Fig. 10E, F) and a bee cell (Fig. 10A, D) from the Eocene-Oligocene Climbing Arrow Formation, Montana. These have a V of 2.45 cm^2 and 0.83 cm^2, respectively. We chose these specimens to test the level of fine detail that could be captured with the MLT scanner. We were particularly interested in a weathered area in the outermost surface of the cocoon that penetrated into the material below (Fig. 10E, F; right of center) and the whorls of the spiral cap of the bee cell (Fig. 10C, D). Both of these features were captured and preserved in the digital models, but the whorls of the spiral cap appear slightly smoothed, suggesting that they are approaching the lower level of detail possible.

Specimens with a lot of surface relief, openings that lead to internal structures, or many branched parts with acute angles of intersection can be difficult to scan because lasers might not be able to reach all parts of specimens. In general, laser scanning is best suited for trace fossils preserved in convex hyporelief and convex epirelief, and casts of modern endogenic traces. Low-relief concave traces can also be scanned easily. We tested the difficulty level of scanning a specimen of *Feoichnus* isp. (Fig. 10G, H), a cup-shaped trace fossil (Krause et al. 2008) we attribute to dung beetles. The specimen has a central hemispherical concavity that was possible to scan but required one 360° scan with six divisions, two bracket scans, and two single scans.

Mounted Specimens.—Mounted specimens are easy to rotate on their base (e.g., Fig. 1B), but a base will obscure the bottom view of a specimen. Many traces we studied are permanently affixed to bases and required multiple single scans from different angles to capture

specimen bottoms; many specimen bottoms could not be seen completely, which resulted in holes in the mesh that had to be patched with software. If possible, specimens should be mounted in such a way that they can be more easily removed from their bases for scanning.

Mounted specimens will have supports that may need to be digitally erased after scanning. Digital removal, however, adds time to the project and results in holes in the mesh that will have to be patched. Mounting supports can also obscure parts of the specimens during scanning, which increases the number of scans needed to completely capture a specimen. Supports can also cast shadows on specimens when the scanner's built-in lights illuminate it for scanning. Shadows in digital photos overlaid on the mesh detract from color fidelity.

Lighting Conditions.—The built-in lights of the MLT scanner illuminate objects consistently for digital photographs, but lighting variations are still possible given ambient lighting conditions and shadows cast by the PartGripper ™ and parts of the object itself. Lighting variations in digital photographs will not affect the appearance of the solid rendered model. When a model mesh overlain with photographs is fused into a single mesh, however, the photographs are stitched together, so lighting variations will result in visible seams on the model. If faithful color representation of an object is important, lighting conditions must be controlled. The MLT scanner and the object being scanned need to be shaded if used outdoors to ensure that light returning to the scanner is not oversaturated by ambient light, because it will interfere with the scanner's detection of the lasers and cause holes in what is captured.

Cropping Digital Models.—We avoided alteration of digital models as much as possible with editing software to retain the accuracy of original specimens. There were cases, however, where we cropped the digital models before calculating physical properties. For example, a large pebble was partially embedded in the surface of the resin cast of a wolf spider (*Geolycosa*

wrightii) burrow. The pebble would have inflated V and SA measurements, so we cropped the pebble out of the digital model and rendered a mesh surface over the hole created by cropping. Also, several ant tunnels intersected the *E. inornata* burrow and were preserved in the resin cast (See Fig. 3E). The ant tunnels are important, and we did not want to physically remove them from the cast before scanning. We were interested only in the V of the skink burrow, so we digitally deleted the ant burrows and sealed the holes left from their deletion (See Fig. 3F). Patching cropped areas typically results in a visible scar with a smoother surface than the original object, so some error may be introduced into measurements; however, they are still more accurate than if we had not cropped the digital models.

Digital Specimens.—Errors introduced by scanning are drawbacks for the preservation, conservation, and dissemination of digital specimens and their perpetuity on websites and in museums as digital specimens. Errors can be introduced while scanning or using the software to produce the digital models. The distance of the specimen from the scanner determines the mesh resolution of the digital model, and the scanner has an ideal range of operation. If the specimen is outside that range, scanning can produce false textures and morphologies. Guidi et al. (2007) raised similar issues for archaeological applications for scanning artifacts at very high resolutions. We found that surfaces perpendicular to the laser stripes are scanned with the highest accuracy. More errors are introduced by scanning surfaces that are parallel or near parallel to the lasers; this happens most commonly at the edges of round, 3D objects.

Scanner errors are compounded when software is used to combine multiple scans; these errors are expressed in overlapped digital models as misaligned regions of the mesh. Misaligned mesh regions can cause incorrect extrapolations of surface textures and produce interference patterns when models are merged with 3D software. We recommend trimming each individual

scan to remove surfaces that were parallel to scanner lasers before aligning an entire model to avoid these errors. This ensures that only the most accurate parts of scans are used to align and merge digital models. Scanning and alignment errors can be analyzed with more sophisticated software, such as RapidWorks (Rapidform Inc. 2007).

Area Exploited.—Traces with a lot of relief will introduce error into the AE, because elevated portions of a trace will produce an overestimation of the proportion of AA used by the tracemaker. Using software to delete the traces from the bedding plane and fill in the holes to produce a flat surface for AA can prevent this problem.

Surface-Area Index.—The smoothing method we used for SAI removes only the finest-scale surface features that can be seen from the smoothed specimens of *Edaphichnium*, which still retain most of their pelleted textures (Fig. 6A–E). The difference in SAI between the *A. camurea* burrow and the slightly rougher *E. colubrinus* burrow is visible at the fine scale (Fig. 6H, I), but this difference may due to the medium in which the burrow was constructed, not behavior. The *E. colubrinus* burrow was constructed in a mixture of coconut fiber and fine- to medium-grained sand, which imparted a rough texture and partially adhered to the plaster cast. The *A. camurea* burrow was constructed in clay-rich soil that did not adhere to the plaster. Burrow features resulting from the lateral motion of *E. colubrinus* while burrowing (Hembree and Hasiotis 2007) and the upward shoveling by the snout of *A. camurea* (Hembree and Hasiotis 2006) are present, but appear to be too coarse to affect SAI greatly. Preservation and the original medium are, therefore, important to consider when applying SAI to traces.

Weathering and geochemical alteration that takes place after a trace fossil is abandoned, filled (completely or partial), and buried, and after it experiences diagenesis, exhumation, and exposure (taphonomic condition) will have a major effect on SAI. Only the best-preserved

specimens should be scanned for this quantitative technique. Although SAI may be useful to quantify such surficially smooth traces as *Psilonichnus* compared to such surficially rough trace fossils as *Ophiomorpha*, the most accurate data will come from the least modified specimens.

Volume Exploited.—This measure cannot provide direct measurements of missing components of burrows and nests. For example, the wasp cocoon (Fig. 10E, F) and bee cell (Fig. 10A–D) were originally part of a larger nest connected to the surface as well as to other cells by one or more tubes (e.g., Hasiotis 2002, 2003). Quantitative data of individual cells and cocoons, however, can more accurately compare similarly sized morphologic features that are more often preserved in the rock record.

Such endogenic traces as backfilled burrows (e.g., *Naktodemasis* isp.) and spreite burrows (e.g., *Diplocraterion*) can be quantified with VE if they weather from the outcrop in full relief (e.g., Bown 1982; Bown and Kraus 1983). Although weathering may remove some of the original diameter and length of a backfilled burrow or thickness of the spreiten between a U-shaped tube, VE provides a minimum quantity of sediment disturbance.

Applications to Research Problems Involving Ichnology

Interpretations of Burrow Cross Sections.—Virtual cross sections of a segment of a fossil burrow cast from the Lower Triassic Fremouw Formation (Fig. 3A–D) show that the same general shape persists throughout the entire burrow length. This supports interpretations of Miller et al. (2001) and Hasiotis et al. (2004) of the tracemaker as a therapsid by comparison with the sectioned therapsid burrows of Groenewald et al. (2001).

Differences in shape between the therapsid burrow cross section (Fig. 3C, D) and the *E. inornata* burrow (Fig. 3G, H) are due most likely to different tracemaker postures. Skinks have a

sprawling posture that gives them a shorter, wider profile than such tetrapods with more erect postures as therapsids and mammals. The skink's limb movements during locomotion are likely responsible for the wing-like extensions of the burrow walls. The fossil burrow is attributed to a therapsid (Hasiotis et al. 2004), which was capable of a more erect posture (Blob 2001) that produced the different cross-sectional burrow shape.

Ratio of Burrow Volume to Surface Area.—Volume-to-surface-area ratios are calculated easily from laser-scanned specimens but may not be informative because the SA of an object increases as the square of its linear dimensions, whereas V increases as the cube of its linear dimensions (Bonner 2006). If, however, a relationship exists between V and SA of burrows of an ontogenetic series of a single taxon and the relationship varies between taxa, then the relationship could be useful for ichnotaxonomy. We hypothesize that this is indeed the case. As a preliminary test, we used a simple linear model to regress published data on modern burrow V and SA for three species of shrimp (*Biffarius arenosus*, *Callianassa subterranea*, *Jaxea nocturna*), one species of crab (*Helice crassa*), and one species of fish (*Lumpenus lampretaeformis*) (Fig. 11). Slopes of the regression lines were compared (Table 5) using a protected least significant difference (LSD) test ($\alpha = 0.05$). Slopes of the burrow data from the three species of shrimp are significantly different from each other. Slopes of the burrow data from the crab and the fish are also significantly different from each other. No difference is detected, however, between the slopes of the burrow data from the crab and *B. arenosus*, or between the slopes of the burrow data from the fish and *C. subterranea*. Results support our hypothesis at low taxonomic levels, but a more robust dataset is needed to determine the nature of the relationship between V and SA for burrows in an ontogenetic series of a taxon.

Spatial Analyses.—Spatial analyses of 3D data can be performed at multiple scales to enhance ichnological interpretations. Spatial analyses of the surfaces of individual trace fossils can be conducted with GIS, morphometric, and landmark analysis software. Such analyses may prove useful for ichnotaxonomy and behavioral interpretations.

Interpretations of assemblages of trace fossils can be improved by incorporating such quantitative measures as SAI, VE, V:SA, and RC if the majority of trace fossils at a locality are preserved suitably for laser scanning. For example, VE can be calculated on a broad scale to compare the sum of V of all trace fossils within a region to the V of the region as measured in the field; this would provide a measure of trace-fossil density that could be related to tracemaker abundance and diversity, deposition rate (or relative duration of discontinuity surfaces), topography, microclimate, paleohydrology, oxygenation, and nutrient availability. Paleoenvironmental influence can also be expressed as groups of trace fossils with similar 3D properties that persist across ichnotaxa; these groupings may constitute suites (*sensu* Bromley and Asgaard 1979) or ichnocoenoses (e.g., Hasiotis 2004, 2008) resulting from different paleoenvironmental conditions at different times in the same location.

Bioturbation Rates.—Volumetric bioturbation rates are difficult to measure directly and are estimated typically by radiotracer diffusion rates (Bentley and Sheremet 2003). MLT technology enables quantification of bioturbation by using burrow and burrow-cast V as estimates for sediment V moved by tracemakers. Bioturbation rates can be determined for modern tracemakers from timed ichnological experiments by casting and scanning experimental burrows where construction time is known; the result is a rate in unit V per unit time.

Bioturbation rates determined from neoichnological experiments can be applied to trace fossils to estimate formation times from trace-fossil V. The time available for bioturbation can

be used to interpret deposition rates, but these interpretations should be made with caution because they assume that ancient behaviors were similar to those of modern tracemakers. Trace-fossil V can also be affected by many local environmental factors, so a comprehensive study of modern bioturbation rates should take these factors into consideration.

Soils and Paleosols.—New quantitative parameters measurable with MLT technology will be useful for interpretations of traces in soils and paleosols. Burrows and roots provide pathways for infiltration, nutrient cycling, aeration, porosity, permeability, translocation, transformation, and aggregate stability (Hole 1981; Butler 1995; Wang et al. 1996). Macropore SA and V created by burrows and roots are not often quantified in soil science because they are difficult to measure. Macropore SA is important for gas exchange, water availability, and mineral weathering (Perret et al. 1999; Buol et al. 2003). Future analyses may quantify relationships between SA of biotic macropores and authigenic clay content and soil respiration.

Volume measurements of macropore casts can be used to quantify relationships with the soil properties they influence. Results can also be applied to paleosols to interpret properties that may be obscured by compaction and diagenesis. Burrow V could be used to supplement interpretations from other paleopedological features. For example, a paleosol interpreted as well drained based on horizon properties, coloration, and rhizolith depth may also have a large total V of pore space created by burrows, now possible to determine with a MLT scanner.

Hydraulic radii of macropores are calculated from V:SA in modern soils (Perret et al. 1999). Hydraulic radius approximates the local minimum in pore-space size. This minimum is important because it controls percolation rates and is the location of maximum capillary pressure in a macropore (Perret et al. 1999). Hydraulic radii of biotic macropores in paleosols can be combined with other paleohydrologic indicators to help interpret original drainage conditions.

Pedoturbation—soil mixing—results from a combination of abiotic and biotic factors and is important for horizon development, ped structure formation, translocation of minerals and nutrients, and aeration (e.g., Buol et al. 2003; Hasiotis 2007). Bioturbation rates calculated from burrow V can help interpret the biotic aspect of pedoturbation. Interpretations of soil mixing can also be improved by measuring V of mounded sediment on ground surfaces created by such soil fauna as earthworms, termites, crayfish, and gophers (Thorp 1949; Hole 1981). Fecal V from exopedonic animals—animals living outside the soil body (Hole 1981)—can aid estimates of rates of additions to the soil. These volumetric data, however, will not provide a complete picture of biotic soil mixing, which must account for older, unmeasurable burrows destroyed by pedoturbation, biotic micropores too small to measure, treethrows, and other soil additions.

Trampling by exopedonic animals effectively compacts soils and affects vegetation, porosity, permeability, infiltration, erosion, bulk density, and aggregate strength (Hole 1981: Pietola et al. 2005). Deformation from footprint formation is accommodated by reduction of porosity, repacking of particles, and displacement of material (Allen 1997). If upward displacement of soil above the original ground surface is disregarded, then footprint V should provide estimates of soil compaction in terms of V for pore space lost.

CONCLUSIONS

MLT scanning technology and 3D software are useful tools for paleoichnology and neoichnology. Benefits fall into three categories: visualization, quantification, and perpetuity, with quantification and perpetuity providing the most opportunity for advancement of these fields. We scanned and analyzed a variety of fossil and modern traces from laboratory and natural field settings. Visualization includes operations that enable qualitative observations of

trace-fossil properties. Traces can be rotated in 3D and saved as movies that can be used for educational purposes and inserted into websites, presentations, and publications. Models with solid rendered surfaces of a uniform color can be used to enhance observations of surface morphology of traces. Cross-sectional shape of scanned traces can be observed easily without cutting actual specimens.

Quantification of trace-fossil properties with MLT technology mainly involves improving accuracy and precision of preexisting treatments of trace fossils, but we introduce new measures as well. Precision of distance measurements of burrows is improved by measuring along a central axis; this also improves calculation of T. Restricting measurement of length to the vertical plane can be used to determine burrowing depth; restricting measurements to the horizontal plane can be used to increase precision of traces created on originally horizontal surfaces, like vertebrate tracks. Angle measurement is improved by restriction to a single plane.

Quantification of surfaces includes generation of contour maps and accurate and precise calculations of AE and burrow SA. Surface area can also be used to quantify surface roughness by calculating a SAI; this is the first application of this index to ichnology. Volume is easy to quantify and is a useful measure for burrows, footprints, and coprolites. We introduce the concept of VE, which compares trace V to the V of a software-generated bounding box; this can be used as a measure of burrow density or efficiency of space usage. We hypothesize that the relationship between SA and V may be unique to specific tracemakers. We plotted V vs. SA for burrows of five species and found significant differences between slopes for some species, but more data are needed to test this thoroughly. Volume and SA can be used to calculate RC, a measure from building physics that we apply to ichnology for the first time.

Perpetuity of specimens is facilitated by MLT technology, which allows digital data to be easily recorded, preserved, and disseminated to researchers, educators, artists, and laypeople interested in organism behavior. Digital models can be used to create physical 3D models for the same purposes. Scanned specimens can be placed in museums and used in cases where actual specimens are too fragile to cast or impossible to collect from the field.

The quality of 3D data is limited by several factors, including the actual specimen, lighting conditions, 3D software, computing power, and the scanner. By considering these factors and planning accordingly, researchers can apply MLT technology to formulate and test a wide range of hypotheses in ichnology. Examples of applications include spatial analyses, calculating bioturbation rates, and quantifying properties of soils and paleosols.

ACKNOWLEDGMENTS

We thank Bill Johnson, Ian Rowell, Josh Schmerge, Jon Smith, NextEngine support staff, Dawn Olson and the staff at the Topeka Zoo, the IchnoBioGeoScience Group at the University of Kansas (KU), and the Society for Sedimentary Geology (SEPM). This project is part of a Ph.D. dissertation by BFP for the University of Kansas Department of Geology. BFP was funded by The Madison and Lila Self Graduate Fellowship, Geological Society of America, Paleontological Society, KU Natural History Museum Panorama fund, KU Geology Department, and Sigma Xi. STH was supported by National Science Foundation Grant EAR-02293000. Vertebrate trace fossils from the Morrison Formation were collected under BLM Permit PA03-WY-107 and we thank Brent Breithaupt and Dale Hanson for their assistance. We also thank Murray Gingras, James MacEachern, and an anonymous reviewer for thoughtful reviews and helpful comments.

REFERENCES

ALLEN, J.R.L., 1989, Short paper: fossil vertebrate tracks and indenter mechanics: Geological Society of London, Journal, v. 146, p. 600–602.

ALLEN, J.R.L., 1997, Subfossil mammalian tracks (Flandrian) in the Severn Estuary, S.W. Britain: mechanics of formation, preservation and distribution: Royal Society of London, Philosophical Transactions, B, v. 352, p. 481–518.

ARAKAWA, Y., AZUMA, Y., KANO, A., TANIJIRI, T., and MIYAMOTO, T., 2002, A new technique to illustrate and analyze dinosaur and bird footprints using 3-D digitizer: Fukui Prefectural Dinosaur Museum, Memoirs, v. 1, p. 7–18.

ATKINSON, R.J.A., and CHAPMAN, C.J., 1984, Resin casting: a technique for investigating burrows in sublittoral sediments: Progress in Underwater Science, v. 9, p. 15–25.

ATKINSON, R.J.A., and NASH, R.D., 1990, Some preliminary observations on the burrows of *Callianassa subterranea* (Montagu) (Decapoda: Thalassinidea) from the west coast of Scotland: Journal of Natural History, v. 24, p. 403–413.

ATKINSON, R.J.A., PELSTER, B., BRIDGES, C.R., TAYLOR, A.C., and MORRIS, S., 1987, Behavioural and physiological adaptations to a burrowing lifestyle in the snake blenny, *Lumpenus lampretaeformis*, and the red band-fish, *Cepola rubescens*: Journal of Fish Biology, v. 31, p. 639–659.

BANCROFT, W.J., HILL, D., and ROBERTS, J.D., 2004, A new method for calculating volume of excavated burrows: the geomorphic impact of wedge-tailed shearwater burrows on Rottnest Island: Functional Ecology, v. 18, p. 752–759.

BATES, K.T., MANNING, P.L., VILA, B., and HODGETTS, D., 2008a, Three-dimensional modeling and analysis of dinosaur trackways: Palaeontology, v. 51, p. 999–1010.

BATES, K.T., RARITY, F., MANNING, P.L., HODGETTS, D., VILA, B., OMS, O., GALOBART, A., and GAWTHORPE, R.L., 2008b, High-resolution LiDAR and photogrammetric survey of the Fumanya dinosaur tracksites (Catalonia): implications for the conservation and interpretation of geological heritage sites: Geological Society of London, Journal, v. 165, p. 115–127.

BENTLEY, S.J., and SHEREMET, A., 2003, New model for the emplacement, bioturbation, and preservation of file-scaled sedimentary strata: Geology, v. 31, p. 725–728.

BERTLING, M., 2007, What's in a name? Nomenclature, systematics, ichnotaxonomy, *in* Miller, W. ed., Trace Fossils: Concepts, Problems, Prospects: Amsterdam, Elsevier, p. 81–91.

BIRD, F.L., and POORE, G.C.B., 1999, Functional burrow morphology of *Biffarius arenosus* (Decapoda: Callianassidae) from southern Africa: Marine Biology, v. 134, p. 77–87.

BLOB, R.W., 2001, Evolution of hindlimb posture in nonmammalian therapsids: biomechanical tests of paleontological hypotheses: Paleobiology, v. 27, p. 14–38.

BONNER, J.T., 2006, Why Size Matters: From Bacteria to Blue Whales: Princeton, New Jersey, Princeton University Press, , 161 p.

BOWN, T.M., 1982, Ichnofossils and rhizoliths of the nearshore fluvial Jebel Qatrani Formation (Oligocene), Fayum Province, Egypt: Palaeogeography, Palaeoclimatology, Palaeoecology, v. 40, p. 255-309.

BOWN, T.M., and KRAUS, M.J., 1983, Ichnofossils of the alluvial Willwood Formation (Lower Eocene), Bighorn Basin, northwest Wyoming, U.S.A.: Palaeogeography, Palaeoclimatology, Palaeoecology, v. 43, p. 95–128.

BOWN, T.M., HASIOTIS, S.T., GENISE, J.F., MALDONADO, F., and BROUWERS, E.M., 1997, Trace fossils of Hymenoptera and other insects, and paleoenvironments of the Claron Formation (Paleocene and Eocene), southwestern Utah: United States, Geological Survey Bulletin 2153, p. 43–58.

BREITHAUPT, B.H., and MATTHEWS, N.A., 2001, Preserving paleontological resources using photogrammetry and geographic information systems: Proceedings of the 11th Conference on Research and Resource Management in Parks and on Public Lands, The George Wright Society, Inc., p. 62–70.

BREITHAUPT, B.H., MATTHEWS, N.A., and NOBLE, T.A., 2004, An integrated approach to three-dimensional data collection at dinosaur tracksites in the Rocky Mountain West: Ichnos, v. 11, p. 11–26.

BROMLEY, R., and ASGAARD, U., 1979, Triassic freshwater ichnocoenoses from Carlsberg Fjord, East Greenland: Palaeogeography, Palaeoclimatology, Palaeoecology, v. 28, p. 39–80.

BUOL, S.W., SOUTHARD, R.J., GRAHAM, R.C., and MCDANIEL, P.A., 2003, Soil Genesis and Classification, Fifth Edition: Ames, Iowa, Iowa State University Press, 494 p.

BUTLER, D.R., 1995, Zoogeomorphology: Cambridge University Press, Cambridge, 231 p.

COHEN, A., LOCKLEY, M., HALFPENNY, J., and MICHEL, A.E., 1991, Modern vertebrate track taphonomy at Lake Manyara, Tanzania: PALAIOS, v. 6, p. 371–389.

DESILVA, J.M., 2010, Revisiting the "midtarsal break": American Journal of Physical Anthropology, v. 141, p. 245–258.

D'URSO, P.S., THOMPSON, R.G., and EARWAKER, W.J., 2000, Stereolithographic (SL) biomodelling in palaeontology: a technical note: Rapid Prototyping Journal, v. 6, p. 212–215.

DWORSCHAK, P.C., 2001, The burrows of *Callianassa tyrrhene* (Petagna 1792) (Decapoda: Thalassinidea): Pubblicazioni della Stazione Zoologica di Napoli: Marine Ecology, v. 22, p. 155–166.

EKDALE, A.A., BROMLEY, R.G., and PEMBERTON, S.G., 1984, Ichnology: the Use of Trace Fossils in Sedimentology and Stratigraphy: SEPM, Short Course 15, 317 p.

EKDALE, A.A., EKDALE, E.G., and COLBERT, M.W., 2006, invertebrate trace fossils inside vertebrate skulls: the worms crawl in, and the worms crawl out (abstract): Geological Society of America, Abstracts with Programs, v. 38, p. 476.

EVITT, W.R., II, 1949, Stereophotography as a tool of the paleontologist: Journal of Paleontology, v. 23, p. 566–570.

FALKINGHAM, P.L., MARGETTS, L., SMITH, I.M., and MANNING, P.L., 2009, Reinterpretation of palmate and semi-palmate (webbed) fossil tracks; insights from finite element modeling: Palaeogeography, Palaeoclimatology, Palaeoecology: v. 271, p. 69–76.

FARLOW, J.O., 1993, The Dinosaurs of Dinosaur Valley State Park: Austin, Texas, Texas Parks and Wildlife Press, 29 p.

FARLOW, J.O., and LOCKLEY, M.G., 1993, An osteometric approach to the identification of the makers of early Mesozoic tridactyl dinosaur footprints, *in* Lucas, S.G., and Morales, M., eds., The Nonmarine Triassic: New Mexico Museum of Natural History and Science, Bulletin 3, p. 123–131.

FIORIOLLO, A.R., HASIOTIS, S.T., KOBAYASHI, Y., and TOMSICH, C.S., 2009, A pterosaur manus track from Denali National Park, Alaska Range, Alaska, United States: PALAIOS, v. 24, p. 466–472.

FREY, R.W., HOWARD, J.D., and PRYOR, W.A., 1978, *Ophiomorpha*: its morphologic, taxonomic, and environmental significance: Palaeogeography, Palaeoclimatology, Palaeoecology, v. 23, p. 199–229.

FU, S., WERNER, F., BROSSMANN, J., 1994, Computed tomography: application in studying biogenic structures in sediment cores: PALAIOS, v. 9, p. 116–119.

GATESY, S.M., 2003, Direct and indirect track features: what sediment did a dinosaur touch?: Ichnos, v. 10, p. 91–98.

GATESY, S.M., MIDDLETON, K.M., JENKINS, F.A., JR., and SHUBIN, N.H., 1999, Three-dimensional preservation of foot movements in Triassic theropod dinosaurs: Nature, v. 399, p. 141–144.

GATESY, S.M., SHUBIN, N.H., and JENKINS, F.A., JR., 2005, Anaglyph stereo imaging of dinosaur track morphology and microtopography: Palaeontologia Electronica, v. 8, no. 1, 814 KB, http://palaeo-electronica.org/2005_1/gatesy10/issue1_05.htm. Checked April 2009.

GERINO, M., and STORA, G., 1991, Analyse quantitative *in vitro* de la bioturbation induite par la polychète *Nereis diversicolor*: Académie des Sciences, Comptes Rendus, Série III, Sciences de la Vie, v. 313, p. 489–494.

GINGRAS, M.K., MACMILLAN, B., BALCOM, B.J., SAUNDERS, T., and PEMBERTON, S.G., 2002, Using magnetic resonance imaging and petrographic techniques to understand the textural attributes and porosity distribution in *Macaronichnus*-burrowed sandstone: Journal of Sedimentary Research, v. 72, p. 552–558.

GRAHAM, R.W., FARLOW, J.O., and VANDIKE, J.E., 1996, Tracking ice age felids: identification of tracks of *Panthera atrox* from a cave in southern Missouri, U.S.A., *in* Stewart, K.M., and Seymour, K.L., eds., Palaeoecology and Palaeoenvironments of Late Cenozoic Mammals: Toronto, University of Toronto Press, p. 331–345.

GRIFFEN, B.D., DEWITT, T.H., and LANGDON, C., 2004, Particle removal rates by the mud shrimp *Upogebia pugettensis*, its burrow, and a commensal clam: effects on estuarine phytoplankton abundance: Marine Ecology Progress Series, v. 269, p. 223–236.

GRIFFIS, R.B., and SUCHANEK, T.H., 1991, A model of burrow architecture and trophic modes in thalassinidean shrimp (Decapoda: Thalassinidea): Marine Ecology Progress Series, v. 79, p. 171–183.

GROENEWALD, G.H., WELMAN, J., and MACEACHERN, J.A., 2001, Vertebrate burrow complexes from the Early Triassic *Cynognathus* Zone (Driekoppen Formation, Beaufort Group) of the Karoo Basin, South Africa: PALAIOS, v. 16, p. 148–160.

GOBETZ, K.E., 2005, Claw impressions in the walls of modern mole (*Scalopus aquaticus*) tunnels as a means to identify fossil burrows and interpret digging movements: Ichnos, v. 12, p. 227–231.

GUIDI, G., REMONDINO, F., MORLANDO, G., DEL MASTIO, A., UCCHEDDU, F., and PELAGOTTI, A., 2007, Performance evaluation of a low cost active sensor for cultural heritage documentation: VIII Conference on Optical 3D Measurement Techniques, Zurich, Switzerland, p. 59–69.

HÄNTZSCHEL, W., 1980, *in* Teichert, C., ed., Treatise on Invertebrate Paleontology, Part W Miscellanea, Supplement 1, Trace Fossils and Problematica, Second Edition: University of Kansas Press and the Geological Society of America, p. W1–W269.

HARRIS, J.D., and LACOVARA, K.J., 2004, Enigmatic fossil footprints from the Sundance Formation (Upper Jurassic) of Bighorn Canyon National Recreation Area, Wyoming: Ichnos, v. 11, p. 151–166.

HASIOTIS, S.T., 2002, Continental Trace Fossils: SEPM, Short Course 51, 134 p.

HASIOTIS, S.T., 2003, Complex ichnofossils of solitary to social soil organisms: understanding their evolution and roles in terrestrial paleoecosystems: Palaeogeography, Palaeoclimatology, Palaeoecology, v. 192, p. 259-320.

HASIOTIS, S.T., 2004, Reconnaissance of Upper Jurassic Morrison Formation ichnofossils, Rocky Mountain region, USA: environmental, stratigraphic, and climatic significance of terrestrial and freshwater ichnocoenoses: Sedimentary Geology, v. 167, p. 277–369.

HASIOTIS, S.T., 2007, Continental ichnology: fundamental processes and controls on trace-fossil distribution, *in* Miller, W., III, ed., Trace Fossils: Concepts, Problems, Prospects: Amsterdam, Elsevier, p. 268–284.

HASIOTIS, S.T., and MITCHELL, C.E., 1993, A comparison of crayfish burrow morphologies: Triassic and Holocene fossil, paleo- and neo-ichnological evidence, and the identification of their burrowing signatures: Ichnos, v. 2, p. 291–314.

HASIOTIS, S.T., MITCHELL, C.E., and DUBIEL, R.F., 1993a, Application of morphologic burrow interpretations to discern continental burrow architects: lungfish or crayfish: Ichnos, v. 2, p. 315–333.

HASIOTIS, S.T., ASLAN, A., and BOWN, T.M., 1993b, Origin, architecture, and paleoecology of the early Eocene continental ichnofossil, *Scaphichnium hamatum*—integration of ichnology and paleopedology: Ichnos, v. 3, p. 1–9.

HASIOTIS, S.T., PLATT, B.F., HEMBREE, D.I., and EVERHART, M.J., 2007, The trace-fossil record of vertebrates, *in* Miller, W., III, ed., Trace Fossils: Concepts, Problems, Prospects: Amsterdam, Elsevier, p. 196–218.

HASIOTIS, S.T., WELLNER, R.W., MARTIN, A.J., and DEMKO, T.M., 2004, Vertebrate burrows from Triassic and Jurassic continental deposits of North America: their paleoenvironmental and paleoecological significance: Ichnos, v. 11, p. 103–124.

HEMBREE, D.I., and HASIOTIS, S.T., 2006, The identification and interpretation of reptile ichnofossils in paleosols through modern studies: Journal of Sedimentary Research, v. 76, p. 575–588.

HEMBREE, D.I., and HASIOTIS, S.T., 2007, Sand-swimming biogenic structures produced by the Kenyan sand boa *Eryx colubrinus*: modern analogs for interpreting continental ichnofossils: Journal of Sedimentary Research, v. 77, p. 389–397.

HIRMAS, D.R., GIMÉNEZ, D., and LI, X., 2009, Characterization of soil structure and pore architecture from the aggregate to horizon scale (abstract): Abstracts, International Annual Meeting, ASA-CSSA-SSSA, Pittsburgh, PA. 1–4 Nov. 2009. American Society of Agronomy-Crop Science Society of America-Soil Science Society of America, Madison, WI.

HOLE, F.D., 1981, The effects of animals on soil: Geoderma, v. 25, p. 75–112.

ISHIGAKI, S., and FUJISAKI, T., 1989, Three dimensional representation of *Eubrontes* by the method of moiré topography, *in* Gillette, D.D., and Lockley, M.G., eds., Dinosaur Tracks and Traces: Cambridge, U.K., Cambridge University Press, p. 421–425.

JESTER, W., and KLIK, A., 2005, Soil surface roughness measurement—methods, applicability, and surface representation: Catena, v. 64, p. 174–192.

KIER, P.M., GRANT, R.E., and YOCHELSON, E.L., 1965, Whitening fossils, *in* Kummel, B., and Raup, D., eds., Handbook of Paleontological Techniques: New York, W.H. Freeman and Company, p. 453–456.

KINOSHITA, K., 2002, Burrow structure of the mud shrimp *Upogebia major* (Decapoda: Thalassinidea: Upogebiidae): Journal of Crustacean Biology, v. 22, p. 474–480.

KNIGHTON, M.S., AGABRA, D.S., MCKINLEY, W.D., ZHENG, J.Z., DROBNIS, D.D., LOGAN, J.D., BAHHOUR, B.F., HAYNIE, J.E., VUONG, K.H., TANDON, A., SIDNEY, K.E., and DIACONESCU, P.L., 2005, Three dimensional digitizer using multiple methods. U.S. Patent 6,980,302 B2, filed September 17, 2003, and issued December 27, 2005.

KOIKE, I., and MUKAI, H., 1983, Oxygen and inorganic nitrogen contents and fluxes in burrows of the shrimps *Callianassa japonica* and *Upogebia major*: Marine Ecology Progress Series, v. 12, p. 185–190.

KRAUSE, J.M., BOWN, T.M., BELLOSI, E.S., and GENISE, J.F., 2008, Trace fossils of cicadas in the Cenozoic of Central Patagonia, Argentina: Palaeontology, v. 51, p. 405–418.

KUBAN, G.J., 1989, Color distinctions and other curious features of dinosaur tracks near Glen Rose, Texas, *in* Gillette, D.D., and Lockley, M.G., eds., Dinosaur Tracks and Traces: Cambridge, U.K., Cambridge University Press, p. 427–440.

LAK, M., AZAR, D., NEL, A., NÉRAUDEAU, D., and TAFFOREAU, P., 2008, The oldest representative of the Trichomyiinae (Diptera: Psychodidae) from the Lower Cenomanian French amber studied with phase-contrast synchrotron X-ray imaging: Invertebrate Systematics, v. 22, p. 471–478.

LANGMAACK, M., SCHRADER, S., RAPP-BERNHARDT, U., and KOTZKE, K., 1999, Quantitative analysis of earthworm burrow systems with respect to biological soil-structure regeneration after soil compaction: Biology and Fertility of Soils, v. 28, p. 219–229.

LEONARDI, G., ed., 1987, Glossary and Manual of Tetrapod Footprint Palaeoichnology: Departmento Nacional da Produção Mineral, Brasilia, 117 p.

LIM, S. –K., YANG, S. –Y., and LOCKLEY, M.G., 1989, Large dinosaur footprint assemblages from the Cretaceous Jindong Formation of Southern Korea, *in* Gillette, D.D., and Lockley, M.G., eds., Dinosaur Tracks and Traces: Cambridge, U.K., Cambridge University Press, p. 421–425.

LIM, S.S.L., 2006, Fiddler crab burrow morphology: how do burrow dimensions and bioturbative activities compare in sympatric populations of *Uca vocans* (Linnaeus, 1758) and *U. annulipes* (H. Milne Edwards, 1837)?: Crustaceana, v. 79, p. 525–540.

MAHDAVI, A., and GURTEKIN, B., 2001, Computational support for the generation and exploration of the design-performance space: Seventh International Building Performance Simulation Association Conference Proceedings, p. 669–676.

MANNING, P.L., 2004, A new approach to the analysis and interpretation of tracks: examples from the Dinosauria, *in* McIlroy, D., ed., The Application of Ichnology to Palaeoenvironmental and Stratigraphic Analysis: Geological Society of London, Special Publication 228, p. 93–123.

MARGETTS, L., LENG, J.M., SMITH, I.M., and MANNING, P.L., 2006, Parallel three dimensional finite element analysis of dinosaur trackway formation, *in* Schweiger, H.F., ed., Numerical Methods in Geotechnical Engineering: London, Taylor & Francis, p. 743–749.

MATTHEWS, N.A., and BREITHAUPT, B.H., 2001, Close-range photogrammetric experiments at Dinosaur Ridge: Mountain Geologist, v. 38, p. 147–153.

MEADOWS, P.S., 1991, The environmental impact of burrows and burrowing animals—conclusions and a model, *in* Meadows, P.S., and Meadows, A., eds., The Environmental Impact of Burrowing Animals and Animal Burrows: The Zoological Society of London: Oxford, U.K., Clarendon Press, p. 327–338.

MILÀN, J., CLEMMENSEN, L.B., and BONDE, N., 2004, Vertical sections through dinosaur tracks (Late Triassic lake deposits, East Greenland)—undertracks and other subsurface deformation structures revealed: Lethaia, v. 37, p. 285–296.

MILLER, M.F., HASIOTIS, S.T., BABCOCK, L.E., ISBELL, J.L., and COLLINSON, J.W., 2001, Tetrapod and large burrows of uncertain origin in Triassic high paleolatitude floodplain deposits, Antarctica: PALAIOS, v. 16, p. 218–232.

MORRISEY, D.J., DEWITT, T.H., ROPER, D.S., and WILLIAMSON, R.B., 1999, Variation in the depth and morphology of burrows of the mud crab *Helice crassa* among different types of intertidal sediment in New Zealand: Marine Ecology Progress Series, v. 182, p. 231–242.

MOSSMAN, D.J., BRÜNING, R., and POWELL, H.P., 2003, Anatomy of a Jurassic theropod trackway from Ardley, Oxfordshire, U.K.: Ichnos, v. 10 p. 195–207.

NARUSE, H., and NIFUKU, K., 2008, Three-dimensional morphology of the ichnofossil *Phycosiphon incertum* and its implication for paleoslope inclination: PALAIOS, v. 23, p. 270–279.

NEXTENGINE, INC., 2009, NextEnging Desktop 3D Scanner TechSpecs, http://www.nextengine.com/HD_DataSheet.pdf. Checked April 2009.

NICKELL, L., and ATKINSON, R.J.A., 1995, Functional morphology of burrows and trophic modes of three thalassinidean shrimp species, and a new approach to the classification of thalassinidean burrow morphology: Marine Ecology Progress Series, v. 128, p. 181–197.

NORTHWOOD, C., 2005, Early Triassic coprolites from Australia and their palaeobiological significance: Palaeontology, v. 48, p. 49–68.

ORR, P.J., 1999, Quantitative approaches to the resolution of taxonomic problems in invertebrate ichnology, *in* Harper, D.A.T., ed., Numerical Paleobiology: West Sussex, U.K., John Wiley & Sons Ltd., p. 395–431.

PEREZ, K.T., DAVEY, E.W., MOORE, R.H., BURN, P.R., ROSOL, M.S., CARDIN, J.A., JOHNSON, R.L., and KOPANS, D.N., 1999, Application of computer-aided tomography (CT) to the study of estuarine benthic communities: Ecological Applications, v. 9, p. 1050–1058.

PERRET, J., PRASHER, S.O., KANTZAS, A., and LANGFORD, C., 1999, Three-dimensional quantification of macropore networks in undisturbed soil cores: Soil Science Society of America, Journal, v. 63, p. 1530–1543.

PIETOLA, L., HORN, R., and YLI-HALLA, M., 2005, Effects of trampling by cattle on the hydraulic and mechanical properties of soil: Soil and Tillage Research, v. 82, p. 99–108.

PLATT, B.F., and HASIOTIS, S.T., 2006, Newly discovered sauropod dinosaur tracks with skin and foot-pad impressions from the Upper Jurassic Morrison Formation, Bighorn Basin, Wyoming, USA: PALAIOS, v. 21, p. 249–261.

PLATT, B.F., and HASIOTIS, S.T., 2008. Modern elephant footprints in alluvium as analogs for sauropod dinosaur tracks in ancient floodplain sediments (abstract): Geological Society of America, Abstracts with Programs, v. 40, p. 101.

PURNELL, M.A., 2003, Casting, replication, and anaglyph stereo imaging of microscopic detail in fossils, with examples from conodonts and other jawless vertebrates: Palaeontologia Electronica, v. 6, no. 2, 704 KB, http://palaeo-electronica.org/2003_2/rubber/issue2_03.htm. Checked June 2009.

R DEVELOPMENT CORE TEAM, 2008, R: A Language and Environment for Statistical Computing, Vienna, Austria, R Foundation for Statistical Computing.

RAPIDFORM INC., 2007, RapidWorks64, version 2.3.5, build version 2.5.13.0, Seoul, South Korea.

RIGHT HEMISPHERE, 2009, Deep View, version 5.7: Pleasanton, California, USA.

ROSSI, A.M., HIRMAS, D.R., GRAHAM, R.C., and STERNBERG, P.D., 2008, Bulk density determination by automated three-dimensional laser scanning: Soil Science Society of America, Journal, v. 72, p. 1591–1593.

RUDNICK, D.A., CHAN, V., and RESH, V.H., 2005, Morphology and impacts of the burrows of the Chinese mitten crab, *Eriocheir sinensis* H. Milne Edwards (Decapoda, Grapsoidea), in south San Francisco Bay, California, U.S.A.: Crustaceana, v. 78, p. 787–807.

SARJEANT, W.A.S., 1975, Fossil tracks and impressions of vertebrates, *in* Frey, R.W., ed., The Study of Trace Fossils: New York, Springer-Verlag, p. 283–324.

SARJEANT, W.A.S., and THULBORN, R.A., 1986, Probable marsupial footprints from the Cretaceous sediments of British Columbia: Canadian Journal of Earth Sciences, v. 23, p. 1223–1227.

SMITH, J.J., HASIOTIS, S.T., WOODY, D.T., and KRAUS, M.J., 2008, Paleoclimatic implications of crayfish-mediated prismatic structures in paleosols of the Paleogene Willwood

Formation, Bighorn Basin, Wyoming, USA.: Journal of Sedimentary Research, v. 78, p. 323–334.

SMITH, N.E., and STRAIT, S.G., 2008, PaleoView3D: from specimen to online digital model: Palaeontologia Electronica v. 11, no. 2, 1.00 MB, http://palaeo-electronica.org/2008_2/134/index.html. Checked April 2009.

SMITH, R.M.H., 1987, Helical burrow casts of therapsid origin from the Beaufort Group (Permian) of South Africa: Palaeogeography, Palaeoclimatology, Palaeoecology, v. 60, p. 155–170.

STICHTING BLENDER FOUNDATION, 2008, Blender, version 2.48a: Amsterdam, the Netherlands.

STIEGLITZ, T., RIDD, P., and MÜLLER, P., 2000, Passive irrigation and functional morphology of crustacean burrows in a tropical mangrove swamp: Hydrobiologia, v. 421, p. 69–76.

STRAIT, S., SMITH, N., and PENKROT, T., 2007, The promise of low cost 3D laser scanners: Journal of Vertebrate Paleontology, v. 27, supplement to no. 3, p. 153A.

THORP, J., 1949, Effects of certain animals that live in soils: Scientific Monthly, v. 68, p. 180-191.

THULBORN, R.A., 1991, Morphology, preservation and palaeobiological significance of dinosaur coprolites: Palaeogeography, Palaeoclimatology, Palaeoecology, v. 83, p. 341–366.

TREWIN, N.H., 1994, A draft system for the identification and description of arthropod trackways: Palaeontology, v. 37, p. 811–823.

UCHMAN, A., 1995, Tiering patterns of trace fossils in the Palaeogene flysch deposits of the Carpathians, Poland: Géobios Mémoire Spécial, v. 18, p. 389–394.

WANG, D., LOWRY, B., NORMAN, J.M., and MCSWEENEY, K., 1996, Ant burrow effects on water flow and soil hydraulic properties of Sparta sand: Soil and Tillage Research, v. 37, p. 83–93.

WELCH, D., 1982, Dung properties and defecation characteristics in some Scottish herbivores, with an evaluation of the dung-volume method of assessing occupance: Acta Theriologica, v. 27, p. 191–212.

WETZEL, A., and UCHMAN, A., 2001, Sequential colonization of muddy turbidites in the Eocene Beloveza Formation, Carpathians, Poland: Palaeogeography, Palaeoclimatology, Palaeoecology, v. 168, p. 178–202.

TABLES

Table 1.—Availability of operations needed for applications described in software used in this paper. *Denotes function is available, but with limited capabilities.

Ichnological application(s)	Software function(s) needed	Function availability		
		ScanStudio HD™	ScanStudio CAD Tools™	Adobe ® 3D Reviewer
Stereo pairs	rotation	*	*	●
Movies	animation			●
Uniform surface images	solid render	●	●	●
Cross-sectional shape	section			●
Measuring distances	distance	*	*	●
Tortuosity index	section			●
	find center of circle			●
	distance	*	*	●
Measuring angles	angle			●
Track topography	spline/section		*	●
Area exploited	trim	●	●	
	surface area	●	●	●
Burrow surface area	surface area	●	●	●
Surface area index	surface area	●	●	●
	CAD surface			●
Burrow, track, & coprolite volume	volume		●	*
Volume exploited	volume		●	*
	bounding box			●
Volume-surface area ratio, relative compactness	volume		●	*
	surface area	●	●	●

Table 2.—Lengths of segments of ghost crab burrow (Fig. 4D–F) used to calculate burrow length and tortuosity index. Subscript indicates segment number from Figure 4D, u = total length of segment, v = straight-line length of segment.

Segment variable	Length (cm)
u_1	14.6
v_1	14.4
u_2	8.1
v_2	7.7
u_3	22.8
v_3	22.6

Table 3.—Quantitative data from digital models of trace fossils. SA = surface area, V = volume, VE = volume exploited, RC = relative compactness. Note surface areas include software-generated enclosing faces over openings in mesh.

Ichnotaxon or trace fossil	Age	Formation	Location	SA (cm^2)	V (cm^3)	VE	RC
Edaphichnium lumbricatum (small)	Eocene	Willwood	Wyoming, USA	20.20	5.15	39.64	0.71
E. lumbricatum (large)	Eocene	Willwood	Wyoming, USA	118.93	51.80	27.35	0.57
Tetrapod burrow segment	Early Triassic	Fremouw	Queen Maud Mtns., Antarctica	143.62	96.45	42.52	0.71
Eatonichnus claronensis (small)	Paleocene-Eocene	Claron	Utah, USA	17.63	5.93	46.73	0.90
E. claronensis (large)	Paleocene-Eocene	Claron	Utah, USA	112.41	66.43	43.38	0.71
Scaphichnium hamatum	Eocene	Willwood	Wyoming, USA	13.09	3.25	44.01	0.81
Wasp cocoon	Paleocene-Eocene	Claron	Utah, USA	9.75	2.45	54.39	0.90
Bee cell	Eocene-Oligocene	Climbing Arrow	Montana, USA	4.77	0.83	52.89	0.90
Feoichnus sp.	Eocene	Willwood	Wyoming, USA	54.48	19.10	31.69	0.63
Tridactyl dinosaur track (latex mold)	Late Jurassic	Morrison	Wyoming, USA	148.20	27.72	15.58	0.30
Tetradactyl dinosaur track cast	Late Jurassic	Morrison	Wyoming, USA	214.73	139.75	25.44	0.61
Coprolite	Eocene	Willwood	Wyoming, USA	40.42	19.16	46.68	0.86
Coprolite	Miocene	Found in float (exact stratigraphic position uncertain)	Washington, USA	124.66	38.12	20.35	0.44

Table 4.—Quantitative data from digital models of modern traces. SA = surface area, V = volume, VE = volume exploited, RC = relative compactness. Note surface areas include software-generated enclosing faces over openings in mesh. *Data from model of skink burrow cast with ant tunnels digitally removed.

Trace description	Tracemaker	Setting	SA (cm^2)	V (cm^3)	VE	RC
Partial burrow network cast	Worm lizard (*Amphisbaena camurea*)	Lab	396.68	145.15	3.82	0.34
Burrow cast	Wolf spider (*Geolycosa wrightii*)	Field	133.23	54.51	11.51	0.52
Burrow cast	Brown scorpion (*Urodacus* sp.)	Field	617.29	246.46	2.38	0.31
Burrow cast	Tiger beetle larva (*Cicindela* sp.)	Field	73.43	13.54	1.16	0.37
Burrow cast	Cobalt blue tarantula (*Haplopelma lividum*)	Lab	507.52	463.05	17.08	0.57
Burrow cast	Ghost crab (*Ocypode quadrata*)	Field	225.54	75.52	2.74	0.38
Burrow cast	Sand boa (*Eryx colubrinus*)	Lab	910.91	516.69	2.80	0.34
Burrow cast	Marsh crab (*Sesarma* sp.)	Field	579.34	332.46	5.39	0.40
Burrow cast	Desert skink (*Egernia inornata*)*	Field	1029.62	548.16	1.93	0.31
Fecal mass	Horse (*Equus ferus caballus*)	Field	73.02	44.54	47.95	0.83
Fecal mass	Asian elephant (*Elephas maximus*)	Zoo	815.60	1682.46	50.71	0.84
Footprint	African elephant (*Loxodonta Africana*)	Zoo	2429.67	2761.75	42.08	0.39

Table 5.—Slopes from surface area vs. volume plot (Fig. 11) with references for data sources. Similar letters after slope values represent non-significant differences at the $\alpha = 0.05$ level. *These data are means of measurements from multiple burrows at different locations.

Species	Reference	Slope
Biffarius arenosus	Bird and Poore, 1999	0.195 a
Callianassa subterranea	Atkinson and Nash, 1990; Nickell and Atkinson, 1995	0.408 b
Jaxea nocturna	Nickell and Atkinson, 1995	0.596 c
Helice crassa	Morrisey et al., 1999*	0.200 a
Lumpenus lampretaeformis	Atkinson et al., 1987	0.443 b

FIGURES

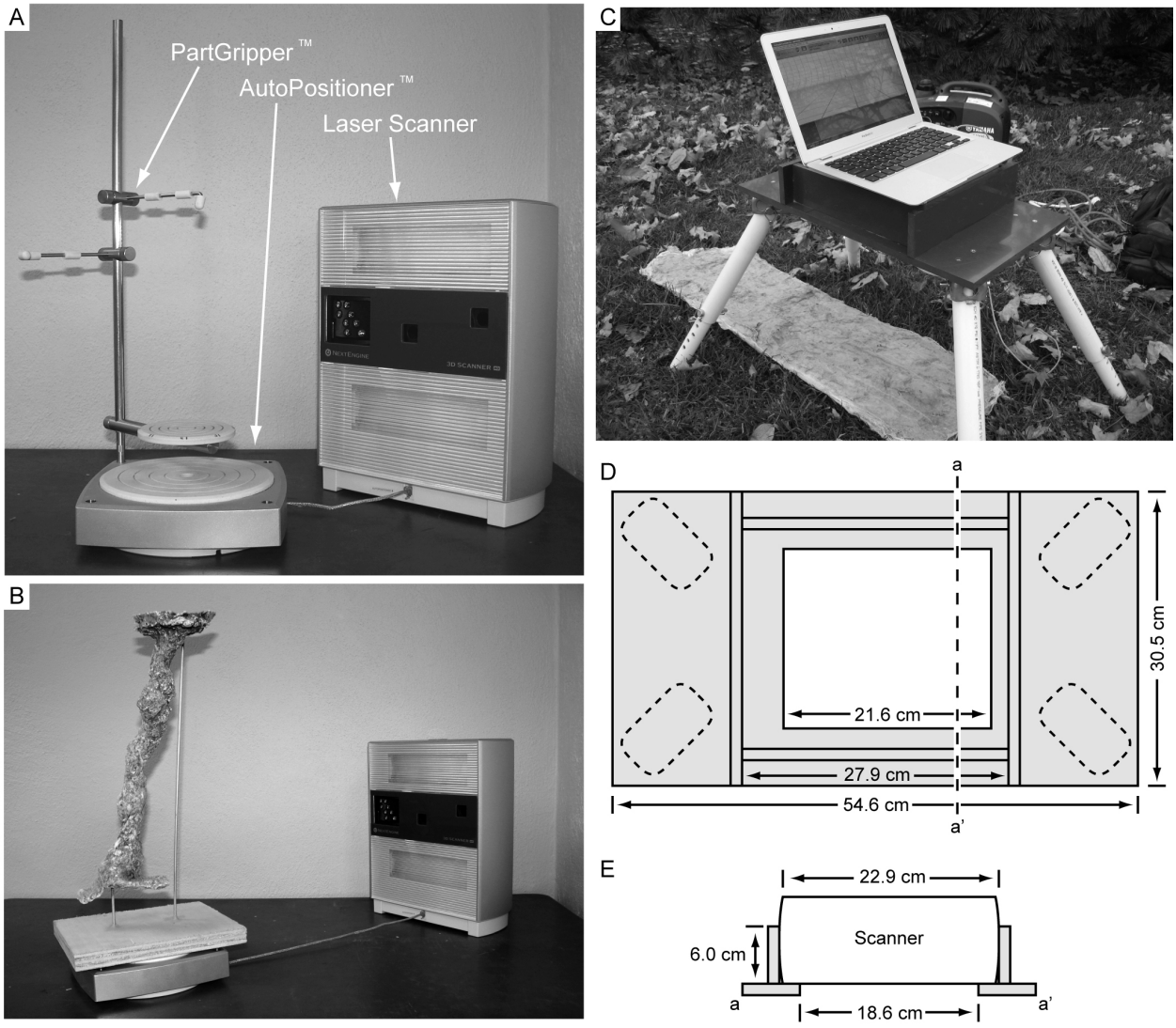

Figure 1.—A) NextEngine™ laser scanner, AutoPositioner™, and PartGripper™. **B)** Mounted plaster cast of marsh crab (*Sesarma* sp.) burrow on AutoPositioner™ with PartGripper™ removed. **C)** Custom-made base for scanner (housed under laptop) use in the field. **D)** Plan view of scanner base showing dimensions; legs underneath base represented by dashed boxes. **E)** Cross section through base along a–a′ in Part D showing scanner position.

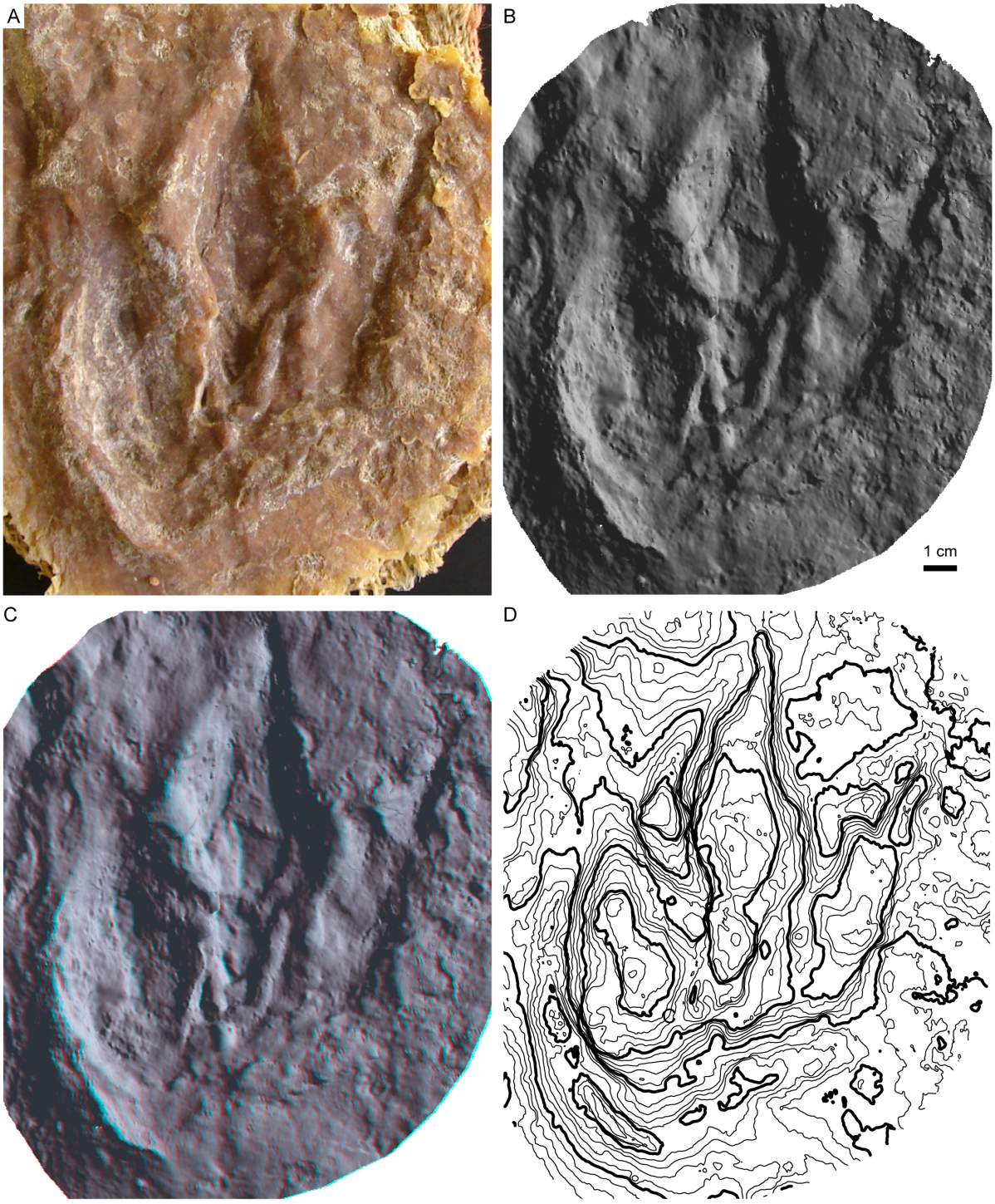
A
B
1 cm
C
D

Figure 2 (previous page).—A) Latex mold of tridactyl dinosaur track from the Upper Jurassic Morrison Formation, Bighorn Basin, Wyoming, USA. **B)** Solid rendered digital model of track in Part A; note improved detail. **C)** Stereo anaglyph image of Part A. **D)** Contour map of Part A; contour interval 1 mm.

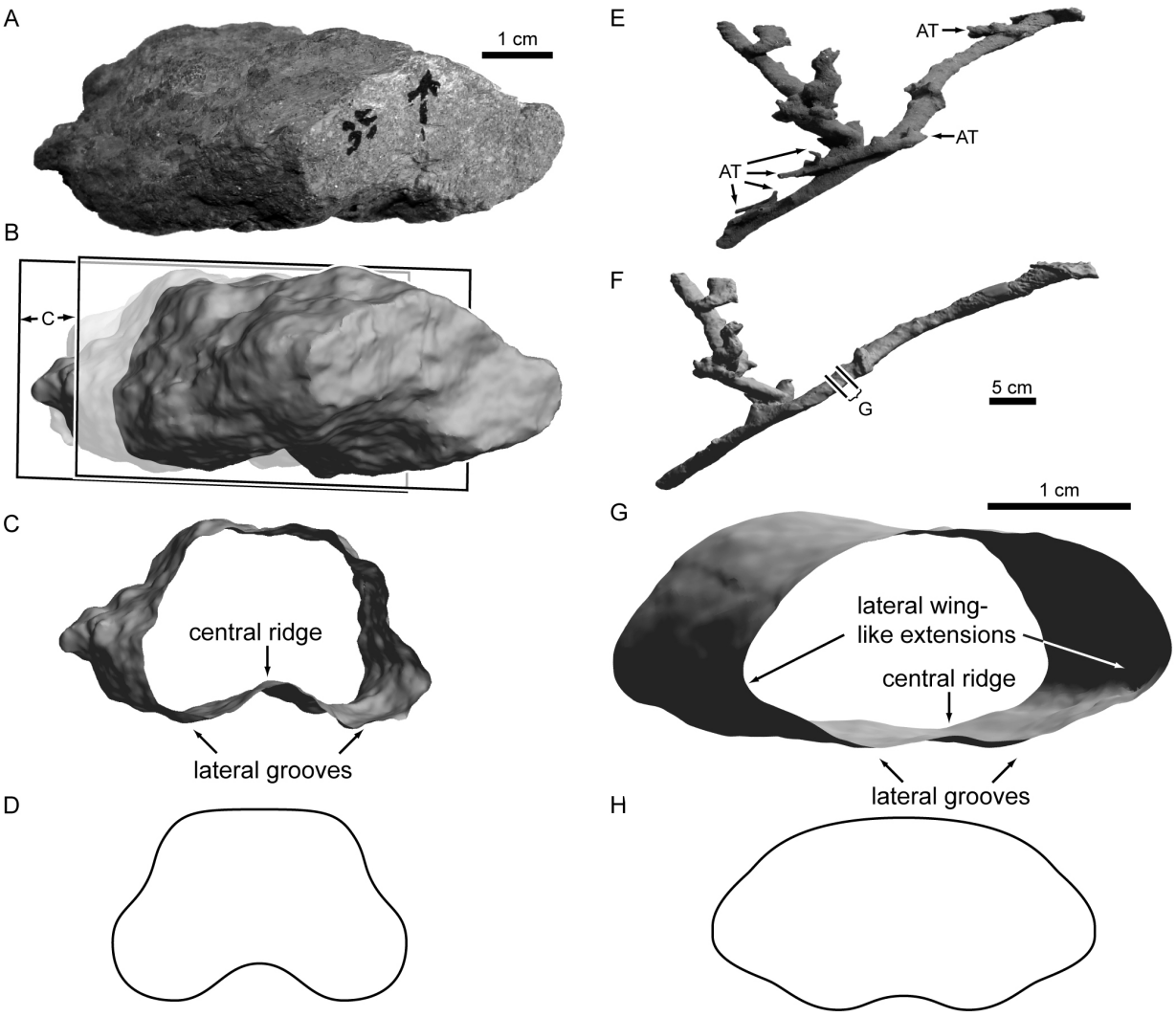

Figure 3.—A) Tetrapod burrow segment from the Lower Triassic Fremouw Formation, Kitching Ridge, Queen Maud Mountains, Antarctica. **B)** Solid rendered digital model of Part A; parallel rectangles represent planes used to create cross section in Part C. **C)** Section through model in Part B showing cross-sectional shape. **D)** Idealized cross-sectional outline of burrow from Part C. **E)** Desert skink (*Egernia inornata*) burrow; AT = ant tunnels. **F)** Solid rendered digital model of Part E with ant tunnels digitally removed. **G)** Cross section through digital model in Part F; compare to Part C. **H)** Idealized cross-sectional outline of burrow in Part G; compare to Part D.

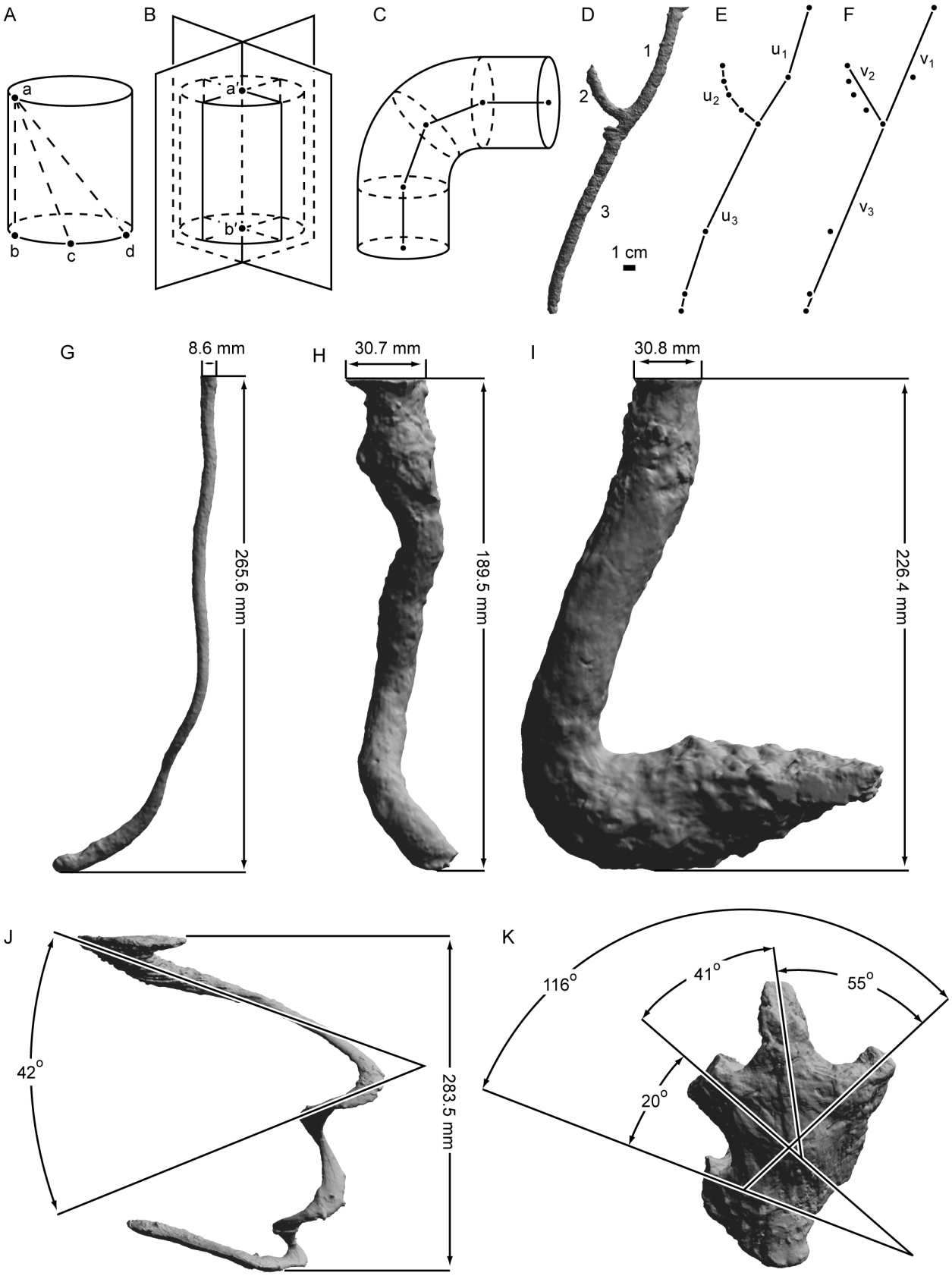
A
a
b
c
d
B
a′
b′
C
D
1
2
3
1 cm
E
u_1
u_2
u_3
F
v_1
v_2
v_3
G
8.6 mm
265.6 mm
H
30.7 mm
189.5 mm
I
30.8 mm
226.4 mm
J
42°
283.5 mm
K
116°
41°
55°
20°

Figure 4 (previous page).—Measurements of distances and angles from digital models. **A)** Example of errors when measuring length of a cylinder; ab = true length, perpendicular to central axis, ad > ac > ab. **B)** Ideal method of measuring true length along central axis a′b′ formed by the intersection of two perpendicular planes that bisect the cylinder. **C) ** Ideal method for measuring a curved cylinder by connecting the central points of circles created by planes perpendicular to the curved cylinder at points of direction change. **D)** Plaster cast of ghost crab (*Ocypode quadrata*) burrow with its three segments numbered. **E)** Measurement of burrow segment lengths; points represent centers of shapes created by the intersections of planes perpendicular to burrow long axes and burrow surface. **F)** Straight-line distances between burrow-segment endpoints used to calculate tortuosity index (See Table 2). **G)** Resin cast of tiger beetle (*Cicindela* sp.) larva burrow, showing opening diameter and depth. **H)** Resin cast of wolf spider (*Geolycosa wrightii*) burrow, showing opening diameter and depth. **I)** Plaster cast of cobalt blue tarantula (*Haplopelma lividum*) burrow, showing opening diameter and depth. **J)** Resin cast of brown scorpion (*Urodacus* sp.) burrow showing depth and ramp angle of uppermost spiral. **K)** Natural sandstone cast of tetradactyl dinosaur track, Upper Jurassic Morrison Formation, showing angles of divarication.

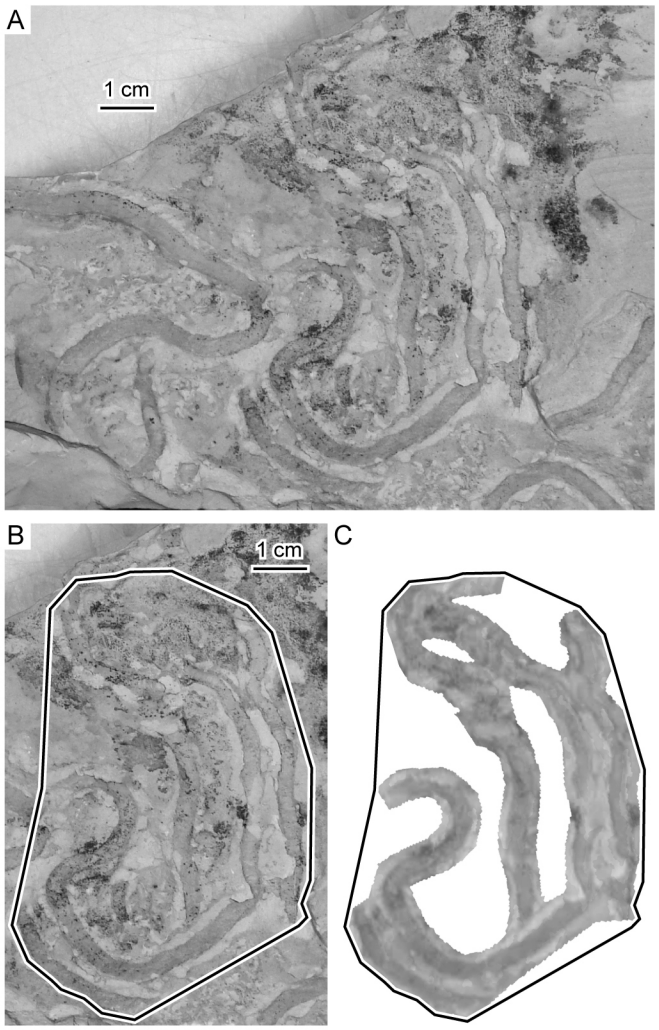

Figure 5.—Area-exploited calculation for *Nerites* specimen from the Eocene Promina Beds, Benkovac, Croatia. **A)** Traces are preserved on multiple bedding planes. **B)** Outline represents area available for traces on a single bedding plane. **C)** Area utilized within outline in Part B.

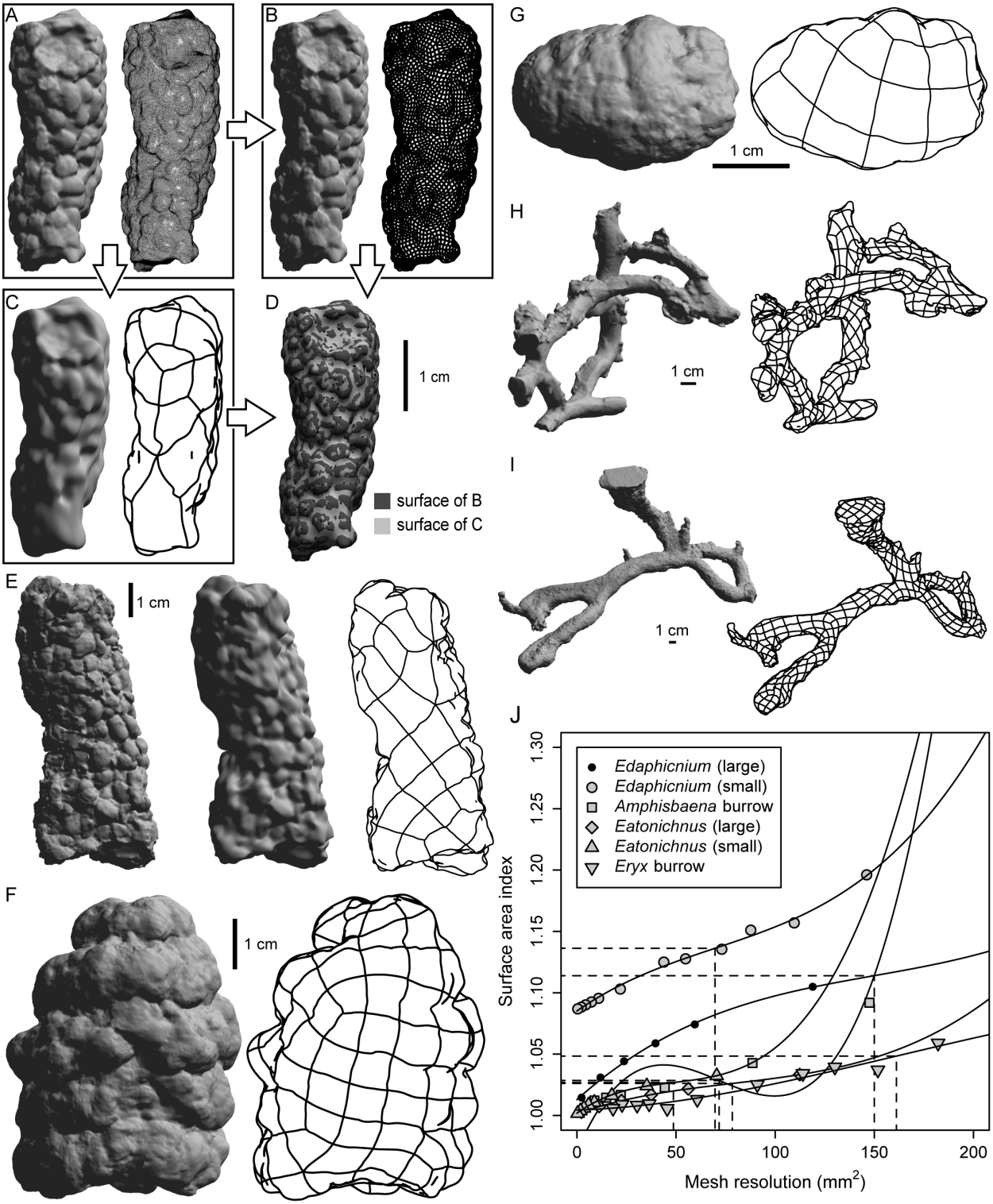
A
B
C
D
1 cm
surface of B
surface of C
E
1 cm
F
1 cm
G
1 cm
H
1 cm
I
1 cm
J
Edaphicnium (large)
Edaphicnium (small)
Amphisbaena burrow
Eatonichnus (large)
Eatonichnus (small)
Eryx burrow
Surface area index
1.00
1.05
1.10
1.15
1.20
1.25
1.30
0
50
100
150
200
Mesh resolution (mm2)

Figure 6 (previous page).—Determination of surface-area index (SAI). **A)** Initial digital model and corresponding mesh view of small specimen of *Edaphichnium*. **B)** Solid render and mesh of model in Part A after wrapping original 3D data with 5000 polygons. Note fidelity to original model in Part A. **C)** Solid render and mesh of model in Part A after smoothing to 29 polygons. **D)** Comparison of models in Parts B and C; models overlapped and shading represents whether Part B or Part C is exposed at the surface, highlighting the parts of the models that have the highest elevations. **E)** Original solid model, smoothed solid model, and smoothed mesh of large specimen of *Edaphichnium.* **F)** Original solid model and smoothed mesh of large specimen of *Eatonichnus*. **G**) Original solid model and smoothed mesh of small specimen of *Eatonichnus*. **H)** Original solid model and smoothed mesh of *Amphisbaena camurea* burrow cast. **I**) Original solid model and smoothed mesh of *Eryx colubrinus* burrow cast. **J)** Plot of SAI and mesh resolution (original surface area/number of polygons in mesh). Y values of inflection points are final SAI values for each trace.

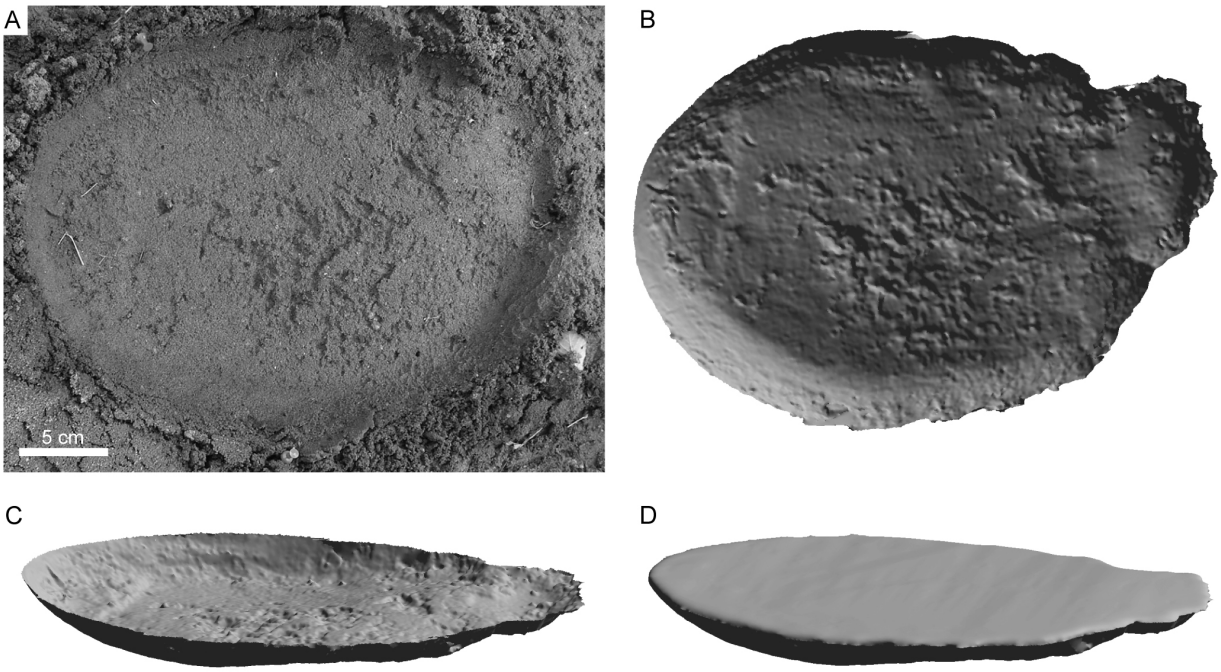

Figure 7.—A) African elephant (*Loxodonta africana*) footprint, Topeka Zoo, Topeka, Kansas, USA. **B)** Digital model of Part A, with ground surface removed. **C)** Oblique view of Part B. **D)** Oblique view of virtual plaster cast—laser scanned elephant footprint with simulated enclosing top surface.

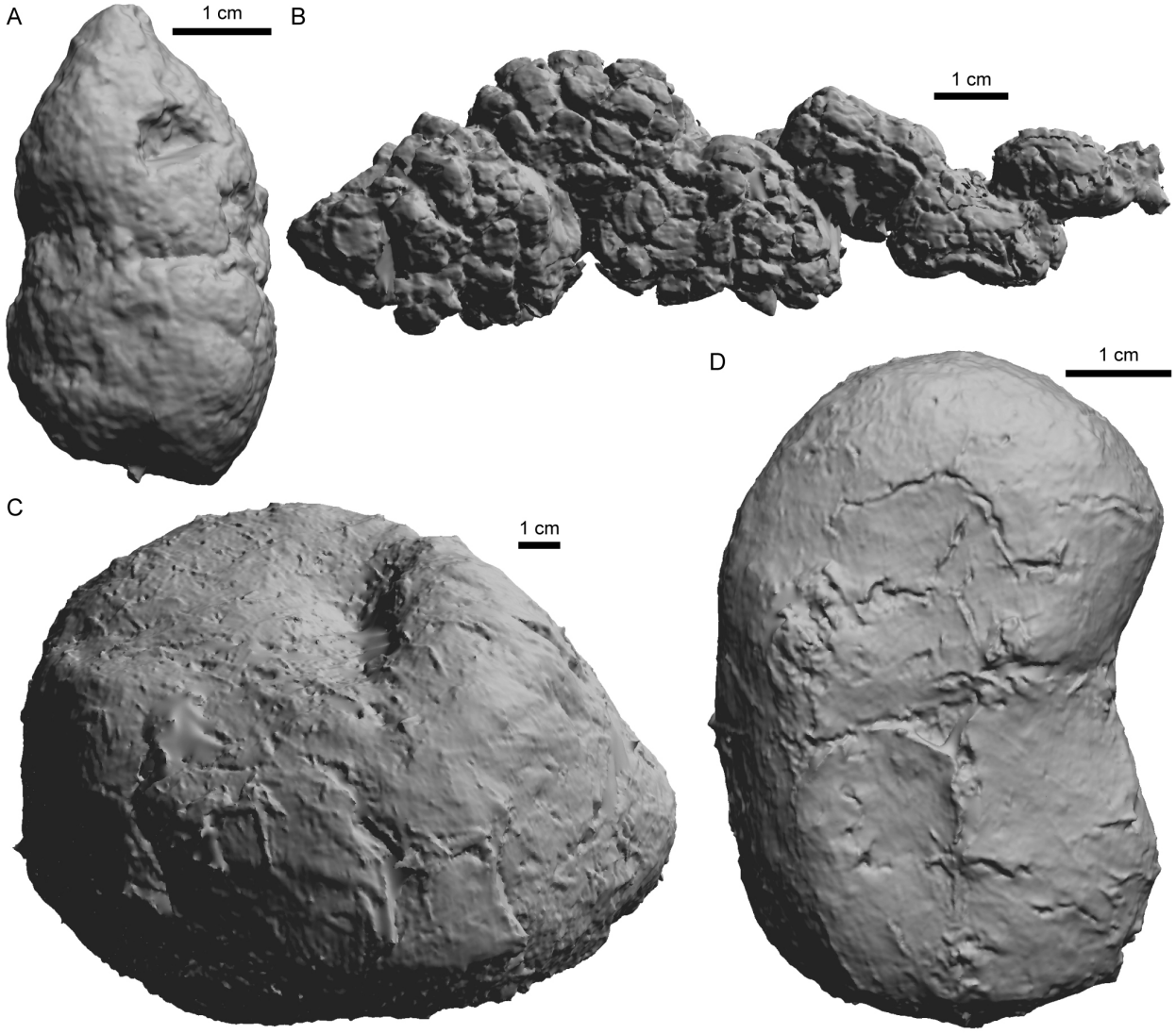

Figure 8.—Digital models of **A)** coprolite from the Eocene Willwood Formation, Wyoming, USA, **B)** coprolite from the Miocene of Washington, USA, **C)** desiccated fecal mass from Asian elephant (*Elephas maximus*), and **D)** desiccated fecal mass from a horse (*Equus ferus caballus*).

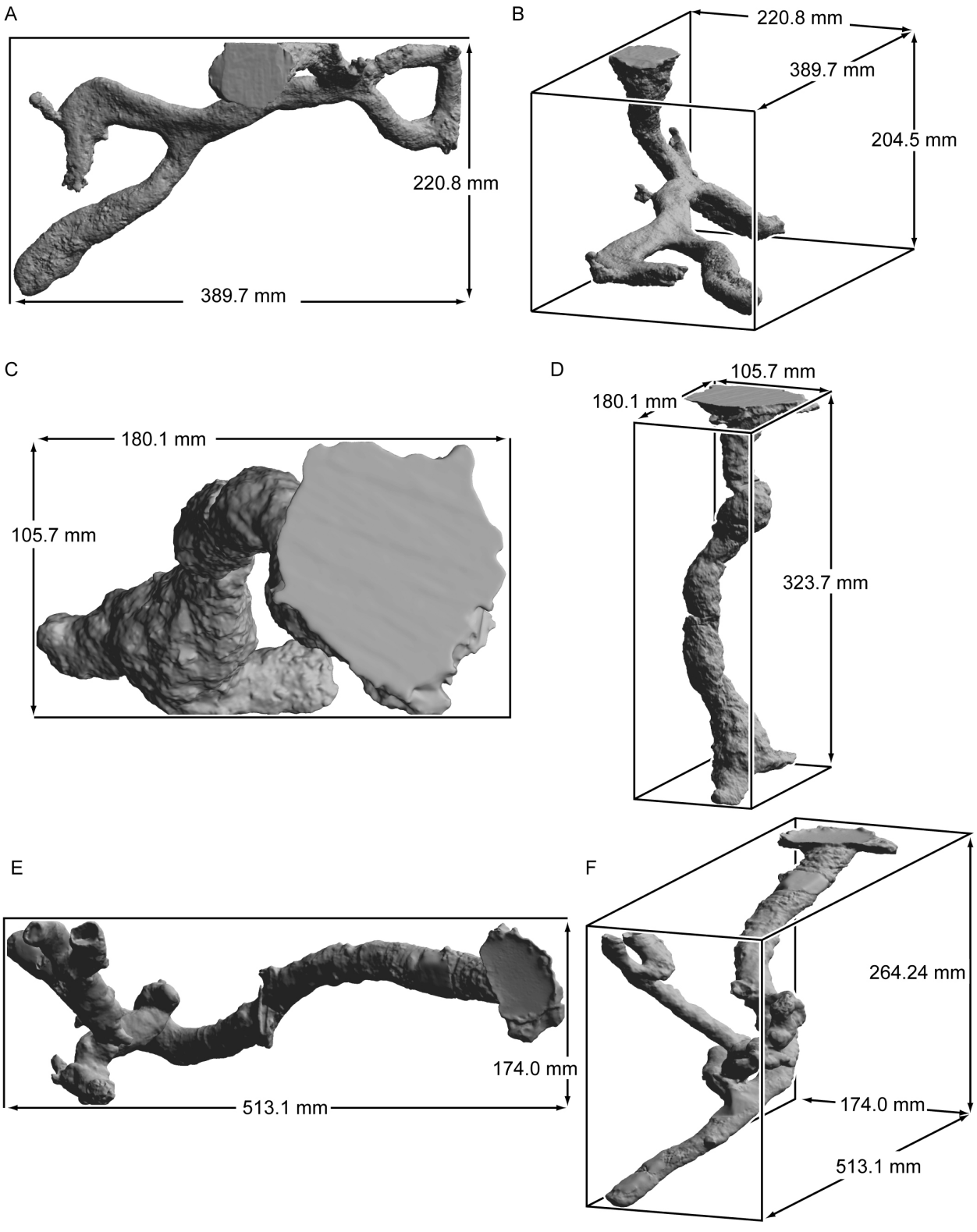
A
220.8 mm
389.7 mm
B
220.8 mm
389.7 mm
204.5 mm
C
180.1 mm
105.7 mm
D
105.7 mm
180.1 mm
323.7 mm
E
174.0 mm
513.1 mm
F
264.24 mm
174.0 mm
513.1 mm

Figure 9 (previous page).—Bounding boxes (modified in Adobe Illustrator®) used to calculate volume exploited. **A)** Top view of digital model of plaster cast of sand boa (*Eryx colubrinus*) burrow with bounding box. **B)** Oblique view of Part A. **C)** Top view of digital model of plaster cast of marsh crab (*Sesarma* sp.) burrow. **D)** Oblique view of Part C. **E)** Top view of digital model of resin cast of desert skink (*Egernia inornata*) burrow with bounding box. **F)** Oblique view of Part D.

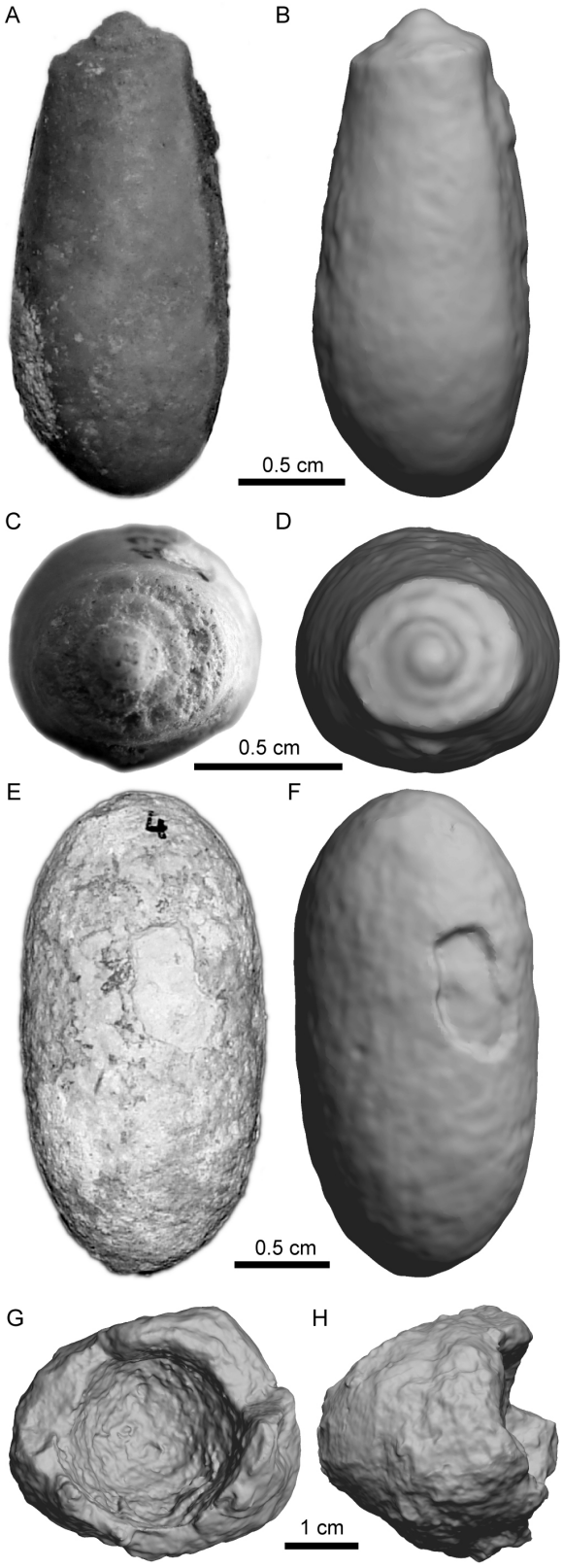
A
B
0.5 cm
C
D
0.5 cm
E
F
0.5 cm
G
H
1 cm

Figure 10 (previous page).—Tests of limitations of MLT scanner with small and concave objects. **A)** Bee cell, Eocene-Oligocene Climbing Arrow Formation, Montana, USA. **B)** Digital model of Part A. **C)** Spiral cap of bee cell in Part A. **D)** Digital model of Part C. **E)** Wasp cocoon, Paleocene-Eocene Claron Formation, Utah, USA. **F)** Digital model of Part E; note weathered patch on surface. **G)** Digital model of *Feoichnus* isp., Eocene Willwood Formation, Wyoming, USA, showing successfully scanned concave center. **H)** Side view of Part G.

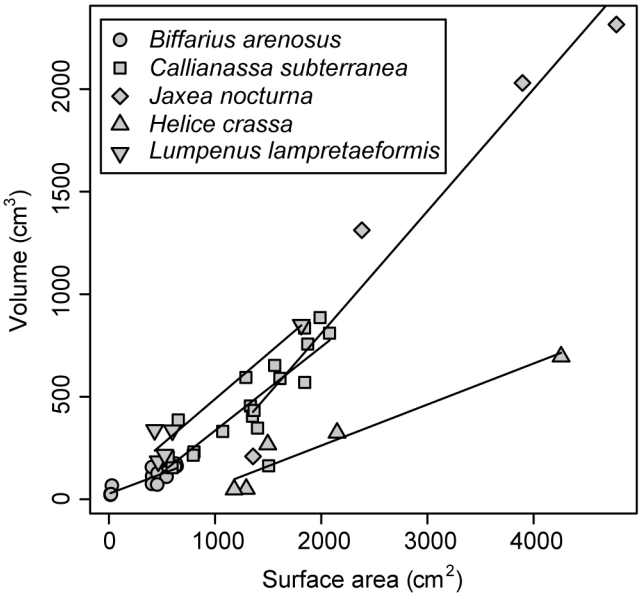

Figure 11.—Plot of burrow surface area and volume data for five species (see Table 5 for slopes).

CHAPTER 3: EMPIRICAL DETERMINATION OF PHYSICAL CONTROLS ON MEGAFAUNAL FOOTPRINT FORMATION THROUGH NEOICHNOLOGICAL EXPERIMENTS WITH ELEPHANTS

Currently in review as:

PLATT, B.F., HASIOTIS, S.T., AND HIRMAS, D.R., Empirical determination of physical controls on megafaunal footprint formation through neoichnological experiments with elephants: PALAIOS.

ABSTRACT

The purpose of this study is to quantify the relationship between physical variables that control megafaunal footprint formation in unconsolidated, sandy sediment. Results of this research can be used to help interpret the physical conditions under which fossil tracks of megafauna were produced in similar ancient sediments. We collected and analyzed empirical data from trackmaking trials with live elephants and experimental sediments. Trials were designed to produce data appropriate for a multiple regression analysis, i.e., one dependent variable and multiple independent variables. Variables measured or calculated for each trial were track volume normalized to track length (V_n), locomotion velocity (v), standing foot pressure (P), time elapsed since sediment deposition (A), sediment dry bulk density (ρ_b), volumetric water content of sediment (θ_v), and phi mean (M_ϕ), standard deviation (σ_ϕ), skewness (S_ϕ), and kurtosis (K_ϕ) of particle size distribution. We removed particle size distribution parameters because they did not meet the assumptions of multiple regression. A second-order polynomial term for θ_v was also added because of a parabolic relationship between θ_v and V_n.

We used multiple regression with a backward elimination technique to obtain the following empirical relationship:

$$V_n = 0.812\theta_v^2 - 26.4\theta_v - 157\rho_b - 20.5v + 518$$

where V_n is measured in cm^2, θ_v and θ_v^2 are in percent, ρ_b is measured in g/cm^3, and v is measured in m/s. We calculated volumes of hypothetical sauropod tracks and solved our equation for θ_v to calculate ancient θ_v and saturation values from fossil sauropod tracks. Results fall mostly within the range of possible results and compare well to elephant track data collected from trials; this shows that our approach is promising for future vertebrate ichnological studies.

INTRODUCTION

The purpose of this study is to conduct neoichnological experiments with elephants to quantify the relationship between physical variables involved in megafaunal footprint formation and morphology. The ultimate goal of this research is to enable calculations of ancient sediment and soil properties for fossil-footprint-bearing siliciclastic sedimentary rocks.

The impetus for this study was a body of research on deep sauropod dinosaur tracks and interpretations of the conditions responsible for their preservation (e.g., Hasiotis, 2002, 2004; Jennings et al., 2006; Platt and Hasiotis, 2006). There are many examples of relatively large, deep footprints that have been attributed to dinosaurs (e.g., Englemann and Hasiotis, 1999; Gatesy et al., 1999; Nadon, 2001; Gatesy, 2003; Jones and Gustason, 2006; Eberth et al., 2010) and mammals (e.g., Laporte and Behrensmeyer, 1980; Loope, 1986; Allen, 1997; Ashley and Liutkus, 2002), including proboscideans (Scrivner and Bottjer, 1986; Roberts et al., 2008).

Lockley (1986) outlined specific uses of fossil dinosaur tracks for interpreting paleoenvironments and original media (= substrate) conditions, but an empirical neoichnological study of megafaunal track formation has, to our knowledge, never before been attempted.

Approaches that interpret physicochemical controls on track formation include field-based observations of modern tracks in natural sediments (Laporte and Behrensmeyer, 1980; Cohen et al., 1991; Genise et al., 2009; Marty et al., 2009; Scott et al., 2010), experiments with controlled media and live trackmakers (Brand, 1996; Gatesy et al., 1999; Milàn, 2006; Milàn and Bromley, 2006), laboratory experiments with controlled sediments and artificial indenters (Allen, 1989, 1997; Gingras and Pemberton, 2000; Schaub et al., 2000; Manning, 2004; Jackson et al., 2009; Falkingham et al., 2010; Scott et al., 2010), cross-sectional and structural interpretations of fossil footprints (Loope, 1986; Milàn et al., 2004; Loope, 2006; Platt and Hasiotis, 2006; Graversen et al., 2007), and finite-element analysis (Margetts et al., 2006; Falkingham et al., 2009, 2010, 2011a, 2011b).

Footprint formation can be viewed in terms of sediment or soil compaction (e.g., Manning, 2004; Falkingham et al., 2010), which has received considerable attention in the engineering and agricultural literature because of construction specifications (Lambe and Whitman, 1969; Hillel, 1980; Lee and Salgado, 2005) and soil issues arising from livestock trampling and heavy machinery operation on arable land (Knoll and Hopkins, 1959; Hillel, 1980; Warren et al., 1986; Russell et al., 2001; Pietola et al., 2005). Experimental determinations of soil compaction in engineering and agriculture focus on applied pressure and do not discuss the dimensions of traces left behind by the indenter; Walker et al. (2005) is a notable exception.

The relatively simple, circular, and elliptical shapes of the soles of elephant feet (Weissengruber et al., 2006) are ideal for an empirical trackmaking study because the effects of

complex edge shapes on media penetration (e.g., Falkingham et al., 2010) are minimized. Elephant trackmaking behavior is also a good analog for that of extinct proboscideans, other large mammals (e.g., rhinoceroses, hippopotami, titanotheres), and sauropod dinosaurs because of anatomical similarities related to graviportal locomotion—movement enabled by physical adaptations for transporting a large body mass over terrestrial settings (e.g., Sikes, 1971; Coombs, 1975; Gallup, 1989; Bonnan, 2003; Carrano, 2005; Miller et al., 2008). We take advantage of this literature by applying our results to published data from fossil sauropod tracks.

METHODS AND MATERIALS

Tracemakers and Facilities

Trackmaking trials were conducted at the Topeka Zoological Park, Topeka, Kansas, USA, with one female African elephant (*Loxodonta africana*) named Tembo, and one female Asian elephant (*Elephas maximus*) named Sunda. Tembo was wild caught in Kenya in 1973, has been at the Topeka Zoo since 1976, has an estimated birth year of 1971 (Olson, 2011), and has a mass of ~4,200 kg. Sunda was wild caught in an unspecified region of Asia in about 1962, has been at the Topeka Zoo since 1966, has an estimated birth year of 1962 (Keele et al., 2010), and a mass of ~3,800 kg. Both elephants have been housed together at the Topeka Zoo since 1976 (D. Olson, personal communication, 2008).

The elephant enclosure at the Topeka Zoo (Fig. 1) consists of two indoor housing facilities connected to an outdoor, fenced yard. One of the housing facilities contains a large built-in weighing scale at floor level (Fig. 1). The outdoor portion of the exhibit consists of a large sand-filled yard. The layer of sand is ~22 cm thick and is underlain by a layer of dense organic-rich clay.

Design and Variables

Experimental Design.—Trackmaking trials were designed to incorporate variables identified in the literature as playing a significant role in track formation. Variables were selected based on trackmaker and sedimentary properties that are most easily measured or estimated from ancient track-bearing sediments, or that would provide the most informative results when solving for an unknown variable. We selected footprint volume (V), rather than depth (D), as our dependent variable because V incorporates track surface area (SA), which affects penetration of a foot into a medium (Falkingham et al., 2010). For purposes of scaling our results to different sized trackmakers, we normalized V by track length (L) because of the link between L and body size; that is, hind L correlates to limb length (Alexander, 1976; Thulborn, 1990; Henderson, 2003) and limb dimensions correlate to body mass (Roth, 1990; Thulburn, 1990). Independent variables included sediment particle-size distribution (PSD), sediment dry bulk density (ρ_b), sediment moisture content (θ_v), sediment aging (A), standing foot pressure applied to the ground (P), and locomotion velocity (v). Note that PSD is described by multiple parameters.

Sediment Provenance and Composition.—The sediment we used in trackmaking trials was derived from the Kansas River and purchased from sand and gravel companies in Topeka, Kansas, USA (Victory Sand Mining & Dredging, L.L.C.; Kansas Sand and Concrete, Inc.). The mineralogy of the Kansas River sands and silts is predominantly quartz with only a minor contribution from feldspars (Brady et al., 1998). The quartz and feldspars are derived largely from the Ogallala Formation and glacial sediments, which originated from granitic rocks in the Rocky Mountains and the Canadian Shield, respectively (Brady et al., 1998). Fine silts and clays

in Kansas River alluvium are derived mostly from glacial sediments and local siliciclastic rocks that outcrop in the drainage basin (Brady et al., 1998). Mixed-layer clays are the dominant clay minerals in Kansas River sediments, but kaolinite, montmorillonite, illite, and amorphous clays are also present (Kennedy, 1963). Logistical challenges with transporting the required large volumes of sediment limited experiments to two main sediment types: unprocessed river sediment and masonry sand, which has a maximum particle size of 0.75 mm (American Society for Testing and Materials Standard C144, 2004).

Normalized Footprint Volume.—We measured *L*, width (*W*), and *D* of each footprint (Fig. 2) and calculated *V* geometrically using the formula for volume of an elliptical cylinder:

$$V = \pi\ 0.5\ L\ 0.5\ W\ D \tag{1}$$

We measured *L* and *W* on the bottom surface of each track to obtain true dimensions (sensu Lockley et al., 2002). Length was measured parallel to the direction of locomotion and *W* was measured perpendicular to *L*. All measurements of *D* were taken between the base of the deepest part of the track and the original ground surface, i.e., excluding expulsion rims. Geometric calculation of volume was necessary because time constraints did not allow us to take plaster casts or laser scans of every track for direct measurement of volume. Normalized track volume (V_n) was calculated as:

$$V_n = V/L \tag{2}$$

Note that V_n is calculable from width and depth of fossil footprints in the field.

Particle-Size Distribution.—Particle-size distribution of experimental sediments was measured by laser defractometry (Mastersizer 2000, Malvern Instruments, Worcestershire, UK) at the University of Kansas in the Soils and Geomorphology Laboratory. Mean (M_ϕ), standard deviation (σ_ϕ), skewness (S_ϕ), and kurtosis (K_ϕ) of particle sizes in Φ-units were calculated using the method of moments described by Krumbein and Pettijohn (1938). Most PSD data were limited, however, to representative samples collected from initial installations of experimental sediments because we did not expect substantial variation once sediment was in place.

Sediment Dry Bulk Density.—Dry bulk density was measured two different ways depending on availability of instrumentation. Most data were collected with a surface nuclear gauge (SNG), either the Troxler 3411-B, 3430, or 3440, in the direct transmission mode of operation. Direct transmission involves lowering a Cs-137 source into the sediment and measuring the intensity of returning gamma radiation with detectors on the gauge; this is related to wet bulk density of the material, which can be converted to ρ_b using a simultaneous measure of moisture content (Randrup and Lichter, 2001; Troxler Electronic Laboratories, Inc., 2009). Surface nuclear gauge data were collected from undisturbed sediment before trampling because we are interested in how original ρ_b affects track volume.

When a SNG was not available, bulk density was determined with a Soil Moisture Model 0200 Soil Core Sampler from the mass of a known volume of oven-dry sediment. Soil core samples were taken from undisturbed sediment adjacent to tracks immediately after a trial. Even though two different methods were used, they produce results that are the same statistically (Timm et al., 2005).

Sediment Water Content.—Similarly to ρ_b, θ_v of the sediment was measured in two ways depending on availability of instrumentation. Most θ_v data were collected with a Troxler

3411-B, 3430, or 3440 operating in direct transmission mode. The direct transmission method for moisture determination uses a neutron source lowered into the sediment and a detector on the gauge to measure neutron thermalization resulting from collisions with hydrogen nuclei within water molecules (Gardner, 1986; Randrup and Lichter, 2001; Troxler Electronic Laboratories, 2009). Data collection with a SNG was performed prior to trampling to assess the θ_v of undisturbed sediment.

When a SNG was not available, sediment water content was determined by gravimetry (Gardner, 1986) and converted to θ_v. Sediment samples for gravimetry were collected from undisturbed sediment adjacent to footprints immediately after a trial. Even though this method differs from SNG data collection, replicate samples evaluated by both methods are consistently highly correlated ($0.8 \leq R^2 \leq 0.9$) (Veenstra et al., 2005).

Sediment Aging.—Experimental sediments were reused multiple times because of the logistical challenges with managing large volumes of sediments in a public park. Sediments were exposed to the elements between trackmaking trials and were regularly accessible to the elephants. The possibility exists, therefore, that repeated wetting and drying, trampling, erosion from adjacent sediments, and additions of organic matter affected sediment properties between trials. Because of the difficulty associated with monitoring each of these factors, we aggregated them into a sediment aging variable, A, which we quantified as the number of days that passed between installation of fresh sediment—representing deposition—and the trackmaking trial from which data were collected. We expected that a correlation between A and V_n would indicate that sedimentary properties were impacted significantly by factors that we did not measure directly.

Foot Pressure.—We use P instead of weight as a variable because weight is not distributed evenly between all limbs of an elephant (Henderson, 2006). Foot pressure also takes

into account the area of the foot in contact with the sediment, which will help scale the relationship to different sized animals. We used standing foot pressure rather than maximum foot pressure during locomotion because standing foot pressure is relatively simple to estimate for extinct trackmakers from footprint areas and reconstructed masses (e.g., Alexander, 1985, 1989). The maximum load borne by an individual foot is determined by the number of feet in contact with the ground and the distribution of weight between those feet (Henderson, 2006). Maximum ground pressure from an individual foot is approximately double the standing foot pressure (Jayes and Alexander, 1978; Alexander, 1985). Standing foot pressure is, therefore, appropriate for our purposes because it is directly proportional to maximum pressure during locomotion. We used the following equation to calculate P:

$$P = m_f g/SA \tag{3}$$

where m_f = body mass supported by the foot responsible for making the track, g = acceleration due to gravity, and SA = surface area of the track as a proxy for the surface area of the foot. We also measured length and width of each foot of the elephant for comparison; these measurements were taken once by holding a tape measure directly up against the sole of each foot.

We measured the mass supported by the anterior limbs (m_a) of each elephant by having them stand with both front feet on the zoo's weighing scale and both hind legs on the ground. We measured the mass supported by the posterior limbs (m_p) by having each elephant stand with both hind feet on the scale and both front feet on the ground. Mass supported by each front limb was calculated as $m_{f(anterior)} = 0.5m_a$ and mass supported by each hind limb was calculated as $m_{f(posterior)} = 0.5m_p$. Total weights of each elephant were recorded for most experiments by

having each elephant stand entirely on the scale. When the scale was unavailable or inoperational, the most recent recorded weights of the elephants were used. Weight distributions were not re-measured for each experiment; instead, total weight was measured and multiplied by the percentage of weight supported by the front and hind limbs.

Locomotion Velocity.—Locomotion velocity was measured from video recorded during the experiments. We recorded the time required for a reference landmark on the elephant (the eye) to travel between stationary reference points (fence posts). We measured the distances between fence posts and calculated a speed for each interval between fence posts. That speed was assigned to all tracks within each interval. Since locomotion was initiated by leading elephants with audible commands and food items, speed could not be manipulated directly.

Trials

We used a standard procedure for each trackmaking trial (Fig. 3). Experimental sediments were placed in a series of pits excavated within the elephant yard. Pits were ~2 m wide, 0.3 m deep, and varied between 2 and 18 m long. Pits were filled with the sediments described previously up to the surface of the existing sediment in the yard. Prior to each experiment, a hose was used to add water to the sediment, a manual tamper was used to alter density, and the sediment surface was raked level. We varied the amount of water added and tamping to obtain tracks in sediments with a range of θ_v and ρ_b. Since it was impossible to know exactly where the elephants would step when they were allowed to walk through the sediment, we superimposed a 1 m by 1 m square grid on the sediment surface and measured θ_v and ρ_b every 1 m^2 with a SNG. Sections of the pit were covered with tarps immediately after measurements were taken to prevent moisture loss by evaporation. Tarps were removed immediately prior to

each trial. When a SNG was not available, a soil core sampler was used to collect sediment samples adjacent to tracks after each trial for θ_v and ρ_b determination.

During each trial, one elephant was encouraged to walk at a steady speed through the experimental sediment. When possible, the weight of each elephant was measured prior to or after each experiment. Video was recorded of the elephants walking by an observer holding a camcorder perpendicular to the anteroposterior axis of the elephant, matching walking speed with that of the elephant.

Following each experiment, trackways were sketched and tracks were described, photographed, and measured. We used the terminology of Allen (1997) for track description (Fig. 2). Any sediment sampling necessary was conducted and plaster casts were taken of select tracks if time permitted. After completion of a field trial, necessary sediment analyses were conducted and recorded video was viewed to determine walking speeds.

Data Analyses

We applied multiple regression techniques to our data because we investigated the relationships between a dependent variable and multiple independent variables (Sokal and Rohlf, 1995). All data analyses were performed in R (R Development Core Team, 2008). Assumptions underlying the multiple regressions (i.e., normality, homogeneity of variance, and linearity) were visually inspected from scatterplot matrices. We examined the data for multicollinearity using a correlation matrix and by calculating variation inflation factors for all independent variables.

Initial inspection of scatterplots revealed a nonlinear relationship between V_n and θ_v (Fig. 4), which we accommodated by including the second-order polynomial term, θ_v^2, in addition to

the other independent variables in the regression. Adding this term to perform a curvilinear regression should provide a better fit to the parabolic-shaped θ_v data (Sokal and Rohlf, 1995).

After inspecting the data for the remaining assumptions and transforming where necessary, we performed a stepwise regression using backward elimination on the appropriate independent variables and V_n as the dependent variable. Following model selection, we performed z-score transformations and determined β weights for the multiple regression to evaluate relative influence of independent variables on V_n (Kachigan, 1982).

RESULTS

Weight and Weight Distribution

We obtained two weights for Tembo (average = 4627 kg; standard deviation = 492 kg) and five weights for Sunda (average = 3757 kg; standard deviation = 321 kg) during our trials. Weight distribution data were collected once and show that 60.4% of Tembo's weight was supported by her front limbs and 39.6% was supported by her hind limbs (Table 1). We found that 59.9% of Sunda's weight was supported by her front limbs and 40.1% was supported by her hind limbs (Table 1). This agrees with results found for other elephants by Henderson (2006) and Alexander (1989). Our results were used to calculate P for each trial.

Observations of Trackmakers and Tracks

Foot Morphology.—The soles of the front feet of both elephants are circular in shape and the soles of the hind feet are elliptical with the long axes oriented anteroposteriorly (Fig. 5A–D). The soles of Sunda's feet are more textured than Tembo's and there is greater expression of the digits and nails. Measurements of feet are given in Table 2.

Locomotion Behavior.—When walking, both elephants step down with their heels and step off of their toes (Fig. 5E–J). During the maximum weight-bearing phase of each step cycle, the foot expands abaxially, this is especially prevalent in the front feet (Fig. 5F, I). As the animal moves forward and the weight is shifted off of the foot, the foot contracts adaxially. Both elephants commonly overstep their own tracks.

Track Morphology.—Consistent with foot morphology, manus prints were circular and pes prints were elliptical in general shape (Fig. 6A–E). Average track dimensions are given in Table 3. Overlapped manus and pes prints were common (Fig. 6F). The anterior and posterior regions of tracks were often impressed more deeply and inclined toward the shaft wall because of the trackmakers' locomotion behavior. Digit and nail impressions were more prominent in Sunda's tracks compared to Tembo's tracks. Some tracks preserved palmar (i.e., front sole) and plantar (i.e., rear sole) textures; grooves and fissures at the perimeters of the soles were most often preserved. Some well-preserved tracks contained detailed impressions of the nails on the shaft walls (Fig. 6F). Expulsion rims with concentric and radial fractures were common around tracks (Fig. 6D, F). Drag marks with associated ejecta were also common in front of the toe impressions of many tracks (Fig. 6F).

Data.—Particle-size parameters for experimental sediments are given in Table 4; these sediments were moderately to very poorly sorted based on σ_ϕ values (Folk and Ward,1957). Because PSD data are limited, descriptive statistics for all other variables (Table 5) are given relative to one of the two sediment types that were used: mason sand and unsieved Kansas River sediment. Track volumes were highly variable, but the majority of tracks had low volumes—i.e., were relatively shallow. Locomotion speeds ranged from 0 m/s—standing still—to 1 m/s. We did not calculate Froude numbers for locomotion because we were unable to obtain hip height

measurements. Dry bulk density varied between 1.4 g/cm^3 and 1.7 g/cm^3. Water content values ranged from 3.8 to 24.2%. The tracks with the largest volumes correspond to sediments with low original θ_v and ρ_b values (Fig. 7).

Multiple Regression Analysis

Assumptions.—Most variables met the assumptions of multiple regression. The PSD parameters (M_ϕ, σ_ϕ, S_ϕ, and K_ϕ), however, did not appear to be normally distributed (even as Φ-values) and failed the assumption of homogeneous variance. The correlation matrix showed that all four PSD parameters are correlated with each other and with A. No other significant correlations exist between independent variables. In addition, variation inflation factor values (which test for multicollinearity) for all four PSD parameters were beyond levels normally considered acceptable. All other independent variables passed these tests.

Accomodations.—Because of problems associated with multicollinearity, we exclude PSD parameters from our analysis; this also eliminates the problem of correlations between PSD parameters and A. Data from overstepped tracks were also omitted because such tracks were assumed to have been subjected to the combined pressure of the manus and pes; these high pressures appeared as outliers in scatterplots.

Analyses.—Data were recorded for 118 tracks; 53 from Sunda and 65 from Tembo, but after omissions and exclusions of partial data, the final sample size was 87. Backward elimination kept the variables that best explain the maximum amount of variation in V_n, while simultaneously maximizing parsimony—v, ρ_b, θ_v, and θ_v^2. Results of the regression with these variables are given in Table 6 and yield an adjusted R^2 value of 0.438. The final regression equation is:

$$V_n = 0.812\theta_v^2 - 26.4\theta_v - 157\rho_b - 20.5v + 518 \quad (4)$$

Locomotion velocity has a P-value of 0.07 and all other independent variables are significant at $P < 0.001$ (Table 6).

Beta weights are also provided in Table 6. Beta weights are the coefficients of z-score-transformed variables and show the relative importance of each independent variable in predicting the dependent variable (Kachigan, 1982). The β weight of speed is low relative to the β weights of the other variables. The θ_v^2 term has the largest β weight relative to the other variables.

DISCUSSION

Relationship Between Water Content and Track Volume

A curvilinear relationship between θ_v and *Vn* (Fig. 4) is not unexpected because all sediments and soils have a maximum compactibility that is reached at an ideal θ_v (Lambe and Whitman, 1969). The concave upward shape of the data in Figure 4, however, is opposite the pattern displayed by typical sediments and soils in compaction tests. We interpret the inflection point on Figure 4 as representing the transition from noncohesive behavior to cohesive behavior in our experimental sediments. Relating the curvilinear relationship between θ_v and V_n to cohesion explains why the deepest tracks were created in sediments with extreme θ_v values (Falkingham et al., 2010). Our interpretation implies that maximum compaction of our sediments did not occur. If the θ_v value required for maximum compaction had been reached, we would expect our curve to include a concave downward portion at high θ_v values. A third-order

polynomial, therefore, may prove to be a better model if a wider range of data is available in the future.

Excluded and Nonsignificant Variables

Particle-Size Distribution.—Elimination of PSD parameters is not problematic because all track data used in our regression analysis were from similar sediment types, i.e., sand. Although our treatment of these data limits the potential applicability of results to tracks preserved in sandy sediments, we view this as a first step towards a comprehensive, empirically derived understanding of the physical factors that affect megafaunal track formation. Future studies should focus on expanding the range of particle sizes used in experiments.

Sediment Aging.—The removal of A through the backward elimination process indicates that there was no significant alteration of experimental sediments related to wetting and drying, erosion from the edges of the trench, and additions of organic matter. We noted, however, an apparent time-related change in sediment response to trampling: tracks created shortly after sediment was emplaced were deeper than tracks created in later trials. The apparent time-related change occurred relatively quickly and was likely the result of low initial densities due to loose packing. In a matter of days after installation, sediment rapidly became more closely packed from settling and trampling until a maximum field density was reached.

Foot Pressure.—Removal of P from our regression is not particularly surprising because both elephants were so similar in mass that there was not a wide range in foot pressures. Without P, V_n is the only term that can be used to scale the model to different sized animals. From a practical perspective, V_n is much easier to arrive at for fossil tracks than P, which

requires estimates of trackmaker mass and mass distribution, which can vary considerably depending on the method used (Henderson, 1999).

Locomotion Velocity.—Walking velocity is included in the final regression model, but has a relatively high P-value. Even though v does not appear to explain as much of the variation in V_n as ρ_b, θ_v, and θ_v^2, it is still important to consider, especially because depths and volumes of individual tracks within fossil trackways have been attributed to changes in trackmaker speed (Mossman et al., 2003; Kim and Huh, 2010). We did not have a large degree of control over v in our experimental trials, so v did not vary greatly and gaits were confined to walking. Gait may be important to consider because elephants transition to a bouncing gait at ~2.2 m/s (Hutchinson et al., 2006; Ren and Hutchinson, 2008; Ren et al., 2008); we hypothesize that the resulting increase in foot pressure would cause an increase in V_n. We recommend that future investigations vary v, if possible, to cover a range of gaits.

Sources of Unexplained Variation

Track Volume.—Treatment of tracks as elliptical cylinders is, admittedly, an oversimplification of true track geometries. Such factors as uneven track floors, sloped shaft walls, and irregularities in track perimeter complicate calculation of V. We calculated V geometrically because time constraints did not allow us to take more detailed measurements in the field. Future studies may incorporate other measurement methods that will increase accuracy of V and improve on our regression model.

Particle-Size Distribution.—Because our data are limited to sandy sediment, PSD parameters are unlikely to not have contributed significantly to V_n. Future studies should include a wider range of particle sizes, if possible, because PSD parameters should, theoretically,

influence track dimensions. Mean particle size, for example, is a primary control on compaction in unconsolidated sands (Meade, 1966) so it should also be a factor in footprint formation. Standard deviation of PSD is a measure of sorting (Folk and Ward, 1957; Folk, 1966) so σ_ϕ may be a useful variable to consider in relation to sediments of different textural maturities. There was a notable difference in S_ϕ between our Kansas River sand and our mason sand, which was also sourced from the Kansas River, but had fines removed. Skewness, therefore, may exert a control over V_n in relation to natural controls on this property, i.e., distance from the channel or postdepositional winnowing of fines. Kurtosis of PSD compares the sorting within the central part of the distribution to the sorting of the extremes and is an indicator of peakedness (Folk and Ward, 1957). Kurtosis may be a significant variable in controlling volume of tracks created in sediments with multimodal particle size distributions.

Particle Morphology.—There are a number of variables that we did not measure in our trials that could have contributed to V_n. Particle shape, roundness, and sphericity play a role in the packing of grains (Fraser, 1935; Meade, 1966) and may, therefore, be important variables for understanding compaction of grains during formation of a track. We did not examine our experimental sands under magnification, but Kansas River sand grains are typically subrounded (Han et al., 2010).

Lithology and Mineralogy.—Lithology and clay mineralogy affect the formation and preservation of tracks (e.g., Scott et al., 2010), which is why we chose to use relatively inert siliciclastic sediments for trackmaking trials. The mineralogy of the minor clay fraction in the sediments we used, however, may have influenced track formation by affecting the cohesion, plasticity, and shear strength of the sediment (Loope, 1986; Scott et al., 2010).

Organic Matter.—Organic matter affects sediment cohesion (Scott et al., 2010) and is another unmeasured variable that may account for some of the unexplained variation in our regression. We did not consider organic matter in our trials because Kansas River sands are very clean (Brady et al., 1998) and substantial organic additions from elephants were not likely incorporated into experimental sediments because solid waste is removed daily from the elephant enclosure.

Relative Influence of Independent Variables on the Dependent Variable

Relative influence of independent variables on V_n is determined by comparing the absolute values of the corresponding variable β weights. Based on our results, v has relatively little influence on V_n, while ρ_b, θ_v, and θ_v^2 exert similar degrees of control on V_n. Results confirm previous suggestions that water content is an important control on track preservation (Laporte and Behrensmeyer, 1980; Platt and Hasiotis, 2006). Perhaps more significant is the high relative contribution of ρ_b, a sediment property that is typically overlooked in vertebrate ichnology literature.

Applications to Fossil Footprints

Sauropod Dinosaur Track Volume Estimation.—We explore how our regression equation would perform with larger trackmakers by calculating the volumes of hypothetical sauropod dinosaur tracks created in the same experimental sediments we used for our trials (Table 7). We used track and v data for a large and a small sauropod from Alexander (1989). We used the average ρ_b of our mason sand (1.7g/cm^3) and minimum and maximum θ_v values of 3.8% and 24.2%, respectively. After calculating V_n, we used L to compute V.

Results (Table 7) seem reasonable when compared to recorded elephant track volumes (Table 5); some elephant tracks were larger than the calculated hypothetical sauropod tracks, but those elephant tracks were created in the lower density sediments. As expected, hypothetical tracks from the small sauropod are lower in volume than tracks from the large sauropod. Hypothetical tracks in sediment with low θ_v, however, are larger than tracks in sediment with high θ_v. The apparent inverse relationship between θ_v and V is the result of the polynomial relationship built into the model, which represents the transition from cohesionless to cohesive sand.

Solving for an Unknown Variable.—The most straightforward application of the regression equation to interpretations of fossil footprints is to solve the equation for one unknown variable using measurements or estimates of the remaining variables. Normalized track volume is easy to calculate using L and V acquired through geometric estimates or the methods of Mossman et al. (2003) or Platt et al. (2010). Bulk density can be estimated from sediment texture (e.g., USDA-NRCS, 2011) or calculated from rock samples and porosity data (Athy, 1930) with corrections made for diagenetic alteration (Houseknecht, 1987). Sediment water content is, perhaps, the most difficult parameter to estimate for ancient sediments, but sediment water content, particularly soil water content, can be extremely informative for paleoclimatic interpretations (Seneviratne et al., 2010). Solving for θ_v can be accomplished by setting the regression equation equal to zero and using the quadratic formula, which yields:

$$\theta_v = (26.4 \pm \sqrt{508\rho_b + 66.7v + 3.25V_n - 987}\,)/1.62 \quad (5)$$

We apply Eq. 5 to unpublished data from large sauropod tracks in the Upper Jurassic Morrison Formation (Platt and Hasiotis, 2006). All tracks are preserved in convex hyporelief on the bases of sheet sandstones. Most tracks were originally created in silt, but one was created in sand. We use ρ_b values based on sediment texture (USDA-NRCS, 2011) and assume a walking gait with a v of 1.0 m/s.

Resulting θ_v values (Table 8) are high relative to θ_v values achieved in our experimental sediments. The values are not unrealistic, however, because θ_v is constrained by the porosity (ϕ) of the sediment and our θ_v estimates fall within the ranges of possible ϕ values for sand and silt (Fetter, 1994). Results can also be converted to degree of saturation (S_w) measures by comparison of θ_v and ϕ according to the following relationships:

$$\phi = 1 - \rho_b/\rho_p \tag{6}$$

$$S_w = \theta_v/\phi \tag{7}$$

where ρ_p = particle density. Substituting equations 5 and 6 into equation 7 yields:

$$S_w = \rho_b(26.4 \pm \sqrt{508\rho_b + 66.7v + 3.25V_n - 987}\,)/1.62(\rho_p - \rho_b) \tag{8}$$

We calculated S_w values based on our θ_v results and a ρ_b of 2.65 g/cm^3 (Table 8). Results mostly fall within the acceptable range of possibilities from 0 to 100%. Two results surpass the upper limit of S_w, but only by a small amount. Overall, these numbers are realistic estimates, especially given the large sizes of the sauropod tracks (Platt and Hasiotis, 2006). We are also encouraged

by the fact that our model produced realistic results for tracks created in silt. Our θ_v results should, however, be viewed as preliminary and further refinement should be pursued through additional empirical data collection and analyses.

Note that reconstructed S_w values from individual fossil footprints provide extremely localized information and represent media conditions at virtually an instant in time. Care should be exercised when making interpretations based on reconstructed S_w and results should be considered within the context of associated sedimentary structures and trace fossils (e.g., Hasiotis, 2004).

Broader Applications

Our observations and regression model, although based on specific conditions, are also informative for predicting track properties from a range of media, environments, and trackmakers. Experimental trials most closely reproduced conditions found in recently deposited, subaerially exposed fluvial sediments in river margin, channel barform, and crevasse-splay environments, but may also be useful analogs for coastal plain, delta plain, tidal flat, and eolian environments. As sediments age, compaction from gravity, trampling, and dewatering should result in shallower tracks through time. Environments with low deposition rates, e.g., distal overbank settings, are likely to contain older sediments that are more compact and even undergoing pedogenesis; such environments are less likely to contain well-formed tracks. For example, tracks and trackways made in recently water-deposited sand bodies with high moisture contents will likely be relatively deep. As deposits become better drained with lower moisture contents, any new tracks produced will likely be shallower. Trampling, surface runoff, and infiltration of water will increase sand-body density, which will record shallower tracks and

trackways through time. Such surfaces will likely continue to resist foot penetration even if increased moisture and surface water is delivered because of increased density of the aging sand body. We hypothesize that if initially cohesive sediments desiccate or experience winnowing of fines to the point of exhibiting cohesionless behavior, deep tracks will result only if high densities have not already been reached.

Although we did not produce completely saturated sediment in field trials, we can predict that increased θ_v would result in deeper penetration of feet into the sediment during locomotion. We also hypothesize that morphologies of tracks created by locomotion through saturated sediment will differ depending on whether sediment was subaerially exposed or completely submerged. We expect both subaerial and submerged saturated sediment to potentially collapse back into a track after the foot is removed, but submerged sediment can become suspended, transported, and redeposited, covering tracks and obscuring detail (e.g., Fairchild and Hasiotis, 2011). Saturated and submerged sediments are also susceptible to meter-scale penetration by trackmakers, resulting in deep bioturbation, especially in finer grained sediment (e.g., Ashley and Liutkus, 2002; Deocampo, 2002). Future studies designed to distinguish between subaerial and subaqueous saturated conditions will be useful for detailed paleoenvironmental and paleohydrological interpretations.

The regression model derived from empirical elephant-track data is well suited for interpreting tracks of large animals with similarly shaped feet, including extant and extinct proboscideans and sauropod dinosaurs. Future expansion of the relationship to include other large, graviportal animals is reasonable because of similarities in foot anatomy and dimensions of appendicular skeletal and muscular systems (e.g., Carrano, 1999). We hypothesize that tracks and trackways produced by such graviportal organisms as large terrestrial ungulates and many

quadrupedal ornithischian dinosaurs should record similar track penetration depths and ranges of morphologies, if all independent variables are equal.

A notable concern about applying our results to a variety of taxa, however, relates to differences in foot shape. Falkingham (2010) found that as edge length of an indenter increases, its penetration into a noncohesive medium increases, while its penetration into a cohesive medium decreases. This information can be used to extrapolate whether our regression model will over- or underestimate a variable if applied to animals with more complex foot shapes. Future empirical investigations may need to include measures of both track volume and foot shape complexity to increase the range of applications to fossil tracks. Cohesive and noncohesive behavior, additionally, are affected by sediment texture (e.g., Loope, 1986) so future investigations should consider different textures of sediment as well.

CONCLUSIONS

This study represents a first attempt to empirically quantify the relationship between the physical variables involved in controlling megafaunal footprint formation. Our goal was to define a relationship between track-forming variables that could be applied relatively easily to fossil tracks and trackways to interpret information about ancient trackmakers or paleoenvironments. We designed a series of footprint-making trials with live elephants and controlled sediments where we measured or calculated V, v, P, A, ρ_b, θ_v, M_*, σ_*, S_*, and K_*. We normalized V by track length to improve scalability to different sized trackmakers. Multiple regression with backward elimination resulted in the following equation (adjusted R^2-value of 0.44):

$$V_n = 0.812\theta_v^2 - 26.4\theta_v - 157\rho_b - 20.5v + 518$$

where V_n is measured in cm^2, θ_v is in percent, ρ_b is measured in g/cm^3, and v is measured in m/s. Beta weights show that velocity exerts relatively little influence over V_n based on our empirical data. All other independent variables in the final regression equation influence V_n to a similar degree. This is particularly important in the case of sediment bulk density because that variable is typically overlooked in vertebrate ichnology studies.

The regression equation can be solved for any one variable and applied to fossil tracks where other variables are measured or estimated. We used data from the literature to calculate the volumes of hypothetical sauropod tracks created in sediments similar to those we used in our trials. We also used the quadratic equation to solve the equation for θ_v and estimate original sediment moisture and saturation from fossil sauropod tracks. Results were very reasonable and show promise for future application of empirically derived relationships in megafaunal vertebrate ichnology.

ACKNOWLEDGMENTS

We thank the Topeka Zoo for their hospitality and support, especially Dawn Olson, Mike Coker, Fawn Moser, Daniel Shute, and Mindy Shute. NRC-licensed operators collected all surface nuclear gauge data. We are grateful to the City of Topeka's Engineering Division for providing their services, especially Shawn Bruns, James Lopez, and Mike Briggs. We thank Sara Platt, Julie Retrum, Celina Suarez, Marina Suarez, and Emily Tremain for their help with fieldwork. We also thank Bill Johnson, Terri Woodburn, Mark Bowen, and John Kelly for additional assistance. This project was completed in partial fulfillment of the requirements for a

PhD by BFP at the University of Kansas (KU). Support for this research was provided to BFP by the Department of Geology at KU, a student grant from the Geological Society of America, a Madison and Lila Self Graduate Fellowship at KU, a Paleontological Society Stephen J. Gould Grant, and a Panorama Small Grant from the KU Biodiversity Research Center. We also extend our thanks to Sunda and Tembo, the two elephants who made this all possible.

REFERENCES

ALEXANDER, R.MCN., 1976, Estimates of speeds of dinosaurs: Nature, v. 261, p. 129–130.

ALEXANDER, R.MCN., 1985, Mechanics of posture and gait of some large dinosaurs: Zoological Journal of the Linnean Society, v. 83, p. 1–25.

ALEXANDER, R.MCN., 1989, Dynamics of Dinosaurs and Other Extinct Giants: New York, Columbia University Press, 167 p.

ALLEN, J.R.L., 1989, Short paper: fossil vertebrate tracks and indenter mechanics: Journal of the Geological Society, London, v. 146, p. 600–602.

ALLEN, J. R. L., 1997, Subfossil mammalian tracks (Flandrian) in the Severn Estuary, S. W. Britain: mechanics of formation, preservation and distribution: Philosophical Transactions of the Royal Society of London B, v. 352, p. 481–518.

AMERICAN SOCIETY FOR TESTING AND MATERIALS STANDARD C144, 2004, Standard specification for aggregate for masonry mortar: American Society for Testing and Materials International, West Conshohocken, PA.

ASHLEY, G.M., and LIUTKUS, C.M., 2002, Tracks, trails and trampling by large vertebrates in a rift valley paleo-wetland, lowermost bed II, Olduvai Gorge, Tanzania: Ichnos, v. 9, p. 23–32.

ATHY, L.F., 1930, Density, porosity, and compaction of sedimentary rocks: American Association of Petroleum Geologists Bulletin, v. 14, p. 1–24.

BONNAN, M.F., 2003, The evolution of manus shape in sauropod dinosaurs: functional morphology, forelimb orientation, and phylogeny: Journal of Vertebrate Paleontology, v. 23, p. 595–613.

BRADY, L.L., GRISAFE, D.A., MCCOULEY, J.R., OHLMACHER, G.C., QUINODOZ, H.A.M., and NELSON, K.A., 1998, The Kansas River corridor—its geologic setting, land use, economic

geology, and hydrology: Kansas Geological Survey Open-file Report 98-2, http://www.kgs.ku.edu/Publications/KR/index.html, checked March 9, 2011.

BRAND, L.R., 1996, Variations in salamander trackways resulting from substrate differences: Journal of Paleontology, v. 70, no. 6, p. 1004–1010.

CARRANO, M. T., 2005, The evolution of sauropod locomotion: morphological diversity of a secondarily quadrupedal radiation, *in* Curry Rogers, K.A., and Wilson, J. A., eds., The Sauropods: Evolution and Paleobiology: University of California Press, Berkeley, p. 229–251.

CARRANO, M.T., 1999, What, if anything is a cursor? Categories versus continua for determining locomotor habit in mammals and dinosaurs: Journal of Zoology, London, v. 247, p. 29–42.

COHEN, A., LOCKLEY, M., HALFPENNY, J., and MICHEL, A. E., 1991, Modern vertebrate track taphonomy at Lake Manyara, Tanzania: PALAIOS, v. 6, p. 371–389.

COOMBS, W.P., Jr., 1975, Sauropod habits and habitats: Palaeogeography, Palaeoclimatology, Palaeoecology, v. 17, p. 1–33.

DEOCAMPO, D.M., 2002, Sedimentary structures generated by *Hippopotamus amphibius* in a lake-margin wetland, Ngorongoro Crater, Tanzania: PALAIOS, v. 17, p. 212–217.

EBERTH, D.A., XING, X., and CLARK, J.M., 2010, Dinosaur death pits from the Jurassic of China: PALAIOS, v. 25, p. 112–125.

ENGELMANN, G., and HASIOTIS, S.T., 1999, Deep dinosaur tracks in the Morrison Formation: sole marks that are really sole marks, *in* Gillette, D.D., ed., Vertebrate Paleontology in Utah: Utah Geological Survey Miscellaneous Publication 99-1, Salt Lake City, p. 179–184.

FAIRCHILD, J.M., and HASIOTIS, S.T., 2011, Terrestrial and aquatic neoichnological laboratory experiments with the freshwater crayfish *Orconectes*: trackways on media of varying grain size, moisture, and inclination: PALAIOS, v. 26, p. 790–804.

FALKINGHAM, P.L., MARGETTS, L., SMITH, I.M., and MANNING, P.L., 2009, Reinterpretation of palmate and semi-palmate (webbed) fossil tracks; insights from finite element modeling: Palaeogeography, Palaeoclimatology, Palaeoecology, v. 271, p. 69–76.

FALKINGHAM, P.L., MARGETTS, L., and MANNING, P.L., 2010, Fossil vertebrate tracks as paleopenetrometers: confounding effects of foot morphology: PALAIOS, v. 25, p. 356–360.

FALKINGHAM, P.L., BATES, K.T., MARGETTS, L., and MANNING, P.L., 2011a, The 'Goldilocks' effect: preservation bias in vertebrate track assemblages: Journal of the Royal Society Interface, v. 8, p. 1142–1154.

FALKINGHAM, P.L., BATES, K.T., MARGETTS, L., and MANNING, P.L., 2011b, Simulating sauropod manus-only trackway formation using finite-element analysis: Biology Letters, v. 7, p. 142–145.

FETTER, C.W., 1994, Applied Hydrogeology, 3rd ed.: Prentice-Hall, Upper Saddle River, New Jersey, 691 p.

FOLK, R.L., 1966, A review of grain-size parameters: Sedimentology, v. 6, p. 73–93.

FOLK, R.L., and WARD, W.C., 1957, Brazos River bar: a study in the significance of grain size parameters: Journal of Sedimentary Petrology, v. 27, p. 3–26.

FRASER, H.J., 1935, Experimental study of the porosity and permeability of clastic sediments: The Journal of Geology, v. 43, p. 910–1010.

GALLUP, M.R., 1989, Functional morphology of the hindfoot of the Texas sauropod *Pleurocoelus* sp. indet., *in* Farlow, J.O., ed., Paleobiology of the Dinosaurs: Geological Society of America Special Paper 238, Boulder, Colorado, p. 71–74.

GARDNER, W.H., Water content, *in* Klute, A., ed., Methods of Soil Analysis, Part 1: Physical and Mineralogical Methods, 2nd ed.: American Society of Agronomy, Inc., Soil Science Society of America, Inc., Madison, Wisconsin, p. 493–544.

GATESY, S.M., 2003, Direct and indirect track features: what sediment did a dinosaur touch?: Ichnos, v. 10, p. 91–98.

GATESY, S.M., MIDDLETON, K.M., JENKINS, F.A., JR., and SHUBIN, N.H., 1999, Three-dimensional preservation of foot movements in Triassic theropod dinosaurs: Nature, v. 399, p. 141–144.

GENISE, J.F., MELCHOR, R.N., ARCHANGELSKY, M., BALA, L.O., STRANECK, R., and DE VALAIS, S., 2009, Application of neoichnological studies to behavioural and taphonomic interpretation of fossil bird-like tracks from lacustrine settings: the Late Triassic-Early Jurassic? Santo Domingo Formation, Argentina: Palaeogeography, Palaeoclimatology, Palaeoecology, v. 272, p. 143–161.

GINGRAS, M.K., and PEMBERTON, S.G., 2000, A field method for determining the firmness of colonized sediment substrates: Journal of Sedimentary Research, v. 70, p. 1341–1344.

GLPM ARCHITECTS, INC., 2005, Topeka Zoological Park Master Plan (map), 1:600: Lawrence, Kansas, USA.

GRAVERSON, O., MILÀN, J., and LOOPE, D.B., 2007, Dinosaur tectonics: a structural analysis of theropod undertracks with a reconstruction of theropod walking dynamics: The Journal of Geology: v, 115, p. 641–654.

HAN, J., POKHAREL, S.K., PARSONS, R.L., LESHCHINSKY, D., and HALAHMI, I., 2010, Effect of infill material on the performance of geocell-reinforced bases: Proceedings, 9th International Conference on Geosynthetics, Brazil, 2010, p. 1503–1506.

HASIOTIS, S.T., 2002, Continental Trace Fossils: SEPM Short Course Notes No. 51, 132 p.

HASIOTIS, S.T., 2004, Reconnaissance of Upper Jurassic Morrison Formation ichnofossils, Rocky Mountain Region, USA: paleoenvironmental, stratigraphic, and paleoclimatic significance of terrestrial and freshwater ichnocoenoses: Sedimentary Geology, v. 167, p. 177–268.

HENDERSON, D.M., 1999, Estimating the masses and centers of mass of extinct animals by 3-D mathematical slicing: Paleobiology, v. 25, p. 88–106.

HENDERSON, D.M., 2003, Footprints, trackways, and hip heights of bipedal dinosaurs - testing hip height predictions with computer models: Ichnos, v. 10, p. 99–114.

HENDERSON, D.M., 2006, Burly gaits: centers of mass, stability, and the trackways of sauropod dinosaurs: Journal of Vertebrate Paleontology, v. 26, no. 4, p. 907–921.

HILLEL, D., 1980, Fundamentals of Soil Physics: Academic Press, New York, 413 p.

HOUSEKNECHT, D.W., 1987, Assessing the relative importance of compaction processes and cementation to reduction of porosity in sandstones: The American Association of Petroleum Geologists Bulletin, v. 71, p. 633–642.

HUTCHINSON, J.R., SCHWERDA, D., FAMINI, D.J., DALE, R.H.I., FISCHER, M.S., and KRAM, R., 2006, The locomotor kinematics of Asian and African elephants: changes with speed and size: The Journal of Experimental Biology, v. 209, p. 3812–3827.

JACKSON, S.J., WHYTE, M.A., and ROMANO, M., 2009, Laboratory-controlled simulations of dinosaur footprints in sand: a key to understanding vertebrate track formation and preservation: PALAIOS, v. 24, p. 222–238.

JAYES, A.S., and ALEXANDER, R.MCN., 1978, Mechanics of locomotion of dogs (*Canis familiaris*) and sheep (*Ovis aries*): Journal of Zoology, London, v. 185, p. 289–308.

JENNINGS, D.S., PLATT, B.F., and HASIOTIS, S.T., 2006, Distribution of vertebrate trace fossils, Upper Jurassic Morrison Formation, Bighorn Basin, Wyoming, USA: implications for differentiating paleoecological and preservational bias: New Mexico Museum of Natural History and Science Bulletin, v. 36, p. 183–192.

JONES, L.S., and GUSTASON, E.R., 2006, Dinosaurs as possible avulsion enablers in the Upper Jurassic Morrison Formation, east-central Utah: Ichnos, v. 13, p. 31–41.

KACHIGAN, S.K., 1982, Multivariate Statistical Analysis: A Conceptual Introduction: Radius Press, New York, 297 p.

KEELE, M., LEWIS, K., and DEVER, K., 2010, Asian Elephant (*Elephas maximus*) North America Regional Studbook: Association of Zoos and Aquariums, 235 p.

KENNEDY, V.C., 1963, Base-exchange capacity and clay mineralogy of some modern stream sediments: International Association of Scientific Hydrology, Commission of Subterranean Waters Publication 64, p. 95–105.

KIM, B.S., and HUH, M., 2010, Analysis of the acceleration phase of a theropod dinosaur based on a Cretaceous trackway from Korea: Palaeogeography, Palaeoclimatology, Palaeoecology, v. 293, p. 1–8.

KNOLL, G., and HOPKINS, H. H., 1959, The effects of grazing and trampling upon certain soil properties: Transactions of the Kansas Academy of Science, v. 62, p. 221–231.

KRUMBEIN, W.C., and PETTIJOHN, F.J., 1938, Manual of Sedimentary Petrography: D. Appleton-Century Company, Inc., New York, 549 p.

LAMBE, T. W., and WHITMAN, R. V., 1969, Soil Mechanics: John Wiley & Sons, Inc., New York, 553 p.

LAPORTE, L.F., and BEHRENSMEYER, A.K., 1980, Tracks and substrate reworking by terrestrial vertebrates in Quaternary sediments of Kenya: Journal of Sedimentary Petrology, v. 50, p. 1337–1346.

LEE, J., and SALGADO, R., 2005, Estimation of bearing capacity of circular footings on sands based on cone penetration test: Journal of Geotechnical and Geoenvironmental Engineering, v. 131, p. 442–452.

LOCKLEY, M.G., 1986, The paleobiological and paleoenvironmental importance of dinosaur footprints: PALAIOS, v. 1, p. 37–47.

LOOPE, D.B., 1986, Recognizing and utilizing vertebrate tracks in cross section: Cenozoic hoofprints from Nebraska: PALAIOS, v. 1, p. 141–151.

LOOPE, D.B., 2006, Dry-season tracks in dinosaur-triggered grainflows: PALAIOS, v. 21, p. 132–142.

MANNING, P. L., 2004, A new approach to the analysis and interpretation of tracks: examples from the dinosaurian, *in* McIlroy, D., ed., The Application of Ichnology to Palaeoenvironmental and Stratigraphic Analysis: The Geological Society, London, p. 93–123.

MARGETTS, L., LENG, J.M., SMITH, I.M., and MANNING, P.L., 2006, Parallel three dimensional finite element analysis of dinosaur trackway formation, *in* Schweiger, H.F., ed., Numerical Methods in Geotechnical Engineering: Taylor & Francis Group, London, p. 743–749.

MARTY, D., STRASSER, A., and MEYER, C.A., 2009, Formation and taphonomy of human footprints in microbial mats of present-day tidal-flat environments: implications for the study of fossil footprints: Ichnos, v. 16, p. 127–142.

MEADE, R.H., 1966, Factors influencing the early stages of the compaction of clays and sands—review: Journal of Sedimentary Petrology, v. 36, p. 1085–1101.

MILÀN, J., 2006, Variations in the morphology of emu (*Dromaius novaehollandiae*) tracks reflecting differences in walking pattern and substrate consistency: ichnotaxonomic implications: Palaeontology, v. 49, no. 2, p. 405–420.

MILÀN, J., and BROMLEY, R.G., 2006, True tracks, undertracks and eroded tracks, experimental work with tetrapod tracks in laboratory and field: Palaeogeography, Palaeoclimatology, Palaeoecology, v. 231, p. 253–264.

MILÀN, J., CLEMMENSEN, L.B., and BONDE, N., 2004, Vertical sections through dinosaur tracks (Late Triassic lake deposits, East Greenland) – undertracks and other subsurface deformation structures revealed: Lethaia, v. 37, p. 285–296.

MILLER, C.E., BASU, C., FRITSCH, G., HILDEBRANDT, T., and HUTCHINSON, J.R., 2008, Ontogenetic scaling of foot musculoskeletal anatomy in elephants: Journal of the Royal Society Interface, v. 5, p. 465–475.

MOSSMAN, D.J., BRÜNING, R., and POWELL, H.P., 2003, Anatomy of a Jurassic theropod trackway from Ardley, Oxfordshire, U.K.: Ichnos, v. 10, p. 195–207.

NADON, G.C., 2001, The impact of sedimentology on vertebrate track studies, *in* Tanke, D.H., and Carpenter, K., eds., Mesozoic Vertebrate Life: Indiana University Press, Bloomington, p. 395–407.

OLSON, D., 2011, North American Region Studbook for the African Elephant: International Elephant Foundation, 44 p.

PIETOLA, L., HORN, R., and YLI-HALLA, M., 2005, Effects of trampling on the hydraulic and mechanical properties of soil: Soil & Tillage Research, v. 82, p. 99–108.

PLATT, B.F., and HASIOTIS, S.T., 2006, Newly discovered sauropod dinosaur tracks with skin and foot-pad impressions from the Upper Jurassic Morrison Formation, Bighorn Basin, Wyoming, U.S.A.: PALAIOS, v. 21, p. 249–261.

PLATT, B.F., HASIOTIS, S.T., and HIRMAS, D.R., 2010, Use of low-cost multistripe laser triangulation (MLT) scanning technology for three-dimensional, quantitative paleoichnological and neoichnological studies: Journal of Sedimentary Research, v. 80, p. 590–610.

R DEVELOPMENT CORE TEAM, 2008, R: A Language and Environment for Statistical Computing, R Foundation for Statistical Computing, Vienna, Austria.

RANDRUP, T.B., and LICHTER, J.M., 2001, Measuring soil compaction on construction sites: a review of surface nuclear gauges and penetrometers: Journal of Arboriculture, v. 27, p. 109–117.

REN, L., and HUTCHINSON, J.R., 2008, The three-dimensional locomotor dynamics of African (*Loxodonta Africana*) and Asian (*Elephas maximus*) elephants reveal a smooth gait transition at moderate speed: Journal of the Royal Society Interface, v. 5, p. 195–211.

REN, L., BUTLER, M., MILLER, C., PAXTON, H., SCHWERDA, D., FISCHER, M.S., and HUTCHINSON, J.R., 2008, the movements of limb segments and joints during locomotion in African and Asian elephants: The Journal of Experimental Biology, v. 211, p. 2735–2751.

ROBERTS, D.L., BATEMAN, M.D., MURRAY-WALLACE, C.V., CARR, A.S., and HOLMES, P.J., 2008, Last interglacial fossil elephant trackways dated by OSL/AAR in coastal aeolianites, Still Bay, South Africa: Palaeogeography, Palaeoclimatology, Palaeoecology, v. 257, p. 261-279.

ROTH, V.L., 1990, Insular dwarf elephants: a case study in body mass estimation and ecological inference, *in* Damuth, J., and MacFadden, B.J., eds., Body Size in Mammalian Paleobiology: Estimation and Biological Implications: Cambridge University Press, Cambridge, p. 151–179.

RUSSELL, J. R., BETTERIDGE, K., COSTALL, D. A., and MACKAY, A. D., 2001, Cattle treading effects on sediment loss and water infiltration: Journal of Range Management, v. 54, p. 184–190.

SCHAUB, M.J., ZALISKO, E.J., and SCHAEFER, J.C., 2000, Another advantage of long sauropod necks: reaching out and over hazardous environments: American Zoologist, v. 40, p. 1200 (abstract).

SCOTT, J.J., RENAUT, R.W., and OWEN, R.B., 2010, Taphonomic controls on animal tracks at saline, alkaline Lake Bogoria, Kenya Rift Valley: impact of salt efflorescence and clay mineralogy: Journal of Sedimentary Research, v. 80, p. 639–665.

SCRIVNER, P.J., and BOTTJER, D.J., 1986, Neogene avian and mammalian tracks from Death Valley National Monument, California: their context, classification and preservation: Palaeogeography, Palaeoclimatology, Palaeoecology, v. 57, p. 285–331.

SENEVIRATNE, S.I., CORTI, T., DAVIN, E. L., HIRSCHI, M., JAEGER, E.B., LEHNER, I., ORLOWSKY, B., and TEULING, A.J., 2010, Investigating soil moisture-climate interactions in a changing climate: a review: Earth-Science Reviews, v. 99, p. 125–161.

SHELDON, N.D., and RETALLACK, G.J., 2001, Equation for compaction of paleosols due to burial: Geology, v. 29, p. 247–250.

SIKES, S.K., 1971, The Natural History of the African Elephant: American Elsevier, New York, 397 p.

SOKAL, R.R., and ROHLF, F.J., 1995, Biometry, 3rd ed.: W.H. Freeman and Company, New York, 887 p.

THULBORN, T., 1990, Dinosaur Tracks: Chapman and Hall, London, 410 p.

TIMM, L.C., PIRES, L.F., REICHARDT, K., ROVERATTI, R., OLIVEIRA, J.C.M., and BACCHI, O.O.S., 2005, Soil bulk density evaluation by conventional and nuclear methods: Australian Journal of Soil Research, v. 43, p. 97–103.

TROXLER ELECTRONIC LABORATORIES, INC., 2009, Manual of Operation and Instruction, Model 3440 Surface Moisture-Density Gauge, Edition 17.7: Troxler Electronic Laboratories, Inc., Research Triangle Park, North Carolina, 210 p.

U.S. DEPARTMENT OF AGRICULTURE, NATURAL RESOURCES CONSERVATION SERVICE, 2011, National Soil Survey Handbook, title 430-VI, http://soils.usda.gov/technical/handbook/. Checked December 2011.

VEENSTRA, M., WHITE, D.J., and SCHAEFER, V.R., 2005, Rapid field testing techniques for determining soil density and water content: Proceedings of the 2005 Mid-Continent Transportation Research Symposium, Ames, Iowa, p. 1–13.

WALKER, M.J., KUTSCH, R., MILLER, W.W., CIRELLI, A.L., and DONALDSON, S., 2005, A consistent hoof impact simulator: Soil Science Society of America Journal, v. 69, p. 257–259.

WARREN, S. D., THUROW, T. L., BLACKBURN, W. H., and GARZA, N. E., 1986, The influence of livestock trampling under intensive rotation grazing on soil hydrologic characteristics: Journal of Range Management, v. 39, p. 491–495.

WEISSENGRUBER, G.E., EGGER, G.F., HUTCHINSON, J.R., GROENEWALD, H.B., ELÄSSER, L., FAMINI, D., and FORSTENPOINTNER, G., 2006, The structure of the cushions in the feet of African elephants (*Loxodonta africana*): Journal of Anatomy, v. 209, p. 781–792.

TABLES

Table 1.—Weight distribution of elephants used in trials.

Name	Species	Forelimbs		Hindlimbs	
		Actual quantity (kg)	Percent of total weight	Actual quantity (kg)	Percent of total weight
Sunda	*Elephas maximus*	1552.2	59.9	1675.6	40.1
Tembo	*Loxodonta africana*	2317.9	60.4	2557.4	39.6

Table 2.—Measurements of elephant foot dimensions in cm; *L* = length, *W* = width.

Elephant	Species	Left manus		Right manus		Left pes		Right pes	
		L	*W*	*L*	*W*	*L*	*W*	*L*	*W*
Sunda	*Elephas maximus*	35	40	37	40	42	27	42	26
Tembo	*Loxodonta africana*	35	32	38	34	43	27	43	28

Table 3.—Average dimensions of tracks; RM = right manus, LM = left manus, RP = right pes, LP = left pes, *L* = length in cm, *W* = width in cm, *n* = number of measurements, *SD* = standard deviation, NA = not applicable.

Foot	Elephant	Species	*L*	*n*	*SD*	*W*	*n*	*SD*
RM	Sunda	*E. maximus*	39	9	2	37	9	2
	Tembo	*L. africana*	39	1	NA	38	1	NA
LM	Sunda	*E. maximus*	38	8	3	37	6	2
	Tembo	*L. africana*	40	1	NA	39	1	NA
RP	Sunda	*E. maximus*	42	11	2	27	11	2
	Tembo	*L. africana*	43	22	2	29	20	1
LP	Sunda	*E. maximus*	42	16	2	28	16	2
	Tembo	*L. africana*	42	17	2	29	17	2

Table 4.—Average particle-size parameters for sediment samples used in experiments.

Property	Mason sand	Unsieved KS River sand
M_ϕ	1.29	3.31
σ_ϕ	1.00	2.20
S_ϕ	1.33	0.62
K_ϕ	13.85	1.67

Table 5.—Descriptive statistics for data obtained in mason sand and unsieved Kansas River sand, *SD* = standard deviation.

Variable	Variable Name	Mason sand				Unsieved KS river sand			
		Min	Max	Mean	*SD*	Min	Max	Mean	*SD*
V (cm^3)	Track volume	455	36,442	6,393	9,511	361	8,619	3,322	1,697
V_n (cm^2)	Normalized V	11.4	911.1	157.6	238.7	9.0	205.2	79.5	39.2
A	Sediment aging	0	72	42	32	0	94	21	32
v (m/s)	Locomotion velocity	0	0.86	0.69	0.23	0	1.0	0.61	0.33
P (kPa)	Foot pressure	76	167	101	32	64	133	95	14
ρ_b (g/cm^3)	Sediment dry bulk density	1.4	1.7	1.6	0.1	1.4	1.6	1.5	0.1
θ_v (%)	Sediment water content	3.8	21.5	12.9	5.0	8.7	24.2	14.7	4.5

Table 6.—Results of multiple regression analysis following backward elimination.

Variable	Variable Name	Units	Coefficient	P-value	β weight
Intercept		none	518	3.94×10^{-12}	-0.386
v	Locomotion velocity	m/s	-20.5	7.63×10^{-2}	-0.149
ρ_b	Sediment dry bulk density	g/cm^3	-157	1.48×10^{-4}	-0.333
θ_v	Sediment water content	%	-26.4	4.98×10^{-7}	-0.307
θ_v^2			0.812	6.88×10^{-6}	0.391

Table 7.—Estimation of hypothetical sauropod track volumes in experimental sediments. Foot length and speed data from Alexander (1989). Foot length calculated as leg length/4.

			Minimum θ_v		Maximum θ_v	
Trackmaker	L (cm)	v (m/s)	V_n (cm^2)	V (cm^3)	V_n (cm^2)	V (cm^3)
Large sauropod	75	1.0	142.9	10,714.4	68.7	5,150.5
Small sauropod	37.5	1.1	140.8	5,280.1	66.6	2,498.2

Table 8.—Calculation of θ_v and S_w of original sauropod-track-bearing sediment based on fossil sauropod tracks, Upper Jurassic Morrison Formation, Bighorn Basin, Wyoming, USA. Saturation values are calculated with Equation 8, assuming a particle density of 2.65 g/cm^3.

V_n (cm^2)	Original sediment texture	Estimated ρ_b (g/cm^3)	Estimated v (m/s)	θ_v (%)	S_w (%)
341.6	sand	1.7	1.0	36.2	101.1
326.7	silt	1.4	1.0	34.2	72.6
410.0	silt	1.4	1.0	36.9	78.2
523.1	silt	1.4	1.0	40.0	84.8
726.5	silt	1.4	1.0	44.8	95.0
903.2	silt	1.4	1.0	48.4	102.6

FIGURES

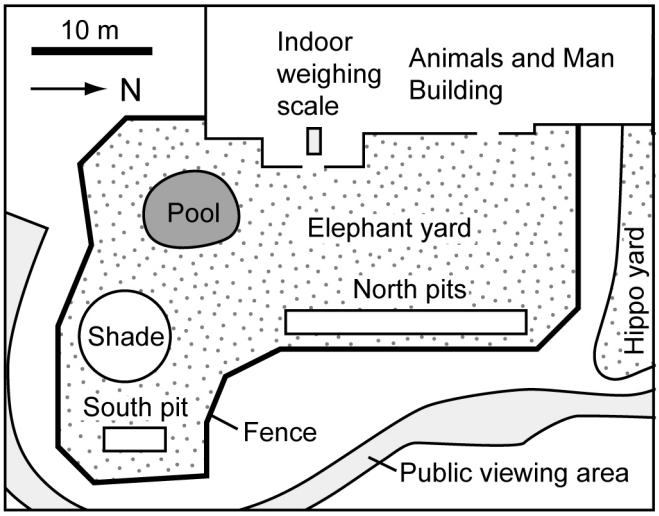

Figure 1.—Map of elephant exhibit at the Topeka Zoo. Modified from Topeka Zoo Master Plan (GLPM Architects, Inc., 2006).

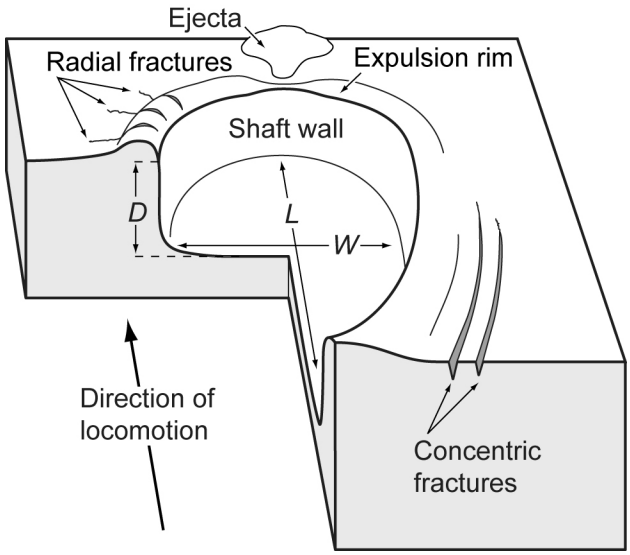

Figure 2.—Illustration of track measurements and terminology of Allen (1997) used in this paper.

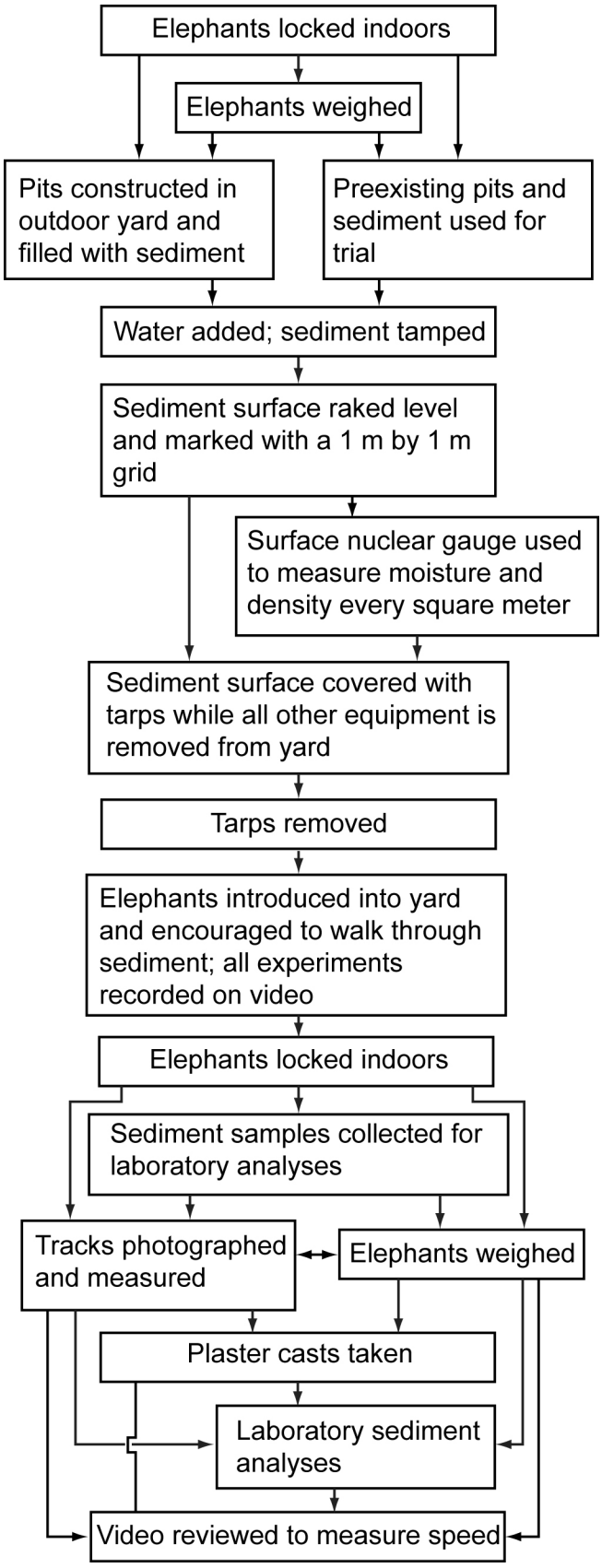
Elephants locked indoors
Elephants weighed
Pits constructed in outdoor yard and filled with sediment
Preexisting pits and sediment used for trial
Water added; sediment tamped
Sediment surface raked level and marked with a 1 m by 1 m grid
Surface nuclear gauge used to measure moisture and density every square meter
Sediment surface covered with tarps while all other equipment is removed from yard
Tarps removed
Elephants introduced into yard and encouraged to walk through sediment; all experiments recorded on video
Elephants locked indoors
Sediment samples collected for laboratory analyses
Tracks photographed and measured
Elephants weighed
Plaster casts taken
Laboratory sediment analyses
Video reviewed to measure speed

Figure 3 (previous page).—Flowchart showing procedures followed for data collection trials.

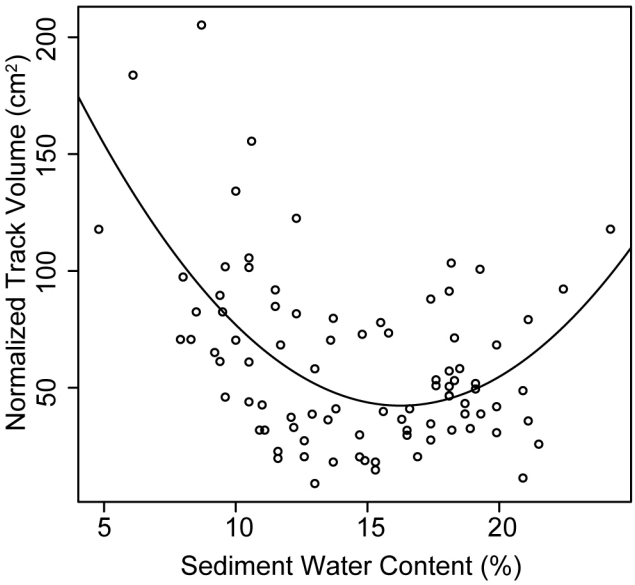

Figure 4.—Normalized track volume plot against sediment volumetric water content with best-fit curve.

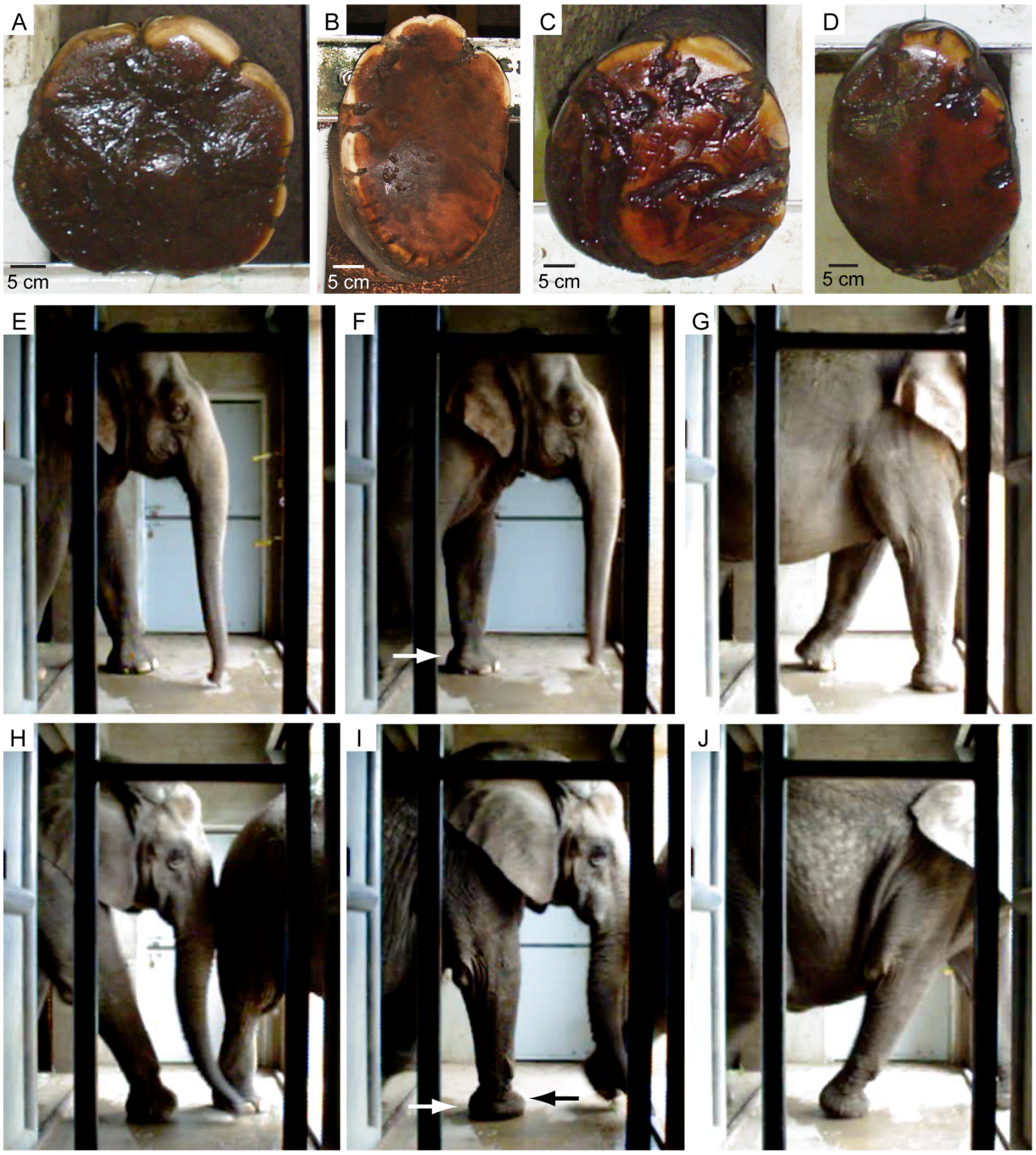

Figure 5.—Morphological and behavioral observations of elephants. Soles of A) Sunda's right manus, B) Sunda's right pes, C) Tembo's right manus, and D) Tembo's right pes, note textures and greater expression of nails in A and B; feet were photographed while wet from being cleaned, which resulted in the contrast and reflections. Anterior is towards the top of the page in A–D. E–G: Still images captured from video of Sunda walking forward. H–J: Still images captured from video of Tembo walking forward. Note outward expansion of feet during weight-bearing phase of locomotion (arrows in F and I).


A
5 cm
B
C
5 cm
D
5 cm
E
5 cm
F
radial fractures
ejecta
nail impressions

Figure 6 (previous page).—Results of trackmaking trials; anterior is towards the top of the frame for all images. A) Shallow impression from Sunda's left manus, B) deeper impression from Sunda's right manus, C) very shallow impressions from Sunda's left pes, D) deep impression from Tembo's right pes, E) Overlapped right manus and pes impressions made by Sunda, F) Detail of shaft wall of a well-preserved left manus impression made by Tembo; photo oblique to ground surface; note nail impressions, toe drag and ejecta (arrow), and radial fractures in expulsion rim.

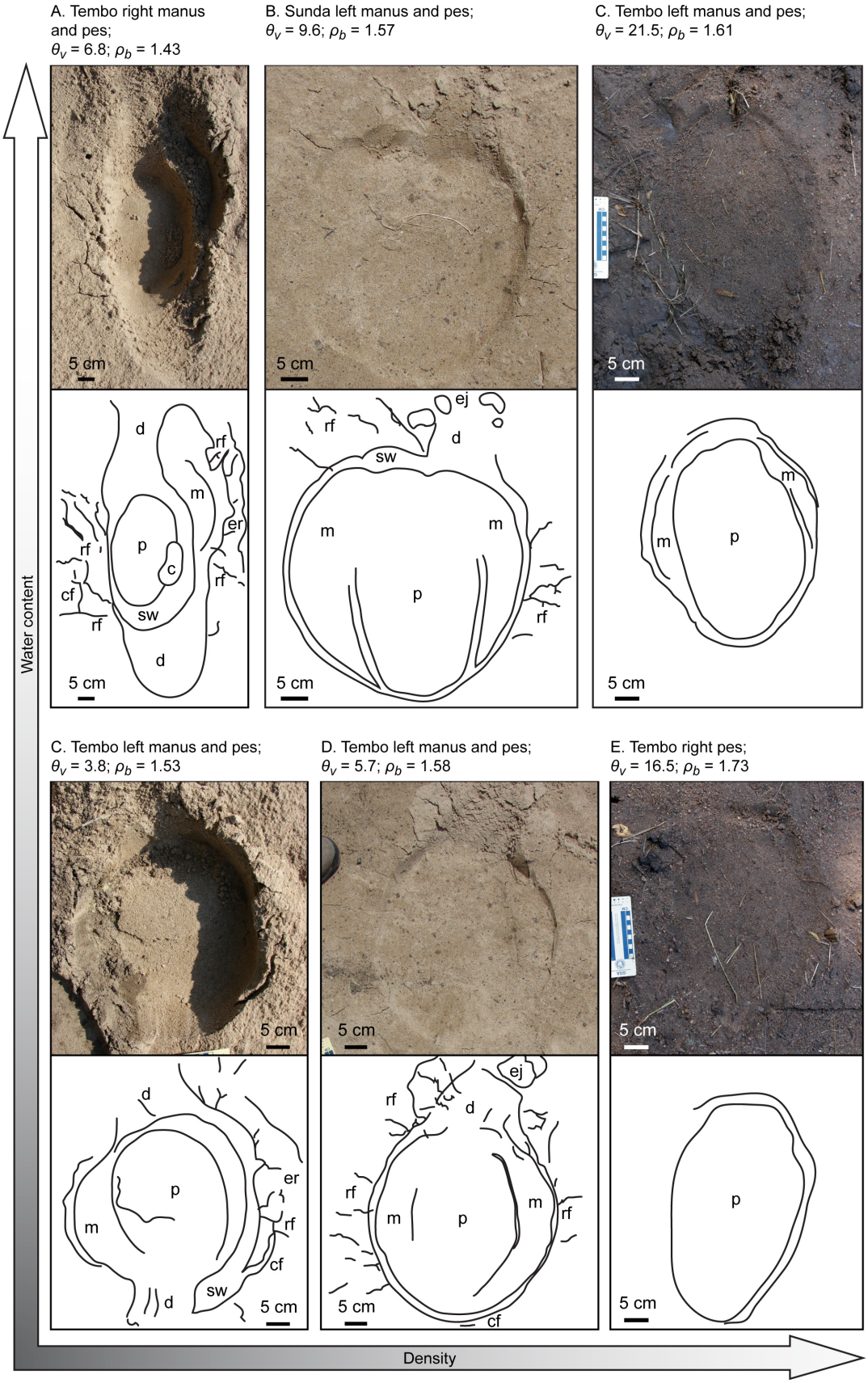
A. Tembo right manus and pes; θ_v = 6.8; ρ_b = 1.43
B. Sunda left manus and pes; θ_v = 9.6; ρ_b = 1.57
C. Tembo left manus and pes; θ_v = 21.5; ρ_b = 1.61
C. Tembo left manus and pes; θ_v = 3.8; ρ_b = 1.53
D. Tembo left manus and pes; θ_v = 5.7; ρ_b = 1.58
E. Tembo right pes; θ_v = 16.5; ρ_b = 1.73
Water content
Density
5 cm
d
rf
m
er
p
c
cf
sw
ej
cf

Figure 7 (previous page).—Range of variation in footprint morphologies in mason sand with different ρ_b and θ_v values; c = collapsed material, cf = concentric fracture, d = drag mark, ej = ejecta, er = expulsion rim, m = manus, p = pes, rf = radial fracture, sw = shaft wall. All tracks are oriented so anterior is towards the top of the figure.

CHAPTER 4: INTEGRATING ICHNOLOGY, PALEOPEDOLOGY, AND SEDIMENTOLOGY TO INTERPRET PALEOENVIRONMENTS AND PALEOHYDROLOGY OF THE UPPER JURASSIC MORRISON FORMATION, BIGHORN BASIN, WYOMING, USA

Currently in preparation as:

PLATT, B. F., HASIOTIS, S.T., KVALE, E.P., AND KRAUS, M.J., Integrating ichnology, paleopedology, and sedimentology to interpret paleoenvironments and paleohydrology of the Upper Jurassic Morrison Formation, Bighorn Basin, Wyoming, USA: Journal of Sedimentary Research.

ABSTRACT

Avulsion deposits in the Upper Jurassic Morrison Formation in northeastern Bighorn Basin, Wyoming, USA, consist of a heterolithic lithofacies bounded below and above by massive mudstone lithofacies. The mudstone lithofacies contains well- and moderately developed paleosols formed on overbank deposits. The heterolithic lithofacies contains thin sheet sandstones, interpreted as crevasse-splay deposits, and ribbon sandstones, interpreted as distributary-splay channels, separated by weakly to moderately developed paleosols. Nineteen ichnofossil types recognized in the mudstone and heterolithic lithofacies constitute six distinct ichnocoenoses classified according to moisture regimes based on ichnofossils and pedogenic characteristics. Cluster analysis of spatial trace-fossil data can aid in the interpretation of ichnocoenoses when a large number of traces are present on a single bedding plane. Vertical trends associated with a single crevassing event reveal a general pattern of dominantly

hygrophilic traces overprinted by dominantly hydrophilic traces, followed by deposition of sheet and ribbon sandstones, which contain traces representative of a range of moisture regimes that may be overprinted by dominantly terraphilic traces.

Lateral moisture profiles, along with vertical trends in ichnocoenoses, provide more detailed paleohydrological information than sedimentology alone. The patterns we document can be used to help interpret avulsion deposits in other rocks because they rely on moisture regimes, as opposed to presence or absence of ichnotaxa. This approach can be useful for interpreting avulsion deposits in areas that do not have significant lateral exposure and in core.

INTRODUCTION

This paper integrates sedimentology, paleopedology, and ichnology to interpret local paleoenvironments and paleohydrology of the Upper Jurassic Morrison Formation (MF) in the Bighorn Basin, Wyoming, USA. We quantitatively identify discrete ichnocoenoses in lateral and vertical successions of ichnofossil assemblages observed from exposures in the study areas. Ichnocoenoses are used as proxies for paleocommunities and provide detailed information about within-facies variations in paleoenvironment and paleohydrologic regime because they are independent of lithology (Hasiotis 2002, 2004, 2007, 2008). The continental realm is unique because postdepositional and physicochemical conditions primarily control the distribution of organisms (Hasiotis 2007; Hasiotis et al. 2007). This degree of resolution of spatial and temporal heterogeneity is not possible with ichnofacies, since one ichnofacies can contain multiple ichnocoenoses, environments, moisture regimes, and ecosystems. Also, recently proposed continental ichnofacies are so broadly defined and poorly constrained that precise and reliable paleoenvironmental interpretations are not possible (Hasiotis 2007, 2008).

Ichnocoenoses have been used to interpret paleoenvironments, paleohydrology, and paleoclimate of the MF in southcentral, southwestern, central, and northwestern parts of the Morrison depositional basin (Hasiotis 2004, 2008). A mosaic of paleohydrologic and paleoenvironmental settings in the MF was controlled largely by temporal and geographic fluctuations in the distribution and amount of effective precipitation (Demko et al. 2004; Hasiotis 2004, 2008; Turner and Peterson 2004).

Exposures of the MF in the northeastern Bighorn basin have attracted attention because of the abundance and quality of vertebrate body fossils (e.g., Brown 1932; Ayer 1999; Kvale et al. 2004). Few studies have focused on the ichnology of these rocks, however, until recent discoveries of abundant and diverse trace-fossil assemblages prompted reassessment of depositional settings in this part of the MF (Kvale et al. 2001; Platt and Hasiotis 2006, 2008).

LOCATION AND GEOLOGIC SETTING

The studied outcrops of MF are in Coyote Basin and Red Gulch, near Shell, Wyoming (Fig. 1). The MF in these locations is ~57 m thick (Platt and Hasiotis 2006) and consists of mostly continental strata deposited between 155 and 148 million years ago (Kimmeridgian–Tithonian) (Kowallis et al. 1998) in the subsiding Cordilleran foreland basin system (Decelles and Burden 1992; DeCelles and Currie 1996). The MF in the Bighorn Basin overlies the Middle Jurassic Sundance Formation (Moberly 1960; Kvale 1986; Winslow and Heller 1987) and unconformably underlies the Lower Cretaceous Cloverly Formation (Winslow and Heller 1987; Pipiringos and O'Sullivan 1978; Heller and Paola 1989).

The upper ~19 m of the MF, the focus of this study (Fig. 2), are dominated by red and greenish gray siltstone, and silty claystone beds with abundant red and greenish gray mottles,

rhizoliths, and carbonate nodules (Moberly 1960; Kvale 1986). These units are interbedded with thin sheet-sandstone beds and sparse, small channel sandstones that decrease upwards in number (Kvale 1986). Sheet and channel sandstones are generally fine- to medium-grained, subarkose to sublitharenite, some of which contain dark chert grains (Kvale 1986; Winslow and Heller 1987). The thickest channel sandstones have large-scale, trough-cross stratification with evidence of midchannel and sidebar accretion (Kvale 1986). Paleocurrent indicators show a northeasterly paleoflow direction (Kvale 1986; Winslow and Heller 1987). Many sheet sandstones are ripple- and climbing ripple-laminated and contain well-preserved invertebrate and vertebrate trace fossils (Kvale et al. 2001; Platt and Hasiotis 2006, 2008). Vertebrate body fossils are locally abundant in the upper MF of the Bighorn Basin, the most famous of which come from the Howe Quarry (Brown 1937; Ayer 1999).

METHODS

Field Methods

We measured a complete section, characterized lithofacies, and recorded trace-fossil data through the MF from outcrop exposures in the field areas. The upper part of the section is well dissected by erosion and presents a unique opportunity to observe excellent lateral exposure of well-preserved, trace-fossil-rich strata. To examine lateral patterns in trace-fossil distribution, we recorded the locations of discrete trace fossils (excluding rhizoliths due to their great abundance) with a Garmin GPS 38™ Personal Navigator™ Global Positioning System (GPS) receiver. GPS locations of slabs in float that could be visually matched to an outcrop were also taken. Well-preserved examples of trace fossils were collected for additional study in the laboratory. All collected vertebrate trace fossils were reposited in the Vertebrate Paleontology

collection in the University of Kansas Natural History Museum (KUVP). All invertebrate trace fossils are housed in the ichnology laboratory in the University of Kansas Geology Department. The specific locality information is available upon request from either the KUVP or the Bureau of Land Management (BLM) head office in Cheyenne, Wyoming.

Treatment of Ichnofossils

We assigned traces with similar architectures and morphologies to numbered trace-fossil types. The numbers are arbitrary but are arranged to generally represent increasing architectural complexity. Trace-fossil types are assigned to ichnotaxa when possible. Our main focus is not ichnotaxonomy, but rather the behaviors, environments, and moisture regimes represented by the trace fossils, based on comparisons to modern homologous and analogous biogenic structures (e.g., Hasiotis and Mitchell 1993; Hasiotis 2002, 2003; Hembree and Hasiotis 2006; Benner et al. 2008; Smith and Hasiotis 2008; Counts and Hasiotis 2009; Knecht et al. 2009; Halfen and Hasiotis 2010; see Table 1). We are, therefore, able to increase the amount of data by not restricting observations to only extremely well-preserved trace fossils. When assigning trace-fossil types, we take into account the range of morphological detail possible due to variations in media (=substrate) consistency (e.g., Platt et al. in review).

Integrative Approach

Our approach to the integration of sedimentology, paleopedology, and ichnology (Fig. 3) draws upon previous studies of controls on pedogenesis and the distribution of soil biota, soil moisture, and the groundwater table. A paleosol representing pedogenesis in a body of sediment during a period of landscape stability, i.e., no substantial deposition or erosion, is considered a

simple paleosol (e.g., Kraus and Aslan 1993). Alluvial paleosols, however, are often complex and can be viewed as the result of a balance between sedimentation and pedogenesis (Kraus 1999). Rapid, non-steady deposition produces vertically stacked, weakly developed soils separated by minimally weathered sediment, preserved as compound paleosols. Composite paleosols exhibit partly overlapping profiles that resulted from rates of pedogenesis that outstripped sedimentation rates. Steady deposition of small increments of sediment that become incorporated into a soil profile by pedogenesis results in cumulative (Kraus 1999), cumulate (Marriott and Wright 1996), or cumulic (Retallack 2001; Smith et al. 2008a) soils and paleosols. Johnson et al. (1987) examined different pedogenic processes, including bioturbation, which act to enhance horizonation (proanisotropic pedoturbation) and destroy horizonation (proisotropic pedoturbation). Pairing this approach with that of Kraus (1999) incorporates sedimentation and erosion, i.e., landscape evolution, with the soil-forming processes responsible for features that are preserved in paleosols. Ichnofossils record organismal behaviors that contributed to the depth and degree of pedogenesis, and are informative for interpreting paleosols because soil moisture and water table levels control the distribution of soil biota (Table 1; e.g., Wallwork 1970; Hasiotis 2002, 2007; Hasiotis et al. 2007). Bioturbation is one of the five major soil-forming factors, whose depth, distribution, and amount of time active in the soil is controlled by the size and behavior of organism(s), zonation of the groundwater profile, and type and seasonality of climate. Combining continental bioturbation patterns with the patterns of Kraus (1999) and Johnson et al. (1987) enables a tripartite approach to pedogenic landscape evolution that unites the controls on the development of soils (preserved as paleosols) in relation to the frequency and magnitude of sedimentation events, biotic and abiotic pedogenesis, and groundwater profile through time in alluvial basinal settings (Hasiotis 2004, 2008).

Ichnological Moisture Regimes

We assigned trace fossil types to one of four moisture regimes, which classifies the tracemaker as 1) epiterraphilic—organisms living on the surface, 2) terraphilic—organisms living above the water table to the upper vadose zone, 3) hygrophilic—organisms living in the vadose zone, or 4) hydrophilic—organisms living below the water table within a soil or living in aquatic settings and make traces on or below the sediment surface in open bodies of water (Hasiotis 2000, 2004, 2008). This moisture-regime classification is based on the well-established concept that in the continental realm, moisture is a major control on the distribution of soil fauna (Hasiotis 2002 and references therein; Hasiotis et al. 2007; Hasiotis 2008; Hasiotis et al. 2012 in press). Even though Bromley et al. (2007) questioned the methods of Hasiotis (2004), an abundance of life history studies of modern tracemakers demonstrate that moisture levels control the behavior, depth, distribution, and reproductive success of continental organisms (Table 1; Hasiotis 2008).

Designation of Ichnocoenoses

To objectively evaluate trace-fossil associations (i.e., ichnocoenoses), GPS data were imported into ArcMap 9.2 (ESRI, Inc.) and divided into layers based on stratigraphic position. We used the Point Distance Analysis tool to generate a distance matrix for all points in each trace-fossil-rich stratigraphic unit. We imported distance matrices into PAST 1.82 (Hammer et al. 2001) and performed cluster analyses to visually represent nearest neighbors on dendrograms. The algorithm used was unweighted pair-group average with Euclidean distance as the similarity measure. Clusters form the basis for ichnocoenosis designations in dense, laterally extensive

trace-fossil assemblages. Ichnocoenoses are named typically for the most abundant trace fossil in each assemblage, but we also considered types and relative abundances of trace fossils within an ichnocoenosis. Multiple clusters composed of similar types and relative abundances of trace fossils may represent recurring paleocommunities associated with specific sets of paleoenvironmental or paleohydrological conditions.

We generated a histogram for each ichnocoenosis that shows the distribution of moisture regimes represented within the ichnocoenosis. Histograms give a general indication of local paleohydrological conditions. Note that for the purpose of paleohydrologic interpretation, surficial traces, i.e., epiterraphilic traces, indicative of saturated media or standing water were classified as hydrophilic. Histograms with disparate results, e.g., abundant hydrophilic and epiterraphilic traces, are interpreted in conjunction with field observations to determine if results represent a single paleocommunity or several overprinted paleocommunities resulting from changing local conditions.

RESULTS

Lithofacies

The upper MF in the study areas comprises a mudstone lithofacies and a heterolithic lithofacies. The heterolithic lithofacies contains thin sheet sandstones, ribbon sandstones, weakly developed paleosols, and moderately developed paleosols. Ribbon sandstones may scour into the mudstone lithofacies. In the study areas, the heterolithic lithofacies is bounded above and below by the mudstone lithofacies (Fig. 2, 4).

Mudstone lithofacies.—The mudstone lithofacies consists of red and greenish gray massive mudstones with varying degrees of red, green, and gray color mottling. Other features

present include carbonate nodules, clay-coated slickensides, and branching, tapering tubular trace fossils. We interpret the combination of features observed in the mudstone lithofacies as evidence of pedogenesis of overbank deposits (e.g., Kraus 1999; Retallack 2001).

Description of paleosols in the mudstone lithofacies.—Paleosol profiles within the mudstone lithofacies usually consist of a red mudstone that is underlain by a slightly coarser grained, green bed. Many paleosols contain multiple, stacked red beds (Fig. 5A) or individual red beds approaching 1 m in thickness (Fig. 5B). Profiles range up to 4 m thick and have well-defined soil horizons. Horizons are massive with no observable primary sedimentary structures. Red beds are characterized by gray mottles and clay-coated slickensides. Rhizoliths are abundant, but animal trace fossils are relatively rare. Carbonate nodules are abundant in the dominantly red beds of the paleosols and are mainly spherical, but some have elongate tubular forms. The nodules are typically < 1 cm in diameter, but some reach 3 cm.

Interpretation of paleosols in the mudstone lithofacies.—Pedogenic features indicate that these paleosols were moderately to well developed and well drained. The thick red horizons are interpreted as B horizons. The red color, which indicates the presence of hematite, along with carbonate nodules imply that the B horizon was at least moderately well drained and oxidized (e.g., Kampf and Schwertmann 1982; Wilding and Tessier 1988; Schwertmann 1993). The mottles and slickensides indicate that the paleosols underwent seasonal wetting and drying (e.g., Stolt et al. 1994; Bigham et al. 2002).

Thick beds of green siltstone and silty mudstone below the red beds represent significant influxes of extrachannel material. These beds are designated as C horizons where they appear to have been substantial enough to have halted pedogenesis in the underlying strata. There appear to be very few preserved A horizons.

We interpret the multiple, stacked red beds as composite paleosols (Fig. 5A), which represent influxes of sediment that were greater than the thickness of the subadjacent horizon, but less than the thickness of the soil profile (Wright and Marriott 1996). Composite paleosols require approximately 10^4 years to develop (Wright and Marriott 1996).

The approximately 1-m-thick red paleosol horizons (Fig. 5B) are interpreted as the result of incorporation of small pulses of sediment into the soil profile over relatively long periods of time. These paleosols represent cumulate soils and require about 10^4–10^5 years to develop (Marriott and Wright 1993; Wright and Marriott 1996; Birkeland 1999).

We interpret the mudstone lithofacies as a distal floodplain environment based on lithology and the low sedimentation rates required to allow development of composite and cumulic paleosols. We interpret the lack of animal trace fossils in these paleosols as the result of proisotropic pedoturbation caused by seasonal wetting and drying (e.g., Johnson et al. 1987).

Sheet sandstones within the heterolithic lithofacies.—The first component of the heterolithic lithofacies, sheet sandstones, are very fine-grained sandstone beds that are thin (typically < 1 m thick) and laterally extensive (> 0.5 km^2). The sandstone beds are categorized as sheet sandstones based on low width-to-thickness (W/T) ratios (Friend et al. 1979; Kraus and Wells 1999). Sandstone grades upward from ripple- and climbing ripple-laminated to planar laminations with primary current lineations (PCL) with a dominant NE–SW orientation. Two major sheet sandstone beds are present in the study areas: a lower sheet sandstone bed at least 9,577 m^2 in area and an upper sheet sandstone bed at least 43,684 m^2 in area. Beds are mainly flat-based with local scours into underlying beds. Trace fossils are most abundant on bedding planes, but many vertical burrows and rhizoliths are also present within beds. Some laterally restricted bedding surfaces contain flat-topped and bifurcating ripples crosscut by trace fossils.

The trace fossils are dense locally, but typically do not crosscut each other. Despite the presence of traces, primary sedimentary structures are relatively undisturbed.

Sheet-sandstone beds are interpreted as crevasse-splay lobes deposited in a proximal floodplain setting (Kvale et al. 2001). The relatively minor bioturbation and lack of crosscutting trace fossils suggest that these units were exposed subaerially for relatively short periods of time (Hasiotis 2002, 2004, 2008). Areas of flat-topped and bifurcating ripples indicate areas of shallow standing water (Allen 1982), perhaps as a result of locally poor drainage.

Ribbon sandstones within the heterolithic lithofacies.—Ribbon sandstones are the second type of sand body within the heterolithic lithofacies. Ribbon sandstones have a lenticular cross section and are composed of very fine-grained sand. They are typically < 2 m thick and, although widths are variable and difficult to measure accurately, most W/T ratios are < 10, placing them in the category of ribbon sandstones (Friend et al. 1979). Ribbon sandstones scour into underlying sheet sandstones and massive mudstones. Ribbon sandstones are more numerous lower in the heterolithic lithofacies. The margins of the ribbon sandstone beds, where exposed, pinch out dramatically. Small-scale, trough cross-stratification is the dominant internal structure. Paleocurrents cannot be measured directly from sedimentary structures, but dissected ribbons correlated between valley walls indicate a dominant NE–SW trend. Some trace fossils are present in the top 10 cm of the ribbon sandstones, but they are sparse. Many of these trace fossils crosscut primary sedimentary structures.

Ribbon sandstones are interpreted as small, shallow channels that traversed the proximal floodplain. None are large enough to be considered trunk channels. The channels represent networks of concentrated overbank flow exploiting topographic lows on the floodplain. Those that are scoured into sheet sandstones may be distributary channels associated with individual

crevasse-splay lobes, but most do not have a clear relationship with sheet sandstones.

Weakly developed paleosols within the heterolithic lithofacies.—Weakly developed paleosols within the heterolithic lithofacies are typically < 1 m thick and consist of a single mudstone, siltstone, or sandstone bed with no evidence of horizons (Fig. 5C). Colors are dominantly green and gray. Carbonate nodules and slickensides are absent. Relict bedding, minor bioturbation, and plant and animal trace fossils are present. Trace fossils do not crosscut each other. Many finer grained paleosols are bounded above and below by sheet and ribbon sandstones. Some green, silty paleosols grade laterally to thin sheet sandstones.

The thickness, presence of relict bedding, and lack of well-developed pedogenic features and crosscutting of trace fossils in heterolithic lithofacies paleosols suggests a relatively short period of pedogenic modification. The time required for a weakly developed soil to form is about 10^1–10^3 years (Wright and Marriott 1996; Birkeland 1999; Brady and Weil 2002), implying high sedimentation rates relative to those that dominated during deposition of the mudstone lithofacies. Each bed likely represents the AC profile of a weakly developed soil (Entisols and Inceptisols). Green and gray colors are interpreted as Fe depletion resulting from poor drainage. We interpret these paleosols as pedogenically modified avulsion deposits in a proximal floodplain setting based on the lateral proximity to sheet sandstone beds, poor drainage, and relatively high sedimentation rates.

Moderately developed paleosols within the heterolithic lithofacies.—Moderately developed paleosols within the heterolithic lithofacies are between about 0.5 m and 2 m thick and contain distinct pedogenic horizons. The thinnest of these paleosols contain two horizons and are red or green with color mottling and rhizoliths. Carbonate nodules and slickensides are rare or absent in the thinnest paleosols (Fig. 5C), but are more abundant in thicker paleosols.

Horizon colors range from greenish gray to red with greenish gray mottles, and to purple with green mottles. These paleosols are bounded above and below by sheet sandstones, ribbon sandstones, or weakly developed paleosols.

Scours up to 1 m deep are present within moderately developed paleosols and are filled by a single bed or multiple beds of mudstone or silty mudstone that onlap the margins of the scour and thicken commonly towards the center (Fig. 5D). The scour fill is typically massive and contains rhizoliths. Some green mudstone fill contains ostracodes and charophytes as well as fossil bone fragments.

The thinnest of the moderately developed paleosols are interpreted as having incipient B horizons. These represent a longer period of soil formation than the weakly developed paleosols in the heterolithic lithofacies. Moderately developed paleosols are interpreted as pedogenically modified floodplain deposits.

Green and purple mudstone and claystone intervals in moderately developed paleosols are interpreted as gleyed horizons resulting from Fe reduction in prolonged saturated conditions or, as in many A horizons, abundant organic matter. The majority of sheet sandstones are underlain by a gleyed horizon suggesting poor drainage of the soils following flooding. Redoximorphic coloration and subsurface gleyed horizons likely represent prolonged high-water tables.

Filled scours resulted from the erosive events during flooding and major precipitation events, and filling events by subsequent floods. Local depressions retained ponded water for a period of time, based on ostracode and charophyte fossils and gleying.

Interpretation of heterolithic lithofacies.—The suite of sheet sandstones, ribbon sandstones, weakly developed paleosols and moderately developed paleosols within the

heterolithic lithofacies resembles avulsion deposits that have been described by Smith et al. (1989) from the modern Saskatchewan River, by Kraus and Aslan (1993) and Kraus (1996) from the Eocene Willwood Formation, and by Jones and Gustason (2006) from the Salt Wash Member of the MF. Avulsion on the Saskatchewan River is carried out by splay systems, which divert flow and sediment from the main channel and prograde out onto the floodplain to form an avulsion complex. As the avulsion continues, splay complexes grow outward so that the avulsion complex eventually covers a large area of the floodplain (up to 500 km^2 in the case of the Saskatchewan River complex). The splay complexes consist of channel networks, in which accumulate sands that range from continuous sheets to isolated ribbons. Fine-grained sediments deposited in interchannel areas surround the sands. If the avulsion goes to completion, a new trunk channel finally develops on the avulsion belt and the old trunk channel is abandoned. Consequently, the avulsion deposits are locally scoured and overlain by the sand deposited by the new trunk channel.

The MF ribbon sandstones, by analogy with modern avulsion deposits, represent ancient splay channels that fed the developing avulsion belt, and the thin sheets formed as sheet floods or overbank deposits from the splay channels. The more strongly developed paleosols in the mudstone lithofacies overlie and underlie the heterolithic lithofacies, and represent a distal floodplain setting with low sedimentation rates resulting in composite and cumulate soils (Fig. 6).

Trace-Fossil Types

Plant, invertebrate, and vertebrate trace fossils are abundant and diverse in the field area. Many trace fossils are preserved in convex hyporelief on the bases of sheet sandstones at the contacts with underlying mudstones; these are natural casts of traces originally created in the

mudstones. When reconstructing ichnocoenoses, we consider the original stratigraphic location of the traces and distinguish traces preserved on the bases of sheet sandstones from traces preserved within sheet sandstones (Table 2).

Type 1a–c—Root traces (Fig. 7A–B).—Vertical to subvertical, branched and unbranched, straight tubes or mottled zones 1 to 150 mm in diameter and from several centimeters to over 1 m long. Three morphotypes are recognized:

(a) Rhizoliths—Hollow, vertical, downward-tapering tubes < 5 cm maximum diameter typically, with walls punctuated by small pits, < 5 mm in diameter (Fig. 7A). Tubes are several centimeters up to 0.5 m long and branching is rare. Type 1a traces are found only in sheet sandstones. Many of the longest Type 1a traces penetrate entire sandstone beds and are associated intimately with the trace fossil cf. *Termitichnus*.

(b) Small Rhizohaloes—Thin, vertical to subvertical zones of lighter color than the matrix; some in dense accumulations. Zones are typically several centimeters long, taper downward, and branch regularly. Colors range from green to purple with lighter colored haloes. Type 1b traces are abundant in paleosols; in many intervals they are the only visible biogenic structures.

(c) Large Rhizohaloes—Vertical, downward-tapering zones of green coloration within red matrix, up to 15 cm maximum width, over 1 m long (Fig. 7B), some branching. Type 1c traces are rare and are found associated with Type 1b traces and thoroughly bioturbated units only in strongly developed paleosols.

Type 1 traces are interpreted as root casts and molds (rhizoliths) and redoximorphic zones produced by roots (rhizohaloes) and, as such, are hygrophilic (Hasiotis 2004, 2008; Kraus and Hasiotis, 2006). The length of the root is the approximate depth to the vadose zone. Type 1a

rhizoliths are interpreted as root molds remaining in the sediment after root decay (Klappa 1980; Kraus and Hasiotis 2006). Pits on the walls may represent rootlets radiating from the main root. Shallow roots represent proximal settings on crevasse splays with shallower water tables, whereas deeper roots represent more distal settings and deeper water tables.

Type 1b and 1c rhizoliths are classified as rhizohaloes (Kraus and Hasiotis 2006). Type 1b rhizoliths are interpreted as reduced zones around shallow roots. Reduction zones were produced during life processes and from decay of the root material after death (Kraus and Hasiotis 2006). Rhizolith abundance suggests a vegetative ground cover was present. The rhizoliths cannot be assigned to a particular group of plants, but Type 1b traces likely represent herbaceous ferns based on the dominant plant macrofossils of the MF (Parrish et al. 2004). Type 1c rhizohaloes (Fig. 7B) probably represent either locations where roots intersected the intermediate vadose zone (Hasiotis 2004, 2008) or taproots that extended down to a seasonally low-water table.

Type 2—*Planolites* isp. (Fig. 7C).—Horizontal, generally straight, unlined, unbranched, smooth-walled tubes; cylindrical to elliptical in cross section with short axes perpendicular to bedding. Maximum long-axis widths range from 0.3 to 1.0 cm. Lengths are variable, from 2.4 to 4.4 cm, and all examples are broken at both ends. Most are filled with the same material as the surrounding matrix. The fill shows no preferential arrangement of grains and typically weathers out as cylindrical casts, leaving behind elongate concavities on the bottoms of beds. These traces are found in sheet and ribbon sandstones and are sparse, rarely intersecting each other. This trace is also present in paleosols within the heterolithic lithofacies, where it is preserved poorly and associated with massive bedding. Type 2 traces in paleosols may be filled with up to sand-sized particles from the overlying sheet sandstone.

Type 2 traces were assigned to *Planolites* isp. We interpret elliptical burrow cross sections as the result of postdepositional compaction of a burrow that was originally circular in cross section. Trace type 2 was likely constructed by a small invertebrate, but the tracemaker cannot be assigned to any taxonomic group because such a simple trace can be constructed by a variety of invertebrates (Bromley 1996; Hasiotis 2002, 2004, 2008). Trace properties suggest that each was an open burrow that was later filled by sediment. The traces are ubiquitous in continental settings and do not appear to be organism or environment specific. The nature of its construction, however, indicates that the tracemakers were living in the vadose zone (hygrophilic behavior) or near the sediment-water interface under bodies of standing water where the water table intersected the surface (hydrophilic behavior) (Hasiotis 2004, 2008).

Type 3—cf. *Scolicia* isp. (Fig. 7D).—Straight to meandering, unbranched, horizontal furrows and furrow casts. Widths are uniform and < 1 cm. Parallel, raised rims flank the margins of some furrows. Trails may be interrupted by deeper, bilaterally symmetrical, ovate depressions that are slightly wider than the width of the trail. Some of these traces are associated with round to spiral depressions in the sediment. Type 3 traces are in convex hyporelief on the bases of sheet sandstone beds, and in epirelief on bedding surfaces of sheet and ribbon sandstones.

Type 3 traces are compound traces and represent multiple behaviors. The morphology of the groove-like portions is consistent with that of locomotion trails made by gastropods (e.g., Yochelson and Fedonkin 1997; Hasiotis 2004, 2008; Fig. 7E). Traces are similar to *Scolicia*, which has two convex ridges separated by a deep, medial groove (Häntzschel 1975). Even though *Scolicia* is typically attributed to echinoids (e.g., Donovan et al. 2005), the basic description fits the observed trace morphology best. Ovate and spiral depressions are likely

resting and feeding traces where the shell or foot pressed into the sediment before the tracemaker continued on its course (Hasiotis 2004, 2008). The depositional setting indicates that the tracemakers were likely freshwater gastropods. Type 3 traces are hydrophilic and were created on saturated sediments in subaqueous environments (Hasiotis 2004, 2008). Traces in convex hyporelief on the bases of sheet sandstones are casts of traces originally made in the underlying mudstone. These traces overprinted the surfaces of weakly and moderately developed paleosols that became flooded during avulsions or extrachannel depositional events.

Type 4—cf. *Steinichnus* (Fig. 7F, G).—Straight to curved, branched and unbranched, horizontal to subhorizontal burrows < 1 cm wide. Individual burrows vary slightly in width along their length. Some burrow walls have narrow, elongate scratches that are parallel or oblique to the length of the furrow (Fig. 7F), although many have smooth walls. Many of these traces are found in relatively dense, intersecting networks and follow the contours of bedding surfaces, especially depressions and dinosaur tracks (Fig. 7G). Size, density, and intersection angles unite all type 4 traces, regardless of surface morphology. Type 4 traces are preserved in sheet sandstones in convex hyporelief on the bottoms of beds, and in epirelief on bedding surfaces.

Type 4 traces are most similar to *Steinichnus* isp. and show morphologic characteristics attributed to mud-loving beetles (Heteroceridae) (Chamberlain 1975; Ratcliffe and Fagerstrom 1980; Hasiotis 2002). Lack of characteristic striations on burrow walls in many examples is likely due to poor preservation. The traces are hygrophilic and were likely excavated at or just above the sediment-water interface in close proximity to the sediment-atmosphere interface (Clark and Ratcliffe 1989; Hasiotis 2004, 2008). Preservation indicates that type 4 traces were created in both sheet sandstones and weak paleosols. Although these traces are found in

depressions, none are associated with desiccation cracks, suggesting that they formed in saturated sediments rather then in evaporating pools of standing water. Those conditions indicate locations proximal to the paleochannel.

Type 5—*Cochlichnus* isp. (Fig. 8A).—Horizontal, sinusoidal furrows and furrow casts of uniform depth and width found on the surfaces of bedding planes. Furrows are < 0.4 cm in diameter and lengths are variable, but sinuosity is regular. The longest observed continuous trace is 98 cm long. Some examples are discontinuous and appear as a series of S-shaped furrows that have been translated diagonally from each other (Fig. 8A). These are presumed to represent segments of the same trace. Type 5 traces are preserved in convex hyporelief on the bases of sheet sandstones, indicating that they were produced in the underlying paleosol. The largest of these traces are preserved in epirelief in sheet sandstones associated with flat-topped current ripples. The traces are sparse where they are present.

Trace type 5 is assigned to *Cochlichnus* isp., which is attributed to the locomotion of an annelid (Hitchcock 1858; Moussa 1970) or insect larvae (Metz 1987). Examples from the MF were likely produced by aquatic oligochaetes, based on the width and length of the trails. The traces are hydrophilic and indicate activity at or just below the sediment-water interface in a film of water probably < 1 mm deep on the sediment surface (Moussa 1970; Hasiotis 2002, 2004, 2008). Discontinuous traces (Fig. 8A) are attributed to saltation during locomotion, indicating slightly deeper water.

Type 6—cf. *Ancorichnus* isp. (Fig. 8B).—Straight, unbranched, horizontal to vertical burrows with meniscate backfill and a discontinuous mantle of sediment. Burrows are 1 cm or less in diameter; a mantle up to 0.2 cm wide may or may not be present. Adjacent burrows may share a mantle (Fig. 8B). In some cases, an individual burrow changes from horizontal to a

vertical orientation at fractures in the host rock. Some examples contain menisci alternating with narrow voids that may have been filled originally with mudstone. This trace is found in sheet sandstones and is relatively rare in the study areas. Type 6 traces are found in areas with low trace-fossil abundances and are associated typically with massive bedding.

Type 6 traces are interpreted as backfilled burrows similar to *Ancorichnus* isp. (Frey et al. 1984) that were created as the tracemaker tunneled through the sediment and pushed excavated material posteriorly. Continental traces with this morphology are attributed to beetles (Coleoptera; Counts and Hasiotis 2009) and are classified as hygrophilic. Cicada nymphs (Hemiptera: Cicadidae) construct similar burrows and are another possible tracemaker (Willis and Roth 1962; Smith and Hasiotis 2008; Smith et al. 2008b). They were probably constructed in soft, cohesive sediments below the sediment-atmosphere interface in subaerially exposed sediment (Hasiotis 2004, 2008).

Type 7—cf. *Cylindricum* isp. (Fig. 8C).—Straight to slightly irregularly sinuous, unbranched, smooth-walled vertical to subvertical tubes. Tubes range from 0.5 to 1.1 cm in diameter and 5 to 27 cm long; width-to-length ratios vary from 1:10 to 1:25. Some tubes have simple, rounded terminations, but many penetrate into less resistant beds, which preserve trace fossils more poorly than more resistant beds. The total depth and termination type are unknown but appear not to be much longer than maximum observed depths, based on examples where tubes in erosive beds terminate at the boundary between the erosive bed and an underlying resistant bed. In many cases, the tubes are filled with massive sandstone, which weathers out as cylindrical casts. Tubes are relatively widely distributed laterally with no apparent dense accumulations. Type 7 traces are found in sheet sandstones and penetrate into underlying mudstone but have been eroded or are not preserved. The traces are typically associated with

and crosscut well-preserved, ripple- and climbing ripple-laminations in the sheet sandstones. The density of associated trace fossils ranges from high to low and tiering is evident locally. For example, where trace type 7 is found with cf. *Termitichnus* (type 9), cf. *Termitichnus* traces penetrate to a depth of more than four times the maximum depth of the type 7 traces.

Burrow dimensions and morphology of type 7 traces are most similar to *Cylindricum* (Linck 1949). Although burrow lengths fall within the range given for *Skolithos*, type 7 burrow diameters are larger than the 15 mm limit for *Skolithos* (Alpert 1974). The ratio of width-to-length, however, may be important in distinguishing *Cylindricum* from burrows that are grossly similar to it in morphology. Type 7 traces cannot be attributed to a particular tracemaker with certainty because many organisms construct vertical burrows, including plant roots, spiders (Araenae), tiger beetle larvae (Coleoptera: Cicindelidae), wasps (Hymenoptera), worms (Annelida), cicadas (Hemiptera: Cicadidae), and crickets (Orthoptera: Gryllidae) (e.g., Chamberlain 1975; Hasiotis 2002; Gregory et al. 2006). Even though the moisture requirements of the tracemaker are unknown, the orientation and preservation of the traces suggest that they were created in the vadose zone (terraphilic and hygrophilic) and their length can be used to infer areas of higher moisture levels or minimum water table depth. Larger diameter tubes could be small crayfish burrows (*Camborygma* isp.) (Hasiotis and Mitchell 1993); however, evidence is inconclusive. Tiering may indicate bioturbation during two paleohydrologic settings or the different moisture preferences of different soil organisms at the same time. Because none of the burrows crosscut each other, their relative timing cannot be established. The morphology of this trace fossil, however, is most similar to burrows produced by tiger beetles based on comparisons to modern burrowing organisms (e.g., Chamberlain 1975; Ratcliffe and Fagerstrom 1980; Pearson and Vogler 2001; Hasiotis 2002; Hasiotis et al. 2012 in press). The orientation and

preservation of these traces, as well as the inferred moisture regime is in line with our interpretation that tiger beetles constructed the burrows in a subaerial setting.

Type 8—cf. *Macanopsis* (Fig. 8D–E).—Vertical, smooth-walled tubes with consistent diameters identical to trace type 7, except each has a hook-shaped termination at the lowermost extent of the burrow. This termination can be a simple horizontal extension, giving the burrow a J-shaped appearance (Fig. 8D) or an upturn followed by a downturn (Fig. 8E). The traces are found associated with ripple and climbing ripple lamination exclusively in sheet sandstones. None of the vertical tubes that penetrate the sheet sandstones are preserved in the underlying mudstones. Some of the tubes may have penetrated the underlying mudstones and had J-shaped terminations that were not preserved.

The morphology of type 8 traces is similar to *Macanopsis* isp. (Macsotay 1967). Modern traces with this morphology are created by rove beetles (Coleoptera: Staphylinidae), dung beetles (Coleoptera: Scarabaeidae), crickets (Orthoptera: Gryllidae), spiders (Araenae), and earthworms (Annelida: Oligochaeta) (Bown and Kraus 1983; Chamberlain 1975; Ratcliffe and Fagerstrom 1980; Hasiotis, unpublished data). The traces are likely hygrophilic and were produced above the water table in moist sediments (Hasiotis 2004, 2008), based on their association with bioturbated ripple-laminated sheet sandstones. The consistency of diameters through direction changes suggests that the traces were created in firm sediment that allowed the burrow to remain open without collapse.

Type 9—cf. *Termitichnus* (Fig. 8F–H).—Mainly straight, vertical to subvertical features that range from small- to large-diameter shafts with distinctive pitted texture on the walls; the pitting is the surficial expression of dense, interconnected and interpenetrating tunnels. In other cases, elongate zones of irregular, interconnected tunnels occur without a distinct boundary and

do not appear to radiate from a central tube. Diameters range from 0.8 to 15 cm and vertical lengths reach 39 cm. Many penetrate entire beds so the total depths are unknown. Some sets of adjacent shafts and zones of interconnected-interpenetrated tunnels appear to be connected by horizontal to subhorizontal single tunnels to multiple tunnels that follow bedding planes. Well-preserved traces of this type contain walls up to 1 cm thick that are composed of reworked matrix material (Fig. 8G, H). The walls of many of these traces appear lighter in color than the surrounding rock. The traces occur in dense clusters locally in sheet sandstones. Primary sedimentary structures adjacent to the traces are not disrupted, except where a wall is present. Many examples appear to have penetrated into the underlying paleosol.

The texture of type 9 traces is similar to the earthen packing of termites (Blattodea; termites; Hadlington 1966; Darlington 2005; Laza 2006; Tschinkel 2010). Trace morphology and orientation are similar to the vertical nests and galleries of *Termitichnus* (Bown 1982; Hasiotis 2002) and the texture is similar to that of *Barberichnus* (Laza 2006), both of which are attributed to the activity of termites. The dominant vertical orientations of these traces may represent termite nests constructed in and around plant stems and downward along plant roots, similar to those constructed by extant termites of the families Rhinotermitidae and Kalotermitidae (e.g., Noirot 1970; Lee and Wood 1971; Hasiotis and Demko 1998; Hasiotis 2002, 2004, 2008; Tschinkel 2010). Some of the termite traces may have been associated with upright vegetation and their roots, which were buried by sand during a flood, and termite nest construction may have followed roots into the sheet sandstones after the death of the tree. These traces are terraphilic (Hasiotis 2004, 2008) and suggest relatively low water tables.

Type 10—cf. *Celliforma* (Fig. 9A).—A single vertical tube similar to trace type 7 terminating in multiple, horizontal to subhorizontal, overprinted cells at the end of subhorizontal

branches from the main tube. The entire trace is up to 18 cm long and five–six distinct cells are visible in cross-section exposed by outcrop. Cells are up to 2 cm long, about 0.5 cm wide, and are roughly cylindrical. Where well preserved, the cells exhibit slight constrictions proximal to the main tube. They are smooth-walled with rounded, convex terminations. Cells appear to be cut longitudinally and obliquely in one single longitudinal exposure suggesting that they radiated from the main shaft in multiple directions. This trace type is found only in sheet sandstones. Examples of cf. *Celliforma* may have been present in soils, but were not preserved due to proisotropic pedoturbation.

The morphology of type 10 traces is most similar to nests created by ground-dwelling, solitary bees and wasps (Hymenoptera; Sakagami and Michener 1962; Ratcliffe and Fagerstrom 1980; O'Neill 2001) and closely resembles the ichnogenera *Celliforma* (Brown 1934; Elliott and Nations 1998) and *Cellicalichnus* (Genise et al 2002). The traces are hygrophilic to terraphilic and were created in moist sediment above the water table (Hasiotis 2002, 2004, 2008). The relatively low number of chambers indicates that these nests were in use for only a short period of time and that the tracemaker was not social (e.g., Michener 1974).

Type 11—cf. *Camborygma*. (Fig. 9B–C).—Vertical, smooth-walled tubes 4 to 11 cm in diameter. The tubes penetrate the entire thickness of the beds in which they are found (up to 0.5 m) so their total length is unknown. Some widen with depth and appear to turn towards the horizontal at depth. The tops of the tubes intersect the upper bedding plane at right angles and produce circular openings. Several closely spaced entrances (tens of centimeters apart) have been observed on a single slab (Fig. 9C). Walls are not smooth but do not contain well-preserved surficial morphology. The traces are found exclusively in sheet sandstones.

The vertical orientation and architecture of type 11 traces are consistent with burrows

constructed by crayfish (Decapoda: Cambaridae and Parastacidae) and are similar to those of the ichnotaxon *Camborygma* isp. (Hasiotis 1993; Hasiotis and Mitchell 1993). The traces cannot be assigned with certainty to this ichnotaxon however, because of a lack of surficial morphology. The trace fossils are similar to burrows from Permian, Triassic, Jurassic, Paleocene, and Eocene strata attributed to crayfish (Hasiotis and Mitchell 1993; Hasiotis and Honey 2000; Hasiotis 2002, 2004, 2008; Smith et al. 2008a). They are also similar to modern crayfish burrows (Hasiotis and Mitchell 1993). These traces are hydrophilic and are used as water table indicators (Hasiotis 2002, 2004, 2008). The cf. *Camborygma* burrows suggest a water-table depth of ~0.5 m locally at the time of burrow emplacement, based on their depths.

Type 12—Y-shaped vertical burrows (Fig. 9D).—Vertical to subvertical, mostly straight, upward-bifurcating tubes with smooth to pitted walls. The tubes are ~1 cm in diameter and show no evidence of substantial narrowing or widening. The angle between the branching tubes is acute, from 20 to 40º. Some appear to divide into two branches of equal size, whereas others appear to have one dominant vertical tube with an angled subordinate branch.

Type 12 traces traces are found only in sheet sandstones and are relatively rare in the study areas. They crosscut primary sedimentary structures and are typically associated with climbing ripple-laminations. Associated traces include cf. *Cylindricum* (type 7), cf. *Macanopsis* (type 8), cf. *Termitichnus* (type 9), and sauropod tracks (type 17).

Type 12 traces are similar in morphology to orthopteran and rove beetle (Coleoptera: Staphylinidae) burrows (Ratcliffe and Fagerstrom 1980; Villani et al. 1999), although other arthropod tracemakers cannot be ruled out. The traces are terraphilic and were likely constructed in relatively moist sediments above the water table because of the sharp boundary between the burrow wall and the burrow fill in the horizontal and vertical components of the burrows

(Hasiotis 2004, 2008).

Type 13—U-shaped tubes—cf. *Arenicolites* isp. (Fig. 8A).—U-shaped, vertical tubes < 0.5 cm in diameter that are up to 3 cm deep. Diameter is fairly consistent throughout the tube length. The traces are rarely exposed in cross section and are seen typically only as paired, round openings or circular casts of equal size in hyporelief on bedding surfaces (Fig. 8A). In cross section, the traces do not have spreiten and may connect to horizontal tubes below the surface. The traces are found only in sheet sandstones and ribbon sandstones, although paired burrow openings in convex hyporelief on the bottoms of sandstone beds likely indicate that U-shaped tubes were present in underlying paleosols. In sandstones, the traces are associated with current ripple laminations.

Type 13 traces are similar to *Arenicolites* isp. and were likely constructed by aquatic insect larvae of chironomids (Diptera) or ephemeropterans (Ephemeroptera) (e.g., Ward 1992; Merritt and Cummins 1996; Hasiotis 2002; Hasiotis 2004, 2008; Gingras et al. 2007). The traces are hydrophilic and represent relatively low-energy environments where surface water was present (Hasiotis 2002; Hasiotis 2004, 2008).

Type 14—cf. *Lockeia* (Fig. 9E, F).—Elliptical bulges up to 6 cm wide, about 9 cm long, and up to 5 cm deep; and bilaterally symmetrical across their long axes. Few contain a longitudinal ridge along the entire length of the long axis. Some of these traces are found adjacent to, and at irregular intervals within, long, unbranched, curved trails with variable widths up to 1 cm (Fig. 9F). The trails are not as deeply penetrating as the bulges. The traces are preserved in convex hyporelief in sheet sandstones. Some are also found in sheet sandstones and in the lateral margins of ribbon sandstones.

The symmetrical bulges composing type 14 traces are interpreted as pelecypod resting

traces similar to *Lockeia* isp. (Häntzschel 1975; Maples and West 1989). We interpret the associated trails as the locomotion trails of pelecypods (Hasiotis 2004, 2008; Lawfield and Pickerill 2006; Hasiotis et al. 2012 in press). Based on the dominant bivalve fossils from the MF, the tracemaker is probably a unionid bivalve (Good 2004). Type 14 traces overprinted the surfaces of weakly and moderately developed paleosols that became flooded and scoured during avulsions or extrachannel depositional events; the traces were filled later with sand as the sand moved along the base of the sheet and ribbon channels. These traces are hydrophilic and represent subaqueous, freshwater conditions that were perennial, based on the physiology and behavior of extant freshwater bivalves (Evanoff et al. 1998; Good 2004; Hasiotis 2004, 2008).

Type 15—cf. *Kouphichnium* isp. (Fig. 9G).—This trace type appears as a series of multiple, elongate depressions to scratches < 2 cm long. Depressions and scratches are arranged in bilaterally symmetrical trails with the long axes of the depressions oriented parallel to the long axis of the trail. The traces are rare and found on the sole of sheet sandstones, suggesting that the traces were made in the sediment of underlying paleosols.

Type 15 traces are interpreted as the locomotion trackways of arthropods. In particular, they resemble *Kouphichnium* isp. and morphologies that grade from *Kouphichnium* isp. to *Limulicubichnus* isp., and are interpreted as the trails of freshwater horseshoe crabs (Eagar et al. 1985; Miller and Knox 1985; Hasiotis and Demko 1996; Hasiotis 2002, 2004, 2008). The traces are hydrophilic and indicate moist to saturated sediment conditions because the scratches within the trails are sharp, well formed, and preserve fine details (Hasiotis 2002, 2004, 2008; Fairchild and Hasiotis 2011).

Type 16—Crocodilian traces—cf. *Hatcherichnus sanjuanensis* (Fig. 10A).—Tetradactyl footprints or groups of four parallel scratches (See trace type 19). None have well-

defined heel impressions. Some are associated with smooth, wide, elongate troughs oriented in the same direction as the long axes of the footprints. The best example of this trace contains impressions of both a forefoot (manus) and hind foot (pes). The manus is 12 cm long and 9 cm wide and has three clear digits. The digits increase in length medially. The pes oversteps the manus and only has three discernable digits, which appear weathered and obscured partially by a possible tail or body trace. The visible portion of the pes print is about 15 cm long and about 14 cm wide. The elongate digits of this footprint curve away from the manus track. The manus–pes set is isolated on a small slab and there is no evidence of an associated trackway. The traces are preserved in convex hyporelief on the soles of sheet sandstones and are presumed to have been created in the underlying paleosols.

The manus–pes set of trace type 16 appears crocodilian and is similar to *Hatcherichnus sanjuanensis* from the MF (Foster and Lockley 1997). The elongate depressions are interpreted as tail or body drag marks; these are associated commonly with crocodile tracks (Foster and Lockley 1997). Possible tracemakers are Goniopholid crocodiles, which are known from skeletal material from the MF (Mook 1933, 1967). The traces are epiterraphilic to hydrophilic (Hasiotis 2004, 2008) and indicate proximity to the paleochannel.

Type 17a–c—Sauropod tracks.—The traces in cross section appear as large convex bulges or downward deformations of bedding (Fig. 10B). Some of the bulges contain parallel, vertical to subvertical striations and rare digit impressions. In plan view, the traces are generally subcircular in shape. Three distinct morphotypes are recognized, though many contain no well-defined features:

(a) Large rounded blocks with a tapered rear end and a wide, blunt or stair-stepped anterior margin 30 to 50 cm long and 29 to 37 cm in maximum width (Platt and Hasiotis 2006).

The anterior portion may contain three to four parallel, vertical to subvertical striations.

(b) Large subcircular depressions, 46 cm long and 50 cm wide, with one pair of opposite sides pinched in toward the middle of the trace. The surface of this trace contains grooves and in some places is offset vertically, dividing it into several distinct pads (Platt and Hasiotis 2006).

(c) Rounded ellipses with a tapered end and a large digital protrusion on one side (Platt and Hasiotis 2006). The traces are preserved mostly in convex hyporelief at the base of sheet sandstone beds. This suggests that the actual trace was a depression created in the underlying mudstone of weak paleosols and filled by sand. There are also several examples of this trace in both the ribbon sandstones and sheet sandstones in the heterolithic lithofacies. Type 17a is the most common morphotype, although types b and c, if preserved poorly, can be mistaken for type a. No trackways are visible in the study areas; all of the traces are isolated examples.

Type 17 traces are interpreted as sauropod dinosaur footprints based on morphology. Examples of type 17a are consistent with sauropod pes prints, including those assigned to *Brontopodus birdi* (Farlow et al. 1989; Thulborn 1990; Lockley et al. 1994). Type 17b is interpreted as a titanosauriform manus track similar to *Brontopodus birdi* (Farlow et al. 1989). Type 17c is interpreted as the impression of a sauropod manus in which digits II to V were bound together in a rigid structure and digit I protruded medially. This morphology is consistent with the manus of a diplodocid sauropod (Bonnan 2003). All of the tracks are epiterraphilic, but their depths indicate moist to near saturated sediments (Platt and Hasiotis 2006; Platt et al. in review).

Type 18 a–b—Tridactyl vertebrate footprints (Fig. 10C–G).—Tridactyl footprints that range from 7 to 51 cm long and 8 to 42 cm wide. Some are indistinct and resemble deep sauropod tracks (type 17), but many have three visible digits and an asymmetrical profile in cross

section. Two morphotypes are recognized:

(a) Tridactyl tracks with long, slender toes with relatively wide angles of divarication from 34º to 57º between individual toes and 74º to 93º total divarication. Some of the traces have associated claw impressions (Fig. 10E) and middle digits that are longer than the marginal digits (Fig. 10C, D), and some have digits that are curved slightly. Well-preserved examples have vertical striations on the sides, and one contains evidence of digit I (Fig. 10G; Platt et al. 2010). Small tracks under 15 cm long are abundant, and large tracks greater than 30 cm long are rare. Intermediate sizes are absent.

(b) Tridactyl tracks with relatively short, thick digits and wider angles between digits. The digits appear to be about the same length and width, except in rare examples where the middle digit is significantly wider than the outer digits. All of these tracks have heel impressions. Most of the traces are preserved in convex hyporelief on the base of sheet sandstones and were created originally in the underlying mudstones of weak paleosols. Rare natural casts weather out and are found in talus slopes below sheet-sandstone outcrops. Rare examples and underprints matching the dimensions of these tracks are found in the sheet sandstones. There is at least one location where a tridactyl track is present in a ribbon sandstone. All examples of this trace type are isolated fossils; no trackways are exposed. Some of the traces are surrounded by concentric fractures (sensu Allen 1997) that mirror footprint morphology (Fig. 10E, F). Some of the tracks also contain radial cracks (Lockley et al. 1989; Nadon 1993).

Type 18a traces are interpreted as the tracks of theropod dinosaurs based on morphology (Thulborn 1990 and references therein). The bimodal size range suggests at least two different trackmakers. Smaller tracks may belong to small theropods like *Ornitholestes*, whereas large tracks may belong to *Allosaurus*. Both of these dinosaurs are known from skeletal material in

the upper MF in the Bighorn basin (Ayer 1999). The tracemaker of type 18b is more uncertain because these track morphologies are less distinct, and, thus, they may belong to theropods or ornithopods. The tracks of these dinosaurs are extremely difficult to differentiate, especially when poor preservation and sediment variation are considered (Thulborn 1990).

Type 18 traces are epiterraphilic (Hasiotis 2004, 2008) and represent locomotion across moist sediments. Concentric fractures and radial cracks may indicate drying, although distinct desiccation cracks are absent. The fractures may also represent areas where the sediment was bound by algal mats.

Type 19—Vertebrate swim traces (Fig. 10H).—Groups of three or four closely spaced, parallel grooves of equal to subequal width. Groove lengths vary from about 1.5 to 3 cm. Adjacent grooves may be offset by a few millimeters. The area between grooves is raised also in some specimens (Fig. 10H). The traces are found in convex hyporelief on the base of sheet sandstones, indicating that they were created on the surfaces of the underlying paleosols.

We interpret type 19 traces as swim tracks produced by the anterior portion of the foot of a vertebrate scraping the sediment surface. The absence of impressions of the posterior margin of the feet suggests that the tracemaker was at least partially supported by water and used its feet to propel itself forward. These traces are, therefore, hydrophilic (Hasiotis 2004, 2008). Some of these tracks may be crocodilian, (See type 16), while others resemble closely turtle traces (Fig. 10H, cf. Foster et al. [1999]). The raised areas present between some of these traces may indicate depressions created by interdigital webbing (Fig. 10H).

Ichnocoenoses

GPS data.—Discrete trace-fossil data comprise four layers, each corresponding to a

different stratigraphic interval within the heterolithic lithofacies. The layers of trace-fossil data, in stratigraphic order, are (1) trace fossils preserved in convex hyporelief on the base of the lower sheet sandstone, (2) trace fossils within the lower sheet sandstone, (3) trace fossils preserved in convex hyporelief on the base of the upper sheet sandstone, and (4) traces within the upper sheet sandstone. Most trace-fossil assemblages within individual layers are not laterally extensive or contain sparse data points and did not benefit from cluster analysis, i.e., we interpret the entire layer as a single ichnocoenosis. Trace fossils preserved in convex hyporelief on the base of the upper sheet sandstone, however, were of sufficient abundance, lateral extent, and density to use cluster analysis to distinguish multiple ichnocoenoses.

In addition to discrete trace-fossil layers, ubiquitous (not amenable to measurement by GPS) trace fossils are present in paleosols in the heterolithic lithofacies and the mudstone lithofacies. Traces within ribbon sandstones are also not included with layers of GPS data because of their limited areal extent.

Rhizohalo Ichnocoenosis.—This ichnocoenosis is present within paleosols in the heterolithic lithofacies and the mudstone lithofacies and it consists of large numbers of relatively dense rhizoliths (type 1b), the majority of which are < 10 cm deep. Type 1c rhizoliths are isolated and rare. *Planolites* (type 2) and cf. *Cylindricum* (type 7) are rare, but present also, in addition to bioturbation.

The massive fabric of the paleosols indicates a high ratio of bioturbation to sedimentation and the influence of proisotropic pedoturbation (Kraus 1999; Hasiotis and Honey 2000; Hasiotis 2004, 2007, 2008). Variation in rhizolith depth indicates water-table fluctuation, although the relationships between the rhizoliths are not clear because of their vertical proximity to each other resulting from low sedimentation rates. The maturity of the paleosols suggests that these

communities persisted for a relatively long time with no major perturbations. Relatively stable conditions would have allowed ample time for significant organism diversification in the original community (e.g., Goulden 1969). For this reason we interpret the small number of trace types as the result of the loss of ichnofossil diversity due to overall pedoturbation—bioturbation and physical pedoturbation (Johnson et al. 1987; Hasiotis 2004, 2007, 2008).

The traces in this ichnocoenosis are predominantly hygrophilic (Fig. 11), indicating that sufficient water was available in the soil to support a vegetative ground cover with little deep fluctuation in the water table. Deeper roots (type 1c) might indicate: 1) deeper, more penetrative wetting fronts and deeper water tables in a distal floodplain setting, or 2) higher moisture-loving plants with roots that penetrate into areas of great moisture or into the water table. The type and maturity of paleosol in which the rhizoliths are found indicate the conditions under which deeper and larger plant roots were produced.

Cf. *Steinichnus* Ichnocoenosis.—This ichnocoenosis is present in two stratigraphic positions: on the base of the lower sheet sandstone (Fig. 11) and on the base of the upper sheet sandstone (Fig. 12). Both examples of this ichnocoenosis have slight differences in trace fossil composition, but the four most abundant traces are cf. *Steinichnus*, *Cochlichnus*, cf. *Lockeia*, and cf. *Arenicolites*. Tridactyl tracks and swim traces are also present in both examples, while the example on the base of the upper sheet sandstone also contains some sauropod tracks, *Planolites*, and cf. *Kouphichnium*. Many of the vertebrate tracks are deeply impressed and indistinct, but some are very well preserved and show detailed foot morphology (e.g., Jennings et al. 2006; Platt and Hasiotis 2006). Some of the deep tracks are lined with networks of cf. *Steinichnus* (Fig. 7G). The mudstones underlying the sheet sandstones do not contain animal traces, but rhizohaloes are abundant.

We interpret the two examples of this ichnocoenosis as two separate occurrences of the same original paleocommunity. Not only is the composition of each trace-fossil assemblage similar, but their moisture profiles also contain two dominant moisture regimes: hydrophilic and hygrophilic (Figs. 9, 11). This ichnocoenosis may, therefore, represent two different suites (*sensu* Bromley and Asgaard 1979), each representing a community living in the same location, at different times under different environmental conditions.

We argue that this trace-fossil assemblage represents a single ichnocoenosis in the sense that the hygrophilic and hydrophilic suites represent a single community of tracemakers within a spectrum of paleohydrological conditions. Cf. *Steinichnus* and *Cochlichnus* likely formed close to the sediment-water-air interface—the same position for these three media—and, therefore, represent saturated but subaerial conditions to extremely shallow standing water (Hasiotis 2002, 2004, 2008). Cf. *Lockeia*, cf. *Arenicolites*, vertebrate swim traces, and cf. *Kouphichnium* indicate deeper standing water. Vertebrate tracks are classified as epiterraphilic, but their preservation suggests saturated to moist sediment (Laporte and Behrensmeyer 1980; Jennings et al. 2006; Platt and Hasiotis 2006; in review). We interpret the hydrophilic suite as representing areas where standing water was present, while the hygrophilic suite represents margins of ponded water, where the water table intersected and fell below the sediment-air interface. We interpret the rhizohaloes as representing a vegetated landscape that was flooded and retained standing water deep enough for the hydrophilic traces to be produced. We interpret the hygrophilic suite of traces as representing a fall in the level of surface water resulting from infiltration into the soil. The timing between the two trace fossil suites is uncertain, but the conditions they represent are likely separated by a relatively short amount of time because they are both preserved on the same surface; this implies relatively short-lived periods of standing

water.

Cf. *Termitichnus* Ichnocoenosis.—The cf. *Termitichnus* ichnocoenosis (Fig. 11) is found exclusively in the lower sheet sandstone, where the trace-fossil assemblage includes cf. *Termitichnus* associated with type 1a rhizoliths, *Planolites*, cf. *Cylindrichum*, tridactyl tracks, *Cochlichnus*, sauropod tracks, cf. *Scolicia*, and vertebrate swim traces. Termite and associated rhizoliths regularly penetrate the entire thickness of the sheet sandstone. Cf. *Cylindrichum* traces form a shallow tier ~6 cm below the top of the sheet sandstone.

Moisture regimes of the trace fossils in this assemblage vary greatly, and we restrict the cf. *Termitichnus* ichnocoenosis to the deep terraphilic traces, i.e., cf. *Termitichnus*, because the moisture regime they represent is mostly incompatible with the moisture regimes represented by the rest of the trace fossils in the assemblage. We assign the hydrophilic, hygrophilic, and shallow terraphilic traces to the *Planolites* ichnocoenosis. Even though cf. *Cylindrichum* may be compatible with cf. *Termitichnus*, we exclude it from the cf. *Termitichnus* ichnocoenosis because cf. *Cylindrichum* occupies a shallow tier that is representative of a higher water table level than cf. *Termitichnus*, and it is a major component of the *Planolites* ichnocoenosis elsewhere in the study area (Fig. 11).

The association of cf. *Termitichnus* and deep rhizoliths (Type 1a) is consistent with formation in the vadose zone with a water table deeper than the ~0.5 m thickness of the sheet sandstones. The ultimate depth of trace fossils in this ichnocoenosis is unknown because the traces presumably continued into the underlying mudstone and were not preserved. We interpret the cf. *Termitichnus* ichnocoenosis as the result of a fall in water table after the period of shallow standing water to saturated sediment represented by the *Planolites* ichnocoenosis. In this interpretation, cf. *Termitichnus* traces represent a unique paleocommunity that occupied the same

position in the sheet sandstone as the paleocommunity represented by the *Planolites* ichnocoenosis. The exact amount of time that passed between the initial group of tracemakers and the next group of tracemakers is uncertain, but enough time must have passed to allow for the establishment of vegetation. The amount of time represented is still relatively short based on the small size and sparse nature of rhizoliths.

***Planolites* Ichnocoenosis.**—This ichnocoenosis (Fig. 11) is present in the upper sheet sandstone, where it comprises, in decreasing order of abundance, *Planolites*, cf. *Cylindrichum*, tridactyl tracks, cf. *Ancorichnus* , cf. *Macanopsis*, cf. *Steinichnus*, cf. *Celliforma*, and cf. *Arenicolites*. The trace-fossil assemblage in the lower sheet sandstone associated with the cf. *Termitichnus* ichnocoenosis shares the same three most abundant traces and is also assigned to the *Planolites* ichnocoenosis. This example of the ichnocoenosis also contains *Cochlichnus*, sauropod tracks, cf. *Scolicia*, and swim traces. All vertically oriented trace fossils originate from the contact between the sheet sandstone and overlying mudstones and are < 20 cm deep. All traces are fairly sparse in distribution with no crosscutting or tiering.

Even though the less common trace types in the two examples of this ichnocoenosis are different, they are still compatible in terms of moisture regimes. For example, both instances of the ichnocoenosis have different hydrophilic traces, but those traces are rare, so their absence in one observed assemblage does not mean they would not present given greater exposure in the field area. The range in moisture regimes represented is greater than that present in the cf. *Steinichnus* ichnocoenosis, but we still argue that this ichnocoenosis represents a single paleocommunity with regular trophic interactions occurring between organisms.

Each sheet sandstone appears to have been deposited in a single, rapid event, preventing colonization during deposition because most of the traces originate from the upper surface of the

sandstone. The low density of traces indicates that the sandstone surface was exposed only for a short time before it was buried below the depth to which bioturbation was occurring or it was below the water table. Minimal exposure time may also explain the lack of rhizoliths. The high gradient in moisture regimes and the short exposure time imply rapid infiltration of standing water. Given enough time, when the water table dropped low enough and arborescent vegetation began to establish itself, termite activity resulted in the cf. *Termitichnus* ichnocoenosis overprinting the *Planolites* ichnocoenosis; the fact that this occurred only in the lower sheet sandstone suggests that the lower sheet sandstone was exposed for a longer period of time than the upper sheet sandstone.

Vertebrate Track Ichnocoenosis.—A combination of sauropod and tridactyl tracks dominate four of the five clusters on the base of the upper sheet sandstone (Figs. 12, 13). Many of these vertebrate tracks are deep with relatively poor preservation. Other traces present are cf. *Steinichnus*, cf. *Lockeia*, cf. *Arenicolites*, *Planolites*, swim traces, *Cochlichnus*, and cf. *Hatcherichnus*. Because preservation of traces on the bases of sheet sandstones implies formation in the underlying mudstone, rhizohaloes must also be included in this ichnocoenosis because they are present in mudstones directly below sheet sandstones.

The range in moisture regimes represented by the vertebrate track ichnocoenosis is similar to that of the cf. *Steinichnus* ichnocoenosis. A hydrophilic suite of traces represents standing water on the floodplain, while a hygrophilic suite represents more marginal settings near and below the air-sediment-moisture interface. Vertebrate tracks, although classified as epiterraphilic, are preserved in a manner that suggests formation in relatively high-moisture sediment (Jennings et al. 2006; Platt and Hasiotis 2006; Platt et al. in review). We assign rhizohaloes underlying the sheet sandstone to the rhizohalo ichnocoenosis and interpret them as

representing vegetation present before water levels increased to the point where the vertebrate track ichnocoenosis was emplaced. Crevassing occurred shortly after these raised water levels.

Cf. *Camborygma* Ichnocoenosis.—This ichnocoenosis (Fig. 14) consists of locally dense accumulations of cf. *Camborygma* and less abundant cf. *Cylindricum*. This ichnocoenosis is found only in ribbon sandstones. No terminations of cf. *Camborygma* burrows were observed; all penetrate the entire thickness of the sandstone in which they are present.

Even though cf. *Camborygma* cannot be identified with certainty, the shape and depth of the burrows indicate that the sediment in which they were constructed was moist, but not saturated. Crayfish burrow to the water table (e.g., Hasiotis and Honey 2000) so incomplete crayfish burrows indicate that the water table was below the sheet sandstone at the time of burrow construction. Burrows likely continued into underlying mudstones, but were not preserved. We interpret the cf. *Camborygma* ichnocoenosis in ribbon sandstones as result of a lowered water table following channel abandonment.

DISCUSSION

Sequence and timing of events

Mudstone lithofacies.—Placing the ichnocoenoses within the context of the lithofacies allows us to use moisture regimes to reconstruct a higher resolution sequence of events than is possible from lithofacies and paleosol interpretations alone (Fig. 14). The heterolithic lithofacies in the field areas contains two laterally extensive sheet sandstones bounded and separated by paleosols. The paleosol underlying the lower sheet sandstone contains the rhizohalo ichnocoenosis and represents a relatively long period of time based on the degree of pedogenic modification and pervasiveness of rhizoliths.

Lower sheet sandstone.—The trace fossils preserved on the base of the lower sheet sandstone represent casts of traces originally created on the surface of the underlying paleosol. The surface experienced an increase in moisture prior to crevassing, which recorded the cf. *Steinichnus* ichnocoenosis. The traces are not crosscut by rhizoliths and are relatively well preserved; this suggests that the sheet sandstone preserved the underlying paleosurface in a single depositional event. The paleosurface likely represents a relatively short amount of time, from days to tens of days, based on modern tetrapod track survivorship data from a floodplain setting (Cohen et al. 1991). Hydrophilic and hygrophilic suites represent areas of standing water that quickly experienced desiccation following lowering of the water table.

The deposition of the lower sheet sandstone was likely relatively rapid, on the order of tens of years (Perez-Arlucea and Smith 1999). Most traces originate from the top of the sheet sandstone so bioturbation most likely began after deposition. The lack of disruption of the basal sandstone-mudstone contact suggests that the deposited sand was thick enough to prevent further bioturbation or the water table was high enough to prevent organisms from burrowing down to this level. Periods of high water tables after crevassing resulted in gleying of the top of the underlying mudstone. The *Planolites* ichnocoenosis within the sheet sandstone indicates relatively well-drained conditions that allowed hydrophilic to terraphilic traces to be constructed over a relatively short period of time. As water levels continued to drop, vegetation became established. This vegetation was eventually exploited by termites, resulting in the emplacement of the cf. *Termitichnus* ichnocoenosis.

Paleosols in the heterolithic lithofacies.—Overbank fines and minor sandsheets were deposited on top of the lower sheet sandstone during multiple pulses of sedimentation and pedogenesis. These paleosols are weakly to moderately well developed and contain the

rhizohalo ichnocoenosis. The degree of soil development suggests at least hundreds of years are represented.

Immediately below the upper sheet sandstone is a paleosurface similar to that preserved on the base of the lower sandstone. The upper sheet sandstone is so laterally extensive and well exposed that two different ichnocoenoses can be identified on its lower paleosurface: the cf. *Steinichnus* ichnocoenosis and the vertebrate track ichnocoenosis. These two ichnocoenoses are similar in terms of moisture regimes and conditions similar to those present prior to deposition of the lower sheet sandstone. The amount of time represented by the trace fossils preserved on the base of the upper sheet sandstone is similar to that interpreted for traces on the base of the lower sheet sandstone: days to tens of days.

Upper sheet sandstone.—The upper sheet sandstone is very similar to the lower sheet sandstone in terms of timing of deposition and the presence of the *Planolites* ichnocoenosis. The upper sheet sandstone, however, represents deposition of a larger volume of sediment, possibly the result of stage II or III splays (Smith et al. 1989). This sheet sandstone was exposed for a shorter period of time than the lower sheet sandstone, based on the lack of rhizoliths and lack of overprinting of multiple generations of trace fossils. Moisture availability after deposition was similar to the lower sheet sandstone in that underlying mudstones were gleyed.

Ribbon sandstones.—Small ribbon sandstones, representing distributary channels associated with crevassing, traversed the floodplain and were eventually abandoned as new channels were established. The water table dropped after a new trunk channel was established outside of the field area, and the cf. *Camborygma* ichnocoenosis became established in abandoned channel deposits. Crayfish likely were present in proximal overbank environments as well, but their burrows were not preserved because of pedoturbation in proximal floodplain

paleosols.

Lateral Paleohydrological Patterns within a Single Stratigraphic Level

The presence of multiple ichnocoenoses preserved on the base of the upper sheet sandstone (Figs. 10, 11) enable interpretations of lateral patterns in paleohydrology on that bedding plane. Even though the cf. *Steinichnus* ichnocoenosis and the vertebrate track ichnocoenosis are the only ichnocoenoses represented at this stratigraphic interval, multiple examples of the vertebrate track ichnocoenosis have slightly different relative abundances of constituent traces. Comparison of the four vertebrate track ichnocoenoses to the cf. *Steinichnus* ichnocoenosis yields a clear difference in the dominant moisture regimes: the cf. *Steinichnus* ichnocoenosis represents relatively more moist conditions based on the abundance of hydrophilic and hygrophilic traces.

Within the four examples of the vertebrate track ichnocoenosis, the eastern clusters have more hygrophilic and hydrophilic traces than the western clusters. Even though epiterraphilic vertebrate tracks can represent high-moisture conditions (Platt et al. in review), we argue that a greater abundance of megafaunal tracks indicates overall more stable, i.e., drier, media conditions more suitable for terrestrial locomotion. Consideration of all ichnocoenoses at this stratigraphic level, therefore, shows a gradient from relatively low moisture in the west to relatively high moisture in the east and southeast. Higher moisture to the southeast may indicate that the trunk channel that supplied the sediment to the floodplain was located in that direction.

Overall Paleohydrology

Ichnologic evidence indicates that sufficient moisture was present during MF deposition

to support relatively diverse communities of organisms in multiple environments. Ichnocoenoses show variation in water table levels, which can be related to infiltration rates and moisture content associated with hydraulic sediment deposition. Multiple moisture regimes within a single ichnocoenosis, however, indicate paleocommunities that were adapted to fluctuating moisture levels. Comparison of the range of moisture regimes represented by ichnocoenoses indicates the degree of water-table fluctuation increased with distance from the channel. Such an interpretation is consistent with seasonally distributed precipitation, which has been proposed previously (Hasiotis 2004, 2008).

The interpreted paleohydrologic conditions, along with rhizolith distribution in the study area and presence of large trees in channel sandstones at Howe Quarry (Ayer 1999), suggest that large trees grew proximal to channels, while smaller shrubs and low-lying vegetation provided groundcover in distal settings. This riparian vegetation shows that, even though there was a seasonal climate, soil moisture did not fall below the wilting coefficient, at least proximal to channels. Vegetation was supported by seasonally distributed precipitation, which often was not sufficient enough to flush all carbonate from the soil profile, as evidenced by abundant carbonate nodules.

CONCLUSIONS

The Upper Jurassic MF in the Bighorn Basin contains a diverse assemblage of ichnofossils, which can be integrated with sedimentology and paleopedology to interpret paleoenvironments and paleohydrology that cannot be determined from lithology and pedogenic features alone.

Two lithofacies are recognized in the study areas: a mudstone lithofacies and a

heterolithic lithofacies. The mudstone lithofacies contains moderately to well-developed paleosols and represents a well-drained, distal floodplain environment. The heterolithic lithofacies contains thin sheet sandstones, ribbon sandstones, and weakly to moderately developed paleosols, which show evidence of poor drainage. The heterolithic lithofacies is bounded above and below by the mudstone lithofacies. This pattern is interpreted as resulting from relatively rapid episodes of avulsion and long periods of slow sedimentation in a distal floodplain setting.

Nineteen types of plant, invertebrate, and vertebrate trace fossils are recognized in the study areas. These are found in distinct associations assigned to six ichnocoenoses. These ichnocoenoses are classified according to the dominant trace fossil. Each ichnocoenosis is represented by a moisture profile that expresses the relative abundances of moisture regimes of constituent trace fossils.

We can summarize patterns in the distribution of ichnocoenoses during avulsion as follows: dominantly hygrophilic traces in floodplain sediments are overprinted by dominantly hydrophilic communities in response to increased moisture availability associated with the onset of avulsion. Following crevassing, sheet sands are colonized by a community composed of organisms with a wide range of moisture preferences, representing paleohydrological instability. Distributary splay channels incise into subjacent sediments and, upon abandonment, may support deep burrowing hydrophilic communities. Given enough time or distance from the avulsive channel, consistently low water-table levels may allow establishment of arborescent vegetation and dominantly terraphilic communities within sheet sands, overprinting traces made by earlier organisms with higher moisture preferences.

We view the observed ichnological patterns as a general model that predicts the

stratigraphic relationships of ichnofossils in avulsion deposits. This ichnocoenoses model can be used to aid in the interpretation of core and strata that do not have significant lateral exposure. Note that the pattern observed in the study areas describes only an avulsive scenario that results in the reestablishment of the channel elsewhere. We expect this pattern to be the most common representation of avulsion in the rock record because the area occupied by the reestablished channel is very small in comparison to the relatively large area of the floodplain.

The relationship between paleohydrology, sedimentology, ichnology, and pedogenesis leads us to formulate a causal mechanism for this avulsive scenario. During particularly wet intervals, the Morrison drainage basin collected a large amount of precipitation, raising water-table levels in lowland discharge areas, which saturated soils and greatly decreased infiltration. During this time, topographic lows were inundated with an influx of water and sediment from overland flow and from the compounded effects of the confluence of tributaries upstream. Channel avulsion was triggered once the avulsion threshold was exceeded (Jones and Schumm 1999). The onset of avulsion resulted in a period of instability marked by crevassing and weak development of paleosols between crevasse-splay deposits. This is also the reason for the rapid transition from dominantly hygrophilic to dominantly hydrophilic ichnocoenoses.

When precipitation levels dropped off, the amount of influent water and sediment fell back within the capacity of the avulsive stream, which was reestablished, possibly within the pre-avulsion channel. Evaporation driven by high temperatures (e.g., Demko and Parrish 1998; Hasiotis 2004, 2008) removed much of the moisture from the soil, but regional groundwater flow prevented complete desiccation in environments proximal to the channel.

Overall, our integrative approach increases the amount of information that can be interpreted from the studied MF deposits and younger and older continental deposits in the rock

record. The patterns we observed were based on ichnological moisture regimes, rather than specific ichnotaxa, which vary through space and time and are subject to misinterpretation. Our approach to the integration of ichnology with sedimentology and paleopedology provides a useful framework for future integrative geological studies.

ACKNOWLEDGMENTS

We thank M. Smeins and A. Huttenlocker for their assistance in the field, R. and C. Manuel for logistical support, J. Farlow for providing feedback on vertebrate tracks, J. Retrum for preparing microfossil samples, R. Goldstein, L. Martin, and the University of Kansas (KU) IchnoBioGeoScience class for their helpful comments, and the Iowa State University field camp for lodging accommodations. We thank A. Aslan, N. Smith, and an anonymous reviewer for helpful comments on an earlier version of this manuscript. This paper is part of a Ph.D. dissertation conducted by BFP at the KU Department of Geology, using data collected during a MS thesis by BFP at KU. This research was funded by the KU Geology Department and Sigma Xi. Vertebrate specimens were collected under BLM Permit PA03-WY-107 and we thank Brent Breithaupt and Dale Hanson for their assistance with permitting.

REFERENCES

ALLEN, J.R.L., 1982, Sedimentary Structures: Their Character and Physical Basis v. 2: New York, Elsevier Scientific Publishing Company, 663 p.

ALLEN, J.R.L., 1997, Subfossil mammalian tracks (Flandrian) in the Severn Estuary, S. W. Britain: mechanics of formation, preservation, and distribution: Philosophical Transactions of the Royal Society of London B, v. 352, p. 481–518.

ALPERT, S.P., 1974, Systematic review of the genus *Skolithos*: Journal of Paleontology, v. 48, p. 661–669.

AYER, J., 1999, The Howe Ranch Dinosaurs: Aathal, Switzerland, Support Society of the Sauriermuseum, 96 p.

BENNER, J.S., RIDGE, J.C., AND TAFT, N.K., Late Pleistocene freshwater fish (Cottidae) trackways from New England (USA) glacial lakes and a reinterpretation of the ichnogenus *Broomichnium* Kuhn: Palaeogeography, Palaeoclimatology, Palaeoecology, v. 260, p. 375–388.

BIGHAM, J.M., FITZPATRICK, R.W., AND SCHULZE, D.G., 2002, Iron oxides, *in* Dixon, J.B., and Schulze, D.G., eds., Soil Mineralogy with Environmental Applications: Madison, Soil Science Society of America Book Series, p. 323–366.

BIRKELAND, P.W., 1999, Soils and Geomorphology, 3rd edition. Oxford University Press, New York, 430 p.

BONNAN, M.F., 2003, The evolution of manus shape in sauropod dinosaurs: implications for functional morphology, forelimb orientation, and phylogeny: Journal of Vertebrate Paleontology, v. 23, p. 595–613.

BOWN, T.M., 1982, Ichnofossils and rhizoliths of the nearshore fluvial Jebel Qatrani Formation

(Oligocene), Fayum Province, Egypt: Palaeogeography, Palaeoclimatology, Palaeoecology, v. 40, p. 255–309.

BOWN, T.M., AND KRAUS, M.J., 1983, Ichnofossils of the alluvial Willwood Formation (Lower Eocene), Bighorn Basin, Northwest Wyoming, U.S.A.: Palaeogeography, Palaeoclimatology, Palaeoecology, v. 43, p. 95–128.

BRADY, N.C., AND WEIL, R.R., 2002, The Nature and Properties of Soils, 13th Edition: Upper Saddle River, Prentice Hall, 960 p.

BROMLEY, R.G., 1996, Trace fossils: Biology and Taphonomy, 2nd Edition: London, Unwin Hyman Ltd., 280 p.

BROMLEY, R. G., BUATOIS, L.A, GENISE, J.F., LABANDEIRA, C.C., MÁNGANO, M.G., MELCHOR, R.N., SCHLIRF, M., AND UCHMAN, A., 2007, Comments on the paper "Reconnaissance of Upper Jurassic Morrison Formation ichnofossils, Rocky Mountain Region, USA: Paleoenvironmental, stratigraphic, and paleoclimatic significance of terrestrial and freshwater ichnocoenoses" by Stephen T. Hasiotis: Sedimentary Geology, v. 200, p. 141–150.

BROWN, B., 1932, Sinclair dinosaur expedition, 1924: Natural History, v. 36, p. 3–15.

BROWN, B., 1937, Excavating the great Jurassic dinosaur quarry of northern Wyoming, 140,000,000 years ago: Roentgen Economist, v. 5, p. 3–6.

BROWN, R.W., 1934, *Celliforma spirifer*, the fossil larval chambers of mining bees: Journal of the Washington Academy of Sciences, v. 24, p. 532–539.

CHAMBERLAIN, C.K., 1975, Recent lebensspuren in nonmarine aquatic environments, *in* Frey, R.W., ed., The Study of Trace Fossils: New York, Springer-Verlag, p. 431–458.

CLARK, G.G., AND RATCLIFFE, B.C., 1989, Observations on the tunnel morphology of

Heterocerus brunneus Melsheimer (Coleoptera: Heteroceridae) and its paleoecological significance: Journal of Paleontology, v. 63, p. 228–232.

CLOUD, P., GUSTAFSON, L.B., AND WATSON, J.A.L., 1980, The works of living social insects as pseudofossils and the age of the oldest known Metazoa: Science, v. 210, p. 1013–1015.

COHEN, A., LOCKLEY, M., HALFPENNY, J., AND MICHEL, A. E., 1991, Modern vertebrate track taphonomy at Lake Manyara, Tanzania: PALAIOS, v. 6, p. 371–389.

COUNTS, J.W., AND HASIOTIS, S.T., 2009, Neoichnological experiments with masked chafer beetles (Coleoptera: Scarabaeidae): implications for backfilled continental trace fossils: PALAIOS, v. 24, p. 74–91.

DARLINGTON, J.P.E.C., 2005, Distinctive fossilized termite nests at Laetoli, Tanzania: Insectes Sociaux, v. 52, p. 408–409.

DECELLES, P.G., AND BURDEN, E.T., 1992, Non-marine sedimentation in the overfilled part of the Jurassic-Cretaceous Cordilleran foreland basin Morrison and Cloverly formations, central Wyoming, USA: Basin Research, v. 4, p. 291–313.

DECELLES, P.G., AND CURRIE, B.S., 1996, Long-term sediment accumulation in the Middle Jurassic-early Eocene Cordilleran retroarc foreland-basin system: Geology, v. 24, p. 591–594.

DEMKO, T.M., AND PARRISH, J.T., 1998, Paleoclimatic setting of the Upper Jurassic Morrison Formation: Modern Geology, v. 22, p. 283–296.

DEMKO, T.M., CURRIE, B.S., AND NICOLL, K.A., 2004, Regional paleoclimatic and stratigraphic implications of paleosols and fluvial/overbank architecture in the Morrison Formation (Upper Jurassic), Western Interior, USA: Sedimentary Geology, v. 167, p. 115–135.

DONOVAN, S.K., RENEMA, W., AND PICKERILL, R.K., 2005, The ichnofossil *Scolicia prisca* de

Quatrefages from the Paleogene of eastern Jamaica and fossil echinoids of the Richmond Formation: Caribbean Journal of Science, v. 41, p. 876–881.

EAGAR, R.M.C., BAINES, J.G., COLLINSON, J.D., HARDY, P.G., OKOLO, S.A., AND POLLARD, J.E., 1985, Trace fossil assemblages and their occurrence in Silesian (Mid-Carboniferous) deltaic sediments of the Central Pennine Basin, England, *in* Curran, H.A., ed., Biogenic Sedimentary Structures: Their Use in Interpreting Depositional Environments: Society of Economic Paleontologists and Mineralogists Special Publication 35, p. 99–149.

EDWARDS, P.B., AND ASCHENBORN, H.H., 1987, Patterns of nesting and dung burial in *Onitis* dung beetles: implications for pasture productivity and fly control: Journal of Applied Ecology, v. 24, p. 837–851.

ELLIOTT, D.K., AND NATIONS, J.D., 1998, Bee burrows in the Late Cretaceous (Late Cenomanian) Dakota Formation, northeastern Arizona: Ichnos, v. 5, p. 243–253.

EVANOFF, E., GOOD, S.C., AND HANLEY, J.H., 1998, An overview of freshwater mollusks of the Jurassic Morrison Formation (Late Jurassic, Western Interior, USA): Modern Geology, v. 22, p. 423–450.

EVANS, H.E., 1957, Comparative ethology of digger wasps of the genus *Bembix*: Ithaca, New York, Comstock Publishing Associates, 248 p.

FAIRCHILD, J.M., AND HASIOTIS, S.T., 2011, Terrestrial and aquatic neoichnological laboratory experiments with the freshwater crayfish *Orconectes*: trackways on media of varying grain size, moisture, and inclination: PALAIOS, v. 26, p. 790–804.

FARLOW, J.O., PITTMAN, J.G., AND HAWTHORNE, J.M., 1989, *Brontopodus birdi*, Lower Cretaceous dinosaur footprints from the U.S. Gulf Coastal Plain, *in* Gillette, D.D., and Lockley, M. G., eds., Dinosaur Tracks and Traces: Cambridge, Cambridge University

Press, p. 371–394.

FOSTER, J.R., AND LOCKLEY, M.G., 1997, Probable crocodilian tracks and traces from the Morrison Formation (Upper Jurassic) of eastern Utah: Ichnos, v. 5, p. 121–129.

FOSTER, J.R., LOCKLEY, M.G., AND BROCKETT, J., 1999, Possible turtle tracks from the Morrison Formation of southern Utah, *in* Gillette, D.D., ed., Vertebrate Paleontology in Utah: Utah Geological Survey, p. 185–191.

FREY, R.W., PEMBERTON, S.G., AND FAGERSTROM, J.A., 1984, Morphological, ethological, and environmental significance of the ichnogenera *Scoyenia* and *Ancorichnus*: Journal of Paleontology, v. 58, p. 511–528.

FRIEND, P.F., SLATER, M.J., AND WILLIAMS, R.C., 1979, Vertical and lateral relationships of river sandstone bodies, Ebro Basin, Spain: Geological Society of London Journal, v. 135, p. 39–46.

GENISE, J.F., SCIUTTO, J.C., LAZA, J.H., GONZÁLEZ, M.G., AND BELLOSI, E.S., 2002, Fossil bee nests, coleopteran pupil chambers and tuffaceous paleosols from the Late Cretaceous Laguna Palacios Formation, central Patagonia (Argentina): Palaeogeography, Palaeoclimatology, Palaeoecology, v. 177, p. 215–235.

GOOD, S.C., 2004, Paleoenvironmental and paleoclimatic significance of freshwater bivalves in the Upper Jurassic Morrison Formation, Western Interior, USA: Sedimentary Geology, v. 167, p. 163–176.

GINGRAS, M.K., LALOND, S.V., AMSKOLD, L., AND KONHAUSER, K.O., 2007, Wintering Chironomids mine oxygen, PALAIOS, v. 22, p. 433–438.

GOULDEN, C.E., 1969, Developmental phases of the biocoenosis: Zoology, v. 62, p. 1066–1073.

GREGORY, M.R., CAMPBELL, K.A., ZURAIDA, R., AND MARTIN, A.J., 2006, Plant traces

resembling *Skolithos*: Ichnos, v. 13, p. 205–216.

HADLINGTON, P., 1966, Australian Termites and other common timber pests, 2nd Edition: New South Wales, New South Wales University Press, 126 p.

HALFEN, A.F., AND HASIOTIS, S.T., 2010, Neoichnological study of the traces and burrowing behaviors of the western harvester ant *Pogonomyrmex occidentalis* (Insecta: Hymenoptera: Formicidae): paleopedogenic and paleoecological implications: PALAIOS, v. 25, p. 703–720.

HAMMER, ∅., HARPER, D.A.T., AND RYAN, P.D., 2001, Paleontological statistics software package for education and data analysis: Palaeontologia Electronica, v. 4, 9 p.

HÄNTZSCHEL, W., 1975, Trace fossils and problematica, *in* Teichert, C., ed., Treatise on Invertebrate Paleontology, Pt. W, Miscellanea, Suppl. 1: Lawrence, Geological Society of America and University of Kansas Press, p. W1–W269.

HASIOTIS, S.T., 1993, Ichnology of Triassic and Holocene cambarid crayfish of North America: An overview of burrowing behavior and morphology as reflected by their morphologies in the geologic record: Freshwater Crayfish, v. 9, p. 399–406.

HASIOTIS, S.T., 2000, The Invertebrate Invasion and Evolution of Mesozoic Soil Ecosystems: The Ichnofossil Record of Ecological Innovations, *in* Gastaldo, R.A. and DiMichele, W.A., eds., Phanerozoic Terrestrial Ecosystems, Paleontological Society Papers, v. 6, p. 141-169

HASIOTIS, S.T., 2002, Continental Trace Fossils: SEPM Short Course Notes, no. 51, 132 p.

HASIOTIS, S.T., 2003, Complex ichnofossils of solitary and social soil organisms: understanding their evolution and roles in terrestrial paleoecosystems: Palaeogeography, Palaeoclimatology, Palaeoecology, v. 192, p. 259–320.

HASIOTIS, S.T., 2004, Reconnaissance of Upper Jurassic Morrison Formation ichnofossils, Rocky Mountain Region, USA: paleoenvironmental, stratigraphic, and paleoclimatic significance of terrestrial and freshwater ichnocoenoses: Sedimentary Geology, v. 167, p. 177–268.

HASIOTIS, S.T., 2007, Continental ichnology: fundamental processes and controls on trace fossil distribution, *in* Miller, W., ed., Trace Fossils: Concepts, Problems, Prospects, Elsevier, p. 268–284.

HASIOTIS, S.T., 2008, Reply to the comments by Bromley et al. of the paper "Reconnaissance of the Upper Jurassic Morrison Formation ichnofossils, Rocky Mountain Region, USA: Paleoenvironmental, stratigraphic, and paleoclimatic significance of terrestrial and freshwater ichnocoenoses" by Stephen T. Hasiotis: Sedimentary Geology, v. 208, p. 61–68.

HASIOTIS, S.T., AND DEMKO, T.M., 1996, Terrestrial and freshwater trace fossils, Upper Jurassic Morrison Formation, Colorado Plateau, *in* Morales, M. ed., The Continental Jurassic: Museum of Northern Arizona Bulletin, v. 60. The Paleontological Society, p. 355–370.

HASIOTIS, S.T., AND HONEY, J.G., 2000, Paleohydrologic and stratigraphic significance of crayfish burrows in continental deposits: examples from several Paleocene Laramide basins in the Rocky Mountains: Journal of Sedimentary Research, v. 70, p. 127–139.

HASIOTIS, S.T., AND MITCHELL, C.E., 1993, A comparison of crayfish burrow morphologies: Triassic and Holocene fossil, paleo- and neo-ichnological evidence, and the identification of their burrowing signatures: Ichnos, v. 2, p. 291–314.

HASIOTIS, S.T., KRAUS, M.J., AND DEMKO, T.M., 2007, Climatic controls on continental trace fossils, *in* Miller, W. ed., Trace Fossils: Concepts, Problems, Prospects, Elsevier, p. 172–

195.

HASIOTIS, S.T., REILLY, M., AMOS, K., LANG, S., KENNEDY, D., TODD, J.A., MICHEL, E., AND PLATT, B.F., in press, Actualistic studies of the spatial and temporal distributions of terrestrial and aquatic organism traces in continental environments to differentiate lacustrine from fluvial, eolian, and marine deposits in the geologic record, *in* Baganz, O.W., Bartov, Y., Bohacs, K., and Nummendal, D., eds., Lacustrine sandstone reservoirs and hydrocarbon systems: American Association of Petroleum Geologists Memoir 95, p. 1–56.

HELLER, P.L., AND PAOLA, C., 1989, The paradox of Lower Cretaceous gravels and the initiation of thrusting in the Sevier Orogenic Belt, western United States interior: Geological Society of America Bulletin, v. 101, p. 864–875.

HEMBREE, D.I., 2009, Neoichnology of burrowing millipedes: linking modern burrow morphology, organism behavior, and sediment properties to interpret continental ichnofossils: PALAIOS, v. 24, p. 425–439.

HEMBREE, D.I., AND HASIOTIS, S.T., 2006, The identification and interpretation of reptile ichnofossils in paleosols through modern studies: Journal of Sedimentary Research, v. 76, p. 575–588.

HEMBREE, D.I., AND HASIOTIS, S.T., 2007, Biogenic structures produced by sand-swimming snakes: a modern analog for interpreting continental ichnofossils: Journal of Sedimentary Research, v. 77, p. 389–397.

HEMBREE, D.I., JOHNSON, L.M., AND TENWALDE, R.W., 2012, Neoichnology of the desert scorpion *Hadrurus arizonensis*: burrows to biogenic cross lamination: Palaeontologia Electronica, v. 15, 34 p.

HITCHCOCK, E., 1858, Ichnology of New England: A Report of the Sandstone of the Connecticut Valley Especially its Footprints: Boston, William White, 220 p.

JOHNSON, D.L., WATSON-STEGNER, D., JOHNSON, D.N., AND SCHAETZL, R.J., 1987, Proisotropic and proanisotropic processes of pedoturbation: Soil Science, v. 143, p. 278–291.

JONES, L.S., AND GUSTASON, E.R., 2006, Dinosaurs as possible avulsion enablers in the Upper Jurassic Morrison Formation, East-Central Utah: Ichnos, v. 13, p. 31–41.

JONES, L.S., AND SCHUMM, S.A., 1999, Causes of avulsion: an overview, *in* Smith, N. D., and Rogers, J., eds., Fluvial Sedimentology VI, Malden, MA, Blackwell Science, p. 171–178.

KAMPF, N., AND SCHWERTMANN, U., 1982, Goethite and hematite in a climosequence in southern Brazil and their application in classification of kaolinitic soils: Geoderma, v. 29, p. 27–39.

KLAPPA, C.F., 1980, Rhizoliths in terrestrial carbonates: classification, recognition, genesis, and significance: Sedimentology, v. 26, p. 613–629.

KNECHT, R.J., BENNER, J.S., ROGERS, D.C., AND RIDGE, J.C., *Surculichnus bifurcauda* n. igen., n. isp., a trace fossil from Late Pleistocene glaciolacustrine varves of the Connecticut River Valley, USA, attributed to notostracan crustaceans based on neoichnological experimentation: Palaeogeography, Palaeoclimatology, Palaeoecology, v. 272, p. 232–239.

KONDO, Y., 1987, Burrowing depth of infaunal bivalves—observation of living species and its relation to shell morphology: Transactions and Proceedings of the Paleontological Society of Japan, v. 148, p. 306–323.

KOWALLIS, B.J., CHRISTIANSEN, E.H., DEINO, A.L., PETERSON, F., TURNER, C.E., KUNK, M.J., AND OBRADOVICH, J.D., 1998, The age of the Morrison Formation: Modern Geology, v. 22, p. 235–260.

KRAUS, M.J., 1996, Avulsion deposits in Lower Eocene alluvial rocks, Bighorn Basin, Wyoming: Journal of Sedimentary Research, v. 66, p. 354–363.

KRAUS, M.J., 1999, Paleosols in clastic sedimentary rocks: their geologic applications: Earth-Science Reviews, v. 47, p. 41–70.

KRAUS, M.J., 2002, Basin-scale changes in floodplain paleosols: implications for interpreting alluvial architecture: Journal of Sedimentary Research, v. 72, p. 500–509.

KRAUS, M.J., AND ASLAN, A., 1993, Eocene hydromorphic paleosols: significance for interpreting ancient floodplain processes: Journal of Sedimentary Petrology, v. 63, p. 453–463.

KRAUS, M.J., AND HASIOTIS, S.T., 2006, Significance of different modes of rhizolith preservation to interpreting paleoenvironmental and paleohydrologic settings: examples from Paleogene paleosols, Bighorn Basin, Wyoming, U.S.A. Journal of Sedimentary Research, v. 76, p. 633-646.

KRAUS, M.J., AND WELLS, T.M., 1999, Recognizing avulsion deposits in the ancient stratigraphical record, *in* Smith, N.D., and Rogers, J., eds., Fluvial Sedimentology VI: Malden, Blackwell Science, Inc., p. 251–268.

KVALE, E.P., 1986, Paleoenvironments and tectonic significance of the Upper Jurassic Morrison/Lower Cretaceous Cloverly Formations, Bighorn Basin, Wyoming. [Unpublished doctoral dissertation]: Iowa State University, Ames, 191 p.

KVALE, E.P., HASIOTIS, S.T., MICKELSON, D.L., AND JOHNSON, G.D., 2001, Middle and Late Jurassic Dinosaur fossil-bearing horizons: implications for dinosaur paleoecology, northeastern Bighorn Basin, Wyoming, *in* Hill, C.L., ed., Guidebook for the Field Trips, Museum of the Rockies Occasional Paper No. 3: Bozeman, Montana, p. 16–45.

KVALE, E.P., MICKELSON, D.L., HASIOTIS, S.T., AND JOHNSON, G.D., 2004, The history of dinosaur footprint discoveries in Wyoming with emphasis on the Bighorn Basin: Ichnos, v. 11, p. 3–9.

LAPORTE, L.F., AND BEHRENSMEYER, A.K., 1980, Tracks and substrate reworking by terrestrial vertebrates in Quaternary sediments of Kenya: Journal of Sedimentary Petrology, v. 50, p. 1337–1346.

LAZA, J.H., 2006, Termiteros del Plioceno y Pleistoceno de la provincia de Buenos Aires, República Argentina. Significación paleoambiental y paleozoogeográfica: Ameghiniana, v. 43, p. 641–648.

LEE, K.E., AND WOOD, T.G., 1971, Termites and Soils: New York, Academic Press, 251 p.

LINCK, O., 1949, Fossile Bohrgänge (*Anobichnium simile* n. g. n. sp.) an einem Keuperholz: Neus Jarbuch fur Mineralogie, Geologie, und Paläontologie, Monatshefte, v. 4–6, p. 180–185.

LOCKLEY, M.G., MATSUKAWA, M., AND OBATA, I., 1989, Dinosaur tracks and radial cracks: unusual footprint features: Bulletin of the National Science Museum, Series C, v. 15, p. 151–160.

LOCKLEY, M.G., MEYER, C., HUNT, A.P., AND LUCAS, S.G., 1994, The distribution of sauropod tracks and trackmakers: Gaia, v. 10, p. 233–248.

MACSOTAY, O., 1967, Huellas problematicas y su valor paleoecologico en Venezuela: Geos, v. 16, p. 7–79.

MAPLES, C.G., AND WEST, R.R., 1989, *Lockeia*, not *Pelecypodichnus*: Journal of Paleontology, v. 63, p. 694–696.

MARRIOTT, S.B., AND WRIGHT, V.P., 1993, Palaeosols as indicators of geomorphic stability in

two Old Red Sandstone alluvial suites, South Wales: Journal of the Geological Society, London, v. 150, p. 1109–1120.

MERRITT, R.W., AND CUMMINS, K.W., eds., 1996, An Introduction to the Aquatic Insects of North America, 3rd ed.: Dubuque, Kendall/Hunt Publishing Company, 862 p.

METZ, R., 1987, Sinusoidal trail formed by a recent biting midge (family Ceratopogonidae): trace fossil implications: Journal of Paleontology, v. 61, p. 312–314.

MICHELIS, I., 2004, Taphonomie des Howe Quarry's (Morrison-Formation, Oberer Jura), Bighorn County, Wyoming, USA. [Unpublished doctoral dissertation]: Rheinischen Friedrich-Wilhelms-Universität Bonn, 41 p.

MICHENER, C.D., 1974, The Social Behavior of the Bees: Cambridge, Harvard University Press, 418 p.

MILLER, M.F., AND KNOX, L.W., 1985, Biogenic structures and depositional environments of a Lower Pennsylvanian coal-bearing sequence, northern Cumberland Plateau, Tennessee, U.S.A., *in* Curran, H.E., ed., Biogenic Structures: Their Use in Interpreting Depositional Environments: Society of Economic Paleontologists and Mineralogists Special Publication 35, p. 67–97.

MOBERLY, R. Jr., 1960, Morrison, Cloverly, and Sykes Mountain Formations, northern Bighorn Basin, Wyoming and Montana: Bulletin of the Geological Society of America, v. 71, p. 1137–1176.

MOOK, C.C., 1933, A crocodilian skeleton from the Morrison Formation at Canyon City, Colorado: American Museum Novitates, v. 671, p. 1–8.

MOOK, C.C., 1967, Preliminary description of a new Goniopholid crocodilian: Kirtlandia, v. 2, p. 1–10.

MOUSSA, M.T., 1970, Nematode trails from the Green River Formation (Eocene) in the Uinta basin, Utah: Journal of Paleontology, v. 44, p. 304– 307.

NADON, G.C., 1993, The association of anastomosed fluvial deposits and dinosaur tracks, eggs, and nests: Implications for the interpretation of floodplain environments and a possible survival strategy for ornithopods: PALAIOS, v. 8, p. 31–44.

NOIROT, C., 1970, The nests of termites, *in* Krishna, K., and Weesner, F.M., eds., Biology of Termites, Volume II: New York, Academic Press, p. 73–126.

O'NEILL, K.M., 2001, Solitary Wasps: Behavior and Natural History: London, Comstock Publishing Associates, 406 p.

PARRISH, J.T., PETERSON, F., AND TURNER, C.E., 2004, Jurassic "savannah"—plant taphonomy and climate of the Morrison Formation (Upper Jurassic, Western USA): Sedimentary Geology, v. 167, p. 137–162.

PEARSON, D.L., AND VOGLER, A.P., 2001, Tiger Beetles: the Evolution, Ecology, and Diversity of the Cicindelids: Ithaca, Comstock Publishing Associates, 333 p.

PÉREZ-ARLUCEA, M., AND SMITH, N.D., 1999, Depositional patterns following the 1870s avulsion of the Saskatchewan River (Cumberland Marshes, Saskatchewan, Canada): Journal of Sedimentary Research, v. 69, p. 62–73.

PERREAULT, J.M. AND WHALEN, J.K., 2006, Earthworm burrowing in laboratory microcosms as influenced by soil temperature and moisture: Pedobiologia, v. 50, p. 397–403.

PIPIRINGOS, G.N., AND O'SULLIVAN, R.B., 1978, Principal unconformities in Triassic and Jurassic rocks—a preliminary survey: U.S. Geological Survey Professional Paper 1035-A., p. A1–A29.

PLATT, B.F., AND HASIOTIS, S.T., 2006, Newly discovered sauropod dinosaur tracks with skin

and foot-pad impressions from the Upper Jurassic Morrison Formation, Bighorn Basin, Wyoming, U.S.A., PALAIOS, v. 21, p. 249–261.

PLATT, B. F., AND HASIOTIS, S.T., 2008, A new system for describing and classifying tetrapod-tail traces with implications for interpreting the dinosaur-tail trace record: PALAIOS, v. 23, p. 3–13.

PLATT, B.F., HASIOTIS, S.T., AND HIRMAS, D.R., in review, Empirical determination of physical controls on megafaunal footprint formation through neoichnological experiments with elephants: PALAIOS, 41 manuscript pages.

POTTER, D.A., 1983, Effect of soil moisture on oviposition, water absorption, and survival of southern masked chafer (Coleoptera: Scarabaeidae) eggs: Environmental Entomology, v. 12, p. 1223–1227.

POTTER, D.A., AND GORDON, F.C., 1984, Susceptibility of *Cyclocephala immaculata* (Coleoptera: Scarabaeidae) eggs and immatures to heat and drought in turf grass: Environmental Entomology, v. 13, p. 794–799.

RATCLIFFE, B.C., AND FAGERSTROM, J.A., 1980. Invertebrate lebensspuren of Holocene floodplain: their morphology, origin, and paleoecological significance. Journal of Paleontology, v. 54, 614–630.

RETALLACK, G., 2001, Soils of the Past: an Introduction to Paleopedology, 2nd Edition, Malden, MA, Blackwell Science, 512 p.

SAKAGAMI, S.F., AND MICHENER, C.D., 1962, The Nest Architecture of the Sweat Bees (Halictinae): Lawrence, The University of Kansas Press, 135 p.

SCHWERTMANN, U., 1993, Relations between iron oxides, soil color, and soil formation: Soil Science Society of America Special Publication 31, p. 51–69.

SMITH, J.J., AND HASIOTIS, S.T., 2007, Traces and burrowing behaviors of the cicada nymph *Melampsalta calliope*: Neoichnology and paleoecological significance of modern soil-dwelling insects: Geological Society of America Abstracts with Programs, v. 39, p. 54.

SMITH, J.J., AND HASIOTIS, S.T., 2008, Traces and burrowing behaviors of the cicada nymph *Cicadetta calliope*: neoichnology and paleoecological significance of extant soil-dwelling insects: PALAIOS, v. 23, p. 503–513.

SMITH, J.J., HASIOTIS, S.T., WOODY, D.T., AND KRAUS, M.J., 2008a, Paleoclimatic implications of crayfish-mediated prismatic structures in paleosols of the Paleogene Willwood Formation, Bighorn Basin, Wyoming, U.S.A.: Journal of Sedimentary Research, v. 78, p. 323–334.

SMITH, J.J., HASIOTIS, S.T., KRAUS, M.J., AND WOODY, D.T., 2008b, *Naktodemasis bowni*: new ichnogenus and ichnospecies for adhesive meniscate burrows (AMB), and paleoenvironmental implications, Paleogene Willwood Formation, Bighorn Basin, Wyoming: Journal of Paleontology, v. 82, p. 267–278.

SMITH, N.D., CROSS, T.A., DUFFICY, J.P., AND CLOUGH, S.R., 1989, Anatomy of an avulsion: Sedimentology, v. 36, p. 1–23.

SOWIG, P., 1996, Brood care in the dung beetle *Onthophagus vacca* (Coleoptera: Scarabaeidae): the effect of soil moisture on time budget, nest structure, and reproductive success: Ecography, v. 19, p. 254–258.

STOLT, M.H., OGG, C.M., AND BAKER, J.C., 1994, Strongly contrasting redoximorphic patterns in Virginia Valley and Ridge paleosols: Soil Science Society of America Journal, v. 58, p. 477–484.

THULBORN, T., 1990, Dinosaur Tracks: New York, Chapman and Hall, 410 p.

TSCHINKEL, W.R., 2010, The foraging tunnel system of the Namabian Desert termite, *Baucaliotermes hainesi*: Journal of Insect Science, v. 10, p. 1–17.

TURNER, C.E., AND PETERSON, F., 2004, Reconstruction of the Upper Jurassic Morrison Formation extinct ecosystem—a synthesis: Sedimentary Geology, v. 167, p. 309–355.

TURNER, S., MARIAS, E., VINTE, M., MUDENGI, A., AND PARK, W., 2006, Termites, water and soils: Agricola, v. 16, p. 40–45.

VILLANI, M.G., ALLEE, L.L., DIAZ, A., AND ROBBINS, P.S., 1999, Adaptive strategies of edaphic arthropods: Annual Review of Entomology, v. 44, p. 233–256.

WARD, J.V., 1992, Aquatic Insect Ecology, 1. Biology and Habitat: New York, John Wiley & Sons, Inc., 438 p.

WILDING, L.P., AND TESSIER, D., 1988, Genesis of vertisols: shrink-swell phenomena, *in* Wilding, L.P., and Puentes, R., eds., Vertisols: Their Distribution, Properties, Classification, and Management: Texas A&M Technical Monograph 18, p. 205–225.

WILLIS, E.R., AND ROTH, L.M., 1962, Soil and moisture relationships of *Scaptocoris divergins* Troeschner (Hemiptera: Cydnidae): Annals of the Entomological Society of America, v. 55, p. 21–32.

WINSLOW, N.S., AND HELLER, P.L., 1987, Evaluation of unconformities in Upper Jurassic and Lower Cretaceous nonmarine deposits, Bighorn Basin, Wyoming and Montana, U.S.A.: Sedimentary Geology, v. 53, p. 181–202.

WRIGHT, V.P., AND MARRIOTT, S.B., 1996, A quantitative approach to soil occurrence in alluvial deposits and its application to the Old Red Sandstone of Britain: Journal of the Geological Society, v. 153, p. 907–913.

YOCHELSON, E.L., AND FEDONKIN, M.A., 1997, The type specimens (Middle Cambrian) of the

trace fossil *Archaeonassa* Fenton and Fenton: Canadian Journal of Earth Sciences, v. 34, p. 1210–1219.

ZHANG, Y., ZHANG, Z., AND LIU, J., 2003, Burrowing rodents as ecosystem engineers: the ecology and management of plateau zokors *Myospalax fontanierii* in alpine meadow ecosystems on the Tibetan Plateau: Mammal Review, v. 33, p. 284–294.

TABLES

Table 1.—Moisture preferences of modern tracemakers.

Tracemaker	Common name	Primary behaviors	Maximum depth	Moisture preference	Reference	Moisture regime
Amphisbaena camurea	worm lizard	locomotion, feeding, dwelling	>60 cm	vadose zone, but not below water table	Hembree and Hasiotis 2006	terraphilic to hygrophilic
Aporrectodea caliginosa (juvenile)	grey worm	dwelling, locomotion, feeding (endogeic)	~23 cm	increased feeding in wet soil (-5 kPa matric potential), increased burrowing in drier soil (-11 kPa matric potential)	Perreault and Whalen 2006	hygrophilic
Archispirostreptus gigas; *Orthoporus ornatus*	giant African millipede; Sonoran Desert millipede, respectively	dwelling	up to 160 mm	prefer moist sediment, ~40% moisture	Hembree 2009	terraphilic
Bembix, various species	sand wasp	nesting	species fall into 3 groups: 9-16 cm; ~20 cm; ~30 cm, with depths up to 54 cm reported for *B. pallidipicta*	species fall into 3 groups: 25% water, 3-5% water, and 1% water	Evans 1957; O'Neill 2001	terraphilic
Cicadetta calliope	prairie cicada	feeding, dwelling, locomotion	~300-500 mm	well-drained soils <26% water content	Smith and Hasiotis 2008	hygrophilic
Cyclocephala immaculata	southern masked chafer beetle	brooding	2-4 cm for oviposition; >34 cm for larvae	>10.3 to 12.5% soil moisture for egg survival; ~15%-27% water for larvae	Potter 1983; Potter and Gordon 1984; Counts and Hasiotis 2010	terraphilic
Eryx colubrinus	Kenyan sand boa	locomotion, feeding, dwelling	~6 cm	loose sediment with little interstitial water	Hembree and Hasiotis 2007	terraphilic

Tracemaker	Common name	Primary behaviors	Maximum depth	Moisture preference	Reference	Moisture regime
Hadrurus arizonensis	giant desert hairy scorpion	dwelling	up to ~8 cm	vadose zone, between 20% and 50% moisture	Hembree et al. 2012	terraphilic
Heterocerus brunneus	variagated mud-loving beetle	feeding	just below the surface	moist mud or sand near the shores of rivers, ponds, and lakes	Clark and Ratcliffe 1989	hygrophilic
Lumbricus terrestris (juvenile)	nightcrawler; common earthworm	dwelling, feeding (anecic)	~28 cm	greater feeding in wet soil (-5 kPa matric potential), greater burrowing in drier soil (-11 kPa matric potential)	Perreault and Whalen 2006	hygrophilic
Macrotermes, various species	African mound-building termite	dwelling	soil disturbance down to 15 m; other termites known to burrow to 100 m	arid soils in regions with as little as 250mm/year rainfall	Turner et al. 2006; Cloud et al. 1980	terraphilic
Myospalax fontanierii	plateau zokor	dwelling, feeding	1.5 to >2 m deep	~20%-~30% soil water content	Zhang et al. 2003	terraphilic
Onitis, various species; *Onthophagus vaccus*	dung beetle	Nesting; Brooding	up to 130 cm, but differs by species; maximum depth limited by water table (*O. vacca*)	moist, sandy soil, 48%-66% dung moisture (Onitis); sand with 4%-8% water content (*O. vacca*)	Edwards and Aschenborn 1987; Sowig 1996	terraphilic to hygrophilic
Pogonomyrmex sp.	harvester ant	dwelling, brooding	~ 2 m	vadose zone	Halfen and Hasiotis 2010 and references therein	terraphilic
Procambarus clarkii; *P. acutus acutus*; *Cambarus diogenes diogenes*	freshwater crayfish	dwelling	1 to 5 m or more	saturated zone	Hasiotis and Mitchell 1993	hydrophilic
Scaptocoris divergens	burrower bug	dwelling, locomotion, feeding	~160 mm	~7%-37% soil moisture	Willis and Roth 1962	hygrophilic

Tracemaker	Common name	Primary behaviors	Maximum depth	Moisture preference	Reference	Moisture regime
various infaunal bivalves		dwelling, feeding	0-40 cm	aquatic environments	Kondo 1987	hydrophilic

Table 2.—Summary of trace-fossil types, vertical distributions, potential tracemakers, moisture regimes, and composition of ichnocoenoses. Surficial traces are considered epiterraphilic by definition, but note that surface traces indicative of saturated conditions, e.g., deep sauropod tracks, or standing water, e.g., vertebrate swim tracks, were considered hydrophilic for the purpose of interpreting paleohydrology.

Type	Name	Depth	Potential tracemaker	Moisture regime	Ichnocoenoses					
					Rhizohalo	cf. *Steinichnus*	cf. *Termitichnus*	*Planolites*	Vertebrate track	cf. *Camborygma*
1a	rhizoliths	>5 cm	plants	hygrophilic			X			
1b	small rhizohaloes	throughout soil profile	low-stature plants	hygrophilic	X					
1c	large rhizohaloes	>1 m	large arborescent plants	hygrophilic	X					
2	*Planolites* isp.	surface to decimeters	unknown invertebrate	hygrophilic to hydrophilic	X	X		X	X	
3	cf. *Scolicia*	surface	gastropods	hydrophilic				X		
4	cf. *Steinichnus*	dominantly on surfaces	heteroceridid beetles	hygrophilic		X		X	X	
5	*Cochlichnus*	surfaces	aquatic oligochaetes	hydrophilic		X		X	X	
6	cf. *Ancorichnus*	~10 cm	beetles, cicada nymphs	hygrophilic				X		
7	cf. *Cylindricum*	up to 27 cm	plants; spiders; tiger beetle larvae; wasps; worms; cicadas; crickets	terraphilic to hygrophilic	X			X		X
8	cf. *Macanopsis*	up to 15 cm	rove beetles; dung beetles; crickets; spiders; earthworms	hygrophilic				X		

Type	Name	Depth	Potential tracemaker	Moisture regime	Ichnocoenoses					
					Rhizohalo	cf. *Steinichnus*	cf. *Termitichnus*	*Planolites*	Vertebrate track	cf. *Camborygma*
9	cf. *Termitichnus*	up to 30 cm	termites	terraphilic			X			
10	cf. *Celliforma*	up to 18 cm	bees or wasps	hygrophilic to terraphilic				X		
11	cf. *Camborygma*	> 50 cm	crayfish	hydrophilic						X
12	Y-shaped vertical burrows	up to 25 cm	orthopteran; rove beetles; other arthropods	terraphilic						
13	cf. *Arenicolites*	up to 3 cm	chironomid larvae; Ephemeroptera	hydrophilic		X		X	X	
14	cf. *Lockeia*	surface	pelecypods	hydrophilic		X			X	
15	cf. *Kouphichnium*	surface	horseshoe crabs	epiterraphilic & hydrophilic		X				
16	cf. *Hatcherichnus sanjuanensis*	surface	crocodilians	epiterraphilic & hydrophilic					X	
17a	sauropod tracks	surface	sauropod dinosaurs	epiterraphilic						
17b	sauropod tracks	surface	sauropod dinosaurs	epiterraphilic		X		X	X	
17c	sauropod tracks	surface	diplodocid sauropod	epiterraphilic						
18a	tridactyl tracks	surface	theropod dinosaurs	epiterraphilic						
18b	tridactyl tracks	surface	theropod or ornithopod dinosaurs	epiterraphilic		X		X	X	

Type	Name	Depth	Potential tracemaker	Moisture regime	Ichnocoenoses					
					Rhizohalo	cf. *Steinichnus*	cf. *Termitichnus*	*Planolites*	Vertebrate track	cf. *Camborygma*
19	vertebrate swim traces	surface	turtles	epiterraphilic & hydrophilic		X		X	X	

FIGURES

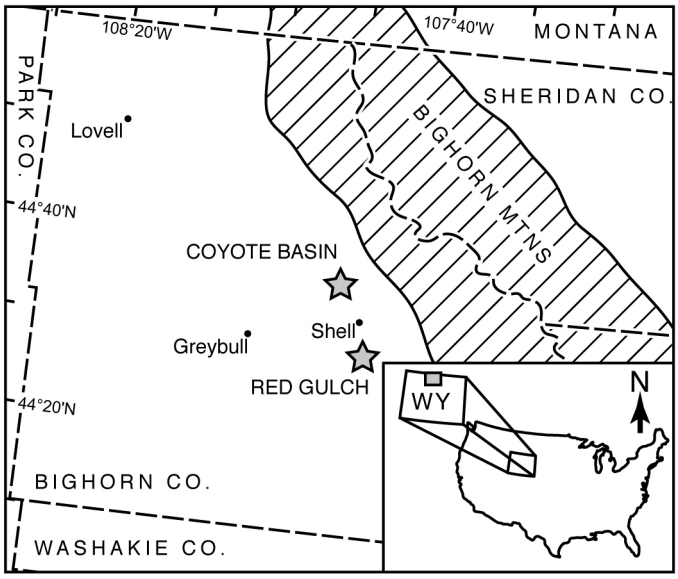

Figure 1.—Map with location of study areas.

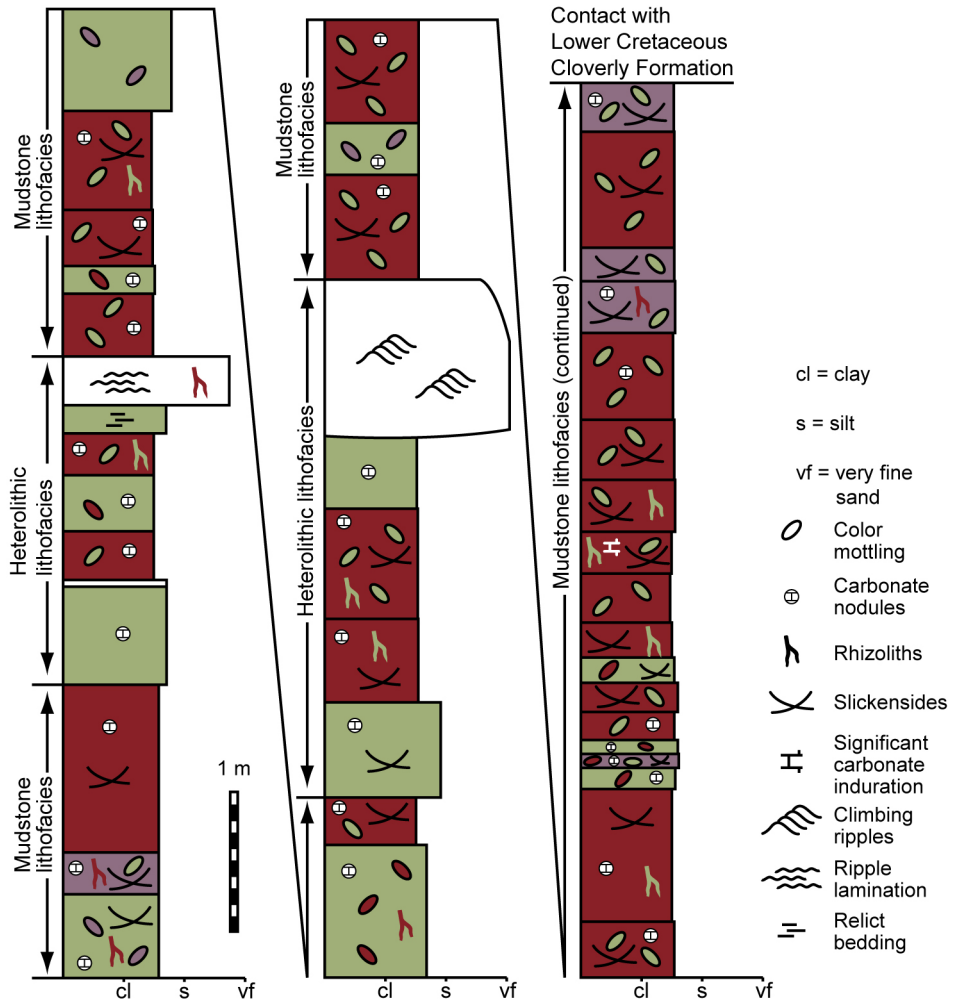

Figure 2.—Stratigraphic section through the upper part of the Upper Jurassic Morrison Formation in the study areas.

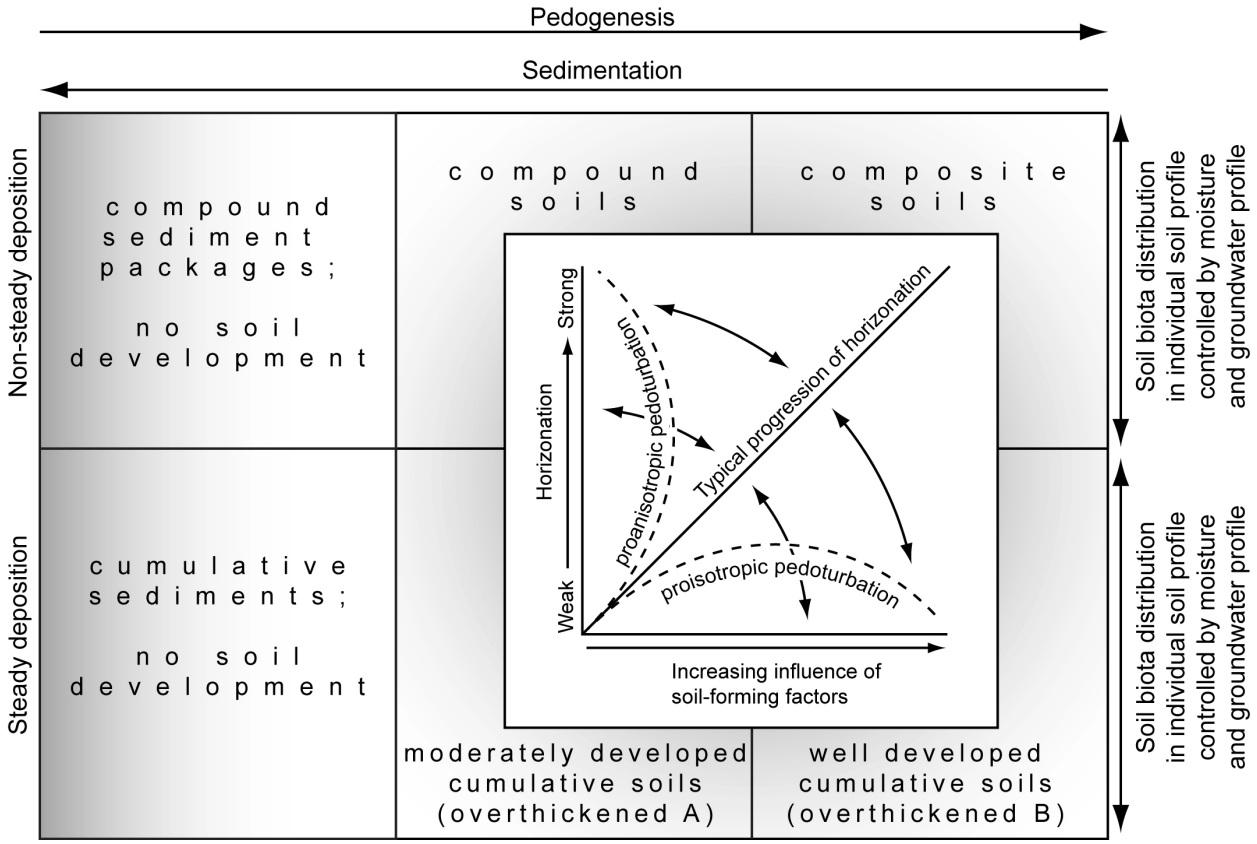

Figure 3.—Paleosol interpretation can be viewed in terms of sedimentation and pedogenesis rates combined with horizonation enhancing and destroying processes and moisture controls on soil biota distribution. Figure is based on concepts from Kraus (1999), Johnson et al. (1987), and Hasiotis (2004, 2007, 2008).

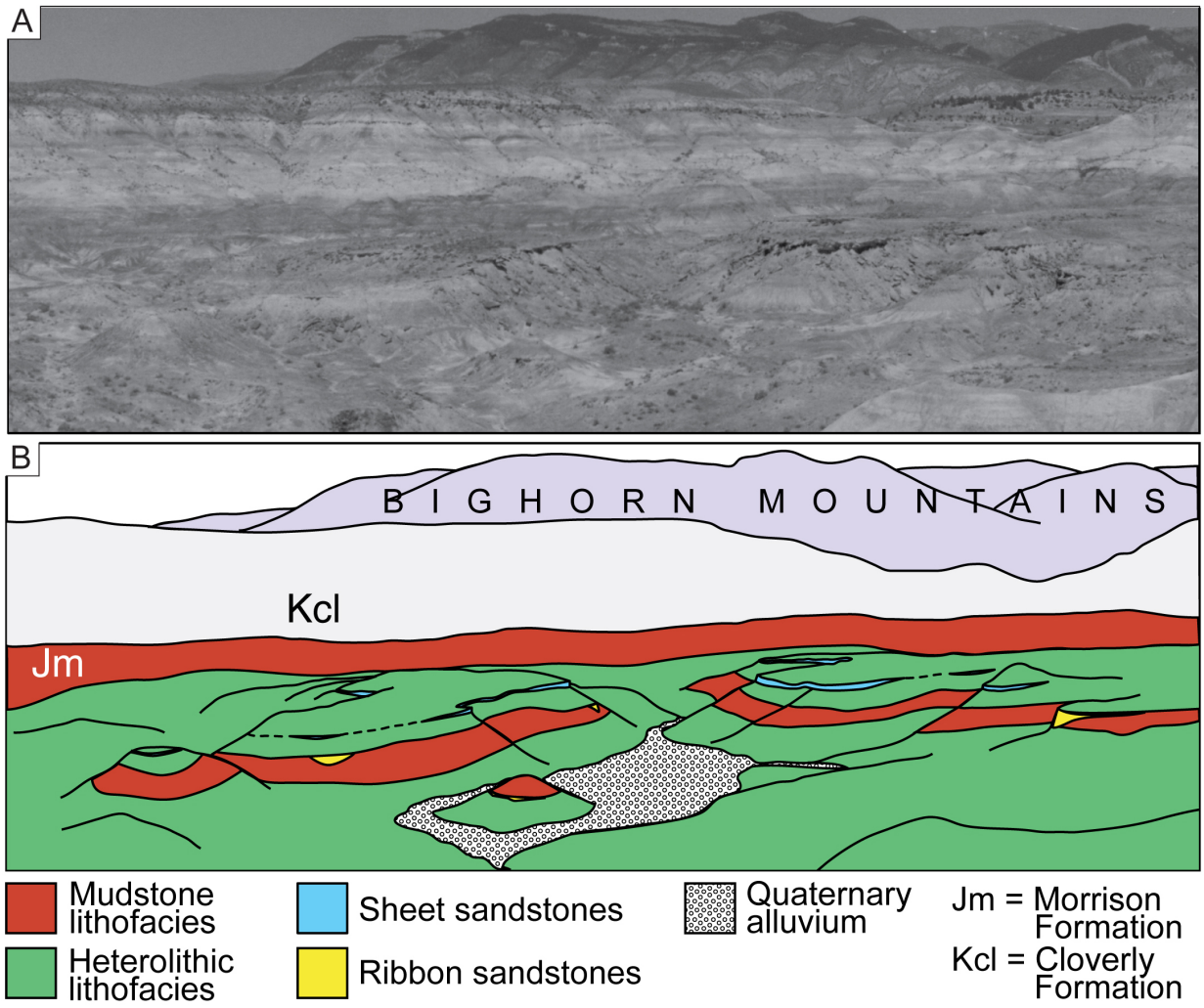

Figure 4.—A) Photomosaic of Coyote Basin, facing north. **B)** Interpretation of lithofacies relationships in A.

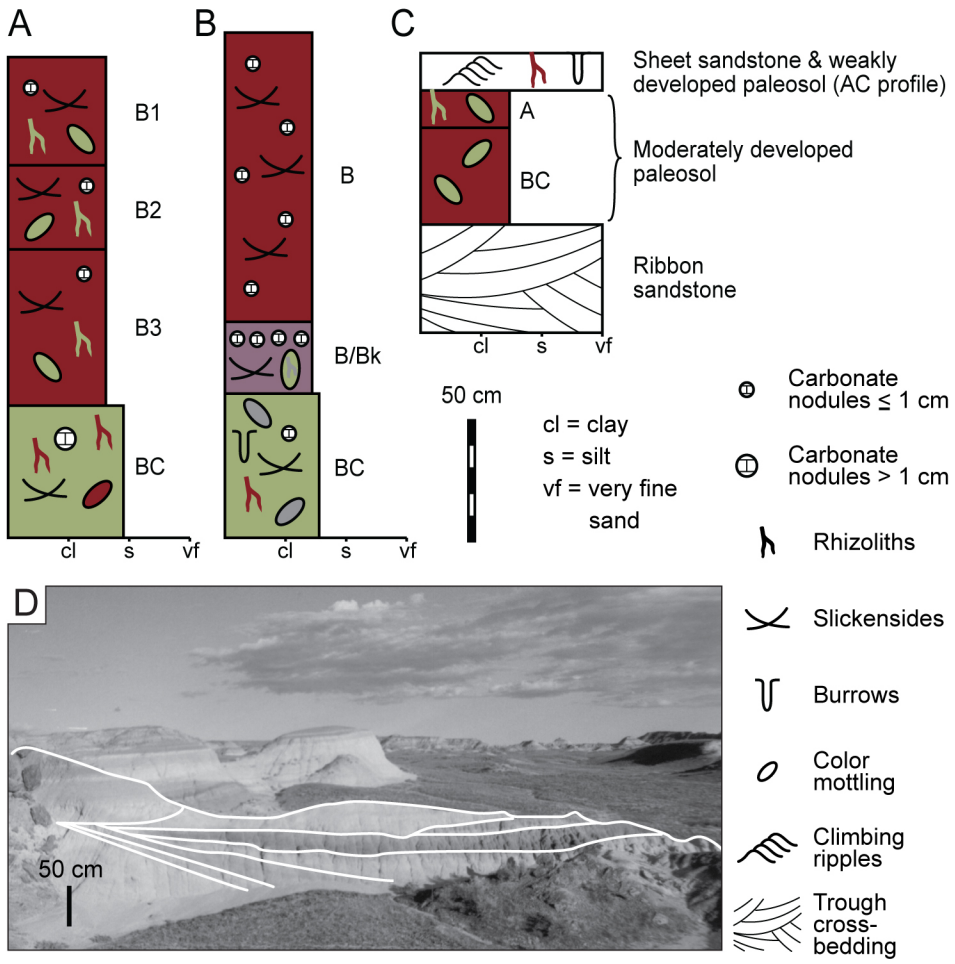

Figure 5.—A) Representative profile of a compound paleosol in the mudstone lithofacies. **B)** Representative profile of a cumulate paleosol in the mudstone lithofacies. **C)** Representative profile of a weakly developed paleosol and a moderately developed paleosol in the heterolithic lithofacies, including typical relationship between paleosols and sheet and ribbon sandstones. **D)** Scour and fill features in the heterolithic lithofacies.

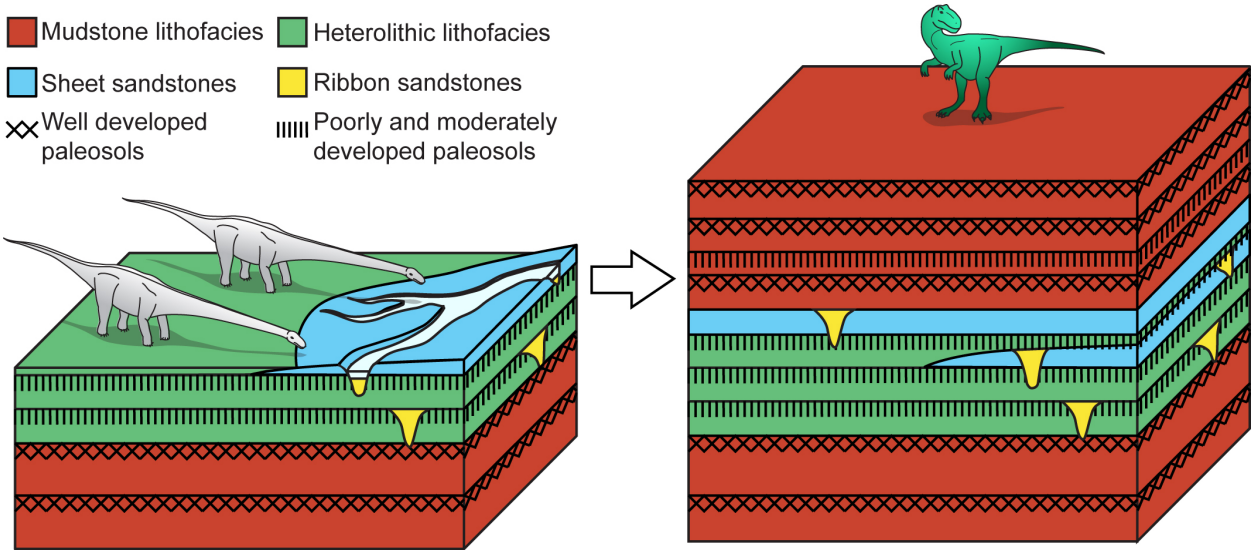

Figure 6.—Lithofacies relationships in the field areas (not to scale, but with substantial vertical exaggeration). Note that the trunk channel is absent from these floodplain cross sections.

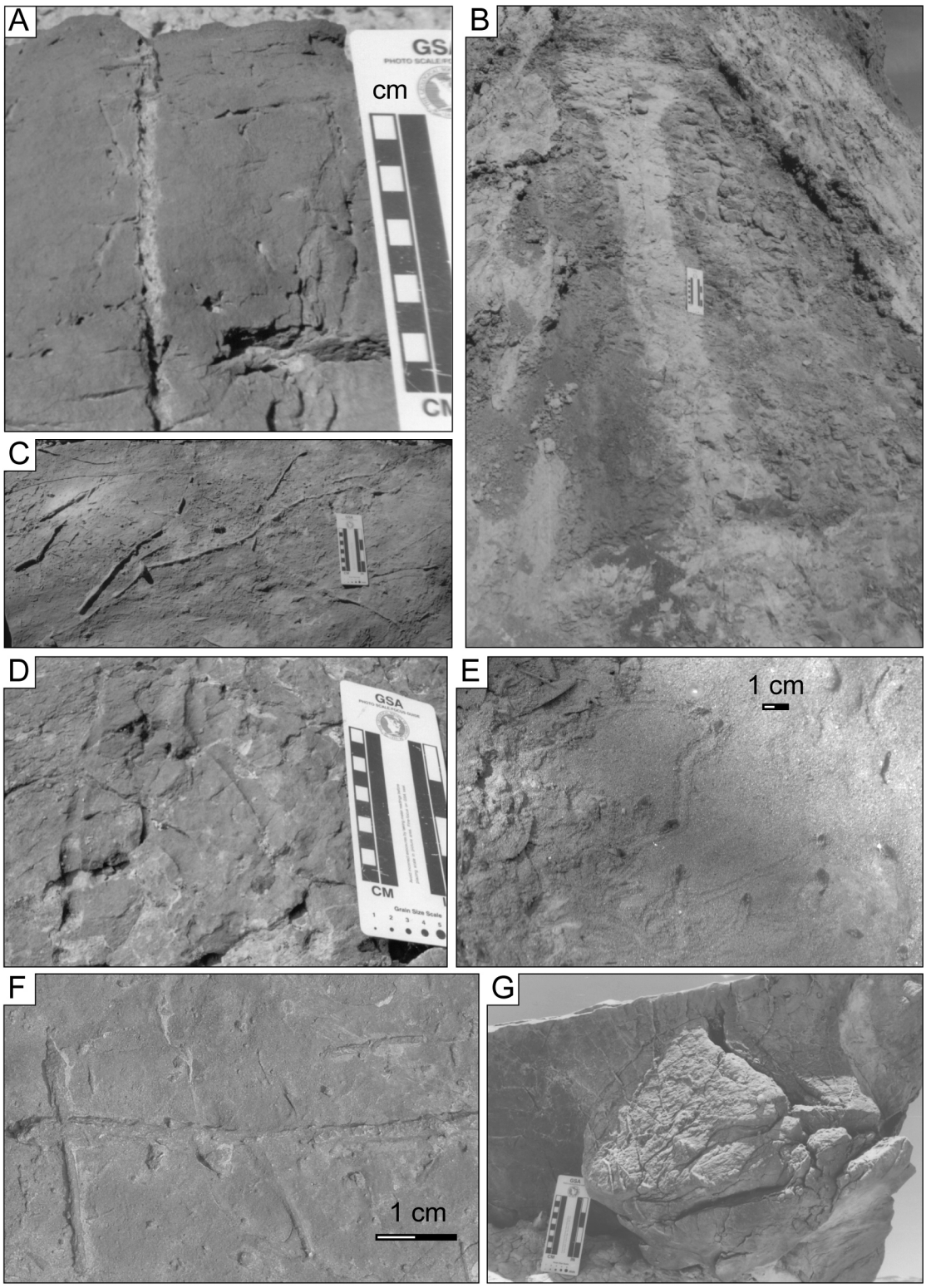
A
cm
B
C
D
GSA
CM
E
1 cm
F
1 cm
G

Figure 7 (previous page).—A) Trace type 1a rhizolith in sheet sandstone. **B)** Large rhizohalo (trace type 1c) in massive mudstone lithofacies. **C)** Trace type 2: *Planolites*. **D)** cf. *Scolicia* isp. (type 3) preserved in epirelief in sheet sandstone. **E)** Modern gastropod trails, Puerto Rico. **F)** Trace type 4: cf. *Steinichnus* isp. on bedding surface, scale bar = 1 cm. **G)** Trace type 4 lining the surface of a sauropod track (type 17).

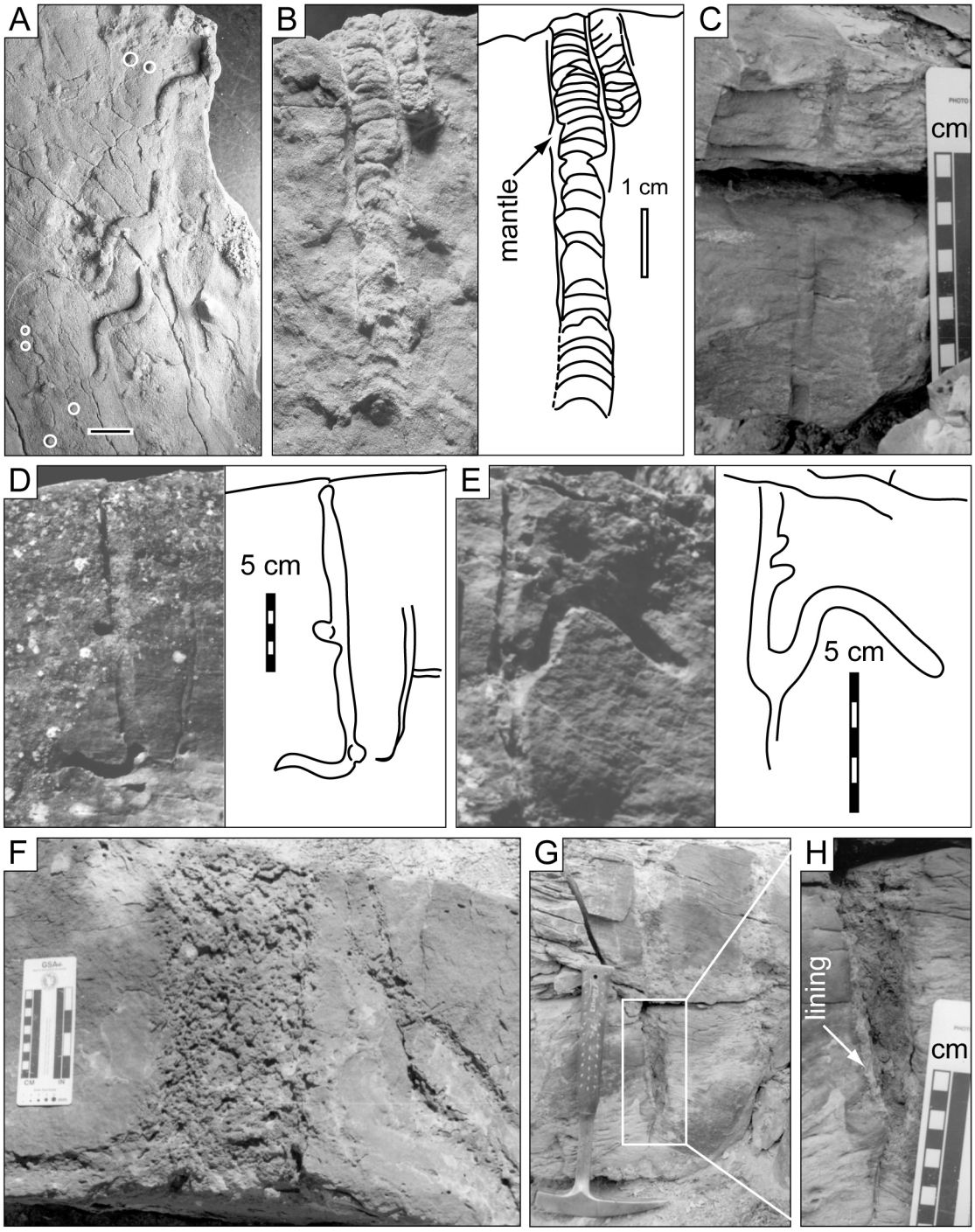

Figure 8.—A) *Cochlichnus* (trace type 5) preserved in convex hyporelief on the bottom surface of a sheet sandstone. Circles represent cf. *Arenicolites* (trace type 13). **B)** Trace type 6: cf. *Ancorichnus* isp. **C)** Trace type 7: cf. *Cylindricum*. **D** and **E)** Trace type 8: cf. *Macanopsis* and interpretive line drawings. **F** to **H**) Trace type 9: cf. *Termitichnus*. Hammer in G is 32 cm long.

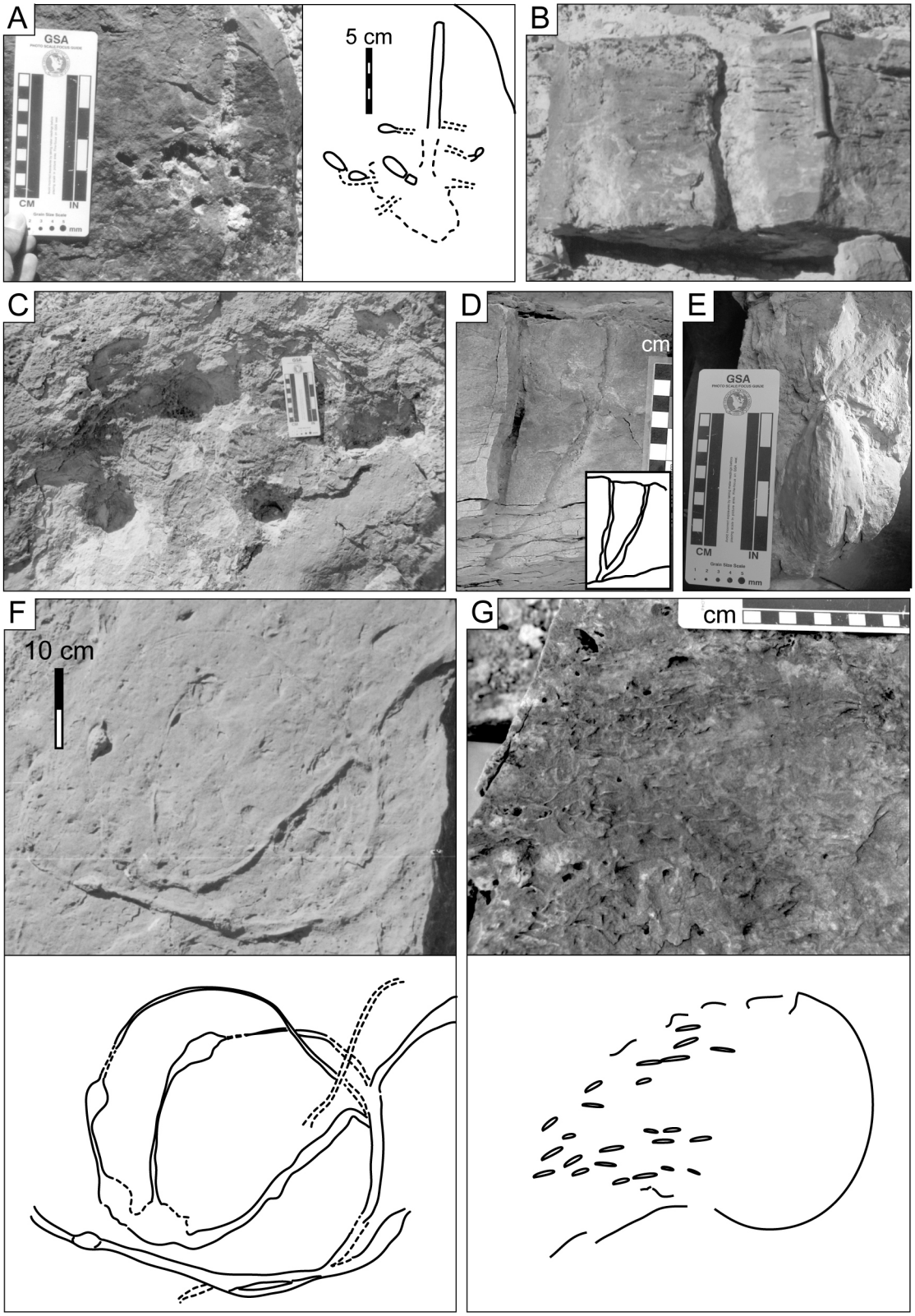
A
GSA
CM
IN
mm
5 cm
B
C
D
cm
E
GSA
CM
IN
mm
F
10 cm
G
cm

Figure 9 (previous page).—A) Trace type 10: cf. *Celliforma* and interpretive line drawing. **B)** Cross-sectional exposure of trace type 11, cf. *Camborygma*. Rock hammer is 32 cm long. **C)** Bedding surface of sheet sandstone with cluster of cf. *Camborygma* burrow openings. **D)** Trace type 12: Y-shaped vertical burrow and interpretive line drawing (inset). **E** and **F)** Trace type 14: Cf. *Lockeia*: pelecypod resting (E) and locomotion (F) traces. **G)** Trace type 15: cf. *Kouphichnium* and interpretative drawing.

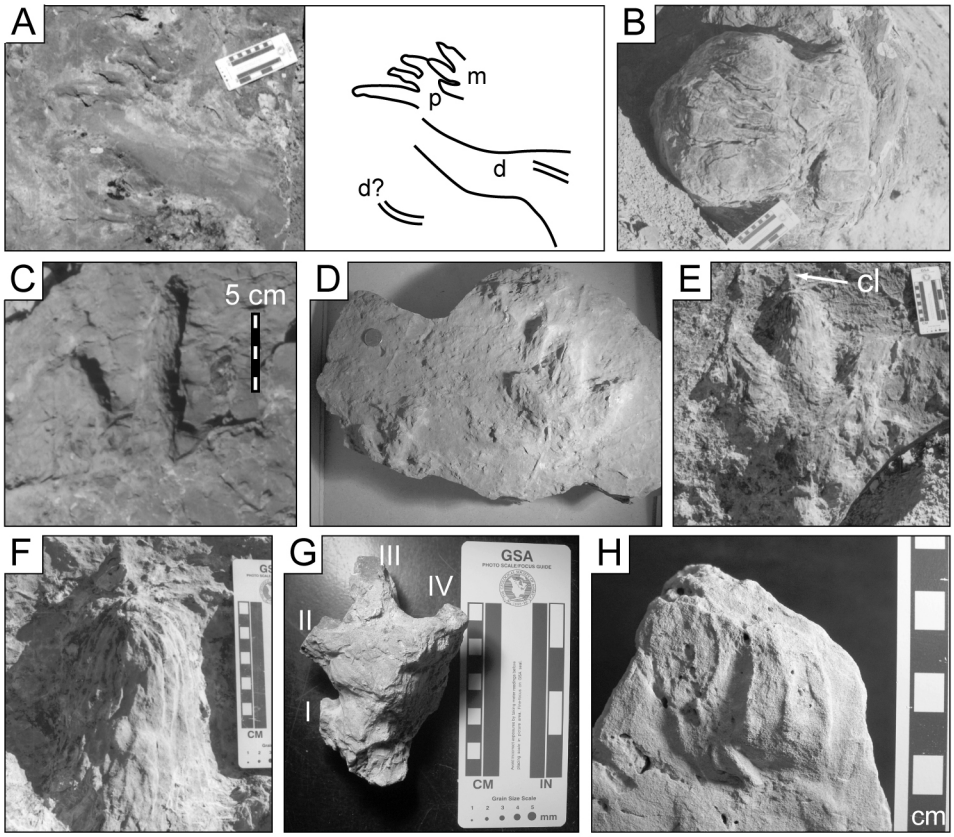

Figure 10.—A) Trace type 16: cf. *Hatcherichnus* isp. and interpretive drawing, p=pes, m=manus, d=drag mark. **B)** Natural cast of sauropod track (trace type 17b) on the base of the upper sheet sandstone (KUVP 152460). **C)** Trace type 18a: tridactyl track. **D)** Slab (KUVP 152457) with examples of trace types 18a (left) and 18b (right), coin diameter is 2.4 cm. **E)** Large tridactyl track in sheet sandstone (KUVP 152456), cl=claw impression. **F)** Close up of middle digit in E showing concentric fractures. **G)** Natural cast of a tetradactyl track (KUVP 152468). **H)** Possible turtle swim track (KUVP 152459; trace type 19), note raised area between digits.

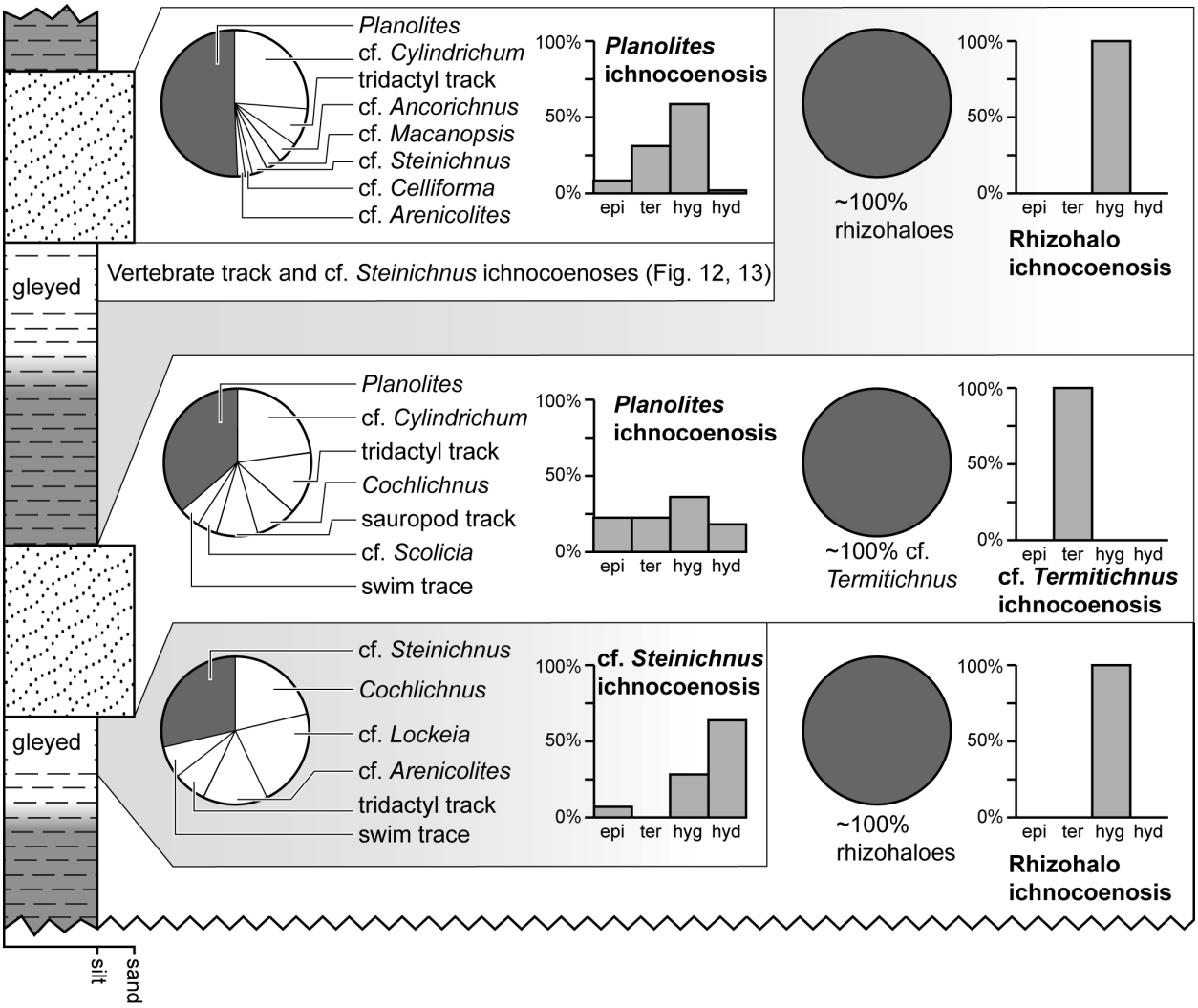

Figure 11.—Generalized stratigraphic section (no vertical scale) of the upper part of the Upper Jurassic Morrison Formation in Coyote Basin with associated ichnocoenoses. Trace fossil abundance in each ichnocoenosis is represented with pie charts; the shaded slices in pie charts represent the most abundant trace fossil in each ichnocoenosis. See Figs. 10 and 11 for ichnocoenoses preserved on the base of the upper sheet sandstone. Histograms show percentages of trace fossils in each ichnocoenosis that represent each moisture regime; X axes are arranged to show increasing moisture from left to right, epi = epiterraphilic, ter = terraphilic, hyg = hygrophilic, hyd = hydrophilic.

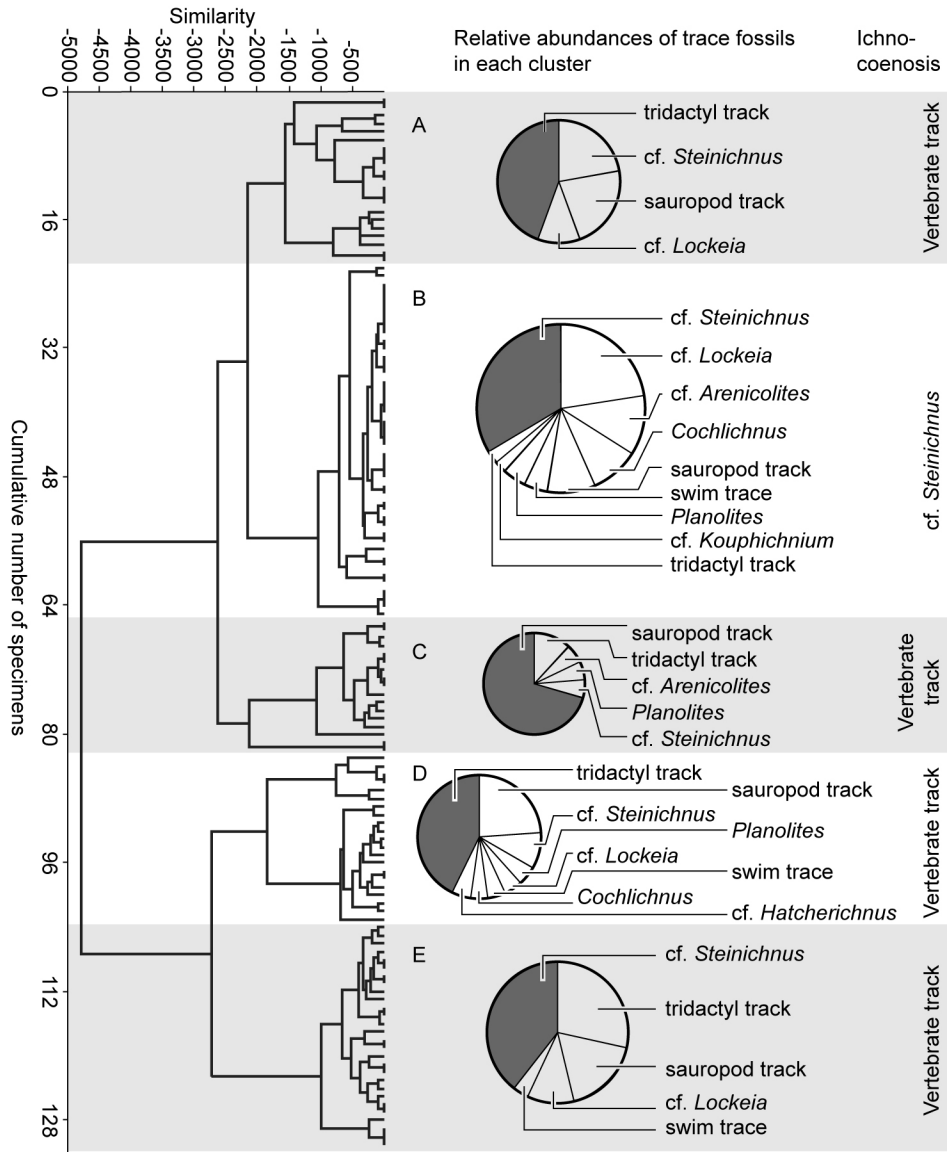

Figure 12.—Dendrogram resulting from cluster analysis of trace fossil GPS data preserved on the base of the upper sheet sandstone in Coyote Basin. Pie charts show the trace fossil composition of each of the clusters. Shaded slices of pie charts represent the most abundant trace fossil in each cluster. Note that even though cf. *Steinichnus* is the most abundant trace fossil in cluster E, when sauropod and tridactyl tracks are combined, they become the dominant traces.

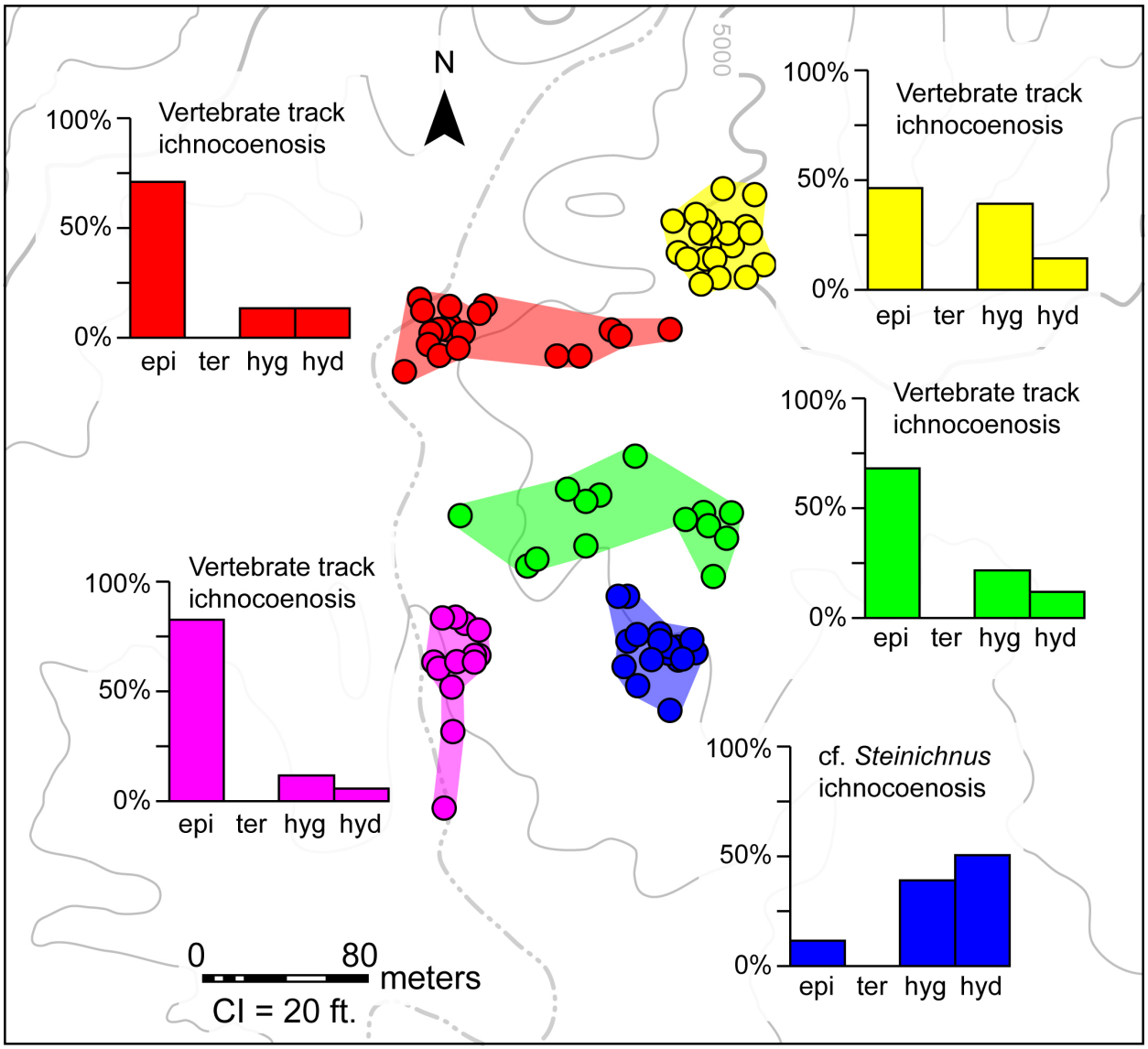

Figure 13.—Map view of clusters preserved on the base of the upper sheet sandstone. Histograms for each of the clusters represent the same information as histograms in Fig. 9. Note that the cf. *Steinichnus* ichnocoenosis represents higher moisture conditions than the other ichnocoenoses. Contours represent present topography.

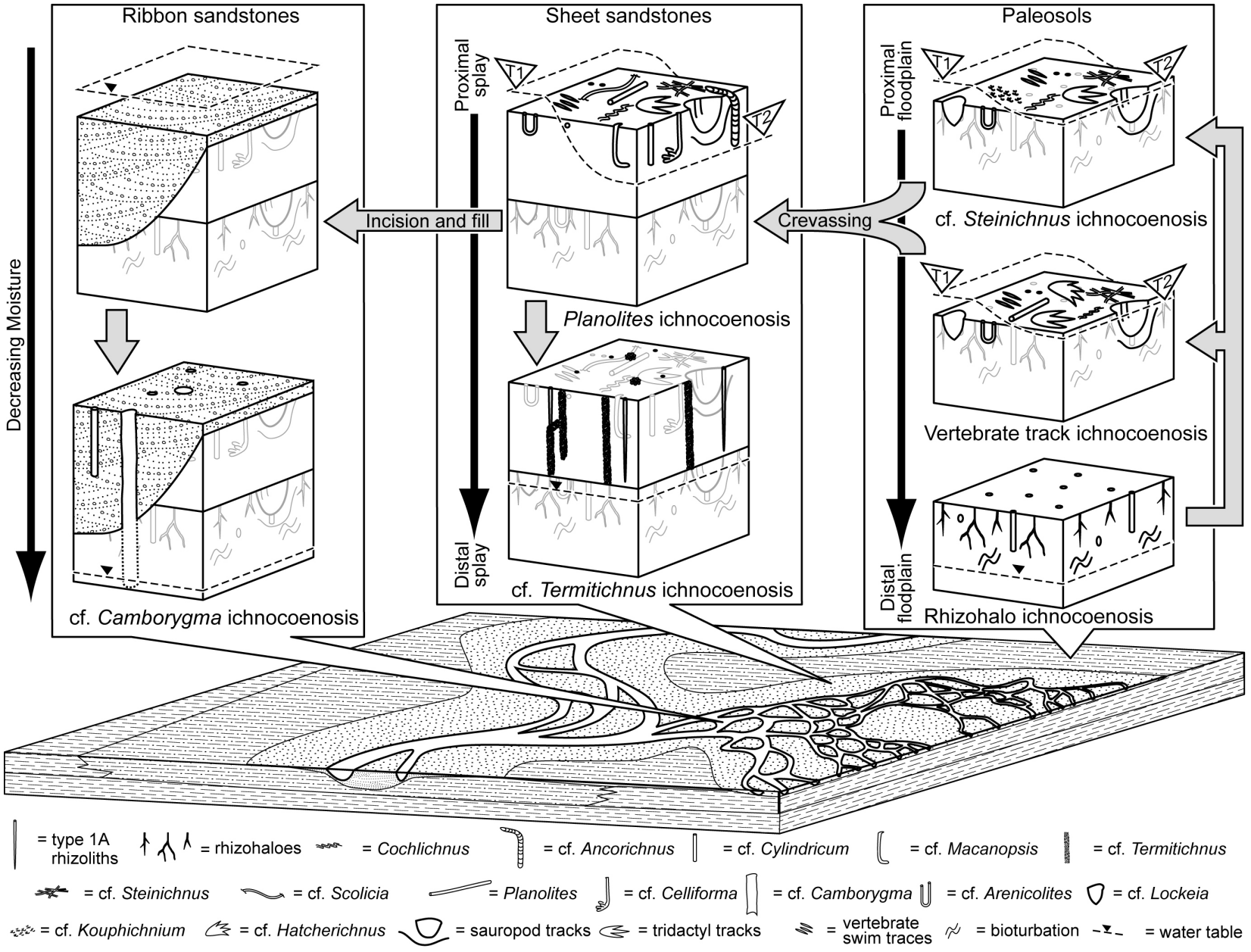
Ribbon sandstones
Sheet sandstones
Paleosols
Proximal splay
Distal splay
Proximal floodplain
Distal floodplain
T1
T2
Incision and fill
Crevassing
Decreasing Moisture
Planolites ichnocoenosis
cf. Steinichnus ichnocoenosis
Vertebrate track ichnocoenosis
cf. Camborygma ichnocoenosis
cf. Termitichnus ichnocoenosis
Rhizohalo ichnocoenosis
= type 1A rhizoliths
= rhizohaloes
= Cochlichnus
= cf. Ancorichnus
= cf. Cylindricum
= cf. Macanopsis
= cf. Termitichnus
= cf. Steinichnus
= cf. Scolicia
= Planolites
= cf. Celliforma
= cf. Camborygma
= cf. Arenicolites
= cf. Lockeia
= cf. Kouphichnium
= cf. Hatcherichnus
= sauropod tracks
= tridactyl tracks
= vertebrate swim traces
= bioturbation
= water table

Figure 14 (previous page).—Summary diagram showing relationship between ichnocoenoses, apparent floodplain position, and avulsion processes. Trace fossils in gray represent an older ichnocoenosis that has been overprinted.

CHAPTER 5: INTEGRATING PALEOPEDOLOGY, ICHNOLOGY, AND STABLE ISOTOPE GEOCHEMISTRY TO INTERPRET PALEOENVIRONMENTS AND PALEOCLIMATE THROUGH THE UPPER JURASSIC MORRISON FORMATION, UTAH, USA

Currently in preparation as:

PLATT, B.F., HASIOTIS, S.T., AND GONZÁLEZ, L.A., Integrating paleopedology, ichnology, and stable isotope geochemistry to interpret paleoenvironments and paleoclimate through the Upper Jurassic Morrison Formation, Utah, USA: Geological Society of America Bulletin.

ABSTRACT

The purpose of this paper is to interpret paleoenvironments, paleohydrology, and paleoclimate during deposition of the Upper Jurassic Morrison Formation by integrating sedimentology, paleopedology, ichnology, and stable isotope geochemistry. We measured a detailed section through the Morrison Formation in Garfield County, Utah, and performed multiple analyses of observed paleopedological and ichnological features and collected rock samples. We recognize nine lithofacies that represent, in stratigraphic order, a lacustrine environment, a fluvially dominated environment represented by thick channel sandstones and proximal overbank deposits, and a dominantly distal floodplain environment represented by thick, pedogenically modified mudstones. Within terrestrial paleoenvironments, we recognize seven pedofacies, representing different degrees of pedogenic modification and paleohydrologic conditions. Fourteen trace-fossil types, which we assign to one of four ichnological moisture regimes, are integrated with abiotic pedogenic properties to define a soil-drainage index. Soil

drainage results are combined with geochemical analyses to construct a multiproxy vertical profile useful for interpreting Morrison Formation deposits, and for correlating within and between the Morrison Formation and other terrestrial and marine stable isotope records. Soil drainage results show a general decrease in soil drainage conditions during deposition and the stable isotope results largely reflect the composition of global atmospheric CO_2 and meteoric water. Recognition of a global stable isotope signal within organic carbon isotopes allows us to draw a correlation to the marine organic carbon isotope record. This is significant because it implies that the previously recognized mid *eudoxus* positive shift represents a global event. We hypothesize that the global event represented by the mid *eudoxus* positive shift corresponds to turnover in Morrison Formation biota; future work on the basal Morrison Formation will determine the nature of the relationship between these data.

INTRODUCTION

The purpose of this paper is to combine sedimentology, ichnology, paleopedology, and geochemistry to interpret paleoenvironments and reconstruct aspects of paleoclimate during deposition of the Upper Jurassic Morrison Formation (MF). Our goal is to construct a detailed stratigraphic profile of the MF that can be compared to stratigraphic patterns in paleontological data. Correlations between paleoclimate change and paleoecology may indicate a biotic response to climate-driven ecological disturbances; better understanding of such scenarios is informative for mitigating predicted anthropogenic environmental impacts on future biodiversity and ecosystems.

The MF is an ideal unit to explore for linked climatic and biotic patterns because well over a century of study has provided a wealth of geological and paleontological data. Initial

scientific interest in the MF during the mid- to late-1800s focused on recovering dinosaur fossils (Foster, 2007), whereas uranium mining prompted substantial geological MF research in the latter part of the 20th century (Chenoweth, 1998). Compilations of paleontological data have established several biostratigraphies based on first and last occurrences of ostracodes and charophytes (Schudack et al., 1998), dinosaurs (Turner and Peterson, 1999), and vertebrates (Foster, 2003, 2007). Apparent biotic turnover suggested by these biostratigraphies has been attributed to environmental or climatic changes (Turner and Peterson, 1999).

Early reconstructions of paleoclimate, particularly moisture availability, during MF deposition yielded conflicting results (Dodson et al., 1980), but Moberly's (1960) interpretation of a strongly seasonal climate explains many of these discrepancies. More recent detailed investigations of temporal paleoclimate trends have identified an up section increase in moisture based on paleosols (Demko et al., 2004), ichnofossils (Hasiotis, 2004, 2008), and plant taphonomy (Parrish et al., 2004). Precise stratigraphic constraints on Late Jurassic climate change in the MF depositional basin, however, are not well resolved. This study represents the first attempt to incorporate vertical trends in stable isotope geochemistry with paleopedological and ichnological data to refine interpretations of paleoclimate during MF deposition.

Our results will be useful for interpreting biostratigraphic patterns, especially biotic response to climate change, which is relevant for predicting future ecosystem impacts from anthropogenic activities. Future economic exploration will also benefit from enhanced correlation possible through chemostratigraphy; this is significant, especially since laterally extensive marker beds are rare in the MF. Comparison of MF isotopes to established marine isotope records may also improve age constraints on timing of deposition and depositional rates, which are limited because of a scarcity of ash beds that can be dated reliably (Kowallis et al.,

1998).

BACKGROUND AND GEOLOGIC SETTING

The Upper Jurassic MF covers >10^6 km^2 of the western interior of North America (Dodson et al., 1980), is up to 237 m thick (Peterson, 1984), and consists of multiple named members that are best known from the Colorado Plateau region (Turner and Peterson, 2004). Morrison Formation strata represent a mosaic of paleoenvironments deposited in mostly continental settings (Dodson et al., 1980) between 30° N and 40° N paleolatitude (Demko and Parrish, 1998), with the four corners region at about 32° N paleolatitude (Turner and Peterson, 2004). There is disagreement about the precise tectonic setting of the MF (Turner and Peterson, 2004), but sedimentary provenance was lower Mesozoic, Paleozoic, and Proterozoic sedimentary rocks in highlands to the west or southwest (Bilodeau, 1986; Currie, 1998).

The MF ranges in age from ~155 Ma to ~148 Ma (latest Oxfordian? to early Tithonian) based on $^{40}Ar/^{39}Ar$ dating of sanidine grains (Kowallis et al., 1998) and U-Pb dating of zircons (Kowallis et al., 2007) from ash beds. These ages are corroborated by paleomagnetic data (Steiner, 1998).

Despite the general agreement about the age of the MF, localized age constraints are typically difficult to establish, as are correlations between locations. Abundant lateral facies changes greatly limit the number of reliable correlative surfaces, and regional correlations typically rely on the J–5 unconformity at the base of the formation (Pipiringos and O'Sullivan, 1978), the K–1 unconformity at the top of the formation (Peterson, 1994), and the clay change—a vertical change in clay mineralogy from illitic mixed-layer clays to smectitic clays attributed to a significant, rapid increase in volcanic ash (Owen et al., 1989). A well-developed paleosol

interpreted to represent a mid-Morrison unconformity is also widespread in the Colorado Plateau region (Demko et al., 2004).

We selected a study area in the Henry Mountains region of Garfield County, Utah (Fig. 1) as the MF is well exposed, relatively thick, and relatively close to sections in Notom, Utah, Hanksville, Utah, and Montezuma Creek, Utah, which have associated radiometric dates (Kowallis et al., 1998, 2007). The Henry Mountains and structural basin all postdate MF deposition (Hunt, 1980). The region has also been the subject of detailed studies—including stable isotope analyses—aimed at understanding local uranium and vanadium mineralization (Northrop and Goldhaber, 1990; Wanty et al., 1990) and sandstone body geometries (Robinson and McCabe, 1997, 1998).

In stratigraphic order, the three members of the MF represented in the study area are the Tidwell, Salt Wash, and Brushy Basin members. The Tidwell Member unconformably (at the J–5 unconformity) overlies the Middle Jurassic Summerville Formation (Peterson, 1980) and includes sandstone, siltstone, and mudstone facies interpreted as lacustrine and fluvial paleoenvironments (Peterson, 1980; Robinson and McCabe, 1997). The Salt Wash Member is composed chiefly of thick fluvial sandstone bodies, with uranium and vanadium concentrated near the base of the member (Northrop and Goldhaber, 1990). The Brushy Basin Member consists of mudstone and less common channel sandstones, and is unconformably overlain (at the K–1 unconformity) either by the Buckhorn Conglomerate of the Lower Cretaceous Cedar Mountain Formation, or the Lower Cretaceous Dakota Sandstone (Robinson and McCabe, 1997; Kowallis et al., 2007).

MATERIALS AND METHODS

Field Methods

We measured, photographed, and described a detailed stratigraphic section through the MF in the study area. Trenching was necessary to expose fresh rock through the entire Brushy Basin Member. Particular attention was paid to ichnofossils and other evidence of paleopedogenesis. We collected rock samples at 0.5 m intervals through the entire section for total organic carbon (TOC) and organic carbon stable isotope ($\delta^{13}C_{org}$) analyses; samples for $\delta^{13}C_{org}$ were also collected wherever organic-rich strata were encountered. Carbonate samples were collected for $\delta^{13}C_{carb}$ and $\delta^{18}O$ analyses where encountered.

Ichnological methods

We describe and interpret discrete trace-fossil types in the study area, and attribute them to ichnotaxa when possible. We assign trace-fossil types to one of four moisture regimes, based on moisture preferences inferred from the structure, pedogenic character of the matrix, and its similarity to structures produced by extant tracemakers (Hasiotis, 2004, 2007, 2008). These four regimes are 1) epiterraphilic—traces created by organisms living on the surface, above the water table, 2) terraphilic—traces made in and above the upper vadose zone by soil-dwelling organisms, 3) hygrophilic—organisms living within the intermediate and lower vadose zone, and 4) hydrophilic—organisms living in the phreatic zone and within saturated media below open bodies of water (Hasiotis, 2004, 2008).

Soil drainage indicators

We defined pedofacies based on distinct sets of paleopedological properties. Individual

paleosol profiles were delineated when possible, and degree of development was assessed, including assignment to one of three paleosol types: 1) simple paleosols—pedogenesis within a body of sediment from a single depositional event, 2) cumulate (or cumulic or cumulative) paleosols—thick profiles resulting from slow, continuous deposition, and 3) composite paleosols—multiple, overlapped soil profiles resulting from episodic deposition of relatively low volumes of sediment (Marriott and Wright, 1993; Kraus, 1999; Retallack, 2001). We used a method modified from Smith et al. (2008) to classify interpreted original soil drainage from paleosols in our measured section. Our classification relies on semiquantitative rankings of three factors: 1) paleosol abiotic features, 2) moisture regimes represented by animal trace fossils, and 3) rhizoliths. These factors are ranked on a scale from 1 to 4, with 1 representing poor drainage conditions and 4 representing well-drained conditions (Table 1). We described colors of paleosols from fresh, dry samples using Munsell Color Charts (Munsell, 2000) and paleosol horizons were ranked individually. The ranks of the three factors were averaged for each paleosol or horizon being considered and plotted against stratigraphic position to create a coarse visual representation of drainage conditions through the measured section. Only those categories present were included in the average, i.e., if a category was absent, it was excluded from the average, rather than assigned a value of zero. We only used evidence from observed categories because absence of features from a particular category cannot be assumed to indicate that the features are truly absent.

Carbonate content

Calcium carbonate equivalent (CCE) values of samples were determined from inorganic carbon content measured with a UIC CM5230 Acidification Module connected to a CM5015

CO_2 coulometer in the University of Kansas Pedology Lab. We also used the coulometer to determine calcite and dolomite fractions according to Hirmas et al. (2012). Calcite-dolomite fraction determinations were limited to samples containing >10% CCE because of the method followed.

Stable isotopes

Stable isotope and TOC analyses were conducted at the W. M. Keck Paleoenvironmental and Environmental Stable Isotope Laboratory at the University of Kansas. All samples for TOC and $\delta^{13}C_{org}$ determinations were powdered; hand samples were drilled along bedding and unconsolidated samples were ground with a mortar and pestle. Powdered samples were decarbonated using a procedure modified after that of Midwood and Boutton (1998). TOC and $\delta^{13}C_{org}$ were analyzed using a Costech EA interfaced to a ThermoFinnigan MAT 253. Precision for TOC values is better than ± 0.30% and for $\delta^{13}C_{org}$ better than ± 0.24‰.

Carbonate stable isotope analysis were performed on bulk carbonate samples containing variable calcite:dolomite ratios. We report, however, only results from bulk samples with carbonate fractions that we could confidently characterize as 100% calcite or 100% dolomite within the limits of the coulometric method. Calcite-dolomite separations of mixed bulk samples were attempted unsuccessfully and detailed separations were beyond the scope of this paper. Carbonate $\delta^{13}C$ and $\delta^{18}O$ analysis were performed on a Kiel III carbonate reaction device connected to the inlet of a ThermoFinnigan MAT 253. Carbonates were roasted in vacuo at 200°C for 1 hour to remove volatile components and then reacted with 100% H_3PO_4 at 75°C. Precision of $\delta^{13}C_{carb}$ is better than ±0.06‰ and for $\delta^{18}O$ is better than ±0.09‰.

We evaluated carbonate nodules by cutting them in half and creating a thin section and

polished thick section from corresponding sides of the cut. Thick and thin sections were examined under cathodoluminescence using a Reliotron III cathodoluminescence chamber at the Kansas Geological Survey. We used a microdrill to mill carbonate powders from the micritic matrix of carbonate nodules.

RESULTS

Lithofacies

We recognize nine lithofacies (A–I; Table 2), including five in the Tidwell Member (Fig. 2A), two in the Salt Wash Member (Fig. 2A,B), and three in the Brushy Basin Member (Fig. 2C). We further divide four of these lithofacies into multiple pedofacies (Table 3) based on evidence for pedogenic modification.

Lithofacies A.— Tabular to undulatory beds of greenish white, very fine to fine-grained, well-rounded, well-sorted sandstone. Beds contain locally abundant green sandy mudstone lenses and red and green, up to medium sand sized chert grains. Beds contain local scours up to 1.5 m wide and 0.5 m deep. Sedimentary structures include tabular planar cross bedding, laminations, asymmetrical ripples, and mudcracks. Bedding planes contain rare horizontal burrows.

This lithofacies represents migrating 2D dunes in a relatively low energy fluvial system infilling the incision represented by the J–5 unconformity. Localized scours represent episodes of incision and fill from small, higher energy channels, possibly small chutes traversing sandbars. Desiccation cracks indicate occasional drying during subaerial exposure.

Lithofacies B.—interbedded, coarsening upward, relatively thin (< 10 cm), tabular beds of mudstone and sandstone; sandstone beds thicken upward. Mudstones are red to brown, tan,

and green with very fine planar to convolute laminations and ripple cross laminations. There is little to no bioturbation. Sandstones are tan and very fine grained. Beds are well cemented locally and cement reacts with HCl. Rare horizontal bands of radial, feathery calcite are observed in thin section.

We interpret this lithofacies as fluvially dominated lacustrine prodelta deposits. The upward increase in grain size and sandstone bed thickness indicates increasing fluvial influence while the lacustrine basin was infilled (Tye and Coleman, 1989). Planar laminations indicate the slow rainout of fine particles. Convolute laminations indicate episodes of turbulent flow (Dzulynski and Smith, 1963) that we interpret as the result of hyperpycnal flow. The calcite crystals may represent influx of calcite-saturated groundwater (Fouke et al., 2000). Sparse trace fossils are consistent with the low ichnodiversity associated with the profundal zone (Hasiotis, 2004, 2008; Hasiotis et al., 2012-in press). Alternatively, the lack of bioturbation may indicate unfavorable conditions for lacustrine biota (Hasiotis et al., 2012-in press).

Lithofacies C.—white to brown tabular beds of silt to fine-grained sandstone; beds coarsen upward. Bedding is dominantly planar, but localized flaser bedding is present. Sedimentary structures include planar laminations, symmetrical and asymmetrical ripples, and ripple cross lamination. Some laminations are contorted, but there is little to no evidence of bioturbation. This lithofacies directly overlies lithofacies B and the transition is gradational.

The increase in grain size from lithofacies B and abundance of ripples indicate an increase in energy consistent with a prograding, shallowly dipping lacustrine delta-front environment (Tye and Coleman, 1989).

Lithofacies D.—Repeated packages of tabular to slightly undulatory beds of very fine-grained, greenish white sandstone that overlay lithofacies C and grade up to red-brown and green

laminated silty sandstone with white sandstone lenses. Sandstone lenses decrease in size and connectivity upward. Sandstones are more resistant than red, siltier intervals; sandstone cement reacts with dilute HCl. Some red silty sandstone contain mudcracks. The thickest tabular sandstone beds contain ripple cross lamination and trough cross bedding.

We interpret lithofacies D as lacustrine delta plain deposits. Sandstone beds represent pulses of relatively high-energy fluvial input and lenses to laminated silty sandstones were deposited in waning flows. The repeated nature of these sediment packages suggests multiple pulses of sedimentation, possibly from an intermittent stream. Desiccation cracks indicate periodic subaerial exposure and desiccation during decreases in lake level.

Lithofacies E.—Interbedded greenish white silty sandstone and wavy to lenticular beds of white, very fine-grained, well-sorted sandstone overlaying lithofacies D. Silty sandstone is massive with rare organic-rich zones. White sandstone beds are well cemented and cement reacts with HCl. Sandstones contain planar and ripple cross lamination. Some laminae are disrupted by bioturbation. Bases of white sandstone beds contain downwardly oriented deformation structures.

We interpret this lithofacies as representing lake margin and lakeshore sediments. The deep deformation structures are reminiscent of dinoturbation and indicate trampling of wet sediment (Jennings et al., 2006; Platt and Hasiotis, 2006).

Lithofacies F.—Scour-based beds of fining upward, fine to medium, white to tan sandstone, often with rip-up mudstone clasts and coarse pebble lags. Trough cross bedding is the dominant sedimentary structure, but planar tabular cross bedding and horizontal plane beds are also present. Trough cross bedding may flatten out to plane beds upward. Some beds contain trace fossils. Fining upward sequences may be capped with green laminated mudstone < 10 cm

thick.

We interpret this lithofacies as channel fill deposits. Scoured bases, coarse grains, and trough cross bedding indicate high-energy flow and 3D dunes at the bases of these beds. Fining upward patterns and transitions to planar tabular cross bedding and plane beds indicate waning flow conditions. Laminated green mudstones are interpreted as slackwater deposits associated with channel abandonment.

Lithofacies G.—Very fine-grained, greenish white sandstone beds 5 to 50 cm thick interbedded with dominantly red mudstone beds 5 to 60 cm thick. Sandstones are typically sharp based, laterally extensive, massively bedded, and well cemented; cement reacts with dilute HCl. Other sedimentary structures in sandstones include trough cross bedding, plane beds, ripple cross lamination, and climbing ripple lamination. Trace fossils are abundant in sandstones and include rhizoliths and burrows. Local scours are present, including one that truncates 30 cm of mudstone. Mudstones are red to purple and are dominantly massive, but green laminations and ripple laminations are also present as are mudcracks. Trace fossils are also abundant in mudstones; some are infilled by subadjacent sandstone and some contain a massive infill that is reactive with dilute HCl. Carbonate nodules are rare and locally present within mudstone beds. Mudcracks are also present in some mudstone beds.

We interpret lithofacies G as levee and proximal overbank deposits. Sandstone beds represent crevasse-splay deposits and interdistributary channels. Mudstones represent levee deposits and pedogenically modified floodplain deposits. As such, this lithofacies represents relatively rapid deposition rates.

Lithofacies H.—Dominantly red, gray, or light green, massive mudstone with one or more of the following features: color banding, color mottling, fracture into small aggregates,

locally abundant glossy, clay-rich surfaces with parallel striations, bioturbation, and locally abundant discrete trace fossils, including rhizoliths. Some color bands occur at changes in grain size. Some beds may contain up to fine-grained sand grains. Mudstone cement reacts with HCl. Beds rarely contain small carbonate nodules or undisturbed remnants of original bedding.

We interpret mudstones as distal overbank deposits and the massive fabric as the result of pedogenesis and bioturbation. A suite of additional soil features also supports an interpretation of pedogenic modification. Color banding represents soil horizons and associated changes in grain size represent results of illuviation. Color mottling represents redoximorphic depletions and concentrations of Fe (e.g., Rabenhorst and Parikh, 2000). Paleosol horizons that fracture into small aggregates may be displaying original ped structures. Glossy, clay-rich, striated surfaces are interpreted as pedogenic slickensides.

Lithofacies I.—white to greenish gray, well-sorted, mostly massive, mudstone with conchoidal fracture on freshly exposed surfaces. Primary sedimentary structures are rare and include horizontal planar laminae and ripple cross stratification. Rare gray siltstone clasts up to 1 cm in diameter are also present and associated with color mottling. Brown and tan color mottling and clay-filled tubes are common in massive beds. Thin sections show locally abundant, conspicuous vermiform kaolinite and rare volcanic glass shards. Rocks do not react with HCl and disaggregate and swell rapidly when introduced to water. This lithofacies is present in the upper half of the Brushy Basin Member where it is expressed on the surface with a popcorn-weathered texture.

The upper Brushy Basin Member is known to contain a large amount of smectite derived from volcanic ash (Turner and Fishman, 1991). The sorting, massive bedding, abundance of smectitic clays, and paucity of ash shards suggest extensive reworking of volcaniclastic sediment.

Relict bedding suggests a fluvial origin for sediments in this lithofacies and particle size indicates a distal floodplain setting. Clay-filled tubes are interpreted as rhizoliths and burrows and, together with color mottling, indicate pedogenic modification. We interpret an overall lack of sedimentary structures and trace fossils as a result of mixing from the high smectite content.

Pedofacies

Pedofacies I (Table 3; Fig. 3A).—These paleosols are found in Lithofacies G, are 10 to 100 cm thick, and are dominantly red to brown with sporadic light gray and light greenish gray mottles. Most show no evidence of horizonation. Other locally abundant features include relict bedding and mudcracks. Trace fossils are locally abundant and include rhizohaloes and vertical and horizontal burrows.

Relict sedimentary structures and lack of evidence of horizonation indicate relatively weakly developed soils; these likely resulted from the rapid deposition rates interpreted for the heterolithic lithofacies. The red coloration and carbonate nodules are typical of well-drained paleosols (e.g., Demko et al., 2004; Smith et al., 2008). Desiccation cracks and rare slickensides indicate limited wetting and drying of soils and possibly more arid conditions relative to pedofacies found in the Brushy Basin Member. We interpret each paleosol in pedofacies I as consisting of an AC profile; this qualifies these paleosols as Entisols (Soil Survey Staff, 2010).

Pedofacies II (Table 3; Fig. 3B).—Similar to pedofacies I, but with incipient or clear horizonation, and presence of such features as slickensides and carbonate nodules. Many carbonate nodules consist of a micritic matrix with centrally located radial veins filled with sparry calcite. Some profiles may be >1 m thick and contain large burrows. Overall, these paleosols represent increased pedogenic development compared to pedofacies I paleosols.

Pedofacies III (Table 3; Fig. 3C).—These paleosols are present within the trough cross-bedded lithofacies and sandstone intervals in the massive mudstone lithofacies. Examples are no more than 0.5 m thick with massive bedding, bioturbation, and discrete, relatively shallow trace fossils, including rhizoliths. There is no evidence of horizonation.

These paleosols represent relatively minimal pedogenic modification of crevasse splay and channel sandstones and are considered Entisols (Soil Survey Staff, 2010). These Entisols likely formed during relatively brief depositional hiatuses.

Pedofacies IV (Table 3; Fig. 3D).—Found in the massive mudstone lithofacies, up to several meters thick, matrix color is generally red and gray color mottling is common. Composed of multiple, distinct horizons with local concentrations of rhizoliths in individual horizons. Some horizon colors, textures, and properties are repeated within a vertical profile. Some boundaries between horizons show a gradation or superimposition of features; for example, concentrated zones of rhizoliths may be superimposed on gray mottles. Relict bedding and sedimentary structures are present at the bases of some profiles. Clay-rich horizons are common and may contain slickensides. Clay-rich rock fractures preferentially into angular, equidimensional to horizontally elongated blocks.

Repeated vertical patterns within profiles suggest stacked paleosols. Overlap between subadjacent paleosols classifies these units as composite paleosols (Wright and Marriott, 1996). Dominant red coloration represents relatively well-drained conditions and gray mottles record redoximorphic features from fluctuating moisture conditions (Kraus and Aslan, 1993). Distinct horizons are present, e.g., clay-rich horizons with slickensides and blocky ped structure represented by natural fracture are interpreted as B or Bt horizons. Distinct horizons show that the soils were relatively mature (Kraus and Brown [*recte* Bown], 1988). Composite paleosols

represent substantial pulses of sediment that became welded to existing soil profiles (Wright and Marriott, 1996); this scenario likely represents deposition in an intermediate portion of the floodplain that was subjected to periodic flooding.

Pedofacies V (Table 3; Fig. 3E).—Units within the massive mudstone lithofacies that are up to several meters thick and dominantly red with distinct horizonation and common gray color mottling. Many horizons are relatively thick and some of these thick horizons coarsen upward. Rare relict bedding is present in some horizons and clay-coated slickensided surfaces are common in clay-rich horizons. Rhizoliths are the most common trace fossils. Bioturbation and small diameter burrows are also present.

Over-thickened horizons and upward coarsening are consistent with fairly high rates of deposition of thin packages of sediment, qualifying paleosols in this pedofacies as cumulate or cumulic paleosols (Wright and Marriott, 1996; Kraus, 1999; Retallack, 2001). Coloration indicates drainage conditions similar to those of pedofacies IV. Greater concentrations of clay and the cumulative nature of these paleosols suggests that they were deposited in a more distal floodplain setting relative to pedofacies IV.

Pedofacies VI (Table 3; Fig. 3F).—Dominantly gray and greenish gray units up to several meters thick within the massive mudstone lithofacies that contain multiple, distinct horizons. Some horizons are relatively thick and gradually coarsen upward. Isolated horizons consist of a red or purple matrix with various amounts of color mottling. Rhizoliths are present throughout but may be concentrated locally in horizontal zones. Rhizoliths are commonly shades of brown with dark haloes and may be clay filled.

The physical properties of these paleosols indicate that they are cumulate, similar to pedofacies V. The abundance of gray colors indicative of reducing conditions (Kraus and Aslan,

1993) and lack of slickensides suggests that these soils were poorly drained. We interpret depositional settings as distal floodplain environments with relatively high, possibly perched water tables.

Pedofacies VII (Table 3; Fig. 3G).—Pedogenic modification in the smectitic mudstone lithofacies falls into this pedofacies. Paleosol thicknesses vary and can be up to several meters. Matrix colors include light greenish gray, white, and pale yellow. Color mottling is common and is typically weak red or greenish gray. There is little to no evidence of horizontaion and rhizoliths are present, but they are dispersed vertically throughout paleosols and are not found in dense concentrations. Rhizoliths are preserved as rhizohaloes, clay-filled rhizoliths, and carbonized root fossils (e.g., Kraus and Hasiotis, 2006).

The thick nature of the paleosols suggests relatively frequent additions of small increments of sediment, classifying these paleosols as cumulic paleosols. The dominant colors and carbonized roots are typical of paleosols formed in reducing conditions and indicate poor drainage conditions (Kraus and Aslan, 1993; Kraus and Hasiotis, 2006; Lal, 2006).

Ichnology

Type 1: Rhizohaloes (Fig. 4A, B).—Thin (< 1 cm thick), vertical to horizontal, isolated to interconnected networks of linear to curvilinear zones of coloration that differ from matrix color. There is no associated change in grain size and branching and tapering are common. These traces are most abundant in pedofacies I, II, and IV–VII. Light, greenish gray and purple are common trace colors within red paleosol horizons. Brown, black, and purple are common colors in gray, green, and white paleosol horizons. One or more thin, concentric zones of a different color surround many of these traces.

We interpret these traces as rhizohaloes, which are Fe- and Mn-depleted zones that formed around roots because of changing soil moisture conditions and organic decay (Kraus and Hasiotis, 2006). Colors of rhizohaloes and rims are indicative of drainage conditions (Table 1; Kraus and Hasiotis, 2006). Horizontal, dense rhizohaloes may be evidence of root mats that developed in A horizons, or at stable water table positions (Cohen, 1982).

Type 2: Rhizoliths (Fig. 4B, C).—Mainly vertically oriented, semicylindrical molds and casts in sandstone and tubular zones of greenish gray and light reddish brown claystone and mudstone with roughly circular cross sections. Diameters are typically < 1 cm when preserved in mudstone, but larger examples preserved in sandstones are up to ~5 cm in diameter. Maximum length is ~50 cm. Branching and tapering are common. No colored haloes were observed surrounding these traces in paleosols, but some discoloration is present on the walls of examples preserved in sandstone. The larger, semicylindrical traces are found in pedofacies III. Clay and mud-filled examples are present in pedofacies V, VI, and VII above the clay change.

We interpret the semicylindrical voids and tubes within sandstones as rhizoliths—the external molds and casts of decayed subsurface roots (Kraus and Hasiotis, 2006). Voids left by roots provided conduits for clay illuviation in clay-rich parent material (e.g., altered ash in lithofacies I in the Brushy Basin Member).

Type 3: Carbonized root fossils and rhizoliths (Fig. 4D).—Vertical to horizontally oriented, black, carbonaceous strands up to 0.5 cm in diameter. Branching and tapering are common. Some carbonaceous strands are rimmed by dark brown zones of matrix coloration. These traces are found exclusively within pedofacies VII.

We interpret these features as carbonized root fossils preserved within their channels rhizoliths. Carbonaceous root fossils are preserved by anoxic conditions from high water tables

and are typically found in very poorly drained paleosols (Kraus and Hasiotis 2006).

Type 4: Horizontal burrows cf. *Planolites* (Fig. 5A).—Mostly horizontal, linear to slightly sinuous tubes and tube casts up to 20 cm long with circular to elliptical cross sections ≤1 cm in diameter. Tubes have a consistent diameter throughout their length and their walls are smooth. There is no evidence of wall linings. Casts typically are composed of the same material as the matrix and are massive.

We interpret these traces as burrows constructed by invertebrates moving horizontally through the sediment. The architecture of these traces is similar to both *Planolites* and *Palaeophycus*, but absence of a wall lining precludes assignment to *Palaeophycus* and a fill that is the same lithology as the matrix excludes a designation of *Planolites* (Häntzschel, 1980; Pemberton and Frey, 1982). We refer to these traces as cf. *Planolites* because we believe the absence of a wall lining is a more relevant to paleoenvironmental interpretation than the composition of the burrow fill. The structureless nature of the burrow fill suggests that sediment was not actively ingested and passed through the gut of the tracemaker as in the original interpretation of *Planolites* (Häntzschel, 1980). Type 4 burrows were likely passively infilled, requiring suitable sediment consistency to maintain an open, unlined burrow. Sufficient sediment consistency requires variably moist conditions, which qualifies these burrows as terraphilic to hygrophilic (Hasiotis, 2004, 2008).

Type 5: Large-diameter, vertical burrows: cf. *Camborygma litonomos* (Fig. 5B, C).—Vertical tubes ~ 2 cm wide and up to ~ 15 cm long, preserved in sandstones and mudstones in the heterolithic lithofacies. Architectures are simple; only single shafts were observed and there is no evidence of branching. Tubes are filled with sediment from subadjacent units and the surrounding matrix. Associated natural casts in float show rarely preserved knobby surficial

textures (Fig. 5C).

Even though no terminal chambers are preserved, the simple architecture and surficial morphology suggest that these traces can be assigned to *Camborygma litonomos* (Hasiotis and Mitchell, 1993). *Camborygma* represents the burrowing behavior of crayfish and this ichnogenus is reported from elsewhere in the MF (Hasiotis et al., 1998; Hasiotis, 2004, 2008). The crayfish responsible for creating burrows with such simple architectures commonly live in open water and burrow for protection, reproduction, and to keep moist during episodes of lowered water tables (Hasiotis and Mitchell, 1993). This is consistent with the near-channel environment interpreted for the heterolithic lithofacies where these burrows are present.

Type 6: J-shaped burrows (Fig. 5D).—Vertical, narrow diameter (~1 cm), J-shaped burrows found in sandstones in lithofacies G and F. Burrow may have a gentle curve at depth, or a sharp hooked shape that becomes more horizontal after it curves back upward. Wall surfaces are typically smooth, but some examples show slight ribbing perpendicular to the burrow axis (Fig. 5D).

Modern invertebrates that construct J-shaped burrows include beetles, spiders, and crickets (Bryson, 1939; Chamberlain, 1975; Ratcliffe and Fagerstrom, 1980; Hasiotis, 2002; Hasiotis unpublished research); however, the observed burrow may just be a J-shaped segment from a larger burrow network. Alternatively, the remnants of ribbing on burrow walls might represent the menisci from active backfilling by such tracemakers as beetle larvae and cicada nymphs, which maintain open cells in the subsurface (Smith and Hasiotis, 2008; Counts and Hasiotis, 2009). Regardless of the specific tracemaker, these traces are terraphilic and represent construction in the vadose zone (Hasiotis, 2004, 2008).

Type 7.—Small-diameter-burrow networks: cf. *Palaeophycus* (Fig. 5E, F).—Small

diameter (< 1 cm), mainly horizontal, straight to slightly curved cylinders in relatively dense accumulations visible on the tops of sandstone beds in lithofacies F. Cylinders are filled with the same material as the host rock and regularly crosscut and intersect each other at T- to Y- shaped junctions. Walls are smooth with a surface lining up to 1 mm thick (Fig. 5F).

These traces are most similar to *Palaeophycus* (Häntzschel, 1980; Pemberton and Frey, 1982), which is typically attributed to worms in marine settings. In continental settings *Palaeophycus* has been attributed to crustaceans and insects (Buatois and Mángano 2002); however, this morphology could be produced by a variety of animals and plant roots. Thin to thick, continuous to discontinuous linings can also be found on a variety of continental burrow morphologies, including the galleries of ant and termite nests (e.g., Krishna and Weesner, 1970; Hasiotis, 2003, 2004; Smith and Hasiotis, 2008; Counts and Hasiotis, 2009; Halfen and Hasiotis, 2010). This burrow morphology likely represents a range of terraphilic to hydrophilic behaviors (Hasiotis, 2004, 2`008).

Type 8.—Rhizolith-associated termite traces (Fig. 6A).—Downward tapering, branching, semicylindrical features with a pitted wall texture within sandstones. Features are up to 5 cm wide and up to 55 cm deep. Associated are horizontally elongated voids. Multiple examples of this trace are found within a single lithofacies G sandstone bed spaced 0.5 m to several meters apart.

These traces have the overall architecture of rhizoliths (Type 2), but with modification of the matrix in and around the root. Similar structures in the MF have been interpreted previously as the result of termites modifying the sediment adjacent to roots (Hasiotis, 2002, 2004; Jones and Gustason, 2006). Some groups of subterranean termites exhibit behaviors similar to those indicated by trace type 8, i.e., exploiting living and dead roots in the subsurface (Thompson

1934; King and Spink 1969; Krishna and Weesner, 1970). Such behavior is terraphilic, based on the moisture requirements of extant termites (Hasiotis, 2004, 2008). The presence of type 8 traces indicates water table levels below maximum trace depth and relatively well-drained conditions.

Type 9.—Large, vertical column of massive, vuggy sandstone—termite traces (Fig. 6B-E).—Large, slightly downward-tapering column of massive sandstone up to 25 cm in diameter and 1.1 m deep. Only one example of this trace type was observed in the study area within plane- and cross-bedded sandstone with white chert gravel lags in lithofacies F. The top of the column is associated with porous, massive sandstone. Adjacent to the column, gravel lags are undisturbed, but they are completely disrupted and chert grains are well sorted within the column.

Structures with this architecture have been attributed to fluid escape, biogenic escape, and subterranean termite activity. We rule out an interpretation of type 9 structures as fluid and biogenic escape because displacement of grains is random, not as in fluid escape structures (e.g., Riese et al., 2011) or biogenic escape structures (e.g., Buck and Goldring, 2003). The morphology is also inconsistent with passively filled large-diameter mammal burrows, which are typically not completely vertical (Riese et al., 2011). We favor an interpretation of the type 9 trace as a termite nest, similar to those constructed by *Microcerotermes parvus* (Hegh, 1922; Grassé, 1984) and *Baucaliotermes hainesi* (Tschinkel, 2010). We interpret the porous sandstone associated with the column as multiple chambers near the paleosurface similar to other fossil termite nests (Grassé, 1986). This particular nest likely supported a very large termite colony because nest size is correlated to number of termites (Josens and Soki, 2010). The depth of the nest provides a minimum estimate of depth to the water table (Frisch, 1974) and represents

terraphilic behavior (Hasiotis, 2004, 2008).

Type 10.—Large-diameter, simple, subhorizontal burrows (Fig. 7A).— Subhorizontally oriented, elongate, circular to elliptical cylindrical tubes with minimum diameters of ~5 cm and up to ~70 cm in length. Burrows are typically preserved within red paleosols (pedofacies I and II) and filled with carbonate and sandstone from an overlying sandstone bed. Angles of intersection with the overlying sandstone bed range from 10° to 50°. Tubes with elliptical cross sections are oriented so the long axis of the ellipse is horizontal. Surficial morphology is typically not well preserved.

Similar burrows in the MF were identified by Hasiotis et al. (2004), who interpreted them as reptile burrows. Elliptical cylindrical cylinders may represent vertical compression of an originally circular tube. These burrows represent terraphilic behavior (Hasiotis, 2004, 2008) and indicate relatively well-drained conditions in pedofacies I and II paleosols.

Type 11.—cf. *Daemonelix* (Fig. 7B, C).—Helical, cylindrical tubes with a consistent diameter and arranged in a tight vertical spiral (Fig. 7B, C). Tube coils are near horizontal so the angle of coiling is very low. Some examples contain a large upper chamber and end in a straight, horizontal to subhorizontal tube with a hemispherical termination (Fig. 7C). Tubes are composed of carbonate-cemented sandstone within pedofacies I and II. Tube surface morphology ranges from smooth to rough with polygonal cracks.

This trace is most similar to the helical trace *Daemonelix*, which is attributed, in North American Cenozoic strata, to the beaver *Palaeocastor* (Martin and Bennett, 1977) and other mammals (Hembree and Hasiotis, 2008). Spiral burrow excavation by vertebrates is known, however, from as early as the Permian (Smith, 1987). The most likely tracemakers of these burrows in the MF are mammals, based on their abundance in the MF (e.g., Englemann and

Callison, 1998; Foster, 2003) and the apparent absence of helical burrowing behavior in reptiles (Riese et al., 2011). This interpretation is also supported by the discovery of a mammal in the MF with unequivocal fossorial features (Luo and Wible, 2005). Burrowing dinosaurs are purported to have created sinuous, burrows (Varricchio et al., 2007), but tight, vertical spirals like those of type 11 traces are not known from that burrow morphotype. Surface morphology is likely the result of a combination of original textures and disruption and cracking due to expansive pressure from carbonate precipitation. Type 11 traces represent terraphilic behavior (Hasiotis, 2004, 2008) and indicate well-drained conditions in pedofacies I and II. Helical burrows also have been interpreted as a method of maintaining a constant burrow temperature and humidity, which would be useful during seasonal climate fluctuations (Meyer, 1999).

Type 12.—Large-diameter burrow complexes (Fig. 7D, E).—Large-diameter (typically > 5 cm), interconnected, cylindrical, and bulbous masses of carbonate cemented sandstone. Segments are mostly circular in cross section and diameter is typically constant throughout lengths of segments, although some expansion and contraction of dimensions was observed. These traces are found within red paleosols (pedofacies I and II) in heterolithic intervals. Surfaces of cylinders are smooth to irregular, with some displaying parallel, linear ridges.

These burrow complexes were described by Hasiotis (2002, 2004) and Hasiotis et al. (2004) who interpreted them as mammal burrows. We continue to support this interpretation, especially in light of the subsequent discovery of a mammal in the MF with unequivocal fossorial features (Luo and Wible, 2005). We interpret parallel ridges as scratch marks from digging behavior. Changes in burrow diameter may represent distortion due to compaction (Hasiotis, 2002; Hasiotis et al., 2004). These burrows represent terraphilic behavior (Hasiotis,

2004, 2008) and, in accordance with other vertebrate burrows in pedofacies I and II paleosols, represent well-drained conditions.

Type 13.—Small vertebrate tracks (Fig. 8A, B).—Groups of up to four parallel, elongate ridges that taper in the same direction; many curve slightly in a uniform direction. Ridges are preserved in convex hyporelief on the base of sandstone beds in lithofacies F. Some sets of ridges are joined at their widest ends by a deeper, rounded protrusion. Traces are found in a regular, repeating pattern along a horizontal, linear axis.

These tracks were reported by Foster et al. (1999), who interpreted them as turtle tracks. The linear marks do not appear to be accurate impressions of digits; rather they are similar to scratch marks made by a tracemaker in saturated media or partially supported by standing water (Wright and Lockley, 2001; Fiorillo, 2005). The tracks represent epiterraphilic organisms but may have been created in a hydrophilic setting based on track preservation (Hasiotis, 2004, 2008). The preservation of such finely detailed traces suggests that low energy conditions dominated during their formation and burial.

Type 14.—Large vertebrate tracks (Fig. 8C, D).—Large, cylindrical sandstone bulges preserved in convex hyporelief on the bases of sandstone beds. Traces penetrate into underlying mudstone beds, but erosion of mudstone from outcrops leaves many examples exposed. Some contain multiple, smaller, rounded protrusions and vertically oriented ridges (Fig. 8C).

We interpret these traces as deeply impressed dinosaur tracks, most likely those of sauropods based on size and morphology. Similarly preserved tracks have been reported from elsewhere in the MF (Engelmann and Hasiotis, 1999; Hasiotis, 2004, 2008; Jennings et al., 2006; Platt and Hasiotis, 2006; Jones and Gustason, 2006). Protrusions and vertical ridges represent digit impressions and scratch marks, respectively. These tracks represent behavior by

epiterraphilic animals, but the deep nature of the tracks suggests high moisture content of the original sediment (Platt and Hasiotis, 2006; Platt et al., in review).

Soil Drainage Indicators

Soil drainage indicators (Fig. 9) show that paleosols in the Salt Wash Member are characterized by relatively well- to moderately well-drained conditions overall. Results for paleosols in the Brushy Basin Member show high variability, but there is an overall upsection trend from well-drained to poorly drained conditions. The majority of poor-drainage indicators correspond to the smectitic mudstone lithofacies (pedofacies VII). The main transition from well-drained to poorly drained paleosols occurs below the smectitic mudstone lithofacies and includes paleosols that belong to pedofacies IV–VI. Above pedofacies VII, better drainage conditions return for a short time before falling back to poorly drained conditions indicated by traces and paleosol features in pedofacies VI.

Local soil drainage is influenced by a number of factors including environmental setting, topography, water table position, parent material, particle size, and climate (Kraus, 1999, 2002; Hasiotis, 2007; Hasiotis et al., 2007; Smith et al., 2008). Any regional- or global-scale climatic interpretations of our soil drainage data must account for environmental factors that may influence local drainage conditions. The mostly well-drained conditions of calcic paleosols in the Salt Wash Member, for example, are informative because their near-channel setting places them in a position to receive a relatively high percentage of total overbank flow. An abundance of sand at depth within the heterolithic lithofacies likely helped increase infiltration, but, nevertheless, the well-drained conditions of paleosols in such a proximal channel setting lead us to interpret seasonally moisture availability during Salt Wash Member deposition.

Multiple facies changes in the Brushy Basin Member complicate interpretations of soil drainage indicators in the study area. Association of poor drainage indicators with the smectitic mudstone lithofacies is not surprising because the abundant smectitic clay content and fine particle size likely limited infiltration substantially. Paleosols in the massive mudstone lithofacies are easier to compare, especially Pedofacies V and VI, because they are the same lithology and represent similar positions on the floodplain. The upward transition from well-drained conditions to more poorly drained conditions does appear to represent an increase in moisture availability rather than a change in channel position or parent material. The observed pattern agrees with previous reports of an up-section increase in moisture attributed to climate based on data from paleosols (Demko et al., 2004), plant fossils (Parrish et al., 2004), and ichnofossils (Hasiotis, 2004, 2008).

Carbonate Content and Composition

Bulk carbonate content.—The amount of carbonate present in bulk samples (Fig. 9) in the Tidwell and Salt Wash members is variable, with fluctuation typically between about 0% and 40% CCE. The majority of carbonate is present as cements. A maximum of 62.4% CCE in the Tidwell Member corresponds to rocks containing feathery calcite in lithofacies B. Carbonate content generally decreases up section towards the top of the Salt Wash Member and is practically absent from the Brushy Basin Member. The greatest carbonate content in the Brushy Basin Member is present as cements in channel sandstones of the trough cross-bedded lithofacies.

Specific interpretations of bulk carbonate content are complicated by the presence of multiple phases of calcite and dolomite cements in the study area (Northrop and Goldhaber, 1990). We can, however, make some general statements regarding carbonate content. The up-

section decrease in carbonate in the Salt Wash Member is consistent with the observations of Robinson and McCabe (1997), who distinguished a lower, better cemented, Salt Wash interval composed of cliff-forming sandstones and an upper recessive interval that is more poorly cemented. The fact that paleosols in the Brushy Basin Member have almost no carbonate in them suggests an absence of original pedogenic carbonate. The pattern of pedogenic carbonate presence in the Salt Wash Member and absence in the Brushy Basin Member, therefore, suggests a change in moisture availability through time.

Pedogenic carbonate nodules.—Carbonate is present in pedofacies II paleosols as cement and as pedogenic nodules. Pedogenic carbonate is generally uncommon in the field area and no distinct Bk horizons were observed. Carbonate nodules are rare and were only observed in and collected from one laterally extensive paleosol near the top of the Salt Wash Member. Carbonate is also abundant in Salt Wash Member paleosols as cements in sand-filled burrows (e.g., Fig. 7).

An absence of soil carbonate horizons is correlated to a minimum mean annual precipitation of 760 mm (Royer, 1999). Absence of a pedogenic carbonate horizon can also indicate that a soil was not mature enough to develop a calcic horizon (Cerling, 1991). The latter is a plausible explanation for the general lack of Bk horizons in Salt Wash Member paleosols because Salt Wash Member paleosols are relatively immature (pedofacies I–III). While we may not be able to say with certainty why most Salt Wash Member paleosols lack carbonate nodules, the presence of carbonate nodules in the laterally extensive paleosol indicates moisture levels sufficient to result in precipitation of isolated carbonate nodules during pedogenesis, but not low enough to result in precipitation of carbonate-rich horizon.

Calcite-dolomite fractions.—Results of calcite and dolomite discrimination show that

calcite is the dominant carbonate mineral in the field area. The most dolomite-rich samples came from the Tidwell Member and the lowest 20 m of the Salt Wash Member; these stratigraphic positions also have higher amplitude oscillations in calcite:dolomite fractions than bulk samples from the remainder of the Salt Wash Member. The lowest ~60 m of the MF has relatively high frequency shifts in calcite fractions, while carbonate cements above that level have lower frequency shifts.

Calcite:dolomite fractions agree with previous determinations based on X-ray diffraction (Northrop and Goldhaber, 1990; Hirmas et al., 2012). Dolomite near the Tidwell Member-Salt Wash Member contact has been interpreted as authigenic and related to ore body mineralization because of the relationship between dolomite cement and rhombs and coffinite, the dominant uranium ore mineral (Northrop and Goldhaber, 1990). Multiple phases of calcite have been identified in U-rich intervals (Northrop and Goldhaber, 1990; Wanty et al., 1990), which complicate interpretations of stable isotopes from bulk samples from these intervals. We should be able to derive more useful stable isotope data from preore calcite cements in nonmineralized Salt Wash Member sandstones because petrography indicates that these are early diagenetic cements (Wanty et al., 1990).

Organic Carbon Content

Total organic carbon results (Figs. 9–10) show that the MF in the field area generally contains very little organic matter. Results for bulk samples display a range of TOC values from 0.01% to 0.24% with a mean of 0.05%. The highest TOC value recorded was 0.48%, but this was taken directly from a carbonized root fossil and associated matrix. In general, mudstones contain the most TOC and sandstones the least; there appears to be no clear temporal trend in

TOC values. There are three closely spaced positive peaks represented by multiple samples in TOC in the Tidwell and basal Salt Wash members (Fig. 9); these are found in the interbedded mudstone and sandstone lithofacies, interbedded muddy sandstone, and very fine-grained sandstone lithofacies, and trough cross-bedded sandstone lithofacies.

The overall paucity and stratigraphic distribution of organic matter agrees with previous findings (Northrop and Goldhaber, 1990). The relatively high TOC value associated with a root fossil confirms that organic matter is preserved, supporting reducing conditions interpreted for associated paleosols. The relatively higher TOC values in the Tidwell and basal Salt Wash members are associated with regressive lacustrine and overlying fluvial environments. High TOC values are common in productive lakes (e.g., Mayer and Schwark, 1999) and in lakes with abundant input of terrestrial vegetation (e.g., Meyers and Lallier-Vergès, 1999). Algae are present in the Tidwell Member (Peterson, 1980) and fossil terrestrial vegetation is common in the base of the Salt Wash Member (Northrop and Goldhaber, 1990). The highest TOC values from the Tidwell Member, however, are < 0.5%, which is lower than typical values from ancient lake deposits (e.g., Gore, 1989; Bohacs et al., 2000). We interpret this as the result of dilution of organic matter from substantial terrigenous clastic input represented by the thick deltaic deposits. We do not think that destruction of organic matter by scavengers was a particularly large contributing factor to the low TOC values because of the rarity of bioturbation in lacustrine sediments.

Stable Isotope Geochemistry

Bulk dolomite samples.—Carbonate samples can be divided into bulk dolomite, bulk calcite, and pedogenic calcite nodules. Only two bulk carbonate samples are composed of 100%

dolomite and both are from the Tidwell Member. Dolomite carbon isotope values are –3.87‰ and –3.00‰. Oxygen isotope values are –12.95‰ and –9.27‰.

Bulk calcite samples.—These represent the majority of carbonate isotope data. Bulk $\delta^{13}C_{carb}$ values range from –6.79‰ to –0.35‰, with a mean of –4.53‰. There are not enough data to properly evaluate stratigraphic trends because of the large number of mixed calcite-dolomite samples through the section. The $\delta^{13}C_{carb}$ value at 18 m is particularly high relative to the rest of the values. Values appear to decrease up section and stabilize between –4.0‰ and –4.5‰, before becoming highly variable at ~60 m.

Bulk calcite $\delta^{18}O$ values range from –12.32‰ to –7.29‰ with a mean of –9.98‰. These values are more variable than $\delta^{13}C_{carb}$ values. Values range between –7.29‰ at 18 m, and –12.20‰ at 36 m. Values appear to shift in a generally positive direction above 36 m, but are highly variable.

Pedogenic carbonate nodules.—Pedogenic $\delta^{18}O$ values range from –9.74‰ to –9.34‰, with a mean of –9.57‰. Pedogenic $\delta^{13}C_{carb}$ values are substantially more depleted compared to other sampled carbonates in the study area (Fig. 9). Values range from –6.79‰ to –6.63‰, with a mean of –6.73‰. Pedogenic carbonate nodules are rare and are present in a single laterally extensive paleosol.

Organic carbon isotopes.—$\delta^{13}C_{org}$ values for the entire measured section range from –30.88‰ to –20.78‰ with a mean of –26.80‰ (Fig. 10). Stratigraphic distribution of $\delta^{13}C_{org}$ (Fig. 9) shows that $\delta^{13}C_{org}$ values start at –28.06‰ at the base of the Tidwell Member and rise in a short vertical distance to a maximum of –22.29‰ at 4.0 m (peak a, Fig. 9). Above 4.0 m, values drop to a minimum of –26.82‰ at 7.5 m, followed by an increase to a maximum of –20.78‰ at 13.0 m (peak b, Fig. 9), near the contact between the Tidwell Member and the Salt

Wash Member. After this maximum, values fall to a minimum of –27.66‰ at 15.5 m, followed by an interval of values between ~–27.5‰ and ~–23.4‰ with two isolated, highly positive values (interval c, Fig. 9). Above this interval, values fall to a minimum of –29.80‰ at 23.5 m (peak d, Fig. 9) and then are highly variable with some isolated positive (peak e, Fig. 9) and negative spikes (peaks f and g, Fig. 9), but remain mostly between ~–28‰ and ~–26‰, up to ~150 m.

A positive shift in $\delta^{13}C_{org}$ values occurs at ~154 m (h, Fig. 9), above which, values remain between ~–26‰ to ~–23‰ until 163.5 m. Above this, values return to between ~–28‰ and ~–26‰ for a short vertical distance, followed by a gradual enrichment that reaches a maximum of –22.41‰ at 180.5 m (peak i, Fig. 9).

DISCUSSION

Stable Isotope Results

Bulk dolomite samples.—Dolomite carbon isotope values are similar in magnitude to previous findings (Northrop and Goldhaber, 1990), but bulk dolomite oxygen isotope values are extremely depleted compared to previously published averages of 16.5‰ for unmineralized dolomites and 20.9‰ for mineralized dolomites in the Tidwell Member (Northrop and Goldhaber, 1990). We do not have enough data for a thorough analysis however, and we will refrain from interpreting these results. Dolomite cement in the Tidwell Member is related to uranium mineralization (Northrop and Goldhaber, 1990) and is not necessarily relevant for interpreting paleoenvironment and paleoclimate during deposition.

Bulk calcite samples.— Bulk $\delta^{13}C_{carb}$ and $\delta^{18}O$ results are comparable to previous results from bedded lacustrine and wetland carbonates throughout the Morrison depositional basin

(Dunagan and Turner, 2004), although our $\delta^{13}C_{carb}$ values are not as negative. Lacustrine and wetland carbonates showed similar $\delta^{18}O$ values, which were interpreted as the result of isotopically depleted meteoric water from progressive eastward rainout over western North America (Dunagan and Turner, 2004; Turner and Peterson, 2004).

The sparse nature of pure bulk calcite data prevents evaluation of detailed curve geometry. Results from bulk mixed calcite-dolomite samples (Appendix D), however, suggest enrichment of $\delta^{13}C_{carb}$ and $\delta^{18}O$ values at ~20 m. This enrichment correlates to a positive excursion in dolomite stable isotopes reported by Northrop and Goldhaber (1990). Additional research is needed, however, to assess the precise position of a positive excursion in carbonate isotopes.

Pedogenic carbonate nodules.—Pedogenic carbonate nodules $\delta^{18}O$ values fall within the range reported from pedogenic carbonate in the MF in the Colorado Plateau (Dunagan and Turner, 2004). The fact that pedogenic $\delta^{18}O$ values are similar to bulk carbonate values is not surprising because both are interpreted as being sourced from meteoric water.

Stable carbon isotope values are more negative than previously reported MF pedogenic $\delta^{13}C_{carb}$ values (Dunagan and Turner, 2004). Pedogenic $\delta^{13}C_{carb}$ values are controlled by soil CO_2 and highly depleted $\delta^{13}C_{carb}$ values could result from such factors as high soil respiration rates, low porosity, and high temperatures (Cerling, 1991; Sharp, 2007). We rule out low porosity as the cause of the depleted $\delta^{13}C_{carb}$ values because pedogenic and ichnological features indicate soils were well drained. If high temperatures (MAT; mean annual temperature) contributed to depleted $\delta^{13}C_{carb}$ values, we would expect $\delta^{18}O$ values to be depleted as well because of their sensitivity to temperature (Cerling, 1984). Increased soil respiration is the preferred explanation, because the pedogenic carbonate nodules are associated with an increase

in TOC (Fig. 9), which has been shown to increase soil respiration rate (Schlesinger and Andrews, 2000).

Organic carbon isotopes.— The range of $\delta^{13}C_{org}$ values (Fig. 10) encompasses the range known for modern C3 plants (Boutton, 1996); this is expected because C4 plants, which have much more positive $\delta^{13}C_{org}$ values, were not abundant until the Paleogene (Cerling, 1991; Urban et al., 2010). The source of organic matter for most lithofacies is interpreted as terrestrial plants because their presence and abundance are indicated by macrofossils and rhizoliths. Organic carbon in lacustrine facies (lithofacies B–E), however, may be derived from planktonic algae, aquatic macrophytes, and terrestrial vegetation, which are the dominant sources of organic matter in lakes (Mayer and Schwark, 1999). Macrophytes have the same average $\delta^{13}C_{org}$ values as terrestrial C3 plants, but planktonic algae typically have lower values (Mayer and Schwark, 1999). Positive excursions in lacustrine deposits, therefore, did not result from shifts in organic carbon sources, but rather, represent changes in atmospheric CO_2.

The positive excursion in the upper half of the Brushy Basin Member (peak h, Fig. 9) differs from the excursion lower in the section in that the positive shift corresponds to a change in lithofacies from lithofacies H to lithofacies I. The association between the lithofacies change and the positive shift in $\delta^{13}C_{org}$ values suggests the possibility that changes in local environment may have resulted in the observed isotope trend. The enrichment is not instantaneous, however, and is recorded by eight data points. One possible interpretation is that the positive excursion was brought about by an increase in volcanism, as suggested by the sudden presence of volcanic ash, but volcanic emissions would have decreased $\delta^{13}C_{org}$ values through time because they are depleted in ^{13}C (Kump and Arthur, 1999). We attribute the Brushy Basin Member isotope trend to other local or regional factors.

Correlation between TOC and $\delta^{13}C_{org}$ in the Tidwell and Salt Wash members

Trends in TOC and $\delta^{13}C_{org}$ values are in phase within the Tidwell and basal Salt Wash members, while the two curves do not appear to correlate higher stratigraphically (Fig. 9). Correlations between TOC and $\delta^{13}C_{org}$ values in lacustrine environments in the Tidwell Member can indicate increased phytoplankton productivity (Tyson, 1995) or microbial activity related to rates of remineralization of organic matter and burial of isotopically light carbon (Talbot and Lærdal, 2000). We favor an interpretation of increased phytoplankton productivity because that explains the continuation of the correlation from the lacustrine environment into the overlying fluvial environments of the Salt Wash Member. Even though the positive peaks may be explained by biological fractionation, the fact that $\delta^{13}C_{org}$ values remain positive relative to values further up section indicates that background values, i.e., atmospheric carbon in the form of CO_2, were isotopically heavier during deposition of the Tidwell and basal Salt Wash members. In other words, the Tidwell and basal Salt Wash members record a positive shift in background $\delta^{13}C_{org}$ values, which may have been further enriched through the activity of lacustrine biota.

Correlation between $\delta^{13}C_{org}$ and carbonate isotopes in the Salt Wash Member

Northrop and Goldhaber (1990) documented a positive trend in carbon and oxygen isotopes of authigenic dolomite cements in association with uranium and vanadium in the Salt Wash Member. Even though uranium content of the MF was not measured in this study, the stratigraphic position of mining activity can be taken as an indication of the location of economic ores; using this information to correlate our section to that of Northrop and Goldhaber (1990), we can state that the positive peak in dolomite cement isotopes correlates to the positive peak in organic carbon isotopes and possibly a positive trend in bulk calcite isotopes. If the dolomite

cement incorporated enriched carbon and oxygen from preore calcite then that would explain the positive stratigraphic trend in dolomite cements. In this interpretation, the positive excursion would be unrelated to uranium mineralization and would represent the recording of a paleoclimatic signal. A paleoclimatic interpretation is also supported by the positive excursion recorded by organic carbon isotopes. The preore calcite was precipitated from meteoric water, which contained enriched carbon derived from atmospheric CO_2 via the soil organic matter and oxygen from the meteoric waters.

Brushy Basin Member datasets

The gradual transition from well-drained soil drainage conditions to relatively poorly drained soils in the Brushy Basin Member is independent of vertical facies changes, and the most poorly drained soil conditions corresponds to the positive shift in $\delta^{13}C_{org}$ data (peak h, Fig. 9). Soil drainage trends and $\delta^{13}C_{org}$ trends are unrelated because increased soil moisture availability should cause depletion of organic carbon isotopes due to an increase in CO_2 diffusion from open stomata of plants living on the soil surface that later become incorporated into the soil as organic matter (Boutton, 1996). The positive $\delta^{13}C_{org}$ excursion, furthermore, does not persist for the entire portion of this section (peak h, Fig. 9). We attribute the positive shift in $\delta^{13}C_{org}$, therefore, to the contribution of enriched carbon from atmospheric CO_2.

Paleoenvironments

Fluvial paleoenvironments.—Fluvial environments are represented in the study area by lithofacies A and F. Lithofacies A represents a relatively low energy fluvial environment the experienced occasional drying. This may have been a low gradient, intermittent stream. Periods

of heavy flow resulted in scours and deposition of chert grains. Shallow scours and smaller scale cross bedding relative to lithofacies F indicate that a lower energy system was responsible for the fluvial deposits in the Tidwell Member compared to the Salt Wash Member.

Lithofacies F records large, braided-river channels that traversed the landscape during deposition of the Salt Wash and lower Brushy Basin members. These rivers provided adjacent environments with enough moisture to sustain a diverse biota, based on associated trace fossils. Large trees, remnants of which are preserved in the base of the Salt Wash Member were supported, at least proximally to channels. A slight increase in average grain size from the base of the Salt Wash Member to ~75 m suggests a slight increase in energy through time.

Lacustrine paleoenvironments.—Lithofacies B–E in the Tidwell Member represent a lacustrine environment. Prograding deltaic and lake-margin deposits appear to have infilled the lacustrine basin with no major changes in accommodation. We interpret this lake as a balanced-fill lake, based on apparent sediment and water supply rates that matched accommodation (Bohacs et al., 2000). The relative abundance of TOC in lacustrine deposits suggests a well-oxygenated, productive lake. In addition to riverine input, the lake may have also been groundwater fed, as evidenced by thin bands of feathery calcite within lithofacies B.

Proximal floodplain paleoenvironments.—Proximal floodplain environments, including levee and pedogenically modified overbank muds, are common between channel sandstones in the Salt Wash Member. Weak to moderate pedogenesis represented by simple paleosols in proximal floodplain deposits suggests deposition of relatively thick packages of sediment followed by relatively short periods of stability and pedogenesis. Relatively high deposition rates prevented substantial pedogenic development and all paleosols in the Salt Wash Member can be classified as Entisols or Inceptisols. Paleosols supported diverse communities of

plants and animals, based on trace fossils and suggestions of high soil respiration rates from TOC and $\delta^{13}C_{org}$ results.

Distal floodplain paleoenvironments.—Distal floodplain environments dominate the Brushy Basin Member, where low deposition rates are represented mostly by composite paleosols and thick cumulate paleosols. Common evidence of gleying indicates poor to moderate drainage, and areas of ponded surface water may have been common. Bedded carbonates from such pond settings are known from elsewhere in the Brushy Basin Member (Dunagan and Turner, 2004), but were not encountered in the field area. Paleosols in the upper third of the Brushy Basin Member incorporate abundant altered ash, giving them a distinct white color. High shrink-swell-potential clays from weathered ash resulted in argilliturbation (Johnson et al., 1987) in soils, which destroyed many traces. Nevertheless, rhizoliths are common and indicate that abundant vegetation was supported in distal floodplains. Despite the rarity of trace fossils, a diverse community of invertebrates and vertebrates was likely present in these environments, based on fossils from numerous localities in the Brushy Basin Member (e.g., Turner and Peterson, 1999; Foster, 2003).

Paleoclimates

Tidwell Member.—We can interpret paleoclimate chronologically through deposition of the MF by integrating all of our observations and data for our entire measured section. Beginning at the base of the Tidwell Member, the relatively low-energy fluvial environment with occasional desiccation represented by lithofacies A shows that enough moisture was available to sustain at least occasional flow. The lower energy of lithofacies A relative to lithofacies F, represents lower precipitation to evaporation (P/E) ratios than lithofacies F. An interpretation of

relatively low P/E ratios during deposition of lithofacies A is consistent with previous interpretations of basal Tidwell Member deposits (Demko et al., 2005), laterally equivalent eolian environments (Peterson, 1980), and higher than current global MAT during the Late Jurassic (e.g., Valdes, 1993; Sellwood et al., 2000).

Stratigraphically above lithofacies A are lithofacies B–E, which record the gradual infilling of a balanced-fill lake. High water availability suggests P/E ratios greater than or equal to that represented by lithofacies A. Mudcracks near the top of the succession show occasional drying, but lake margin sediments contain deep sauropod tracks indicative of near saturated conditions (Platt and Hasiotis, 2006; Platt et al., in review).

Salt Wash Member.—Large channel sandstones in the Salt Wash Member indicate high energy fluvial systems fed by precipitation levels sufficient to maintain perennial flow. Floodplains received enough moisture to support abundant vegetation and diverse communities of invertebrates and vertebrates, based on common trace fossils. The well-drained nature of pedofacies I–III paleosols represents rapid infiltration in soils developed on abandoned channel sands and floodplain deposits. Absence of gleyed horizons and presence of hygrophilic and terraphilic traces suggests relatively low water table levels. Redoximorphic coloration in paleosols, however, indicates fluctuating water tables, perhaps as a result of seasonally distributed precipitation. Mean annual precipitation was high enough to prevent accumulation of pedogenic carbonate horizons, which form at MAP levels < 760 mm/year (Royer, 1999). The highest MAP was likely close to 1,200 mm, based on comparisons to present-day analogous ecosystems with high diversity megafauna, megaherbivores, and overall biodiversity in such biomes (e.g., Kendall, 1969; East, 1984).

Brushy Basin Member.—Several thick channel sandstones and well-drained paleosols

in the base of the Brushy Basin Member suggest paleoclimatic conditions similar to those during deposition of the Salt Wash Member. Most of the Brushy Basin Member, however, is dominated by mudstones with paleosols that belong to pedofacies IV–VII. These compound and cumulic paleosols represent smaller packages of sediment deposited less often than paleosols in the Salt Wash Member. While the presence of compound and cumulic paleosols may be a result of extremely distal floodplain positions, a number of features indicate increased moisture availability compared to Salt Wash paleosols. Abundant evidence of gleying, an extreme lack of carbonate, and an upward decrease in soil drainage conditions suggest greater moisture availability through time. Redoximorphic coloration and slickensides indicate continued seasonality of precipitation. Paleosols, however, do not contain enough vertic features to be interpreted as Vertisols, even with their substantial smectitic clay component. We, therefore, argue that seasonal extremes in precipitation and temperatures were less pronounced during deposition of the upper Brushy Basin Member than during deposition of the Salt Wash and lower Brushy Basin members. Even though abundant clay and volcanic ash would have decreased infiltration, we interpret the upward increase in moisture availability as the result of increased P/E ratios.

Changes in P/E ratios may represent global climate change, but more likely correspond to tectonic migration of the Morrison Formation depositional basin. During deposition of the Brushy Basin Member, North America was moving northward (Bazard and Butler, 1994), which could have brought the depositional basin into cooler latitudes with lower P/E ratios.

Correlation to the Late Jurassic marine isotope record

Meaningful comparison of our results to marine isotope curves requires reliable time

constraints for our measured section. Unfortunately, no ash beds suitable for radiometric dating are present in our field area. Correlation of our measured section to sections in Notom, Utah, and Montezuma Creek, Utah, with associated radiometric dates, restricts the time interval represented by our section to ~149.3 to 154.8 Ma (Kowallis et al., 1998). Comparison of MF $\delta^{13}C_{org}$ values to Late Jurassic marine data from the appropriate time interval (Morgans-Bell et al., 2001; Jenkyns et al., 2002) reveals distinct correlative excursions (Fig. 11). The basal multipeaked positive excursion (peaks a–c, Fig. 11) appears to correspond to the onset of the mid *eudoxus* positive shift (Morgans-Bell et al., 2001; Jenkyns et al., 2002). The mid *eudoxus* positive shift has been recognized in multiple deposits in Europe and is interpreted as the isotopic response to increases in organic carbon burial (Jenkyns et al., 2002). If the basal MF records the mid *eudoxus* positive shift, then it implies that the event was global in scale. Global increases in organic carbon burial have been interpreted as driving mechanisms for decreased MAT (e.g., Arthur et al., 1988).

According to our correlation, the MF in the study area does not capture the global isotopic signal recorded in the *baylei* through mid *eudoxus* ammonite zones. Future research on organic carbon isotopes associated with the J–5 unconformity may be informative for quantifying the amount of missing time represented.

We tentatively draw other correlations, including an interval bounded by peaks f and g in the basal *autissiodorensis* zone, followed by an increase in $\delta^{13}C_{org}$ values, which peak and then decrease upward in the *autissiodorensis* zone (Fig. 11). A highly variable interval that persists from the upper *autissiodorensis* zone to the basal *scitulus* zone may correlate to the isotope curve in the upper Salt Wash (Fig. 11), but interpretations are limited by unconformities in our field area. Finally, the interval from the base of the upper MF positive excursion (peak h) through the

top of our measured section appears to correlate to the *wheatleyensis* through mid *hudlestoni* zones in the Kimmeridge Clay (Fig. 11).

The overall trend in bulk calcite $\delta^{13}C_{carb}$ towards more depleted values corresponds to the trend seen in the Tithonian in the marine isotope record and attributed to a decrease in organic carbon sedimentation (Padden et al., 2002; Dera et al., 2011). This is useful information for correlation and provides the possibility of calculating relative MF sedimentation rates based on slopes of isotopic trends; a more robust dataset is needed for this, however.

Implications for biotic patterns

The basal $\delta^{13}C_{org}$ positive excursion is particularly interesting because its stratigraphic position low in the MF potentially corresponds to a unique biostratigraphic zone (biozone 1 in Foster, 2003, 2007). Biozone 1 contains a dinosaurian fauna with several unique taxa that are not found higher in the MF, as opposed to younger taxa in the MF that persist through several biostratigraphic zones before going extinct (Foster, 2003, 2007). We propose that the unique faunal composition in the basal MF correlates to the time interval spanned by the basal MF positive excursion. We also propose that initial MF paleocommunities were adapted to changing global conditions, possibly cooling, represented by the mid *eudoxus* positive shift. Following this, more stable conditions allowed initial MF paleocommunities to be supplanted by the biota that reigned during the remainder of MF deposition. Testing of these hypotheses, however, is complicated by a lack of sampling and time constraints, so future work in the MF will benefit from studies of the basal MF biota, chronostratigraphy, and more detailed stable isotope geochemistry in other locations within the MF.

CONCLUSIONS

We combined sedimentology, paleopedology, ichnology, and stable isotope geochemistry to reconstruct a paleoenvironmental and paleoclimatic record through the Upper Jurassic MF in the Henry Mountains region of south-central Utah. We recognize nine lithofacies and seven pedofacies in the study area. We also report 14 trace-fossil morphotypes, including three kinds of root trace fossils (rhizoliths). Inferred paleohydrology of trace fossils and paleosols were combined to create a soil drainage index for paleosols within a measured section. Geochemical samples were collected from the measured section and analyzed for carbonate content, calcite:dolomite ratio, $\delta^{13}C_{carb}$ and $\delta^{18}O$ of calcites and dolomites, total organic carbon (TOC) content, and $\delta^{13}C_{org}$.

Combined results, in stratigraphic order, indicate that the basal-most Tidwell Member represents a transition from a fluvial environment to a lacustrine setting, which was gradually infilled, as indicated by shallowing-upward facies shifts. Positive peaks in TOC and $\delta^{13}C_{org}$ show that the lake experienced periods of high productivity. Positive background $\delta^{13}C_{org}$ values persist throughout the lacustrine deposits vertically into the overlying fluvial deposits of the basal Salt Wash Member. We interpret this basal positive excursion as recording a global signal that may have been further enriched through biological activity. We argue that the excursion is unrelated to uranium mineralization. Carbonate isotope results are too sparse to evaluate trends, but a previous study reported a similar positive excursion in dolomite isotopes at the same stratigraphic position as our $\delta^{13}C_{org}$ excursion. The timing of this excursion roughly correlates to the mid-*eudoxus* positive shift reported from the Late Jurassic marine stable isotope record, suggesting that this was a global event useful for chemistratigraphic correlation.

The Salt Wash Member is dominated by fluvial sandstones and also contains heterolithic

intervals with poorly to moderately developed paleosols. Soil drainage index results show that mostly moderately well-drained to well-drained conditions prevailed. Carbonate nodules are rare, which agrees with drainage indications of abundant moisture. Following the basal positive shift in organic carbon isotopes, $\delta^{13}C_{org}$ values fluctuate mostly between ~ –28‰ and ~ –26‰. Several distinct peaks, however, indicate that the MF organic carbon isotope curve is correlative to the marine $\delta^{13}C_{org}$ record from the *autissiodorensis* through *elegans* ammonite zones. Carbonate isotope data are sparse, but an overall upward decrease in $\delta^{13}C_{carb}$ values corresponds to the trend observed in the Kimmeridgian and Tithonian marine $\delta^{13}C_{carb}$ record. Bulk carbonate samples yielded relatively depleted $\delta^{18}O$ values, similar in magnitude to previous findings that suggest that meteoric water was depleted due to the continental effect from the inland position of the depositional basin.

Pedogenically modified distal floodplain deposits dominate the Brushy Basin Member, so it has the most extensive drainage index record. Drainage indicators show that a transition from well-drained to poorly drained conditions occurred in the lower half of the member. The transition does appear to represent an increase in available moisture. Organic carbon isotopes do not support this interpretation, however, but we argue that $\delta^{13}C_{org}$ values represent a global signal that dominates any local environmental signal. The $\delta^{13}C_{org}$ curve for the Brushy Basin in the field area potentially correlates to the marine $\delta^{13}C_{org}$ record from the *scitulus* through *hudlestoni* ammonite zones.

These new data are important because paleosols and trace fossils corroborate other lines of evidence for increased moisture availability towards the end of MF deposition. Stable isotope data are not particularly informative about local paleoclimate, but their potential correlation to marine isotope records implies that events recorded in various oceanic basin sediments may have

been global in scale. Detection of these global patterns is useful for establishing general time constraints on deposition of the MF and for correlation between locations. Perhaps most intriguing is the potential correlation between the basal $\delta^{13}C_{org}$ positive excursion and a unique MF fauna. This particular interval of the MF warrants additional study because its conclusion may contain evidence of biotic response to global climate change.

ACKNOWLEDGMENTS

We thank A. Bonilla, G. Cane, D. Hirmas, G. Ludvigson, C. Suarez, and M. Suarez for help with laboratory work and J. Schmerge and C. Motter for help with fieldwork. We thank A. Coe for providing useful references. This research is part of a Ph.D. dissertation by B.F.P. at the University of Kansas (KU). Support was provided to B.F.P. by the American Association of Petroleum Geologists Grants-in-Aid Program, the Jurassic Foundation, the KU Geology Department, a Leaman Harris Scholarship from the KU Biodiversity Institute, a Madison and Lila Self Graduate Fellowship at KU, and a Stephen J. Gould student grant from the Paleontological Society.

REFERENCES

Arthur, M.S., Dean, W.E., and Pratt, L.M., 1988, Geochemical and climatic effects of increased marine organic carbon burian at the Cenomanian/Turonian boundary: Nature, v. 335, p. 714–717.

Bazard, D.R., and Butler, R.F., 1994, Paleomagnetism of the Brushy Basin Member of the Morrison Formation: implications for Jurassic apparent polar wander: Journal of Geophysical Research, v. 99, p. 6695–6710.

Bilodeau, W.L., 1986, The Mesozoic Mogollon Highlands, Arizona: an Early Cretaceous rift shoulder: Journal of Geology, v. 94, p. 724–735.

Bohacs, K.M., Carroll, A.R., Neal, J.E., and Mankiewicz, P.J., 2000, Lake-basin type, source potential, and hydrocarbon character: an integrated-sequence-stratigraphic-geochemical framework, *in* Gierlowski-Kordesch, E.H., and Kelts, K.R., eds., Lake basins through space and time: AAPG Studies in Geology 46, p. 3–34.

Boutton, T.W., 1996, Stable carbon isotope ratios of soil organic matter and their use as indicators of vegetation and climate change, *in* Yamasaki, S.-I, and Boutton, T.W., eds., Mass Spectrometry of Soils: New York, Marcel Dekker, Inc., p. 47–82.

Bryson, H.R., 1939, The identification of soil insects by their burrow characteristics: Transactions of the Kansas Academy of Science, v. 42, p. 245–254.

Buatois, L.A., and Mángano, M.G., 2002, Trace fossils from Carboniferous floodplain deposits in western Argentina: implications for ichnofacies models of continental environments: Palaeogeography, Palaeoclimatology, Palaeoecology, v. 183, p. 71–86.

Buck, S.G., and Goldring, R., 2003, Conical sedimentary structures, trace fossils or not? Observations, experiments, and review: Journal of Sedimentary Research, v. 73, p. 338–353.

Cerling, T.E., 1984, The stable isotopic composition of modern soil carbonates and its relationship to climate: Earth and Planetary Science Letters, v. 71, p. 229–240.

Cerling, T.E., 1991, Carbon dioxide in the atmosphere: evidence from Cenozoic and Mesozoic paleosols: American Journal of Science, v. 291, p. 377–400.

Chamberlain, C.K., 1975, Recent lebensspuren in nonmarine aquatic environments, *in* Frey, R.W., ed., The study of trace fossils: a synthesis of principles, problems, and procedures in ichnology: Springer-Verlag, New York, p. 431–457.

Chenoweth, W.L., 1998, Uranium mining in the Morrison Formation: Modern Geology, v. 23, p. 427–439.

Cohen, A.S., 1982, Paleoenvironments of root casts from the Koobi Fora Formation, Kenya: Journal of Sedimentary Petrology, v. 52, p. 401–414.

Counts, J.W., and Hasiotis, S.T., 2009, Neoichnological experiments with masked chafer beetles (Coleoptera: Scarabaeidae): implications for backfilled continental trace fossils: PALAIOS, v. 24, p. 74–91.

Currie, B.S., 1998, Upper Jurassic-Lower Cretaceous Morrison and Cedar Mountain Formations, NE Utah-NW Colorado: relationships between nonmarine deposition and early Cordilleran foreland-basin development: Journal of Sedimentary Research, v. 68, p. 632–652.

Demko, T.M., and Parrish, J.T., 1998, Paleoclimatic setting of the Upper Jurassic Morrison Formation: Modern Geology, v. 22, p. 283–296.

Demko, T.M., Currie, B.S., and Nicoll, K.A., 2004, Regional paleoclimatic and stratigraphic implications of paleosols and fluvial/overbank architecture in the Morrison Formation (Upper Jurassic), Western Interior, USA: Sedimentary Geology, v. 167, p. 115–135.

Demko, T.M., Nicoll, K., Beer, J.J., Hasiotis, S.T., and Park, L.E., 2005, Mesozoic Lakes of the Colorado Plateau: *in* Pederson, J., and Dehler, C.M., eds., Interior Western United States: Geological Society of America Field Guide 6, 28 p.

Dera, G., Brigaud, B., Monna, F., Laffont, R., Pucéat, E., Deconinck, J.-F., Pellenard, P., Joachimski, M.M., and Durlet, C., 2011, Climatic ups and downs in a disturbed Jurassic world: Geology, v. 39, p. 215–218.

Dodson, P., Behrensmeyer, A.K., Bakker, R.T., and McIntosh, J.S., 1980, Taphonomy and paleoecology of the dinosaur beds of the Jurassic Morrison Formation: Paleobiology, v. 6, p. 208–232.

Dunagan, S.P., and Turner, C.E., 2004, Regional paleohydrologic and paleoclimatic setting of wetland/lacustrine depositional systems in the Morrison Formation (Upper Jurassic), Western Interior, USA: Sedimentary Geology, v. 167, p. 269–296.

Dzulynski, S., and Smith, A.J., 1963, Convolute lamination, its origin, preservation, and directional significance: Journal of Sedimentary Petrology, v. 33, p. 616–627.

East, R., 1984, Rainfall, soil nutrient status and biomass of large African savanna mammals: African Journal of Ecology, v. 22, p. 245–270.

Engelmann, G.F., and Callison, G., 1998, Mammalian faunas of the Morrison Formation: Modern Geology, v. 23, p. 343–379.

Engelmann, G.F., and Hasiotis, S.T., 1999, Deep dinosaur tracks in the Morrison Formation: sole marks that are really sole marks, *in* Gillette, D.D., ed., Vertebrate Paleontology in Utah: Utah Geological Survey Miscellaneous Publication 99-1, p. 179–183.

Fiorillo, A.R., 2005, Turtle tracks in the Judith River Formation (Upper Cretaceous) of south-central Montana: Palaeontologia Electronica, v. 8, p. 1–11.

Foster, J.R., Lockley, M.G., and Brockett, J., 1999, Possible turtle tracks from the Morrison Formation of southern Utah, *in* Gillette, D.D., ed., Vertebrate Paleontology in Utah: Utah Geological Survey Miscellaneous Publication 99-1, p. 185–191.

Foster, J.R., 2003, Paleoecological analysis of the vertebrate fauna of the Morrison Formation (Upper Jurassic), Rocky Mountain region, U.S.A., New Mexico Museum of Natural History and Science Bulletin 23, 95 p.

Foster, J.R., 2007, Jurassic West: Indiana University Press, Bloomington, Indiana, 389 p.

Fouke, B.W., Farmer, J.D., Des Marias, D.J., Pratt, L., Sturchio, N.C., Burns, P.C., and Discipulo, M.K., 2000, Depositional facies and aqueous-solid geochemistry of travertine-depositing hot springs (Angel Terrace, Mammoth Hot Springs, Yellowstone National Park, U.S.A.): Journal of Sedimentary Research, v. 70, p. 565–585.

Frisch, K.v., 1974, Animal Architecture: Harcourt, New York, 306 p.

Gore, P.J.W., 1989, Toward a model for open- and closed-basin deposition in ancient lacustrine sequences: the Newark Supergroup (Triassic–Jurassic), eastern North America: Palaeogeography, Palaeoclimatology, Palaeoecology, v. 70, p. 29–51.

Grassé, P.-P., 1984, Termitologia, Tome II: Fondation des Sociétés – Construction: Masson, Paris, 613 p.

Grassé, P.-P., 1986, Termitologia, Tome III: Comportement – Socialité – Écologie – Évolution – Systématique: Masson, Paris, 715 p.

Häntzschel, W., ed., 1980, Treatise on Invertebrate Paleontology: Part W Miscellanea, Supplement 1: Trace Fossils and Problematica, 2nd ed., 2nd printing, The Geological Society of America: Boulder, Colorado, 269 p.

Hasiotis, S.T., 2002, Continental Trace Fossils: SEPM Short Course Notes No. 51, 132 p.

Hasiotis, S.T., 2004, Reconnaissance of Upper Jurassic Morrison Formation ichnofossils, Rocky Mountain region, USA: paleoenvironmental, stratigraphic, and paleoclimatic significance of terrestrial and freshwater ichnocoenoses: Sedimentary Geology, v. 167, p. 177–268.

Hasiotis, S.T., Kirkland, J.I., and Callison, G., 1998, Crayfish fossils and burrows from the Upper Jurassic Morrison Formation of western Colorado: Modern Geology, v. 22, p. 481–491.

Hasiotis, S.T., and Mitchell, C.E., 1993, A comparison of crayfish burrow morphologies: Triassic and Holocene fossil, paleo- and neo-ichnological evidence, and the identification of their burrowing signatures: Ichnos, v. 2, p. 291–314.

Hasiotis, S.T., Wellner, R.W., Martin, A.J., and Demko, T.M., 2004, Vertebrate burrows from Triassic and Jurassic continental deposits of North America and Antarctica: their paleoenvironmental and paleoecological significance: Ichnos, v. 11, p. 103–124.

Hegh, E., 1922, Les Termites: Louis Desmet-Verteneuil, Brussels, Belgium, 756 p.

Hembree, D.I., and Hasiotis, S.T., 2008, Miocene vertebrate and invertebrate burrows defining compound paleosols in the Pawnee Creek Formation, Colorado, U.S.A.: Palaeogeography, Palaeoclimatology, Palaeoecology, v. 270, p. 349–365.

Hirmas, D.R., Platt, B.F., and Hasiotis, S.T., 2012, Determination of calcite and dolomite content in soils and paleosols by continuous coulometric titration: Soil Science Society of America Journal, 19 manuscript pages, doi: 10.2136/sssaj2011.0278.

Hunt, C.B., 1980, Structural and igneous geology of the Henry Mountains, Utah, *in* Picard, M.D., ed., Henry Mountains Symposium: Utah Geological Association, pg. 25–106.

Hunt, C.B., Averitt, P., and Miller, R.L., 1953, Geology and Geography of the Henry Mountains Region Utah: Geological Survey Professional Paper 228, United States Government Printing Office, Washington, D.C., 234 p.

Jenkyns, H.C., Jones, C.E., Gröcke, D.R., Hesselbo, S.P., and Parkinson, D.N., 2002, Chemostratigraphy of the Jurassic system: applications, limitations and implications for palaeoceanography: Journal of the Geological Society, London, v. 159, p. 351–378.

Jennings, D.S., Platt, B.F., and Hasiotis, S.T., 2006, Distribution of vertebrate trace fossils, Upper Jurassic Morrison Formation, Bighorn Basin, Wyoming, USA: implications for differentiating paleoecological and preservational bias: New Mexico Museum of Natural History and Science Bulletin, v. 36, p. 183–192.

Johnson, D.L., Watson-Stegner, D., Johnson, D.N., and Schaetzl R.J., 1987, Proisotropic and proanisotropic processes of pedoturbation: Soil Science, v. 143, p. 278–292.

Jones, L.S., and Gustason, E.R., 2006, Dinosaurs as possible avulsion enablers in the Upper Jurassic Morrison Formation, East-Central Utah: Ichnos, v. 13, p. 31–41.

Josens, G., and Soki, K., 2012, Relation between termite numbers and the size of their mounds: Insectes Sociaux, v. 57, p. 303–316.

Kendall, R.L., 1969, An ecological history of the Lake Victoria Basin: Ecological Monographs, v. 39, p. 121–176.

King, E.G., and Spink, W.T., 1969, Foraging galleries of the Formosan subterranean termite, *Coptotermes formosanus*, in Louisiana: Annals of the Entomological Society of America, v. 62, p. 536–542.

Kowallis, B.J., Britt, B.B., Greenhalgh, B.W., and Sprinkel, D.A., 2007, New U-Pb zircon ages from an ash bed in the Brushy Basin Member of the Morrison Formation near Hanksville, Utah, *in* Willis, G.C., Hylland, M.D., Clark, D.L., and Chidsey, T.C., Jr., eds., Central Utah—Diverse Geology of a Dynamic Landscape: Salt Lake City, Utah Geological Association Publication 36, p. 75–80.

Kowallis, B.J., Christiansen, E.H., Deino, A.L., Turner, C.E., Kunk, M.J., and Obradovich, J.D., 1998, The age of the Morrison Formation: Modern Geology, v. 22, p. 235–260.

Kraus, M.J., 1999, Paleosols in clastic sedimentary rocks: their geologic applications: Earth-Science Reviews, v. 47, p. 41–70.

Kraus, M.J., 2002, Basin-scale changes in floodplain paleosols: implications for interpreting alluvial architecture: Journal of Sedimentary Research, v. 72, p. 500–509.

Kraus, M.J., and Aslan, A., 1993, Eocene hydromorphic paleosols: significance for interpreting ancient floodplain processes: Journal of Sedimentary Petrology, v. 63, p. 453–463.

Kraus, M.J., and Brown, T.M., 1988, Pedofacies analysis; a new approach to reconstructing ancient fluvial sequences, in Reinhardt, J., and Sigleo, W.R., eds., Paleosols and Weathering Through Geologic Time: Principles and Applications: The Geological Society of America, Boulder, pg. 143–152.

Kraus, M.J., and Hasiotis, S.T., 2006, Significance of different modes of rhizolith preservation to interpreting paleoenvironmental and paleohydrological settings: examples from

Paleogene paleosols, Bighorn Basin, Wyoming, U.S.A.: Journal of Sedimentary Research, v. 76, p. 633–646.

Kump, L.R., and Arthur, M.A., 1999, Interpreting carbon-isotope excursions: carbonates and organic matter: Chemical Geology, v. 161, p. 181–198.

Lal, 2006, ed., Encyclopedia of Soil Science, v. I: Taylor and Francis, Boca Raton.

Luo, Z.-X., and Wible, J.R., 2005, A Late Jurassic digging mammal and early mammalian diversification: Science, v. 308. P. 103–107.

Marriott, S.B., and Wright, V.P., 1993, Palaeosols as indicators of geomorphic stability in two Old Red Sandstone alluvial suites, South Wales: Journal of the Geological Society, London, v. 150, p. 1109–1120.

Martin, A.J., 2009, Dinosaur burrows in the Otway Group (Albian) of Victoria, Australia, and their relation to Cretaceous polar environments: Cretaceous Research, v. 30, p. 1223–1237.

Martin, L.D., and Bennett, D.K., 1977, The burrows of the Miocene beaver *Palaeocastor*, western Nebraska, U.S.A.: Palaeogeography, Palaeoclimatology, Palaeoecology, v. 22, p. 173–193.

Mayer, B., and Schwark, L., 1999, A 15,000-year stable isotope record form sediments of Lake Steisslingen, Southwest Germany: Chemical Geology, v. 161, p 315–337.

Meyer, R.C., 1999, Helical burrows as a palaeoclimate response: *Daimonelix* by *Palaeocastor*: Palaeogeography, Palaeoclimatology, Palaeoecology, v. 147, p. 291–298.

Meyers, P.A., and Lallier-Vergès, E., 1999, Lacustrine sedimentary organic matter records of Late Quaternary paleoclimates: Journal of Paleolimnology, v. 21, p. 345–372.

Midwood, A., and Boutton, T., 1989, Soil carbonate decomposition by acid has little effect on $\delta^{13}C$ of organic matter: Soil Biology and Biochemistry, v. 30, p. 1301–1307.

Moberly, R. Jr., 1960, Morrison, Cloverly, and Sykes Mountain Formations, northern Bighorn Basin, Wyoming and Montana: Bulletin of the Geological Society of America, v. 71, p. 1137–1176.

Morgans-Bell, H.S., Coe, A.L., Hesselbo, S.P., Jenkyns, H.C., Weedon, G.P., Marshall, J.E.A., Tyson, R.V., and Williams, C.J., 2001, Integrated stratigraphy of the Kimmeridge Clay Formation (Upper Jurassic) based on exposures and boreholes in south Dorset, UK: Geological Magazine, v. 138, p. 511–539.

Munsell Color, 2000, Munsell Soil Color Charts: Munsell Color, Grand Rapids, 29 p.

Northrop, H.R., and Goldhaber, M.B., eds., 1990, Genesis of the tabular-type vanadium-uranium deposits of the Henry Basin, Utah: Economic Geology, v. 85, p. 215–269.

Owen, D. E., Turner-Peterson, C. E., and Fishman, N. S., 1989, X-ray diffraction studies of the <0.5 μm fraction from the Brushy Basin Member of the Upper Jurassic Morrison Formation, Colorado Plateau: U.S. Geological Survey Bulletin 1808-G, 25 p.

Padden, M., Weissert, H., Funk, H., Schneider, S., and Gansner, C., 2002, Late Jurassic lithological evolution and carbon-isotope stratigraphy of the western Tethys: Eclogae Geologicae Helvetiae, v. 95, p. 333–346.

Parrish, J.T., Peterson, F., and Turner, C.E., 2004, Jurassic "savannah"—plant taphonomy and climate of the Morrison Formation (Upper Jurassic, western USA): Sedimentary Geology, v. 167, p. 137–162.

Pemberton, S.G., and Frey, R.W., 1982, Trace fossil nomenclature and the *Planolites*-*Palaeophycus* dilemma: Journal of Paleontology, v. 56, p. 843–881.

Peterson, F., 1980, Sedimentology of the uranium-bearing Salt Wash Member and Tidwell Unit of the Morrison Formation in the Henry and Kaiparowits Basins, Utah, *in* Picard, M.D., ed., Henry Mountains Symposium: Utah Geological Association, p. 305–322.

Peterson, F., 1984, Fluvial sedimentation on a quivering craton: influence of slight crustal movements on fluvial processes, Upper Jurassic Morrison Formation, western Colorado Plateau: Sedimentary Geology, v. 38, p. 21–49.

Peterson, F., 1994, Sand dunes, sabkhas, streams, and shallow seas: Jurassic paleogeography in the southern part of the Western Interior Basin, in Caputo, M. V., Peterson, J. A., Franczyk, K. J., eds., Mesozoic Systems of the Rocky Mountain Region, USA, Denver, Rocky Mountain Section SEPM, p. 233–272.

Pipiringos, G. N., and O'Sullivan, R. B., 1978, Principal unconformities in Triassic and Jurassic rocks, Western Interior United States—A preliminary survey, U. S. Geological Survey Professional Paper 1035-A, p. A1–A29.

Platt, B.F., and Hasiotis, S.T., 2006, Newly discovered sauropod dinosaur tracks with skin and foot-pad impressions from the Upper Jurassic Morrison Formation, Bighorn Basin, Wyoming, USA: PALAIOS, v. 21, p. 249–261.

Platt, B.F., Hasiotis, S.T., and Hirmas, D.R., in review, Empirical determination of physical controls on megafaunal footprint formation through neoichnological experiments with elephants: PALAIOS, 41 manuscript pages.

Rabenhorst, M.C., and Parikh, S., 2000, Propensity of soils to develop redoximorphic color changes: Soil Science Society of America Journal, v. 64, p. 1904–1910.

Ratcliffe, B.C., and Fagerstrom, J.A., 1980, Invertebrate lebensspuren of Holocene floodplains: their morphology, origin and paleoecological significance: Journal of Paleontology, v. 54, p. 614–630.

Riese, D.J., Hasiotis, S.T., and Odier, G.P., 2011, Synapsid burrows and associated trace fossils in the Lower Jurassic Navajo Sandstone, southeastern Utah, U.S.A., indicates a diverse community living in a wet desert ecosystem: Journal of Sedimentary Research, v. 81, p. 299–321.

Robinson, J.W., and McCabe, P.J., 1997, Sandstone-body and shale-body dimensions in a braided fluvial system: Salt Wash Sandstone Member (Morrison Formation), Garfield County, Utah: AAPG Bulletin, v. 81, p. 1267–1291.

Robinson, J.W., and McCabe, P.J., 1998, Evolution of a braided river system: the Salt Wash Member of the Morrison Formation (Jurassic) in southern Utah, *in* Shanley, K.W., and McCabe, P.J., eds., Relative Role of Eustacy, Climate, and Tectonism in Continental Rocks: Tulsa, SEPM, p. 93–107.

Royer, D.L., 1999, Depth to pedogenic carbonate horizon as a paleoprecipitation indicator?: Geology, v. 27, p. 1123–1126.

Schlesinger, W.H., and Andrews, J.A., 2000, Soil respiration and the global carbon cycle: Biogeochemistry, v. 48, p. 7–20.

Schudack, M.E., Turner, C.E., and Peterson, F., 1998, Biostratigraphy, paleoecology, and biogeography of charophytes and ostracodes from the Upper Jurassic Morrison Formation, western interior, USA: Modern Geology, v. 22, p. 379–414.

Selby, D., 2007, Direct rhenium-osmium age of the Oxfordian-Kimmeridgian boundary, Staffin Bay, Isle of Skye, U.K., and the Late Jurassic time scale: Norwegian Journal of Geology, v. 87, p. 291–299.

Sellwood, B.W., Valdes, P.J., and Price, G.D., 2000, Geological evaluation of multiple general circulation model simulations of Late Jurassic palaeoclimate: Palaeogeography, Palaeoclimatology, Palaeoecology, v. 156, p. 147–160

Sharp, Z., 2007, Principles of Stable Isotope Geochemistry: Upper Saddle River, Pearson Prentice Hall, 360 p.

Smith, J.J., and Hasiotis, S.T., 2008, Traces and burrowing behaviors of the cicada nymph *Cicadetta calliope*: Neoichnology and paleoecological significance of extant soil-dwelling insects: PALAIOS, v. 23, p. 503–513.

Smith, J.J., Hasiotis, S.T., Kraus, M.J., and Woody, D.T., 2008, Relationship of floodplain ichnocoenoses to paleopedology, paleohydrology, and paleoclimate in the Willwood Formation, Wyoming, during the Paleocene-Eocene thermal maximum: PALAIOS, v. 23, p. 683–699.

Smith, R.M.H., 1987, Helical burrow casts of therapsid origin from the Beaufort Group (Permian) of South Africa: Palaeogeography, Palaeoclimatology, Palaeoecology, v. 60, p. 155–170.

Soil Survey Staff, 2010, Keys to Soil Taxonomy, 11th ed., United States Department of Agriculture, Natural Resources Conservation Service, 338 p.

Steiner, M.B., 1998, Age, correlation, and tectonic implications of Morrison Formation paleomagnetic data, including rotation of the Colorado Plateau: Modern Geology, v. 22, p. 261–281.

Talbot, M.R., and Lærdal, T., 2000, The Late Pleistocene – Holocene palaeolimnology of Lake Victoria, East Africa, based upon elemental and isotopic analyses of sedimentary organic matter: Journal of Paleolimnology, v. 23, p. 141–164.

Thompson, W.L., 1934, Notes on *Neotermes castaneus* Burm: The Florida Entomologist, v. 18, p. 33–39.

Tschinkel, W.R., 2010, The foraging tunnel system of the Namibian Desert termite, *Baucaliotermes hainesi*: Journal of Insect Science, v. 10, p. 1–17.

Turner, C.E., and Fishman, N.S., 1991, Jurassic Lake T'oo'dichi': a large alkaline, saline lake, Morrison Formation, eastern Colorado Plateau: Geological Society of America Bulletin, v. 103, p. 538–558.

Turner, C.E., and Peterson, F., 1999, Biostratigraphy of dinosaurs in the Upper Jurassic Morrison Formation of the western interior, U.S.A., *in* Gillette, D.D., ed., Vertebrate Paleontology in Utah: Utah Geological Survey Miscellaneous Publication 99-1, p. 77–114.

Turner, C.E., and Peterson, F., 2004, Reconstruction of the Upper Jurassic Morrison Formation extinct ecosystem—a synthesis: Sedimentary Geology, v. 167, p. 309–355.

Tye, R.S., and Coleman, J.M., 1989, Depositional processes and stratigraphy of fluvially dominated lacustrine deltas: Mississippi delta plain: Journal of Sedimentary Petrology, v. 59, p. 973–996.

Tyson, R.V., 1995, Sedimentary Organic Matter: Organic Facies and Palynofacies: Chapman & Hall, London, 615 p.

Urban, M.A., Nelson, D.M., Jiménez-Moreno, Châteauneuf, J.-J, Pearson, A., and Hu, F.S., 2010, Isotopic evidence of C_4 grasses in southwestern Europe during the Early Oligocene–Middle Miocene: Geology, v. 38, p. 1091–1094.

Valdes, P., 1993, Atmospheric general circulation models of the Jurassic: Philosophical Transactions of the Royal Society of London, B, v. 341, p. 317–326.

Varricchio, D.J., Martin, A.J., and Katsura, Y., 2007, First trace and body fossil evidence of a burrowing, denning dinosaur: Proceedings of the Royal Society B, v. 274, p. 1361–1368.

Wanty, R.B., Goldhaber, M.B., and Northrop, H.R., 1990, Geochemistry of vanadium in an epigenetic, sandstone-hosted vanadium-uranium deposit, Henry Basin, Utah: Economic Geology, v. 85, p. 270–284.

Weedon, G.P., Coe, A.L., and Gallois, R., 2004, Cyclostratigraphy, orbital tuning and inferred productivity for the type Kimmeridge Clay (Late Jurassic), southern England: Journal of the Geological Society, London, v. 161, p. 655–666.

Wright, J., and Lockley, M., 2001, Dinosaur and turtle tracks from the Laramie/Arapahoe Formations (Upper Cretaceous) near Denver, Colorado, USA: Cretaceous Research, v. 22, p. 365–376.

Wright, V.P., and Marriott, S.B., 1996, A quantitative approach to soil occurrence in alluvial deposits and its application to the Old Red Sandstone of Britain: Journal of the Geological Society, London, v. 153, p. 907–913.

TABLES

Table 1.—Features used for ranking estimated drainage conditions. Many features represent a spectrum of conditions so ranks were assigned based on interpretations of all available evidence.

Numeric rank	Estimated conditions	Animal trace fossils	Rhizolith features	Paleosol features
1	poor	• Hydrophilic traces[1] • Shallow traces[1]	• Carbonized roots[2] • Sediment filled rhizoliths[4] • Shallow roots and root mats[6]	• Grey colors; evidence of gleying[3, 4] • Pale yellow coloration[5] • Finer particle size and greater distance from channel[2, 3]
2	imperfect	• Hygrophilic traces[1]	• Sediment filled rhizoliths[4] • Shallow roots[6] • Gray rhizohaloes with yellow-brown Fe rich rims[2]	• Purple colors[3, 4] • Iron oxide nodules[3]
3	moderate	• Terraphilic traces[1]	• Gray rhizohaloes with red Fe rich rims[2] • Deep roots[6]	• $CaCO_3$ accumulation[2, 7] • Slickensides[2, 7] • Red matrix with yellow brown mottles[2]
4	well	• Epiterraphilic traces[1]	• Gray rhizohaloes[2] • Deep roots[6]	• $CaCO_3$ accumulation[7] • Red coloration[4] • Coarser particle size and greater proximity to channel[3]

[1]Hasiotis (2004, 2008)
[2]Kraus and Hasiotis (2006)
[3]Kraus and Aslan (1993)
[4]Smith et al. (2008)
[5]Lal (2006)
[6]Cohen (1982)
[7]Demko et al. (2004)

Table 2.—Lithofacies summary of MF deposits in the study area.

Lithofacies	Sedimentary structures	Interpretation
A) Greenish white very fine- to fine-grained, well-rounded, well-sorted sandstone with up to medium-grained, red and green chert clasts	Low angle planar-tabular cross-stratification, planar to undulatory laminations, ripples, and mudcracks; surfaces planar- to scour-based	2D dune migration in a relatively low energy, possibly intermittent, fluvial system
B) Coarsening upward, interbedded red-brown, tan, and green mudstone, and tan, well-cemented, very fine-grained siltstone	Thin, tabular bedding (<10 cm) with siltstone beds thickening upward, siltstone is massive, mudstone contains planar laminations with local convolute and ripple laminations	Fluvially dominated, lacustrine prodelta deposits
C) Coarsening upward, white to brown siltstone to fine sandstone	Tabular, planar bedding, local flaser bedding, planar laminations, symmetrical and asymmetrical ripples, and ripple cross-laminations	Prograding, shallowly dipping, lacustrine delta-front deposits
D) Greenish white, very fine sandstone, grading up to red-brown and green silt and silty sandstone	Very fine sandstone bedding is tabular to slightly undulatory; silt and silty sandstone contain laminations, mudcracks, and white, thin sandstone lenses that decrease in size and connectivity upward	Delta plain and interdistributary channel deposits
E) White to greenish white, well-sorted, very fine sandstone	Wavy to lenticular bedding, planar and ripple cross-lamination, bioturbation	Fluvially influenced lake-margin deposits
F) White to tan, fining upward, fine to coarse sandstone, rarely fining upward to green mudstone	Scour-based with trough and planar-tabular cross-bedding transitioning upward to horizontal, planar bedding; coarse clasts and green mudstone clasts are present at the bases of many beds; green mudstones contain planar laminations	Braided stream channel-fill deposits; coarse-grained channel bases represent lag deposits with rip-up clasts; laminated green mudstones represent slackwater deposits associated with channel abandonment

Lithofacies	Sedimentary structures	Interpretation
G) Interbedded, white, very fine sandstone and red to purple mudstone with rare carbonate nodules	Sandstones are relatively thin, sharp-based, laterally extensive with trough cross-bedding, horizontal planar bedding, ripple cross-lamination, climbing ripple lamination, and abundant bioturbation; mudstones are massively bedded with less common planar laminations, ripple laminations, and mudcracks	Levee and proximal overbank deposits with varying degrees of pedogenic modification
H) Red, gray, or light green mudstone with common color mottling	Massive, many internal, striated, clay-coated surfaces, and abundant bioturbation	Pedogenically modified distal floodplain deposits
I) White to greenish gray, high shrink-swell potential mudstone with brown and tan color mottling	Massive, conchoidal fracture, rare planar laminations, ripple cross-stratification, and gravel-sized mudstone clasts	Pedogenically modified distal floodplain deposits with substantial altered volcanic ash component

Table 3.—Pedofacies summary of MF deposits. Paleosol Designations: (*) U.S Soil Taxonomy and (+) Mack et al (1993).

Pedofacies	Paleopedologic features	Interpretation	Paleosol Designation(s)
I) Red to brown mottled mudstone	Relict bedding, mudcracks, rhizohaloes, carbonate-filled burrows	Poorly developed, simple paleosols developed on proximal floodplain deposits	*Entisol +Protosol
II) Red to brown and purple mottled mudstone	Massive, faint to distinct horizontal intervals with unique properties, including color, presence of rare carbonate nodules and rare slickensides, common rhizohaloes and burrows	Moderately well-developed, simple paleosols with incipient horizonation, in proximal to intermediate floodplain deposits	*Inceptisol +Protosol
III) Massive, bioturbated sandstone	Massive or with primary sedimentary structures disrupted by trace fossils	Weak pedogenic modification of fluvial deposits into simple paleosols	*Entisol +Protosol
IV) Red and gray mottled mudstone with clay-rich intervals	Distinct horizontal intervals with unique colors and other properties including irregular to elongate, vertically oriented gray mottles and rhizoliths and clay-rich intervals that fracture preferentially into equidimensional to horizontally elongated blocks and contain slickensides; some superimposition of properties within intervals	Well-drained, relatively mature, composite paleosols with well-developed horizons; clay rich horizons typical of Bt horizons experiencing shrinking and swelling	*Alfisol +Argillisol

Pedofacies	Paleopedologic features	Interpretation	Paleosol Designation(s)
V) Red mottled mudstone	Thick, horizontal intervals with distinct matrix properties, including color, gray mottling, rhizoliths, and high clay content associated with slickensides	Well-drained, relatively mature, cumulate paleosols with well developed horizons; clay rich horizons with slickensides typical of Bt horizons that experience shrinking and swelling	*Alfisol or Ultisol +Argillisol
VI) Dominantly gray mottled mudstone	Beds up to several meters thick with thick, horizontal intervals with distinct properties, including matrix color, red and gray color mottling, rhizoliths, and rare Fe nodules	Poorly drained, relatively mature, cumulate paleosols with well-developed horizons; gray coloration and Fe nodules indicative of reducing conditions from poor drainage	*Aqualf (Alfisol) +Gleysol
VII) Light greenish gray, white, and light yellow mudstones and claystones	Beds up to several meters thick, rare relict bedding, conchoidal fracture, sparse zones of irregular, weak red and greenish gray mottling, rhizoliths, rhizohaloes, and carbonized roots	Poorly drained, moderately to well-developed, cumulate paleosols formed in lithofacies I; carbonized roots and dominantly gray, white, and yellow redoximorphic coloration indicate reducing conditions from poor drainage	*Inceptisol or Andisol +Protosol or Gleysol

FIGURES

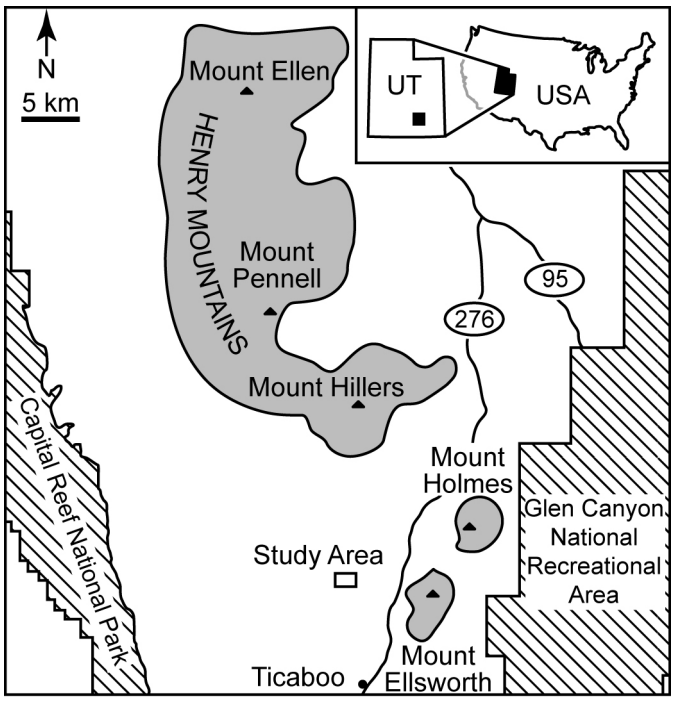

Figure 1.—Location map of study area. Shaded mountainous regions follow physiographic province boundaries of Hunt et al. (1953).

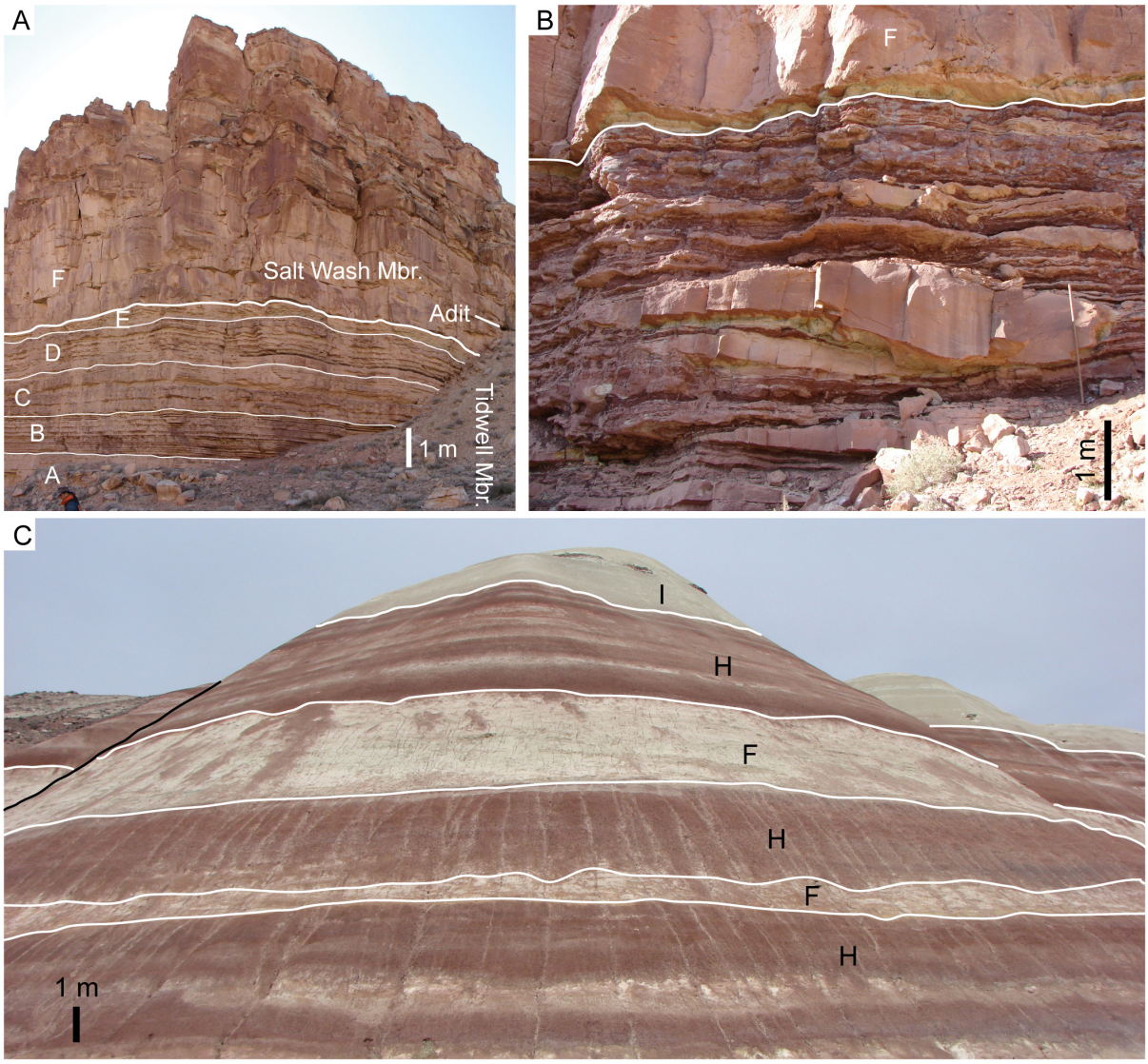

Figure 2.—Field photographs showing examples of members and lithofacies in the study area. A) Tidwell and basal Salt Wash members, showing lithofacies A–F. Adit located at the U-rich interval at the base of the Salt Wash Member. Image is a photomosaic assembled with Microsoft ICE. B) Heterolithic lithofacies within the Salt Wash Member. C) Typical outcrop expression of the Brushy Basin Member, which contains examples of lithofacies F, H, and I.

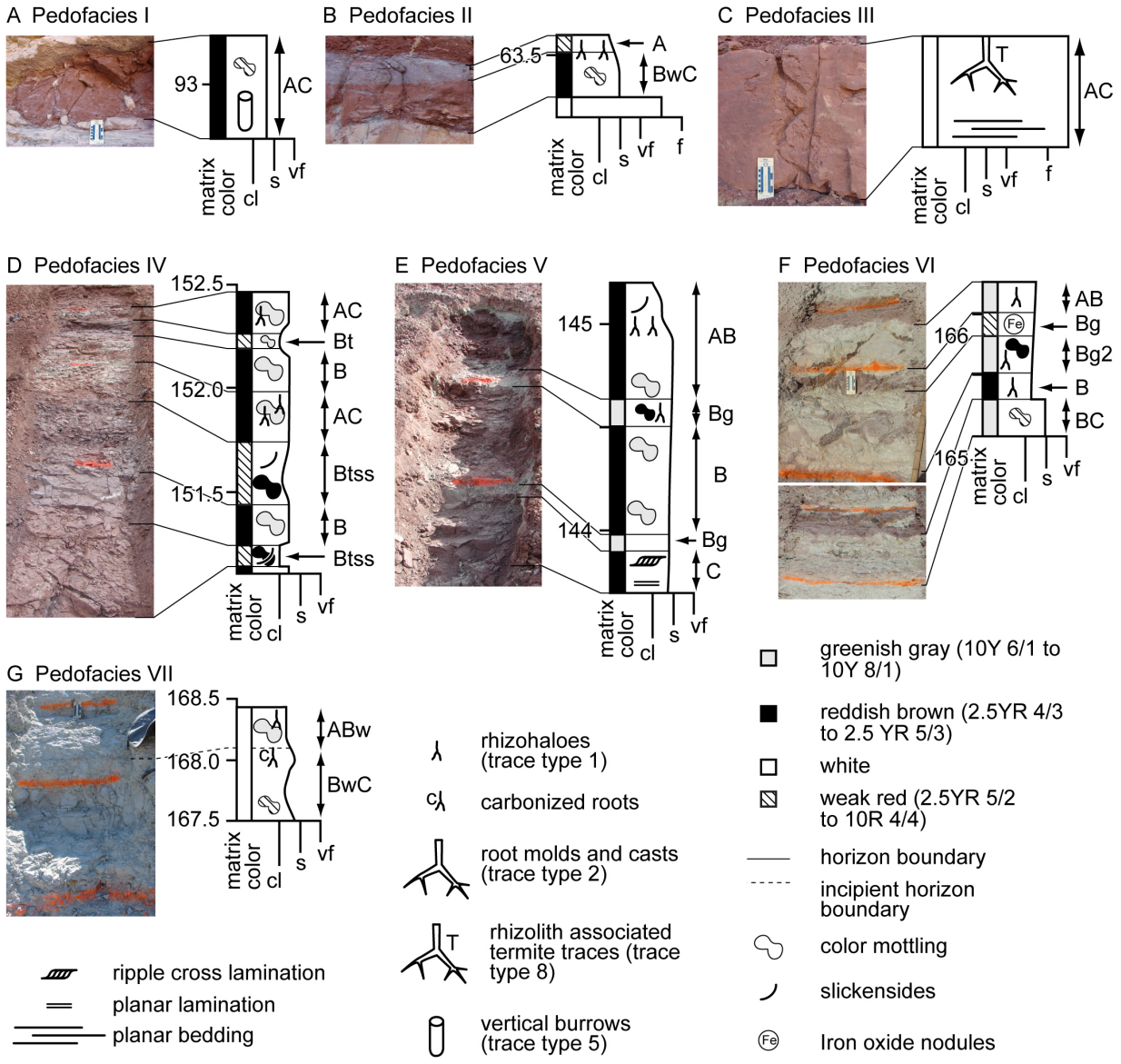

Figure 3.—Field photographs and corresponding interpretations of representative profiles from pedofacies A) I, B) II, C) III, D) IV, E) V, F) VI, and G) VII. Orange lines in photographs represent 0.5-m vertical intervals measured in the field. Interpretations of paleosol horizons are shown associated with arrows adjacent to profiles.

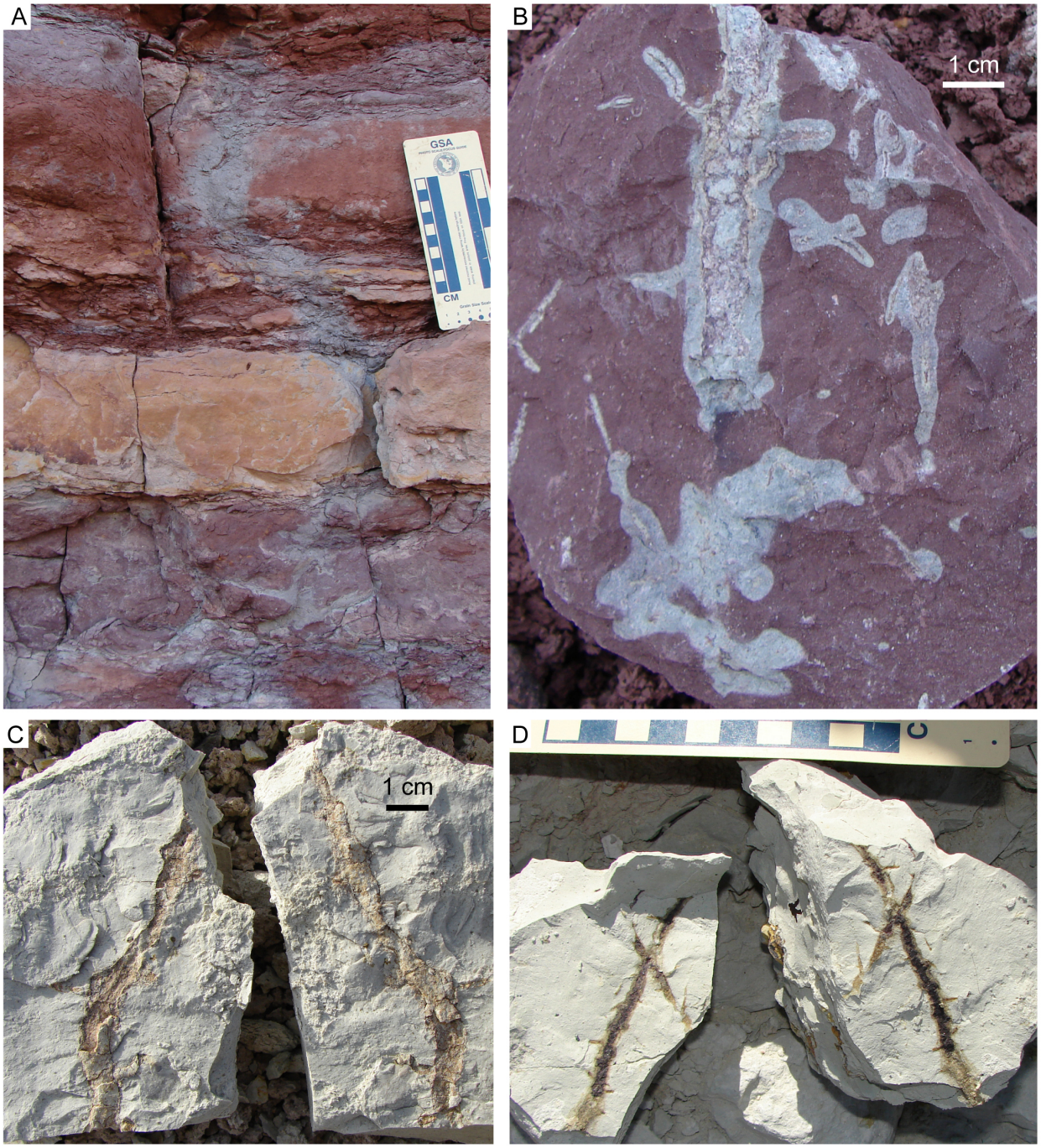

Figure 4.—Root traces. A) Large rhizohalo (type 1) and associated sandstone mold (type 2) in pedofacies II. B) Trace type 1: rhizohaloes associated with root cast in pedofacies V. C) Root mold and cast in pedofacies VII. D) Carbonized root fossil and rhizohalo in pedofacies VII).

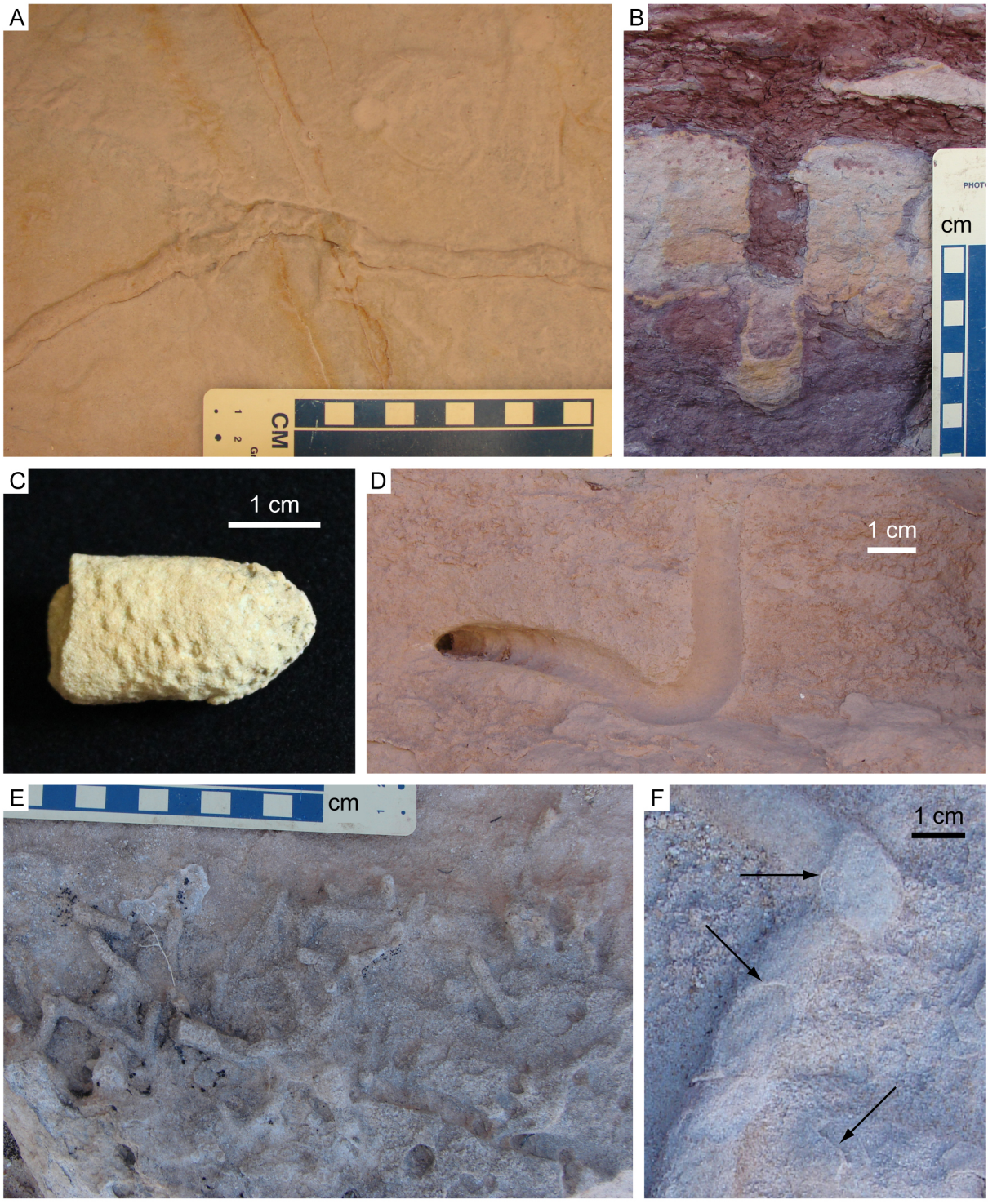

Figure 5.—Small- and medium-diameter burrows. A) cf. *Planolites* (type 4) in the Salt Wash Member. B) Vertical burrows (type 5) in lithofacies G. Note downward displacement of matrix material. C) Sandstone cast attributed to trace type 5. D) J-shaped burrow (type 6). E) cf. *Palaeophycus* (type 7), detail of wall lining exposed in fractured surface in F (arrows).

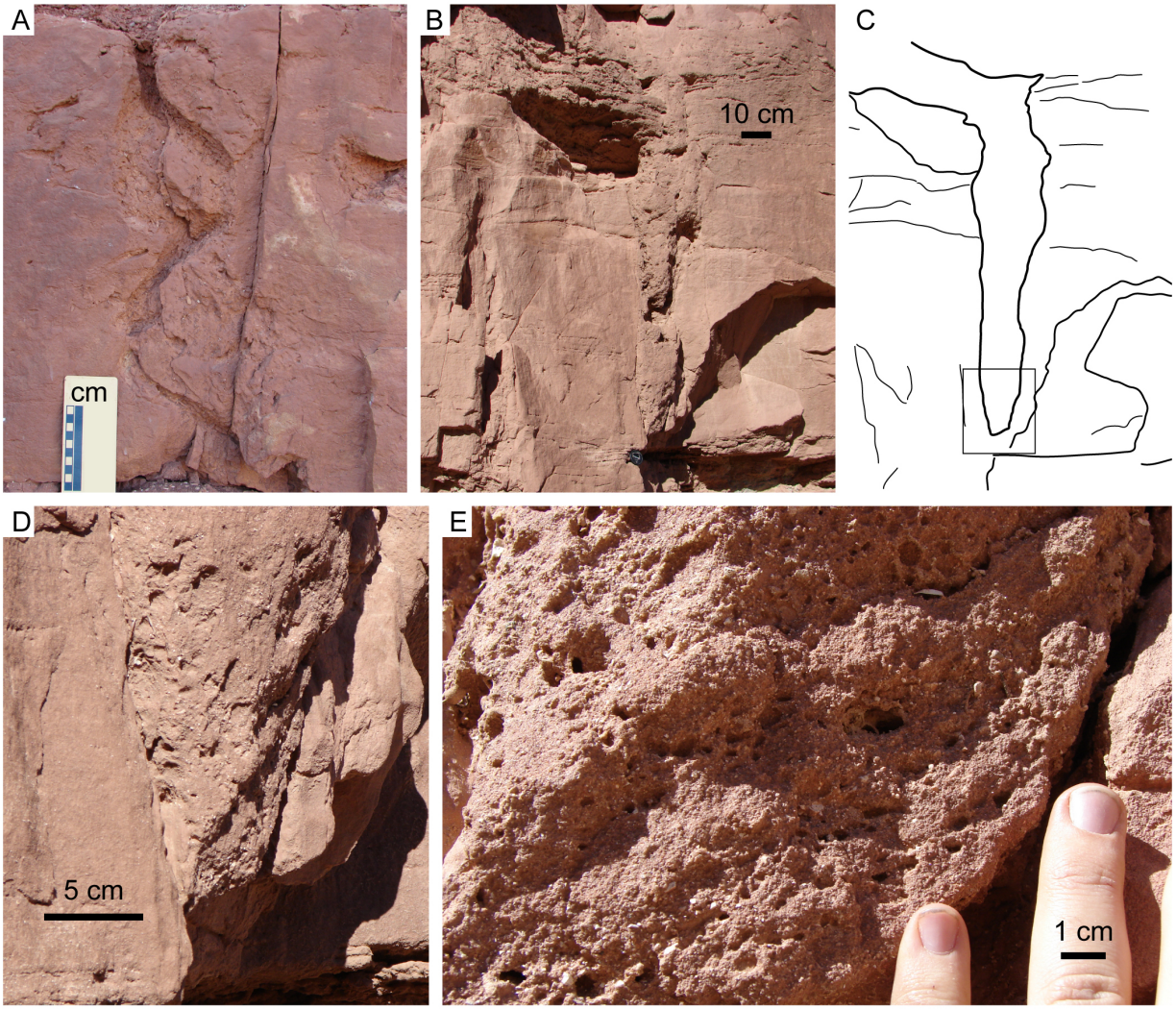

Figure 6.—Termite traces. A) rhizolith-associated termite traces (type 8). B) Large termite nest (type 9) in lithofacies F. C) Interpretation of structure in B. D) close up of lower, tapered end of the vertical column, note difference in texture and sorting of gravel compared to adjacent matrix. E) Close up of texture within termite nest, showing pitting interpreted as chambers.

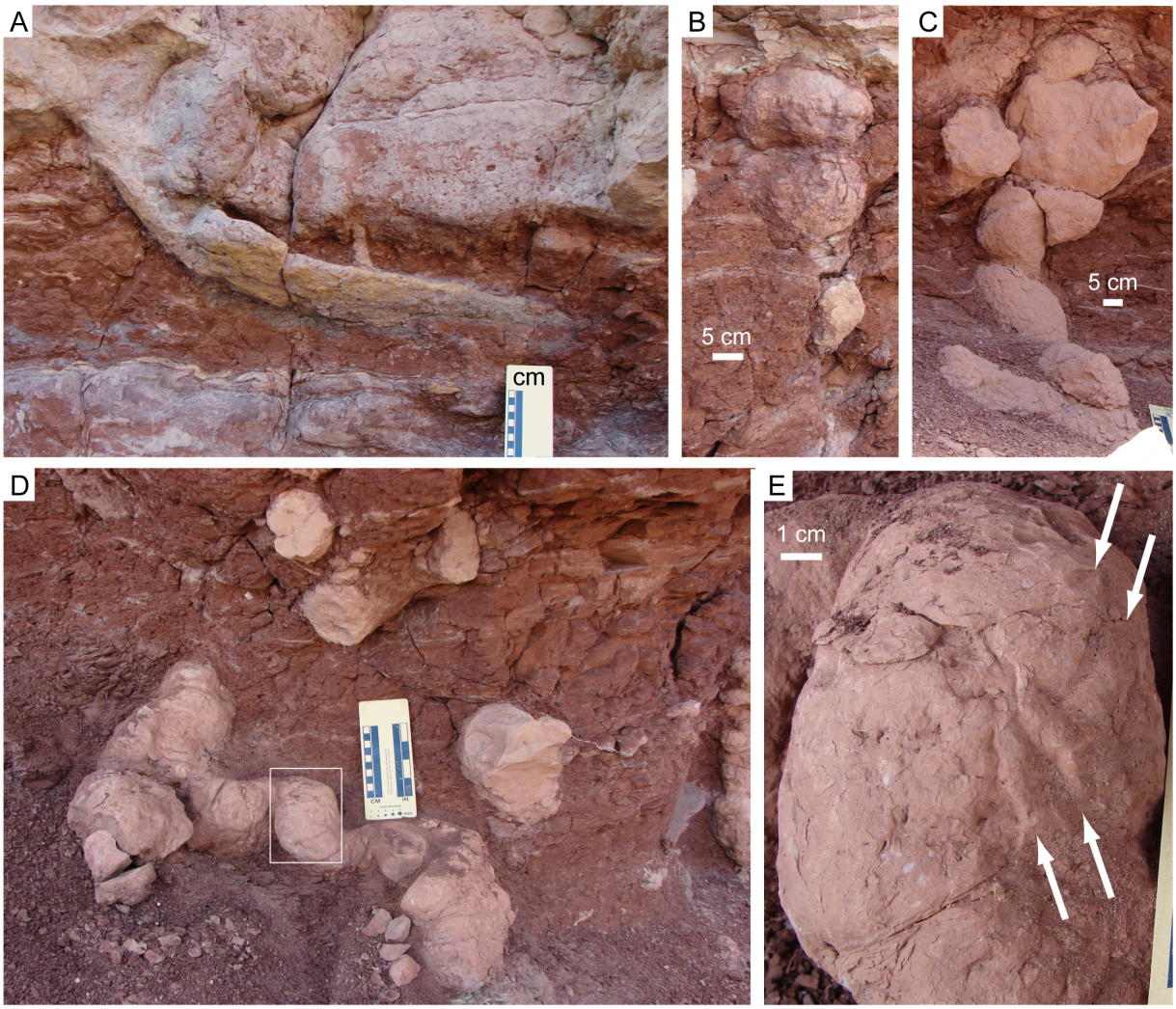

Figure 7.—Large-diameter vertebrate burrows. A) Simple type 10 burrow. B, C) cf. *Daemonelix* in laterally extensive paleosol in lithofacies G. Note terminal subhorizontal chamber in C. D) partial burrow complex (type 12) in the same laterally extensive paleosol. E) close-up of boxed region in D showing parallel, linear ridges on surface (arrows).

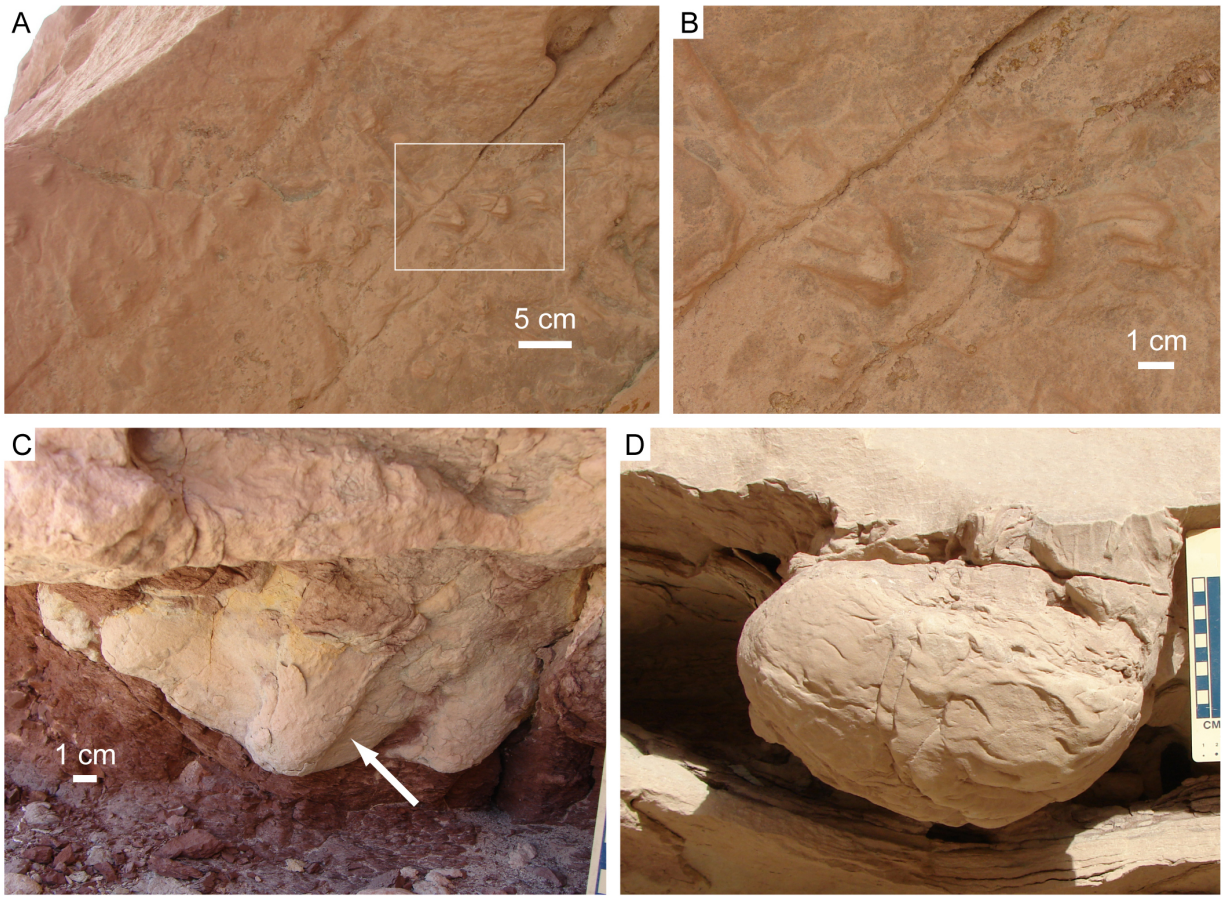

Figure 8.—Vertebrate tracks. A) Turtle trackway (type 13). B) Close up of trackway in A, showing individual tracks. C, D) Sauropod dinosaur tracks (type 14).

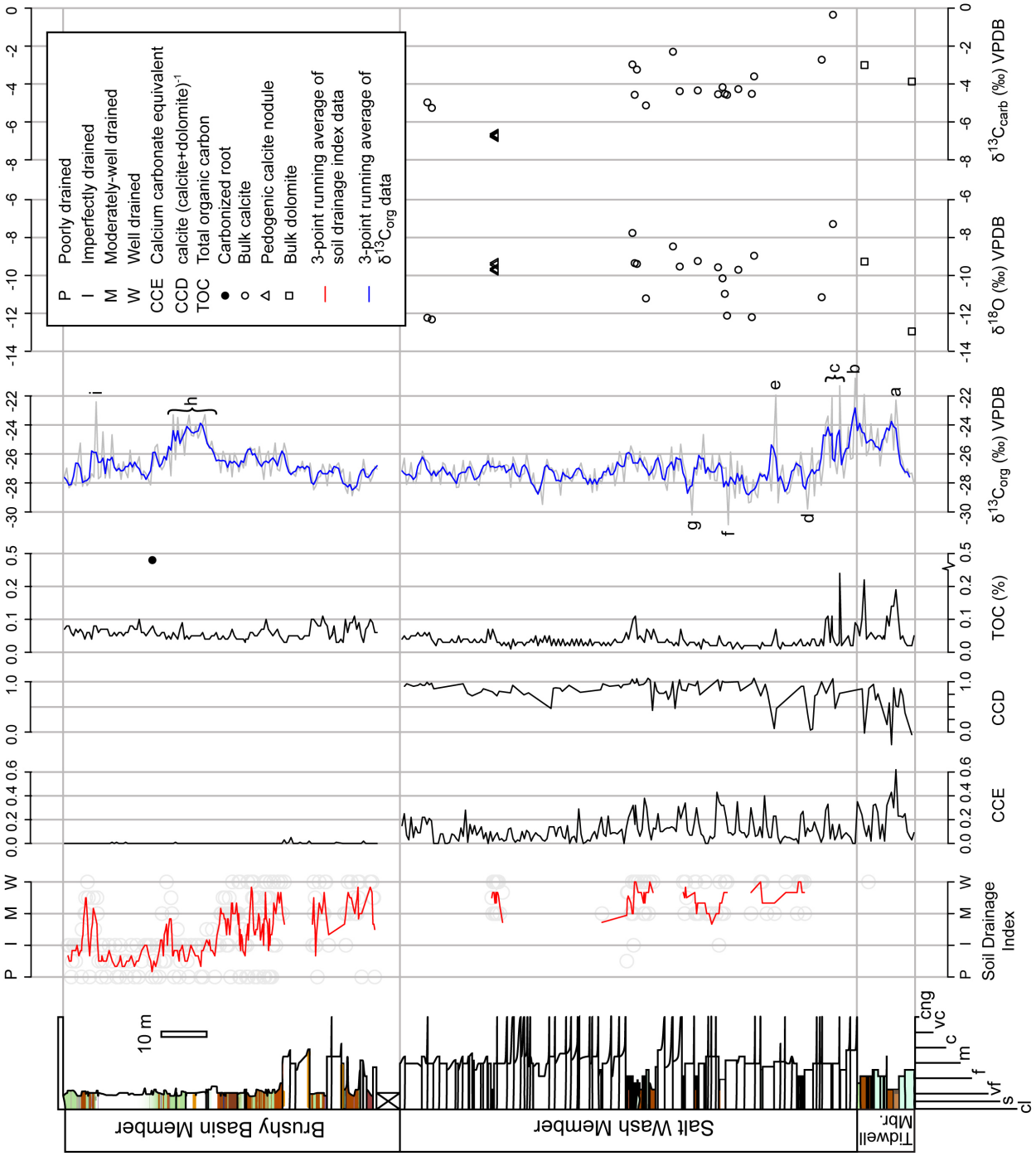

Figure 9.—Analytical results, including stratigraphic section, soil drainage index, calcium carbonate equivalent (CCE), calcium fraction (calcite/(calcite+dolomite)) of carbonate fraction of samples (CCD), total organic carbon (TOC), $\delta^{13}C_{org}$, $\delta^{18}O$, and $\delta^{13}C_{carb}$.

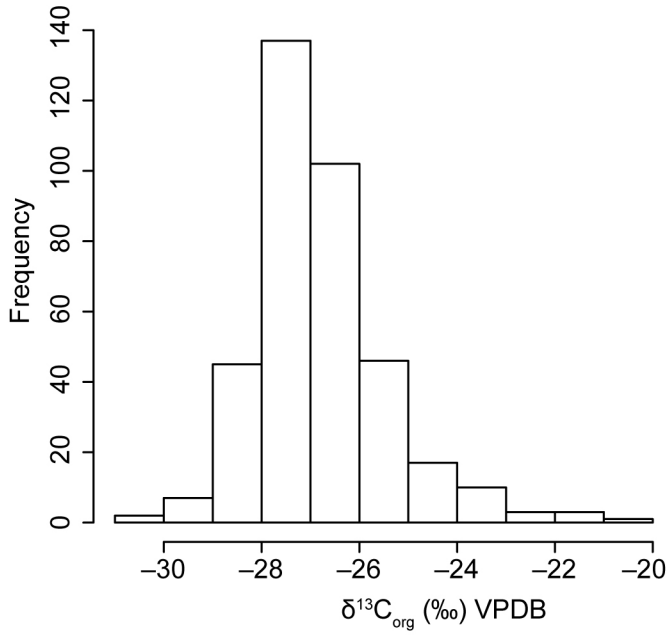

Figure 10.—Histogram of $\delta^{13}C_{org}$ values from the entire MF.

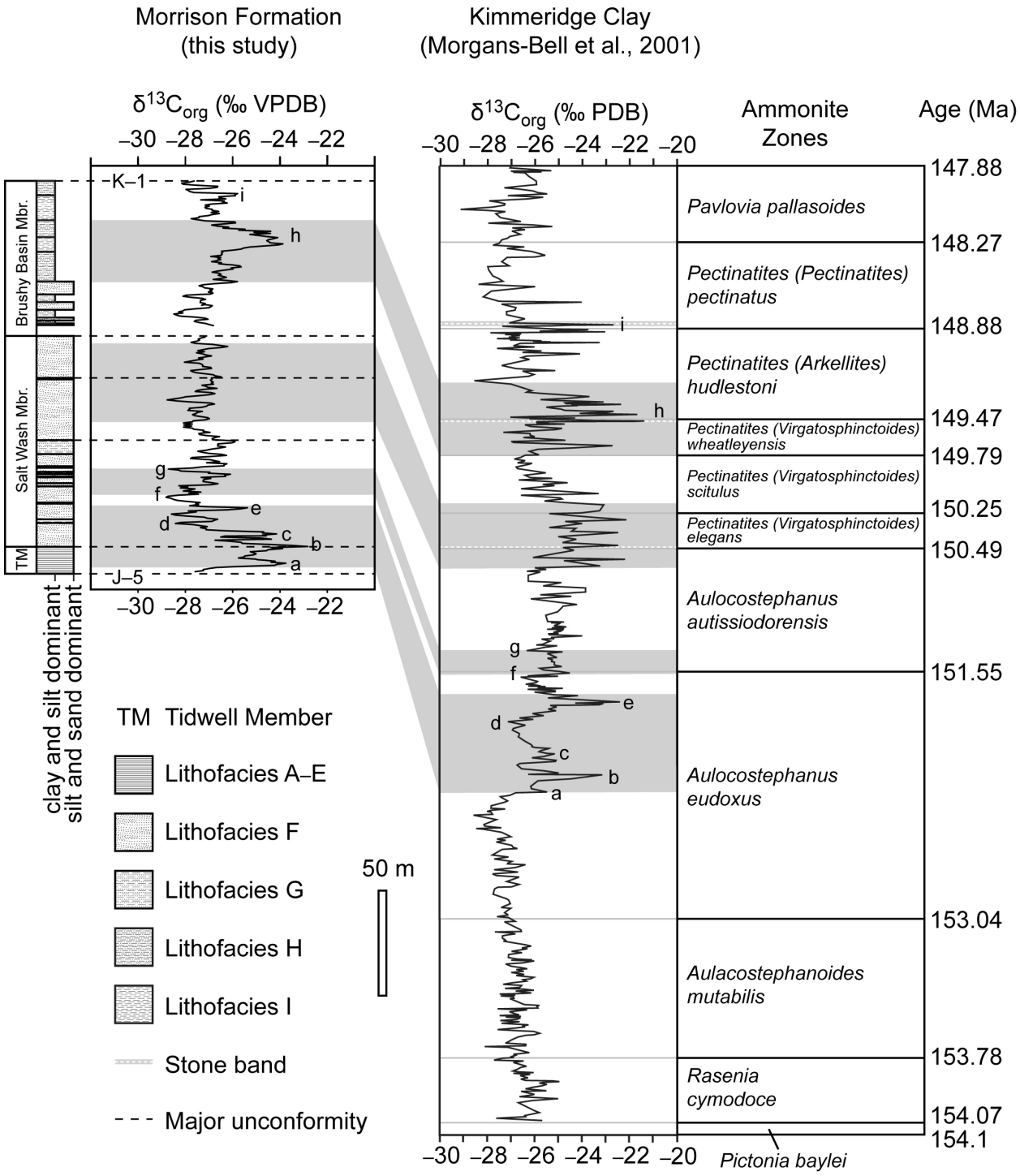

Figure 11.—Proposed isotope correlation between $\delta^{13}C_{org}$ values from the MF and marine $\delta^{13}C_{org}$ from the Kimmeridge Clay Formation, south Dorset, UK from Morgans-Bell et al. (2001). Age of base of *baylei* ammonite zone from Selby (2007). Ages of all other ammonite zone boundaries are minimum estimates from cyclostratigraphy (Weedon et al., 2004).

CHAPTER 6: ROBUST FOOD WEBS LED TO DINOSAUR SUCCESS

Currently in preparation as:

PLATT, B.F., AND HASIOTIS, S.T., Robust food webs led to dinosaur success: Geology.

ABSTRACT

Dinosaur-dominated ecosystems persisted for ~145 million years despite biotic turnover and climate change; however, little is known as to why they were so successful. Established biostratigraphy, extensive fossil assemblage data, and paleoclimate records of the Upper Jurassic Morrison Formation (North America) allow us to test the hypothesis that climate shifts correlate to episodes of biotic turnover. Food-web network analyses of Late Jurassic paleocommunities show that the same robust food-web structure persisted unchanged for about five million years despite climate change through that time. Patterns of vulnerability to food web collapse from simulated extinctions of constituent taxa are most similar to those observed in the African Serengeti ecosystem, a proposed analog. Paleoecosystem responses to environmental perturbations may provide perspectives on the success of Mesozoic dinosaur-dominated ecosystems.

INTRODUCTION

Exceptional concentrations of vertebrate fossils preserved in the geological record provide unique windows into extinct ecosystems and their evolution through time (Roopnarine, 2010). Well over a century of paleontological research in the Upper Jurassic Morrison Formation (MF), western interior North America, has produced extensive fossil data that enable

detailed reconstructions of ancient, dinosaur-dominated landscapes. Invertebrate and vertebrate biostratigraphies of the MF suggest multiple episodes of biotic turnover during deposition (Turner and Peterson, 1999), but paleoecological analyses of faunal assemblages suggest relatively stable paleocommunities (Foster, 2003, 2007). Quantitative food-web network analyses of the trophic relationships of MF biota have not been attempted. Here we show that, with the potential exception of the oldest biostratigraphic interval, the same food-web structure persisted virtually unchanged throughout MF deposition, despite geological evidence for paleoclimate change through that time. We found that the MF food webs did not follow the pattern typical of modern ecosystems, which are vulnerable to the extinction of the most connected taxa. Our results suggest that the highly robust and persistent food webs—a pattern that characterizes the analogous megafaunal-dominated African Serengeti ecosystem (Van Valkenburgh and Molnar, 2002; Hasiotis, 2004)—contributed to success of dinosaur-dominated ecosystems throughout the Mesozoic.

The MF covers > 10^6 km^2 of the western interior of North America (Dodson et al., 1980) and comprises a mosaic of laterally extensive sedimentary lithofacies of varying thicknesses (Turner and Peterson, 2004). Radiometric dating from multiple localities has established an age of ~148–155 Ma (?latest Oxfordian–Kimmeridgian) (Kowallis et al., 1998, 2007). Depositional settings represented by lithofacies include channel, levee, floodplain, lacustrine, eolian, palustrine, coastal plain, and shallow marine environments, many of which coexist in, or exclusively define, formally named members (Peterson, 1994; Turner and Peterson, 2004). Paleontological investigations have produced an exceptional abundance of fossils, most famously those of dinosaurs, preserved within terrestrial and freshwater aquatic deposits (Nudds and Selden, 2008). Paleoclimate during MF deposition is interpreted as warm, tropical wet-dry

or semiarid with seasonally distributed precipitation (Demko and Parrish, 1998; Hasiotis, 2004; Parrish et al., 2004; Hasiotis, 2008). An increase in humidity through time is indicated by paleopedology (Demko et al., 2004), ichnology (Hasiotis, 2004, 2008), and paleobotany (Parrish et al., 2004). Biostratigraphic zones (biozones) have been established based on first and last occurrences of ostracodes and charophytes (Schudack et al., 1998) and dinosaurs (Turner and Peterson, 1999). Modification of the dinosaur biostratigraphy to include all fossil vertebrates yielded six biozones (Foster, 2003), which we follow herein (Fig. 1). Two of the vertebrate biozone boundaries correspond to ostracode and charophyte biozone boundaries and may, therefore, represent particularly significant turnover events.

We test the hypothesis that paleocommunity structure changed significantly throughout deposition of the formation, as suggested by the apparent biotic turnover events marking biozone boundaries. Biostratigraphic data are considered in terms of both the entire terrestrial–freshwater aquatic ecosystem (whole ecosystem; WE) and a subset of the ecosystem—terrestrial taxa (terrestrial subset; TS)—excluding aquatic organisms, which are not as well represented by fossil data. Changes in food web topology (i.e., structure) between biozones are of particular interest because they may indicate ecosystem response to environmental or climatic perturbations, which could be tested with correlative geological proxy data from the MF. Alternatively, no substantial changes in food webs through time may indicate that the basic MF paleocommunity structure was resilient. Temporal food-web patterns may be explained partially by their robustness, a measure of food-web sensitivity to constituent extinctions (Dunne et al., 2002b). Food webs that experience major topological changes from extinctions at terminal biozone boundaries may be explained by low robustness values. No significant changes in food-web properties at biozone boundaries may be the result of highly robust food webs that were not substantially affected by

extinctions.

METHODS

Approach

We approached the entire continental biota of the MF as a single ecosystem because fossil evidence shows that a large number of terrestrial taxa had a cosmopolitan distribution (Dodson et al., 1980; Foster, 2000, 2003), and there is no evidence of major geographic barriers within the depositional basin (Turner and Peterson, 2004). Many aquatic taxa and geochemical data also show connectivity between lentic and lotic systems (Evanoff et al., 1998; Kirkland, 1998; Dunagan and Turner, 2004; Good, 2004).

Potential evidence of endemism comes from palynomorphs (Hotton and Baghai-Riding, 2010), the bivalve *Hadrodon* (Evanoff et al., 1998), the mammal *Docodon* (Foster et al., 2006), some sauropod dinosaurs (Harris and Dodson, 2004), and cluster analysis of Late Jurassic dinosaur assemblages (Noto and Grossman, 2010). We argue that consideration of all MF taxa in food web analyses is valid because most taxa with limited distributions will group with cosmopolitan taxa with similar ecological roles during analyses, i.e., they are the same kinds of organisms and fill the same niches (Cohen, 1978).

Environmental Categories

We distinguished between different paleoenviornmental settings within the MF as interpreted from different lithofacies. Paleoenvironmental distinctions allow for segregation of taxa confined to a particular habitat while accounting for links between contiguous habitats; such links can have substantial influences on food web dynamics (Nakano and Murakami, 2001). For

the purposes of this study, we divided the MF ecosystem into five broad paleoenvironmental settings: lentic, lotic, terrestrial, lentic-terrestrial ecotone (LeTE), and lotic-terrestrial ecotone (LoTE). Lentic settings are characterized by standing water and include all lacustrine and palustrine environments. Lotic settings are characterized by flowing water and include all fluvial environments. Terrestrial settings include all distal floodplain and upland environments. Levee and proximal floodplain deposits constitute LoTE settings. Marginal lacustrine and palustrine environments are considered LeTE settings.

Taxonomic Data

We compiled a database of terrestrial and freshwater aquatic body and trace fossils from an extensive literature search and assigned biozone and paleoenvironmental attributes to each taxon when possible (Table E7). All taxonomic data fall into one of three categories: plant and algae fossils, animal trace fossils, and animal body fossils. We treated each type of data differently because of differences in the nature of the fossils and reconstructions of representative biota.

Algae are represented in the MF by palynomorphs (Litwin et al., 1998) and fossilized gyrogonites of charophytes (Schudack et al., 1998). Algae were included in the broadly defined nodes phytoplankton and phytobenthos. Charophytes and other macroscopic benthic algae were assigned to an additional node.

Plant megafossil and palynomorph data (Ash and Tidwell, 1998; Litwin et al., 1998; Chure et al., 2006; Hotton and Baghai-Riding, 2010) were grouped at the ordinal or familial level because of uncertainties about identifications and whole-plant reconstructions from form taxa. Grouped plants were further consolidated based on reconstructed stature and morphology

(Stevens and Parrish, 2005; Chure et al., 2006; Hotton and Baghai-Riding, 2010) and inferred habitat preferences based on preferences of modern relatives (Hotton and Baghai-Riding, 2010) and depositional environment and taphonomy of plant fossils (Tidwell, 1990; Parrish et al., 2004). We chose to bin plants by stature and environment because we used reconstructed feeding heights and environmental preferences of consumers to determine feeding links between plants and herbivores.

Trace fossils are abundant throughout the MF, and record environmental preferences of tracemakers and the presence of animals not represented by body fossils (Hasiotis, 2002, 2004; Jennings et al., 2006; Platt and Hasiotis, 2006; Hasiotis, 2008). We included ichnotaxa, depositional environments, and tracemaker interpretations in our database. High taxonomic resolution is not possible for tracemaker interpretations, which are typically limited to the ordinal or familial level (Hasiotis 2004, 2007, 2008). When trace fossils indicated the presence of a taxon not represented by body fossils, that taxon was added to the list of animal taxa represented by body fossils. Taxa represented only by trace fossils are mostly terrestrial and aquatic insects. Trace fossils could not always be assigned with certainty to a particular biozone, but we assume that representatives of major groups of Mesozoic insects were present in favorable environments throughout MF time.

Animal body fossils in the MF are limited almost exclusively to invertebrates with hard parts (e.g., mollusks, ostracodes, conchostracans) and vertebrate skeletal remains. We populated our database at the generic level because there is not enough evidence to suggest that multiple species within any single genus maintained distinct enough lifestyles to warrant assigning each species to a different node. Also, taxonomic status of many species is uncertain (e.g., Carpenter, 2010). The majority of the data were taken from previously compiled faunal lists (Foster, 2003,

Chure et al., 2006; Foster, 2007). All taxa were assigned to biozones and preferred environments. Environmental preferences were determined from interpretations of depositional environments, morphological characteristics, and environmental preferences of modern analogs and extant relatives (Table E7).

Juveniles and adults of a single taxon were treated as distinct nodes when evidence showed ontogenetic dietary or lifestyle changes. We created two nodes to represent hatchling herbivorous and hatchling carnivorous dinosaurs of unspecified taxa since these may have been a food source for a number of predators (Kirkland, 1996). A single prey taxon was divided into juvenile and adult nodes when a change in prey body size allowed different predators to exploit the resource; this includes all sauropod dinosaurs.

We did not include eggs as nodes in our database because they would occupy the same trophic level as plants. If an animal was interpreted as ovivorous (i.e., egg eating), we assigned hatchling nodes as its resources. Similarly, parasites without predators would occupy the top trophic level with carnivores. We excluded these parasitic nodes because of limited information about their presence and host taxa.

Certain nodes were inferred to be present that were not represented by fossils—bacteria (i.e., prokaryotes)—because of their long and ubiquitous presence on Earth (Dunne et al., 2008). Also, detritus was included as a basal node because it is such an important resource. For our purposes, detritus included dung and was assigned as a resource for any coprophagous nodes.

Feeding Relationships—Links

Direct evidence of primary consumer-autotroph interactions is rare in the MF and includes insect borings in plant body fossils (Tidwell and Ash, 1990; Hasiotis, 2004, 2008),

dinosaur gut contents (Bird, 1985), and dinosaur coprolites (Chin and Kirkland, 1998); the insect traces and coprolites are not attributable with certainty to a particular taxon. Links between plant and animal taxa were assigned based on dentition (Fiorillo, 1998), reconstructed bite force (Reichel, 2010), diets of modern analogs and extant relatives, shared environmental preferences between plants and herbivores, and reconstructed feeding heights and plant stature (Stevens and Parrish, 2005).

Specific plant preferences of large, herbivorous dinosaurs have been interpreted from tooth wear patterns and tooth and skull morphology (Fiorillo, 1998; Whitlock, 2011) and plant nutrition and herbivore metabolic requirements (Hummel et al., 2008). Although there is evidence that some herbivores fed preferentially on certain plants, these herbivores still likely ingested a range of plant material (Sander et al., 2010), which is confirmed by coprolites with plant debris from a range of taxa (Chin and Kirkland, 1998).

Primary evidence of predator-prey relationships came from ichnological and paleopathological evidence, although such evidence is rare (Chure et al., 1998; Hasiotis, 2004; Carpenter et al., 2005; Britt et al., 2008; Bader et al., 2009). Inferences about trophic interactions were made from dentition (Henderson, 1998), body size (Farlow and Pianka, 2002; Van Valkenburgh and Molnar, 2002), shed carnivore teeth associated with taxa (Bakker and Bir, 2004), associated taxa within multitaxonomic assemblages (Dodson et al., 1980), comparison with modern analogs (Farlow, 1976), and diets of extant relatives (Kirkland, 1987). Links incorporate all inferred prey, regardless of mode of acquisition, i.e., scavenged or actively hunted. *Allosaurus* juveniles, for example, were likely cursorial hunters that fed differently than adults based on limb proportions and jaw kinematics (Therrien et al., 2005; Foster and Chure, 2006). Small tooth marks and shed teeth, however, show that juveniles also fed on large dinosaurs,

which presumably were killed or scavenged initially by *Allosaurus* adults (Bakker and Bir, 2004; Jennings and Hasiotis, 2006).

We placed all MF taxa in a single master spreadsheet (Table E7), regardless of biozone, and established rules for consumer-resource relationships based on the link criteria presented here. Environmental affiliations were used as guides for link assignment, but consideration was given to situations that would create interactions between environments—e.g., transportation of lotic bivalves and fish into floodplain ponds (Kirkland, 1998; Good, 2004). The master spreadsheet was used to create a spreadsheet for each biozone that was restricted to only the taxa in that biozone; this ensured consistent link assignment across biozones.

Analyses

Each biozone spreadsheet was used to generate a whole-ecosystem (WE) consumer-resource list for each biozone (Tables E8–E13). We also created a terrestrial subset (TS) consumer-resource list for each biozone (Tables E14–E19) to facilitate comparison to modern terrestrial food webs. We used Network3D (Williams, 2010) to aggregate, visualize, and analyze consumer-resource list data. Aggregation collapses multiple nodes with the same sets of consumers and resources into a single node. Data aggregation results were used for all analyses, which quantified 21 properties for WE and TS webs for all biozones (Table E1). We also quantified degree distributions (DD) (Dunne et al., 2002a; Dunne, 2009) for each food web.

We used R (R Development Core Team, 2011) for statistical analyses. We performed linear regressions on each property through the six biozones to look for unidirectional temporal trends. Time data were obtained by extrapolating a date for the midpoint of each biozone from the stratigraphically closest radiometric dates. We transformed the best-fit curves for DD results

to fit linear models and performed an F test to evaluate the null hypotheses that slopes of all six WE models are equal and slopes of all six TS models are equal.

We quantified robustness (Dunne et al., 2002b) by removing nodes from each MF food web in three different ways: in order of increasing connectivity, in order of decreasing connectivity, and randomly—performing 1000 random deletion sequences for each food web. Results for each food web were a list of fractions of nodes deleted—primary extinctions—and a list of fractions of nodes lost due to resource elimination from node deletions—secondary extinctions. For each deletion sequence, robustness was identified as the fraction of primary extinctions that, when added to its corresponding fraction of secondary extinctions, resulted in a sum ≥ 0.5.

Comparisons to Other Food Webs

We compare food web analytical results from each biozone to an analysis of Quarry 9, Como Bluff, Wyoming, USA, a well-sampled MF quarry, to rule out effects of erroneously inflated paleocommunity size from long-term time averaging and assumptions of cosmopolitan distributions. Quarry 9 is in a lenticular claystone interpreted as a pond or oxbow lake (Carrano and Velez-Juarbe, 2006). Precise time constraints are lacking, but the deposit represents a much shorter time interval than all of biozone 5, within which the quarry is located. We apply the same reconstructive methods to the published Quarry 9 faunal list (Carrano and Velez-Juarbe, 2006) that we apply to the six MF biozones.

We also compare our results to modern food web properties to ensure our values are reasonable and to look for potential modern analogs for the extinct MF ecosystem. Published network analytical data for modern terrestrial food webs are available for four ecosystems

(Dunne et al., 2004). The Coachella Valley food web represents a ~780 km^2 desert community of plants, invertebrates, and vertebrates in California, U.S.A. (Polis, 1991). The United Kingdom Grassland site is ~0.97 km^2 and consists of herbivores, omnivores, parasitoids, predators, and pathogens based on a single species of plant, *Cytisus scoparius* (Memmott et al., 2000). The St. Martin food web considers all organisms on the ~87 km^2 island of St. Martin in the Lesser Antilles (Goldwasser and Roughgarden, 1993). The El Verde food web includes the ~0.01 km^2 forested portion of the El Verde Field Station in Puerto Rico (Brown et al., 1983), where birds, reptiles, and amphibians are the dominant vertebrates and greatly outnumber mammals (Reagan and Waide, 1996). Data are also available for the modern Serengeti food web in the ~25,000 km^2 Serengeti National Park, Tanzania, Africa (de Visser et al., 2011). We used Network3D (Williams, 2010) to subject the Serengeti data to the same analyses as the MF food webs.

RESULTS AND DISCUSSION

We performed food-web network analyses (Shipitalo and Gibbs, 2000) of reconstructed MF WE and TS food webs to quantify 21 basic node and network properties (Table E1; supporting online text). Overall, biozones 2–6 have similar properties, but many biozone 1 values are noticeably different from corresponding biozone 2–6 values (Tables E2 and E3). Nine of the 21 biozone 1 WE properties do not fall within two standard deviations (2σ) of the means of biozone 2–6 WE values, and ten of the 21 biozone 1 TS properties fall outside 2σ of the means of biozone 2–6 TS values. This agrees with previous paleoecological analyses of MF biozones (Foster, 2003, 2007).

We performed a food-web network analysis of fossil data from a single MF quarry

(Quarry 9 (Carrano and Velez-Juarbe, 2006)) to rule out effects of time averaging and assumptions of cosmopolitan paleobiogeography. Results yield values that fall within the range of values for MF biozones 1–6, except for the fraction of cannibalistic nodes, which is slightly lower in Quarry 9 than in all the MF biozones (Table E2) but falls within 2σ of the mean of biozone 1–6 values. We, therefore, conclude that our treatment of the MF biota within nongeographically differentiated biozones is valid. The fraction of cannibals in our Quarry 9 web is not substantially different from the values obtained from the six biozone food webs and is likely the result of the particular sample of the MF ecosystem preserved in the quarry.

Most values for TS MF food webs fall within the range of published values obtained from analyses of modern terrestrial food webs (Table 1). All MF biozones have higher links per node (L/S) values than reported for modern terrestrial L/S values. MF biozones 1 and 3 have lower mean trophic level values and higher fractions of basal nodes than published terrestrial webs. All MF food-web properties, however, do fall within the range of values reported from modern ecosystems in all environments, including aquatic ecosystems (Dunne et al., 2002a). We, therefore, consider our values reasonable estimates for reconstructions of extinct ecosystems. There is no single modern terrestrial food web in which all properties are similar in magnitude to those of MF TS webs, but this is not surprising because modern analogs for dinosaurs are limited and relatively few modern terrestrial food webs have been rigorously studied and analyzed.

We performed linear regressions to evaluate unidirectional trends in individual food-web properties. All regressions have nonsignificant slopes except for the fraction of herbivores, the fraction of omnivores, and the fraction of nodes found in feeding loops, which have slopes significantly different from zero at the $\alpha = 0.05$ level (Tables E4 and E5). Significant slopes, however, appear to result from extreme biozone 1 values and results are nonsignificant when

biozone 1 data are removed. This implies that the same basic food-web structure persisted throughout deposition of the MF with the possible exception of biozone 1, as indicated by its substantially different topological properties.

We also quantified degree distributions (DD)—the fractions of nodes with a given number of links to other nodes (Dunne, 2009)—for all MF food webs. Results of DD are all best fit by exponential curves (Fig. 2). Curves were natural logarithm transformed to fit linear models (Fig. 2). The results of an F test on the slopes of the transformed WE data show no significant differences between DD slopes for zones 1–6 at the $\alpha = 0.05$ level (Table E6). There is also no significant difference between DD slopes of TS food webs (Table E6). The nonsignificant differences in DD between biozones indicate that losses and additions of taxa between biozones did not substantially alter this particular food-web property through time.

We deleted nodes in three different orders to simulate extinctions of MF biota and evaluate food-web robustness (Table 2). Robustness values determined by deleting nodes in order from most to least connected are the highest for biozones 2–6, some approaching and reaching the maximum possible value of 0.5 (Dunne et al., 2002b). Robustness values based on random species deletions are also relatively high. Robustness values for biozones 2–6 determined by node deletions ordered from least to most connected are mainly much lower than values determined from the other two deletion methods. Low robustness associated with deletions of the least connected nodes is likely a result of loss of basal nodes or loss of a node with one consumer that serves as a resource for multiple consumers (Dunne et al., 2002b). The former may have caused the results obtained for MF biozones 2–6 food webs because the basal nodes are generally the least connected nodes (see link density between the first and second trophic levels in Fig. 1). Low robustness resulting from extinction of the least connected nodes

is uncommon in modern food webs, which are typically vulnerable to loss of the most connected nodes (Dunne, 2002b), and is reported only from two aquatic food webs (Dunne et al., 2002b). The only modern terrestrial ecosystem documented to be experiencing extinction of the least connected nodes is the African Serengeti (de Visser et al., 2011), which has been proposed as a modern analog for the MF ecosystem (Van Valkenburgh and Molnar, 2002; Hasiotis, 2004). The Serengeti, however, was found to have moderately high robustness in response to extinctions of the least connected nodes, which are attributed to human impacts (de Visser et al., 2011). Robustness results from deletion of the least connected nodes in the MF food webs are comparable in magnitude to the same deletion scenario for the Serengeti ecosystem (Table 2; De Visser et al., 2011). Deletions of the most connected nodes in the MF yielded the highest robustness values for the MF food webs, which is opposite the pattern seen in modern food webs (Dunne, 2002b).

Biozone 1 robustness results are mostly different than those of the other MF biozones. Biozone 1 has noticeably lower robustness values than the other biozones for deletions ordered by decreasing connectivity and random deletions, but has higher values than most other zones when nodes are deleted by increasing connectivity. The differences in robustness results for biozone 1 and biozones 2–6 agrees with node and food web network property results that suggest a major change in food web structure at the boundary between biozones 1 and 2. This boundary is marked by concurrent species originations and extinctions in vertebrates, ostracodes, and charophytes (Fig. 1). Our results may be evidence for a significant event or a transition from an initial paleocommunity structure that was eventually supplanted to produce the food web structure that persisted for the remainder of MF deposition. This interpretation is supported by a unique faunal composition in biozone 1 that contains several exclusive dinosaur taxa (Foster,

2007). Biozone 1, however, is poorly sampled (Turner and Peterson, 1999) so we cannot rule out small sample size as the cause of our results. Additional research focused on the basal MF fauna may help clarify whether the biozone 1 food web was significantly different from the biozone 2–6 food webs.

CONCLUSIONS

Overall, the robustness data agree with basic food-web network property results and previous interpretations of MF paleoecology (Foster, 2003). For the most part, many primary extinctions would be required to cause substantial secondary extinctions in MF food webs; this is a result of the high degree of connectivity between taxa based on the nondiscriminant dietary selection behavior interpreted for many MF dinosaurs (Van Valkenburgh and Molnar, 2002). The robustness of MF food webs may explain the longevity of constituent taxa that persist through multiple biozones. Similar results from future food web network analyses of other dinosaur-dominated ecosystems may indicate that robust food-web structure played a large role in the success of dinosaur-dominated paleocommunities throughout the most of the Mesozoic. The predators in these communities may have also shared non-discriminant feeding behaviors that would have produced high robustness, resulting in a strong buffer to loss of the most connected nodes through secondary extinctions. Perhaps the most telling result of our MF study may be that Mesozoic dinosaur-dominated ecosystems were extremely robust in response to extinction of the most connected taxa; a pattern opposite modern terrestrial ecosystems, which exhibit high vulnerability in response to similar extinction scenarios.

ACKNOWLEDGMENTS

This research is part of a PhD dissertation by B.F.P. at the University of Kansas (KU). We thank J. Dunne and R. Williams for access to and assistance with Network3D software, D. Hirmas for assistance with R code, and B. Lieberman and J. Smith for helpful comments. Support was provided to B.F.P. by the Jurassic Foundation, the KU Geology Department, a Leaman Harris Scholarship from the KU Biodiversity Institute, a Madison and Lila Self Graduate Fellowship at KU, and a Stephen J. Gould student grant from the Paleontological Society.

REFERENCES

Ash, S.R., and Tidwell, W.D., 1998, Plant megafossils from the Brushy Basin Member of the Morrison Formation near Montezuma Creek Trading Post, southeastern Utah: Modern Geology, v. 22, p. 321-339.

Bader, K.S., Hasiotis, S.T., and Martin, L.D., 2009, Application of forensic science techniques to trace fossils on dinosaur bones from a quarry in the Upper Jurassic Morrison Formation, northeast Wyoming: PALAIOS, v. 24, p. 140-158.

Bakker, R.T., and Bir, G., 2004, Dinosaur crime scene investigations: theropod behavior at Como Bluff, Wyoming, and the evolution of birdness, *in* Currie, P.J., Koppelhus, E.B., Shugar, M.A., and Wright, J.L., eds., Feathered Dragons: Bloomington, Indiana, Indiana University Press, p. 301-342.

Bird, R.T., 1985, Bones for Barnum Brown: Adventures of a Dinosaur Hunter: Fort Worth, Texas, Texas Christian University Press, 225 p.

Britt, B.B., Scheetz, R.D., and Dangerfield, A., 2008, A suite of dermestid beetle traces on dinosaur bone from the Upper Jurassic Morrison Formation, Wyoming, USA: Ichnos, v. 15, p. 59-71.

Brown, S., Lugo, A.E., Silander, S., and Liegel, L., 1983, Research history and opportunities in the Luquillo Experimental Forest: New Orleans, Louisiana, p. 132.

Carpenter, K., 2010, Species concept in North American stegosaurs: Swiss Journal of Geosciences, v. 103, p. 155-162.

Carpenter, K., Sanders, F., McWhinney, L.A., and Wood, L., 2005, Evidence for predator-prey relationshops: examples for *Allosaurus* and *Stegosaurus*, *in* Carpenter, K., ed., The Carnivorous Dinosaurs: Bloomington, Indiana, Indiana University Press, p. 325-350.

Carrano, M.T., and Velez-Juarbe, J., 2006, Paleoecology of the Quarry 9 vertebrate assemblage from Como Bluff, Wyoming (Morrison Formation, Late Jurassic): Palaeogeography, Palaeoclimatology, Palaeoecology, v. 237, p. 147-159.

Chin, K., and Kirkland, J.I., 1998, Probable herbivore coprolites from the Upper Jurassic Mygatt-Moore Quarry, western Colorado: Modern Geology, v. 23, p. 249-275.

Chure, D.J., Fiorillo, A.R., and Jacobsen, A., 1998, Prey bone utilization by predatory dinosaurs in the Late Jurassic of North America, with comments on prey bone use by dinosaurs throughout the Mesozoic: Gaia, v. 15, p. 227-232.

Chure, D.J., Litwin, R., Hasiotis, S.T., Evanoff, E., and Carpenter, K., 2006, The fauna and flora of the Morrison Formation: 2006: New Mexico Museum of Natural History and Science Bulletin, v. 36, p. 233-249.

Cohen, J.E., 1978, Food Webs and Niche Space: Princeton, New Jersey, Princeton University Press, 189 p.

de Visser, S.N., Freymann, B.P., and Olff, H., 2011, The Serengeti food web: empirical quantification and analysis of topological changes under increasing human impact: Journal of Animal Ecology, v. 80, p. 484-494.

Demko, T.M., Currie, B.S., and Nicoll, K.A., 2004, Regional paleoclimatic and stratigraphic implications of paleosols and fluvial/overbank architecture in the Morrison Formation (Upper Jurassic), Western Interior, USA: Sedimentary Geology, v. 167, p. 115-135.

Demko, T.M., and Parrish, J.T., 1998, Paleoclimatic setting of the Upper Jurassic Morrison Formation: Modern Geology, v. 22, p. 283-296.

Dodson, P., Behrensmeyer, A.K., Bakker, R.T., and McIntosh, J.S., 1980, Taphonomy and paleoecology of the dinosaur beds of the Jurassic Morrison Formation: Paleobiology, v. 6, p. 208-232.

Dunagan, S.P., and Turner, C.E., 2004, Regional paleohydrologic and paleoclimatic settings of wetland/lacustrine depositional systems in the Morrison Formation (Upper Jurassic), Western Interior, USA: Sedimentary Geology, v. 167, p. 269-296.

Dunne, J.A., 2009, Food webs, *in* Meyers, R.A., ed., Encyclopedia of Complexity and Systems Science: New York, Springer, p. 3661-3682.

Dunne, J.A., Williams, R.J., and Martinez, N.D., 2002a, Food-web structure and network theory: the role of connectance and size: Proceedings of the National Academy of Sciences, v. 99, p. 12917-12922.

Dunne, J.A., Williams, R.J., and Martinez, N.D., 2002b, Network structure and biodiversity loss in food webs: robustness increases with connectance: Ecology Letters, v. 5, p. 558-567.

Dunne, J.A., Williams, R.J., and Martinez, N.D., 2004, Network structure and robustness of marine food webs: Marine Ecology Progress Series, v. 273, p. 291-302.

Dunne, J.A., Williams, R.J., Martinez, N.D., Wood, R.A., and Erwin, D.H., 2008, Compilation and network analyses of Cambrian food webs: Plos Biology, v. 6, p. 693-708.

Evanoff, E., Good, S.C., and Hanley, J.H., 1998, An overview of the freshwater mollusks from the Morrison Formation (Upper Jurassic, Western Interior, USA): Modern Geology, v. 22, p. 423-450.

Farlow, J.O., 1976, Speculations about the diet and foraging behavior of large carnivorous dinosaurs: American Midland Naturalist, v. 95, p. 186-191.

Farlow, J.O., and Pianka, E.R., 2002, Body size overlap, habitat partitioning and living space requirements of terrestrial vertebrate predators: implications for the paleoecology of large theropod dinosaurs: Historical Biology, v. 16, p. 21-40.

Fiorillo, A.R., 1998, Dental microwear patterns of the sauropod dinosaurs *Camarasaurus* and *Diplodocus*: evidence for resource partitioning in the Late Jurassic of North America: Historical Biology, v. 13, p. 1-16.

Foster, J.R., 2000, Paleobiogeographic homogeneity of dinosaur faunas during the Late Jurassic in western North America: New Mexico Museum of Natural History and Science Bulletin, v. 17, p. 47-50.

Foster, J.R., 2003, Paleoecological Analysis of the Vertebrate Fauna of the Morrison Formation (Upper Jurassic), Rocky Mountain Region, U.S.A., v. 23: Albuquerque, NM, New Mexico Museum of Natural History of Science, 95 p.

Foster, J.R., 2007, Jurassic West: Bloomington, Indiana, Indiana University Press, 416 p.

Foster, J.R., and Chure, D.J., 2006, Hindlimb allometry in the Late Jurassic theropod dinosaur *Allosaurus*, with comments on its abundance and distribution: New Mexico Museum of Natural History and Science Bulletin, v. 36, p. 119-122.

Foster, J.R., Trujillo, K.C., Madsen, S.K., and Martin, J.E., 2006, The Late Jurassic mammal *Docodon*, from the Morrison Formation of the Black Hills, Wyoming: implications for abundance and biogeography of the genus: New Mexico Museum of Natural History and Science Bulletin, v. 36, p. 165-169.

Goldwasser, L., and Roughgarden, J., 1993, Construction and analysis of a large Caribbean Food Web: Ecology, v. 74, p. 1216-1233.

Good, S.C., 2004, Paleoenvironmental and paleoclimatic significance of freshwater bivalves in the Upper Jurassic Morrison Formation, Western Interior, USA: Sedimentary Geology, v. 167, p. 163-176.

Harris, J.D., and Dodson, P., 2004, A new diplodocid sauropod dinosaur from the Upper Jurassic Morrison Formation of Montana, USA: Acta Palaeontologica Polonica, v. 49, p. 197-210.

Hasiotis, S.T., 2002, Continental Trace Fossils: SEPM Short Course Notes, v. 51, 132 p.

Hasiotis, S.T., 2004, Reconnaissance of Upper Jurassic Morrison Formation ichnofossils, Rocky Mountain Region, USA: paleoenvironmental, stratigraphic, and paleoclimatic significance of terrestrial and freshwater ichnocoenoses: Sedimentary Geology, v. 167, p. 177-268.

Hasiotis, S.T., 2007, Continental ichnology: fundamental processes and controls on trace fossil distribution, *in* Miller, W.I., ed., Trace Fossils: Concepts, Problems, Prospects: Amsterdam, Elsevier, p. 268-284.

Hasiotis, S.T., 2008, Reply to the comments by Bromley et al. of the paper "Reconnaissance of the Upper Jurassic Morrison Formation ichnofossils, Rocky Mountain Region, USA: Paleoenvironmental, stratigraphic, and paleoclimatic significance of terrestrial and freshwater ichnocoenoses" by Stephen T. Hasiotis: Sedimentary Geology, v. 208, p. 61-68.

Henderson, D.M., 1998, Skull and tooth morphology as indicators of niche partitioning in sympatric Morrison Formation theropods: Gaia, v. 15, p. 219-226.

Hotton, C.L., and Baghai-Riding, N.L., 2010, Paylnological evidence for conifer dominance within a heterogeneous landscape in the Late Jurassic Morrison Formation, U.S.A., *in*

Gee, C.T., ed., Plants in Mesozoic Time: Morphological Innovations, Phylogeny, Ecosystsms: Bloomington, Indiana, Indiana University Press, p. 294-328.

Hummel, J., Gee, C.T., Südekum, K.-H., Sander, P.M., Nogge, G., and Clauss, M., 2008, *In vitro* digestibility of fern and gymnosperm foliage: implications for sauropod feeding ecology and diet selection: Proceedings of the Royal Society B, v. 275, p. 1015-1021.

Jennings, D.S., and Hasiotis, S.T., 2006, Taphonomic analysis of a dinosaur feeding site using geographic information systems (GIS), Morrison Formation, southern Bighorn Basin, Wyoming, USA: Palaios, v. 21, p. 480-492.

Jennings, D.S., Platt, B.F., and Hasiotis, S.T., 2006, Distribution of vertebrate trace fossils, Upper Jurassic Morrison Formation, Bighorn Basin, Wyoming, USA: implications for differentiating paleoecological and preservational bias: New Mexico Museum of Natural History and Science Bulletin, v. 36, p. 183-192.

Kirkland, J.I., 1987, Upper Jurassic and Cretaceous lungfish tooth plates from the western interior, the last dipnoan faunas of North America: Hunteria, v. 2, p. 1-16.

Kirkland, J.I., 1996, Predation of dinosaur nests by terrestrial crocodilians, *in* Carpenter, K., Hirsch, K.F., and Horner, J.R., eds., Dinosaur Eggs and Babies: New York, New York, Cambridge University Press, p. 124-133.

Kirkland, J.I., 1998, Morrison fishes: Modern Geology, v. 22, p. 503-533.

Kowallis, B.J., Britt, B.B., Greenhalgh, B.W., and Sprinkel, D.A., 2007, New U-Pb zircon ages from an ash bed in the Brushy Basin Member of the Morrison Formation near Hanksvile, Utah, *in* Willis, G.C., Hylland, M.D., Clark, D.L., and Chidsey, T.C., Jr., eds., Central Utah—Diverse Geology of a Dynamic Landscape, Utah Geological Association, p. 75-80.

Kowallis, B.J., Christiansen, E.H., Deino, A.L., Peterson, F., Turner, C.E., Kunk, M.J., and Obradovich, J.D., 1998, The age of the Morrison Formation: Modern Geology, v. 22, p. 235-260.

Litwin, R.J., Turner, C.E., and Peterson, F., 1998, Palynological evidence on the age of the Morrison Formation, Western Interior U.S.: Modern Geology, v. 22, p. 297-319.

Memmott, J., Martinez, N.D., and Cohen, J.E., 2000, Predators, parasitoids and pathogens: species richness, trophic generality and body sizes in a natural food web: Journal of Animal Ecology, v. 69, p. 1-15.

Nakano, S., and Murakami, M., 2001, Recripocal subsidies: dynamic interdependence between terrestrial and aquatic food webs: Proceedings of the National Academy of Sciences, v. 98, p. 166-170.

Noto, C.R., and Grossman, A., 2010, Broad-scale patterns of Late Jurassic dinosaur paleoecology: PLoS one, v. 5, p. 1-11.

Nudds, J.R., and Selden, P., 2008, Fossil ecosystems of North America: a Guide to their Sites and their Extraordinary Biotas, Manson Publishing Ltd., 288 p.

Parrish, J.T., Peterson, F., and Turner, C.E., 2004, Jurassic "savannah"--plant taphonomy and climate of the Morrison Formation (Upper Jurassic, Western USA): Sedimentary Geology, v. 167, p. 137-162.

Peterson, F., 1994, Sand dunes, sabkhas, streams, and shallow seas: Jurassic paleogeography in the southern part of the Western Interior Basin, *in* Caputo, M.V., Peterson, J.A., and Franczyk, K.J., eds., Mesozoic Systems of the Rocky Mountain Region, USA, SEPM, p. 233-272.

Polis, G.A., 1991, Complex trophic interactions in deserts: an emperical critique of food-web theory: American Naturalist, v. 138, p. 123-155.

R Development Core Team, 2011, R: A Language and Environment for Statistical Computing: Vienna, Austria, R Foundation for Statistical Computing.

Reagan, D.P., and Waide, R.B., 1996, The Food Web of a Tropical Rain Forest, University of Chicago Press.

Reichel, M., 2010, A model for the bite mechanics in the herbivorous dinosaur *Stegosaurus* (Ornithischia, Stegosauridae): Swiss Journal of Geosciences, v. 103, p. 235-240.

Riede, J.P., Rall, B.C., Banasek-Richter, C., Navarrete, S.A., Wieters, E.A., Emmerson, M.C., Jacob, U., and Brose, U., 2010, Scaling of food-web properties with diversity and complexity across ecosystems, *in* Woodward, G., ed., Advances in Ecological Research: Burlington, Academic Press, p. 139-170.

Roopnarine, P.D., 2010, Networks, extinction and paleocommunity food webs, *in* Alroy, J., and Hunt, G., eds., Quantitative methods in paleobiology, The Paleontological Society, p. 143-161.

Sander, P.M., Gee, C.T., Hummel, J., and Clauss, M., 2010, Mesozoic plants and dinosaur herbivory, *in* Gee, C.T., ed., Plants in Mesozoic Time: Morphological Innovations, Phylogeny, Ecosystems: Bloomington, Indiana, Indiana University Press, p. 330-359.

Schudack, M.E., Turner, C.E., and Peterson, F., 1998, Biostratigraphy, paleoecology, and biogeography of charophytes and ostracodes from the Upper Jurassic Morrison Formation, western interior, USA: Modern Geology, v. 22, p. 379-414.

Shipitalo, M.J., and Gibbs, F., 2000, Potential of earthworm burrows to transmit injected animal wastes to tile drains: Soil Science Society of America Journal, v. 64, p. 2103-2109.

Stevens, K.A., and Parrish, J.M., 2005, Digital reconstructions of sauropod dinosaurs and implications for feeding, *in* Curry Rogers, K.A., and Wilson, J.A., eds., The Sauropods: Evolution and Paleobiology: Berkeley, California, University of California Press, p. 178-200.

Therrien, F., Henderson, D.M., and Ruff, C.B., 2005, Bite me: biomechanical models of theropod mandibles and implications for feeding behavior, *in* Carpenter, K., ed., The Carnivorous Dinosaurs: Bloomington, Indiana, Indiana University Press, p. 179-237.

Tidwell, W.D., 1990, Preliminary report on the megafosil flora of the Upper Jurassic Morrison Formation: Hunteria, v. 2, p. 3-12.

Tidwell, W.D., and Ash, S.R., 1990, On the Upper Jurassic stem *Hermanophyton* and its species from Colorado and Utah, USA: Palaeontographica Abteilung B, v. 218, p. 77-92.

Turner, C.E., and Peterson, F., 1999, Biostratigraphy of dinosaurs in the Upper Jurassic Morrison Formation of the western interior, U.S.A., *in* Gillette, D.D., ed., Vertebrate Paleontology in Utah, Utah Geological Survey, p. 77-114.

Turner, C.E., and Peterson, F., 2004, Reconstruction of the Upper Jurassic Morrison Formation extinct ecosystem-a synthesis: Sedimentary Geology, v. 167, p. 309-355.

Van Valkenburgh, B., and Molnar, R.E., 2002, Dinosaurian and mammalian predators compared: Paleobiology, v. 28, p. 527-543.

Whitlock, J.A., 2011, Inferences of diplodocoid (Sauropoda: Dinosauria) feeding behavior from snout shape and microwear analyses: PLoS one, v. 6, p. 1-20.

Williams, R.J., 2010, Network3D Software: Cambridge, UK, Microsoft Research.

Williams, R.J., and Martinez, N.D., 2004, Limits to trophic levels and omnivory in complex food webs: theory and data: The American Naturalist, v. 163, p. 458-468.

TABLES

Table 1.—Comparison of select properties of Morrison TS food webs and modern terrestrial food webs. Abbreviations: MF, Morrison Formation; S, number of nodes; C, connectance; L/S, links per node; TL, mean trophic level; Path, characteristic path length; Top, fraction of top nodes; Int, fraction of intermediate nodes; Bas, fraction of basal nodes; Can, fraction of cannibals; Omn, fraction of omnivores. Food webs are listed in order of increasing S. Values for MF food webs that fall outside the range of modern terrestrial food webs are in bold.

Food web	S	C	L/S	TL	Path	Top	Int	Bas	Can	Omn
Coachella Valley (Williams and Martinez 2004)	29	0.31	9.0	3.0	1.4	0	0.90	0.10	0.66	0.76
MF biozone 1	33	0.14	4.6	**2.1**	1.9	0	0.73	**0.27**	0.18	0.33
St. Martin Island (Williams and Martinez 2004)	42	0.12	4.9	2.4	2.4	0.17	0.69	0.14	0	0.60
MF biozone 3	47	0.18	8.3	**2.3**	1.8	0	0.81	**0.19**	0.23	0.47
MF biozone 6	53	0.17	9.2	2.5	1.8	0	0.83	0.17	0.19	0.55
MF biozone 2	57	0.19	**10.6**	2.5	1.7	0	0.84	0.16	0.26	0.54
MF biozone 5	58	0.18	**10.3**	2.6	1.8	0	0.84	0.16	0.21	0.57
UK Grassland (Memmott et al. 2000)	61	0.03	1.6	2.6	2.6	0.31	0.56	0.13	0	0.21
MF biozone 4	63	0.17	**11.0**	2.6	1.8	0	0.86	0.14	0.21	0.59
Serengeti (de Visser et al. 2011)	85	0.08	6.4	2.7	2.2	0.18	0.75	0.07	0.13	0.67
El Verde (Reagan and Waide 1996)	155	0.06	9.7	2.5	2.5	0.13	0.69	0.18	0.01	0.57

Table 2.—Robustness results for three node deletion treatments of Morrison Formation food webs. Abbreviations: WE, whole ecosystem food webs; TS, terrestrial subset food webs; a, node deletions in order of ascending connectivity; d, node deletions in order of decreasing connectivity; r, 1,000 random node deletion sequences. Biozones arranged in stratigraphic order. Maximum possible robustness is 0.5 (Dunne et al., 2002b).

Biozone	WEa	TSa	WEd	TSd	WEr	TSr
6	0.35	0.32	0.48	0.49	0.44	0.47
5	0.25	0.33	0.48	0.50	0.45	0.47
4	0.30	0.33	0.48	0.49	0.45	0.48
3	0.33	0.40	0.48	0.50	0.43	0.47
2	0.30	0.33	0.49	0.50	0.44	0.47
1	0.43	0.39	0.38	0.45	0.43	0.45

FIGURES

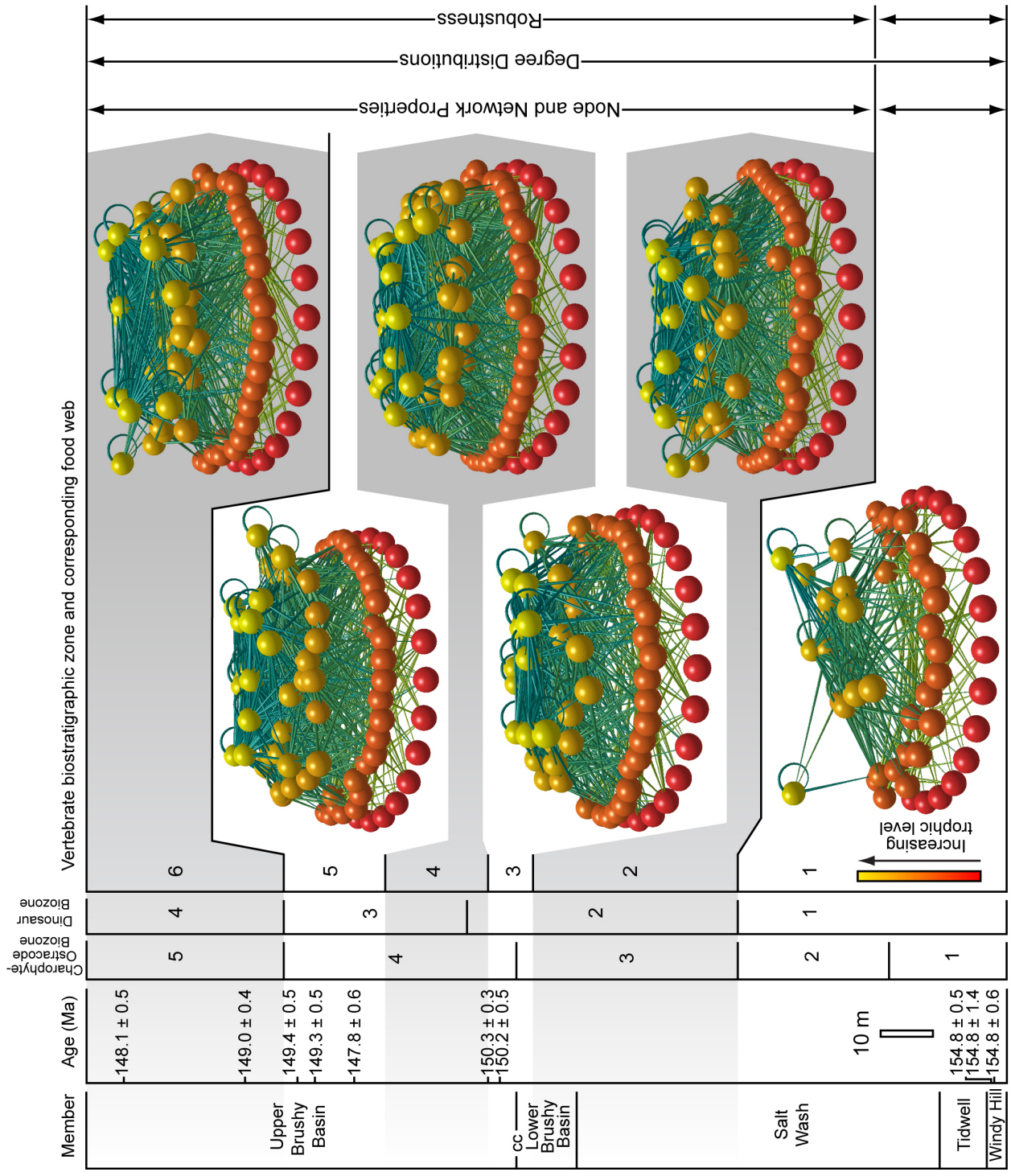
Member
Age (Ma)
Charophyte-Ostracode Biozone
Dinosaur Biozone
Vertebrate biostratigraphic zone and corresponding food web
Node and Network Properties
Degree Distributions
Robustness
Increasing trophic level
10 m
Upper Brushy Basin
cc
Lower Brushy Basin
Salt Wash
Tidwell
Windy Hill
148.1 ± 0.5
149.0 ± 0.4
149.4 ± 0.5
149.3 ± 0.5
147.8 ± 0.6
150.3 ± 0.3
150.2 ± 0.5
154.8 ± 0.5
154.8 ± 1.4
154.8 ± 0.6

Figure 1 (previous page).—Summary of Morrison Formation members, biostratigraphy, and reconstructed food webs. Food webs were reconstructed for time intervals represented by vertebrate biostratigraphy (Foster, 2003); biostratigraphic zone number in upper right hand corner of food web. Thicknesses of biostratigraphic zones are given relative to members and radiometric ages in a master stratigraphic section at Dinosaur National Monument (Turner and Peterson, 1999); WH, Windy Hill Member; LBB, lower Brushy Basin Member. Bold lines represent concurrent boundaries in ostracode, charophyte, dinosaur, and vertebrate biostratigraphies. Food web images generated with Network3D software (Williams, 2010).

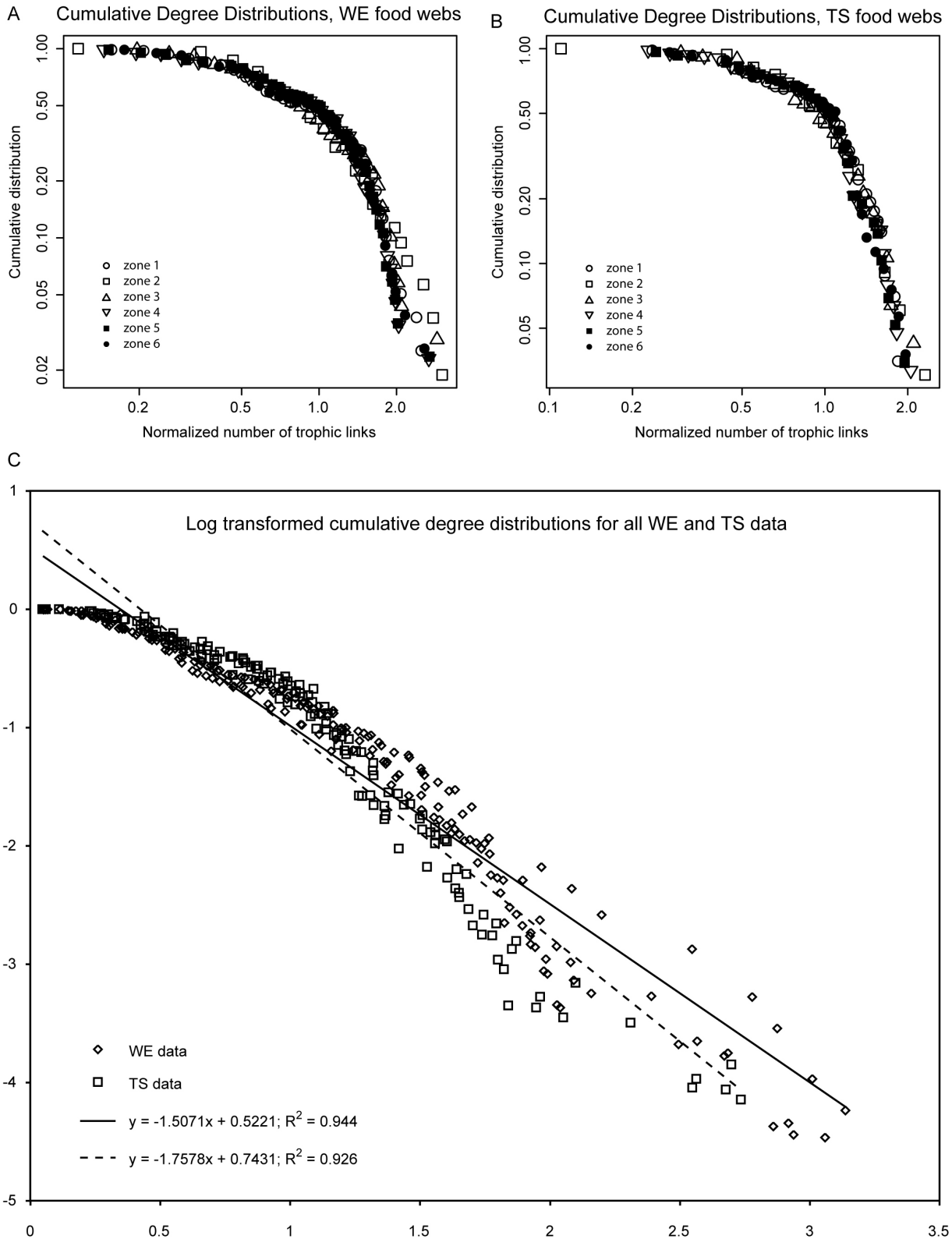
A
Cumulative Degree Distributions, WE food webs
Cumulative distribution
1.00
0.50
0.20
0.10
0.05
0.02
zone 1
zone 2
zone 3
zone 4
zone 5
zone 6
0.2
0.5
1.0
2.0
Normalized number of trophic links
B
Cumulative Degree Distributions, TS food webs
Cumulative distribution
1.00
0.50
0.20
0.10
0.05
zone 1
zone 2
zone 3
zone 4
zone 5
zone 6
0.1
0.2
0.5
1.0
2.0
Normalized number of trophic links
C
Log transformed cumulative degree distributions for all WE and TS data
1
0
-1
-2
-3
-4
-5
WE data
TS data
y = -1.5071x + 0.5221; R2 = 0.944
y = -1.7578x + 0.7431; R2 = 0.926
0
0.5
1
1.5
2
2.5
3
3.5

Figure 2 (previous page).—Degree distributions for A) WE and B) TS food webs for all biozones. C) Log transformed DD data for pooled WE and pooled TS DD data fit with linear regressions. Regression slopes are significantly different at the $\alpha = 0.05$ level, reinforcing the idea that the scale at which ecosystems are approached can affect study outcomes.

CHAPTER 7: CONCLUSIONS

The preceding five chapters represent a multifaceted approach to analyzing ichnological, sedimentological, paleopedological, and geochemical data to reconstruct paleoenvironments, paleoecology, and paleoclimate during deposition of the Upper Jurassic Morrison Formation (MF). The purpose of this chapter is to summarize findings and synthesize results to draw broader conclusions. I approached the MF at multiple scales and organized my dissertation to move roughly from narrow to broad approaches to problems. I first approached problems with quantifying properties of individual trace fossils using multistripe laser triangulation (MLT) scanning. I built upon my MLT research by approaching a single kind of trace fossil—sauropod tracks—that is common in the MF. I worked with live elephants as modern analogs for sauropods, collecting data from elephant tracks to enable better interpretations of fossil megafaunal tracks. Sauropod tracks were just one of the many trace fossils I considered in chapter four, when I interpreted moisture regimes in avulsion deposits in the MF in Bighorn County, Wyoming. In chapter five, I took a vertical approach to ichnological moisture regimes and combined those data with paleopedological observations and geochemistry to interpret multiple aspects of the MF through time. Lastly, in chapter six, I reconstructed food webs from six biostratigraphic zones throughout the MF to look for changes in paleoecology through time.

MLT SCANNING

The results of chapter two show that MLT scanning can be a valuable complement to traditional ichnological methods. I used a NextEngine MLT scanner to make 3D digital models of modern and fossil invertebrate and vertebrate traces, from which I explored ichnological

applications of MLT technology. Even though the resolutions of my digital models did not reach the manufacturer's claims of maximum possible resolutions, results were quite satisfactory and provided potential for advances in three categories: 1) visualization, 2) quantification, and 3) perpetuity of specimens. Visualization of traces is improved by representing multicolored surfaces in a single color, which makes surficial morphology more easily visible. Expression of 3D features in two dimensions is also enhanced through use of digital models to create stereo pairs, stereo anaglyph images, and moving point-of-view movies. One final visual application of MLT technology is the use of software to view the cross-sectional shape of a scanned trace.

Quantification of trace properties from digital models includes improvements in precision of traditional techniques for measuring distances, angles, surface areas, and volumes. Such preexisting techniques as creating contour maps, calculating tortuosity index, and calculating area exploited are improved by the increased precision available through treatments of digital models. I also introduced the new ichnological methods of surface-area index, volume exploited, and relative compactness. These quantitative methods will improve interpretations of bioturbation rates in sediments and biotic contributions to pedogenesis. Ichnotaxonomy can also be aided by quantitative measurements. I found preliminary evidence, for example, that burrow volume to surface area ratios are characteristic of specific tracemakers.

Perpetuity of specimens is facilitated through archiving of digital models captured from physical specimens. Virtual data are useful for recording fossil sites that are threatened by weathering, vandalism, or development. Sharing of digital models between colleagues is easy, as is incorporation of images and movies into online and classroom geoscience lessons at all educational levels. Finally, digital models can be used to create physical copies of original specimens by printing them with a 3D printer. Printed copies are durable and can be safely

incorporated into hands-on educational lessons.

ELEPHANT NEOICHNOLOGY

Chapter three presents results of neoichnological experiments with elephants to quantify the relationship between empirical trackmaking data. I was interested in understanding better the influences of physical and sedimentological properties on footprint formation so that fossil tracks could be used to reconstruct original sedimentary properties, e.g., original sediment moisture content. I designed experiments wherein trenches were excavated in the elephant exhibit yard at the Topeka Zoo, Topeka, Kansas, and filled with experimental sediments up to ground level. Measurements of sedimentary variables and elephant weights were taken before the elephants walked through the sediments. I recorded video while zoo staff encouraged the elephants to walk through the sediment, after which I measured and photographed footprints.

I chose track volume normalized by length (V_n) as the independent variable for all trials. Measurement of track volume in the field was challenging and attempts to use MLT technology produced volume data, but the lengthy scanning time involved and oversaturated lighting conditions made this method unfeasible for data collection for this particular project. Instead, I performed geometric calculations of track volume, incorporating track length, width, and depth measures into the formula for volume of an elliptical cylinder.

I selected locomotion velocity (v) foot pressure (P), sediment aging (A), sediment bulk density (ρ_b), volumetric water content of sediment (θ_v), and mean (M_ϕ), standard deviation (σ_ϕ), skewness (S_ϕ), and kurtosis (K_ϕ) of phi-transformed particle-size distribution as the dependent variables. Velocity was measured from recorded video, P was calculated from weights and weight distributions, A represented the amount of time that passed between installation of

experimental sediment and data collection, ρ_b and θ_v were measured with a nuclear density gauge or from sediment samples collected and analyzed in the soils lab, and particle-size distribution parameters were measured with a laser diffractometer.

Data were analyzed by multiple regression with backward elimination, which yielded the following equation (adjusted R^2-value of 0.44):

$$V_n = 0.812\theta_v^2 - 26.4\theta_v - 157\rho_b - 20.5v + 518$$

where V_n is measured in cm^2, θ_v is in percent, ρ_b is measured in g/cm^3, and v is measured in m/s. Beta weights showed that v exerts relatively little influence over V_n. All other independent variables in the final regression equation influence V_n to a similar degree. This is particularly important in the case of sediment bulk density, which is typically overlooked in vertebrate ichnology studies.

I used data from the literature to calculate the volumes of hypothetical sauropod tracks created in sediments similar to those used in experiments. I also solved the equation for θ_v and estimated original sediment moisture and saturation from deep fossil sauropod tracks from the MF. Results showed that deep tracks represent near saturated conditions, which is important because these results imply that animal tracks, which are classified as epiterraphilic traces (Hasiotis, 2004, 2008), can represent high-moisture conditions. Megafaunal track preservation, therefore, is important to consider when using ichnofossil assemblages to interpret paleohydrology.

MOISTURE REGIMES OF ICHNOFOSSILS IN MORRISON FORMATION AVULSION DEPOSITS

Chapter four shows the utility of ichnological moisture regimes for interpreting the paleohydrological, paleoenvironmental, and paleoclimatic conditions under which avulsion packages were deposited in the upper part of the MF in Coyote Basin. I combined field observations with laboratory analyses of unpublished GPS data to identify and evaluate ichnocoenoses in floodplain paleosols, sheet sandstones, and ribbon sandstones. I recognized 19 different trace types in six different ichnocoenoses, each with a distinct moisture regime profile. Results of chapter three were taken into consideration when interpreting moisture profiles of ichnocoenoses with abundant megafaunal tracks.

The basic vertical pattern that emerged from my analysis was a sequence of moisture regime patterns associated with crevassing during avulsion. An initial suite of dominantly hygrophilic traces was overprinted by dominantly hydrophilic traces immediately before crevassing. After deposition of sheet sands, a suite of traces with a wide range of moisture preferences was dominant, representing instability in moisture availability. Eventually, a dominantly terraphilic suite of traces overprinted other traces in at least one sheet sand. Ribbon sands became inhabited by deep hydrophilic tracemakers following channel abandonment. These general patterns in moisture regime changes can be useful for interpreting avulsion deposits from ichnofossils, which provide more detail than sedimentology alone.

I also showed that ichnology can be useful for evaluating lateral patterns within single trace-fossil-bearing beds. Cluster analysis of abundant traces on a single bedding plane revealed multiple ichnocoenoses that indicate lateral differences in paleohydrological conditions. An overall gradient could be seen, with the wettest conditions representing the most proximal setting

to the main trunk channel.

MULTIPROXY STRATIGRAPHIC PROFILE THROUGH THE MORRISON FORMATION

Chapter five built upon the moisture regime approach applied in chapter four to construct a vertical, semiquantitative, graphical representation of soil drainage conditions through the MF at a field site in Garfield County, Utah, USA. In addition, analyses of carbonate content, carbonate mineralogy, total organic carbon, $\delta^{13}C_{org}$, $\delta^{13}C_{carb}$, and $\delta^{18}O$ were combined to create a detailed stratigraphic profile that is useful for paleoenvironmental and paleoclimatic interpretations, as well as correlations to marine isotope records and stratigraphic profiles of the MF at other locations.

Three members of the MF are recognized in the field area: the Tidwell Member, the Salt Wash Member, and the Brushy Basin Member. I recognized nine lithofacies that included lacustrine, fluvial, and floodplain paleoenvironments. Many deposits contain evidence of pedogenic modification and I recognized seven pedofacies that represent differing degrees of development and drainage conditions. Fourteen types of trace fossils were also present, including root traces, invertebrate burrows and nests, vertebrate burrows, and vertebrate tracks.

Soil drainage indicators combined moisture regime information from trace fossils with ratings of paleosol drainage conditions inferred from abiotic pedogenic features. Overall, the MF exhibited a general up section decrease in soil drainage conditions, which is consistent with patterns observed in previous studies of paleosols (Demko et al., 2004), plant fossils (Parrish et al., 2004), and ichnofossils (Hasiotis, 2004, 2008).

Notable geochemical patterns included a gradual up section decrease in $\delta^{18}O$ values, which corresponds to the trend observed in the Kimmeridgian and Tithonian marine $\delta^{18}O$ record

(Padden et al., 2002). Also, vertical trends in MF $\delta^{13}C_{org}$ data appeared to correlate to the Kimmeridgian and Tithonian marine $\delta^{13}C_{org}$ record (Morgans-Bell et al., 2001), which suggests that Late Jurassic isotope trends previously interpreted as regional (Jenkyns et al., 2002) may have been global in scale.

As far as improving understanding of the MF, correlations between the continental and marine isotope records have important implications for establishing age constraints and interpreting deposition rates. Preservation of a global signal in MF stable isotope data suggests that global isotopic signals overpowered any localized paleoclimatic effects. Furthermore, a $\delta^{13}C_{carb}$ excursion near the Tidwell Member-Salt Wash Member contact previously interpreted as the result of local uranium mineralization, may, in fact, represent a shift in the isotopic composition of global CO_2, specifically, the mid *eudoxus* positive shift (Jenkyns et al., 2002). Further refinement of my correlation between MF stable isotopes and marine stable isotopes will require future attempts at establishing radiometric dates for the MF.

MORRISON FORMATION FOOD WEBS

In chapter six, I compiled paleobiological data from the literature to reconstruct food webs for the six biostratigraphic zones (biozones) in the MF. For each biostratigraphic zone, I created two versions of its food web: a whole-ecosystem (WE) web, which included all aquatic and terrestrial taxa, and a terrestrial subset (TS) web, which was restricted to terrestrial taxa and their resources. Using Network3D software, I generated ball and stick models of the food webs and performed multiple quantitative network analyses. Analyses for each food web included measurement of 21 basic node and network properties, degree distribution—the fractions of nodes with a given number of links to other nodes, and robustness—the fraction of primary

extinctions that, when added to its corresponding fraction of secondary extinctions, results in a sum ≥0.5.

Two major conclusions from this research were reached. First, the WE and TS foodwebs in biozone 1 are substantially different than the foodwebs in biozones 2–6. In particular, nine of the 21 biozone 1 WE properties fall outside two standard deviations (2σ) of the means of biozone 2–6 WE values, and ten of the 21 biozone 1 TS properties fall outside 2σ of the means of biozone 2–6 TS values. Biozone 1 robustness results were mostly different than those of the other MF biozones. Also, biozone 1 had lower robustness values compared to other biozones for deletions ordered by decreasing connectivity and random deletions, but had higher values than most other zones when nodes were deleted by increasing connectivity. Degree distributions were not significantly different for all biozones.

I interpreted the differences between biozone 1 properties and the other biozones as the result of a substantial change in food web structure at the biozone 1- biozone 2 boundary. This is significant because the boundary between biozones 1 and 2 is marked by biotic turnover in a large number of taxa. Also, biozone 1 has several unique taxa that go extinct at the boundary, whereas biozones 2–6 contain a large number of taxa that span multiple biozones. If biozone 1 is truly different from all subsequent biozones, then perhaps it represents biotic response to a substantial paleoecological or paleoenvironmental perturbation. Evidence for such a perturbation may be preserved in the rock record so future studies should focus on collecting data from biozone 1. Correlation between a climatic or environmental event and biotic turnover in the MF would be informative for understanding long-term impacts of anthropogenic climate change and environmental degradation on modern ecosystems. Stable isotope results from chapter five do suggest a shift in the global carbon budget near the beginning of MF deposition,

but whether this trend correlates to biozone 1 remains to be seen.

My second major conclusion was that foodwebs in biozones 2 through 6 were extremely stable and resistant to collapse based on consistent node and network properties, degree distributions, and robustness determinations. Robustness results showed that MF food webs were most resistant to collapse from loss of the most connected nodes, a pattern opposite of that observed in modern terrestrial ecosystems (Dunne et al., 2002). I attributed robustness results to the high interconnectedness of MF taxa, many of which exhibited nondiscriminatory feeding behavior (Van Valkenburgh and Molnar, 2002). Similar patterns, if documented from other dinosaur-dominated ecosystems, may indicate that robust foodwebs contributed to the success of dinosaurs during the Mesozoic.

In conclusion, considering all of the contents of this dissertation, regardless of scale, reveals important lessons for the future of ichnological and paleontological research. First, incorporation of new technologies into research projects can both enhance existing techniques and contribute novel methodologies that can, ultimately, increase our ability to retrodict past events and ecological relationships. In turn, better understanding of patterns in deep time will improve predictions of future global conditions. Second, approaches to research in the geosciences will always benefit from integrative, multidisciplinary studies, as exemplified by the conclusions I was able to draw by building upon the expertise and guidance from leaders in multiple fields during my time at the University of Kansas. The scale of a particular study does not limit the potential implications and applications of results derived from that study. Finally, in the time-honored tradition of a uniformitarian approach to earth science, modern-analog studies provide a valuable testing ground for theoretically formulated hypotheses. From beetle larvae burrows to elephant tracks to the Serengeti ecosystem, there is no substitute for direct

observations of the natural world. Continued innovation in the geosciences, tempered by traditional field- and laboratory-based experimentation and data collection, will ensure long-term prosperity and productivity in our shared fields of scientific inquiry.

REFERENCES

Demko, T.M., Currie, B.S., and Nicoll, K.A., 2004, Regional paleoclimatic and stratigraphic implications of paleosols and fluvial/overbank architecture in the Morrison Formation (Upper Jurassic), Western Interior, USA: Sedimentary Geology, v. 167, p. 115–135.

Dunne, J.A., Williams, R.J., and Martinez, N.D., 2002, Network structure and robustness of marine food webs: Marine Ecology Progress Series, v. 273, p. 291-302.

Hasiotis, S.T., 2004, Reconnaissance of Upper Jurassic Morrison Formation ichnofossils, Rocky Mountain region, USA: paleoenvironmental, stratigraphic, and paleoclimatic significance of terrestrial and freshwater ichnocoenoses: Sedimentary Geology, v. 167, p. 177–268.

Jenkyns, H.C., Jones, C.E., Gröcke, D.R., Hesselbo, S.P., and Parkinson, D.N., 2002, Chemostratigraphy of the Jurassic system: applications, limitations and implications for palaeoceanography: Journal of the Geological Society, London, v. 159, p. 351–378.

Morgans-Bell, H.S., Coe, A.L., Hesselbo, S.P., Jenkyns, H.C., Weedon, G.P., Marshall, J.E.A., Tyson, R.V., and Williams, C.J., 2001, Integrated stratigraphy of the Kimmeridge Clay Formation (Upper Jurassic) based on exposures and boreholes in south Dorset, UK: Geological Magazine, v. 138, p. 511–539.

Padden, M., Weissert, H., Funk, H., Schneider, S., and Gansner, C., 2002, Late Jurassic lithological evolution and carbon-isotope stratigraphy of the western Tethys: Eclogae Geologicae Helvetiae, v. 95, p. 333–346.

Parrish, J.T., Peterson, F., and Turner, C.E., 2004, Jurassic “savannah”—plant taphonomy and climate of the Morrison Formation (Upper Jurassic, western USA): Sedimentary Geology, v. 167, p. 137–162.

Van Valkenburgh, B., and Molnar, R.E., 2002, Dinosaurian and mammalian predators compared: Paleobiology, v. 28, p. 527–543.

APPENDIX A: DERIVATION OF RELATIVE COMPACTNESS EQUATION

SA_s = surface area of a sphere
V_s = volume of a sphere
V = volume of an object, e.g., a burrow
SA = surface area of an object, e.g., a burrow
r = radius of a sphere

$V_s = (4/3)\pi r^3$
$SA_s = 4\pi r^2$

Solving for r:

$r = \sqrt[3]{V_s /(4\pi/3)}$

Substituting:
$SA_s = 4\pi\ (V_s /(4\pi/3))^{2/3}$

To compare the volume/surface area ratios of an object and a sphere:
$(V/SA) / (V_s/SA_s)$
$= V \cdot SA_s/SA \cdot V_s$

Relative compactness (RC) is the comparison of the volume/surface area ratio of an object and a sphere of equivalent volume:

For $V = V_s$:
$RC = V \cdot SA_s/SA \cdot V$
$= SA_s/SA$
$= SA_s \cdot SA^{-1}$

and

$A_s = 4\pi\ (V /(4\pi/3))^{2/3}$

Substituting and simplifying:
$RC = 4\pi\ (V/(4\pi/3))^{2/3} SA^{-1}$
$= 4\pi \cdot V^{2/3} \cdot 1/(4\pi/3)^{2/3} \cdot SA^{-1}$
$\approx V^{2/3} \cdot 4.84 \cdot SA^{-1}$

APPENDIX B: DATA USED IN REGRESSION ANALYSES

A	P	v	V	ρ_b	θ_v	M_ϕ	σ_ϕ	S_ϕ	K_ϕ	V_n
0	101.6	0.7	3402.3	1.57	9.4	2.35	1.50	1.14	6.79	89.5
0	94.5	0.7	2450.4	1.57	9.4	2.35	1.50	1.14	6.79	61.3
0	101.7	0.7	2266.7	1.55	13.0	2.35	1.50	1.14	6.79	58.1
0	106.8	0.7	361.3	1.55	13.0	2.35	1.50	1.14	6.79	9.0
0	102.3	0.7	3381.1	1.48	9.5	2.35	1.50	1.14	6.79	82.5
0	83.6	0.7	1847.3	1.55	10.5	2.35	1.50	1.14	6.79	44.0
0	89.6	0.7	3859.4	1.50	11.5	2.35	1.50	1.14	6.79	91.9
0	91.0	0.7	3392.9	1.50	11.5	2.35	1.50	1.14	6.79	84.8
0	96.5	0.7	4778.4	1.53	12.3	2.35	1.50	1.14	6.79	122.5
0	94.5	0.7	3267.3	1.53	12.3	2.35	1.50	1.14	6.79	81.7
0	95.6	0.0	7208.3	1.17	5.7	4.91	1.47	0.81	2.96	175.8
0	88.9	0.7	2401.4	1.62	18.1	2.35	1.50	1.14	6.79	57.2
7	81.8	0.0	2052.7	1.62	18.1	2.35	1.50	1.14	6.79	46.7
7	85.6	0.7	2137.5	1.59	17.6	2.35	1.50	1.14	6.79	50.9
7	115.1	0.7	1781.3	1.56	19.1	2.35	1.50	1.14	6.79	49.5
7	90.7	0.0	2136.3	1.59	17.6	2.35	1.50	1.14	6.79	53.4
7	133.2		1710.6	1.56	19.1	2.35	1.50	1.14	6.79	51.8
7	91.1	0.7	2176.8	1.55	18.3	2.35	1.50	1.14	6.79	53.1
7	90.7	0.7	3518.6	1.59	17.4	2.35	1.50	1.14	6.79	88.0
7	125.9	0.7	995.3	1.59	17.4	2.35	1.50	1.14	6.79	27.6
7	93.0	0.7	1347.7	1.59	17.4	2.35	1.50	1.14	6.79	34.6
7	100.5	0.7	1360.9	1.56	21.1	2.35	1.50	1.14	6.79	35.8
7	111.9	0.7	2850.1	1.56	21.1	2.35	1.50	1.14	6.79	79.2
72	84.9	0.7	1400.5	1.62	18.9	1.29	1.00	1.33	13.85	32.6
72	91.2	0.7	1112.5	1.61	21.5	1.29	1.00	1.33	13.85	25.9
72	92.2	0.7	1217.2	1.73	16.5	1.29	1.00	1.33	13.85	29.7
72	94.7	0.8	1668.3	1.65	19.3	1.29	1.00	1.33	13.85	38.8
72		0.8				1.29	1.00	1.33	13.85	
72	91.2	0.8	455.5	1.62	20.9	1.29	1.00	1.33	13.85	11.4
72	84.9	0.8	1860.8	1.62	18.7	1.29	1.00	1.33	13.85	43.3
72	89.0	0.8	840.5	1.61	16.9	1.29	1.00	1.33	13.85	20.5
72	82.0	0.8	2938.2	1.52	19.9	1.29	1.00	1.33	13.85	68.3
72	86.9	0.7	1339.3	1.46	18.2	1.29	1.00	1.33	13.85	31.9
72		0.7				1.29	1.00	1.33	13.85	
72	94.5	0.7	1231.5	1.52	19.9	1.29	1.00	1.33	13.85	30.8
72	90.0	0.7	1570.2	1.61	12.1	1.29	1.00	1.33	13.85	37.4
72	86.9	0.7	1387.1	1.59	12.2	1.29	1.00	1.33	13.85	33.0
72	84.9	0.7	881.5	1.68	12.6	1.29	1.00	1.33	13.85	20.5
72	91.2	0.7	1093.3	1.64	12.6	1.29	1.00	1.33	13.85	27.3
72	108.9	0.7	1164.0	1.64	14.7	1.29	1.00	1.33	13.85	29.8
72	104.4	0.7	796.4	1.64	14.7	1.29	1.00	1.33	13.85	20.4
72	86.0	0.7	1497.4	1.66	16.3	1.29	1.00	1.33	13.85	36.5
72	82.0	0.7	2502.5	1.72	18.5	1.29	1.00	1.33	13.85	58.2

A	P	v	V	ρ_b	θ_v	M_ϕ	σ_ϕ	S_ϕ	K_ϕ	V_n
72	97.3	0.0	3744.4	1.67	18.1	1.29	1.00	1.33	13.85	91.3
72	77.4	0.0	1906.3	1.67	18.1	1.29	1.00	1.33	13.85	46.5
72	100.7	0.0	1820.9	1.67	18.1	1.29	1.00	1.33	13.85	50.6
72	85.4	0.7	2146.0	1.62	20.9	1.29	1.00	1.33	13.85	48.8
72	92.9	0.7	1629.5	1.62	18.7	1.29	1.00	1.33	13.85	38.8
72	85.8	0.7	1801.7	1.52	19.9	1.29	1.00	1.33	13.85	41.9
72	79.5	0.7	1753.8	1.54	15.6	1.29	1.00	1.33	13.85	39.9
72	87.9	0.0	3084.3	1.58	15.8	1.29	1.00	1.33	13.85	73.4
72	84.3	0.0	1560.3	1.57	13.5	1.29	1.00	1.33	13.85	36.3
72	81.4	0.0	3427.9	1.63	13.7	1.29	1.00	1.33	13.85	79.7
72	84.3	0.7	3026.0	1.58	13.6	1.29	1.00	1.33	13.85	70.4
72	89.5	0.7	2734.3	1.70	9.2	1.29	1.00	1.33	13.85	65.1
72	87.4	0.7	1978.7	1.61	9.6	1.29	1.00	1.33	13.85	46.0
72	86.3	0.7	2955.6	1.57	10.0	1.29	1.00	1.33	13.85	70.4
72	84.3	0.7	1834.5	1.60	11.0	1.29	1.00	1.33	13.85	42.7
53	89.1	0.7	653.1	1.70	15.3	1.29	1.00	1.33	13.85	14.8
53		0.7				1.29	1.00	1.33	13.85	
53	87.1	0.9	1431.4	1.66	16.5	1.29	1.00	1.33	13.85	31.8
53		0.9				1.29	1.00	1.33	13.85	
53	82.9	0.9	1803.9	1.62	16.6	1.29	1.00	1.33	13.85	41.0
53	84.9	0.9	783.5	1.65	13.7	1.29	1.00	1.33	13.85	18.2
53	80.2	0.9	829.4	1.67	14.9	1.29	1.00	1.33	13.85	18.8
53	86.9	0.9	765.3	1.66	15.3	1.29	1.00	1.33	13.85	18.2
53	82.9	0.8	1803.9	1.61	13.8	1.29	1.00	1.33	13.85	41.0
53	86.9	0.8	1626.2	1.61	12.9	1.29	1.00	1.33	13.85	38.7
53	89.0	0.8	1307.4	1.65	11.1	1.29	1.00	1.33	13.85	31.9
53	92.2	0.8	811.5	1.44	11.6	1.29	1.00	1.33	13.85	19.8
53	86.9	0.8	1339.3	1.60	10.9	1.29	1.00	1.33	13.85	31.9
53	84.9	0.8	979.4	1.66	11.6	1.29	1.00	1.33	13.85	22.8
53		0.8				1.29	1.00	1.33	13.85	
4	78.4	0.7	5301.4	1.56	4.8	1.29	1.00	1.33	13.85	117.8
4		0.7		1.57	8.5	1.29	1.00	1.33	13.85	
4	77.6	0.8	4285.1	1.61	8.0	1.29	1.00	1.33	13.85	97.4
4	80.2	0.8	3110.2	1.59	8.3	1.29	1.00	1.33	13.85	70.7
4		0.8		1.56	6.2	1.29	1.00	1.33	13.85	
4		0.8		1.57	9.6	1.29	1.00	1.33	13.85	
4	84.9	0.8	3134.1	1.57	14.8	1.29	1.00	1.33	13.85	72.9
4	91.2	0.5	2733.2	1.61	11.7	1.29	1.00	1.33	13.85	68.3
4	75.6	0.7	3298.7	1.57	8.5	1.29	1.00	1.33	13.85	82.5
4	78.4	0.8	3180.9	1.57	7.9	1.29	1.00	1.33	13.85	70.7
4		0.8		1.61	8.2	1.29	1.00	1.33	13.85	
4		0.8		1.57	8.4	1.29	1.00	1.33	13.85	
4		0.8		1.58	5.7	1.29	1.00	1.33	13.85	
4	77.6	0.8	3428.1	1.62	15.5	1.29	1.00	1.33	13.85	77.9
4	103.5	0.7	7351.3	1.62	6.1	1.29	1.00	1.33	13.85	183.8

A	P	v	V	ρ_b	θ_v	M_ϕ	σ_ϕ	S_ϕ	K_ϕ	V_n
0	167.0	0.8	28902.7	1.49	5.3	1.29	1.00	1.33	13.85	722.6
0	167.0	0.8	21362.8	1.53	3.8	1.29	1.00	1.33	13.85	534.1
0	167.0	0.8	27646.0	1.45	4.9	1.29	1.00	1.33	13.85	691.2
0	167.0	0.8	23876.1	1.48	4.5	1.29	1.00	1.33	13.85	596.9
0	167.0	0.8	36442.5	1.44	6.6	1.29	1.00	1.33	13.85	911.1
0	167.0	0.8	21362.8	1.48	6.1	1.29	1.00	1.33	13.85	534.1
0	167.0	0.8	25132.7	1.48	6.6	1.29	1.00	1.33	13.85	628.3
0	167.0	0.8	26389.4	1.52	6.6	1.29	1.00	1.33	13.85	659.7
0	167.0	0.8	26389.4	1.45	5.4	1.29	1.00	1.33	13.85	659.7
0	167.0	0.8	25132.7	1.44	7.2	1.29	1.00	1.33	13.85	628.3
0	167.0	0.8	23876.1	1.43	6.8	1.29	1.00	1.33	13.85	596.9
0	167.0	0.8	25132.7	1.48	4.4	1.29	1.00	1.33	13.85	628.3
0		0.8	0.0	1.44	4.9	1.29	1.00	1.33	13.85	
0		0.8	0.0	1.45	6.5	1.29	1.00	1.33	13.85	
0	167.0	0.8		1.43	6.1	1.29	1.00	1.33	13.85	
25	89.6	0.0	8619.4	1.39	8.7	2.35	1.50	1.14	6.79	205.2
25		1.0		1.47	11.3	2.35	1.50	1.14	6.79	
25	99.4	1.0	6375.9	1.60	10.6	2.35	1.50	1.14	6.79	155.5
25	88.8	1.0	4173.3	1.53	9.6	2.35	1.50	1.14	6.79	101.8
25	119.8	1.0	3944.7	1.45	10.0	2.35	1.50	1.14	6.79	
25	90.0	1.0	5231.7	1.45	10.0	2.35	1.50	1.14	6.79	134.1
25	72.2	0.0	4058.9	1.40	10.5	2.35	1.50	1.14	6.79	101.5
25	81.6	0.0	4539.0	1.40	10.5	2.35	1.50	1.14	6.79	105.6
25	96.5	0.0	6570.2	1.40	10.5	2.35	1.50	1.14	6.79	
25	101.7	0.0	2380.0	1.40	10.5	2.35	1.50	1.14	6.79	61.0
94	99.0	0.7	4134.3	1.38	18.2	2.88	1.96	0.83	2.52	103.4
94	81.8	0.7	4230.5	1.45	19.3	2.97	1.94	0.79	2.28	100.7
94	73.0	0.7	2924.8	1.39	18.3	3.35	2.31	0.55	0.41	71.3
94	81.8	0.9	3874.3	1.44	22.4	4.44	2.73	0.15	-1.07	92.2
94	64.4	0.9	5068.5	1.58	24.2	3.86	2.74	0.23	-0.90	117.9

APPENDIX C: GPS DATA FOR TRACE FOSSILS IN COYOTE BASIN

Appendix C-1. GPS data for trace fossils. Trace types: 1 = rhizolith, 2 = *Planolites*, 3 = cf. *Scolicia*, 4 = cf. *Steinichnus*, 5 = *Cochlichnus*, 6 = cf. *Ancorichnus*, 7 = cf. *Cylindrichum*, 8 = cf. *Macanopsis*, 9 = cf. *Termitichnus*, 10 = cf. *Celliforma*, 11 = cf. *Camborygma*, 12 = Y-shaped burrows, 13 = cf. *Arenicolites*, 14 = clam traces, 15 = cf. *Kouphichnium*, 16 = cf. *Hatcherichnus*, 17 = sauropod tracks, 18 = tridactyl tracks, 19 = vertebrate swim traces. Layers: 2 = base of lower sheet sandstone, 3 = lower sheet sandstone, 4 = base of upper sheet sandstone, 5 = upper sheet sandstone. Latitude and longitude are in decimal degrees (DD).

Trace Type	Layer	Latitude (DD)		Longitude (DD)	
19	4	44.656750	N	107.843528	W
2	5	44.656750	N	107.843528	W
18	4	44.656889	N	107.843472	W
18	4	44.656889	N	107.843472	W
18	4	44.656722	N	107.843500	W
18	5	44.656722	N	107.843500	W
18	4	44.656889	N	107.843472	W
7	5	44.656806	N	107.843444	W
7	5	44.656583	N	107.843639	W
2	5	44.656722	N	107.843417	W
17	4	44.656583	N	107.843417	W
17	4	44.656528	N	107.843694	W
18	5	44.656528	N	107.843667	W
4	4	44.656917	N	107.843667	W
2	5	44.656722	N	107.843722	W
7	5	44.656667	N	107.843611	W
4	4	44.656667	N	107.843611	W
18	4	44.656528	N	107.843528	W
4	4	44.656528	N	107.843528	W
8	5	44.656806	N	107.843806	W
7	5	44.656806	N	107.843806	W
4	4	44.656778	N	107.843778	W
10	5	44.656778	N	107.843722	W
2	5	44.656861	N	107.843694	W
4	4	44.656667	N	107.843667	W
17	4	44.656750	N	107.843750	W
4	4	44.656750	N	107.843750	W
7	5	44.656750	N	107.843750	W
4	4	44.656778	N	107.843722	W
2	5	44.656750	N	107.843750	W
18	4	44.656722	N	107.843806	W
2	4	44.656306	N	107.844000	W
18	4	44.656722	N	107.843639	W
4	4	44.656500	N	107.843806	W
14	4	44.656500	N	107.843806	W

Trace Type	Layer	Latitude (DD)		Longitude (DD)	
18	4	44.656611	N	107.843722	W
8	5	44.656556	N	107.843750	W
17	4	44.656611	N	107.843778	W
17	4	44.656611	N	107.843889	W
2	5	44.656722	N	107.843556	W
2	5	44.656722	N	107.843556	W
2	5	44.656722	N	107.843806	W
4	4	44.656806	N	107.843833	W
14	4	44.656806	N	107.843833	W
4	4	44.656778	N	107.843972	W
2	5	44.656778	N	107.843972	W
4	4	44.656639	N	107.843944	W
14	4	44.656639	N	107.843944	W
4	4	44.656722	N	107.843500	W
2	5	44.656722	N	107.843500	W
7	5	44.656722	N	107.843500	W
18	4	44.656450	N	107.845533	W
18	4	44.655500	N	107.845300	W
18	4	44.655500	N	107.845300	W
18	4	44.656317	N	107.845417	W
18	4	44.656400	N	107.845517	W
19		44.654650	N	107.842883	W
18	4	44.656133	N	107.845633	W
16	4	44.656317	N	107.845367	W
17	4	44.656300	N	107.845467	W
18	4	44.656417	N	107.845350	W
5	4	44.656333	N	107.845350	W
7	5	44.656317	N	107.845417	W
7	5	44.656317	N	107.845417	W
18	4	44.656233	N	107.845300	W
14	4	44.656233	N	107.845300	W
18	4	44.656383	N	107.845167	W
19	4	44.656417	N	107.845133	W
18	4	44.656200	N	107.845417	W
17	4	44.656250	N	107.845483	W
17	4	44.656300	N	107.845267	W
2	5	44.656300	N	107.845267	W
7	5	44.656306	N	107.844694	W
17	4	44.656194	N	107.844694	W
17		44.656250	N	107.844806	W
19	3	44.656444	N	107.844917	W
9	3	44.656444	N	107.844917	W
9	3	44.656444	N	107.844917	W
7	3	44.656444	N	107.844917	W
18	3	44.656250	N	107.844750	W

Trace Type	Layer	Latitude (DD)		Longitude (DD)	
18	3	44.656250	N	107.844556	W
2	3	44.656194	N	107.844806	W
2	3	44.656361	N	107.844833	W
9	3	44.656333	N	107.844806	W
7	3	44.656333	N	107.844806	W
9	3	44.656333	N	107.844806	W
9	3	44.656333	N	107.844806	W
9	3	44.656333	N	107.844806	W
9	3	44.656333	N	107.844806	W
9	3				
4	2	44.656306	N	107.844722	W
2	3	44.656417	N	107.844722	W
19	2	44.656417	N	107.844722	W
2	3	44.656417	N	107.844722	W
2	5	44.656194	N	107.844639	W
7	5	44.656250	N	107.844583	W
18	5	44.656250	N	107.844639	W
2	5	44.656250	N	107.844639	W
7	5	44.656250	N	107.844639	W
7	5	44.656278	N	107.844528	W
4	5	44.656167	N	107.844500	W
6	5	44.656167	N	107.844500	W
18	4	44.656194	N	107.844556	W
18	4	44.655306	N	107.844833	W
18	4	44.655278	N	107.844889	W
2	5	44.654528	N	107.845000	W
7	5	44.656333	N	107.844528	W
7	3	44.655833	N	107.844444	W
7	3	44.655917	N	107.844556	W
1	3	44.655917	N	107.844556	W
9	3	44.656000	N	107.844417	W
7	3	44.656000	N	107.844417	W
17	4	44.656278	N	107.844306	W
7	5	44.656278	N	107.844306	W
17	4	44.654750	N	107.845361	W
4	4	44.654750	N	107.845361	W
4	4	44.656306	N	107.844361	W
4	4	44.656306	N	107.844361	W
17	4	44.655750	N	107.844222	W
2	5	44.655333	N	107.844417	W
7	5	44.655333	N	107.844417	W
1	5	44.655333	N	107.844417	W
14	4	44.655361	N	107.844528	W
18	5	44.655667	N	107.844361	W

Trace Type	Layer	Latitude (DD)		Longitude (DD)	
4	5	44.655667	N	107.844361	W
18	4	44.655583	N	107.844444	W
4	4	44.655583	N	107.844444	W
17	4	44.655583	N	107.844444	W
18	4	44.655611	N	107.844639	W
2	5	44.655611	N	107.844639	W
4	4	44.655611	N	107.844639	W
4	4	44.655611	N	107.844639	W
4	4	44.655556	N	107.844528	W
5	4	44.655556	N	107.844528	W
17	4	44.654944	N	107.844278	W
17	4	44.655139	N	107.844278	W
4	4	44.655139	N	107.844278	W
4	4	44.654972	N	107.844222	W
17	4	44.654833	N	107.844306	W
17	4	44.655472	N	107.843917	W
9	3	44.655222	N	107.844000	W
17	3	44.655222	N	107.844000	W
14	4	44.655139	N	107.844333	W
17	4	44.655139	N	107.844278	W
4	4	44.655500	N	107.843639	W
2		44.655083	N	107.843944	W
2	5	44.655083	N	107.843917	W
18		44.655194	N	107.843889	W
14	4	44.654889	N	107.844028	W
4	4	44.654889	N	107.844028	W
5	4	44.654889	N	107.844028	W
14	4	44.654861	N	107.843972	W
4	4	44.654861	N	107.843972	W
5	4	44.654861	N	107.843972	W
4	4	44.654861	N	107.843972	W
4	4	44.654861	N	107.843972	W
18	4	44.655444	N	107.843778	W
14	4	44.654917	N	107.844028	W
4	4	44.654917	N	107.844028	W
2	5	44.654861	N	107.843944	W
5	4	44.654861	N	107.843944	W
2	4	44.654861	N	107.843944	W
4	4	44.654861	N	107.843944	W
13	4	44.654861	N	107.843944	W
14	4	44.654889	N	107.843861	W
2	4	44.654889	N	107.843861	W
4	4	44.654889	N	107.843861	W
13	4	44.654889	N	107.843861	W
19	4	44.654972	N	107.844083	W

Trace Type	Layer	Latitude (DD)		Longitude (DD)	
4	4	44.654972	N	107.844083	W
5	4	44.654917	N	107.843972	W
4	4	44.654917	N	107.843972	W
14	4	44.654917	N	107.843972	W
4	4	44.654750	N	107.844222	W
14	4	44.654750	N	107.844222	W
13	4	44.654861	N	107.844139	W
15	4	44.654861	N	107.844139	W
19	4	44.654889	N	107.844028	W
14	4	44.654889	N	107.844028	W
4	4	44.654889	N	107.844028	W
13	4	44.654889	N	107.844028	W
18	4	44.655500	N	107.843806	W
18	4	44.654944	N	107.843889	W
4	4	44.654944	N	107.843889	W
14	4	44.654639	N	107.844028	W
2	5	44.654639	N	107.844028	W
13	4	44.654639	N	107.844028	W
17	3	44.654694	N	107.844056	W
4	4	44.654944	N	107.844083	W
14	4	44.654944	N	107.844083	W
18	5	44.654833	N	107.843944	W
17	4	44.655389	N	107.843667	W
4	4	44.655222	N	107.843750	W
14	4	44.655222	N	107.843750	W
4	2	44.655056	N	107.844056	W
2	3	44.655167	N	107.844000	W
2	3	44.654528	N	107.843917	W
13	2	44.654528	N	107.843917	W
17	4	44.654528	N	107.843278	W
3	4	44.654444	N	107.843167	W
14	2	44.654167	N	107.845000	W
14	2	44.654167	N	107.845000	W
20	2	44.654167	N	107.845000	W
2	3	44.654167	N	107.845000	W
5	2	44.654167	N	107.845000	W
13	5	44.654194	N	107.845167	W
2	5	44.653917	N	107.845278	W
2	5	44.653972	N	107.845222	W
2	5	44.654028	N	107.845556	W
2	4	44.654222	N	107.845417	W
13	4	44.654222	N	107.845417	W
17	4	44.654861	N	107.845222	W
17	4	44.655028	N	107.845278	W
17	4	44.654889	N	107.845194	W

Trace Type	Layer	Latitude (DD)		Longitude (DD)	
17	4	44.655000	N	107.845194	W
2	5	44.655028	N	107.845361	W
17	4	44.655056	N	107.845333	W
17	4	44.655056	N	107.845417	W
17	4	44.654833	N	107.845444	W
18	4	44.654861	N	107.845472	W
17	4	44.654556	N	107.845361	W
17	4	44.654889	N	107.845222	W
17	4	44.654861	N	107.845333	W
18	4	44.654889	N	107.845222	W
17	4	44.654861	N	107.845222	W
6	3	44.638889	N	107.846222	W
7	3	44.638889	N	107.846222	W
2	5	44.655556	N	107.845917	W
2	5	44.655556	N	107.845917	W
6	5	44.655556	N	107.845917	W
5	3	44.653944	N	107.847167	W
3	3	44.653944	N	107.847167	W
18	3	44.653944	N	107.847167	W
18	2	44.654083	N	107.846167	W
14	2	44.654000	N	107.846194	W
2	3	44.654000	N	107.846194	W
4	2	44.653944	N	107.847167	W
17	4	44.654000	N	107.847167	W
2	5	44.654000	N	107.847167	W
4	2	44.653806	N	107.846972	W
5	3	44.653806	N	107.846972	W
5	2	44.653944	N	107.846861	W
5	2	44.653667	N	107.846528	W
13	2	44.654139	N	107.846417	W
5	4	44.653722	N	107.848806	W
2	5	44.653694	N	107.848750	W
7	5	44.653694	N	107.848750	W
6	5	44.653694	N	107.848750	W
4	4	44.653833	N	107.848806	W
2	5	44.653833	N	107.848806	W
17	4	44.654778	N	107.850444	W
4	4	44.654778	N	107.850444	W
2	5	44.654250	N	107.845972	W
2	5	44.653444	N	107.845667	W
2	5	44.653250	N	107.845611	W
18	4	44.653250	N	107.845611	W
18	4	44.653389	N	107.845778	W
17	4	44.653444	N	107.845556	W

APPENDIX D: SOIL MOISTURE AND GEOCHEMICAL DATA FROM GARFIELD COUNTY, UTAH

Key: SP = stratigraphic position in meters, CCE = calcium carbonate equivalent, CCD = calcite:dolomite ratio, CST = carbonate sample type, 1 = bulk dolomite, 2 = bulk calcite, 3 = pedogenic calcite nodule, 4 = bulk sample of mixed calcite and dolomite, 5 = bulk carbonate sample where calcite:dolomite ratio is unknown, SDI = soil drainage index.

Sample ID	SP	CCE	CCD	$\delta^{13}C_{carb}$	$\delta^{18}O$	CST	$\delta^{13}C_{org}$	TOC	SDI
T-01	0.0	0.09					-28.06	0.05	
T-02	0.5	0.03	-0.05	-3.87	-12.95	1	-27.33	0.02	
T-03	1.0	0.06					-27.37	0.02	
T-04	1.5	0.10					-27.02	0.02	
T-05	2.0	0.25	0.38	-3.94	-11.61	4	-27.35	0.03	
T-06	2.5	0.22	0.72	-4.01	-11.97	4	-26.60	0.05	
T-07	3.0	0.23	0.86	-5.27	-14.18	4	-26.10	0.04	
T-08	3.5	0.23	0.50				-24.33	0.11	
T-09	4.0	0.62	0.52				-22.29	0.19	
T-10	4.5	0.30	0.88				-25.73	0.14	
T-11	5.0	0.43	-0.25				-23.25	0.14	
T-12	5.5		0.58				-24.15	0.08	
T-12DUP	5.5								
T-13	6.0	0.32	0.15				-25.22	0.11	
T-13B	6.1								
T-14	6.5								
T-14DUP	6.5	0.02					-24.67	0.04	
T-14B	6.7						-24.94	0.05	
T-15	7.0	0.16		-3.55	-14.51	4	-25.51	0.04	
T-16	7.5	0.04					-26.82	0.05	
T-17	8.0	0.26	0.76	-5.28	-10.75	4	-24.25	0.05	
T-18	8.5	0.33	0.64	-2.91	-12.10	4	-25.38	0.04	
T-19	9.0	0.32	0.95				-25.72	0.05	
T-20	9.5	0.02					-23.93	0.06	
T-21	10.0	0.15	0.87	-6.64	-10.52	4	-25.71	0.05	4.0
T-22	10.5	0.06					-26.12	0.04	
T-23	11.0	0.13	-0.02	-3.00	-9.27	1	-21.90	0.22	
T-24	11.5	0.24	0.86				-25.46	0.10	
T-25	12.0						-24.32	0.05	
T-26	12.5	0.35					-23.38	0.08	
SW-01	13.0	0.00					-20.78	0.09	
SW-02	13.5	0.00					-26.28	0.02	
SW-03	14.0	0.05					-26.36	0.02	
SW-04	14.5	0.07					-24.14	0.05	

Sample ID	SP	CCE	CCD	$\delta^{13}C_{carb}$	$\delta^{18}O$	CST	$\delta^{13}C_{org}$	TOC	SDI
SW-05	15.0	0.09					-26.44	0.04	
SW-06	15.5	0.07					-27.66	0.03	
SW-07	16.0	0.04					-26.13	0.02	
SW-07B	16.4						-21.30	0.24	
SW-08	16.5	0.16	0.77	-2.54	-10.83	4	-25.67	0.03	
SW-09	17.0	0.07					-27.36	0.02	
SW-10	17.5	0.03	0.47	-1.68	-9.39	4	-26.48	0.03	
SW-11	18.0	0.16	1.06	-0.35	-7.29	2	-25.15	0.05	
SW-11B	18.1						-22.12	0.11	
SW-12	18.5	0.04					-26.93	0.03	
SW-13	19.0	0.33	0.87				-23.39	0.11	
SW-14	19.5	0.28	0.77				-23.92	0.10	
SW-15	20.0	0.06					-26.77	0.02	
SW-15B	20.2								
SW-16	20.5	0.01	1.00	-2.72	-11.15	2	-28.16	0.04	
SW-17	21.0	0.07					-26.44	0.02	
SW-18	21.5	0.12	0.75	-3.02	-12.69	4	-26.76	0.02	
SW-19	22.0	0.18	0.72	-0.55	-9.08	4	-28.89	0.04	
SW-20	22.5	0.11	0.06	-1.45	-10.06	4	-25.58	0.04	
SW-21	23.0	0.10	0.04				-27.69	0.02	
SW-22	23.5	0.13	0.30				-29.80	0.03	
SW-23	24.0	0.06					-27.77	0.02	
	24.1								3.0
	24.2								4.0
SW-24	24.5	0.27	0.91	-3.88	-12.47	4	-26.97	0.02	
	24.7								4.0
SW-25	25.0	0.24	0.91	-3.57	-9.13	4	-25.89	0.04	4.0
	25.4								4.0
SW-26	25.5	0.00					-27.49	0.03	4.0
	25.8								3.0
SW-27	26.0	0.04					-26.53	0.02	
SW-28	26.5	0.03		-0.45	-6.31	4	-27.20	0.03	
	28.3								4.0
SW-29	27.0	0.04		-1.02	-8.51	4	-27.86	0.02	
SW-30	27.5	0.05					-28.62	0.02	
SW-31	28.0	0.05					-28.76	0.02	
SW-32	28.5	0.06					-28.38	0.02	
SW-33	29.0	0.04		-0.90	-7.95	4	-26.77	0.03	
SW-34	29.5	0.00					-27.48	0.01	
SW-35	30.0	0.05					-29.37	0.02	
SW-36	30.5	0.23	0.47	-2.66	-7.07	4	-21.94	0.07	
	30.8								3.0

Sample ID	SP	CCE	CCD	$\delta^{13}C_{carb}$	$\delta^{18}O$	CST	$\delta^{13}C_{org}$	TOC	SDI
SW-37	31.0	0.23	0.07				-25.64	0.04	
SW-38	31.5	0.05		-2.29	-11.32	4	-28.55	0.02	
SW-39	32.0	0.05		-1.86	-10.09	4	-27.07	0.02	
SW-40BAD									
SW-40	32.5	0.14	0.78	-3.72	-12.12	4	-27.83	0.02	3.0
SW-41	33.0	0.40	0.95	-3.43	-9.73	4	-27.43	0.02	
SW-42	33.5	0.05					-27.43	0.03	4.0
	33.7								4.0
	33.9								4.0
SW-43	34.0	0.14	0.72	-3.87	-15.30	4	-27.27	0.01	
SW-44	34.5	0.07					-29.02	0.02	
SW-45	35.0	0.06					-28.71	0.02	
SW-46	35.5	0.18	1.07	-3.60	-8.96	2	-27.78	0.02	
SW-47	36.0	0.30	0.97	-4.52	-12.20	2	-29.30	0.02	3.0
SW-48	36.5	0.08		-2.27	-9.68	5	-29.37	0.02	
SW-49	37.0	0.05					-27.54	0.02	
SW-50	37.5	0.09					-28.00	0.02	
SW-51	38.0	0.09					-26.82	0.01	
SW-52	38.5	0.11	0.82				-28.72	0.02	
SW-53	39.0	0.35	1.00	-4.27	-9.70	2	-26.50	0.03	
SW-54	39.5	0.09					-29.04	0.02	
SW-55	40.0	0.07					-27.88	0.01	
SW-56	40.5	0.09					-25.87	0.03	
SW-57	41.0	0.09					-30.88	0.03	
	41.3								4.0
SW-58	41.5	0.22	0.99	-4.57	-12.12	2	-26.94	0.02	
	41.7								4.0
SW-59	42.0	0.32	0.99	-4.52	-10.97	2	-27.00	0.02	3.0
SW-60	42.5	0.32	1.01	-4.17	-10.15	2	-26.80	0.03	3.0
	42.9								4.0
SW-61	43.0	0.35	0.82				-26.07	0.05	
	43.1								2.0
SW-62	43.5	0.43	1.04	-4.54	-9.57	2	-27.85	0.02	
	43.7								3.0
SW-63	44.0	0.06		-2.76	-9.95	4	-27.82	0.02	
SW-64	44.5	0.04		-2.85	-10.29	4	-26.08	0.02	
	44.7								3.0
SW-65	45.0	0.06					-27.74	0.02	
	45.3								3.0
SW-66	45.5	0.00					-26.97	0.03	
	45.8								3.0
SW-67	46.0	0.00					-27.28	0.03	

Sample ID	SP	CCE	CCD	$\delta^{13}C_{carb}$	$\delta^{18}O$	CST	$\delta^{13}C_{org}$	TOC	SDI
	46.2								4.0
SW-68	46.5	0.06					-24.66	0.04	
SW-69	47.0	0.08		-4.49	-12.07	5	-27.06	0.01	
	47.4								3.0
SW-70	47.5	0.17	0.74	-4.66	-10.03	4	-26.57	0.03	
	47.8								3.0
SW-71	48.0	0.30	1.01	-4.34	-9.24	2	-27.46	0.02	
	48.1								3.0
	48.2								4.0
	48.4								3.0
	48.5								4.0
SW-72	48.5	0.17	0.92	-3.61	-11.98	4	-26.87	0.03	
SW-73	49.0	0.07					-30.21	0.03	
SW-74	49.5	0.07					-27.78	0.03	
SW-75	50.0	0.11	0.96	-4.49	-11.41	4	-28.15	0.02	
	50.3								3.5
SW-76	50.5	0.34	0.82	-3.82	-11.72	4	-27.17	0.03	4.0
	50.7								3.0
SW-77	51.0						-26.60	0.04	4.0
SW-78	51.5	0.21	0.84	-3.38	-11.90	4	-25.33	0.07	
SW-79	52.0	0.31	1.04	-4.38	-9.53	2	-27.16	0.02	
SW-80	52.5	0.10	0.83				-26.25	0.03	
SW-81	53.0	0.13	0.47	-3.91	-10.37	4	-27.89	0.02	
SW-82	53.5	0.14	1.00	-2.30	-8.47	2	-25.52	0.03	
SW-83	54.0	0.13	0.75	-2.38	-8.26	4	-26.89	0.03	
SW-84	54.5	0.13	0.65	-2.16	-8.09	4	-28.51	0.04	
SW-85	55.0	0.12	0.81	-4.03	-9.75	4	-27.94	0.03	
SW-86	55.5	0.10	0.77	-3.27	-10.51	4	-26.67	0.03	
SW-87	56.0	0.10					-26.07	0.03	
SW-88	56.5	0.25	0.77	-4.89	-10.17	4	-26.05	0.03	
SW-89	57.0	0.12	0.82				-27.28	0.05	
SW-90	57.5	0.13	0.99				-27.74	0.07	
	57.7								4.0
SW-91	58.0	0.03	0.43	-4.64	-10.81	4	-26.84	0.04	
	58.4								4.0
SW-92	58.5	0.12	1.03				-27.83	0.06	
	58.7								3.0
SW-93	59.0	0.30	1.07				-26.64	0.07	
	59.3								4.0
SW-94	59.5	0.38	0.99	-5.13	-11.21	2	-26.22	0.03	3.0
	59.7								4.0
	59.8								3.0

Sample ID	SP	CCE	CCD	$\delta^{13}C_{carb}$	$\delta^{18}O$	CST	$\delta^{13}C_{org}$	TOC	SDI
SW-95	60.0	0.12	0.95				-26.85	0.04	
	60.3								4.0
SW-96	60.5	0.06					-25.84	0.05	
SW-97	61.0	0.12	0.93				-27.23	0.04	4.0
SW-98	61.5	0.32	1.06	-3.24	-9.39	2	-26.77	0.11	4.0
SW-98B	61.6	0.16	0.99						
	61.8								4.0
SW-99	62.0	0.32	0.97	-4.57	-9.35	2	-25.89	0.10	2.0
	62.1								3.0
	62.3								4.0
SW-100	62.5	0.27	1.05	-2.97	-7.76	2	-25.45	0.07	
	62.6								3.0
SW-101	63.0	0.22	0.96				-26.37	0.04	
	63.2								3.7
	63.4								3.7
SW-102	63.5	0.13	0.95	-3.09	-8.44	4	-26.16	0.06	1.5
SW-103	64.0	0.00					-28.02	0.04	
SW-103E	64.0								
SW-104	64.5	0.12	0.94	-5.13	-11.77	4	-26.43	0.03	
SW-104E	64.5								
SW-105	65.0		0.88	-5.19	-12.01	4	-25.84	0.03	
SW-106	65.5	0.08	0.93	-4.01	-8.78	4	-27.40	0.03	
SW-107	66.0	0.09		-3.15	-8.91	5	-28.19	0.04	
SW-108	66.5	0.09		-4.99	-10.08	5	-26.64	0.03	
SW-109	67.0	0.08					-27.46	0.02	
SW-110	67.5	0.23	0.91	-5.88	-9.55	4	-26.78	0.03	
SW-111	68.0	0.06					-27.50	0.02	
SW-112	68.5	0.08		-4.60	-9.94	5	-27.40	0.03	
SW-113	69.0	0.22	0.96	-5.88	-11.42	4	-28.04	0.02	3.0
SW-114	69.5	0.14	0.84	-5.49	-12.21	4	-27.67	0.03	
SW-115	70.0	0.04					-28.52	0.03	
SW-116	70.5	0.10					-27.03	0.03	
SW-117	71.0	0.07					-28.65	0.02	
SW-118	71.5	0.02					-27.45	0.04	
SW-119	72.0	0.03					-28.14	0.02	
SW-120	72.5	0.01					-27.55	0.03	
SW-121	73.0	0.00					-27.30	0.02	
SW-122	73.5	0.08					-26.63	0.04	
SW-123	74.0	0.29	0.79	-5.64	-9.48	4	-27.03	0.02	
SW-124	74.5	0.01					-27.48	0.04	
SW-125	75.0	0.06					-27.46	0.02	
SW-126	75.5	0.05					-27.91	0.04	

Sample ID	SP	CCE	CCD	$\delta^{13}C_{carb}$	$\delta^{18}O$	CST	$\delta^{13}C_{org}$	TOC	SDI
SW-127	76.0	0.00					-27.72	0.02	
SW-128	76.5	0.15	0.93	-5.95	-12.27	4	-27.01	0.03	
SW-129	77.0	0.04					-27.78	0.02	
SW-130	77.5	0.06		-4.63	-10.80	5	-27.06	0.04	
SW-131	78.0	0.14	0.81	-5.69	-10.34	4	-28.84	0.02	
SW-132	78.5	0.13	0.87	-5.62	-9.80	4	-27.54	0.04	
SW-133	79.0	0.06					-27.13	0.02	
SW-134	79.5	0.14	0.88				-27.22	0.04	
SW-135	80.0	0.14	0.87				-26.96	0.02	
SW-136	80.5	0.14	0.47				-26.98	0.05	
SW-137	81.0	0.04		-4.88	-11.60	5	-26.38	0.03	
SW-138	81.5	0.02					-27.36	0.05	
SW-139	82.0	0.03					-29.48	0.03	
SW-140	82.5	0.06					-28.23	0.04	
SW-141	83.0	0.07					-28.60	0.02	
SW-142	83.5	0.09					-28.58	0.05	
SW-142B	84.0								
SW-143	84.0	0.06					-27.32	0.03	
SW-144	84.5	0.02					-28.04	0.04	
SW-145	85.0	0.09					-26.94	0.03	
SW-146	85.5	0.11	0.78				-25.97	0.03	
SW-147	86.0	0.04					-27.35	0.02	
SW-148	86.5	0.10	0.74				-27.43	0.03	
SW-149	87.0	0.02					-27.96	0.03	
SW-150	87.5	0.03		-3.82	-10.93	5	-27.13	0.03	
SW-151	88.0	0.01					-26.66	0.02	
SW-152	88.5	0.04					-26.21	0.04	
SW-153	89.0	0.13	0.93				-28.30	0.01	
SW-154	89.5	0.12	0.78	-4.91	-9.80	4	-26.85	0.03	
SW-155	90.0	0.03					-26.74	0.02	
SW-156	90.5	0.02					-26.84	0.03	
SW-157	91.0	0.04		-4.60	-11.98	5	-27.13	0.02	3.7
SW-158	91.5	0.03					-26.50	0.03	
	91.6								3.0
	91.9								4.0
SW-159	92.0	0.09	0.81				-27.09	0.03	
	92.1								4.0
	92.2								3.0
	92.3								4.0
	92.4								3.0
SW-160	92.5	0.06	0.72				-27.22	0.05	4.0
	92.7								3.0

Sample ID	SP	CCE	CCD	$\delta^{13}C_{carb}$	$\delta^{18}O$	CST	$\delta^{13}C_{org}$	TOC	SDI
SW-162-0-6a	92.9			-6.63	-9.34	3			4.0
SW-162-0-6b	92.9			-6.71	-9.44	3			
SW-162-0-6c	92.9			-6.77	-9.72	3			
SW-162-0-6d	92.9			-6.77	-9.74	3			
SW-162-0-6e	92.9			-6.79	-9.64	3			
SW-161	93.0	0.02					-26.27	0.07	
	93.1								4.0
	93.2								3.0
	93.4								3.5
SW-162	93.5	0.10	0.80				-27.21	0.04	
SW-162-0-5	93.0								
SW-162-1	92.5								
SW-162-1-5	92.0								
SW-162-2	91.5								
SW-162-2-5	91.0								
SW-163	94.0	0.00					-25.98	0.07	
SW-164	94.5	0.09					-27.05	0.03	
SW-165	95.0	0.04					-27.41	0.03	
SW-166	95.5	0.14	0.86				-27.06	0.04	
SW-167	96.0	0.10	0.80				-28.17	0.03	
SW-168	96.5	0.07					-27.89	0.03	
SW-169	97.0	0.15	0.76				-27.27	0.04	
SW-170	97.5	0.08					-26.92	0.03	
SW-171	98.0	0.16	0.72				-26.50	0.03	
SW-172	98.5	0.01					-27.36	0.04	
SW-173	99.0	0.28	0.77				-27.96	0.04	
SW-174	99.5	0.06					-26.45	0.04	
SW-175	100.0	0.13	0.96				-27.51	0.03	
SW-176	100.5	0.02					-28.29	0.05	
SW-177	101.0	0.04					-28.32	0.03	
SW-178	101.5	0.07					-26.76	0.03	
SW-179	102.0	0.08					-27.55	0.04	
SW-180	102.5	0.01					-27.44	0.03	
SW-181	103.0	0.00					-27.33	0.03	
SW-182	103.5	0.00					-26.75	0.03	
SW-183	104.0	0.08					-26.60	0.03	
SW-184	104.5	0.08					-28.10	0.04	
SW-185	105.0	0.00					-27.13	0.04	
SW-186	105.5	0.00					-27.35	0.02	
SW-187	106.0	0.00					-27.11	0.03	
SW-188	106.5	0.19	0.86				-27.96	0.04	
SW-189	107.0	0.21	0.97	-5.26	-12.32	2	-26.66	0.06	

Sample ID	SP	CCE	CCD	$\delta^{13}C_{carb}$	$\delta^{18}O$	CST	$\delta^{13}C_{org}$	TOC	SDI
SW-190	107.5	0.16	0.94				-26.46	0.05	
SW-191	108.0	0.22	0.99	-4.97	-12.23	2	-26.37	0.06	
SW-192	108.5	0.22	0.93				-25.81	0.05	
SW-193	109.0	0.09	0.93				-27.40	0.05	
SW-194	109.5	0.09	0.96				-27.31	0.06	
SW-195	110.0	0.14	0.93				-28.03	0.05	
SW-196	110.5	0.05					-27.94	0.05	
SW-197	111.0	0.22	0.91				-26.60	0.05	
SW-198	111.5	0.03					-27.66	0.04	
SW-199	112.0	0.07					-28.11	0.04	
SW-200	112.5	0.25	0.96				-26.29	0.05	
SW-201	113.0	0.15	0.91				-27.11	0.04	
BB-01	118.5	0.00					-27.04	0.06	
BB-02	119.0						-26.86	0.06	
	119.3								1.0
BB-03	119.5	0.00					-27.55	0.09	3.5
	119.7								3.5
	119.9								4.0
BB-04	120.0	0.00					-27.92	0.10	
	120.3								4.0
BB-05	120.5	0.00					-27.40	0.08	
BB-06	121.0	0.00					-27.35	0.07	
BB-07	121.5	0.02					-26.38	0.03	
BB-08	122.0	0.00					-27.71	0.05	
	122.2								1.0
BB-09	122.5	0.00					-28.54	0.09	
	122.7								4.0
	122.9								3.5
BB-10	123.0	0.00					-28.39	0.07	4.0
BB-10-5	123.2								3.0
	123.4								3.0
BB-11	123.5						-28.19	0.11	
	123.7								3.0
BB-12	124.0	0.00					-28.88	0.09	3.5
BB-13	124.5						-27.25	0.09	4.0
	124.8								3.0
BB-14	125.0	0.00					-28.72	0.06	
	125.2								4.0
BB-15	125.5	0.00					-28.34	0.10	3.0
	125.7								2.0
BB-16	126.0	0.00					-27.05	0.03	3.0
BB-17	126.5						-27.34	0.04	

Sample ID	SP	CCE	CCD	$\delta^{13}C_{carb}$	$\delta^{18}O$	CST	$\delta^{13}C_{org}$	TOC	SDI
BB-18	127.0						-26.62	0.03	
BB-19	127.5	0.01					-26.81	0.03	
BB-20	128.0	0.00					-27.16	0.08	
BB-21B	128.2						-27.22	0.06	
BB-21	128.5	0.00					-27.55	0.05	
BB-22	129.0	0.00					-26.71	0.04	
BB-22B	129.4								
BB-23	129.5	0.00					-28.19	0.08	2.0
BB-24	130.0	0.00					-27.19	0.09	
	130.1								4.0
	130.3								4.0
BB-25	130.5	0.00					-26.71	0.11	3.0
	130.7								3.0
BB-26	131.0	0.00					-27.54	0.08	3.0
BB-27	131.5	0.00					-27.64	0.08	
	131.6								4.0
BB-28	132.0	0.00					-28.19	0.09	1.0
	132.2								2.0
	132.4								2.0
BB-29	132.5						-28.47	0.10	3.5
	132.7								3.0
	132.8								4.0
BB-30	133.0	0.00					-27.24	0.10	2.0
	133.1								2.0
BB-30-5	133.3						-26.64	0.07	
BB-31	133.5	0.02					-26.97	0.05	
BB-32	134.0	0.00					-26.89	0.05	
BB-33	134.5	0.00					-27.23	0.05	
BB-34	135.0	0.00					-26.50	0.04	
BB-35	135.5	0.01					-27.16	0.04	
BB-36	136.0	0.00					-26.86	0.05	
BB-37	136.5	0.00					-27.55	0.05	
BB-38	137.0	0.00					-27.35	0.05	
BB-39	137.5	0.05					-27.36	0.05	
BB-40	138.0	0.01					-27.01	0.05	
BB-41	138.5	0.00					-25.91	0.03	
BB-42E	139.0								
	139.3								4.0
BB-43E	139.5								
	139.7								3.0
BB-44E	140.0								
BB-42	139.0	0.03					-25.26	0.03	

Sample ID	SP	CCE	CCD	$\delta^{13}C_{carb}$	$\delta^{18}O$	CST	$\delta^{13}C_{org}$	TOC	SDI
BB-43	139.5	0.00					-26.23	0.04	
BB-44	140.0	0.00					-27.17	0.05	
	140.1								4.0
	140.4								3.0
BB-45	140.5	0.00					-27.06	0.07	
	140.7								4.0
BB-46	141.0	0.00					-25.25	0.06	
	141.2								2.0
BB-47	141.5	0.00					-26.50	0.05	
	141.7								4.0
	141.8								2.0
BB-48	142.0	0.00					-27.52	0.06	
	142.1								1.0
	142.4								4.0
BB-49	142.5	0.00					-25.81	0.07	1.0
	142.6								3.5
	142.8								1.0
BB-50	143.0	0.00					-26.15	0.10	3.5
	143.3								4.0
BB-51	143.5	0.00					-27.76	0.07	3.5
	143.6								1.0
	143.8								4.0
	143.9								1.0
BB-52	144.0	0.00					-26.69	0.07	
	144.1								3.0
BB-53	144.5	0.00					-25.50	0.06	
	144.6								2.5
	144.8								3.0
BB-54	145.0	0.00					-26.81	0.05	3.5
	145.3								1.0
BB-55	145.5	0.00					-25.64	0.05	
	145.6								3.0
	145.8								3.0
	145.9								1.0
BB-56	146.0	0.00					-25.75	0.06	
	146.1								3.5
	146.2								4.0
	146.4								3.5
BB-57	146.5	0.00					-25.54	0.06	
	146.6								4.0
	146.8								2.5
	146.9								3.0

Sample ID	SP	CCE	CCD	$\delta^{13}C_{carb}$	$\delta^{18}O$	CST	$\delta^{13}C_{org}$	TOC	SDI
BB-58	147.0	0.00					-25.80	0.04	
	147.3								1.0
	147.4								4.0
BB-59	147.5	0.00					-26.80	0.04	
BB-59A	147.6						-25.98	0.03	2.0
	147.7								1.0
BB-60	148.0	0.00					-26.97	0.04	2.0
BB-61	148.5	0.00					-26.47	0.04	2.5
	148.6								2.0
	148.8								2.5
BB-62	149.0	0.00					-27.23	0.04	1.0
	149.1								4.0
	149.2								1.0
	149.4								4.0
BB-63	149.5	0.00					-26.34	0.04	3.0
	149.9								3.0
BB-64	150.0	0.00					-25.95	0.05	
	150.2								3.0
	150.3								3.0
BB-65	150.5						-27.58	0.07	3.0
	150.7								3.0
	150.8								4.0
BB-66	151.0	0.00					-25.98	0.05	3.0
	151.2								1.0
	151.4								3.0
BB-67	151.5	0.00					-27.21	0.04	3.5
	151.8								2.0
	151.9								3.0
BB-68	152.0	0.00					-26.31	0.04	
	152.1								2.0
	152.4								3.5
BB-69	152.5	0.00					-25.82	0.05	
	152.6								3.0
	152.8								2.5
	152.9								3.5
BB-70	153.0	0.00					-27.30	0.04	
	153.2								3.0
	153.4								3.0
BB-71	153.5	0.00					-26.15	0.04	
	153.7								2.0
BB-72	154.0	0.00					-25.96	0.06	
	154.2								2.0

Sample ID	SP	CCE	CCD	$\delta^{13}C_{carb}$	$\delta^{18}O$	CST	$\delta^{13}C_{org}$	TOC	SDI
BB-73	154.5	0.00					-25.86	0.05	
	154.7								1.0
BB-74	155.0	0.00					-25.12	0.05	
	155.3								2.5
BB-75	155.5	0.00					-25.63	0.04	
	155.6								2.0
	155.9								2.0
BB-76	156.0	0.00					-25.08	0.04	2.0
BB-77	156.5	0.00					-23.29	0.04	2.5
BB-78	157.0	0.00					-23.86	0.06	
	157.3								1.0
BB-79	157.5	0.00					-24.49	0.05	
	157.6								2.0
	157.8								1.0
BB-80	158.0	0.00					-24.91	0.05	
	158.4								2.0
BB-81	158.5	0.00					-24.00	0.05	
BB-82	159.0	0.00					-24.77	0.05	2.0
BB-83	159.5	0.00					-24.71	0.05	
BB-84	160.0	0.00					-23.33	0.04	2.0
BB-85	160.5	0.00					-24.26	0.05	1.0
	160.8								1.5
BB-86	161.0	0.00					-26.09	0.04	
	161.3								2.0
BB-87	161.5	0.00					-24.33	0.09	
	161.7								2.0
	161.9								2.0
BB-88	162.0	0.00					-25.40	0.07	
	162.3								1.5
BB-89	162.5	0.00					-23.49	0.04	2.0
BB-89SE	162.5								
	162.6								1.0
BB-90	163.0	0.01					-26.40	0.05	2.5
BB-91	163.5	0.00					-23.30	0.06	2.0
	163.7								1.0
	163.9								2.0
BB-92	164.0	0.00					-27.51	0.04	
	164.1								2.0
	164.2								3.0
	164.4								3.5
BB-93	164.5	0.00					-25.62	0.05	
	164.7								2.0

Sample ID	SP	CCE	CCD	$\delta^{13}C_{carb}$	$\delta^{18}O$	CST	$\delta^{13}C_{org}$	TOC	SDI
BB-94	165.0	0.00					-26.09	0.04	2.0
	165.2								2.0
	165.4								4.0
BB-95	165.5	0.00					-26.81	0.06	
	165.6								1.5
	165.9								1.5
BB-96	166.0	0.00					-27.09	0.06	
	166.1								2.0
	166.4								3.0
BB-97	166.5	0.00					-26.76	0.05	
	166.7								1.5
BB-98	167.0	0.00					-25.34	0.05	1.0
BB-99	167.5	0.00					-25.54	0.06	2.0
	167.8								1.0
BB-100	168.0	0.00					-26.84	0.08	
BB-100-1	168.1						-26.50	0.48	
	168.2								1.5
BB-100-95	168.5								
BB-101	168.5	0.00					-28.14	0.07	
	168.6								1.0
	168.9								2.0
BB-102	169.0	0.00					-27.76	0.06	
	169.3								2.0
BB-103	169.5	0.00					-27.36	0.05	
	169.8								2.0
BB-104	170.0	0.00					-27.17	0.06	
	170.2								2.0
BB-105	170.5	0.00					-27.73	0.06	
	170.9								1.5
BB-105-97	171.0								
BB-106	171.0	0.00					-26.19	0.10	
BB-106-02	171.0								
BB-106-1	171.1								
BB-106-3	171.3								
BB-107	171.5	0.00					-26.69	0.07	
	171.6								1.0
BB-108	172.0	0.00					-26.81	0.07	2.0
BB-109	172.5	0.00					-27.23	0.08	1.0
BB-110	173.0	0.00					-25.74	0.08	
	173.2								2.0
BB-111	173.5	0.00					-27.64	0.06	
	173.7								1.5

Sample ID	SP	CCE	CCD	$\delta^{13}C_{carb}$	$\delta^{18}O$	CST	$\delta^{13}C_{org}$	TOC	SDI
BB-112	174.0	0.01					-27.23	0.06	
	174.2								1.0
BB-113	174.5	0.00					-26.54	0.05	
	174.7								1.5
BB-114	175.0	0.00					-27.75	0.06	
	175.2								1.5
BB-115	175.5	0.00					-26.68	0.06	
	175.6								2.0
	175.8								1.0
BB-116	176.0	0.01					-27.06	0.05	
	176.4								1.0
BB-117	176.5	0.00					-26.96	0.06	
	176.8								2.0
BB-118	177.0	0.01					-24.68	0.05	
	177.4								1.5
BB-119	177.5	0.00					-27.66	0.05	
BB-120	178.0	0.00					-26.73	0.07	
	178.1								2.0
BB-121	178.5	0.00					-27.66	0.07	
	178.7								1.0
BB-122	179.0	0.00					-24.48	0.07	1.5
	179.4								2.0
BB-123	179.5	0.00					-27.56	0.07	
	179.7								1.5
	179.8								1.0
BB-124	180.0	0.00					-27.71	0.06	2.0
	180.4								1.5
BB-125	180.5	0.00					-22.41	0.08	
	180.7								3.0
	180.8								3.5
BB-126	181.0	0.00					-27.60	0.08	
	181.3								2.5
BB-127	181.5	0.00					-27.36	0.04	
	181.6								3.5
	181.8								2.0
BB-128	182.0	0.00					-27.92	0.06	2.0
	182.3								2.0
	182.4								1.0
BB-129	182.5	0.00					-28.18	0.06	
	182.7								3.5
	182.9								4.0
BB-130	183.0	0.00					-27.51	0.04	

Sample ID	SP	CCE	CCD	$\delta^{13}C_{carb}$	$\delta^{18}O$	CST	$\delta^{13}C_{org}$	TOC	SDI
	183.2								3.0
	183.3								3.5
BB-131	183.5	0.00					-28.23	0.06	3.0
	183.8								2.0
	183.9								2.0
BB-132	184.0	0.00					-25.25	0.07	
	184.1								2.5
	184.2								1.0
	184.4								2.0
BB-133	184.5	0.00					-26.48	0.06	
	184.8								2.0
BB-134	185.0	0.00					-28.17	0.07	
	185.2								2.0
BB-135	185.5	0.00					-27.97	0.05	1.5
	185.7								2.0
BB-136	186.0	0.00					-28.15	0.06	2.0
	186.3								1.5
BB-137	186.5	0.00					-28.34	0.08	1.0
	186.9								2.0
BB-138	187.0	0.00					-26.98	0.08	
	187.2								2.0
BB-139	187.5	0.00					-27.56	0.07	
KD-01	188.4								

APPENDIX E: MORRISON FORMATION FOOD-WEB DATA

1) Table E1. Definitions of node and network properties.
2) Table E2. Fundamental and taxonomic properties for all food webs.
3) Table E3. Web network structure properties.
4) Table E4. Results of regression analyses of slopes of food web properties for all biozones of WE webs.
5) Table E5. Results of regression analyses of slopes of food web properties for all biozones of TS webs.
6) Table E6. F test results for slopes of cumulative degree distributions.
7) Table E7. Database of Morrison Formation biota, environmental categories, basic reconstructed diets, biostratigraphic zones, and references.
8) Table E8. WE consumer-resource list for biozone 1.
9) Table E9. WE consumer-resource list for biozone 2.
10) Table E10. WE consumer-resource list for biozone 3.
11) Table E11. WE consumer-resource list for biozone 4.
12) Table E12. WE consumer-resource list for biozone 5.
13) Table E13. WE consumer-resource list for biozone 6.
14) Table E14. WE consumer-resource list for Quarry 9 (Carrano and Velez-Juarbe 2006).
15) Table E15. TS consumer-resource list for biozone 1.
16) Table E16. TS consumer-resource list for biozone 2.
17) Table E17. TS consumer-resource list for biozone 3.

Table E1.—Definitions of node and network properties.

Property	Definition	Reference
Original number of nodes	Total number of taxa before aggregation	(Dunne et al. 2008)
Number of aggregated nodes (S)	Total number of nodes after unifying taxa with the same set of consumers and resources	(Dunne 2009)
Number of links (L)	Total number of feeding links between nodes	(Dunne 2009)
Links per node	L/S	(Dunne 2009)
Connectance	Fraction of actual links compared to all possible links in a network; L/S^2	(Dunne 2009)
Fraction of top nodes	Fraction of nodes with no consumers	(Dunne 2009)
Fraction of intermediate nodes	Fraction of nodes with both consumers and resources	(Dunne 2009)
Fraction of basal nodes	Fraction of nodes with no resources	(Dunne 2009)
Fraction of herbivores	Fraction of nodes that consume only basal nodes	(Dunne 2009)
Fraction of cannibals	Fraction of nodes that feed on themselves	(Dunne 2009)
Fraction of omnivores	Fraction of nodes that feed at multiple trophic levels	(Dunne 2009)
Fraction of nodes in feeding loops	Fraction of nodes that occur twice in a single food chain	(Dunne 2009)
Mean trophic level	Mean number of steps energy takes to go from an energy source to a node	(Dunne 2009)
Mean shortest chain length	Mean shortest chain of links from a node to a basal node	(Riede et al. 2010)
Standard deviation of links	Standard deviation of links per node	(Dunne 2009)
Standard deviation of generality	Standard deviation of resources per node	(Dunne 2009)
Standard deviation of vulnerability	Standard deviation of consumers per node	(Dunne 2009)
Maximum node similarity	Mean of similarity of each node to other nodes	(Dunne 2009)
Diet discontinuity	Fraction of triplets of nodes with an irreducible gap in feeding links / number of possible triplets	(Dunne 2009)
Clustering coefficient	Average fraction of node pairs that are one link away from another pair of linked nodes	(Dunne et al. 2002a)
Characteristic path length	Average shortest path length between all pairs of nodes	(Dunne et al. 2002a)

Table E2.—Fundamental and taxonomic properties for all food webs, Z = MF biozone, WE = whole ecosystem, TS = terrestrial subset, Q9 = Quarry 9, S = number of nodes, L = number of links, C = connectance, Top = fraction of top nodes, Int = fraction of intermediate nodes, Bas = fraction of basal nodes, Herb = fraction of herbivores, Can = fraction of cannibals, Omn = fraction of omnivores, Loop = fraction of nodes in feeding loops. Biozone 1 values that fall outside of 2 standard deviations of the mean of biozone 2–6 values are in italics. Q9 values that fall outside the range of values from MF biozones 1–6 are shown in bold. See table E1 for definitions.

Web	Taxa	S	L	L/S	C	Top	Int	Bas	Herb	Can	Omn	Loop
$Z6_{WE}$	96	77	660	8.57	0.111	0	0.81	0.19	0.31	0.18	0.49	0.36
$Z5_{WE}$	121	85	839	9.87	0.116	0	0.82	0.18	0.29	0.19	0.53	0.38
$Z4_{WE}$	110	87	896	10.30	0.118	0	0.83	0.17	0.30	0.18	0.53	0.39
$Z3_{WE}$	87	69	528	7.65	0.111	0	0.78	0.22	0.35	0.20	0.43	0.30
$Z2_{WE}$	97	79	760	9.62	0.122	0	0.81	0.19	0.33	0.22	0.48	0.35
$Z1_{WE}$	64	*53*	*229*	*4.32*	*0.082*	0	*0.72*	*0.28*	0.40	0.17	*0.32*	*0.19*
Q9	99	75	659	8.79	0.117	0	0.80	0.20	0.32	**0.16**	0.49	0.36
$Z6_{TS}$	74	53	486	9.17	0.173	0	0.83	0.17	0.28	0.19	0.55	0.51
$Z5_{TS}$	96	58	596	10.28	0.177	0	0.84	0.16	0.28	0.21	0.57	0.53
$Z4_{TS}$	88	63	691	10.97	0.174	0	0.86	0.14	0.27	0.21	0.59	0.52
$Z3_{TS}$	67	47	392	8.34	0.177	0	0.81	0.19	0.34	0.23	0.47	0.43
$Z2_{TS}$	76	57	604	10.60	0.186	0	0.84	0.16	0.30	0.26	0.54	0.49
$Z1_{TS}$	45	*33*	*150*	*4.55*	*0.138*	0	*0.73*	*0.27*	0.39	0.18	*0.33*	*0.30*

Table E3.—Web network structure properties, Z = MF biozone, WE = whole ecosystem, TS = terrestrial subset, Q9 = Quarry 9, TL = mean trophic level, ShCh = mean shortest chain length, LinkSD = standard deviation of links per node, GenSD = standard deviation of the number of resources per node, VulSD = standard deviation of the number of consumers per node, MaxSim = maximum similarity, Ddiet = diet discontinuity, Cl = clustering coefficient, Path = characteristic path length. Biozone 1 values that fall outside of 2 standard deviations of the mean of biozone 2–6 values are in italics. See table E1 for definitions.

Web	TL	ShCh	LinkSD	GenSD	VulSD	MaxSim	Ddiet	Cl	Path
$Z6_{WE}$	2.40	2.17	0.65	1.16	0.60	0.69	0.06	0.22	2.04
$Z5_{WE}$	2.50	2.24	0.62	1.12	0.52	0.72	0.07	0.22	2.02
$Z4_{WE}$	2.48	2.22	0.64	1.13	0.56	0.72	0.07	0.23	2.00
$Z3_{WE}$	2.23	2.00	0.69	1.24	0.44	0.69	0.03	0.25	2.10
$Z2_{WE}$	2.40	2.15	0.66	1.14	0.51	0.70	0.07	0.24	2.01
$Z1_{WE}$	2.05	1.92	0.67	1.26	0.49	0.60	0.02	0.19	*2.28*
Q9	2.39	2.17	0.62	1.13	0.57	0.70	0.05	0.21	2.11
$Z6_{TS}$	2.47	2.19	0.52	1.00	0.59	0.76	0.10	0.22	1.76
$Z5_{TS}$	2.56	2.22	0.52	1.01	0.49	0.77	0.09	0.25	1.76
$Z4_{TS}$	2.58	2.25	0.53	1.02	0.53	0.78	0.08	0.24	1.75
$Z3_{TS}$	2.29	2.02	0.56	1.07	0.36	0.77	0.05	0.27	1.78
$Z2_{TS}$	2.53	2.19	0.53	1.00	0.44	0.78	0.11	0.27	1.74
$Z1_{TS}$	2.09	1.94	0.53	1.05	0.46	*0.66*	0.03	0.18	*1.93*

Table E4.—Results of regression analyses of slopes of food web properties for all biozones of WE webs. S = number of nodes, L = number of links, C = connectance, Top = fraction of top nodes, Int = fraction of intermediate nodes, Bas = fraction of basal nodes, Herb = fraction of herbivores, Can = fraction of cannibals, Omn = fraction of omnivores, Loop = fraction of nodes in feeding loops, TL = mean trophic level, ShCh = mean shortest chain length, LinkSD = standard deviation of links per node, GenSD = standard deviation of the number of resources per node, VulSD = standard deviation of the number of consumers per node, MaxSim = maximum similarity, Ddiet = diet discontinuity, Cl = clustering coefficient, Path = characteristic path length. See table E1 for definitions. Values in bold are significant at the α=0.05 level.

Property	Coefficient	Std. Error	t value	p value
Taxa	-0.06955	0.03011	-2.31	0.082
S	-0.10969	0.04682	-2.343	0.0791
L	-0.005203	0.002607	-1.996	0.117
L/S	-0.5948	0.2793	-2.13	0.100
C	-87.67	45.13	-1.943	0.124
Top	NA	NA	NA	NA
Int	-36.26	13.10	-2.768	0.0504
Bas	36.258	13.100	2.768	0.0504
Herb	38.659	11.117	3.477	**0.0254**
Can	-7.50	50.34	-0.149	0.889
Omn	-18.795	6.402	-2.936	**0.0426**
Loop	-20.197	6.651	-3.037	**0.0385**
TL	-8.131	3.305	-2.46	0.0697
ShCh	-10.487	4.706	-2.228	0.0898
LinkSD	34.41	32.96	1.044	0.35542
GenSD	18.69	11.82	1.581	0.18908
VulSD	-17.013	13.870	-1.277	0.287
MaxSim	-32.651	11.997	-2.722	0.0529
Ddiet	-49.211	31.685	-1.553	0.195
Cl	-41.628	38.250	-1.088	0.338
Path	13.225	5.303	2.494	0.067204

Table E5.—Results of regression analyses of slopes of food web properties for all biozones of TS webs. S = number of nodes, L = number of links, C = connectance, Top = fraction of top nodes, Int = fraction of intermediate nodes, Bas = fraction of basal nodes, Herb = fraction of herbivores, Can = fraction of cannibals, Omn = fraction of omnivores, Loop = fraction of nodes in feeding loops, TL = mean trophic level, ShCh = mean shortest chain length, LinkSD = standard deviation of links per node, GenSD = standard deviation of the number of resources per node, VulSD = standard deviation of the number of consumers per node, MaxSim = maximum similarity, Ddiet = diet discontinuity, Cl = clustering coefficient, Path = characteristic path length. See table E1 for definitions. Values in bold are significant at the α=0.05 level.

Property	Coefficient	Std. Error	t value	p value
Taxa	-0.07676	0.03344	-2.295	0.0834
S	-0.12080	0.05932	-2.036	0.111
L	-0.006124	0.003480	-1.76	0.153
L/S	-0.5368	0.2679	-2.004	0.116
C	-74.074	39.280	-1.886	0.132
Top	NA	NA	NA	NA
Int	-30.530	12.190	-2.504	0.0664
Bas	30.530	12.190	2.504	0.0664
Herb	32.407	10.721	3.023	**0.0391**
Can	-3.306	31.363	-0.105	0.921
Omn	-15.471	5.279	-2.931	**0.0428**
Loop	-17.730	5.269	-3.365	**0.0282**
TL	-6.730	3.263	-2.063	0.108
ShCh	-10.309	5.086	-2.027	0.113
LinkSD	21.38	60.41	0.354	0.7412
GenSD	27.11	28.26	0.959	0.3918
VulSD	-10.429	10.197	-1.023	0.364
MaxSim	-29.783	12.574	-2.369	0.077
Ddiet	-36.197	23.104	-1.567	0.192
Cl	-23.824	23.475	-1.015	0.368
Path	20.04	7.70	2.603	0.05988

Table E6.—F test results for slopes (β) of cumulative degree distributions; WEx = whole ecosystem zone x; TSx = terrestrial subset zone x; WE = all zones in WE webs; TS = all zones in TS webs; dfn = numerator degrees of freedom; dfd = denominator degrees of freedom. The significant difference between β_{WE} and β_{TS} shows that the scale at which ecosystems are approached influences study outcomes.

H_0	F	dfn	dfd	F critical, α=0.05	p	Result
$\beta_{WE1} = \beta_{WE2} = \beta_{WE3} = \beta_{WE4} = \beta_{WE5} = \beta_{WE6}$	1.400	10	184	1.882	0.183	accept H_0
$\beta_{TS1} = \beta_{TS2} = \beta_{TS3} = \beta_{TS4} = \beta_{TS5} = \beta_{TS6}$	0.285	10	144	1.897	0.984	accept H_0
$\beta_{WE} = \beta_{TS}$	15.824	2	348	3.022	0.000	reject H_0

Table E7.—Database of Morrison Formation biota, environmental categories, basic reconstructed diets, biostratigraphic zones, and references.

ID Number	Node	EfP	Ter	LeTE	LoTE	Le	Lo	Diet	Biozone 1	Biozone 2	Biozone 3	Biozone 4	Biozone 5	Biozone 6	References
1	benthic detritus	Im				X	X	NF	Im	Im	Im	Im	Im	Im	
2	terrestrial detritus	Im	X	X	X			NF	Im	Im	Im	Im	Im	Im	
3	bacteriobenthos	T				X	X	NF	Im	Im	Im	Im	Im	Im	Dunagan, 2000; Dunagan and Turner, 2004; Hasiotis, 2004
4	bacterioplankton	Im				X	X	NF	Im	Im	Im	Im	Im	Im	
5	fungi	B, T	X	X	X			Pw, Vb	Im	Im	Im	Im	Im	Im	Ash and Tidwell, 1998; Britt et al., 2003; Chure et al., 2006; Hasiotis, 2004; Tidwell, 1990
6	phytoplankton	B, P				X	X	NF	Im	Im	Im	Im	Im	Im	Chure et al., 2006; Litwin et al., 1998; Sheath and Hambrook, 1990
7	phytobenthos	Im				X	X	NF	Im	Im	Im	Im	Im	Im	
8	charophytes	B				X		NF	X	X	X	X	X	X	Schudack et al., 1998
9	bryophytes	B, P		X	X			NF	X	X	X	X	X	X	Ash and Tidwell, 1998; Chure et al., 2006; Hotton and Baghai-Riding, 2010; Litwin et al., 1998; Parrish et al., 2004; Raven et al., 1999
11	aquatic, low stature plants	B, P		X	X	X		NF	X	X	X	X	X	X	Ash and Tidwell, 1998; Chure et al., 2006; Hotton and Baghai-Riding, 2010; Parrish et al., 2004; Tidwell, 1990; Tidwell et al., 2006; Turner and Peterson, 1999

ID Number	Node	EfP	Ter	LeTE	LoTE	Le	Lo	Diet	Biozone 1	Biozone 2	Biozone 3	Biozone 4	Biozone 5	Biozone 6	References
12	low stature lete+lote plants	B, P		X	X			NF	X	X	X	X	X	X	Ash and Tidwell, 1998; Chure et al., 2006; Hotton and Baghai-Riding, 2010; Litwin et al., 1998; Parrish et al., 2004; Taylor et al., 2009; Wesley 1973
13	low stature ter plants	B, P	X					NF	X	X	X	Im	Im	X	Ash and Tidwell, 1998; Chure et al., 2006; Hotton and Baghai-Riding, 2010; Litwin et al., 1998; Parrish et al., 2004; Tidwell et al., 2006
14	low stature ter+lete+lote plants	P	X	X	X			NF	X	X	X	X	X	X	Chure et al., 2006; Hotton and Baghai-Riding, 2010; Litwin et al., 1998
15	moderate stature lete+lote plants	B, P		X	X			NF	X	X	X	X	X	X	Ash and Tidwell, 1998; Chure et al., 2006; Hotton and Baghai-Riding, 2010; Large and Braggins, 2004; Litwin et al., 1998; Parrish, 2004; Tidwell, 1990
16	shrub ter plants	P	X					NF	Im	Im	Im	Im	Im	Im	Chure et al., 2006; Hotton and Baghai-Riding, 2010

ID Number	Node	EfP	Ter	LeTE	LoTE	Le	Lo	Diet	Biozone 1	Biozone 2	Biozone 3	Biozone 4	Biozone 5	Biozone 6	References
17	shrubby ter+lete+lote	B, P	X	X	X			NF	X	X	X	X	X	X	Ash and Tidwell, 1998; Chure et al., 2006; Hotton and Baghai-Riding, 2010; Litwin et al., 1998; Parrish et al., 2004; Tidwell, 1990
18	tallest lete+lote plants	B, P		X	X			NF	X	X	X	X	X	X	Ash and Tidwell, 1998; Chure et al., 2006; Hotton and Baghai-Riding, 2010; Parrish et al., 2004; Royer et al., 2003
19	tallest ter+lete+lote plants	B, P	X	X	X			NF	X	X	X	X	X	X	Ash and Tidwell, 1998; Carpenter, 2006; Chure et al., 2006; Gee and Tidwell, 2010; Hotton and Baghai-Riding, 2010; Kirkland, 2006; Litwin et al., 1998; Parrish et al., 2004; Tidwell, 1990
20	zooplankton	Im				X	X	P	X	X	X	X	X	X	
21	freshwater sponges	B				X		De, P	X	X	X	X	X	X	Dunagan, 1999; Dunagan, 2000; Dunagan and Turner, 2004; Reiswig et al., 2010
22	lentic unionid bivalves	B, Im, T				X		P	X	X	X	X	X	X	Evanoff et al., 1998; Good, 2004; Good, 2004; Hasiotis, 2004
23	lentic unionid glochidia	Ipc				X		Vf	X	X	X	X	X	X	Good, 2004
24	lotic unionid bivalves	B, Im, T					X	P	X	X	X	X	X	X	Evanoff et al., 1998; Good, 2004; Hasiotis, 2004

ID Number	Node	EfP	Ter	LeTE	LoTE	Le	Lo	Diet	Biozone 1	Biozone 2	Biozone 3	Biozone 4	Biozone 5	Biozone 6	References
25	lotic unionig glochidia	Ipc					X	Vf	X	X	X	X	X	X	Good, 2004; Kirkland, 1998
26	freshwater gastropods	B, T		X		X		De, Isp, P	X	X	X	X	X	X	Chure et al., 2006; Evanoff et al., 1998; Hasiotis, 2004; Kirkland, 2006
27	terrestrial Oligochaeta	T	X	X	X			De	Im	Im	Im	Im	Im	Im	Hasiotis, 2004
28	leeches	T				X		Ian, Imo	Im	Im	Im	Im	Im	Im	Ash and Tidwell, 1998; Govedich et al., 2010
29	freshwater ostracodes	B				X		De, P	X	X	X	X	X	X	Chure et al., 1998; Dodds, 2002; Sames et al 2010; Schudack et al., 1998; Smith and Delorme, 2010
30	conchostracans	B				X		P	?	X	X	X	X	X	Chure et al., 2006; Dodson et al., 2010; Kirkland, 2006; Lucas and Kirkland, 1998
31	crayfish	B, T		X	X	X	X	De, Ian, Iar, Isp, P	Im	Im	Im	Im	Im	Im	Hasiotis, 2004; Hasiotis et al., 1998; Huner, 1994
32	horseshoe crabs	T				X		Iar, Imo	Im	Im	Im	Im	Im	Im	Hasiotis, 2004; Jennings et al., 2006; Walls et al., 2002
33	trichoptera larvae	T				X	X	P	Im	Im	Im	Im	Im	Im	Gorman et al., 2008; Hasiotis, 2004; Hasiotis et al., 1998b; Slack, 1936; Wiggins, 2005
34	adult trichoptera	Is		X	X			NF	Im	Im	Im	Im	Im	Im	Gorman et al, 2008; Hasiotis, 2004; Hasiotis et al 1998b
35	chironomid larvae	T		X	X	X	X	De, Iar, P	Im	Im	Im	Im	Im	Im	Armitage et al., 1995; Hasiotis 1998; Hasiotis, 2004

ID Number	Node	EfP	Ter	LeTE	LoTE	Le	Lo	Diet	Biozone 1	Biozone 2	Biozone 3	Biozone 4	Biozone 5	Biozone 6	References
36	adult chironomids	Is		X	X			NF	Im	Im	Im	Im	Im	Im	Coffman and Ferrington, 1995; Hasiotis 1998; Hasiotis, 2004
37	*Parapleurites* and orthopterans	B, T	X	X	X			P	Im	Im	Im	Im	Im	Im	Hasiotis, 2004; Smith et al., 2011
38	hemipterans	T	X	X	X	X		P	Im	Im	Im	Im	Im	Im	Hasiotis, 2004
39	beetle larvae	T			X			De	Im	Im	Im	Im	Im	Im	Hasiotis, 2004
40	heterocid beetles	T		X	X			De, P	Im	Im	Im	Im	Im	Im	Hasiotis, 2004; Kaufmann and Stansly, 1979
41	tiger beetles	T		X	X			De, Iar, P	Im	Im	Im	Im	Im	Im	Hasiotis, 2004; Hori, 1982; Lövei and Sunderland 1996; Pearson and Vogler, 2001
42	staphylinid beetles	T	X	X	X			Iar	Im	Im	Im	Im	Im	Im	Bohac, 1999; Hasiotis, 2004
43	dung beetles	T	X	X	X			De	Im	Im	Im	Im	Im	Im	Hasiotis, 2004
44	wood-boring and engraver beetles	T	X					Pw	Im	Im	Im	Im	Im	Im	Hasiotis, 2004; Tidwell and Ash, 1990
45	dermestid beetles	T	X	X	X			Vb	Im	Im	Im	Im	Im	Im	Bader et al., 2009; Britt et al., 2008; Hasiotis, 2004; Hasiotis et al., 1999
46	ants	T	X	X	X			Iar	Im	Im	Im	Im	Im	Im	Hasiotis, 2004; Hölldobler and Wilson, 1990
47	non-formicid hymenoptera	T	X	X	X			Iar	Im	Im	Im	Im	Im	Im	Hasiotis, 2004; Labandeira, 2002
50	termites	T	X	X	X			Pw	Im	Im	Im	Im	Im	Im	Hasiotis, 2004; Traniello and Leuthold, 2000
51	cicada nymphs	T	X	X	X			P	Im	Im	Im	Im	Im	Im	Hasiotis, 2004; White and Strehl, 1978
52	adult cicadas	Is	X	X	X			P	Im	Im	Im	Im	Im	Im	Hasiotis, 2004
53	inferred lentic fish	Ip				X	X	Va, Vf	Ip	Ip	Ip	Ip	Ip	Ip	
54	inferred lotic fish	Ip				X	X	Va, Vf	Ip	Ip	Ip	Ip	Ip	Ip	

ID Number	Node	EfP	Ter	LeTE	LoTE	Le	Lo	Diet	Biozone 1	Biozone 2	Biozone 3	Biozone 4	Biozone 5	Biozone 6	References
55	*Morrolepis*	B				X		Ian, Iar, Va, Vf					X		Foster, 2003; Foster, 2007; Kirkland, 1998
56	*Hulettia*	B				X		Ian, Iar, Va					X		Foster, 2003; Foster, 2007; Kirkland, 1998
57	Amiiformes	B				X	X	Ian, Iar, Va, Vf		X	X	X			Chure et al., 2006; Foster, 2003; Foster, 2007; Kirkland, 1998
58	Pycnodontoidea	B				X	X	Ian, Iar, Va				X			Chure et al., 2006; Foster, 2003; Foster, 2007; Kirkland, 1998
59	Cf. *Leptolepis*	B				X		Ian, Iar, Va, Vf					X		Foster, 2003; Foster, 2007; Kirkland, 1998
61	*Ceratodus* (adult)	B				X		Iar, Imo , P, Va, Vf		X	X	X	X	X	Foster, 2003; Foster, 2007; Kirkland, 1987; Kirkland, 1998
62	*Ceratodus* (juvenile)	B, Is				X		Ian, Iar, P		X	X	X	X	X	Foster, 2003; Kirkland, 1987
64	*Cteniogenys*	B		X	X	X	X	Iar, Va, Vf		X	Ib	Ib	X	X	Chure and Evans, 1998; Chure et al., 2006; Foster, 2003; Foster, 2007
68	*Ophiopsis*	B				X	X	Ian, Iar, P, Va					X		Chure et al., 2006; Foster, 2003; Foster, 2007; Prothero, 1981
69	*Enneabatrachus*	B		X	X	X	X	Ian, Iar, P, Va					X		Chure et al., 2006; Evans and Milner, 1993; Foster, 2003; Henrici, 1998
70	*Rhadinosteus*	B		X		X		Ian, Iar, P, Va						X	Chure, et al., 2006; Foster, 2003; Foster 2007

ID Number	Node	EfP	Ter	LeTE	LoTE	Le	Lo	Diet	Biozone 1	Biozone 2	Biozone 3	Biozone 4	Biozone 5	Biozone 6	References
71	unnamed Pelobatidae	B		X	X	X	X	Ian, Iar, P, Va					X	X	Chure et al., 2006; Evans and Milner, 1993; Foster, 2003
72	tadpoles	Is				X		De, P		X		X	X	X	Hoff et al., 1999
73	Anura indet.	B	X	X	X			Ian, Iar, P, Va		X		X			Foster, 2003
74	*Iridotriton*	B	X	X	X			Ian, Iar, P, Va						X	Evans et al., 2005; Foster, 2003; Foster, 2007
96	*Comonecturoides*	B	X	X	X			Ian, Iar, P, Va					X		Chure et al., 2006; Evans et al., 2005; Foster, 2003
75	Caudata B	B	X	X	X			Ian, Iar, P, Va						X	Foster, 2003
76	Caudata indet.	B	X	X	X			Ian, Iar, P, Va		X		X	X		Foster, 2003
77	*Glyptops*	B		X	X	X	X	Ian, Iar, Imo, P, Va, Vf	X	X	X	X	X	X	Bakker and Bir, 2004; Foster, 2003; Foster, 2007; Kirkland, 2006; Lucas et al., 2006
78	*Dinochelys*	B		X	X	X	X	Ian, Iar, Imo, P, Va, Vf		X	Ib	X	Ib	X	Bakker and Bir, 2004; Chure et al., 2006; Foster, 2003; Foster, 2007
79	*Uluops*	B		X	X	X	X	Ian, Iar, Imo, P, Va, Vf						X	Bakker and Bir, 2004; Chure et al., 2006; Foster, 2003; Foster, 2007
80	*Dorsetochelys*	B		X	X	X	X	Ian, Iar, Imo, P, Va, Vf						X	Bakker and Bir, 2004; Chure et al., 2006; Foster, 2003; Foster, 2007

ID Number	Node	EfP	Ter	LeTE	LoTE	Le	Lo	Diet	Biozone 1	Biozone 2	Biozone 3	Biozone 4	Biozone 5	Biozone 6	References
81	Chelonia indet.	B		X	X	X	X	Ian, Iar, Imo, P, Va, Vf	X	X	X	X	X	X	Bakker and Bir, 2004; Foster, 2003; Foster, 2007
82	*Opisthias*	B	X	X	X			Ian, Iar, Imo, Va, Vr		X	Ib	X	X	X	Chure et al., 2006; Foster, 2003; Foster, 2007; Walls, 1981
83	*Theretairus*	B	X	X	X			Ian, Iar, Imo, Va, Vr					X	X	Chure et al., 2006; Foster, 2003; Foster, 2007
84	*Eilenodon*	B	X	X	X			P, Va, Vr				X			Chure et al., 2006; Foster, 2003; Foster, 2007; Kirkland, 1996
85	Sphenodontia indet.	B	X	X	X			P, Va, Vr		X	X	X	X	X	Foster, 2003; Foster, 2007
86	*Dorsetisaurus*	B	X	X	X			Ian, Iar, Va		X	Ib	X	X		Chure et al., 2006; Foster, 2003; Foster, 2007
87	*Parviraptor*	B	X	X	X			Ian, Iar, Va				X			Chure et al., 2006; Foster, 2003; Foster, 2007
88	*Paramacellodus*	B	X	X	X			Ian, Iar, Va				X	X		Chure et al., 2006; Evans and Chure, 1999; Foster, 2003; Foster, 2007
89	*Saurillodon*	B	X	X	X			Ian, Iar, Va				X			Chure et al., 2006; Foster, 2003; Foster, 2007
90	*Schilleria*	B	X	X	X			Ian, Iar, Va					?		Chure et al., 2006; Evans and Chure, 1999; Foster, 2003; Foster, 2007

ID Number	Node	EfP	Ter	LeTE	LoTE	Le	Lo	Diet	Biozone 1	Biozone 2	Biozone 3	Biozone 4	Biozone 5	Biozone 6	References
95	Squamata indet.	B	X	X	X			Ian, Iar, Va		X		X		X	Foster, 2003; Foster, 2007
97	*Hallopus*	B	X	X	X			Va, Ve, Vr						X	Foster, 2003; Foster, 2007; Kirkland, 1996; Walker, 1970
98	"Fruitachampsa"	B	X	X	X			Va, Ve, Vr		?		X			Foster, 2003; Foster, 2007
99	*Goniopholis* (adults)	B		X	X	X	X	Va, Vd, Vf, Vr		X	X	X	X	X	Bakker and Bir, 2004; Foster, 2003; Foster, 2006; Foster, 2007; Foster and Martin, 1994
100	*Goniopholis* (juveniles)	B, Is		X	X	X	X	Ian, Iar, Va, Vf		X	X	X	X	X	Bakker and Bir, 2004; Foster, 2003; Foster, 2006
101	*Eutretauranosuchus*	B		X	X	X	X	Iar, Va, Vd, Vf, Vr	X	Ib	X	Ib	X	X	Foster, 2003; Foster, 2007
102	*Macelognathus*	B	X	X	X			Va, Vr				X	X		Chure et al., 2006; Foster, 2003; Foster, 2007; Gohlich et al., 2005; Ostrom, 1971
103	*Hoplosuchus*	B	X	X	X			Va, Vr					X		Chure et al., 2006; Foster, 2003; Foster, 2007
104	*Dermodactylus*	B	X	X	X			Ian, Iar, Va, Vf					X		Foster, 2007; King et al., 2006; Marsh, 1878; Marsh, 1881
105	*Mesadactylus*	B	X	X	X			Ian, Iar, Va, Vf				X			Foster, 2007; Jensen and Ostrom, 1977; King et al., 2006
106	*Kepodactylus*	B	X	X	X			Ian, Iar, Va, Vf				X			Foster, 2007; Harris and Carpenter, 1996; King et al., 2006

ID Number	Node	EfP	Ter	LeTE	LoTE	Le	Lo	Diet	Biozone 1	Biozone 2	Biozone 3	Biozone 4	Biozone 5	Biozone 6	References
107	*Comodactylus*	B	X	X	X			Ian, Iar, Va, Vf					X		Foster, 2007; Galton, 1981; King et al., 2006; Smith et al., 2004
108	*Harpactognathus*	B	X	X	X			Ian, Iar, Va, Vf		X					Carpenter et al., 2003; Foster, 2007; King et al., 2006
110	Pterosauria indet.	B	X	X	X			Ian, Iar, Va, Vf		X		X	X	X	Foster, 2007; King et al., 2006
111	*Laopteryx*	B	X	X	X			Ian, Iar, Va, Vf					X		King et al., 2006; Marsh, 1881; Ostrom, 1986; Turner and Peterson, 1999
112	*Allosaurus* (adults)	B	X	X	X			Vd, Vf, Vr	X	X	X	X	X	X	Bader et al., 2009; Bakker, 1986; Bakker, 1998; Bakker and Bir, 2004; Carpenter, 2002; Carpenter et al., 2005a; Chure et al., 2006; Colbert, 1961; Dodson et al., 1980; Farlow 1976; Fastovsky and Smith, 2004; Foster, 2003; Foster, 2007; Foster and Martin, 1994; Gates, 2005; Henderson, 1998; Ikejiri et al., 2006; Madsen, 1976; Myers and Storrs, 2007; Rayfield et al., 2001

ID Number	Node	EfP	Ter	LeTE	LoTE	Le	Lo	Diet	Biozone 1	Biozone 2	Biozone 3	Biozone 4	Biozone 5	Biozone 6	References
113	*Allosaurus* (juvenile)	B, Is	X	X	X			Iar, Vd, Vf, Vm, Vr	X	X	X	X	X	X	Bakker and Bir, 2004; Farlow, 1976; Foster and Chure, 2006; Jennings and Hasiotis, 2006; Therrien et al., 2005
114	*Ceratosaurus* (adults)	B	X	X	X			Vd, Vf, Vr		X	Ib	X	X	X	Bakker, 1986; Bakker, 1998; Bakker and Bir, 2004; Chure et al., 1998b; Chure et al., 2006; Foster, 2003; Foster, 2007; Fastovsky and Smith, 2004; Gates, 2005; Henderson, 1998
115	*Ceratosaurus* (juveniles)	B, Is	X	X	X			Iar, Va, Vf, Vm, Vr		X	Ib	X	X	X	Bakker and Bir, 2004
116	*Saurophaganax*	B	X	X	X			Vd, Vr					X		Chure et al., 2006; Foster, 2003; Foster, 2007
117	*Torvosaurus*	B	X	X	X			Vd, Vr			X	Ib	X		Bader et al., 2009; Chure et al., 1998b; Chure et al., 2006; Foster, 2003; Foster, 2007; Van Valkenburgh and Molnar, 2002
118	*Marshosaurus*	B	X	X	X			Vd, Vr			X	Ib	X		Chure et al., 2006; Foster, 2003; Foster, 2007
119	*Stokesosaurus*	B	X	X	X			Va, Vd, Vr		?			X		Foster, 2003; Foster, 2007

ID Number	Node	EfP	Ter	LeTE	LoTE	Le	Lo	Diet	Biozone 1	Biozone 2	Biozone 3	Biozone 4	Biozone 5	Biozone 6	References
120	*Ornitholestes*	B	X	X	X			Iar, Va, Vd, Vm, Vr		X			?		Bakker, 1996; Bakker and Bir, 2004; Carpenter et al., 2005b; Foster, 2003; Foster, 2007
121	*Coelurus*	B	X	X	X			Iar, Va, Vd, Vm, Vr		X	Ib	Ib	X		Bakker, 1986; Carpenter, 2002; Carpenter et al., 2005b; Foster, 2003; Foster, 2007
122	*Tanycolagreus*	B	X	X	X			Iar, Va, Vd, Vm, Vr		X			?		Carpenter et al., 2005c; Foster, 2007
123	*Elaphrosaurus*	B	X	X	X			Vd, Vm, Vr		X	X	X			Chure et al., 2006; Foster, 2003; Foster, 2007
125	*Koparion*	B	X	X	X			Va, Vd, Vm, Vr						X	Chure et al., 2006; Foster, 2003; Foster, 2007
127	*Brachiosaurus* (adults)	B	X	X	X			P		X	X	X			Christian and Dzemski, 2007; Chure et al., 2006; Fiorillo, 1998b; Foster, 2003; Foster, 2007; Foster and Martin, 1994; Stevens and Parrish, 2005; Weaver, 1983; Weishampel, 1984
128	*Brachiosaurus* (juveniles)	Is	X	X	X			P		X	X	X			

ID Number	Node	EfP	Ter	LeTE	LoTE	Le	Lo	Diet	Biozone 1	Biozone 2	Biozone 3	Biozone 4	Biozone 5	Biozone 6	References
129	*Camarasaurus* (adults)	B	X	X	X			P		X	X	X	X	X	Britt and Naylor, 1994; Carpenter, 1998a; Chatterjee and Zheng, 2005; Chure et al., 2006; Dodson et al., 1980; Fiorillo, 1991; Fiorillo 1994; Fiorillo, 1998a; Fiorillo, 1998b; Foster, 2003; Foster, 2007; Foster and Martin, 1994; Weishampel, 1984
130	*Camarasaurus* (juveniles)	B, Is	X	X	X			P		X	X	X	X	X	Fiorillo, 1998b
131	*Haplocanthosaurus* (adults)	B	X	X	X			P	X	X	Ib	X			Chure et al., 2006; Foster, 2003; Foster, 2007; Weishampel, 1984
132	*Haplocanthosaurus* (juveniles)	Is	X	X	X			P	X	X	Ib	X			
133	*Diplodocus* (adults)	B	X	X	X			P		X	X	X	X	X	Carpenter, 1998a; Carpenter, 2006; Chure et al., 2006; Dodson et al., 1980; Fiorillo, 1991; Fiorillo, 1994; Fiorillo, 1998b; Foster, 2003; Foster, 2007; Foster and Martin, 1994; Stevens and Parrish, 1999; Stevens and Parrish, 2005; Weishampel, 1984
134	*Diplodocus* (juveniles)	B, Is	X	X	X			P		X	X	X	X	X	

ID Number	Node	EfP	Ter	LeTE	LoTE	Le	Lo	Diet	Biozone 1	Biozone 2	Biozone 3	Biozone 4	Biozone 5	Biozone 6	References
135	*Barosaurus* (adults)	B	X	X	X			P		X	X	X	X		Carpenter, 2006; Chure et al., 2006; Foster, 2003; Foster, 2007; Foster and Martin, 1994; Weishampel, 1984
136	*Barosaurus* (juveniles)	B, Is	X	X	X			P		X	X	X	X		
137	*Apatosaurus* (adults)	B	X	X	X			P		X	X	X	X	X	Bakker, 1998; Carpenter, 2006; Chure et al., 2006; Dodson et al., 1980; Foster, 2003; Foster, 2007; Foster and Martin, 1994; Stevens and Parrish, 1999; Stevens and Parrish, 2005; Weishampel, 1984
138	*Apatosaurus* (juveniles)	B, Is	X	X	X			P		X	X	X	X		
139	*Supersaurus* (adults)	B	X	X	X			P			X				Carpenter, 2006; Chure et al., 2006; Foster, 2003; Foster, 2007; Weishampel, 1984
140	*Supersaurus* (juveniles)	Is	X	X	X			P			X				
141	*Dystrophaeus* (adults)	B	X	X	X			P	X						Carpenter, 2006; Chure et al., 2006; Foster, 2003; Foster, 2007; Weishampel, 1984
142	*Dystrophaeus* (juveniles)	Is	X	X	X			P	X						

ID Number	Node	EfP	Ter	LeTE	LoTE	Le	Lo	Diet	Biozone 1	Biozone 2	Biozone 3	Biozone 4	Biozone 5	Biozone 6	References
143	*Amphicoelias* (adults)	B	X	X	X			P						X	Carpenter, 2006; Foster, 2003; Foster, 2007; Weishampel, 1984
144	*Amphicoelias* (juveniles)	Is	X	X	X			P						X	
145	*Suuwassea* (adults)	B	X	X	X			P						?	Carpenter, 2006; Foster, 2003; Harris and Dodson, 2004; Weishampel, 1984
146	*Suuwassea* (juveniles)	Is	X	X	X			P						?	
147	*Stegosaurus*	B	X	X	X			P	?	X	X	X	X	X	Carpenter, 1998b; Chure et al., 2006; Dodson et al., 1980; Farlow et al., 1976; Foster, 2007; Lockley and Hunt, 1998; Reichel, 2010; Weishampel, 1984
148	*Hesperosaurus*	B	X	X	X			P	X						Chure et al., 2006; Foster, 2003; Foster, 2007; Weishampel, 1984
149	*Mymoorapelta*	B	X	X	X			P				X	X		Chure et al., 2006; Foster, 2003; Foster, 2007; Kirkland and Carpenter, 1994; Molnar and Clifford, 2000; Weishampel, 1984

ID Number	Node	EfP	Ter	LeTE	LoTE	Le	Lo	Diet	Biozone 1	Biozone 2	Biozone 3	Biozone 4	Biozone 5	Biozone 6	References
150	*Gargoyleosaurus*	B	X	X	X			P		X					Chure et al., 2006; Foster, 2003; Foster, 2007; Molnar and Clifford, 2000; Weishampel, 1984
151	Ankylosauria indet.	B	X	X	X			P	X			X			Foster, 2003; Kirkland, et al., 1998; Molnar and Clifford, 2000; Weishampel, 1984
152	cf. *Echinodon*	B	X	X	X			Iar, P				X			Chure et al., 2006; Foster, 2003; Foster, 2007; Weishampel, 1984
153	*Othnielosaurus*	B	X	X	X			P		X	X	X	X		Bakker, 1998; Foster, 2003; Foster, 2007; Galton, 2006; Weishampel, 1984
154	*Drinker*	B	X	X	X			P					X	X	Bakker, 1998; Chure et al., 2006; Foster, 2003; Foster, 2007; Weishampel, 1984
155	*Dryosaurus*	B	X	X	X			P	X	X	X	X	X	X	Chure et al., 2006; Foster, 2003; Foster, 2007; Kirkland, 1996; Weishampel, 1984

ID Number	Node	EfP	Ter	LeTE	LoTE	Le	Lo	Diet	Biozone 1	Biozone 2	Biozone 3	Biozone 4	Biozone 5	Biozone 6	References
156	*Camptosaurus*	B	X	X	X			P	X	X	X	X	X	X	Bakker, 1998; Chure et al., 1994; Chure et al., 2006; Dodson et al., 1980; Foster, 2003; Foster, 2007; Foster and Lockley, 2006; Weishampel, 1984
157	*Fruitadens*	B	X					Iar, P				X			Butler et al., 2010; Weishampel, 1984
158	*Docodon*	B		X	X			Iar, P, Va, Vr	X	X	X	X	X	X	Foster, 2007; Foster et al., 2006; Gingerich, 1973; Kielan-Jawaoroska et al., 2004
159	*Fruitafossor*	B	X					Ian, Iar				X			Chure et al., 2006; Foster, 2007; Luo and Wible, 2005
160	*Ctenacodon*	B	X					Ian, Iar, P		?			X		Chure et al., 2006; Foster, 2003; Foster, 2007
161	*Psalodon*	B	X					Ian, Iar, P		X	Ib	Ib	X		Chure et al., 2006; Foster, 2003; Foster, 2007
162	*Glirodon*	B	X					Ian, Iar, P				X	Ib	X	Chure et al., 2006; Engelmann and Callison, 1999; Foster, 2003; Foster, 2007
163	*Zofiabaatar*	B	X					Ian, Iar, P						X	Bakker and Bir, 2004; Chure et al., 2006; Foster, 2003; Foster, 2007
164	*Triconolestes*	B	X					Ian, Iar				X			Chure et al., 2006; Foster, 2003; Foster, 2007

ID Number	Node	EfP	Ter	LeTE	LoTE	Le	Lo	Diet	Biozone 1	Biozone 2	Biozone 3	Biozone 4	Biozone 5	Biozone 6	References
165	*Aploconodon*	B	X					Ian, Iar					X		Chure et al., 2006; Foster, 2003; Foster, 2007
166	*Comodon*	B	X					Ian, Iar					X		Chure et al., 2006; Foster, 2007
167	*Priacodon*	B	X					Ian, Iar, Va, Vr				X	X	X	Foster, 2003; Foster, 2007
168	*Trioracodon*	B	X					Ian, Iar, Va, Vr					X		Foster, 2003; Foster, 2007
170	*Amphidon*	B	X					Ian, Iar					X		Chure et al., 2006; Foster, 2003; Foster, 2007
171	*Tinodon*	B	X					Ian, Iar					X		Chure et al., 2006; Foster, 2003; Foster, 2007
172	*Araeodon*	B	X					Ian, Iar					X		Carpenter and Bakker, 1990; Chure et al., 2006; Foster, 2003; Foster, 2007
173	*Archaeotrigon*	B	X					Ian, Iar					X		Carpenter and Bakker, 1990; Chure et al., 2006; Foster, 2003; Foster, 2007
174	*Euthlastus*	B	X					Ian, Iar					X	X	Carpenter and Bakker, 1990; Chure et al., 2006; Foster, 2003; Foster, 2007
175	*Paurodon*	B	X					Ian, Iar					X		Carpenter and Bakker, 1990; Chure et al., 2006; Foster, 2003; Foster, 2007

ID Number	Node	EfP	Ter	LeTE	LoTE	Le	Lo	Diet	Biozone 1	Biozone 2	Biozone 3	Biozone 4	Biozone 5	Biozone 6	References
176	*Comotherium*	B	X					Ian, Iar					X		Carpenter and Bakker, 1990; Chure et al., 2006; Foster, 2003; Foster, 2007
177	*Tathiodon*	B	X					Ian, Iar					X		Carpenter and Bakker, 1990; Chure et al., 2006; Foster, 2003; Foster, 2007
178	*Foxraptor*	B	X					Ian, Iar, Va, Vr						X	Carpenter and Bakker, 1990; Chure et al., 2006; Foster, 2003; Foster, 2007
179	*Laolestes*	B	X					Ian, Iar					X	X	Chure et al., 2006; Foster, 2003; Foster, 2007
180	*Dryolestes*	B	X					Ian, Iar		X	Ib	Ib	X	X	Chure et al., 2006; Foster, 2007
181	*Amblotherium*	B	X					Ian, Iar		X	X	Ib	X		Chure et al., 2006; Foster, 2003; Foster, 2007
184	hatchling herbivorous dinosaurs	Is	X					P	Is	Is	Is	Is	Is	Is	
185	hatchling carnivorous dinosaurs	Is	X					Iar	Is	Is	Is	Is	Is	Is	

TABLE LEGEND

Headings: EfP = evidence for presence; Ter = terrestrial; LeTE = lentic-terrestrial ecotone; LoTE = lotic-terrestrial ecotone; Le = lentic; Lo = lotic

EfP: B = body fossils; Im = inferred based on modern ecosystem analog; Ip = inferred host based on presence of parasite taxa; Ipc = inferred based on phylogenetic conservation; Is = Inferred life stage of taxon known to be present; P = palynomorphs; T = trace fossils

Diet: De = detritus; Ian = annelids; Iar = arthropods; Imo = mollusks; Isp = sponges; NF = nonfeeding; P = plants or other autotrophs; Pw =woody parts of plants; Va = amphibians; Vb = vertebrate bone; Vd = dinosaurs; Ve = vertebrate eggs; Vf = fish; Vm = mammals; Vr = reptiles

Biozones: ? = presence uncertain; Ib = no fossils known from biozone, but presence is inferred because biozone is bracketed by presences of this taxon; Im = presence inferred based on modern ecosystem analog; Ip = presence inferred from presence of host-specific parasites; Is = presence inferred from fossil evidence of other life stages of taxon; X = present based on fossil evidence

Missing ID numbers are intentional. Note plants are aggregated based on reconstructed environmental preferences and statures

TABLE REFERENCES

Armitage, P.D., Pinder, L.C., and Cranston, P.S., eds., 1995, The Chironomidae: Biology and Ecology of Non-biting Midges: Chapman & Hall, London, 572 p.

Ash, S.R., and Tidwell, W.D., 1998, Plant megafossils from the Brushy Basin Member of the Morrison Formation near Montezuma Creek Trading Post, southeastern Utah: Modern Geology, v. 22, p. 321-339.

Bader, K.S., Hasiotis, S.T., and Martin, L.D., 2009, Application of forensic science techniques to trace fossils on dinosaur bones from a quarry in the Upper Jurassic Morrison Formation, northeastern Wyoming: PALAIOS, v. 24, p. 140-158.

Bakker, R.T., 1986, The Dinosaur Heresies: William Morrow and Company, Inc., New York, 165 p.

Bakker, R.T., 1996, The real Jurassic Park: dinosaurs and habitats at Como Bluff, Wyoming, in Morales, M., ed., The Continental Jurassic: Museum of Northern Arizona Bulletin 60, p. 35-49.

Bakker, R.T., 1998, Brontosaur killers: Late Jurassic allosaurids as sabre-tooth cat analogs: Gaia, v. 15, p. 145-158.

Bakker, R.T., and Bir, G., 2004, Dinosaur crime scene investigations: theropod behavior at Como Bluff, Wyoming, and the evolution of birdness: in Currie, P.J., Koppelhus, E.B., Shugar, M.A., and Wright, J.L., eds., Feathered Dragons: Studies on the Transition from Dinosaurs to Birds: Indiana University Press, Bloomington, p. 301-342.

Bohac, J., 1999, Staphylinid beetles as bioindicators: Agriculture, Ecosystems and Environment, v. 74, p. 357-372.

Britt, B.B, and Naylor B.G. 1994, An embryonic Camarasaurus (Dinosauria, Sauropoda) from the Upper Jurassic Morrison Formation (Dry Mesa Quarry, Colorado), in, Carpenter K, Hirsch K.F, and Horner J.R, eds., Dinosaur eggs and babies: Cambridge University Press, Cambridge, p. 256–264.

Britt, B.B., Scheetz, R., Stadtman, K., and Chure, D.J., 2003, Relicts of soft tissue and osteophagous fungi in partially ossified tendons of Ceratosaurus (Theropoda, Dinosauria): Journal of Vertebrate Paleontology, v. 23, supplement to no. 3, p. 36A.

Britt, B.B., Scheetz, R.D., and Dangerfield, A., 2008, A suite of dermestid beetle traces on dinosaur bone from the Upper Jurassic Morrison Formation, Wyoming, USA: Ichnos, v. 15, p. 59-71.

Butler, R.J., Galton, P.M., Porro, L.B., Chiappe, L.M., Henderson, D.M., and Erickson, G.M., 2010, Lower limits of ornithschian dinosaur body size inferred from a new Upper Jurassic heterodontosaurid from North America: Proceedings of the Royal Society B, v. 277, p. 375-381.

Carpenter, K., 1998a, Vertebrate biostratigraphy of the Morrison Formation near Cañon City, Colorado: Modern Geology, v. 23, p. 407-426.

Carpenter, K., 1998b, Armor of Stegosaurus stenops, and the taphonomic history of a new specimen from Garden Park, Colorado: Modern Geology, v. 23, p. 127-144.

Carpenter, K., 2002, Forelimb biomechanics of nonavian theropod dinosaurs in predation: Senckenbergiana Lethaea, v. 82, p. 59-76.

Carpenter, K., 2006, Biggest of the big: a critical re-evaluation of the mega-sauropod Amphicoelias fragillimus: New Mexico Museum of Natural History and Science Bulletin, v. 36, p. 131-138.

Carpenter, K., and Bakker, R.T., 1990, A new latest Jurassic vertebrate fauna, from the highest levels of the Morrison Formation at Como Bluff, Wyoming with comments on Morrison biochronology: Part III the mammals: a new multituberculate and a new paurodont: Hunteria, v. 2, p. 4-19.

Carpenter, K., Unwin, D., Cloward, K., Miles, C., and Miles, C., 2003, A new scaphognathine like pterosaur from the Upper Jurassic Morrison Formation of Wyoming, USA: in Buffetaut, E., and Mazin, J.-M., eds., Evolution and Paleobiology of Pterosaurs: Geological Society of America Special Publication no. 217, p. 45-54.

Carpenter, K., Sanders, F., McWhinney, L.A., and Wood, L., 2005a, Evidence for predator-prey relationships: examples for Allosaurus and Stegosaurus: in Carpenter, K., ed., The Carnivorous Dinosaurs: Indiana University Press, Bloomington, p. 325-350.

Carpenter, K., Miles, C., Ostrom, J.H., and Cloward, K., 2005b, Redescription of the small maniraptoran theropods Ornitholestes and Coelurus from the Upper Jurassic Morrison Formation of Wyoming in Carpenter, K., ed., The Carnivorous Dinosaurs: Indiana University Press, Bloomington, p. 49-71.

Carpenter, K., Miles, C., and Cloward, K., 2005c, New small theropod from the Upper Jurassic Morrison Formation of Wyoming, in Carpenter, K., ed., The Carnivorous Dinosaurs: Indiana University Press, Bloomington, p. 23-48.

Chatterjee, S. and Zheng, Z., 2005, Neuroanatomy and dentition of Camarasaurus lentus, Tidwell, V., and Carpenter, K., eds., Thunder-lizards: The Sauropodomorph Dinosaurs: Indiana University Press, Bloomington, p. 99-211.

Christian, A., and Dzemski, G., 2007, Reconstruction of the cervical skeleton posture of Brachiosaurus brancai Janensch, 1914 by an analysis of the intervertebral stress along the neck and a comparison with the results of different approaches: Fossil Record, v. 10, p. 38-49.

Chure, D.J., and Evans, S.E., 1998, A new occurrence of Cteniogenys, with comments on its distribution and abundance: Modern Geology, v. 23, p. 49-55.
Chure, D., Turner, C., and Peterson, F., 1994, An embryo of Camptosaurus from the Morrison Formation (Jurassic, Middle Tithonian) in Dinosaur National Monument, Utah, in, Carpenter K, Hirsch K.F, and Horner J.R, eds., Dinosaur eggs and babies: Cambridge University Press, Cambridge, p. 298-311.
Chure, D.J., Fiorillo, A.R., and Jacobsen, A., 1998a, Prey bone utilization by predatory dinosaurs in the Late Jurassic of North America, with comments on prey bone use by dinosaurs throughout the Mesozoic: Gaia, v. 15, p. 227-232.
Chure, D.J., Carpenter, K., Litwin, R., Hasiotis, S., and Evanoff, E., 1998b, Appendix. The fauna and flora of the Morrison Formation: Modern Geology, v. 23, p. 507-537.
Chure, D.J., Litwin, R., Hasiotis, S.T., Evanoff, E., and Carpenter, K., 2006, The fauna and flora of the Morrison Formation: 2006: New Mexico Museum of Natural History and Science Bulletin, v. 36, p. 233-249.
Coffman, W.P. and Ferrington Jr., L.C., 1995, Chironomidae, in Merritt, R.W., and Cummins, K.W., eds., An introduction to the aquatic insects of North America: Kendall/Hunt Publishing Company, Dubuque, Iowa, p. 635-754.
Colbert, E.H., 1961, Dinosaurs: their discovery and their world: Dutton, New York, 300 p.
Dodds, K., 2002, Freshwater Ecology: Concepts and Environmental Applications: Academic Press, San Diego, 569 p.
Dodson, P., Behrensmeyer, A.K., Bakker, R.T., and McIntosh, J.S., 1980, Taphonomy and paleoecology of the dinosaur beds of the Jurassic Morrison Formation: Paleobiology, v. 6, p. 208-232.
Dodson, S.L., Cáceres, C.E., and Rogers, D.C., 2010, Cladocera and other Branchiopoda, in Thorp, J.H., and Covich, A.P., eds., Ecology and Classification of North American Freshwater Invertebrates, 3rd ed.: Academic Press, Amsterdam, p. 773-827.
Dunagan, S.P., 1999, A North American freshwater sponge (Eospongilla morrisonensis new genus and species) from the Morrison Formation (Upper Jurassic), Colorado: Journal of Paleontology, v. 73, p. 389-393.
Dunagan, S.P., 2000, Lacustrine carbonates of the Morrison Formation (Upper Jurassic, Western Interior), east-central Colorado, U.S.A., in Geirlowski-Kordesch, E.H., and Kelts, K.R., eds., Lake Basins Through Space and Time: AAPG Studies in Geology, p. 181-188.
Dunagan, S.P., and Turner, C.E., 2004, Regional paleohydrologic and paleoclimatic settings of wetland/lacustrine depositional systems in the Morrison Formation (Upper Jurassic), Western Interior, USA: Sedimentary Geology, v. 167, p. 269-296.
Engelmann, G.F., and Callison, G., 1999, Glirodon grandis, a new multituberculate mammal from the Upper Jurassic Morrison Formation, in Gillette D.D., ed., Vertebrate Paleontology in Utah: Utah Geological Survey, Miscellaneous Publication 99-1, p. 161-177.
Evanoff, E., Good, S.C., and Hanley, J.H., 1998, An overview of the freshwater mollusks from the Morrison Formation (Upper Jurassic, Western Interior, USA): Modern Geology, v. 22, p. 423-450.
Evans, S.E., and Chure, D.J., 1999, Upper Jurassic lizards from the Morrison Formation of Dinosaur National Monument, Utah, in Gillette D.D., ed., Vertebrate Paleontology in Utah: Utah Geological Survey, Miscellaneous Publication 99-1, p. 151-159.
Evans, S.E., and Milner, A.R., 1993, Frogs and salamanders from the Upper Jurassic Morrison Formation (Quarry Nine, Como Bluff) of North America: Journal of Vertebrate Paleontology, v. 13, p. 24-30.
Evans, S.E., Lally, C., Chure, D.C., Elder, A., and Maisano, J.A., 2005, A Late Jurassic salamander (Amphibia: Caudata) from the Morrison Formation of North America: Zoological Journal of the Linnean Society, v. 143, p. 599-616.
Farlow, J.O., 1976, Speculations about the diet and foraging behavior of large carnivorous dinosaurs: American Midland Naturalist, v. 95, p. 186-191.
Farlow, J.O., Thompson, C.V., and Rosner, D.E., 1976, Plates of the dinosaur Stegosaurus: forced convection heat loss fins?: Science, v. 192, p. 1123-1125.
Fastovsky, D.E., and Smith, J.B., 2004, Dinosaur paleoecology, in, Weishampel, D.B., Dodson, P., and Osmólska, H., The Dinosauria, 2nd ed.: University of California Press, Berkeley, p. 614-626.
Fiorillo, A.R., 1991, Dental microwear on the teeth of Camarasaurus and Diplodocus: implications for sauropod paleoecology, in Kielan-Jawowowska, Z., Heintz, N., and Nakrem, H.A., eds., Fifth Symposium on Mesozoic Terrestrial Ecosystsms and Biota: Oslo, Contributions from the Paleontological Museum, University of Oslo, no. 30, p. 23-24.

Fiorillo, A.R., 1998a, Bone modification features on sauropod remains (Dinosauria) from the Freezeout Hills Quarry N (Morrison Formation) of southeastern Wyoming and their contribution to fine-scale paleoenvironmental interpretation: Modern Geology, v. 23, p. 111-126.

Fiorillo, A.R., 1998b, Dental microwear patterns of the sauropod dinosaurs Camarasaurus and Diplodocus: evidence for resource partitioning in the Late Jurassic of North America: Historical Biology, v. 13, p. 1-16.

Foster, J.R., 2003, Paleoecological analysis of the vertebrate fauna of the Morrison Formation (Upper Jurassic), Rocky Mountain Region, U.S.A.: New Mexico Museum of Natural History and Science Bulletin 23: Albuquerque, New Mexico Museum of Natural History and Science, 95 p.

Foster, J.R., 2006, The mandible of a juvenile goniopholidid (Crocodyliformes) from the Morrison Formation (Upper Jurassic) of Wyoming: Bulletin of the New Mexico Museum of Natural History and Science, v. 36, p 101-105.

Foster, J., 2007, Jurassic West: Indiana University Press, Bloomington, 389 p.

Foster, J.R., and Chure, D.J., 2006, Hindlimb allometry in the Late Jurassic theropod dinosaur Allosaurus, with comments on its abundance and distribution: Bulletin of the New Mexico Museum of Natural History and Science, v. 36, p. 119-122.

Foster, J.R., and Lockley, M.G., 2006, The vertebrate ichnological record of the Morrison Formation (Upper Jurassic, North America): Bulletin of the New Mexico Museum of Natural History and Science, v. 36, p. 203-216.

Foster, J.R., and Martin, J.E., 1994, Late Jurassic dinosaur localities in the Morrison Formation of northeastern Wyoming, in Nelson, G.E., ed., The Dinosaurs of Wyoming: Wyoming Geological Association Guidebook, 44th Annual Field Conference, p. 115-126.

Foster, J.R., Trujillo, K.C., Madsen, S.K., and Martin, J.E., 2006, The Late Jurassic mammal Docodon, from the Morrison Formation of the Black Hills, Wyoming: Implications for abundance and biogeography of the genus: Bulletin of the New Mexico Museum of Natural History and Science, v. 36, p. 165-169.

Galton, P.M., 1981, A rhamphorhynchoid pterosaur from the Upper Jurassic of North America: Journal of Paleontology, v. 55, p. 1117-1122.

Galton, P.M., 2006, Teeth of ornithischian dinosaurs (mostly Ornithopoda) from the Morrison Formation (Upper Jurassic) of the western Unites States, in Carpenter, K., ed., Horns and Beaks: Ceratopsian and Ornithopod Dinosaurs: Indiana University Press, Bloomington ,384 p.

Gates, T.A., 2005, The Late Jurassic Cleveland-Lloyd Dinosaur Quarry as a drought-induced assemblage: PALAIOS, v. 20, p. 363-375.

Gee and Tidwell, 2010, A mosaic of characters in a new whole-plant Araucaria, A. delevoryasii Gee sp. nov., from the Late Jurassic Morrison Formation of Wyoming, U.S.A., in Gee, C.T., ed., Plants in Mesozoic Time: Morphological Innovations, Phylogeny, Ecosystems: Indiana University Press, Bloomington, p. 67-96.

Gingerich, P.D., 1973, Molar occlusion and function in the Jurassic mammal Docodon: Journal of Mammalogy, v. 54, p. 1008-1013.

Göhlich, U.B., Chiappe, L.M., Clark, J.M., and Sues, H.-D., 2005, The systematic position of the Late Jurassic alleged dinosaur Macelognathus (Crocodylomorpha: Sphenosuchia): Canadian Journal of Earth Sciences, v. 42, p. 307-321.

Good, S.C., 2004, Paleoenvironmental and paleoclimatic significance of freshwater bivalves in the Upper Jurassic Morrison Formation, Western Interior, USA: Sedimentary Geology, v. 167, p. 163-176.

Gorman, M.A.I., Miller, I.M., Pardo, J.D., and Small, B.J., 2008, Plants, fish, turtles, and insects from the Morrison Formation: a Late Jurassic ecosystem near Cañon City, Colorado, in Raynolds, R.G., ed., Roaming the Rocky Mountains and Environs: Geological Field Trips: Geological Society of America Field Guide: The Geological Society of America, p. 295-310.

Govedich, F.R., Bain, B.A., Moser, W.E., Gelder, S.R., Davies, R.W., and Brinkhurst, R.O., 2010, Annelida (Clitellata): Oligochaeta, Branchiobdellida, Hirudinida, and Acanthobdellida, in Thorp, J.H., and Covich, A.P., eds., Ecology and Classification of North American Freshwater Invertebrates, 3rd ed., Academic Press, Amsterdam, p. 385-436.

Harris, J.D., and Carpenter, K., 1996, A large pterodactyloid from the Morrison Formation (Late Jurassic) of Garden Park, Colorado: Neues Jahrbuch der Geologie, Paläontologie, Montash, v. 8, p. 473-484.

Harris, J.D., and Dodson, P., 2004, A new diplodocid sauropod dinosaur from the Upper Jurassic Morrison Formation of Montana, USA: Acta Palaeontologica Polonica, v. 49, p. 197-210.

Hasiotis, S.T., 1998, Continental trace fossils as the key to understanding Jurassic terrestrial and freshwater ecosystems: Modern Geology, v. 22, p. 451-459.

Hasiotis, S.T., 2004, Reconnaissance of Upper Jurassic Morrison Formation ichnofossils, Rocky Mountain Region, USA: paleoenvironmental, stratigraphic, and paleoclimatic significance of terrestrial and freshwater ichnocoenoses: Sedimentary Geology, v. 167, p. 177-268.

Hasiotis, S.T., Kirkland, J.I., and Callison, G., 1998a, Crayfish fossils and burrows from the Upper Jurassic Morrison Formation of western Colorado: Modern Geology, v. 22, p. 481-491.

Hasiotis, S.T., Kirkland, J.I., Windscheffel, G.W., and Safris, C., 1998b, Fossil caddisfly cases (Insecta: Trichoptera), Upper Jurassic Morrison Formation, Fruita Paleontological Area, Colorado: Modern Geology, v. 22, p. 493-502.

Hasiotis, S.T., Fiorillo, A.R., and Hanna, R.R., 1999, Preliminary report on borings in Jurassic dinosaur bones: Evidence for invertebrate-vertebrate interactions, in Gillette, D. G., ed., Vertebrate paleontology in Utah: Miscellaneous Publication – Utah Geological Survey, 99-1; p. 193–200.

Henderson, D.M., 1998, Skull and tooth morphology as indicators of niche partitioning in sympatric Morrison Formation theropods: Gaia, v. 15, p. 219-226.

Henrici, A.C., 1998, New anurans from the Rainbow Park microsite, Dinosaur National Monument, Utah: Modern Geology, v. 23, p. 1-16.

Hölldobler, B., and Wilson, E.O., 1990, The Ants: Belknap Press of Harvard University Press, Cambridge, 732 p.

Hoff, K.vS., Blaustein, A.R., McDiarmid, R.W., and Altig, R., 1999, Behavior: Interactions and their consequences, in McDiarmid, R.W., and Altig, R., eds., Tadpoles: the Biology of Anuran Larvae: University of Chicago Press, Chicago, p. 215-239.

Hori, M., 1982, The biology and population dynamics of the tiger beetle Cicindela japonica (Thunberg): Physiology and Ecology Japan, v. 19, p. 77-212.

Hotton, C.L., and Baghai-Riding, N.L., 2010, Palynological evidence for conifer dominance within a heterogeneous landscape in the Late Jurassic Morrison Formation, U.S.A., in Gee, C.T., ed., Plants in Mesozoic Time: Morphological Innovations, Phylogeny, Ecosystems: Indiana University Press, Bloomington, p. 294-328.

Huner, J., 1994, Freshwater Crayfish Aquaculture in North America, Europe, and Australia: Families Astacidae, Cambaridae, and Parastacidae: Food Products Press, Binghamton, New York, 336 p.

Ikejiri, T., Watkins, P.S., and Gray, D.J., 2006, Stratigraphy, sedimentology, and taphonomy of a sauropod quarry from the Upper Jurassic Morrison Formation of Thermopolis, central Wyoming: New Mexico Museum of Natural History and Science Bulletin, v. 36, p. 39-46.

Jennings, D.S., and Hasiotis, S.T., 2006, Taphonomic analysis of a dinosaur feeding site using geographic information systems (GIS), Morrison Formation, southern Bighorn Basin, Wyoming, USA: PALAIOS, v. 21, p. 480-492.

Jennings, D.S., Platt, B.F., and Hasiotis, S.T., 2006, Distribution of vertebrate trace fossils, Upper Jurassic Morrison Formation, Bighorn Basin, Wyoming, USA: implications for differentiating paleoecological and preservational bias: New Mexico Museum of Natural History and Science Bulletin, v. 36, p.183-192.

Jensen, J.A., and Ostrom, J.H., 1977, A second Jurassic pterosaur from North America: Journal of Paleontology, v. 51, p. 867-870.

Kaufmann, T., and Stansly, P., 1979, Bionomics of Neoheterocerus pallidus Say (Coleoptera: Heteroceridae) in Oklahoma: Journal of the Kansas Entomological Society, v. 52, p. 565-577.

Kielan-Jawaoroska, Z., Cifelli, R.L., and Luo, Z.-X., 2004, Mammals from the Age of Dinosaurs: Columbia University Press, New York, 630 p.

King, L.R., Foster, J.R., Scheetz, R.D., 2006, New pterosaur specimens from the Morrison Formation and a summary of the Late Jurassic pterosaur record of the Rocky Mountain region: New Mexico Museum of Natural History and Science Bulletin, v. 36, p.109-113.

Kirkland, J.I., 1987, Upper Jurassic and Cretaceous lungfish tooth plates from the Western Interior, the last dipnoan faunas of North America: Hunteria, v. 2, p. 1-16.

Kirkland, J.I., 1996, Predation of dinosaur nests by terrestrial crocodilians, in Carpenter, K., Hirsch, K.F., and Horner, J.R., eds., Dinosaur Eggs and Babies: Cambridge University Press, New York, p. 124-133.

Kirkland, J.I., 1998, Morrison Fishes: Modern Geology, v. 22, p. 503-533.

Kirkland, J.I., 2006, Fruita Paleontological Area (Upper Jurassic, Morrison Formation), western Colorado: an example of terrestrial taphofacies analysis: New Mexico Museum of Natural History and Science Bulletin, v. 36, p. 57-65.

Kirkland, J.I., and Carpenter, K., 1994, North America's first pre-Cretaceous ankylosaur (Dinosauria) from the Upper Jurassic Morrison Formation of western Colorado: Brigham Young University Geology Studies, v. 40, p. 25-42.

Kirkland, J.I., Carpenter, K., Hunt, A.P., and Scheetz, R.D., 1998, Ankylosaur (Dinosauria) specimens from the Upper Jurassic Morrison Formation: Modern Geology, v. 23, p. 145-177.
Labandeira, C.C., 2002, Paleobiology of predators, parasitoids, and parasites: death and accomodation in the fossil record of continental invertebrates, in Kowalewski, M., and Kelley, P.H., eds., The Fossil Record of Predation: The Paleontological Society Papers, v. 8, p. 211-250.
Large, M.F., and Braggins, J.E., 2004, Tree Ferns: Timber Press, Portland, 360 p.
Litwin, R.J., Turner, C.E., and Peterson, F., 1998, Palynological evidence on the age of the Morrison Formation, Western Interior U.S.: Modern Geology, v. 22, p. 297-319.
Lockley, M.G., and Hunt, A.P., 1998, A probable stegosaur track from the Morrison Formation of Utah: Modern Geology, v. 23, p. 331-342.
Lövei, G.L., and Sunderland, K.D., 1996, Ecology and behavior of ground beetles (Coleoptera: Carabidae): Annual Reviews of Entomology, v. 41, p. 231-256.
Lucas, S.G., and Kirkland, J.I., 1998, Preliminary report on conchostraca from the Upper Jurassic Morrison Formation, western United States: Modern Geology, v. 22, p. 415-422.
Lucas, S.G., Rhinehart, L.F., and Heckert, A.B., 2006, Glyptops (Testudines, Pleurosternidae) from the Upper Jurassic Morrison Formation, New Mexico: New Mexico Museum of Natural History and Science Bulletin, v. 36, p. 97-99.
Luo, Z.-X., and Wible, J.R., 2005, A Late Jurassic digging mammal and early mammalian diversification: Science, v. 308, p. 103-107.
Madsen J.H.,Jr., 1976, Allosaurus fragilis: A Revised Osteology: Utah Geological Survey, 163 p.
Marsh, O.C., 1878, New pterodactyl from the Jurassic of the Rocky Mountains: American Journal of Science, v. 16, p. 233-234.
Marsh, O.C., 1881, Discovery of a fossil bird in the Jurassic of Wyoming: American Journal of Science, v. 21, p. 341-342.
Molnar, R.E., and Clifford, T., 2000, Gut contents of a small ankylosaur: Journal of Vertebrate Paleontology, v. 20, p. 194-196.
Myers, T.S., and Storrs, G.W., 2007, Taphonomy of the Mother's Day Quarry, Upper Jurassic Morrison Formation, south-central Montana, USA: PALAIOS, v. 22, p. 651-666.
Ostrom, J.H., 1971, On the systematic position of Macelognathus vagans: Postilla, v. 153, p. 1-10.
Ostrom, J.H., 1986, The Jurassic "bird" Laopteryx priscus re-examined: Contributions to Geology, University of Wyoming, Special Paper, v. 3, p. 11-19.
Pardo, J.D., Huttenlocker, A.K., Small, B.J., and Gorman, M.A.I., 2010, The cranial morphology of a new genus of lungfish (Osteichthyes: Dipnoi) from the Upper Jurassic Morrison Formation of North America: Journal of Vertebrate Paleontology, v. 30, p. 1352-1359.
Parrish, J.T., Peterson, F., and Turner, C.E., 2004, Jurassic “savannah”—plant taphonomy and climate of the Morrison Formation (Upper Jurassic, Western USA): Sedimentary Geology, v. 167, p. 137-162.
Pearson, D.L. and Vogler, A.P., 2001, Tiger Beetles: The Evolution, Ecology, and Diversity of the Cicindelids: Cornell University Press, Ithaca, 333 p.
Prothero, D.R., 1981, New Jurassic mammals from Como Bluff, Wyoming, and the interrelationships of non-tribosphenic Theria: Bulletin of the American Museum of Natural History, v. 167, p. 277-326.
Raven, P.H., Evert, Ray F., and Eichhorn, S.E., 1999, Biology of Plants, 6th ed.: W.H. Freeman, New York, 944 p.
Rayfield, E.J., Norman, D.B., Horner, C.C., Horner, J.R., Smith, P.M., Thomason, J., and Upchurch, P., 2001, Cranial design and function in a large theropod dinosaur: Nature, v. 409, p. 1033-1037.
Reichel, M., 2010, A model for the bite mechanics in the herbivorous dinosaur Stegosaurus (Ornithischia, Stegosauridae): Swiss Journal of Geosciences, v. 103, p. 235-240.
Reiswig, H.M., Frost, T.M., and Ricciardi, A., 2010, Porifera, in Thorp, J.H., and Covich, A.P., eds., Ecology and Classification of North American Freshwater Invertebrates, 3rd ed., Academic Press, Amsterdam, p. 91-123.
Royer, D.L., Hickey. L.J., and Wing, S.L., 2003, Ecological conservatism in the "living fossil" Ginkgo: Paleobiology, v. 29, p. 84-104
Sames, B., Whatley, R., and Schudack, M.E., 2010, Praecypridea: a new non-marine ostracod genus from the Jurassic and Early Cretaceous of Europe, North and South America, and Africa: Journal of Micropalaeontology, v. 29, p. 163-176.
Schudack, M.E., Turner, C.E., and Peterson, F., 1998, Biostratigraphy, paleoecology and biogeography of charophytes and ostracodes from the Upper Jurassic Morrison Formation, Western Interior, USA: Modern Geology, v. 22, p. 379-414.

Sheath, R.G., and Hambrook, J.A., 1990, Freshwater Ecology, in Cole, K.M., and Sheath, R.G., eds., Biology of the Red Algae: Cambridge University Press, Cambridge, p. 423-454.
Slack, H.D., 1936, The food of caddis fly (Trichoptera) larvae: Journal of Animal Ecology, v. 5, p. 105-115.
Smith, A.J., and Delorme, L. D., 2010, Ostracoda, in Thorp, J.H., and Covich, A.P., eds., Ecology and Classification of North American Freshwater Invertebrates, 3rd ed.: Academic Press, Amsterdam, p. 725-771.
Smith, D.K., Sanders, R.K., and Stadtman, K.L., 2004, New material of Mesadactylus ornithosphyos, a primitive pterodactyloid pterosaur from the Upper Jurassic of Colorado: Journal of Vertebrate Paleontology, v. 24, p. 850-856.
Smith, D.M., Gorman, M.A.I., Pardo, J.D., and Small, B.J., 2011, First fossil orthoptera from the Jurassic of North America: Journal of Paleontology, v. 85, p. 102-105.
Stevens, K.A., and Parrish, J.M., 1999, Neck posture and feeding behavior of two Jurassic sauropod dinosaurs: Science, v. 284, p. 798-800.
Stevens, K.A., and Parrish, J.M., 2005, Digital reconstructions of sauropod dinosaurs and implications for feeding, in Curry Rogers, K.A., and Wilson, J.A. eds., The Sauropods: Evolution and Paleobiology: University of California Press, Berkeley, p. 178-200.
Taylor, T.N., Taylor, E.L., and Krings, M., 2009, Paleobotany: the Biology and Evolution of Fossil Plants: Elsevier, Amsterdam, 1230 p.
Therrien, F., Henderson, D.M., and Ruff, C.B., 2005, Bite me: biomechanical models of theropod mandibles and implications for feeding behavior, in Carpenter, K., ed., The Carnivorous Dinosaurs: Indiana University Press, Bloomington, p. 179-237.
Thorp, J.P., and Covich, A.P., 2001, Ecology and Classification of North American Freshwater Invertebrates: Academic Press, San Diego, 1038 p.
Tidwell, W.D., 1990, Preliminary report on the megafossil flora of the Upper Jurassic Morrison Formation: Hunteria, v. 2, p. 3-12.
Tidwell W.D., and Ash, S.R., 1990, On the Upper Jurassic stem Hermanophyton and its species from Colorado and Utah, USA: Palaeontolographica Abteilung B. v, 218, p. 77-92.
Tidwell, W.D., Connely, M., and Britt, B.B., 2006, A flora from the base of the Upper Jurassic Morrison Formation near Como Bluff, Wyoming, USA: New Mexico Museum of Natural History and Science Bulletin, v. 36, p. 171-181.
Traniello, J.F.A., and Leuthold, R.H., 2000, Behavior and ecology of foraging in termites, in Abe, T., Bignell, D.E., and Higashi, M., eds., Termites: Evolution, Sociality, Symbioses, Ecology: Kluwer Academic Publishers, Dordrecht, Netherlands, p. 141-168.
Turner, C.E., and Peterson, F., 1999, Biostratigraphy of dinosaurs in the Upper Jurassic Morrison of the Western Interior, U.S.A., in Gillette, D.D., ed., Vertebrate Paleontology in Utah: Utah Geological Survey Miscellaneous Publication 99-1, p. 77-114.
Van Valkenburgh, B., and Molnar, R.E., 2002, Dinosaurian and mammalian predators compared: Paleobiology, v. 28, p. 527-543.
Walker, A.D., 1970, A revision of the Jurassic reptile Hallopus victor (Marsh), with remarks on the classification of crocodiles: Philosophical Transactions of the Royal Society of London. Series B, v. 257, p. 323-372.
Walls, G.Y., 1981, Feeding ecology of the tuatara (Sphenodon punctatus) on Stephens Island, Cook Strait: New Zealand Journal of Ecology, v. 4, p. 89-97.
Walls, E.A., Berkson, J., and Smith, S.A., 2002, The horseshoe crab, Limulus polyphemus: 200 millions years of existence, 100 years of study: Reviews in Fisheries Science, v. 10, p. 39-73.
Weishampel, D.B., 1984, Interactions between Mesozoic plants and vertebrates: fructifications and seed predation: Neues Jahrbuch für Geologie und Palaeontologie, Abhandlungen, v. 167, p. 224-250.
Weaver, J.C., 1983, The improbable endotherm: the energetics of the sauropod dinosaur Brachiosaurus: Paleobiology, v. 9, p. 173-182.
Wesley, A., 1973, Jurassic Plants, in Hallam, A., ed., Atlas of Paleobiography: Elsevier, Amsterdam, p. 329-338.
White, J., and Strehl, C., 1978, Xylem feeding by periodical cicada nymphs on tree roots: Ecological Entomology, v. 3, p. 323-327.
Wiggins, G.B., 2005, Caddisflies: The Underwater Architects: University of Toronto Press, Toronto, 300 p.

Table E8.—WE consumer-resource list for biozone 1. See Table E7 for master list of taxonomic ID numbers.

PredatorID	PreyID
20	6
21	3
21	4
22	6
24	6
26	1
26	3
26	7
26	21
27	2
28	26
28	28
29	1
29	6
29	7
30	4
30	6
31	1
31	3
31	6
31	7
31	8
31	9
31	11
31	20
31	21
31	27
31	28
31	29
31	30
31	31
31	33
31	35
31	39
31	40
32	22
32	31
33	6
35	1
35	6
35	7
35	8
35	11
35	20
35	29
35	30
37	12
37	13
37	14
37	15
37	16
37	17
38	12
38	13
38	14
38	15
38	16
38	17
38	18
38	19
39	2
40	1
40	2
40	6
41	2
41	9
41	12
41	13
41	14
41	37
41	38
41	39
41	40
41	41
41	42
41	43
41	44
41	45
41	46
41	47
41	50
41	52
42	37
42	38
42	39
42	40
42	41
42	42
42	43
42	44
42	45
42	46
42	47
42	50
42	52
43	2
44	15
44	18
45	112
45	113
45	131
45	132
45	141
45	142
45	147
45	148
45	151
45	155
45	156
46	37
46	38
46	39
46	40
46	41
46	42
46	43
46	44
46	45
46	46
46	47

PredatorID	PreyID
46	50
46	52
47	37
47	38
47	39
47	40
47	41
47	42
47	43
47	44
47	45
47	46
47	47
47	50
47	52
50	15
50	16
50	17
50	18
50	19
51	12
51	13
51	14
51	15
51	16
51	17
51	18
51	19
52	12
52	13
52	14
52	15
52	16
52	17
52	18
52	19
53	53
53	29
53	30
53	31
53	35
53	33

PredatorID	PreyID
53	21
54	54
54	29
54	31
54	35
54	33
77	8
77	11
77	22
77	24
77	26
77	27
77	28
77	31
77	33
77	35
77	37
77	38
77	39
77	40
77	41
77	42
77	43
77	45
77	46
77	47
77	52
77	53
77	54
81	8
81	11
81	22
81	24
81	26
81	27
81	28
81	31
81	33
81	35
81	37
81	38
81	39

PredatorID	PreyID
81	40
81	41
81	42
81	43
81	45
81	46
81	47
81	52
81	53
81	54
101	31
101	32
101	53
101	54
101	77
101	81
101	101
101	109
101	113
101	158
109	27
109	31
109	37
109	38
109	39
109	40
109	41
109	42
109	43
109	44
109	45
109	46
109	47
109	52
109	53
109	54
112	77
112	81
112	101
112	109
112	112
112	113

PredatorID	PreyID
112	131
112	132
112	141
112	142
112	147
112	148
112	151
112	155
112	156
112	184
112	185
113	37
113	38
113	39
113	40
113	41
113	42
113	43
113	45
113	46
113	47
113	50
113	52
113	77
113	81
113	101
113	109
113	112
113	113
113	131
113	132
113	141
113	142
113	147
113	148
113	151
113	155
113	156
113	158
113	184
113	185
131	15

PredatorID	PreyID
131	16
131	17
132	12
132	13
132	14
132	16
132	17
141	12
141	13
141	14
141	15
141	16
141	17
142	12
142	13
142	14
142	16
142	17
147	9
147	13
147	14
147	16
147	17
148	9
148	13
148	14
148	16
148	17
151	9
151	13
151	14
151	16
151	17
155	12
155	13
155	14
155	16
155	17
156	12
156	13
156	14
156	16

PredatorID	PreyID
156	17
158	11
158	31
158	32
158	33
158	35
158	37
158	38
158	39
158	40
158	41
158	42
158	43
158	44
158	45
158	46
158	47
158	50
158	51
158	52
184	9
184	12
184	13
184	14
185	37
185	38
185	39
185	40
185	41
185	42
185	43
185	45
185	46
185	47
185	50
185	52

Table E9.—WE consumer-resource list for biozone 1. See Table E7 for master list of taxonomic ID numbers.

PredatorID	PreyID
20	6
21	3
21	4
22	6
24	6
26	1
26	3
26	7
26	21
27	2
28	26
28	28
29	1
29	6
29	7
30	4
30	6
31	1
31	3
31	6
31	7
31	8
31	9
31	11
31	20
31	21
31	27
31	28
31	29
31	30
31	31
31	33
31	35
31	39
31	40
32	22
32	31
33	6
35	1
35	6
35	7
35	8
35	11
35	20
35	29
35	30
37	12
37	13
37	14
37	15
37	16
37	17
38	12
38	13
38	14
38	15
38	16
38	17
38	18
38	19
39	2
40	1
40	2
40	6
41	2
41	9
41	12
41	13
41	14
41	37
41	38
41	39
41	40
41	41
41	42
41	43
41	44
41	45
41	46
41	47
41	50
41	52
42	37
42	38
42	39
42	40
42	41
42	42
42	43
42	44
42	45
42	46
42	47
42	50
42	52
43	2
44	15
44	18
45	112
45	113
45	114
45	115
45	119
45	120
45	121
45	122
45	123
45	127
45	128
45	129
45	130
45	131
45	132
45	133
45	134
45	135
45	136
45	137
45	138
45	147

PredatorID	PreyID
45	150
45	153
45	155
45	156
46	37
46	38
46	39
46	40
46	41
46	42
46	43
46	44
46	45
46	46
46	47
46	50
46	52
47	37
47	38
47	39
47	40
47	41
47	42
47	43
47	44
47	45
47	46
47	47
47	50
47	52
50	15
50	16
50	17
50	18
50	19
51	12
51	13
51	14
51	15
51	16
51	17
51	18

PredatorID	PreyID
51	19
52	12
52	13
52	14
52	15
52	16
52	17
52	18
52	19
57	20
57	27
57	28
57	29
57	30
57	33
57	35
57	57
57	64
57	72
61	11
61	22
61	26
61	31
61	57
61	62
61	64
61	72
62	11
62	20
62	27
62	28
62	29
62	30
62	31
62	33
62	35
62	40
62	72
64	33
64	35
64	37
64	38

PredatorID	PreyID
64	39
64	40
64	41
64	42
64	43
64	45
64	46
64	47
64	50
64	52
64	62
64	64
64	72
64	73
64	76
64	77
64	78
72	1
72	6
72	7
73	20
73	27
73	28
73	29
73	30
73	33
73	35
73	39
73	40
73	72
76	20
76	27
76	28
76	29
76	30
76	33
76	35
76	39
76	40
76	41
76	42
76	43

PredatorID	PreyID
76	45
76	46
76	72
77	8
77	11
77	22
77	24
77	26
77	27
77	28
77	31
77	33
77	35
77	37
77	38
77	39
77	40
77	41
77	42
77	43
77	45
77	46
77	47
77	52
77	62
77	64
77	72
77	73
77	76
77	77
77	78
78	8
78	11
78	22
78	24
78	26
78	27
78	28
78	31
78	33
78	35
78	37

PredatorID	PreyID
78	38
78	39
78	40
78	41
78	42
78	43
78	45
78	46
78	47
78	52
78	62
78	64
78	72
78	73
78	76
78	77
78	78
81	8
81	11
81	22
81	24
81	26
81	27
81	28
81	31
81	33
81	35
81	37
81	38
81	39
81	40
81	41
81	42
81	43
81	45
81	46
81	47
81	52
81	62
81	64
81	72
81	73

PredatorID	PreyID
81	76
81	77
81	78
82	26
82	27
82	31
82	37
82	38
82	39
82	40
82	41
82	42
82	43
82	44
82	45
82	46
82	47
82	50
82	51
82	52
82	73
82	76
82	77
82	78
82	86
82	95
85	9
85	12
85	13
85	14
85	73
85	76
85	77
85	78
85	86
85	95
86	27
86	37
86	38
86	39
86	40
86	41

PredatorID	PreyID
86	42
86	43
86	44
86	45
86	46
86	47
86	50
86	73
86	76
86	77
86	78
95	27
95	37
95	38
95	39
95	40
95	41
95	42
95	43
95	44
95	45
95	46
95	47
95	50
95	73
95	76
95	77
95	78
98	73
98	76
98	77
98	78
98	81
98	82
98	86
98	95
98	98
98	100
98	101
98	158
98	160
98	161

PredatorID	PreyID
98	180
98	181
98	184
98	185
99	22
99	24
99	26
99	31
99	32
99	57
99	61
99	62
99	64
99	73
99	76
99	77
99	78
99	81
99	82
99	85
99	86
99	95
99	98
99	99
99	100
99	101
99	108
99	110
99	112
99	113
99	114
99	115
99	119
99	120
99	121
99	122
99	123
99	127
99	128
99	129
99	130
99	131

PredatorID	PreyID
99	132
99	133
99	134
99	135
99	136
99	137
99	138
99	147
99	150
99	153
99	155
99	156
99	158
99	160
99	161
99	180
99	181
100	27
100	28
100	31
100	33
100	35
100	37
100	38
100	39
100	40
100	41
100	42
100	43
100	45
100	46
100	47
100	50
100	52
100	62
100	64
100	72
100	73
100	76
100	77
100	78
101	31

PredatorID	PreyID
101	32
101	57
101	62
101	64
101	73
101	76
101	77
101	78
101	81
101	82
101	85
101	86
101	95
101	98
101	100
101	101
101	108
101	110
101	113
101	114
101	115
101	153
101	158
101	160
101	161
101	180
101	181
108	27
108	31
108	32
108	37
108	38
108	39
108	40
108	41
108	42
108	43
108	44
108	45
108	46
108	47
108	52

PredatorID	PreyID
108	62
108	72
108	73
108	76
108	77
108	78
110	27
110	31
110	37
110	38
110	39
110	40
110	41
110	42
110	43
110	44
110	45
110	46
110	47
110	52
110	62
110	72
110	73
110	76
110	77
110	78
112	64
112	77
112	78
112	81
112	82
112	85
112	86
112	98
112	99
112	100
112	101
112	108
112	110
112	112
112	113
112	114

PredatorID	PreyID
112	115
112	119
112	120
112	121
112	122
112	123
112	127
112	128
112	129
112	130
112	131
112	132
112	133
112	134
112	135
112	136
112	137
112	138
112	147
112	150
112	153
112	155
112	156
112	184
112	185
113	37
113	38
113	39
113	40
113	41
113	42
113	43
113	45
113	46
113	47
113	50
113	52
113	73
113	76
113	77
113	78
113	81

PredatorID	PreyID
113	82
113	85
113	86
113	95
113	98
113	99
113	100
113	101
113	108
113	110
113	112
113	113
113	114
113	115
113	119
113	120
113	121
113	122
113	123
113	127
113	128
113	129
113	130
113	131
113	132
113	133
113	134
113	135
113	136
113	137
113	138
113	147
113	150
113	153
113	155
113	156
113	158
113	160
113	161
113	180
113	181
113	184

PredatorID	PreyID
113	185
114	61
114	64
114	77
114	78
114	81
114	82
114	85
114	86
114	98
114	99
114	100
114	101
114	108
114	110
114	112
114	113
114	114
114	115
114	119
114	120
114	121
114	122
114	123
114	127
114	128
114	129
114	130
114	131
114	132
114	133
114	134
114	135
114	136
114	137
114	138
114	147
114	150
114	153
114	155
114	156
114	184

PredatorID	PreyID
114	185
115	31
115	32
115	37
115	38
115	39
115	40
115	41
115	42
115	43
115	45
115	46
115	47
115	50
115	52
115	61
115	62
115	64
115	73
115	76
115	77
115	78
115	81
115	82
115	85
115	86
115	95
115	98
115	99
115	100
115	101
115	108
115	110
115	112
115	113
115	114
115	115
115	119
115	120
115	121
115	122
115	123

PredatorID	PreyID
115	127
115	128
115	129
115	130
115	131
115	132
115	133
115	134
115	135
115	136
115	137
115	138
115	147
115	150
115	153
115	155
115	156
115	158
115	160
115	161
115	180
115	181
115	184
115	185
119	73
119	76
119	77
119	78
119	81
119	82
119	85
119	86
119	95
119	98
119	100
119	101
119	108
119	110
119	113
119	114
119	115
119	119

PredatorID	PreyID
119	120
119	121
119	122
119	123
119	128
119	130
119	132
119	134
119	136
119	138
119	153
119	155
119	158
119	160
119	161
119	180
119	181
119	184
119	185
120	32
120	73
120	76
120	77
120	78
120	81
120	82
120	85
120	86
120	95
120	98
120	100
120	101
120	110
120	113
120	114
120	115
120	153
120	158
120	160
120	161
120	180
120	181

PredatorID	PreyID
120	184
120	185
121	32
121	73
121	76
121	77
121	78
121	81
121	82
121	85
121	86
121	95
121	98
121	100
121	101
121	110
121	113
121	114
121	115
121	153
121	158
121	160
121	161
121	180
121	181
121	184
121	185
122	32
122	73
122	76
122	77
122	78
122	81
122	82
122	85
122	86
122	95
122	98
122	100
122	101
122	110
122	113

PredatorID	PreyID
122	114
122	115
122	153
122	158
122	160
122	161
122	180
122	181
122	184
122	185
123	77
123	78
123	81
123	82
123	85
123	86
123	95
123	100
123	101
123	108
123	110
123	113
123	114
123	115
123	119
123	120
123	121
123	122
123	123
123	128
123	130
123	132
123	134
123	136
123	138
123	153
123	155
123	158
123	160
123	161
123	180
123	181

PredatorID	PreyID
123	184
123	185
127	15
127	18
127	19
128	12
128	13
128	14
128	16
128	17
129	15
129	16
129	17
130	12
130	13
130	14
130	16
130	17
131	15
131	16
131	17
132	12
132	13
132	14
132	16
132	17
133	12
133	13
133	14
133	15
133	16
133	17
134	12
134	13
134	14
134	16
134	17
135	12
135	13
135	14
135	15
135	16

PredatorID	PreyID
135	17
136	12
136	13
136	14
136	16
136	17
137	12
137	13
137	14
137	15
137	16
137	17
138	12
138	13
138	14
138	16
138	17
147	9
147	13
147	14
147	16
147	17
150	9
150	13
150	14
150	16
150	17
153	12
153	13
153	14
155	12
155	13
155	14
155	16
155	17
156	12
156	13
156	14
156	16
156	17
158	11
158	31

PredatorID	PreyID
158	32
158	33
158	35
158	37
158	38
158	39
158	40
158	41
158	42
158	43
158	44
158	45
158	46
158	47
158	50
158	51
158	52
158	73
158	76
158	77
158	78
158	86
160	12
160	13
160	14
160	27
160	37
160	38
160	39
160	40
160	41
160	42
160	43
160	44
160	45
160	46
160	50
160	52
161	12
161	13
161	14
161	27

PredatorID	PreyID
161	37
161	38
161	39
161	40
161	41
161	42
161	43
161	44
161	45
161	46
161	50
161	52
180	27
180	37
180	38
180	39
180	40
180	41
180	42
180	43
180	44
180	45
180	46
180	50
181	27
181	37
181	38
181	39
181	40
181	41
181	42
181	43
181	44
181	45
181	46
181	50
184	9
184	12
184	13
184	14
185	37
185	38

PredatorID	PreyID
185	39
185	40
185	41
185	42
185	43
185	45
185	46
185	47
185	50
185	52

Table E10.—WE consumer-resource list for biozone 3. See Table E7 for master list of taxonomic ID numbers.

PredatorID	PreyID
20	6
21	3
21	4
22	6
24	6
26	1
26	3
26	7
26	21
27	2
28	26
28	28
29	1
29	6
29	7
30	4
30	6
31	1
31	3
31	6
31	7
31	8
31	9
31	11
31	20
31	21
31	27
31	28
31	29
31	30
31	31
31	33
31	35
31	39
31	40
32	22
32	31
33	6
35	1
35	6
35	7
35	8
35	11
35	20
35	29
35	30
37	12
37	13
37	14
37	15
37	16
37	17
38	12
38	13
38	14
38	15
38	16
38	17
38	18
38	19
39	2
40	1
40	2
40	6
41	2
41	9
41	12
41	13
41	14
41	37
41	38
41	39
41	40
41	41
41	42
41	43
41	44
41	45
41	46
41	47
41	50
41	52
42	37
42	38
42	39
42	40
42	41
42	42
42	43
42	44
42	45
42	46
42	47
42	50
42	52
43	2
45	112
45	113
45	114
45	115
45	117
45	118
45	121
45	123
45	127
45	128
45	129
45	130
45	131
45	132
45	133
45	134
45	135
45	136
45	137
45	138
45	139
45	140
45	147
45	153

PredatorID	PreyID
45	155
45	156
46	37
46	38
46	39
46	40
46	41
46	42
46	43
46	44
46	45
46	46
46	47
46	50
46	52
47	37
47	38
47	39
47	40
47	41
47	42
47	43
47	44
47	45
47	46
47	47
47	50
47	52
50	15
50	16
50	17
50	18
50	19
51	12
51	13
51	14
51	15
51	16
51	17
51	18
51	19
52	12

PredatorID	PreyID
52	13
52	14
52	15
52	16
52	17
52	18
52	19
57	20
57	27
57	28
57	29
57	30
57	33
57	35
57	57
61	11
61	22
61	26
61	31
61	57
61	62
62	11
62	20
62	27
62	28
62	29
62	30
62	31
62	33
62	35
62	40
77	8
77	11
77	22
77	24
77	26
77	27
77	28
77	31
77	33
77	35
77	37

PredatorID	PreyID
77	38
77	39
77	40
77	41
77	42
77	43
77	45
77	46
77	47
77	52
77	62
78	8
78	11
78	22
78	24
78	26
78	27
78	28
78	31
78	33
78	35
78	37
78	38
78	39
78	40
78	41
78	42
78	43
78	45
78	46
78	47
78	52
78	62
81	8
81	11
81	22
81	24
81	26
81	27
81	28
81	31
81	33

PredatorID	PreyID
81	35
81	37
81	38
81	39
81	40
81	41
81	42
81	43
81	45
81	46
81	47
81	52
81	62
82	26
82	27
82	31
82	37
82	38
82	39
82	40
82	41
82	42
82	43
82	44
82	45
82	46
82	47
82	50
82	51
82	52
82	86
85	9
85	12
85	13
85	14
85	86
86	27
86	37
86	38
86	39
86	40
86	41

PredatorID	PreyID
86	42
86	43
86	44
86	45
86	46
86	47
86	50
99	22
99	24
99	26
99	31
99	32
99	57
99	61
99	62
99	77
99	78
99	81
99	82
99	85
99	86
99	99
99	100
99	112
99	113
99	114
99	115
99	117
99	118
99	121
99	123
99	127
99	128
99	129
99	130
99	131
99	132
99	133
99	134
99	135
99	136
99	137

PredatorID	PreyID
99	138
99	139
99	140
99	147
99	153
99	155
99	156
99	158
99	161
99	180
99	181
99	147
99	153
99	155
99	156
99	158
99	161
99	180
99	181
100	27
100	28
100	31
100	33
100	35
100	37
100	38
100	39
100	40
100	41
100	42
100	43
100	45
100	46
100	47
100	50
100	52
100	62
112	77
112	78
112	81
112	82
112	85

PredatorID	PreyID
112	86
112	99
112	100
112	112
112	113
112	114
112	115
112	117
112	118
112	121
112	123
112	127
112	128
112	129
112	130
112	131
112	132
112	133
112	134
112	135
112	136
112	137
112	138
112	139
112	140
112	147
112	153
112	155
112	156
112	184
112	185
113	37
113	38
113	39
113	40
113	41
113	42
113	43
113	45
113	46
113	47
113	50

PredatorID	PreyID
113	52
113	77
113	78
113	81
113	82
113	85
113	86
113	99
113	100
113	112
113	113
113	114
113	115
113	117
113	118
113	121
113	123
113	127
113	128
113	129
113	130
113	131
113	132
113	133
113	134
113	135
113	136
113	137
113	138
113	139
113	140
113	147
113	153
113	155
113	156
113	158
113	161
113	180
113	181
113	184
113	185
114	61

PredatorID	PreyID
114	77
114	78
114	81
114	82
114	85
114	86
114	99
114	100
114	112
114	113
114	114
114	115
114	117
114	118
114	121
114	123
114	127
114	128
114	129
114	130
114	131
114	132
114	133
114	134
114	135
114	136
114	137
114	138
114	139
114	140
114	147
114	153
114	155
114	156
114	184
114	185
115	31
115	32
115	37
115	38
115	39
115	40

PredatorID	PreyID
115	41
115	42
115	43
115	45
115	46
115	47
115	50
115	52
115	61
115	62
115	77
115	78
115	81
115	82
115	85
115	86
115	99
115	100
115	112
115	113
115	114
115	115
115	117
115	118
115	121
115	123
115	127
115	128
115	129
115	130
115	131
115	132
115	133
115	134
115	135
115	136
115	137
115	138
115	139
115	140
115	147
115	153

PredatorID	PreyID
115	155
115	156
115	158
115	161
115	180
115	181
115	184
115	185
117	82
117	85
117	86
117	99
117	100
117	112
117	113
117	114
117	115
117	117
117	118
117	121
117	123
117	127
117	128
117	129
117	130
117	131
117	132
117	133
117	134
117	135
117	136
117	137
117	138
117	139
117	140
117	147
117	153
117	155
117	156
117	184
117	185
118	82

PredatorID	PreyID
118	85
118	86
118	100
118	113
118	115
118	118
118	121
118	123
118	128
118	130
118	132
118	134
118	136
118	138
118	140
118	153
118	155
118	184
118	185
121	32
121	77
121	78
121	81
121	82
121	85
121	86
121	100
121	113
121	115
121	153
121	158
121	161
121	180
121	181
121	184
121	185
123	77
123	78
123	81
123	82
123	85
123	86

PredatorID	PreyID
123	100
123	113
123	115
123	118
123	121
123	123
123	128
123	130
123	132
123	134
123	136
123	138
123	140
123	153
123	155
123	158
123	161
123	180
123	181
123	184
123	185
127	15
127	18
127	19
128	12
128	13
128	14
128	16
128	17
129	15
129	16
129	17
130	12
130	13
130	14
130	16
130	17
131	15
131	16
131	17
132	12
132	13

PredatorID	PreyID
132	14
132	16
132	17
133	12
133	13
133	14
133	15
133	16
133	17
134	12
134	13
134	14
134	16
134	17
135	12
135	13
135	14
135	15
135	16
135	17
136	12
136	13
136	14
136	16
136	17
137	12
137	13
137	14
137	15
137	16
137	17
138	12
138	13
138	14
138	16
138	17
139	12
139	13
139	14
139	15
139	16
139	17

PredatorID	PreyID
140	12
140	13
140	14
140	16
140	17
147	9
147	13
147	14
147	16
147	17
153	12
153	13
153	14
155	12
155	13
155	14
155	16
155	17
156	12
156	13
156	14
156	16
156	17
158	11
158	31
158	32
158	33
158	35
158	37
158	38
158	39
158	40
158	41
158	42
158	43
158	44
158	45
158	46
158	47
158	50
158	51
158	52

PredatorID	PreyID
158	86
161	12
161	13
161	14
161	27
161	37
161	38
161	39
161	40
161	41
161	42
161	43
161	44
161	45
161	46
161	50
161	52
180	27
180	37
180	38
180	39
180	40
180	41
180	42
180	43
180	44
180	45
180	46
180	50
181	27
181	37
181	38
181	39
181	40
181	41
181	42
181	43
181	44
181	45
181	46
181	50
184	9

PredatorID	PreyID
184	12
184	13
184	14
185	37
185	38
185	39
185	40
185	41
185	42
185	43
185	45
185	46
185	47
185	50
185	52

Table E11.—WE consumer-resource list for biozone 4. See Table E7 for master list of taxonomic ID numbers.

PredatorID	PreyID
20	6
21	3
21	4
22	6
24	6
26	1
26	3
26	7
26	21
27	2
28	26
28	28
29	1
29	6
29	7
30	4
30	6
31	1
31	3
31	6
31	7
31	8
31	9
31	11
31	20
31	21
31	27
31	28
31	29
31	30
31	31
31	33
31	35
31	39
31	40
32	22
32	31
33	6
35	1
35	6
35	7
35	8
35	11
35	20
35	29
35	30
37	12
37	13
37	14
37	15
37	16
37	17
38	12
38	13
38	14
38	15
38	16
38	17
38	18
38	19
39	2
40	1
40	2
40	6
41	2
41	9
41	12
41	13
41	14
41	37
41	38
41	39
41	40
41	41
41	42
41	43
41	44
41	45
41	46
41	47
41	50
41	52
42	37
42	38
42	39
42	40
42	41
42	42
42	43
42	44
42	45
42	46
42	47
42	50
42	52
43	2
44	15
44	18
45	112
45	113
45	114
45	115
45	117
45	118
45	121
45	122
45	123
45	127
45	128
45	129
45	130
45	131
45	132
45	133
45	134
45	135
45	136
45	137
45	138
45	147

PredatorID	PreyID
45	149
45	151
45	152
45	153
45	155
45	156
46	37
46	38
46	39
46	40
46	41
46	42
46	43
46	44
46	45
46	46
46	47
46	50
46	52
47	37
47	38
47	39
47	40
47	41
47	42
47	43
47	44
47	45
47	46
47	47
47	50
47	52
50	15
50	16
50	17
50	18
50	19
51	12
51	13
51	14
51	15
51	16

PredatorID	PreyID
51	17
51	18
51	19
52	12
52	13
52	14
52	15
52	16
52	17
52	18
52	19
57	20
57	27
57	28
57	29
57	30
57	33
57	35
57	57
57	64
57	72
57	58
58	20
58	27
58	28
58	29
58	30
58	33
58	35
58	72
61	11
61	22
61	26
61	31
61	57
61	58
61	62
61	64
61	72
62	11
62	20
62	27

PredatorID	PreyID
62	28
62	29
62	30
62	31
62	33
62	35
62	40
62	72
64	33
64	35
64	37
64	38
64	39
64	40
64	41
64	42
64	43
64	45
64	46
64	47
64	50
64	52
64	58
64	62
64	72
64	73
64	76
72	1
72	6
72	7
73	20
73	27
73	28
73	29
73	30
73	33
73	35
73	39
73	40
73	72
76	20
76	27

PredatorID	PreyID
76	28
76	29
76	30
76	33
76	35
76	39
76	40
76	41
76	42
76	43
76	45
76	46
76	72
77	8
77	11
77	22
77	24
77	26
77	27
77	28
77	31
77	33
77	35
77	37
77	38
77	39
77	40
77	41
77	42
77	43
77	45
77	46
77	47
77	52
77	58
77	62
77	64
77	72
77	73
77	76
78	8
78	11

PredatorID	PreyID
78	22
78	24
78	26
78	27
78	28
78	31
78	33
78	35
78	37
78	38
78	39
78	40
78	41
78	42
78	43
78	45
78	46
78	47
78	52
78	58
78	62
78	64
78	72
78	73
78	76
81	8
81	11
81	22
81	24
81	26
81	27
81	28
81	31
81	33
81	35
81	37
81	38
81	39
81	40
81	41
81	42
81	43

PredatorID	PreyID
81	45
81	46
81	47
81	52
81	58
81	62
81	64
81	72
81	73
81	76
82	26
82	27
82	31
82	37
82	38
82	39
82	40
82	41
82	42
82	43
82	44
82	45
82	46
82	47
82	50
82	51
82	52
82	73
82	76
82	86
82	87
82	88
82	89
82	95
84	9
84	12
84	13
84	14
84	73
84	76
84	86
84	87

PredatorID	PreyID
84	88
84	89
84	95
85	9
85	12
85	13
85	14
85	73
85	76
85	86
85	87
85	88
85	89
85	95
86	27
86	37
86	38
86	39
86	40
86	41
86	42
86	43
86	44
86	45
86	46
86	47
86	50
86	73
86	76
87	27
87	37
87	38
87	39
87	40
87	41
87	42
87	43
87	44
87	45
87	46
87	47
87	50

PredatorID	PreyID
87	73
87	76
88	27
88	37
88	38
88	39
88	40
88	41
88	42
88	43
88	44
88	45
88	46
88	47
88	50
88	73
88	76
89	27
89	37
89	38
89	39
89	40
89	41
89	42
89	43
89	44
89	45
89	46
89	47
89	50
89	73
89	76
95	27
95	37
95	38
95	39
95	40
95	41
95	42
95	43
95	44
95	45

PredatorID	PreyID
95	46
95	47
95	50
95	73
95	76
98	73
98	76
98	77
98	78
98	81
98	86
98	87
98	88
98	89
98	95
98	98
98	100
98	157
98	158
98	159
98	161
98	162
98	164
98	167
98	180
98	181
98	184
98	185
99	22
99	24
99	26
99	31
99	32
99	57
99	58
99	61
99	62
99	64
99	73
99	76
99	77
99	78

PredatorID	PreyID
99	81
99	82
99	84
99	85
99	86
99	87
99	88
99	89
99	95
99	98
99	99
99	100
99	101
99	102
99	105
99	106
99	110
99	112
99	113
99	114
99	115
99	117
99	118
99	121
99	122
99	123
99	127
99	128
99	129
99	130
99	131
99	132
99	133
99	134
99	135
99	136
99	137
99	138
99	147
99	149
99	151
99	152

PredatorID	PreyID
99	153
99	155
99	156
99	157
99	158
99	159
99	161
99	162
99	164
99	167
99	180
99	181
100	27
100	28
100	31
100	33
100	35
100	37
100	38
100	39
100	40
100	41
100	42
100	43
100	45
100	46
100	47
100	50
100	52
100	58
100	62
100	72
100	73
100	76
101	31
101	32
101	57
101	58
101	62
101	64
101	73
101	76

PredatorID	PreyID
101	77
101	78
101	81
101	82
101	84
101	85
101	86
101	87
101	88
101	89
101	95
101	98
101	100
101	101
101	102
101	105
101	106
101	110
101	113
101	115
101	152
101	153
101	157
101	158
101	159
101	161
101	162
101	164
101	167
101	180
101	181
102	73
102	76
102	86
102	87
102	88
102	89
102	95
102	100
102	158
102	159
102	161

PredatorID	PreyID
102	162
102	164
102	167
102	180
102	181
102	184
102	185
105	27
105	31
105	37
105	38
105	39
105	40
105	41
105	42
105	43
105	44
105	45
105	46
105	47
105	52
105	58
105	62
105	72
105	73
105	76
106	27
106	31
106	32
106	37
106	38
106	39
106	40
106	41
106	42
106	43
106	44
106	45
106	46
106	47
106	52
106	58

PredatorID	PreyID
106	62
106	72
106	73
106	76
110	27
110	31
110	37
110	38
110	39
110	40
110	41
110	42
110	43
110	44
110	45
110	46
110	47
110	52
110	58
110	62
110	72
110	73
110	76
112	64
112	77
112	78
112	81
112	82
112	84
112	85
112	98
112	99
112	100
112	101
112	102
112	105
112	106
112	110
112	112
112	113
112	114
112	115

PredatorID	PreyID
112	117
112	118
112	121
112	122
112	123
112	127
112	128
112	129
112	130
112	131
112	132
112	133
112	134
112	135
112	136
112	137
112	138
112	147
112	149
112	151
112	152
112	153
112	155
112	156
112	157
112	184
112	185
113	37
113	38
113	39
113	40
113	41
113	42
113	43
113	45
113	46
113	47
113	50
113	52
113	73
113	76
113	77

PredatorID	PreyID
113	78
113	81
113	82
113	84
113	85
113	86
113	87
113	88
113	89
113	95
113	98
113	99
113	100
113	101
113	102
113	105
113	106
113	110
113	112
113	113
113	114
113	115
113	117
113	118
113	121
113	122
113	123
113	127
113	128
113	129
113	130
113	131
113	132
113	133
113	134
113	135
113	136
113	137
113	138
113	147
113	149
113	151

PredatorID	PreyID
113	152
113	153
113	155
113	156
113	157
113	158
113	159
113	161
113	162
113	164
113	167
113	180
113	181
113	184
113	185
114	61
114	64
114	77
114	78
114	81
114	82
114	84
114	85
114	98
114	99
114	100
114	101
114	102
114	105
114	106
114	110
114	112
114	113
114	114
114	115
114	117
114	118
114	121
114	122
114	123
114	127
114	128

PredatorID	PreyID
114	129
114	130
114	131
114	132
114	133
114	134
114	135
114	136
114	137
114	138
114	147
114	149
114	151
114	152
114	153
114	155
114	156
114	157
114	184
114	185
115	31
115	32
115	37
115	38
115	39
115	40
115	41
115	42
115	43
115	45
115	46
115	47
115	50
115	52
115	61
115	62
115	64
115	73
115	76
115	77
115	78
115	81

PredatorID	PreyID
115	82
115	84
115	85
115	86
115	87
115	88
115	89
115	95
115	98
115	99
115	100
115	101
115	102
115	105
115	106
115	110
115	112
115	113
115	114
115	115
115	117
115	118
115	121
115	122
115	123
115	127
115	128
115	129
115	130
115	131
115	132
115	133
115	134
115	135
115	136
115	137
115	138
115	147
115	149
115	151
115	152
115	153

PredatorID	PreyID
115	155
115	156
115	157
115	158
115	159
115	161
115	162
115	164
115	167
115	180
115	181
115	184
115	185
117	64
117	82
117	84
117	85
117	98
117	99
117	100
117	101
117	102
117	105
117	106
117	110
117	112
117	113
117	114
117	115
117	117
117	118
117	121
117	122
117	123
117	127
117	128
117	129
117	130
117	131
117	132
117	133
117	134

PredatorID	PreyID
117	135
117	136
117	137
117	138
117	147
117	149
117	151
117	152
117	153
117	155
117	156
117	157
117	184
117	185
118	82
118	84
118	85
118	98
118	100
118	101
118	102
118	105
118	106
118	110
118	113
118	115
118	118
118	121
118	122
118	123
118	128
118	130
118	132
118	134
118	136
118	138
118	153
118	155
118	157
118	184
118	185
121	32

PredatorID	PreyID
121	73
121	76
121	77
121	78
121	81
121	82
121	84
121	85
121	86
121	87
121	88
121	89
121	95
121	98
121	100
121	101
121	102
121	105
121	110
121	113
121	115
121	152
121	153
121	157
121	158
121	159
121	161
121	162
121	164
121	167
121	180
121	181
121	184
121	185
122	32
122	73
122	76
122	77
122	78
122	81
122	82
122	84

PredatorID	PreyID
122	85
122	86
122	87
122	88
122	89
122	95
122	98
122	100
122	101
122	102
122	105
122	110
122	113
122	115
122	152
122	153
122	157
122	158
122	159
122	161
122	162
122	164
122	167
122	180
122	181
122	184
122	185
123	77
123	78
123	81
123	82
123	84
123	85
123	86
123	87
123	88
123	89
123	95
123	100
123	101
123	102
123	105

PredatorID	PreyID
123	106
123	110
123	113
123	115
123	118
123	121
123	122
123	123
123	128
123	130
123	132
123	134
123	136
123	138
123	152
123	153
123	155
123	157
123	158
123	159
123	161
123	162
123	164
123	167
123	180
123	181
123	184
123	185
127	15
127	18
127	19
128	12
128	13
128	14
128	16
128	17
129	15
129	16
129	17
130	12
130	13
130	14

PredatorID	PreyID
130	16
130	17
131	15
131	16
131	17
132	12
132	13
132	14
132	16
132	17
133	12
133	13
133	14
133	15
133	16
133	17
134	12
134	13
134	14
134	16
134	17
135	12
135	13
135	14
135	15
135	16
135	17
136	12
136	13
136	14
136	16
136	17
137	12
137	13
137	14
137	15
137	16
137	17
138	12
138	13
138	14
138	16

PredatorID	PreyID
138	17
147	9
147	13
147	14
147	16
147	17
149	9
149	13
149	14
149	16
149	17
151	9
151	13
151	14
151	16
151	17
152	12
152	13
152	14
152	37
152	38
152	39
152	40
152	41
152	42
152	43
152	45
152	46
152	47
152	50
152	52
153	12
153	13
153	14
155	12
155	13
155	14
155	16
155	17
156	12
156	13
156	14

PredatorID	PreyID
156	16
156	17
157	12
157	13
157	14
157	37
157	38
157	39
157	40
157	41
157	42
157	43
157	45
157	46
157	47
157	50
157	52
158	11
158	31
158	32
158	33
158	35
158	37
158	38
158	39
158	40
158	41
158	42
158	43
158	44
158	45
158	46
158	47
158	50
158	51
158	52
158	73
158	76
158	86
158	87
158	88
158	89

PredatorID	PreyID
159	27
159	37
159	38
159	39
159	40
159	41
159	42
159	43
159	46
159	50
159	51
161	12
161	13
161	14
161	27
161	37
161	38
161	39
161	40
161	41
161	42
161	43
161	44
161	45
161	46
161	50
161	52
162	12
162	13
162	14
162	27
162	37
162	38
162	39
162	40
162	41
162	42
162	43
162	44
162	45
162	46
162	50

PredatorID	PreyID
162	52
164	27
164	37
164	38
164	39
164	40
164	41
164	42
164	43
164	44
164	45
164	46
164	50
164	52
167	27
167	37
167	38
167	39
167	40
167	41
167	42
167	43
167	44
167	45
167	46
167	50
167	52
167	73
167	76
167	86
167	87
167	88
167	89
167	159
167	161
167	162
167	164
167	181
180	27
180	37
180	38
180	39

PredatorID	PreyID
180	40
180	41
180	42
180	43
180	44
180	45
180	46
180	50
181	27
181	37
181	38
181	39
181	40
181	41
181	42
181	43
181	44
181	45
181	46
181	50
184	9
184	12
184	13
184	14
185	37
185	38
185	39
185	40
185	41
185	42
185	43
185	45
185	46
185	47
185	50
185	52

Table E12.—WE consumer-resource list for biozone 5. See Table E7 for master list of taxonomic ID numbers.

PredatorID	PreyID
20	6
21	3
21	4
22	6
24	6
26	1
26	3
26	7
26	21
27	2
28	26
28	28
29	1
29	6
29	7
30	4
30	6
31	1
31	3
31	6
31	7
31	8
31	9
31	11
31	20
31	21
31	27
31	28
31	29
31	30
31	31
31	33
31	35
31	39
31	40
32	22
32	31
33	6
35	1
35	6
35	7
35	8
35	11
35	20
35	29
35	30
37	12
37	13
37	14
37	15
37	16
37	17
38	12
38	13
38	14
38	15
38	16
38	17
38	18
38	19
39	2
40	1
40	2
40	6
41	2
41	9
41	12
41	13
41	14
41	37
41	38
41	39
41	40
41	41
41	42
41	43
41	44
41	45
41	46
41	47
41	50
41	52
42	37
42	38
42	39
42	40
42	41
42	42
42	43
42	44
42	45
42	46
42	47
42	50
42	52
43	2
44	15
44	18
45	112
45	113
45	114
45	115
45	116
45	117
45	118
45	119
45	120
45	121
45	122
45	129
45	130
45	133
45	134
45	135
45	136
45	137
45	138
45	147
45	149
45	153

PredatorID	PreyID
45	154
45	155
45	156
46	37
46	38
46	39
46	40
46	41
46	42
46	43
46	44
46	45
46	46
46	47
46	50
46	52
47	37
47	38
47	39
47	40
47	41
47	42
47	43
47	44
47	45
47	46
47	47
47	50
47	52
50	15
50	16
50	17
50	18
50	19
51	12
51	13
51	14
51	15
51	16
51	17
51	18
51	19

PredatorID	PreyID
52	12
52	13
52	14
52	15
52	16
52	17
52	18
52	19
54	54
54	72
55	20
55	27
55	28
55	29
55	30
55	33
55	35
55	55
55	56
55	59
55	72
56	20
56	27
56	28
56	29
56	30
56	33
56	35
56	72
59	20
59	27
59	28
59	29
59	30
59	33
59	35
59	56
59	72
61	11
61	22
61	26
61	31

PredatorID	PreyID
61	55
61	56
61	59
61	62
61	64
61	68
61	72
62	11
62	20
62	27
62	28
62	29
62	30
62	31
62	33
62	35
62	40
62	72
64	33
64	35
64	37
64	38
64	39
64	40
64	41
64	42
64	43
64	45
64	46
64	47
64	50
64	52
64	54
64	55
64	56
64	59
64	62
64	69
64	71
64	72
64	76
68	20

PredatorID	PreyID
68	27
68	28
68	29
68	30
68	33
68	35
68	72
69	20
69	27
69	28
69	29
69	30
69	33
69	35
69	39
69	40
69	72
71	20
71	27
71	28
71	29
71	30
71	33
71	35
71	39
71	40
71	72
72	1
72	6
72	7
76	20
76	27
76	28
76	29
76	30
76	33
76	35
76	39
76	40
76	41
76	42
76	43

PredatorID	PreyID
76	45
76	46
76	72
77	8
77	11
77	22
77	24
77	26
77	27
77	28
77	31
77	33
77	35
77	37
77	38
77	39
77	40
77	41
77	42
77	43
77	45
77	46
77	47
77	52
77	54
77	55
77	56
77	59
77	62
77	64
77	69
77	71
77	72
77	76
77	96
78	8
78	11
78	22
78	24
78	26
78	27
78	28

PredatorID	PreyID
78	31
78	33
78	35
78	37
78	38
78	39
78	40
78	41
78	42
78	43
78	45
78	46
78	47
78	52
78	54
78	55
78	56
78	59
78	62
78	64
78	69
78	71
78	72
78	76
78	96
81	8
81	11
81	22
81	24
81	26
81	27
81	28
81	31
81	33
81	35
81	37
81	38
81	39
81	40
81	41
81	42
81	43

PredatorID	PreyID
81	45
81	46
81	47
81	52
81	54
81	55
81	56
81	59
81	62
81	64
81	69
81	71
81	72
81	76
81	96
82	26
82	27
82	31
82	37
82	38
82	39
82	40
82	41
82	42
82	43
82	44
82	45
82	46
82	47
82	50
82	51
82	52
82	69
82	71
82	76
82	86
82	88
82	90
82	96
83	26
83	27
83	31

PredatorID	PreyID
83	37
83	38
83	39
83	40
83	41
83	42
83	43
83	44
83	45
83	46
83	47
83	50
83	51
83	52
83	69
83	71
83	76
83	86
83	88
83	90
83	96
85	9
85	12
85	13
85	14
85	69
85	71
85	76
85	86
85	88
85	90
85	96
86	27
86	37
86	38
86	39
86	40
86	41
86	42
86	43
86	44
86	45

PredatorID	PreyID
86	46
86	47
86	50
86	69
86	71
86	76
88	27
88	37
88	38
88	39
88	40
88	41
88	42
88	43
88	44
88	45
88	46
88	47
88	50
88	69
88	71
88	76
90	27
90	37
90	38
90	39
90	40
90	41
90	42
90	43
90	44
90	45
90	46
90	47
90	50
90	69
90	71
90	76
96	20
96	27
96	28
96	29

PredatorID	PreyID
96	30
96	33
96	35
96	39
96	40
96	41
96	42
96	43
96	45
96	46
96	72
99	22
99	24
99	26
99	31
99	32
99	54
99	55
99	56
99	59
99	61
99	62
99	64
99	68
99	69
99	71
99	76
99	77
99	78
99	81
99	82
99	83
99	85
99	86
99	88
99	90
99	96
99	99
99	100
99	101
99	102
99	103

PredatorID	PreyID
99	104
99	107
99	110
99	111
99	112
99	113
99	114
99	115
99	116
99	117
99	118
99	119
99	120
99	121
99	122
99	129
99	130
99	133
99	134
99	135
99	136
99	137
99	138
99	147
99	149
99	153
99	154
99	155
99	156
99	158
99	160
99	161
99	162
99	165
99	166
99	167
99	168
99	170
99	171
99	172
99	173
99	174

PredatorID	PreyID
99	175
99	176
99	177
99	179
99	180
99	181
100	27
100	28
100	31
100	33
100	35
100	37
100	38
100	39
100	40
100	41
100	42
100	43
100	45
100	46
100	47
100	50
100	52
100	54
100	55
100	56
100	59
100	62
100	69
100	71
100	72
100	76
101	31
101	32
101	54
101	55
101	56
101	59
101	62
101	64
101	69
101	71

PredatorID	PreyID
101	76
101	77
101	78
101	81
101	82
101	83
101	85
101	86
101	88
101	90
101	96
101	100
101	101
101	102
101	103
101	104
101	107
101	110
101	111
101	113
101	115
101	153
101	154
101	158
101	160
101	161
101	162
101	165
101	166
101	167
101	168
101	170
101	171
101	172
101	173
101	174
101	175
101	176
101	177
101	179
101	180
101	181

PredatorID	PreyID
102	69
102	71
102	76
102	86
102	88
102	90
102	96
102	100
102	158
102	160
102	161
102	162
102	165
102	166
102	167
102	168
102	170
102	171
102	172
102	173
102	174
102	175
102	176
102	177
102	179
102	180
102	181
102	184
102	185
103	69
103	71
103	76
103	86
103	88
103	90
103	96
103	100
103	158
103	160
103	161
103	162
103	165

PredatorID	PreyID
103	166
103	167
103	168
103	170
103	171
103	172
103	173
103	174
103	175
103	176
103	177
103	179
103	180
103	181
103	184
103	185
104	27
104	31
104	37
104	38
104	39
104	40
104	41
104	42
104	43
104	44
104	45
104	46
104	47
104	52
104	54
104	55
104	56
104	62
104	69
104	71
104	72
104	76
107	27
107	31
107	32
107	37

PredatorID	PreyID
107	38
107	39
107	40
107	41
107	42
107	43
107	44
107	45
107	46
107	47
107	52
107	54
107	55
107	56
107	62
107	69
107	71
107	72
107	76
110	27
110	31
110	37
110	38
110	39
110	40
110	41
110	42
110	43
110	44
110	45
110	46
110	47
110	52
110	54
110	55
110	56
110	62
110	69
110	71
110	72
110	76
111	27

PredatorID	PreyID
111	31
111	37
111	38
111	39
111	40
111	41
111	42
111	43
111	44
111	45
111	46
111	47
111	52
111	54
111	55
111	56
111	62
111	69
111	71
111	72
111	76
112	64
112	77
112	78
112	81
112	82
112	83
112	85
112	99
112	100
112	101
112	102
112	103
112	104
112	107
112	110
112	111
112	112
112	113
112	114
112	115
112	116

PredatorID	PreyID
112	117
112	118
112	119
112	120
112	121
112	122
112	129
112	130
112	133
112	134
112	135
112	136
112	137
112	138
112	147
112	149
112	153
112	154
112	155
112	156
112	184
112	185
113	37
113	38
113	39
113	40
113	41
113	42
113	43
113	45
113	46
113	47
113	50
113	52
113	69
113	71
113	76
113	77
113	78
113	81
113	82
113	83

PredatorID	PreyID
113	85
113	86
113	88
113	90
113	96
113	99
113	100
113	101
113	102
113	103
113	104
113	107
113	110
113	111
113	112
113	113
113	114
113	115
113	116
113	117
113	118
113	119
113	120
113	121
113	122
113	129
113	130
113	133
113	134
113	135
113	136
113	137
113	138
113	147
113	149
113	153
113	154
113	155
113	156
113	158
113	160
113	161

PredatorID	PreyID
113	162
113	165
113	166
113	167
113	168
113	170
113	171
113	172
113	173
113	174
113	175
113	176
113	177
113	179
113	180
113	181
113	184
113	185
114	61
114	64
114	77
114	78
114	81
114	82
114	83
114	85
114	99
114	100
114	101
114	102
114	103
114	104
114	107
114	110
114	111
114	112
114	113
114	114
114	115
114	116
114	117
114	118

PredatorID	PreyID
114	119
114	120
114	121
114	122
114	129
114	130
114	133
114	134
114	135
114	136
114	137
114	138
114	147
114	149
114	153
114	154
114	155
114	156
114	184
114	185
115	31
115	32
115	37
115	38
115	39
115	40
115	41
115	42
115	43
115	45
115	46
115	47
115	50
115	52
115	61
115	62
115	64
115	69
115	71
115	76
115	77
115	78

PredatorID	PreyID
115	81
115	82
115	83
115	85
115	86
115	88
115	90
115	96
115	99
115	100
115	101
115	102
115	103
115	104
115	107
115	110
115	111
115	112
115	113
115	114
115	115
115	116
115	117
115	118
115	119
115	120
115	121
115	122
115	129
115	130
115	133
115	134
115	135
115	136
115	137
115	138
115	147
115	149
115	153
115	154
115	155
115	156

PredatorID	PreyID
115	158
115	160
115	161
115	162
115	165
115	166
115	167
115	168
115	170
115	171
115	172
115	173
115	174
115	175
115	176
115	177
115	179
115	180
115	181
115	184
115	185
116	64
116	82
116	83
116	85
116	99
116	100
116	101
116	102
116	103
116	104
116	107
116	110
116	111
116	112
116	113
116	114
116	115
116	116
116	117
116	118
116	119

PredatorID	PreyID
116	120
116	121
116	122
116	129
116	130
116	133
116	134
116	135
116	136
116	137
116	138
116	147
116	149
116	153
116	154
116	155
116	156
116	184
116	185
117	64
117	82
117	83
117	85
117	99
117	100
117	101
117	102
117	103
117	104
117	107
117	110
117	111
117	112
117	113
117	114
117	115
117	116
117	117
117	118
117	119
117	120
117	121

PredatorID	PreyID
117	122
117	129
117	130
117	133
117	134
117	135
117	136
117	137
117	138
117	147
117	149
117	153
117	154
117	155
117	156
117	184
117	185
118	82
118	83
118	85
118	100
118	101
118	102
118	103
118	104
118	107
118	110
118	111
118	113
118	115
118	118
118	119
118	120
118	121
118	122
118	130
118	134
118	136
118	138
118	153
118	154
118	155

PredatorID	PreyID
118	184
118	185
119	69
119	71
119	76
119	77
119	78
119	81
119	82
119	83
119	85
119	86
119	88
119	90
119	96
119	100
119	101
119	102
119	103
119	104
119	107
119	110
119	111
119	113
119	115
119	119
119	120
119	121
119	122
119	130
119	134
119	136
119	138
119	153
119	154
119	155
119	158
119	160
119	161
119	162
119	165
119	166

PredatorID	PreyID
119	167
119	168
119	170
119	171
119	172
119	173
119	174
119	175
119	176
119	177
119	179
119	180
119	181
119	184
119	185
120	32
120	69
120	71
120	76
120	77
120	78
120	81
120	82
120	83
120	85
120	86
120	88
120	90
120	96
120	100
120	101
120	102
120	103
120	104
120	110
120	111
120	113
120	115
120	153
120	154
120	158
120	160

PredatorID	PreyID
120	161
120	162
120	165
120	166
120	167
120	168
120	170
120	171
120	172
120	173
120	174
120	175
120	176
120	177
120	179
120	180
120	181
120	184
120	185
121	32
121	69
121	71
121	76
121	77
121	78
121	81
121	82
121	83
121	85
121	86
121	88
121	90
121	96
121	100
121	101
121	102
121	103
121	104
121	110
121	111
121	113
121	115

PredatorID	PreyID
121	153
121	154
121	158
121	160
121	161
121	162
121	165
121	166
121	167
121	168
121	170
121	171
121	172
121	173
121	174
121	175
121	176
121	177
121	179
121	180
121	181
121	184
121	185
122	32
122	69
122	71
122	76
122	77
122	78
122	81
122	82
122	83
122	85
122	86
122	88
122	90
122	96
122	100
122	101
122	102
122	103
122	104

PredatorID	PreyID
122	110
122	111
122	113
122	115
122	153
122	154
122	158
122	160
122	161
122	162
122	165
122	166
122	167
122	168
122	170
122	171
122	172
122	173
122	174
122	175
122	176
122	177
122	179
122	180
122	181
122	184
122	185
129	15
129	16
129	17
130	12
130	13
130	14
130	16
130	17
133	12
133	13
133	14
133	15
133	16
133	17
134	12

PredatorID	PreyID
134	13
134	14
134	16
134	17
135	12
135	13
135	14
135	15
135	16
135	17
136	12
136	13
136	14
136	16
136	17
137	12
137	13
137	14
137	15
137	16
137	17
138	12
138	13
138	14
138	16
138	17
147	9
147	13
147	14
147	16
147	17
149	9
149	13
149	14
149	16
149	17
153	12
153	13
153	14
154	12
154	13
154	14

PredatorID	PreyID
155	12
155	13
155	14
155	16
155	17
156	12
156	13
156	14
156	16
156	17
158	11
158	31
158	32
158	33
158	35
158	37
158	38
158	39
158	40
158	41
158	42
158	43
158	44
158	45
158	46
158	47
158	50
158	51
158	52
158	69
158	71
158	76
158	86
158	88
158	90
158	96
160	12
160	13
160	14
160	27
160	37
160	38

PredatorID	PreyID
160	39
160	40
160	41
160	42
160	43
160	44
160	45
160	46
160	50
160	52
161	12
161	13
161	14
161	27
161	37
161	38
161	39
161	40
161	41
161	42
161	43
161	44
161	45
161	46
161	50
161	52
162	12
162	13
162	14
162	27
162	37
162	38
162	39
162	40
162	41
162	42
162	43
162	44
162	45
162	46
162	50
162	52

PredatorID	PreyID
165	27
165	37
165	38
165	39
165	40
165	41
165	42
165	43
165	44
165	45
165	46
165	50
165	52
166	27
166	37
166	38
166	39
166	40
166	41
166	42
166	43
166	44
166	45
166	46
166	50
166	52
167	27
167	37
167	38
167	39
167	40
167	41
167	42
167	43
167	44
167	45
167	46
167	50
167	52
167	69
167	71
167	76

PredatorID	PreyID
167	86
167	88
167	90
167	96
167	160
167	161
167	162
167	165
167	166
167	170
167	171
167	172
167	173
167	174
167	175
167	176
167	177
167	179
167	181
168	27
168	37
168	38
168	39
168	40
168	41
168	42
168	43
168	44
168	45
168	46
168	50
168	52
168	69
168	71
168	76
168	86
168	88
168	90
168	96
168	160
168	161
168	162

PredatorID	PreyID
168	165
168	166
168	170
168	171
168	172
168	173
168	174
168	175
168	176
168	177
168	179
168	181
170	27
170	37
170	38
170	39
170	40
170	41
170	42
170	43
170	44
170	45
170	46
170	50
171	27
171	37
171	38
171	39
171	40
171	41
171	42
171	43
171	44
171	45
171	46
171	50
172	27
172	37
172	38
172	39
172	40
172	41

PredatorID	PreyID
172	42
172	43
172	44
172	45
172	46
172	50
172	52
173	27
173	37
173	38
173	39
173	40
173	41
173	42
173	43
173	44
173	45
173	46
173	50
173	52
174	27
174	37
174	38
174	39
174	40
174	41
174	42
174	43
174	44
174	45
174	46
174	50
174	52
175	27
175	37
175	38
175	39
175	40
175	41
175	42
175	43
175	44

PredatorID	PreyID
175	45
175	46
175	50
175	52
176	27
176	37
176	38
176	39
176	40
176	41
176	42
176	43
176	44
176	45
176	46
176	50
176	52
177	27
177	37
177	38
177	39
177	40
177	41
177	42
177	43
177	44
177	45
177	46
177	50
177	52
179	27
179	37
179	38
179	39
179	40
179	41
179	42
179	43
179	44
179	45
179	46
179	50

PredatorID	PreyID
180	27
180	37
180	38
180	39
180	40
180	41
180	42
180	43
180	44
180	45
180	46
180	50
181	27
181	37
181	38
181	39
181	40
181	41
181	42
181	43
181	44
181	45
181	46
181	50
184	9
184	12
184	13
184	14
185	37
185	38
185	39
185	40
185	41
185	42
185	43
185	45
185	46
185	47
185	50
185	52

Table E13.—WE consumer-resource list for biozone 6. See Table E7 for master list of taxonomic ID numbers.

PredatorID	PreyID
20	6
21	3
21	4
22	6
24	6
26	1
26	3
26	7
26	21
27	2
28	26
28	28
29	1
29	6
29	7
30	4
30	6
31	1
31	3
31	6
31	7
31	8
31	9
31	11
31	20
31	21
31	27
31	28
31	29
31	30
31	31
31	33
31	35
31	39
31	40
32	22
32	31
33	6
35	1
35	6
35	7
35	8
35	11
35	20
35	29
35	30
37	12
37	13
37	14
37	15
37	16
37	17
38	12
38	13
38	14
38	15
38	16
38	17
38	18
38	19
39	2
40	1
40	2
40	6
41	2
41	9
41	12
41	13
41	14
41	37
41	38
41	39
41	40
41	41
41	42
41	43
41	44
41	45
41	46
41	47
41	50
41	52
42	37
42	38
42	39
42	40
42	41
42	42
42	43
42	44
42	45
42	46
42	47
42	50
42	52
43	2
44	15
44	18
45	112
45	113
45	114
45	115
45	125
45	129
45	130
45	133
45	134
45	137
45	143
45	144
45	145
45	146
45	147
45	154
45	155
45	156
46	37
46	38
46	39
46	40

PredatorID	PreyID
46	41
46	42
46	43
46	44
46	45
46	46
46	47
46	50
46	52
47	37
47	38
47	39
47	40
47	41
47	42
47	43
47	44
47	45
47	46
47	47
47	50
47	52
50	15
50	16
50	17
50	18
50	19
51	12
51	13
51	14
51	15
51	16
51	17
51	18
51	19
52	12
52	13
52	14
52	15
52	16
52	17
52	18

PredatorID	PreyID
52	19
53	53
53	72
54	54
54	72
61	11
61	22
61	26
61	31
61	53
61	62
61	64
61	72
62	11
62	20
62	27
62	28
62	29
62	30
62	31
62	33
62	35
62	40
62	72
64	33
64	35
64	37
64	38
64	39
64	40
64	41
64	42
64	43
64	45
64	46
64	47
64	50
64	52
64	53
64	54
64	62
64	70

PredatorID	PreyID
64	71
64	72
64	74
64	75
70	20
70	27
70	28
70	29
70	30
70	33
70	35
70	39
70	40
70	72
71	20
71	27
71	28
71	29
71	30
71	33
71	35
71	39
71	40
71	72
72	1
72	6
72	7
74	20
74	27
74	28
74	29
74	30
74	33
74	35
74	39
74	40
74	41
74	42
74	43
74	45
74	46
74	72

PredatorID	PreyID
75	20
75	27
75	28
75	29
75	30
75	33
75	35
75	39
75	40
75	41
75	42
75	43
75	45
75	46
75	72
77	8
77	11
77	22
77	24
77	26
77	27
77	28
77	31
77	33
77	35
77	37
77	38
77	39
77	40
77	41
77	42
77	43
77	45
77	46
77	47
77	52
77	53
77	54
77	62
77	64
77	70
77	71

PredatorID	PreyID
77	72
77	74
77	75
78	8
78	11
78	22
78	24
78	26
78	27
78	28
78	31
78	33
78	35
78	37
78	38
78	39
78	40
78	41
78	42
78	43
78	45
78	46
78	47
78	52
78	53
78	54
78	62
78	64
78	70
78	71
78	72
78	74
78	75
79	8
79	11
79	22
79	24
79	26
79	27
79	28
79	31
79	33

PredatorID	PreyID
79	35
79	37
79	38
79	39
79	40
79	41
79	42
79	43
79	45
79	46
79	47
79	52
79	53
79	54
79	62
79	64
79	70
79	71
79	72
79	74
79	75
80	8
80	11
80	22
80	24
80	26
80	27
80	28
80	31
80	33
80	35
80	37
80	38
80	39
80	40
80	41
80	42
80	43
80	45
80	46
80	47
80	52

PredatorID	PreyID
80	53
80	54
80	62
80	64
80	70
80	71
80	72
80	74
80	75
81	8
81	11
81	22
81	24
81	26
81	27
81	28
81	31
81	33
81	35
81	37
81	38
81	39
81	40
81	41
81	42
81	43
81	45
81	46
81	47
81	52
81	53
81	54
81	62
81	64
81	70
81	71
81	72
81	74
81	75
82	26
82	27
82	31

PredatorID	PreyID
82	37
82	38
82	39
82	40
82	41
82	42
82	43
82	44
82	45
82	46
82	47
82	50
82	51
82	52
82	70
82	71
82	74
82	75
82	95
83	26
83	27
83	31
83	37
83	38
83	39
83	40
83	41
83	42
83	43
83	44
83	45
83	46
83	47
83	50
83	51
83	52
83	70
83	71
83	74
83	75
83	95
85	9

PredatorID	PreyID
85	12
85	13
85	14
85	70
85	71
85	74
85	75
85	95
95	27
95	37
95	38
95	39
95	40
95	41
95	42
95	43
95	44
95	45
95	46
95	47
95	50
95	70
95	71
95	74
95	75
97	70
97	71
97	74
97	75
97	95
97	97
97	100
97	158
97	162
97	163
97	167
97	174
97	178
97	179
97	180
97	184
97	185

PredatorID	PreyID
99	22
99	24
99	26
99	31
99	32
99	53
99	54
99	61
99	62
99	64
99	70
99	71
99	74
99	75
99	77
99	78
99	79
99	80
99	81
99	82
99	83
99	85
99	95
99	97
99	99
99	100
99	101
99	110
99	112
99	113
99	114
99	115
99	125
99	129
99	130
99	133
99	134
99	137
99	143
99	144
99	145
99	146

PredatorID	PreyID
99	147
99	154
99	155
99	156
99	158
99	162
99	163
99	167
99	174
99	178
99	179
99	180
100	27
100	28
100	31
100	33
100	35
100	37
100	38
100	39
100	40
100	41
100	42
100	43
100	45
100	46
100	47
100	50
100	52
100	53
100	54
100	62
100	70
100	71
100	72
100	74
100	75
101	31
101	32
101	53
101	54
101	62

PredatorID	PreyID
101	64
101	70
101	71
101	74
101	75
101	77
101	78
101	79
101	80
101	81
101	82
101	83
101	85
101	95
101	97
101	100
101	101
101	110
101	113
101	115
101	154
101	158
101	162
101	163
101	167
101	174
101	178
101	179
101	180
110	27
110	31
110	37
110	38
110	39
110	40
110	41
110	42
110	43
110	44
110	45
110	46
110	47

PredatorID	PreyID
110	52
110	53
110	54
110	62
110	70
110	71
110	72
110	74
110	75
112	64
112	77
112	78
112	79
112	80
112	81
112	82
112	83
112	85
112	97
112	99
112	100
112	101
112	110
112	112
112	113
112	114
112	115
112	125
112	129
112	130
112	133
112	134
112	137
112	143
112	144
112	145
112	146
112	147
112	154
112	155
112	156
112	184

PredatorID	PreyID
112	185
113	37
113	38
113	39
113	40
113	41
113	42
113	43
113	45
113	46
113	47
113	50
113	52
113	70
113	71
113	74
113	75
113	77
113	78
113	79
113	80
113	81
113	82
113	83
113	85
113	95
113	97
113	99
113	100
113	101
113	110
113	112
113	113
113	114
113	115
113	125
113	129
113	130
113	133
113	134
113	137
113	143

PredatorID	PreyID
113	144
113	145
113	146
113	147
113	154
113	155
113	156
113	158
113	162
113	163
113	167
113	174
113	178
113	179
113	180
113	184
113	185
114	61
114	64
114	77
114	78
114	79
114	80
114	81
114	82
114	83
114	85
114	97
114	99
114	100
114	101
114	110
114	112
114	113
114	114
114	115
114	125
114	129
114	130
114	133
114	134
114	137

PredatorID	PreyID
114	143
114	144
114	145
114	146
114	147
114	154
114	155
114	156
114	184
114	185
115	31
115	32
115	37
115	38
115	39
115	40
115	41
115	42
115	43
115	45
115	46
115	47
115	50
115	52
115	61
115	62
115	64
115	70
115	71
115	74
115	75
115	77
115	78
115	79
115	80
115	81
115	82
115	83
115	85
115	95
115	97
115	99

PredatorID	PreyID
115	100
115	101
115	110
115	112
115	113
115	114
115	115
115	125
115	129
115	130
115	133
115	134
115	137
115	143
115	144
115	145
115	146
115	147
115	154
115	155
115	156
115	158
115	162
115	163
115	167
115	174
115	178
115	179
115	180
115	184
115	185
125	70
125	71
125	74
125	75
125	82
125	83
125	85
125	95
125	100
125	110
125	113

PredatorID	PreyID
125	115
125	154
125	158
125	162
125	163
125	167
125	174
125	178
125	179
125	180
125	184
125	185
129	15
129	16
129	17
130	12
130	13
130	14
130	16
130	17
133	12
133	13
133	14
133	15
133	16
133	17
134	12
134	13
134	14
134	16
134	17
137	12
137	13
137	14
137	15
137	16
137	17
143	12
143	13
143	14
143	15
143	16

PredatorID	PreyID
143	17
144	12
144	13
144	14
144	16
144	17
145	12
145	13
145	14
145	15
145	16
145	17
146	12
146	13
146	14
146	16
146	17
147	9
147	13
147	14
147	16
147	17
154	12
154	13
154	14
155	12
155	13
155	14
155	16
155	17
156	12
156	13
156	14
156	16
156	17
158	11
158	31
158	32
158	33
158	35
158	37
158	38

PredatorID	PreyID
158	39
158	40
158	41
158	42
158	43
158	44
158	45
158	46
158	47
158	50
158	51
158	52
158	70
158	71
158	74
158	75
162	12
162	13
162	14
162	27
162	37
162	38
162	39
162	40
162	41
162	42
162	43
162	44
162	45
162	46
162	50
162	52
163	12
163	13
163	14
163	27
163	37
163	38
163	39
163	40
163	41
163	42

PredatorID	PreyID
163	43
163	44
163	45
163	46
163	50
163	52
167	27
167	37
167	38
167	39
167	40
167	41
167	42
167	43
167	44
167	45
167	46
167	50
167	52
167	70
167	71
167	74
167	75
167	162
167	163
167	174
167	178
167	179
174	27
174	37
174	38
174	39
174	40
174	41
174	42
174	43
174	44
174	45
174	46
174	50
174	52
178	27

PredatorID	PreyID
178	37
178	38
178	39
178	40
178	41
178	42
178	43
178	44
178	45
178	46
178	50
178	52
178	70
178	71
178	74
178	75
179	27
179	37
179	38
179	39
179	40
179	41
179	42
179	43
179	44
179	45
179	46
179	50
180	27
180	37
180	38
180	39
180	40
180	41
180	42
180	43
180	44
180	45
180	46
180	50
184	9
184	12

PredatorID	PreyID
184	13
184	14
185	37
185	38
185	39
185	40
185	41
185	42
185	43
185	45
185	46
185	47
185	50
185	52

Table E14.—WE consumer-resource list for Quarry 9 (Carrano and Velez-Juarbe, 2006). See Table E7 for master list of taxonomic ID numbers.

Predator ID	Prey ID
20	6
22	6
26	1
26	3
26	7
27	2
28	26
28	28
29	1
29	6
29	7
30	4
30	6
31	1
31	3
31	6
31	7
31	8
31	9
31	11
31	20
31	27
31	28
31	29
31	30
31	31
31	33
31	35
31	39
31	40
32	22
32	31
33	6
35	1
35	6
35	7
35	8
35	11
35	20
35	29
35	30
37	12
37	13
37	14
37	15
37	16
37	17
38	12
38	13
38	14
38	15
38	16
38	17
38	18
38	19
39	2
40	1
40	2
40	6
41	2
41	9
41	12
41	13
41	14
41	37
41	38
41	39
41	40
41	41
41	42
41	43
41	44
41	45
41	46
41	47
41	50
41	52
42	37
42	38
42	39
42	40
42	41
42	42
42	43
42	44
42	45
42	46
42	47
42	50
42	52
43	2
44	15
44	18
45	112
45	113
45	114
45	115
45	119
45	120
45	121
45	127
45	128
45	133
45	134
45	147
45	153
45	155
45	156
46	37
46	38
46	39
46	40
46	41
46	42
46	43
46	44
46	45
46	46
46	47
46	50

Predator ID	Prey ID
46	52
47	37
47	38
47	39
47	40
47	41
47	42
47	43
47	44
47	45
47	46
47	47
47	50
47	52
50	15
50	16
50	17
50	18
50	19
51	12
51	13
51	14
51	15
51	16
51	17
51	18
51	19
52	12
52	13
52	14
52	15
52	16
52	17
52	18
52	19
53	53
53	72
61	11
61	22
61	26
61	31
61	53

Predator ID	Prey ID
61	62
61	64
61	68
61	72
62	11
62	20
62	27
62	28
62	29
62	30
62	31
62	33
62	35
62	40
62	72
64	33
64	35
64	37
64	38
64	39
64	40
64	41
64	42
64	43
64	45
64	46
64	47
64	50
64	52
64	53
64	62
64	69
64	70
64	71
64	72
64	76
68	20
68	27
68	28
68	29
68	30
68	33

Predator ID	Prey ID
68	35
68	72
69	20
69	27
69	28
69	29
69	30
69	33
69	35
69	39
69	40
69	72
70	20
70	27
70	28
70	29
70	30
70	33
70	35
70	39
70	40
70	72
71	20
71	27
71	28
71	29
71	30
71	33
71	35
71	39
71	40
71	72
72	1
72	6
72	7
76	20
76	27
76	28
76	29
76	30
76	33
76	35

Predator ID	Prey ID
76	39
76	40
76	41
76	42
76	43
76	45
76	46
76	72
77	8
77	11
77	22
77	26
77	27
77	28
77	31
77	33
77	35
77	37
77	38
77	39
77	40
77	41
77	42
77	43
77	45
77	46
77	47
77	52
77	53
77	62
77	64
77	69
77	70
77	71
77	72
77	76
77	96
78	8
78	11
78	22
78	26
78	27

Predator ID	Prey ID
78	28
78	31
78	33
78	35
78	37
78	38
78	39
78	40
78	41
78	42
78	43
78	45
78	46
78	47
78	52
78	53
78	62
78	64
78	69
78	70
78	71
78	72
78	76
78	96
82	26
82	27
82	31
82	37
82	38
82	39
82	40
82	41
82	42
82	43
82	44
82	45
82	46
82	47
82	50
82	51
82	52
82	69

Predator ID	Prey ID
82	70
82	71
82	76
82	86
82	88
82	96
83	26
83	27
83	31
83	37
83	38
83	39
83	40
83	41
83	42
83	43
83	44
83	45
83	46
83	47
83	50
83	51
83	52
83	69
83	70
83	71
83	76
83	86
83	88
83	96
86	27
86	37
86	38
86	39
86	40
86	41
86	42
86	43
86	44
86	45
86	46
86	47

Predator ID	Prey ID
86	50
86	69
86	70
86	71
86	76
88	27
88	37
88	38
88	39
88	40
88	41
88	42
88	43
88	44
88	45
88	46
88	47
88	50
88	69
88	70
88	71
88	76
96	20
96	27
96	28
96	29
96	30
96	33
96	35
96	39
96	40
96	41
96	42
96	43
96	45
96	46
96	72
99	22
99	26
99	31
99	32
99	53

Predator ID	Prey ID
99	61
99	62
99	64
99	68
99	69
99	70
99	71
99	76
99	77
99	78
99	82
99	83
99	86
99	88
99	96
99	99
99	100
99	102
99	111
99	112
99	113
99	114
99	115
99	119
99	120
99	121
99	127
99	128
99	133
99	134
99	147
99	153
99	155
99	156
99	158
99	160
99	161
99	165
99	166
99	167
99	168
99	170

Predator ID	Prey ID
99	171
99	172
99	173
99	174
99	175
99	176
99	177
99	179
99	180
99	181
99	183
100	27
100	28
100	31
100	33
100	35
100	37
100	38
100	39
100	40
100	41
100	42
100	43
100	45
100	46
100	47
100	50
100	52
100	53
100	62
100	69
100	70
100	71
100	72
100	76
102	69
102	70
102	71
102	76
102	86
102	88
102	96

Predator ID	Prey ID
102	100
102	158
102	160
102	161
102	165
102	166
102	167
102	168
102	170
102	171
102	172
102	173
102	174
102	175
102	176
102	177
102	179
102	180
102	181
102	183
102	184
102	185
111	27
111	31
111	37
111	38
111	39
111	40
111	41
111	42
111	43
111	44
111	45
111	46
111	47
111	52
111	53
111	62
111	69
111	70
111	71
111	72

Predator ID	Prey ID
111	76
112	64
112	77
112	78
112	82
112	83
112	99
112	100
112	102
112	111
112	112
112	113
112	114
112	115
112	119
112	120
112	121
112	127
112	128
112	133
112	134
112	147
112	153
112	155
112	156
112	184
112	185
113	37
113	38
113	39
113	40
113	41
113	42
113	43
113	45
113	46
113	47
113	50
113	52
113	69
113	70
113	71

Predator ID	Prey ID
113	76
113	77
113	78
113	82
113	83
113	86
113	88
113	96
113	99
113	100
113	102
113	111
113	112
113	113
113	114
113	115
113	119
113	120
113	121
113	127
113	128
113	133
113	134
113	147
113	153
113	155
113	156
113	158
113	160
113	161
113	165
113	166
113	167
113	168
113	170
113	171
113	172
113	173
113	174
113	175
113	176
113	177

Predator ID	Prey ID
113	179
113	180
113	181
113	183
113	184
113	185
114	61
114	64
114	77
114	78
114	82
114	83
114	99
114	100
114	102
114	111
114	112
114	113
114	114
114	115
114	119
114	120
114	121
114	127
114	128
114	133
114	134
114	147
114	153
114	155
114	156
114	184
114	185
115	31
115	32
115	37
115	38
115	39
115	40
115	41
115	42
115	43

Predator ID	Prey ID
115	45
115	46
115	47
115	50
115	52
115	61
115	62
115	64
115	69
115	70
115	71
115	76
115	77
115	78
115	82
115	83
115	86
115	88
115	96
115	99
115	100
115	102
115	111
115	112
115	113
115	114
115	115
115	119
115	120
115	121
115	127
115	128
115	133
115	134
115	147
115	153
115	155
115	156
115	158
115	160
115	161
115	165

Predator ID	Prey ID
115	166
115	167
115	168
115	170
115	171
115	172
115	173
115	174
115	175
115	176
115	177
115	179
115	180
115	181
115	183
115	184
115	185
119	69
119	70
119	71
119	76
119	77
119	78
119	82
119	83
119	86
119	88
119	96
119	100
119	102
119	111
119	113
119	115
119	119
119	120
119	121
119	128
119	134
119	153
119	155
119	158
119	160

Predator ID	Prey ID
119	161
119	165
119	166
119	167
119	168
119	170
119	171
119	172
119	173
119	174
119	175
119	176
119	177
119	179
119	180
119	181
119	183
119	184
119	185
120	32
120	69
120	70
120	71
120	76
120	77
120	78
120	82
120	83
120	86
120	88
120	96
120	100
120	102
120	111
120	113
120	115
120	153
120	158
120	160
120	161
120	165
120	166

Predator ID	Prey ID
120	167
120	168
120	170
120	171
120	172
120	173
120	174
120	175
120	176
120	177
120	179
120	180
120	181
120	183
120	184
120	185
121	32
121	69
121	70
121	71
121	76
121	77
121	78
121	82
121	83
121	86
121	88
121	96
121	100
121	102
121	111
121	113
121	115
121	153
121	158
121	160
121	161
121	165
121	166
121	167
121	168
121	170

Predator ID	Prey ID
121	171
121	172
121	173
121	174
121	175
121	176
121	177
121	179
121	180
121	181
121	183
121	184
121	185
127	15
127	18
127	19
128	12
128	13
128	14
128	16
128	17
133	12
133	13
133	14
133	15
133	16
133	17
134	12
134	13
134	14
134	16
134	17
147	9
147	13
147	14
147	16
147	17
153	12
153	13
153	14
155	12
155	13

Predator ID	Prey ID
155	14
155	16
155	17
156	12
156	13
156	14
156	16
156	17
158	11
158	31
158	32
158	33
158	35
158	37
158	38
158	39
158	40
158	41
158	42
158	43
158	44
158	45
158	46
158	47
158	50
158	51
158	52
158	69
158	70
158	71
158	76
158	86
158	88
158	96
160	12
160	13
160	14
160	27
160	37
160	38
160	39
160	40

Predator ID	Prey ID
160	41
160	42
160	43
160	44
160	45
160	46
160	50
160	52
161	12
161	13
161	14
161	27
161	37
161	38
161	39
161	40
161	41
161	42
161	43
161	44
161	45
161	46
161	50
161	52
165	27
165	37
165	38
165	39
165	40
165	41
165	42
165	43
165	44
165	45
165	46
165	50
165	52
166	27
166	37
166	38
166	39
166	40

Predator ID	Prey ID
166	41
166	42
166	43
166	44
166	45
166	46
166	50
166	52
167	27
167	37
167	38
167	39
167	40
167	41
167	42
167	43
167	44
167	45
167	46
167	50
167	52
167	69
167	70
167	71
167	76
167	86
167	88
167	96
167	160
167	161
167	165
167	166
167	170
167	171
167	172
167	173
167	174
167	175
167	176
167	177
167	179
167	181

Predator ID	Prey ID
167	183
168	27
168	37
168	38
168	39
168	40
168	41
168	42
168	43
168	44
168	45
168	46
168	50
168	52
168	69
168	70
168	71
168	76
168	86
168	88
168	96
168	160
168	161
168	165
168	166
168	170
168	171
168	172
168	173
168	174
168	175
168	176
168	177
168	179
168	181
168	183
170	27
170	37
170	38
170	39
170	40
170	41

Predator ID	Prey ID
170	42
170	43
170	44
170	45
170	46
170	50
171	27
171	37
171	38
171	39
171	40
171	41
171	42
171	43
171	44
171	45
171	46
171	50
172	27
172	37
172	38
172	39
172	40
172	41
172	42
172	43
172	44
172	45
172	46
172	50
172	52
173	27
173	37
173	38
173	39
173	40
173	41
173	42
173	43
173	44
173	45
173	46

Predator ID	Prey ID
173	50
173	52
174	27
174	37
174	38
174	39
174	40
174	41
174	42
174	43
174	44
174	45
174	46
174	50
174	52
175	27
175	37
175	38
175	39
175	40
175	41
175	42
175	43
175	44
175	45
175	46
175	50
175	52
176	27
176	37
176	38
176	39
176	40
176	41
176	42
176	43
176	44
176	45
176	46
176	50
176	52
177	27

Predator ID	Prey ID
177	37
177	38
177	39
177	40
177	41
177	42
177	43
177	44
177	45
177	46
177	50
177	52
179	27
179	37
179	38
179	39
179	40
179	41
179	42
179	43
179	44
179	45
179	46
179	50
180	27
180	37
180	38
180	39
180	40
180	41
180	42
180	43
180	44
180	45
180	46
180	50
181	27
181	37
181	38
181	39
181	40
181	41

Predator ID	Prey ID
181	42
181	43
181	44
181	45
181	46
181	50
183	27
183	37
183	38
183	39
183	40
183	41
183	42
183	43
183	44
183	45
183	46
183	50
184	9
184	12
184	13
184	14
185	37
185	38
185	39
185	40
185	41
185	42
185	43
185	45
185	46
185	47
185	50
185	52

Table E15.—TS consumer-resource list for biozone 1. See Table E7 for master list of taxonomic ID numbers.

PredatorID	PreyID
27	2
31	9
31	27
31	31
31	35
31	39
31	40
37	12
37	13
37	14
37	15
37	16
37	17
38	12
38	13
38	14
38	15
38	16
38	17
38	18
38	19
39	2
40	2
41	2
41	9
41	12
41	13
41	14
41	37
41	38
41	39
41	40
41	41
41	42
41	43
41	44
41	45
41	46
41	47
41	50

PredatorID	PreyID
41	52
42	37
42	38
42	39
42	40
42	41
42	42
42	43
42	44
42	45
42	46
42	47
42	50
42	52
43	2
44	15
44	18
45	112
45	113
45	131
45	132
45	141
45	142
45	147
45	148
45	151
45	155
45	156
46	37
46	38
46	39
46	40
46	41
46	42
46	43
46	44
46	45
46	46
46	47
46	50

PredatorID	PreyID
46	52
47	37
47	38
47	39
47	40
47	41
47	42
47	43
47	44
47	45
47	46
47	47
47	50
47	52
50	15
50	16
50	17
50	18
50	19
51	12
51	13
51	14
51	15
51	16
51	17
51	18
51	19
52	12
52	13
52	14
52	15
52	16
52	17
52	18
52	19
77	27
77	31
77	35
77	37
77	38

PredatorID	PreyID
77	39
77	40
77	41
77	42
77	43
77	45
77	46
77	47
77	52
81	27
81	31
81	35
81	37
81	38
81	39
81	40
81	41
81	42
81	43
81	45
81	46
81	47
81	52
101	31
101	77
101	81
101	101
101	109
101	113
101	158
109	27
109	31
109	37
109	38
109	39
109	40
109	41
109	42
109	43
109	44
109	45
109	46

PredatorID	PreyID
109	47
109	52
112	77
112	81
112	101
112	109
112	112
112	113
112	131
112	132
112	141
112	142
112	147
112	148
112	151
112	155
112	156
112	184
112	185
113	37
113	38
113	39
113	40
113	41
113	42
113	43
113	45
113	46
113	47
113	50
113	52
113	77
113	81
113	101
113	109
113	112
113	113
113	131
113	132
113	141
113	142
113	147

PredatorID	PreyID
113	148
113	151
113	155
113	156
113	158
113	184
113	185
131	15
131	16
131	17
132	12
132	13
132	14
132	16
132	17
141	12
141	13
141	14
141	15
141	16
141	17
142	12
142	13
142	14
142	16
142	17
147	9
147	13
147	14
147	16
147	17
148	9
148	13
148	14
148	16
148	17
151	9
151	13
151	14
151	16
151	17
155	12

PredatorID	PreyID
155	13
155	14
155	16
155	17
156	12
156	13
156	14
156	16
156	17
158	31
158	35
158	37
158	38
158	39
158	40
158	41
158	42
158	43
158	44
158	45
158	46
158	47
158	50
158	51
158	52
184	9
184	12
184	13
184	14
185	37
185	38
185	39
185	40
185	41
185	42
185	43
185	45
185	46
185	47
185	50
185	52

Table E16.—TS consumer-resource list for biozone 2. See Table E7 for master list of taxonomic ID numbers.

PredatorID	PreyID
27	2
31	9
31	27
31	31
31	35
31	39
31	40
37	12
37	13
37	14
37	15
37	16
37	17
38	12
38	13
38	14
38	15
38	16
38	17
38	18
38	19
39	2
40	2
41	2
41	9
41	12
41	13
41	14
41	37
41	38
41	39
41	40
41	41
41	42
41	43
41	44
41	45
41	46
41	47
41	50

PredatorID	PreyID
41	52
42	37
42	38
42	39
42	40
42	41
42	42
42	43
42	44
42	45
42	46
42	47
42	50
42	52
43	2
44	15
44	18
45	112
45	113
45	114
45	115
45	119
45	120
45	121
45	122
45	123
45	127
45	128
45	129
45	130
45	131
45	132
45	133
45	134
45	135
45	136
45	137
45	138
45	147
45	150

PredatorID	PreyID
45	153
45	155
45	156
46	37
46	38
46	39
46	40
46	41
46	42
46	43
46	44
46	45
46	46
46	47
46	50
46	52
47	37
47	38
47	39
47	40
47	41
47	42
47	43
47	44
47	45
47	46
47	47
47	50
47	52
50	15
50	16
50	17
50	18
50	19
51	12
51	13
51	14
51	15
51	16
51	17

PredatorID	PreyID
51	18
51	19
52	12
52	13
52	14
52	15
52	16
52	17
52	18
52	19
64	35
64	37
64	38
64	39
64	40
64	41
64	42
64	43
64	45
64	46
64	47
64	50
64	52
64	64
64	73
64	76
64	77
64	78
73	27
73	35
73	39
73	40
76	27
76	35
76	39
76	40
76	41
76	42
76	43
76	45
76	46
77	27

PredatorID	PreyID
77	31
77	35
77	37
77	38
77	39
77	40
77	41
77	42
77	43
77	45
77	46
77	47
77	52
77	64
77	73
77	76
77	77
77	78
78	27
78	31
78	35
78	37
78	38
78	39
78	40
78	41
78	42
78	43
78	45
78	46
78	47
78	52
78	64
78	73
78	76
78	77
78	78
81	27
81	31
81	35
81	37
81	38
81	39
81	40
81	41
81	42
81	43
81	45
81	46
81	47
81	52
81	64
81	73
81	76
81	77
81	78
82	27
82	31
82	37
82	38
82	39
82	40
82	41
82	42
82	43
82	44
82	45
82	46
82	47
82	50
82	51
82	52
82	73
82	76
82	77
82	78
82	86
82	95
85	9
85	12
85	13
85	14
85	73
85	76

PredatorID	PreyID
85	77
85	78
85	86
85	95
86	27
86	37
86	38
86	39
86	40
86	41
86	42
86	43
86	44
86	45
86	46
86	47
86	50
86	73
86	76
86	77
86	78
95	27
95	37
95	38
95	39
95	40
95	41
95	42
95	43
95	44
95	45
95	46
95	47
95	50
95	73
95	76
95	77
95	78
98	73
98	76
98	77
98	78

PredatorID	PreyID
98	81
98	82
98	86
98	95
98	98
98	100
98	101
98	158
98	160
98	161
98	180
98	181
98	184
98	185
99	31
99	64
99	73
99	76
99	77
99	78
99	81
99	82
99	85
99	86
99	95
99	98
99	99
99	100
99	101
99	108
99	110
99	112
99	113
99	114
99	115
99	119
99	120
99	121
99	122
99	123
99	127
99	128

PredatorID	PreyID
99	129
99	130
99	131
99	132
99	133
99	134
99	135
99	136
99	137
99	138
99	147
99	150
99	153
99	155
99	156
99	158
99	160
99	161
99	180
99	181
100	27
100	31
100	35
100	37
100	38
100	39
100	40
100	41
100	42
100	43
100	45
100	46
100	47
100	50
100	52
100	64
100	73
100	76
100	77
100	78
101	31
101	64

PredatorID	PreyID
101	73
101	76
101	77
101	78
101	81
101	82
101	85
101	86
101	95
101	98
101	100
101	101
101	108
101	110
101	113
101	114
101	115
101	153
101	158
101	160
101	161
101	180
101	181
108	27
108	31
108	37
108	38
108	39
108	40
108	41
108	42
108	43
108	44
108	45
108	46
108	47
108	52
108	73
108	76
108	77
108	78
110	27

PredatorID	PreyID
110	31
110	37
110	38
110	39
110	40
110	41
110	42
110	43
110	44
110	45
110	46
110	47
110	52
110	73
110	76
110	77
110	78
112	64
112	77
112	78
112	81
112	82
112	85
112	86
112	98
112	99
112	100
112	101
112	108
112	110
112	112
112	113
112	114
112	115
112	119
112	120
112	121
112	122
112	123
112	127
112	128
112	129

PredatorID	PreyID
112	130
112	131
112	132
112	133
112	134
112	135
112	136
112	137
112	138
112	147
112	150
112	153
112	155
112	156
112	184
112	185
113	37
113	38
113	39
113	40
113	41
113	42
113	43
113	45
113	46
113	47
113	50
113	52
113	73
113	76
113	77
113	78
113	81
113	82
113	85
113	86
113	95
113	98
113	99
113	100
113	101
113	108

PredatorID	PreyID
113	110
113	112
113	113
113	114
113	115
113	119
113	120
113	121
113	122
113	123
113	127
113	128
113	129
113	130
113	131
113	132
113	133
113	134
113	135
113	136
113	137
113	138
113	147
113	150
113	153
113	155
113	156
113	158
113	160
113	161
113	180
113	181
113	184
113	185
114	64
114	77
114	78
114	81
114	82
114	85
114	86
114	98

PredatorID	PreyID
114	99
114	100
114	101
114	108
114	110
114	112
114	113
114	114
114	115
114	119
114	120
114	121
114	122
114	123
114	127
114	128
114	129
114	130
114	131
114	132
114	133
114	134
114	135
114	136
114	137
114	138
114	147
114	150
114	153
114	155
114	156
114	184
114	185
115	31
115	37
115	38
115	39
115	40
115	41
115	42
115	43
115	45

PredatorID	PreyID
115	46
115	47
115	50
115	52
115	64
115	73
115	76
115	77
115	78
115	81
115	82
115	85
115	86
115	95
115	98
115	99
115	100
115	101
115	108
115	110
115	112
115	113
115	114
115	115
115	119
115	120
115	121
115	122
115	123
115	127
115	128
115	129
115	130
115	131
115	132
115	133
115	134
115	135
115	136
115	137
115	138
115	147

PredatorID	PreyID
115	150
115	153
115	155
115	156
115	158
115	160
115	161
115	180
115	181
115	184
115	185
119	73
119	76
119	77
119	78
119	81
119	82
119	85
119	86
119	95
119	98
119	100
119	101
119	108
119	110
119	113
119	114
119	115
119	119
119	120
119	121
119	122
119	123
119	128
119	130
119	132
119	134
119	136
119	138
119	153
119	155
119	158

PredatorID	PreyID
119	160
119	161
119	180
119	181
119	184
119	185
120	73
120	76
120	77
120	78
120	81
120	82
120	85
120	86
120	95
120	98
120	100
120	101
120	110
120	113
120	114
120	115
120	153
120	158
120	160
120	161
120	180
120	181
120	184
120	185
121	73
121	76
121	77
121	78
121	81
121	82
121	85
121	86
121	95
121	98
121	100
121	101

PredatorID	PreyID
121	110
121	113
121	114
121	115
121	153
121	158
121	160
121	161
121	180
121	181
121	184
121	185
122	73
122	76
122	77
122	78
122	81
122	82
122	85
122	86
122	95
122	98
122	100
122	101
122	110
122	113
122	114
122	115
122	153
122	158
122	160
122	161
122	180
122	181
122	184
122	185
123	77
123	78
123	81
123	82
123	85
123	86

PredatorID	PreyID
123	95
123	100
123	101
123	108
123	110
123	113
123	114
123	115
123	119
123	120
123	121
123	122
123	123
123	128
123	130
123	132
123	134
123	136
123	138
123	153
123	155
123	158
123	160
123	161
123	180
123	181
123	184
123	185
127	15
127	18
127	19
128	12
128	13
128	14
128	16
128	17
129	15
129	16
129	17
130	12
130	13
130	14

PredatorID	PreyID
130	16
130	17
131	15
131	16
131	17
132	12
132	13
132	14
132	16
132	17
133	12
133	13
133	14
133	15
133	16
133	17
134	12
134	13
134	14
134	16
134	17
135	12
135	13
135	14
135	15
135	16
135	17
136	12
136	13
136	14
136	16
136	17
137	12
137	13
137	14
137	15
137	16
137	17
138	12
138	13
138	14
138	16

PredatorID	PreyID
138	17
147	9
147	13
147	14
147	16
147	17
150	9
150	13
150	14
150	16
150	17
153	12
153	13
153	14
155	12
155	13
155	14
155	16
155	17
156	12
156	13
156	14
156	16
156	17
158	31
158	35
158	37
158	38
158	39
158	40
158	41
158	42
158	43
158	44
158	45
158	46
158	47
158	50
158	51
158	52
158	73
158	76

PredatorID	PreyID
158	77
158	78
158	86
160	12
160	13
160	14
160	27
160	37
160	38
160	39
160	40
160	41
160	42
160	43
160	44
160	45
160	46
160	50
160	52
161	12
161	13
161	14
161	27
161	37
161	38
161	39
161	40
161	41
161	42
161	43
161	44
161	45
161	46
161	50
161	52
180	27
180	37
180	38
180	39
180	40
180	41
180	42

PredatorID	PreyID
180	43
180	44
180	45
180	46
180	50
181	27
181	37
181	38
181	39
181	40
181	41
181	42
181	43
181	44
181	45
181	46
181	50
184	9
184	12
184	13
184	14
185	37
185	38
185	39
185	40
185	41
185	42
185	43
185	45
185	46
185	47
185	50
185	52

Table E17.—TS consumer-resource list for biozone 3. See Table E7 for master list of taxonomic ID numbers.

PredatorID	PreyID
27	2
31	9
31	27
31	31
31	35
31	39
31	40
37	12
37	13
37	14
37	15
37	16
37	17
38	12
38	13
38	14
38	15
38	16
38	17
38	18
38	19
39	2
40	2
41	2
41	9
41	12
41	13
41	14
41	37
41	38
41	39
41	40
41	41
41	42
41	43
41	44
41	45
41	46
41	47
41	50
41	52
42	37
42	38
42	39
42	40
42	41
42	42
42	43
42	44
42	45
42	46
42	47
42	50
42	52
43	2
45	112
45	113
45	114
45	115
45	117
45	118
45	121
45	123
45	127
45	128
45	129
45	130
45	131
45	132
45	133
45	134
45	135
45	136
45	137
45	138
45	139
45	140
45	147
45	153
45	155
45	156
46	37
46	38
46	39
46	40
46	41
46	42
46	43
46	44
46	45
46	46
46	47
46	50
46	52
47	37
47	38
47	39
47	40
47	41
47	42
47	43
47	44
47	45
47	46
47	47
47	50
47	52
50	15
50	16
50	17
50	18
50	19
51	12
51	13
51	14
51	15
51	16
51	17
51	18
51	19

PredatorID	PreyID
52	12
52	13
52	14
52	15
52	16
52	17
52	18
52	19
77	27
77	31
77	35
77	37
77	38
77	39
77	40
77	41
77	42
77	43
77	45
77	46
77	47
77	52
78	27
78	31
78	35
78	37
78	38
78	39
78	40
78	41
78	42
78	43
78	45
78	46
78	47
78	52
81	27
81	31
81	35
81	37
81	38
81	39

PredatorID	PreyID
81	40
81	41
81	42
81	43
81	45
81	46
81	47
81	52
82	27
82	31
82	37
82	38
82	39
82	40
82	41
82	42
82	43
82	44
82	45
82	46
82	47
82	50
82	51
82	52
82	86
85	9
85	12
85	13
85	14
85	86
86	27
86	37
86	38
86	39
86	40
86	41
86	42
86	43
86	44
86	45
86	46
86	47

PredatorID	PreyID
86	50
99	31
99	77
99	78
99	81
99	82
99	85
99	86
99	99
99	100
99	112
99	113
99	114
99	115
99	117
99	118
99	121
99	123
99	127
99	128
99	129
99	130
99	131
99	132
99	133
99	134
99	135
99	136
99	137
99	138
99	139
99	140
99	147
99	153
99	155
99	156
99	158
99	161
99	180
99	181
99	147
99	153

PredatorID	PreyID
99	155
99	156
99	158
99	161
99	180
99	181
100	27
100	31
100	35
100	37
100	38
100	39
100	40
100	41
100	42
100	43
100	45
100	46
100	47
100	50
100	52
112	77
112	78
112	81
112	82
112	85
112	86
112	99
112	100
112	112
112	113
112	114
112	115
112	117
112	118
112	121
112	123
112	127
112	128
112	129
112	130
112	131

PredatorID	PreyID
112	132
112	133
112	134
112	135
112	136
112	137
112	138
112	139
112	140
112	147
112	153
112	155
112	156
112	184
112	185
113	37
113	38
113	39
113	40
113	41
113	42
113	43
113	45
113	46
113	47
113	50
113	52
113	77
113	78
113	81
113	82
113	85
113	86
113	99
113	100
113	112
113	113
113	114
113	115
113	117
113	118
113	121

PredatorID	PreyID
113	123
113	127
113	128
113	129
113	130
113	131
113	132
113	133
113	134
113	135
113	136
113	137
113	138
113	139
113	140
113	147
113	153
113	155
113	156
113	158
113	161
113	180
113	181
113	184
113	185
114	77
114	78
114	81
114	82
114	85
114	86
114	99
114	100
114	112
114	113
114	114
114	115
114	117
114	118
114	121
114	123
114	127

PredatorID	PreyID
114	128
114	129
114	130
114	131
114	132
114	133
114	134
114	135
114	136
114	137
114	138
114	139
114	140
114	147
114	153
114	155
114	156
114	184
114	185
115	31
115	37
115	38
115	39
115	40
115	41
115	42
115	43
115	45
115	46
115	47
115	50
115	52
115	77
115	78
115	81
115	82
115	85
115	86
115	99
115	100
115	112
115	113

PredatorID	PreyID
115	114
115	115
115	117
115	118
115	121
115	123
115	127
115	128
115	129
115	130
115	131
115	132
115	133
115	134
115	135
115	136
115	137
115	138
115	139
115	140
115	147
115	153
115	155
115	156
115	158
115	161
115	180
115	181
115	184
115	185
117	82
117	85
117	86
117	99
117	100
117	112
117	113
117	114
117	115
117	117
117	118
117	121

PredatorID	PreyID
117	123
117	127
117	128
117	129
117	130
117	131
117	132
117	133
117	134
117	135
117	136
117	137
117	138
117	139
117	140
117	147
117	153
117	155
117	156
117	184
117	185
118	82
118	85
118	86
118	100
118	113
118	115
118	118
118	121
118	123
118	128
118	130
118	132
118	134
118	136
118	138
118	140
118	153
118	155
118	184
118	185
121	77

PredatorID	PreyID
121	78
121	81
121	82
121	85
121	86
121	100
121	113
121	115
121	153
121	158
121	161
121	180
121	181
121	184
121	185
123	77
123	78
123	81
123	82
123	85
123	86
123	100
123	113
123	115
123	118
123	121
123	123
123	128
123	130
123	132
123	134
123	136
123	138
123	140
123	153
123	155
123	158
123	161
123	180
123	181
123	184
123	185

PredatorID	PreyID
127	15
127	18
127	19
128	12
128	13
128	14
128	16
128	17
129	15
129	16
129	17
130	12
130	13
130	14
130	16
130	17
131	15
131	16
131	17
132	12
132	13
132	14
132	16
132	17
133	12
133	13
133	14
133	15
133	16
133	17
134	12
134	13
134	14
134	16
134	17
135	12
135	13
135	14
135	15
135	16
135	17
136	12

PredatorID	PreyID
136	13
136	14
136	16
136	17
137	12
137	13
137	14
137	15
137	16
137	17
138	12
138	13
138	14
138	16
138	17
139	12
139	13
139	14
139	15
139	16
139	17
140	12
140	13
140	14
140	16
140	17
147	9
147	13
147	14
147	16
147	17
153	12
153	13
153	14
155	12
155	13
155	14
155	16
155	17
156	12
156	13
156	14

PredatorID	PreyID
156	16
156	17
158	31
158	35
158	37
158	38
158	39
158	40
158	41
158	42
158	43
158	44
158	45
158	46
158	47
158	50
158	51
158	52
158	86
161	12
161	13
161	14
161	27
161	37
161	38
161	39
161	40
161	41
161	42
161	43
161	44
161	45
161	46
161	50
161	52
180	27
180	37
180	38
180	39
180	40
180	41
180	42

PredatorID	PreyID
180	43
180	44
180	45
180	46
180	50
181	27
181	37
181	38
181	39
181	40
181	41
181	42
181	43
181	44
181	45
181	46
181	50
184	9
184	12
184	13
184	14
185	37
185	38
185	39
185	40
185	41
185	42
185	43
185	45
185	46
185	47
185	50
185	52

Table E18.—TS consumer-resource list for biozone 4. See Table E7 for master list of taxonomic ID numbers.

PredatorID	PreyID
27	2
31	9
31	27
31	31
31	35
31	39
31	40
37	12
37	13
37	14
37	15
37	16
37	17
38	12
38	13
38	14
38	15
38	16
38	17
38	18
38	19
39	2
40	2
41	2
41	9
41	12
41	13
41	14
41	37
41	38
41	39
41	40
41	41
41	42
41	43
41	44
41	45
41	46
41	47
41	50

PredatorID	PreyID
41	52
42	37
42	38
42	39
42	40
42	41
42	42
42	43
42	44
42	45
42	46
42	47
42	50
42	52
43	2
44	15
44	18
45	112
45	113
45	114
45	115
45	117
45	118
45	121
45	122
45	123
45	127
45	128
45	129
45	130
45	131
45	132
45	133
45	134
45	135
45	136
45	137
45	138
45	147
45	149

PredatorID	PreyID
45	151
45	152
45	153
45	155
45	156
46	37
46	38
46	39
46	40
46	41
46	42
46	43
46	44
46	45
46	46
46	47
46	50
46	52
47	37
47	38
47	39
47	40
47	41
47	42
47	43
47	44
47	45
47	46
47	47
47	50
47	52
50	15
50	16
50	17
50	18
50	19
51	12
51	13
51	14
51	15

PredatorID	PreyID
51	16
51	17
51	18
51	19
52	12
52	13
52	14
52	15
52	16
52	17
52	18
52	19
64	35
64	37
64	38
64	39
64	40
64	41
64	42
64	43
64	45
64	46
64	47
64	50
64	52
64	73
64	76
73	27
73	35
73	39
73	40
76	27
76	35
76	39
76	40
76	41
76	42
76	43
76	45
76	46
77	27
77	31

PredatorID	PreyID
77	35
77	37
77	38
77	39
77	40
77	41
77	42
77	43
77	45
77	46
77	47
77	52
77	64
77	73
77	76
78	27
78	31
78	35
78	37
78	38
78	39
78	40
78	41
78	42
78	43
78	45
78	46
78	47
78	52
78	64
78	73
78	76
81	27
81	31
81	35
81	37
81	38
81	39
81	40
81	41
81	42
81	43

PredatorID	PreyID
81	45
81	46
81	47
81	52
81	64
81	73
81	76
82	27
82	31
82	37
82	38
82	39
82	40
82	41
82	42
82	43
82	44
82	45
82	46
82	47
82	50
82	51
82	52
82	73
82	76
82	86
82	87
82	88
82	89
82	95
84	9
84	12
84	13
84	14
84	73
84	76
84	86
84	87
84	88
84	89
84	95
85	9

PredatorID	PreyID
85	12
85	13
85	14
85	73
85	76
85	86
85	87
85	88
85	89
85	95
86	27
86	37
86	38
86	39
86	40
86	41
86	42
86	43
86	44
86	45
86	46
86	47
86	50
86	73
86	76
87	27
87	37
87	38
87	39
87	40
87	41
87	42
87	43
87	44
87	45
87	46
87	47
87	50
87	73
87	76
88	27
88	37

PredatorID	PreyID
88	38
88	39
88	40
88	41
88	42
88	43
88	44
88	45
88	46
88	47
88	50
88	73
88	76
89	27
89	37
89	38
89	39
89	40
89	41
89	42
89	43
89	44
89	45
89	46
89	47
89	50
89	73
89	76
95	27
95	37
95	38
95	39
95	40
95	41
95	42
95	43
95	44
95	45
95	46
95	47
95	50
95	73

PredatorID	PreyID
95	76
98	73
98	76
98	77
98	78
98	81
98	86
98	87
98	88
98	89
98	95
98	98
98	100
98	157
98	158
98	159
98	161
98	162
98	164
98	167
98	180
98	181
98	184
98	185
99	31
99	64
99	73
99	76
99	77
99	78
99	81
99	82
99	84
99	85
99	86
99	87
99	88
99	89
99	95
99	98
99	99
99	100

PredatorID	PreyID
99	101
99	102
99	105
99	106
99	110
99	112
99	113
99	114
99	115
99	117
99	118
99	121
99	122
99	123
99	127
99	128
99	129
99	130
99	131
99	132
99	133
99	134
99	135
99	136
99	137
99	138
99	147
99	149
99	151
99	152
99	153
99	155
99	156
99	157
99	158
99	159
99	161
99	162
99	164
99	167
99	180
99	181

PredatorID	PreyID
100	27
100	31
100	35
100	37
100	38
100	39
100	40
100	41
100	42
100	43
100	45
100	46
100	47
100	50
100	52
100	73
100	76
101	31
101	64
101	73
101	76
101	77
101	78
101	81
101	82
101	84
101	85
101	86
101	87
101	88
101	89
101	95
101	98
101	100
101	101
101	102
101	105
101	106
101	110
101	113
101	115
101	152

PredatorID	PreyID
101	153
101	157
101	158
101	159
101	161
101	162
101	164
101	167
101	180
101	181
102	73
102	76
102	86
102	87
102	88
102	89
102	95
102	100
102	158
102	159
102	161
102	162
102	164
102	167
102	180
102	181
102	184
102	185
105	27
105	31
105	37
105	38
105	39
105	40
105	41
105	42
105	43
105	44
105	45
105	46
105	47
105	52

PredatorID	PreyID
105	73
105	76
106	27
106	31
106	37
106	38
106	39
106	40
106	41
106	42
106	43
106	44
106	45
106	46
106	47
106	52
106	73
106	76
110	27
110	31
110	37
110	38
110	39
110	40
110	41
110	42
110	43
110	44
110	45
110	46
110	47
110	52
110	73
110	76
112	64
112	77
112	78
112	81
112	82
112	84
112	85
112	98

PredatorID	PreyID
112	99
112	100
112	101
112	102
112	105
112	106
112	110
112	112
112	113
112	114
112	115
112	117
112	118
112	121
112	122
112	123
112	127
112	128
112	129
112	130
112	131
112	132
112	133
112	134
112	135
112	136
112	137
112	138
112	147
112	149
112	151
112	152
112	153
112	155
112	156
112	157
112	184
112	185
113	37
113	38
113	39
113	40

PredatorID	PreyID
113	41
113	42
113	43
113	45
113	46
113	47
113	50
113	52
113	73
113	76
113	77
113	78
113	81
113	82
113	84
113	85
113	86
113	87
113	88
113	89
113	95
113	98
113	99
113	100
113	101
113	102
113	105
113	106
113	110
113	112
113	113
113	114
113	115
113	117
113	118
113	121
113	122
113	123
113	127
113	128
113	129
113	130

PredatorID	PreyID
113	131
113	132
113	133
113	134
113	135
113	136
113	137
113	138
113	147
113	149
113	151
113	152
113	153
113	155
113	156
113	157
113	158
113	159
113	161
113	162
113	164
113	167
113	180
113	181
113	184
113	185
114	64
114	77
114	78
114	81
114	82
114	84
114	85
114	98
114	99
114	100
114	101
114	102
114	105
114	106
114	110
114	112

PredatorID	PreyID
114	113
114	114
114	115
114	117
114	118
114	121
114	122
114	123
114	127
114	128
114	129
114	130
114	131
114	132
114	133
114	134
114	135
114	136
114	137
114	138
114	147
114	149
114	151
114	152
114	153
114	155
114	156
114	157
114	184
114	185
115	31
115	37
115	38
115	39
115	40
115	41
115	42
115	43
115	45
115	46
115	47
115	50

PredatorID	PreyID
115	52
115	64
115	73
115	76
115	77
115	78
115	81
115	82
115	84
115	85
115	86
115	87
115	88
115	89
115	95
115	98
115	99
115	100
115	101
115	102
115	105
115	106
115	110
115	112
115	113
115	114
115	115
115	117
115	118
115	121
115	122
115	123
115	127
115	128
115	129
115	130
115	131
115	132
115	133
115	134
115	135
115	136

PredatorID	PreyID
115	137
115	138
115	147
115	149
115	151
115	152
115	153
115	155
115	156
115	157
115	158
115	159
115	161
115	162
115	164
115	167
115	180
115	181
115	184
115	185
117	64
117	82
117	84
117	85
117	98
117	99
117	100
117	101
117	102
117	105
117	106
117	110
117	112
117	113
117	114
117	115
117	117
117	118
117	121
117	122
117	123
117	127

PredatorID	PreyID
117	128
117	129
117	130
117	131
117	132
117	133
117	134
117	135
117	136
117	137
117	138
117	147
117	149
117	151
117	152
117	153
117	155
117	156
117	157
117	184
117	185
118	82
118	84
118	85
118	98
118	100
118	101
118	102
118	105
118	106
118	110
118	113
118	115
118	118
118	121
118	122
118	123
118	128
118	130
118	132
118	134
118	136

PredatorID	PreyID
118	138
118	153
118	155
118	157
118	184
118	185
121	73
121	76
121	77
121	78
121	81
121	82
121	84
121	85
121	86
121	87
121	88
121	89
121	95
121	98
121	100
121	101
121	102
121	105
121	110
121	113
121	115
121	152
121	153
121	157
121	158
121	159
121	161
121	162
121	164
121	167
121	180
121	181
121	184
121	185
122	73
122	76

PredatorID	PreyID
122	77
122	78
122	81
122	82
122	84
122	85
122	86
122	87
122	88
122	89
122	95
122	98
122	100
122	101
122	102
122	105
122	110
122	113
122	115
122	152
122	153
122	157
122	158
122	159
122	161
122	162
122	164
122	167
122	180
122	181
122	184
122	185
123	77
123	78
123	81
123	82
123	84
123	85
123	86
123	87
123	88
123	89

PredatorID	PreyID
123	95
123	100
123	101
123	102
123	105
123	106
123	110
123	113
123	115
123	118
123	121
123	122
123	123
123	128
123	130
123	132
123	134
123	136
123	138
123	152
123	153
123	155
123	157
123	158
123	159
123	161
123	162
123	164
123	167
123	180
123	181
123	184
123	185
127	15
127	18
127	19
128	12
128	13
128	14
128	16
128	17
129	15

PredatorID	PreyID
129	16
129	17
130	12
130	13
130	14
130	16
130	17
131	15
131	16
131	17
132	12
132	13
132	14
132	16
132	17
133	12
133	13
133	14
133	15
133	16
133	17
134	12
134	13
134	14
134	16
134	17
135	12
135	13
135	14
135	15
135	16
135	17
136	12
136	13
136	14
136	16
136	17
137	12
137	13
137	14
137	15
137	16

PredatorID	PreyID
137	17
138	12
138	13
138	14
138	16
138	17
147	9
147	13
147	14
147	16
147	17
149	9
149	13
149	14
149	16
149	17
151	9
151	13
151	14
151	16
151	17
152	12
152	13
152	14
152	37
152	38
152	39
152	40
152	41
152	42
152	43
152	45
152	46
152	47
152	50
152	52
153	12
153	13
153	14
155	12
155	13
155	14

PredatorID	PreyID
155	16
155	17
156	12
156	13
156	14
156	16
156	17
157	12
157	13
157	14
157	37
157	38
157	39
157	40
157	41
157	42
157	43
157	45
157	46
157	47
157	50
157	52
158	31
158	35
158	37
158	38
158	39
158	40
158	41
158	42
158	43
158	44
158	45
158	46
158	47
158	50
158	51
158	52
158	73
158	76
158	86
158	87

PredatorID	PreyID
158	88
158	89
159	27
159	37
159	38
159	39
159	40
159	41
159	42
159	43
159	46
159	50
159	51
161	12
161	13
161	14
161	27
161	37
161	38
161	39
161	40
161	41
161	42
161	43
161	44
161	45
161	46
161	50
161	52
162	12
162	13
162	14
162	27
162	37
162	38
162	39
162	40
162	41
162	42
162	43
162	44
162	45

PredatorID	PreyID
162	46
162	50
162	52
164	27
164	37
164	38
164	39
164	40
164	41
164	42
164	43
164	44
164	45
164	46
164	50
164	52
167	27
167	37
167	38
167	39
167	40
167	41
167	42
167	43
167	44
167	45
167	46
167	50
167	52
167	73
167	76
167	86
167	87
167	88
167	89
167	159
167	161
167	162
167	164
167	181
180	27
180	37

PredatorID	PreyID
180	38
180	39
180	40
180	41
180	42
180	43
180	44
180	45
180	46
180	50
181	27
181	37
181	38
181	39
181	40
181	41
181	42
181	43
181	44
181	45
181	46
181	50
184	9
184	12
184	13
184	14
185	37
185	38
185	39
185	40
185	41
185	42
185	43
185	45
185	46
185	47
185	50
185	52

Table E19.—TS consumer-resource list for biozone 5. See Table E7 for master list of taxonomic ID numbers.

PredatorID	PreyID
27	2
31	9
31	27
31	31
31	35
31	39
31	40
37	12
37	13
37	14
37	15
37	16
37	17
38	12
38	13
38	14
38	15
38	16
38	17
38	18
38	19
39	2
40	2
41	2
41	9
41	12
41	13
41	14
41	37
41	38
41	39
41	40
41	41
41	42
41	43
41	44
41	45
41	46
41	47
41	50
41	52
42	37
42	38
42	39
42	40
42	41
42	42
42	43
42	44
42	45
42	46
42	47
42	50
42	52
43	2
44	15
44	18
45	112
45	113
45	114
45	115
45	116
45	117
45	118
45	119
45	120
45	121
45	122
45	129
45	130
45	133
45	134
45	135
45	136
45	137
45	138
45	147
45	149
45	153
45	154
45	155
45	156
46	37
46	38
46	39
46	40
46	41
46	42
46	43
46	44
46	45
46	46
46	47
46	50
46	52
47	37
47	38
47	39
47	40
47	41
47	42
47	43
47	44
47	45
47	46
47	47
47	50
47	52
50	15
50	16
50	17
50	18
50	19
51	12
51	13
51	14
51	15
51	16
51	17
51	18

PredatorID	PreyID
51	19
52	12
52	13
52	14
52	15
52	16
52	17
52	18
52	19
64	35
64	37
64	38
64	39
64	40
64	41
64	42
64	43
64	45
64	46
64	47
64	50
64	52
64	69
64	71
64	76
69	27
69	35
69	39
69	40
71	27
71	35
71	39
71	40
76	27
76	35
76	39
76	40
76	41
76	42
76	43
76	45
76	46

PredatorID	PreyID
77	27
77	31
77	35
77	37
77	38
77	39
77	40
77	41
77	42
77	43
77	45
77	46
77	47
77	52
77	64
77	69
77	71
77	76
77	96
78	27
78	31
78	35
78	37
78	38
78	39
78	40
78	41
78	42
78	43
78	45
78	46
78	47
78	52
78	64
78	69
78	71
78	76
78	96
81	27
81	31
81	35
81	37

PredatorID	PreyID
81	38
81	39
81	40
81	41
81	42
81	43
81	45
81	46
81	47
81	52
81	64
81	69
81	71
81	76
81	96
82	27
82	31
82	37
82	38
82	39
82	40
82	41
82	42
82	43
82	44
82	45
82	46
82	47
82	50
82	51
82	52
82	69
82	71
82	76
82	86
82	88
82	90
82	96
83	27
83	31
83	37
83	38

PredatorID	PreyID
83	39
83	40
83	41
83	42
83	43
83	44
83	45
83	46
83	47
83	50
83	51
83	52
83	69
83	71
83	76
83	86
83	88
83	90
83	96
85	9
85	12
85	13
85	14
85	69
85	71
85	76
85	86
85	88
85	90
85	96
86	27
86	37
86	38
86	39
86	40
86	41
86	42
86	43
86	44
86	45
86	46
86	47

PredatorID	PreyID
86	50
86	69
86	71
86	76
88	27
88	37
88	38
88	39
88	40
88	41
88	42
88	43
88	44
88	45
88	46
88	47
88	50
88	69
88	71
88	76
90	27
90	37
90	38
90	39
90	40
90	41
90	42
90	43
90	44
90	45
90	46
90	47
90	50
90	69
90	71
90	76
96	27
96	35
96	39
96	40
96	41
96	42

PredatorID	PreyID
96	43
96	45
96	46
99	31
99	64
99	69
99	71
99	76
99	77
99	78
99	81
99	82
99	83
99	85
99	86
99	88
99	90
99	96
99	99
99	100
99	101
99	102
99	103
99	104
99	107
99	110
99	111
99	112
99	113
99	114
99	115
99	116
99	117
99	118
99	119
99	120
99	121
99	122
99	129
99	130
99	133
99	134

PredatorID	PreyID
99	135
99	136
99	137
99	138
99	147
99	149
99	153
99	154
99	155
99	156
99	158
99	160
99	161
99	162
99	165
99	166
99	167
99	168
99	170
99	171
99	172
99	173
99	174
99	175
99	176
99	177
99	179
99	180
99	181
100	27
100	31
100	35
100	37
100	38
100	39
100	40
100	41
100	42
100	43
100	45
100	46
100	47

PredatorID	PreyID
100	50
100	52
100	69
100	71
100	76
101	31
101	64
101	69
101	71
101	76
101	77
101	78
101	81
101	82
101	83
101	85
101	86
101	88
101	90
101	96
101	100
101	101
101	102
101	103
101	104
101	107
101	110
101	111
101	113
101	115
101	153
101	154
101	158
101	160
101	161
101	162
101	165
101	166
101	167
101	168
101	170
101	171

PredatorID	PreyID
101	172
101	173
101	174
101	175
101	176
101	177
101	179
101	180
101	181
102	69
102	71
102	76
102	86
102	88
102	90
102	96
102	100
102	158
102	160
102	161
102	162
102	165
102	166
102	167
102	168
102	170
102	171
102	172
102	173
102	174
102	175
102	176
102	177
102	179
102	180
102	181
102	184
102	185
103	69
103	71
103	76
103	86

PredatorID	PreyID
103	88
103	90
103	96
103	100
103	158
103	160
103	161
103	162
103	165
103	166
103	167
103	168
103	170
103	171
103	172
103	173
103	174
103	175
103	176
103	177
103	179
103	180
103	181
103	184
103	185
104	27
104	31
104	37
104	38
104	39
104	40
104	41
104	42
104	43
104	44
104	45
104	46
104	47
104	52
104	69
104	71
104	76

PredatorID	PreyID
107	27
107	31
107	37
107	38
107	39
107	40
107	41
107	42
107	43
107	44
107	45
107	46
107	47
107	52
107	69
107	71
107	76
110	27
110	31
110	37
110	38
110	39
110	40
110	41
110	42
110	43
110	44
110	45
110	46
110	47
110	52
110	69
110	71
110	76
111	27
111	31
111	37
111	38
111	39
111	40
111	41
111	42

PredatorID	PreyID
111	43
111	44
111	45
111	46
111	47
111	52
111	69
111	71
111	76
112	64
112	77
112	78
112	81
112	82
112	83
112	85
112	99
112	100
112	101
112	102
112	103
112	104
112	107
112	110
112	111
112	112
112	113
112	114
112	115
112	116
112	117
112	118
112	119
112	120
112	121
112	122
112	129
112	130
112	133
112	134
112	135
112	136

PredatorID	PreyID
112	137
112	138
112	147
112	149
112	153
112	154
112	155
112	156
112	184
112	185
113	37
113	38
113	39
113	40
113	41
113	42
113	43
113	45
113	46
113	47
113	50
113	52
113	69
113	71
113	76
113	77
113	78
113	81
113	82
113	83
113	85
113	86
113	88
113	90
113	96
113	99
113	100
113	101
113	102
113	103
113	104
113	107

PredatorID	PreyID
113	110
113	111
113	112
113	113
113	114
113	115
113	116
113	117
113	118
113	119
113	120
113	121
113	122
113	129
113	130
113	133
113	134
113	135
113	136
113	137
113	138
113	147
113	149
113	153
113	154
113	155
113	156
113	158
113	160
113	161
113	162
113	165
113	166
113	167
113	168
113	170
113	171
113	172
113	173
113	174
113	175
113	176

PredatorID	PreyID
113	177
113	179
113	180
113	181
113	184
113	185
114	64
114	77
114	78
114	81
114	82
114	83
114	85
114	99
114	100
114	101
114	102
114	103
114	104
114	107
114	110
114	111
114	112
114	113
114	114
114	115
114	116
114	117
114	118
114	119
114	120
114	121
114	122
114	129
114	130
114	133
114	134
114	135
114	136
114	137
114	138
114	147

PredatorID	PreyID
114	149
114	153
114	154
114	155
114	156
114	184
114	185
115	31
115	37
115	38
115	39
115	40
115	41
115	42
115	43
115	45
115	46
115	47
115	50
115	52
115	64
115	69
115	71
115	76
115	77
115	78
115	81
115	82
115	83
115	85
115	86
115	88
115	90
115	96
115	99
115	100
115	101
115	102
115	103
115	104
115	107
115	110

PredatorID	PreyID
115	111
115	112
115	113
115	114
115	115
115	116
115	117
115	118
115	119
115	120
115	121
115	122
115	129
115	130
115	133
115	134
115	135
115	136
115	137
115	138
115	147
115	149
115	153
115	154
115	155
115	156
115	158
115	160
115	161
115	162
115	165
115	166
115	167
115	168
115	170
115	171
115	172
115	173
115	174
115	175
115	176
115	177

PredatorID	PreyID
115	179
115	180
115	181
115	184
115	185
116	64
116	82
116	83
116	85
116	99
116	100
116	101
116	102
116	103
116	104
116	107
116	110
116	111
116	112
116	113
116	114
116	115
116	116
116	117
116	118
116	119
116	120
116	121
116	122
116	129
116	130
116	133
116	134
116	135
116	136
116	137
116	138
116	147
116	149
116	153
116	154
116	155

PredatorID	PreyID
116	156
116	184
116	185
117	64
117	82
117	83
117	85
117	99
117	100
117	101
117	102
117	103
117	104
117	107
117	110
117	111
117	112
117	113
117	114
117	115
117	116
117	117
117	118
117	119
117	120
117	121
117	122
117	129
117	130
117	133
117	134
117	135
117	136
117	137
117	138
117	147
117	149
117	153
117	154
117	155
117	156
117	184

PredatorID	PreyID
117	185
118	82
118	83
118	85
118	100
118	101
118	102
118	103
118	104
118	107
118	110
118	111
118	113
118	115
118	118
118	119
118	120
118	121
118	122
118	130
118	134
118	136
118	138
118	153
118	154
118	155
118	184
118	185
119	69
119	71
119	76
119	77
119	78
119	81
119	82
119	83
119	85
119	86
119	88
119	90
119	96
119	100

PredatorID	PreyID
119	101
119	102
119	103
119	104
119	107
119	110
119	111
119	113
119	115
119	119
119	120
119	121
119	122
119	130
119	134
119	136
119	138
119	153
119	154
119	155
119	158
119	160
119	161
119	162
119	165
119	166
119	167
119	168
119	170
119	171
119	172
119	173
119	174
119	175
119	176
119	177
119	179
119	180
119	181
119	184
119	185
120	69

PredatorID	PreyID
120	71
120	76
120	77
120	78
120	81
120	82
120	83
120	85
120	86
120	88
120	90
120	96
120	100
120	101
120	102
120	103
120	104
120	110
120	111
120	113
120	115
120	153
120	154
120	158
120	160
120	161
120	162
120	165
120	166
120	167
120	168
120	170
120	171
120	172
120	173
120	174
120	175
120	176
120	177
120	179
120	180
120	181

PredatorID	PreyID
120	184
120	185
121	69
121	71
121	76
121	77
121	78
121	81
121	82
121	83
121	85
121	86
121	88
121	90
121	96
121	100
121	101
121	102
121	103
121	104
121	110
121	111
121	113
121	115
121	153
121	154
121	158
121	160
121	161
121	162
121	165
121	166
121	167
121	168
121	170
121	171
121	172
121	173
121	174
121	175
121	176
121	177

PredatorID	PreyID
121	179
121	180
121	181
121	184
121	185
122	69
122	71
122	76
122	77
122	78
122	81
122	82
122	83
122	85
122	86
122	88
122	90
122	96
122	100
122	101
122	102
122	103
122	104
122	110
122	111
122	113
122	115
122	153
122	154
122	158
122	160
122	161
122	162
122	165
122	166
122	167
122	168
122	170
122	171
122	172
122	173
122	174

PredatorID	PreyID
122	175
122	176
122	177
122	179
122	180
122	181
122	184
122	185
129	15
129	16
129	17
130	12
130	13
130	14
130	16
130	17
133	12
133	13
133	14
133	15
133	16
133	17
134	12
134	13
134	14
134	16
134	17
135	12
135	13
135	14
135	15
135	16
135	17
136	12
136	13
136	14
136	16
136	17
137	12
137	13
137	14
137	15

PredatorID	PreyID
137	16
137	17
138	12
138	13
138	14
138	16
138	17
147	9
147	13
147	14
147	16
147	17
149	9
149	13
149	14
149	16
149	17
153	12
153	13
153	14
154	12
154	13
154	14
155	12
155	13
155	14
155	16
155	17
156	12
156	13
156	14
156	16
156	17
158	31
158	35
158	37
158	38
158	39
158	40
158	41
158	42
158	43

PredatorID	PreyID
158	44
158	45
158	46
158	47
158	50
158	51
158	52
158	69
158	71
158	76
158	86
158	88
158	90
158	96
160	12
160	13
160	14
160	27
160	37
160	38
160	39
160	40
160	41
160	42
160	43
160	44
160	45
160	46
160	50
160	52
161	12
161	13
161	14
161	27
161	37
161	38
161	39
161	40
161	41
161	42
161	43
161	44

PredatorID	PreyID
161	45
161	46
161	50
161	52
162	12
162	13
162	14
162	27
162	37
162	38
162	39
162	40
162	41
162	42
162	43
162	44
162	45
162	46
162	50
162	52
165	27
165	37
165	38
165	39
165	40
165	41
165	42
165	43
165	44
165	45
165	46
165	50
165	52
166	27
166	37
166	38
166	39
166	40
166	41
166	42
166	43
166	44

PredatorID	PreyID
166	45
166	46
166	50
166	52
167	27
167	37
167	38
167	39
167	40
167	41
167	42
167	43
167	44
167	45
167	46
167	50
167	52
167	69
167	71
167	76
167	86
167	88
167	90
167	96
167	160
167	161
167	162
167	165
167	166
167	170
167	171
167	172
167	173
167	174
167	175
167	176
167	177
167	179
167	181
168	27
168	37
168	38

PredatorID	PreyID
168	39
168	40
168	41
168	42
168	43
168	44
168	45
168	46
168	50
168	52
168	69
168	71
168	76
168	86
168	88
168	90
168	96
168	160
168	161
168	162
168	165
168	166
168	170
168	171
168	172
168	173
168	174
168	175
168	176
168	177
168	179
168	181
170	27
170	37
170	38
170	39
170	40
170	41
170	42
170	43
170	44
170	45

PredatorID	PreyID
170	46
170	50
171	27
171	37
171	38
171	39
171	40
171	41
171	42
171	43
171	44
171	45
171	46
171	50
172	27
172	37
172	38
172	39
172	40
172	41
172	42
172	43
172	44
172	45
172	46
172	50
172	52
173	27
173	37
173	38
173	39
173	40
173	41
173	42
173	43
173	44
173	45
173	46
173	50
173	52
174	27
174	37

PredatorID	PreyID
174	38
174	39
174	40
174	41
174	42
174	43
174	44
174	45
174	46
174	50
174	52
175	27
175	37
175	38
175	39
175	40
175	41
175	42
175	43
175	44
175	45
175	46
175	50
175	52
176	27
176	37
176	38
176	39
176	40
176	41
176	42
176	43
176	44
176	45
176	46
176	50
176	52
177	27
177	37
177	38
177	39
177	40

PredatorID	PreyID
177	41
177	42
177	43
177	44
177	45
177	46
177	50
177	52
179	27
179	37
179	38
179	39
179	40
179	41
179	42
179	43
179	44
179	45
179	46
179	50
180	27
180	37
180	38
180	39
180	40
180	41
180	42
180	43
180	44
180	45
180	46
180	50
181	27
181	37
181	38
181	39
181	40
181	41
181	42
181	43
181	44
181	45

PredatorID	PreyID
181	46
181	50
184	9
184	12
184	13
184	14
185	37
185	38
185	39
185	40
185	41
185	42
185	43
185	45
185	46
185	47
185	50
185	52

Table E20.—TS consumer-resource list for biozone 6. See Table E7 for master list of taxonomic ID numbers.

PredatorID	PreyID
27	2
31	9
31	27
31	31
31	35
31	39
31	40
37	12
37	13
37	14
37	15
37	16
37	17
38	12
38	13
38	14
38	15
38	16
38	17
38	18
38	19
39	2
40	2
41	2
41	9
41	12
41	13
41	14
41	37
41	38
41	39
41	40
41	41
41	42
41	43
41	44
41	45
41	46
41	47
41	50
41	52
42	37
42	38
42	39
42	40
42	41
42	42
42	43
42	44
42	45
42	46
42	47
42	50
42	52
43	2
44	15
44	18
45	112
45	113
45	114
45	115
45	125
45	129
45	130
45	133
45	134
45	137
45	143
45	144
45	145
45	146
45	147
45	154
45	155
45	156
46	37
46	38
46	39
46	40
46	41
46	42
46	43
46	44
46	45
46	46
46	47
46	50
46	52
47	37
47	38
47	39
47	40
47	41
47	42
47	43
47	44
47	45
47	46
47	47
47	50
47	52
50	15
50	16
50	17
50	18
50	19
51	12
51	13
51	14
51	15
51	16
51	17
51	18
51	19
52	12
52	13
52	14
52	15
52	16
52	17

PredatorID	PreyID
52	18
52	19
64	35
64	37
64	38
64	39
64	40
64	41
64	42
64	43
64	45
64	46
64	47
64	50
64	52
64	70
64	71
64	74
64	75
70	27
70	35
70	39
70	40
71	27
71	35
71	39
71	40
74	27
74	35
74	39
74	40
74	41
74	42
74	43
74	45
74	46
75	27
75	35
75	39
75	40
75	41
75	42

PredatorID	PreyID
75	43
75	45
75	46
77	27
77	31
77	35
77	37
77	38
77	39
77	40
77	41
77	42
77	43
77	45
77	46
77	47
77	52
77	64
77	70
77	71
77	74
77	75
78	27
78	31
78	35
78	37
78	38
78	39
78	40
78	41
78	42
78	43
78	45
78	46
78	47
78	52
78	64
78	70
78	71
78	74
78	75
79	27

PredatorID	PreyID
79	31
79	35
79	37
79	38
79	39
79	40
79	41
79	42
79	43
79	45
79	46
79	47
79	52
79	64
79	70
79	71
79	74
79	75
80	27
80	31
80	35
80	37
80	38
80	39
80	40
80	41
80	42
80	43
80	45
80	46
80	47
80	52
80	64
80	70
80	71
80	74
80	75
81	27
81	31
81	35
81	37
81	38

PredatorID	PreyID
81	39
81	40
81	41
81	42
81	43
81	45
81	46
81	47
81	52
81	64
81	70
81	71
81	74
81	75
82	27
82	31
82	37
82	38
82	39
82	40
82	41
82	42
82	43
82	44
82	45
82	46
82	47
82	50
82	51
82	52
82	70
82	71
82	74
82	75
82	95
83	27
83	31
83	37
83	38
83	39
83	40
83	41

PredatorID	PreyID
83	42
83	43
83	44
83	45
83	46
83	47
83	50
83	51
83	52
83	70
83	71
83	74
83	75
83	95
85	9
85	12
85	13
85	14
85	70
85	71
85	74
85	75
85	95
95	27
95	37
95	38
95	39
95	40
95	41
95	42
95	43
95	44
95	45
95	46
95	47
95	50
95	70
95	71
95	74
95	75
97	70
97	71

PredatorID	PreyID
97	74
97	75
97	95
97	97
97	100
97	158
97	162
97	163
97	167
97	174
97	178
97	179
97	180
97	184
97	185
99	31
99	64
99	70
99	71
99	74
99	75
99	77
99	78
99	79
99	80
99	81
99	82
99	83
99	85
99	95
99	97
99	99
99	100
99	101
99	110
99	112
99	113
99	114
99	115
99	125
99	129
99	130

PredatorID	PreyID
99	133
99	134
99	137
99	143
99	144
99	145
99	146
99	147
99	154
99	155
99	156
99	158
99	162
99	163
99	167
99	174
99	178
99	179
99	180
100	27
100	31
100	35
100	37
100	38
100	39
100	40
100	41
100	42
100	43
100	45
100	46
100	47
100	50
100	52
100	70
100	71
100	74
100	75
101	31
101	64
101	70
101	71

PredatorID	PreyID
101	74
101	75
101	77
101	78
101	79
101	80
101	81
101	82
101	83
101	85
101	95
101	97
101	100
101	101
101	110
101	113
101	115
101	154
101	158
101	162
101	163
101	167
101	174
101	178
101	179
101	180
110	27
110	31
110	37
110	38
110	39
110	40
110	41
110	42
110	43
110	44
110	45
110	46
110	47
110	52
110	70
110	71

PredatorID	PreyID
110	74
110	75
112	64
112	77
112	78
112	79
112	80
112	81
112	82
112	83
112	85
112	97
112	99
112	100
112	101
112	110
112	112
112	113
112	114
112	115
112	125
112	129
112	130
112	133
112	134
112	137
112	143
112	144
112	145
112	146
112	147
112	154
112	155
112	156
112	184
112	185
113	37
113	38
113	39
113	40
113	41
113	42

PredatorID	PreyID
113	43
113	45
113	46
113	47
113	50
113	52
113	70
113	71
113	74
113	75
113	77
113	78
113	79
113	80
113	81
113	82
113	83
113	85
113	95
113	97
113	99
113	100
113	101
113	110
113	112
113	113
113	114
113	115
113	125
113	129
113	130
113	133
113	134
113	137
113	143
113	144
113	145
113	146
113	147
113	154
113	155
113	156

PredatorID	PreyID
113	158
113	162
113	163
113	167
113	174
113	178
113	179
113	180
113	184
113	185
114	64
114	77
114	78
114	79
114	80
114	81
114	82
114	83
114	85
114	97
114	99
114	100
114	101
114	110
114	112
114	113
114	114
114	115
114	125
114	129
114	130
114	133
114	134
114	137
114	143
114	144
114	145
114	146
114	147
114	154
114	155
114	156

PredatorID	PreyID
114	184
114	185
115	31
115	37
115	38
115	39
115	40
115	41
115	42
115	43
115	45
115	46
115	47
115	50
115	52
115	64
115	70
115	71
115	74
115	75
115	77
115	78
115	79
115	80
115	81
115	82
115	83
115	85
115	95
115	97
115	99
115	100
115	101
115	110
115	112
115	113
115	114
115	115
115	125
115	129
115	130
115	133

PredatorID	PreyID
115	134
115	137
115	143
115	144
115	145
115	146
115	147
115	154
115	155
115	156
115	158
115	162
115	163
115	167
115	174
115	178
115	179
115	180
115	184
115	185
125	70
125	71
125	74
125	75
125	82
125	83
125	85
125	95
125	100
125	110
125	113
125	115
125	154
125	158
125	162
125	163
125	167
125	174
125	178
125	179
125	180
125	184

PredatorID	PreyID
125	185
129	15
129	16
129	17
130	12
130	13
130	14
130	16
130	17
133	12
133	13
133	14
133	15
133	16
133	17
134	12
134	13
134	14
134	16
134	17
137	12
137	13
137	14
137	15
137	16
137	17
143	12
143	13
143	14
143	15
143	16
143	17
144	12
144	13
144	14
144	16
144	17
145	12
145	13
145	14
145	15
145	16

PredatorID	PreyID
145	17
146	12
146	13
146	14
146	16
146	17
147	9
147	13
147	14
147	16
147	17
154	12
154	13
154	14
155	12
155	13
155	14
155	16
155	17
156	12
156	13
156	14
156	16
156	17
158	31
158	35
158	37
158	38
158	39
158	40
158	41
158	42
158	43
158	44
158	45
158	46
158	47
158	50
158	51
158	52
158	70
158	71

PredatorID	PreyID
158	74
158	75
162	12
162	13
162	14
162	27
162	37
162	38
162	39
162	40
162	41
162	42
162	43
162	44
162	45
162	46
162	50
162	52
163	12
163	13
163	14
163	27
163	37
163	38
163	39
163	40
163	41
163	42
163	43
163	44
163	45
163	46
163	50
163	52
167	27
167	37
167	38
167	39
167	40
167	41
167	42
167	43

PredatorID	PreyID
167	44
167	45
167	46
167	50
167	52
167	70
167	71
167	74
167	75
167	162
167	163
167	174
167	178
167	179
174	27
174	37
174	38
174	39
174	40
174	41
174	42
174	43
174	44
174	45
174	46
174	50
174	52
178	27
178	37
178	38
178	39
178	40
178	41
178	42
178	43
178	44
178	45
178	46
178	50
178	52
178	70
178	71

PredatorID	PreyID
178	74
178	75
179	27
179	37
179	38
179	39
179	40
179	41
179	42
179	43
179	44
179	45
179	46
179	50
180	27
180	37
180	38
180	39
180	40
180	41
180	42
180	43
180	44
180	45
180	46
180	50
184	9
184	12
184	13
184	14
185	37
185	38
185	39
185	40
185	41
185	42
185	43
185	45
185	46
185	47
185	50
185	52